BRITISH COLUMBIA
Canada's Pacific Gateway

GEOLOGICAL FIELDWORK 2010

A SUMMARY OF FIELD ACTIVITIES AND CURRENT RESEARCH

Paper 2011-1

BRITISH COLUMBIA
Canada's Pacific Gateway

GEOLOGICAL FIELDWORK 2010

A Summary of Field Activities and Current Research

Ministry of Forests, Mines and Lands
British Columbia Geological Survey

Paper 2011-1

Ministry of Forests, Mines and Lands
Mines and Mineral Resources Division
British Columbia Geological Survey

Parts of this publication may be quoted or reproduced if source and authorship are acknowledged.
The following is the recommended format for referencing individual works contained in this publication:

Logan, J.M., Mihalynuk, M.G., Friedman, R.M. and Creaser, R.A. (2011): Age Constraints of Mineralization at the Brenda and Woodjam Cu-Mo±Au Porphyry Deposits – An Early Jurassic Calcalkaline Event, South-central British Columbia; *in* Geological Fieldwork 2010, *BC Ministry of Forests, Mines and Lands*, Paper 2011-1, pages 129–144.

COVER PHOTO: *Left – Ray Lett soil sampling at the Watson Bar property 40 kilometres north of Lillooet; Emeritus Geochemist, British Columbia Geological Survey*

Right – Nick Massey looking at diorite and pyroxenite intrusive into Nicola Group sediments in the Lawless Creek area northwest of Princeton; Emeritus Geoscientist, British Columbia Geological Survey

BACK PHOTO: *Scott Caldwell (L) and Paul Schiarizza (R) (British Columbia Geological Survey) mapping structure and stratigraphy in the Kutcho Creek volcanogenic massive sulphide district.*

This publication is also available, free of charge, as colour digital files, in Adobe Acrobat® PDF format, from the BC Ministry of Forests, Mines and Lands website at:

http://www.empr.gov.bc.ca/Mining/Geoscience/PublicationsCatalogue/Fieldwork

British Columbia Cataloguing in Publication Data

Main entry under title:

Geological Fieldwork: - 1974 -

Annual.

Issuing body varies

Vols. For 1978-1996 issued in series: Paper / British Columbia. Ministry of Energy, Mines and Petroleum Resources; vols for 1997-1998, Paper / British Columbia. Ministry of Employment and Investment; vols for 1999-2004, Paper / British Columbia Ministry of Energy and Mines; vols for 2005- , Paper / British Columbia Ministry of Energy, Mines and Petroleum Resources.

Includes Bibliographical references.

ISSN 0381-243X=Geological Fieldwork

1. Geology - British Columbia - Periodicals. 2. Mines and mineral resources - British Columbia - Periodicals. 3. Geology - Fieldwork - Periodicals. 4. Geology, Economic - British Columbia - Periodicals. 5. British Columbia. Geological Survey Branch - Periodicals. I. British Columbia. Geological Division. II. British Columbia. Geological Survey Branch. III. British Columbia. Geological Survey Branch. IV. British Columbia. Dept. of Mines and Petroleum Resources. V. British Columbia. Ministry of Energy, Mines and Petroleum Resources. VI. British Columbia. Ministry of Employment and Investment. VII. British Columbia Ministry of Energy and Mines. VIII. Series: Paper (British Columbia. Ministry of Energy, Mines and Petroleum Resources). IX. Series: Paper (British Columbia. Ministry of Employment and Investment). X. Series: Paper (British Columbia Ministry of Energy and Mines). XI. Series: Paper (British Columbia Ministry of Energy, Mines and Petroleum Resources).

QE187.46 622.1'09711 C76-083084-3 (Rev.)

VICTORIA
BRITISH COLUMBIA
CANADA

JANUARY 2011

FOREWORD

Geological Fieldwork 2010

The **British Columbia Geological Survey** (BCGS) presents here the results of 2010 field surveys and geoscience research in the thirty-sixth edition of **Geological Fieldwork**. The articles profile some of the considerable staff expertise housed in the Survey. The provision of new geoscience data about British Columbia is a key activity of the BCGS that leads to mineral tenure acquisition and increased mineral exploration activity in the Province. Most articles are contributions by Survey staff to the understanding of the geology, geochemistry, and mineral deposits of the Province. The volume also includes contributions from the Geoscience and Natural Gas Development Branch of the Ministry of Energy and other professional geoscientists.

Late in 2010, the government of British Columbia reorganized the natural resource sector ministries. The BCGS moved to the new Ministry of Forests, Mines and Lands along with the Mineral Policy Branch, while the regional geologists and the remaining Mines and Minerals Division staff of the former Ministry of Energy, Mines and Petroleum Resources moved to the new Ministry of Natural Resource Operations.

British Columbia Geological Survey Successes

- The BCGS, in partnership with Geoscience BC, continued with the second year of a surficial geology and till geochemistry sampling program in the Colleymount map area southeast of Houston. The aim of the fieldwork is two-fold: to reconstruct the region's glacial and ice-flow history and assess the economic potential of covered bedrock.
- The second season of the North Coast project, jointly delivered with the Geological Survey of Canada (GSC), covered a map area of 30 by 50 kilometres. Mapping in 2010 focused on the southern end of the Alexander terrane near Klemtu. One highlight of this work is that the Grenville Channel fault is a mid-Cretaceous sinistral fault of regional extent (>150 km).
- The Iskut River project followed up on the 2009 summer program with mapping in the Hoodoo Mountain area north of the Rock and Roll volcanogenic massive sulphide deposit. This project is a partnership between Pacific North West Capital Corp., the University of Victoria, the GSC, and the BCGS.
- The new Kutcho Creek project is a two-year bedrock mapping program initiated by the BCGS in 2010 in partnership with the Geological Survey of Canada and Kutcho Mining Corp.
- The BCGS and the GSC began collaborating on a multi-year province-wide study of rare metals. This project falls under the renewed Targeted Geoscience Initiative program (TGI-4) of the GSC.
- Our online interface MapPlace and its supporting site now exceed 11,000 web pages. This interface is used 24 hours a day, 7 days a week by the exploration community world wide and plays an essential and growing role in attracting investment to the province.
- Sixteen mineral resource assessments were completed to facilitate treaty negotiations and government land use planning.
- The Property File database now features more than 25,000 documents online.
- MINFILE continues to improve with 171 MINFILE occurrences updated and 20 new ones identified.
- Staff of the BC Mineral Development Office in Vancouver hosted international investor delegations and led the mining Asia Investment Mission in November.
- The BCGS initiated a new Emeritus Scientist program with two new members in 2010.
- In 2010, the BCGS restarted its 8 member Advisory Subcommittee after a 6-year hiatus. The subcommittee includes 4 industry representatives from Geoscience's BC Technical Advisory Committee and 4 independent industry members that together provide advice on the technical activities of the Survey.
- Survey geologists were key presenters at conferences and workshops around the province including Roundup, KEG, Minerals South, Minerals North, Smither's Rock Talk, and led multiple industry field trips to the North Vancouver Island, Nechako, and Merritt areas.
- The BCGS hosted a sold-out International Workshop on the Geology of Rare Metals in Victoria on Nov. 9th and 10th. The workshop was held in lieu of a fall BCGS Open House.

D.V. Lefebure
Chief Geologist
British Columbia Geological Survey

TABLE OF CONTENTS

Rowins, S.M., Jones, L., Lefebure, D.V. and Fredericks, J.: British Columbia Geological Survey Activities in 2010 1

NORTHERN BRITISH COLUMBIA

Ferri, F., Hickin, A. and Huntley, D.: Bedded Barite-Pyrite Occurrences in upper Besa River Formation, western Liard Basin, British Columbia and Regional Correlations with Devonian to Mississippian Sub-surface Formations..... 13

Hora, Z.D., Langrová, A. and Pivec, E.: Nickeliferous Minerals in the Cassiar Asbestos Deposit, Northern British Columbia (NTS 104P/05) - Relevance for Nickel Exploration 31

Mihalynuk, M.G., Logan, J.M., Zagorevski, A. and Joyce, N.: Geology and Mineralization of the Hoodoo Mountain Area (NTS 104B/14E)..... 37

Mihalynuk, M.G., Ambrose, T.K., Devine, F.A.M. and Johnston, S.T.: Atlin Placer Gold Nuggets Containing Mineral and Rock Matter: Implications for Lode Gold Exploration 65

Nelson, J.L., Diakow, L.J., Karl, S., Mahoney, J.B., Gehrels, G.E., Pecha, M. and van Staal, C.: Geology and Mineral Potential of the Southern Alexander Terrane and western Coast Plutonic Complex near Klemtu, Northwestern British Columbia 73

Schiarizza, P.: Geology of the Kutcho Assemblage between Kutcho Creek and the Tucho River, Northern British Columbia (NTS 104I/01)..... 99

CENTRAL BRITISH COLUMBIA

Ferbey, T.: Quaternary Geology and Till Geochemistry of the Colleymount Map Area (NTS 093L/01), West-Central British Columbia..... 119

Logan, J.M., Mihalynuk, M.G., Friedman, R.M. and Creaser, R.A.: Age Constraints of Mineralization at the Brenda and Woodjam Cu-Mo±Au Porphyry Deposits – An Early Jurassic Calcalkaline Event, South-Central British Columbia 129

SOUTHERN BRITISH COLUMBIA

Massey, N.W.D.: Southern Nicola Project: Geochemistry of Volcanic Rocks of the Nicola Group West of the Boundary Fault (Parts of NTS 092H/02, 07 and 10)..... 145

PROVINCE-WIDE

Cui, Y.: Improving the Efficiency in the Maintenance of the Provincial Geological Database 159

Cui, Y: Regional Geochemical Survey: Validation and Refitting of Stream Sample Locations 169

Lett, R.E. and Paterson, K: A Comparison of Several Commercially Available Methods for the Geochemical Analysis of Rare Earth, Rare Metal and High Field Strength Elements in Geological Samples..... 181

Paradis, S. and Simandl, G.J.: Carbonate-hosted, Nonsulphide Zn–Pb (supergene) Mineral Deposit Profile B09..... 189

MINISTRY OF FORESTS, MINES AND LANDS

MINISTRY OF ENERGY

www.empr.gov.bc.ca/geology

British Columbia Geological Survey Activities in 2010

by S.M. Rowins, L. Jones, D.V. Lefebure and J. Fredericks

INTRODUCTION

The British Columbia Geological Survey (BCGS) continued to play a leading role in the creation of a thriving, safe, and sustainable mining industry in British Columbia (BC) in 2010. This was accomplished by providing world-class geoscience expertise and data to government, industry, and the general public. These diverse groups use our expertise and data in different ways, but an underlying interest of all groups is to see the province position itself as a favoured destination for investment by the mineral exploration and mining industry. A great attribute of the BCGS in the fast-paced world of today is its ability to consistently deliver standardized high quality geological maps, geoscience reports, and online interactive geoscience databases in a very short timeframe. All geoscience products are made available online via MapPlace, the award-winning internet portal of the BCGS.

The mineral exploration and mining industry continued to perform well throughout the 2008-10 recession and helped lead the economic recovery in BC. Exploration expenditures in 2010 are estimated between $220 and $300 million, a significant increase over the $154 million spent in 2009. Nevertheless, funding levels for the BCGS in 2010 were similar to those in 2009. This resulted in the BCGS continuing to focus on creating new geoscience products from existing data and developing innovative programs that involved cooperative partnerships with universities, industry, and other public geoscience agencies. The BCGS continued its long collaboration with the Geological Survey of Canada (GSC) by participating in four joint field projects in 2010. Three field mapping projects were delivered as part of the GSC's Geo-mapping for Energy and Minerals (GEM) program and a new multi-year rare metals project started under the auspices of the renewed Targeted Geoscience Initiative program (TGI-4). This rare metals project is a national initiative co-lead by George Simandl of the BCGS. Its overall objective is to develop new exploration methodologies and technologies in the search for rare metal deposits. Rare metals are important in the manufacturing of automobiles and many high-tech products such as cell phones and computers. Other important BCGS partners included Geoscience BC (GBC). In 2010, the BCGS and GBC collaborated on the delivery of a surficial mapping and till sampling program southeast of Houston in the Tahtsa Lake district of west-central BC. Finally, as in past years, university students were employed as co-op interns and geoscience assistants throughout the year. Their help with the delivery of our field programs and work on improving our digital geoscience databases is greatly appreciated.

This publication is also available, free of charge, as colour digital files in Adobe Acrobat® PDF format from the BC Ministry of Forests, Mines and Lands website at http://www.empr.gov.bc.ca/Mining/Geoscience/PublicationsCatalogue/Fieldwork.

BCGS FIELD ACTIVITIES

A main priority of the BCGS is to generate new geoscience data and products, including bedrock and surficial geology maps and targeted mineral deposit studies. The locations of the 2010 field projects are shown in Figure 1. Projects are typically chosen with the objective of helping to diversify local economies by attracting mineral exploration activity that may lead to the opening of new mines. In many parts of the province, mineral exploration and mining are essential drivers of local employment and tax revenue, and directly support the development of regional infrastructure.

Field mapping studies (Figure 1) continued in the North Coast (Nelson *et al.*, this volume), Iskut River (Mihalynuk *et al.*, this volume), and Tahtsa Lake (Ferbey, this volume) areas of the province. A new two-year GEM "Edges" project in northern British Columbia started in 2010 with mapping in the Kutcho Creek area near the Kutcho Creek volcanogenic massive sulphide deposit (Schiarizza, this volume).

In addition to these 2010 mapping projects, several other mineral deposit-related studies were brought to completion. These include age determinations of mineralization and porphyritic intrusive rocks at the Brenda and Woodjam porphyry Cu-Mo (Au) deposits (Logan *et al.*, this volume), the creation of a new Mineral Deposit Profile for carbonate-hosted, nonsulphide Zn-Pb deposits in BC (Paradis and Simandl, this volume), a preliminary study of nickeliferous minerals in the Cassiar asbestos deposit (Hora *et al.*, this volume), an investigation of placer gold nuggets with implications for bedrock sources from the Atlin placer camp (Mihalynuk *et al.*, this volume), a study of the mineral potential of the western Liard Basin in northeastern BC (Ferri *et al.*, this volume) and a discussion of the geochemistry of Permo-Triassic volcanic rocks of the southern Nicola Group west

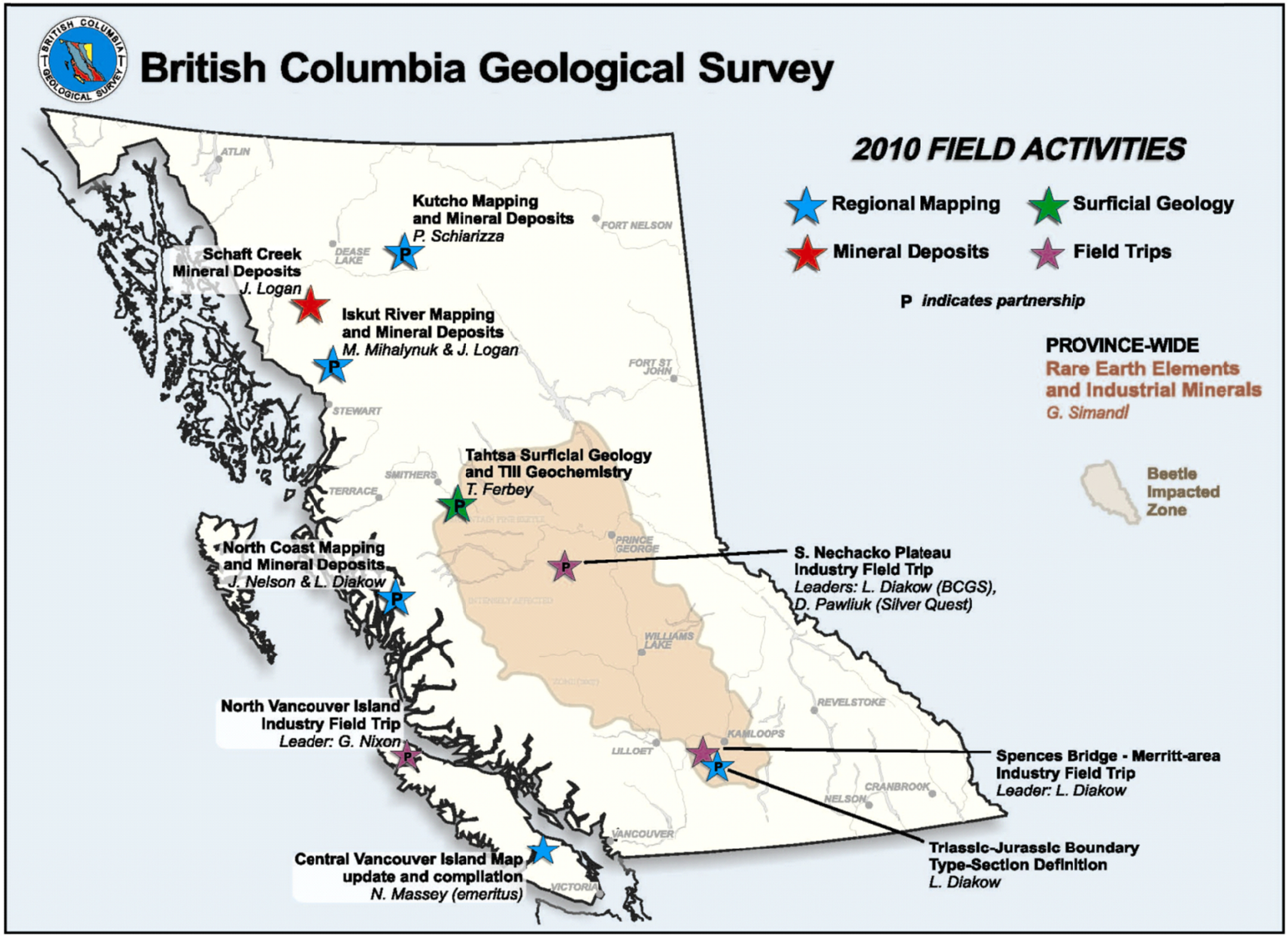

Figure 1. British Columbia Geological Survey 2010 field project areas.

of the Boundary fault near Princeton (Massey, this volume). The western Liard shale basin study is a welcome contribution from the Geoscience and Natural Gas Development Branch of the Ministry of Energy. A technical report by Cui (this volume) on the validation and refitting of stream sample locations in Regional Geochemical Surveys (RGS), together with a another paper by Cui (this volume) on the best practices for maintaining geological databases, highlight the importance of data integrity in public geoscience reporting. A technical paper comparing analytical methods for rare earth, rare metal, and high field strength elements in geological samples (Lett and Paterson, this volume) rounds out the contributions (Figure 2).

Several smaller field projects were also completed by Survey staff over the summer. The Schaft Creek porphyry Cu-Mo-Au deposit in northwest BC was visited by Jim Logan and Regional Geologist Paul Wojdak out of the Smithers office (Figure 1). They investigated the various styles of mineralization and types of alteration at Schaft Creek in an effort to draw comparisons and contrasts with other porphyry systems in the province. Larry Diakow visited the Spences Bridge–Merritt area and mapped type sections of the Nicola Group containing conodonts that accurately define the Triassic-Jurassic timescale boundary (Figure 1).

Ongoing Projects

Edges – Modeling the Evolution of the Northern Cordillera Resource Environment from the Edges of Exotic Terranes

Edges is a highly focused multi-year geological mapping initiative involving formal collaboration between the Government of Canada, the Province of British Columbia, the Yukon Territory, Geoscience BC, the United States Geological Survey, and the Alaska Division of Geological and Geophysical Surveys. It began field operations in 2009 in British Columbia and will last until 2013. It is a key project in the Federal GEM program. Support is being contributed by all participating agencies.

Figure 2. Ray Lett collecting stream samples that contains various pathfinder elements used by exploration geochemists to discover mineral deposits.

The ultimate goal of the initiative is to improve the effectiveness of resource exploration and discovery in the northern Cordillera by outlining resource-rich environments in British Columbia, the Yukon, and Alaska. The geological targets are the exotic outer terranes with their enclosed pre-accretionary syngenetic and epigenetic deposits and the metal-rich Triassic through Paleogene magmatic arcs and associated accretion zones that resulted from interaction of the terranes with the western margin of ancient North America. The target areas include parts of northern and central British Columbia where the geological map base is either several decades out of date or at insufficiently large scale to evaluate mineral potential using modern tectonic interpretations.

North Coast Partnership Project (Edges)

JoAnne Nelson and Larry Diakow returned from a successful second field season mapping along the northern coastal region of BC. In 2009, the first year of the North Coast project, geological mapping began on and near Porcher Island, at the northern end of the Alexander terrane south of Prince Rupert (Figure 1). Mapping in 2010 focused on the southern end of the terrane near Klemtu. In 2011, sparse exposures of pre-plutonic stratified rocks in the intervening region will be documented. JoAnne and Larry's activities were done with help from Brian Mahoney (and his graduate students) from the University of Wisconsin, George Gehrels and Mark Pecha of the University of Arizona, and Cees van Staal from the Geological Survey of Canada. The North Coast project achieved the following in its second year of operation:

- completion of geological map coverage of a 30 by 50 kilometre area covering the channels and islands between Return Channel and northern Princess Royal Island, in eastern Laredo Sound map area.
- rock units of the Alexander terrane of southeastern Alaska can be traced into northwestern British Columbia, including those that are known to host volcanogenic massive sulphide (VMS) mineralization. Farther south, in the 2010 map area, the Alexander terrane is represented by younger, probably Devonian, clastic-carbonate strata.
- the Grenville Channel fault is a mid-Cretaceous sinistral fault of regional extent (>150 km).

Iskut River Partnership Project (Edges)

Mitch Mihalynuk, Jim Logan, and Alex Zagorevski of the GSC returned to the Coast Belt of northwest BC and the area surrounding the Rock and Roll volcanogenic massive sulphide deposit (Figure 3). This was the second

Figure 3. Mitch Mihalynuk using geological intuition to identify areas of high mineral potential in the Iskut.

Figure 4. A structurally engaged Jim Logan with Hoodoo Mountain shrouded in clouds in the background.

field season of a partnership between Pacific North West Capital Corp., the University of Victoria, the GSC, and the BCGS. The short-term goal of the project is to determine the stratigraphic and structural setting of the Rock and Roll deposit. The longer term goal is to evaluate the potential for similar mineralization within the Iskut and adjacent regions. Follow up work in 2010 revealed that the stratigraphic sequence, which hosts the Rock and Roll deposit, is similar to that which hosts the Granduc volcanogenic massive sulphide deposit to the south. Mapping in the Hoodoo Mountain area north of Rock and Roll also led to the discovery of numerous copper-gold showings in intrusive rocks that share similarities with the alkalic porphyry Cu-Au style mineralization at the Galore Creek deposit (Figure 4).

Tahtsa Lake Partnership Project

Travis Ferbey, in partnership with Geoscience BC, returned to the Tahtsa Lake district to complete a till geochemistry survey northeast of Huckleberry Mine in the Colleymount map area (NTS 093L/1) that hosts the past producing Equity Silver Mine (Figure 1). This is an area that has high potential to host porphyry Cu+/-Mo+/-Au and polymetallic vein occurrences, and possibly volcanogenic massive sulphide deposits. This is the second and final year of the program and builds upon previous Quaternary geology and till geochemistry work by Ferbey in 2009. Quaternary till cover presents a challenge to traditional prospecting and makes the area ideally suited for a mineral potential assessment using till geochemistry. During the 2010 field season, 85 basal till samples were collected for analysis. An additional 18 till samples were collected for separation and analysis of heavy mineral concentrates and gold-grain counts.

Observations made at field stations suggest that Quaternary sediments within the study area may not be as thick or areally extensive as previously hypothesized. Therefore, sedimentary cover may not be as significant a hindrance to mineral exploration in the map area.

Southern Nicola Project

Geochemical highlights from Nick Massey on Nicola Group rocks (this volume) follow up on the coordinated mapping projects in 2008 and 2009 by Massey and his colleagues. The present study utilized samples of Nicola Group volcanic and volcaniclastic rocks collected during these years (Figure 5). The results of the geochemical analyses confirm correlation of the Nicola Group rocks west of the Boundary fault with the “Western Belt”. This correlation may have implications for mineralization in the project area. Specifically, felsic volcanic rocks in the “Western Belt” are potential hosts to volcanogenic massive sulphide deposits, although felsic volcanic rocks have not yet been identified in the project area.

Figure 5. Nick Massey examining volcanic rocks of the Nicola Group, Princeton, southern British Columbia.

Major New Projects

Kutcho Partnership Project (Edges)

The Kutcho project is a two-year bedrock mapping program initiated by the BCGS in 2010 in partnership with the Geological Survey of Canada (Edges project) and Kutcho Mining Corp. (formerly Capstone Mining Corporation). The aim of this project is to gain a better understanding of, and provide more detailed geological maps for, the Permo-Triassic Kutcho assemblage, which hosts the Kutcho Creek volcanogenic massive sulphide deposit.

Rare Metals TGI-4 Partnership Project

The BCGS and GSC began collaborating on a multi-year province-wide study of rare metals. The term "rare metals" refers mainly to uncommon, nonferrous metals used in small quantities, typically <150 000 tonnes/year, or derived from geographically restricted areas. The Rare Metals TGI-4 Program will study ore deposits in terms of geological setting, mineralizing processes, applied mineralogy, exploration methods, and metallurgical constraints. The results will address some of the major knowledge gaps related to these deposits and are expected to help the Canadian mining industry tap domestic sources of rare metals. This will contribute directly to supporting the existing and newly developing segments of the high technology industry in North America and help ensure adequate global supply. George Simandl of the BCGS is the national science leader for the Rare Metals TGI-4 Program.

MAPPLACE AND DATABASE ACTIVITIES

MapPlace

MapPlace, our internet portal and one of the most effective geoscience online map systems globally, continues to improve with the addition of new data layers and improved interface tools. MapPlace has provided clients with efficiencies in research time, data costs and analysis. Data themes and applications available on MapPlace include mineral potential, bedrock and surficial geology, publications, mineral and petroleum tenure, MINFILE, assessment reports, geochemistry and geophysical surveys. Yao Cui and Pat Desjardins contributed geomatic expertise to MapPlace data and application enhancements and integration of servers. MapPlace became active on a new web server in October 2009 and steps are being taken to upgrade maps to MapGuide Enterprise.

New data and updates on MapPlace in 2010 include:

- update to regional geochemistry catchment basins and RGS locations snapped to 1:20 000-scale rivers;
- mineral tenure archives for January 2010 and January 2011;
- Natural Resource Sector Boundaries and First Nations Treaty Areas;
- new BCGS Publication Search Application without imbedded MapPlace map plus Google searches for various parts of the web, databases and reports;
- Mineral Economy map updates with current mines and 2009 exploration properties;
- dynamic update of MINFILE and ARIS with the GeoBC Geographic Warehouse (LRDW);
- Till Geochemistry of the Nadina River Map Area (NTS 093E/15), BCGS Open File 2010-07;
- Relative Drift Thickness Map, North-Central BC, Geoscience BC Report 2010-14;
- QUEST-South Airborne Gravity Survey, Geoscience BC Report 2010-6;
- Regional Drainage Sediment and Water Geochemical Data, Central BC, Geoscience BC Report 2009-11;
- re-analysis of archived stream and lake sediment samples covering NTS map sheets, Sample Reanalysis (NTS 082E, 082L, 082M, 092H, 092I, 092J, 092O, 092P) QUEST-South Project, Geoscience BC Report 2010-4;
- QUEST-South Regional Geochemical Data, in-fill sampling and the reanalysis of archived sediment pulps from NTS map sheets 092H, 092I, 092J, Geoscience BC Report 2010-13;
- Open File 2008-4, Rock Properties table downloads and display;
- additional infrastructure, including airport and port locations, and hydro lines; and
- updated BCGS CGKN Data Catalogue totalling 3900 records.

Property File, Databases, Innovation and Mineral Resource Evaluations

During 2010 Property File, a collection of over 63 000 unique industry documents and maps, continued to grow. Recent Property File donations were made by Andre Panteleyev, Tom Schroeter and the estate of W.G. Hainsworth. As of December, 2010, over 25 000 property file documents were available online, including 403 Falconbridge, 1649 Cyprus-Anvil, 304 Chevron, 476 Placer Dome, 1328 Rimfire, 2969 Mine Plans, 9888 Tom Schroeter project files and 9000 Library items. These are retrieved through a search application or through links from MINFILE, http://www.propertyfile.gov.bc.ca and http://www.minfile.ca, respectively. Kirk Hancock is the Property File contact. Sarah Meredith-Jones is the MINFILE contact and this year approved update of 171 occurrences and additions of 20 new occurrences.

Users can now access over 30 900 company mineral assessment reports using the ARIS database over the web. Allan Wilcox and Ted Fuller work with clients to approve reports. The mining industry is encouraged to submit assessment reports in digital form to the Mineral Titles Branch. Benefits include higher quality, more efficient digital reports; quicker approval; and lower costs for printing, mailing, storage, scanning and processing. During the year 930 reports were submitted, of which 911 were approved. Of these, 592 or 65% were submitted digitally. The total value of the assessment reports off confidential for 2010 was $156.6 million. The total reported value of assessment work from January 2008 to December 2010 was $459.6 million and the number of reports off confidential for same period is 2295. Laura de Groot continues to manage 11 000 web pages and keeps staff on track with database management plans and needs.

Yao Cui continues development of his high-performance algorithm for delineating catchment basins and presenting dynamic spatial data on Google Earth using free and open source tools. A newly released *Geofile 2010-14: QUEST-South Regional Geochemical Survey: catchment basins for 2009 stream samples* and a provincial catchment database for download and MapPlace are results of this work. Yao also created tools to evaluate the positional uncertainty of the Regional Geochemical Survey (RGS) stream sample sites, resulting in a refit of locations from the streams on the original paper-based National Topographic System maps, to their equivalent or matching 1:20 000 scale TRIM streams. The known positional uncertainty and refitted locations on TRIM streams can result in a more meaningful delineation of catchment basins, enhancing the values and advancing the applications of the RGS geochemical results in more detailed geochemical modeling, leveling and mineral prospective mapping. The article, *Regional Geochemical Survey: validation and refitting of stream sample locations*, in this Fieldwork volume provides more details on this project. Yao received the Deputy Minister's Golden Glo Innovation Award for his work in *Delineation of Catchment Basins for Regional Geochemical Survey with High Performance Web Services* (Figure 6).

Over the past year Kirk Hancock, Larry Jones and Sarah Meredith-Jones provided 16 mineral resource assessments of different areas of British Columbia for the Ministry of Aboriginal Relations and Reconciliation to assist with treaty negotiations and 3 for other government business. Staff worked with the Mineral Policy and Regional Geology staff developing economic and social assessments and exploration activity products.

BC's Digital Bedrock Geology Map: BCGeology Map

The province's bedrock geology map for industry and government clients is a critical source of information for deciding on areas for exploration and assessing mineral potential. Updating is an important, ongoing task to weave the new data into the digital provincial product, BCGeologyMap. Yao Cui and Pat Desjardins are working with mapping geologists and advanced geospatial technology to improve the efficiency in the maintenance of geological maps. A geology operational database environment (GODE) is being developed to reduce the redundancy in map compilation and data integration while enhancing the data quality. The article, *Improving the Efficiency in the Maintenance of the Provincial Geological Database*, in this Fieldwork volume describes the operational environment and some of the best practices being promoted by the BCGS.

A draft copy of the digital BCGeology Map, updated to include new information from the Bedrock Geology of the QUEST area map, is available for download. This draft, which is the starting point to streamline integration of past and future geological mapping results into the provincial database, is available at: http://www.empr.gov.bc.ca/Mining/Geoscience/BedrockMapping/Pages/BCGeoMap.aspx.

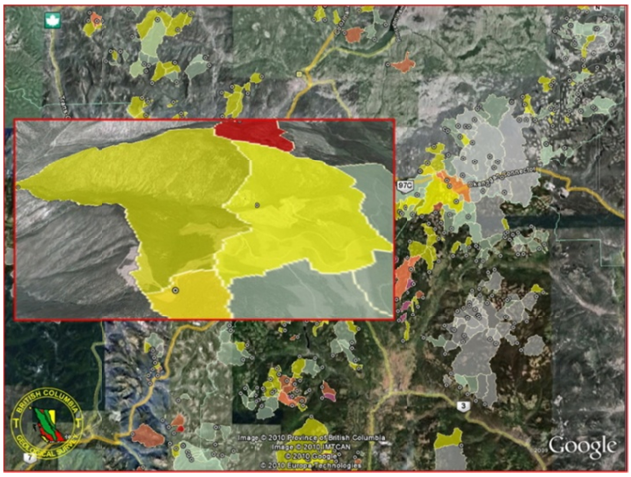

Figure 6. KML data for QUEST South RGS catchment basins.

TECHNICAL MARKETING

BCGS International Workshop on the Geology of Rare Metals

The BCGS hosted almost 200 participants at the International Workshop on the Geology of Rare Metals held in Victoria on November 9th and 10th , 2010 (Figure 7). It was organized by the British Columbia Geological Survey in collaboration with the Geological Survey of Canada and the Pacific Section of the Geological Association of Canada. The Workshop focused on various aspects of rare earth elements (lanthanides, Y and Sc) and other rare metals (mainly Nb, Ta, Li, Be, Zr, Hf). The program consisted of 26 oral presentations, 6 poster displays and an extended abstracts volume that is online on the BCGS website. The Workshop was the first deliverable of the Rare Metals Project that is part of phase four of the Targeted Geoscience Initiative (TGI-4).

Conferences, Workshops and Field Trips

Staff participated in numerous conferences and workshops during 2010, as organizers, speakers and attendees. Highlights from conferences and meetings included:

- presentations by George Simandl and Larry Diakow at the Mineral Exploration Roundup 2010 in Vancouver;
- participation in the Prospectors and Developer's Association of Canada (PDAC) convention in Toronto by hosting a Ministry booth on the trade show floor and helping host an Asian investor luncheon (Figure 8);
- presentations by Larry Diakow and JoAnne Nelson at the 2010 KEG annual meeting in Kamloops;
- Smithers Exploration Group "Rock Talk" presentations by Paul Schiarizza and Travis Ferbey in February. Travis also gave a seminar on regional till geochemistry at a Geoscience BC-sponsored workshop at Rock Talk;
- a workshop on the Life Cycle of a BC Mine presented at Minerals North by Dave Lefebure, and a presentation on regional till surveys by Travis Ferbey;
- a presentation by Steve Rowins at the annual GACMAC conference in Calgary (GeoCanada 2010) on the linkages between porphyry and epithermal deposits in the Toodoggone district. Steve also co-chaired a special technical session on "Hydrothermal Processes in Ore Genesis and Mineral Deposit Discovery" at the conference;
- workshop presentation by Steve Rowins on iron-oxide copper-gold deposits at the BC Geophysical Society's one-day workshop "Economic Geology for Geophysicists" in May;
- Kirk Hancock presented *Innovations with the BCGS and Publishing Technical Document on the Internet* at the Association of Earth Science Editors in September;
- presentation by Steve Rowins on mid-Tertiary porphyry Cu-Au-Mo deposits in the Cordillera at a Vancouver Island Exploration Group (VIX) meeting in Nanaimo in April;
- Sarah Meredith-Jones presented *New BCGS Data on MapPlace* at Minerals South in November 2010. At the same conference Larry Diakow presented an update on the geology and gold potential of the Nicola and Spences Bridge groups near Merritt.

Figure 7. International Workshop on the Geology of Rare Metals organized by the BCGS in Victoria attracted a sell-out audience.

Figure 8. Jay Fredericks, Larry Jones, and Karina Brino ready to promote British Columbia's mineral resources at the PDAC in Toronto, March 2010.

Staff also shared expertise by leading three field trips in 2010. Graham Nixon kicked off the field season with a two-day field trip for industry and government geologists to Northern Vancouver Island (Figure 9). The participants were treated to a detailed explanation of the evolution of the volcanic sequence and related intrusions and

Figure 9. Graham Nixon expounding on the geology and mineral deposits on northern Vancouver Island to field trip participants.

mineralization. In June, Larry Diakow led a group of industry geologists into the Nechako Plateau region south of Vanderhoof to visit the Blackwater-Davidson and Capoose precious metal properties and see the regional geological setting. In October, Larry led another two-day field trip for BCGS and industry participants to the Merritt area where Nicola and Spences Bridge stratigraphy with related exhalative and epithermal mineralization were examined.

Earthbound Lectures

The BCGS hosts geoscience lectures throughout the year under the banner "Earthbound". Invited speakers in 2010 included:

- Dec. 17, 2010: Chris Adams, Ministry of Energy, Oil and Gas Division: Exploration and development activity in northeast BC's shale gas areas.
- Nov. 26, 2010: Kirk Hancock, BCGS: Climate change: A critical review of the data.
- Nov. 12, 2010: Andrew Kerr, Newfoundland & Labrador Geological Survey: Rare-metal renaissance in the Canadian Shield of Labrador: Geological context of active exploration programs.
- Oct. 29, 2010: Alan Galley, GSC: Targeted Geoscience Initiative 4: Increasing exploration effectiveness.
- Oct. 15, 2010: Ray Lett, BCGS Emeritus Scientist: Rare earth element analysis – options & opportunities.
- April 30, 2010: Joanne Nelson, BCGS: Trolling the North Coast for salmon, showings, and schists from Scandinavia.
- April 16, 2010: Duncan McLeish, University of Victoria: Geology of the Aley Creek area, northeastern BC: A record of Mississippian orogenesis in the Cordilleran Foreland Belt?
- March 26, 2010: Bob Anderson, GSC: Some of TGI-3 Cordilleran Project's 'Greatest Hits:' A year five summary of progress.
- March 19, 2010: Steve Rowins, BCGS: The role of Neoproterozoic granitoids in the genesis of the giant Telfer Gold deposit in Western Australia and implications for regional exploration.
- March 5, 2010: Bruce Archibald, Simon Fraser University: McAbee - Climate change and the assembly of the modern world.

Publications

Over the past year, the BCGS published *Geological Fieldwork 2009*, 12 Open File maps and reports, 3 Geoscience Maps, 10 GeoFile maps, reports and data files, and 5 Information Circulars. Various technical papers were also published by staff in external peer-reviewed journals.

With the Regional Geologists as principal authors, the Survey published *Exploration and Mining in British Columbia 2009* and *British Columbia Mines and Mineral Exploration Overview 2009* and coordinated articles on provincial industry activities in the other external publications.

All geoscience publications are available on line at the BCGS website:
http://www.empr.gov.bc.ca/Mining/Geoscience/.

New BCGS Advisory Subcommittee

The BCGS has always appreciated feedback on its program from clients. In order to generate advice regarding the Survey's complete geoscience program, committees of client representatives have been used over the years. These representatives are charged with speaking on behalf of their sector while incorporating an understanding of the BCGS government mandate. For example, a Technical Liaison Committee (TLC) composed of mineral industry and university representatives operated from 1984 until 2004.

In 2010, the BCGS was able to start a new Advisory Subcommittee (AS) by working with Geoscience BC to tap four members from their Technical Advisory Committee (TAC) of mineral industry and university representatives. These four members have been joined by another four independent mineral industry representatives to create a balanced AS that reports to the Assistant Deputy Minister of the Mines and Mineral Resources Division of the Ministry of Forests, Mines and Lands (MFML). The AS meets twice a year and consists of Andrew Davies (Chair), Mike Cathro, Steve Cook, Craig Hart, Ward Kilby, Pat McAndless, Dave McClelland, and Jason Weber.

BC MINERAL DEVELOPMENT OFFICE

The role of the BC Mineral Development Office (MDO) in Vancouver is to promote investment in the province's mineral exploration and mining industry, both domestically and internationally. This includes delivering a multifaceted technical campaign to highlight the province's superior coal and mineral potential, renowned geoscience database and expertise, and attractive business climate. The MDO interacts with decision-makers in industry, including executive management, geologists and prospectors, and forms part of the wider marketing efforts of the MFML. The MDO also hosts incoming national and international companies and government representatives, and provides leadership for government trade missions.

Examples of MDO activities in the past year include acting as a key player to profile information on BC's mineral resources, investment procedures and specific mineral commodities to Asian investors, including the Asia Investment Mission to Hong Kong and China, and the Pacific Gateway initiative Mission to Japan in November; preparing articles on BC's mineral resources and exploration and mining activity for numerous ministry and industry publications to promote the province; profiling BC mineral industry investment opportunities at numerous conferences, including the Mineral Exploration Roundup, the Prospectors and Developers Association of Canada (PDAC) convention, the China Mining Conference and the KEG annual meeting; responding on a daily basis to requests for assistance from prospectors, geologists, companies and the public; working on various land-use issues, including those associated with referrals from Mineral Titles; delivering presentations to mining associations in southeast BC and the Community Coal Forum in Chetwynd; and updating publications such as Gold in BC, Copper in BC, and Opportunities to Explore – British Columbia Mining and Minerals.

Marketing Coal and Minerals to Asia-Pacific Region

The MFML continued an active Asia-Pacific marketing strategy to attract direct investment from Asia in BC exploration and mining projects. Asian countries are leading consumers of the province's coal and metal ores, and have a record of investment in BC's minerals industry (Table 1). Key selling points are BC's rich geology, expert geoscience information, interactive online databases, continuing demand for commodities such as copper and coal, a Pacific Rim gateway, modern infrastructure and a skilled workforce. The BCGS provides the MFML with most of the technical expertise and professional delegates for international presentations and meetings with Asian companies. It is the point of contact for incoming international investors through the BC Mineral Development Office in Vancouver.

Regional Geologists

Regional Geologists are a vital component of the MFML's ability to provide detailed geological knowledge of the region in which they live and work, and gather information on industry exploration and mining activity. In late 2010, the regional geologists changed ministries to Natural Resources Operations as part of the reorganization of the natural resource sector of government.

Regional Geologist	Office	Region
Paul Wojdak	Smithers	Northwest
Vacant	Prince George	North-Central and Northeast
Bruce Madu	Kamloops	South-Central
Dave Grieve	Cranbrook	Southeast
Bruce Northcote	Vancouver	Southwest

The MDO works closely with the regional geologists in attracting investment to BC and in preparing various publications.

STAFF UPDATE

Numerous staff changes occurred in 2010 (Figure 10). Katharine Benning started as the new Administrative Assistant in July filling the position vacated by Arlene Veenhof who left in the same month. Another welcome addition was Ted Fuller. Ted joined the BCGS as a Mineral Assessment Geoscientist in July 2010. Ted, formerly with the Health and Safety Branch, works with Allan Wilcox in assessment report review and providing support for data analysis in the Resource Information Section. Ted's earlier career was as an exploration geologist in BC, Yukon, and other parts of Canada. He also worked with the Geological Survey of Canada and the Canada/Yukon Geoscience Office. Other staff members either moved on or retired. Tania Demchuk, the Manager of Geoscience Marketing and Partnerships, left the Survey in July to start work as an Environmental Geoscientist in the Health and Safety Branch of the Ministry of Natural Resources Operations. Jay Fredericks,

Figure 10. Staff of the British Columbia Geological Survey in 2010.

Table 1. Recent investments from Asia in BC-based companies.

Year	Asian Company	Country	BC Company	Dollar Amount
2000	Korea Zinc Company	Korea	Teck Cominco	US$6.1 million
2005	POSCO	Korea	Elk Valley Corp.	US$25 million
2005	Zijin Mining Group	China	Pinnacle Mines	$1.95 million
2007	Northwest Non-Ferrous Int'l Investment	China	Yukon Nevada Gold Corp.	$3 million
2007	Sojitz	Japan	Thompson Creek Mining	$100 million
2007	Chinalco	China	Peru Copper	US$792 million
2008	Mitsubishi Materials	Japan	Copper Mountain	$28.7 million
2008	Daewon Chemical Co.	Korea	Nanika Resources	$5 million
2008	Jingduicheng Molybdenum Group/NWF	China	Yukon Zinc	$100 million
2008	Itochu Corp and LG Int'l Investment	Japan Korea	Compliance Clean Energy	US$11 million
2008	Kauilan Clean Coal Ltd.	China	Canadian Dehua	US$5.5 million
2008	Jilin Jien Nickel Industry Co. - China	China	Goldbrook Ventures Inc.	$45 million
2009	Toshiba Corp, Tokyo Electric, Japan Bank	Japan	Uranium One Inc.	US$221.4 million
2009	Daewon Chemical Co. Ltd.	Korea	Nanika Resources Inc.	$5 million
2009	China Gas Holdings Ltd. (HK)	China	IMW Industries Ltd.	$20 million
2009	Tongling Nonferrous Metals Group Holdings Co. Ltd.	China	Canada Zinc Metals Corp.	$4.9 million
2009	China Investment Corporation	China	Teck Resources Limited	$1.74 billion
	Minco Gold Corporation	China	Accel China Growth Fund	$4.44 million
2009	Korea Zinc Company	Korea	Selwyn Resources Ltd.	$3 million
2009	Zijin Mining Group	China	Continental Minerals Corporation	$25 million
2009	Yunnan Chihong Zinc & Germanium Co. Ltd. of China	China	Selwyn Resources Ltd.	$100 million
2009	Tianjin Huakan Group Co. Ltd.	China	Merit Mining	$15.5 million
2010	JOGMEC	Japan	Lomiko Resources	US$2.5 million
2010	State Grid International Development Ltd.	China	Quadra Mining Ltd.	$1 billion
2010	Jiangxi Copper Company (JCC)	China	BioteQ Enviromental Technologies Inc.	$2 million
2010	Japanese Consortium (Sojitz Corporation 50%, Dowa Metals & Mining Co., Ltd. 25%, Furukawa Co., Ltd. 25%)	Japan	Taseko Mines Ltd.	$187 million
2010	Anthill	China	Yellowhead Mining	$5.4 million
2010	Investment in Bingay property	China	Centermount Coal Ltd.	$6 million
2010	Huiyong and Kailun companies	China	Canadian Dehua International Mining	$20 million

the Director of the Mineral Development Office in Vancouver also left the Survey at the end of the year to work as Vice President for Hathor Exploration Limited.

Andrew Legun, Nick Massey, and Ray Lett all retired in 2010 after long and distinguished careers with the BCGS. Andrew had worked as both a coal geologist and regional mapper, while Nick focused on mapping parts of southern British Columbia, particularly on Vancouver Island. Ray made major contributions to the regional geochemical data, completed numerous topical studies, and provided laboratory support for the BCGS staff and students. On a positive note, Nick and Ray became the first two Emeritus Scientists with the BCGS. The new Emeritus Scientist program recognizes their tremendous contribution to the Survey and people of British Columbia over the years, and allows for their continued collaboration with Survey personnel on various projects.

NEED MORE INFORMATION? WANT TO COMMENT?

BCGS staff has considerable expertise and welcome the chance to share it. Our contact list is online at: http://www.empr.gov.bc.ca/Mining/Geoscience/Staff/Pages/default.aspx.

We always appreciate your input regarding our many programs and activities. Please email us at Geological.Survey@gov.bc.ca or call 250-952-0429.

To learn about new publications, data releases and upcoming events, join the BCGS release notification list by emailing Geological.Survey@gov.bc.ca. Approximately 15-20 emails are sent per year.

Bedded Barite-Pyrite Occurrences in upper Besa River Formation, western Liard Basin, British Columbia and Regional Correlations with Devonian to Mississippian Sub-surface Formations

by F. Ferri[1], A. Hickin[1] and D. Huntley[2]

KEYWORDS: Liard Basin, Horn River Basin, Liard River, Toad River, Caribou Range, Besa River Formation, gamma ray, oil, gas, pyrite, barite, mineralization, Earn Group, Kechika Trough

INTRODUCTION

The Geoscience and Natural Gas Development Branch of the British Columbia Ministry of Energy, in conjunction with the Geological Survey of Canada, undertook an examination of outcrop exposures of Middle Devonian to Early Mississippian siltstone sequences of the Besa River Formation which are equivalent, in part, to rocks currently being exploited for natural gas resources in the Horn River Basin and to sections being examined for similar potential in the Liard Basin (Figures 1, 2). The main objective was to delineate shale gas-equivalent horizons in outcrop so that they could be used as potential reference sections to aid in understanding of the subsurface geological setting in Horn River Basin. Characterization of the section was accomplished through lithologic description and collection of samples for lithologic and organic geochemistry, and geochronological analysis. In addition, a gamma ray spectroscopic survey of the outcrop was performed for use in correlating the section with subsurface sequences in the Liard and Horn River basins. During the course of this investigation several horizons of bedded and disseminated pyrite, together with a horizon of nodular barite, were observed within the upper part of the Besa River section. This report summarizes findings related to this sulphide-barite mineralization. A more in depth description of the results as they pertain to the natural gas potential of the sequence can be found in Ferri *et al.* (2011).

This study is part of a collaborative program between the Geological Survey of Canada and the British

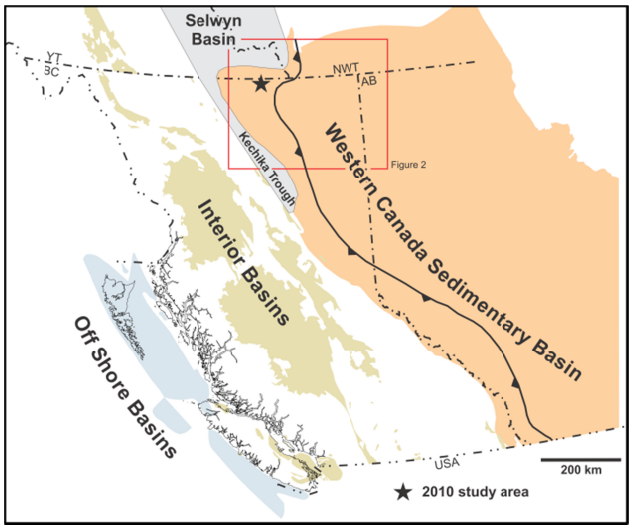

Figure 1. Location of the Liard Basin with respect to the principal sedimentary basins of western Canada. Also shown are the Lower Paleozoic off-shelf depocentres of the Selwyn Basin and Kechika Trough. Red box outlines area of Figure 2.

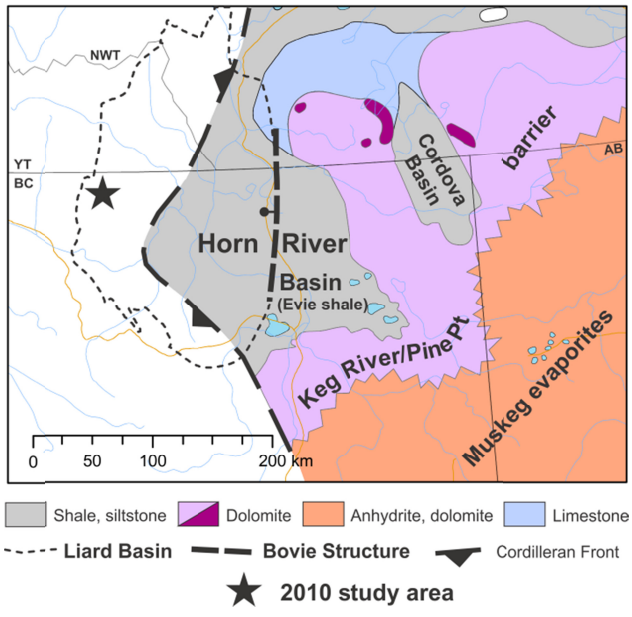

Figure 2. Schematic representation of the Horn River Basin (and Codorva Basin) during upper Keg River times (Givetian). Superimposed on this is the outline of the Liard Basin. This reef/carbonate/shale basin configuration persisted until the end of Slave Point times (end of Givetian; modified from Meijer Drees, 1994; outline of Liard Basin from Mossop *et al.*, 2004).

[1] *Geoscience and Natural Gas Development Branch, BC Ministry of Energy, Victoria, BC*

[2] *Geological Survey of Canada, Natural Resources Canada, Vancouver, BC*

This publication is also available, free of charge, as colour digital files in Adobe Acrobat® PDF format from the BC Ministry of Forests, Mines and Lands website at http://www.empr.gov.bc.ca/Mining/Geoscience/PublicationsCatalogue/Fieldwork.

Columbia Ministry of Energy, and is under the umbrella of the federal government's Geo-mapping for Energy and Minerals program (GEM) that is specifically examining petroleum related geoscience of the Liard and Horn River basins. A major focus of this program has involved mapping of resources associated with surficial geology that are used during drilling and completion of shale gas wells (Huntley and Sidwell, 2010; Huntley and Hickin, 2010).

LOCATION AND REGIONAL GEOLOGY

The Liard Basin is located in northeastern British Columbia, straddling the British Columbia – Yukon – Northwest Territories border (Figures 1, 2), spanning NTS map sheets 094N and O, and 095B and C. It is traversed by the Liard River and defines a relatively high plateau between the southern Selwyn Mountains and northern Rocky Mountains. Highway 77 runs along the eastern half of the basin and joins with the Alaska Highway, which cuts across the southern margin. Numerous petroleum development roads and forestry access roads extend from these two main highways across parts of the basin. Vehicle access across the Liard River is provided by a barge which originates at Fort Liard, Northwest Territories and terminates south of the confluence of La Biche River, where a road connects to the Beaver River gas field (Figure 3).

The Liard Basin was originally defined on the basis of the thick Late Paleozoic succession in southeastern Yukon by Gabrielse (1967) and extended into northeastern British Columbia by Morrow *et al.* (1993) and Richards *et al.* (1994; Figures 4, 5). The Liard Basin formed subsequent to the Horn River Basin and is superimposed on the western part of the Horn River Basin Figure 2). The Bovie Lake structure marks the eastern margin of the Liard Basin, west of which is found an anomalously thick section of the Mississippian Mattson Formation (Figure 4). Subsequent Late Cretaceous movement on this fault has also preserved a thick sequence of Early to Late Cretaceous rocks within the confines of the basin (Leckie *et al.*, 1991). Although development of the Liard Basin had no influence on depositional facies and thicknesses within pre-Mattson Formation units with shale gas potential (*i.e.* Muskwa, Horn River formations), its initiation has effectively marked the current western limit of shale gas development in the Horn River Basin. Prospective shale horizons in eastern Horn River Basin (Figure 2) have been dropped deeper by some 2000 m west of the Bovie fault (Figure 4), imposing drilling and completion challenges. A consequence of this within the Liard Basin, has been a shift to the exploitation of the stratigraphically higher Exshaw Formation, which is at a depth and thermal maturation that potentially can be economically developed for its shale gas resources.

The Middle Devonian to Middle Mississippian Besa River Formation represents the western basinal equivalents of predominantly carbonate successions between the Upper Keg River and Debolt Formation (Figures 4, 5). Further west, in the Selwyn basin and Kechika Trough, these rocks correlate with the Devono-Mississippian Earn Group (Figure 6). Selwyn Basin and Kechika Trough are deep water equivalents to Early Paleozoic carbonate shelf deposition along the Western Canada Sedimentary Basin (MacDonald Platform; Ferri *et al.*, 1999) and are filled primarily by shales and siltstones of the Kechika and Road River groups.

In the study area, Besa River shales and siltstones sit above carbonates of the Middle Devonian Dunedin Formation, which can be traced westward into the subsurface where it is equivalent to parts of the Chinchaga and Lower Keg River formations (Meijer Drees, 1994; Figure 5). During Upper Keg River and Slave Point deposition, a well defined barrier reef complex developed that marked the eastern limit of the Horn River Basin (Oldale and Munday, 1994; Figure 2). West of the barrier edge, shales of the Horn River Formation include two members, a lower radioactive, bituminous shale assigned to the Evie Member, overlain by shales of the Otter Park Member (Figures 4, 5). A transgression followed Slave Point deposition and pushed the shallow carbonate edge eastward (Leduc facies), leading to deposition of highly bituminous shales of the Muskwa Formation (Duvernay equivalent; Switzer *et al.*, 1994). Carbonate conditions were re-established to the west during Frasnian and Famennian times, resulting in deposition of Kakiska to Kotcho formations along a broad shelf (Figures 4, 5). A major transgression occurs across the Devono-Mississippian boundary, represented by deposition of the highly radioactive and bituminous shales of the Exshaw Formation. Carbonate deposition again migrated westward in Early Carboniferous times, with the deposition of the Banff Formation and succeeding Rundle Group.

In the subsurface, shales of the Fort Simpson Formation encompass the westward shale-out of carbonate units above the Muskwa Formation. Carbonates of the Banff Formation and Rundle Group disappear into basinal shales above the Exshaw Formation and transition into the Besa River Formation (Figures 4 and 5). Approximately 300 m of Besa River siltstones and shales equates to over 2000 m of carbonate and siltstone section along the Keg River barrier edge.

The upper part of the Besa River Formation interfingers with the Middle to Late Mississippian sandstones, siltstones and minor carbonates of the Mattson Formation. These exceed 1000 m in thickness within the Liard Basin west of the Bovie fault structure. This fault has been interpreted as a Late Paleozoic extensional structure that was later re-activated during Laramide compression (Wright *et al.*, 1994). This is based on the preservation of thick Mattson sands, and succeeding Kindle Formation, below the Permian Fantasque Formation west of the Bovie fault whereas only a thin Mattson section occurs below the Fantasque Formation east of the fault (Monahan, 2000; MacLean

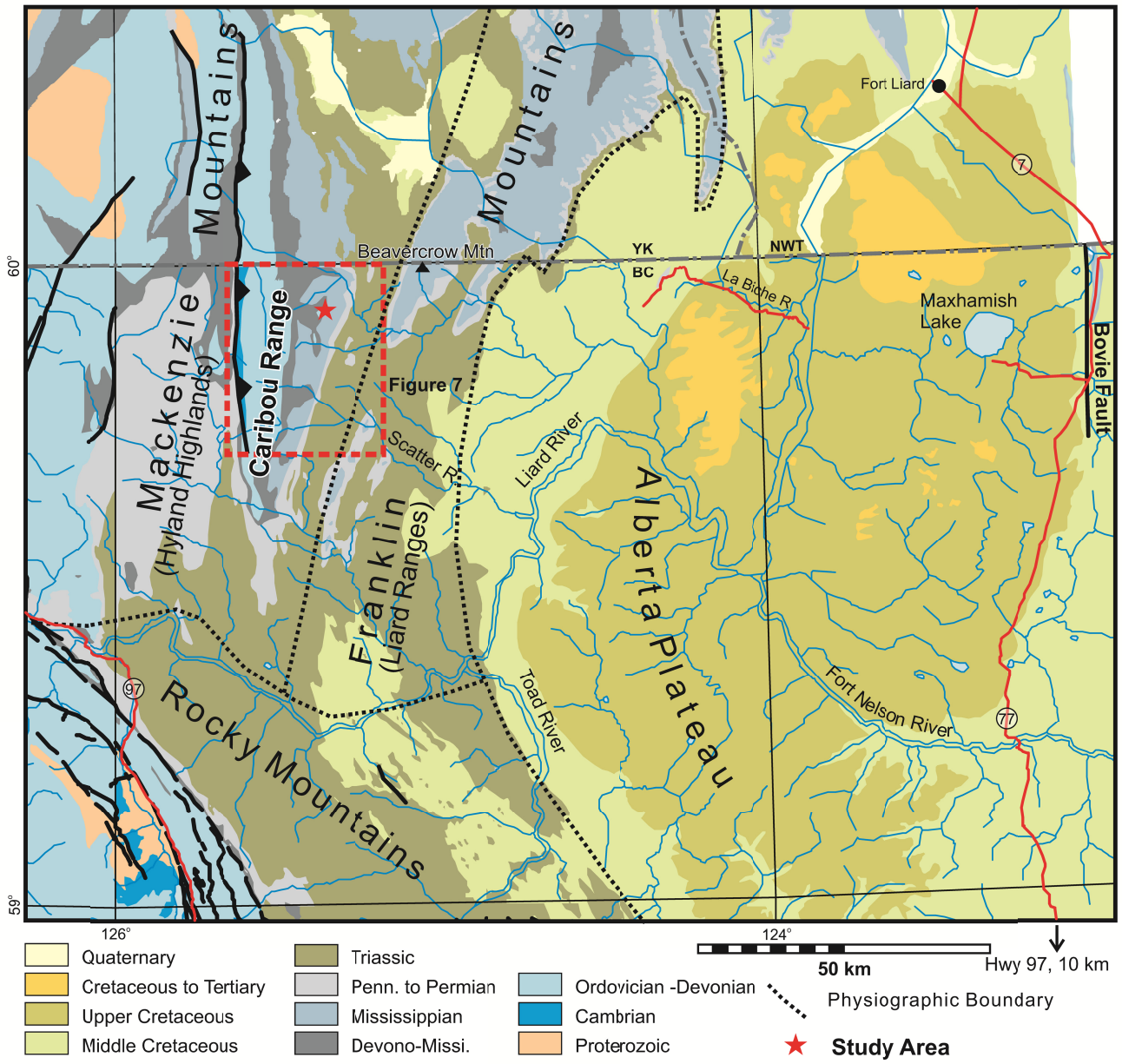

Figure 3. Geology of the western portion of the Liard Basin. Box outlines the geology depicted in Figure 7. Geology from MapPlace.ca (URL: http://www.mapplace.ca/).

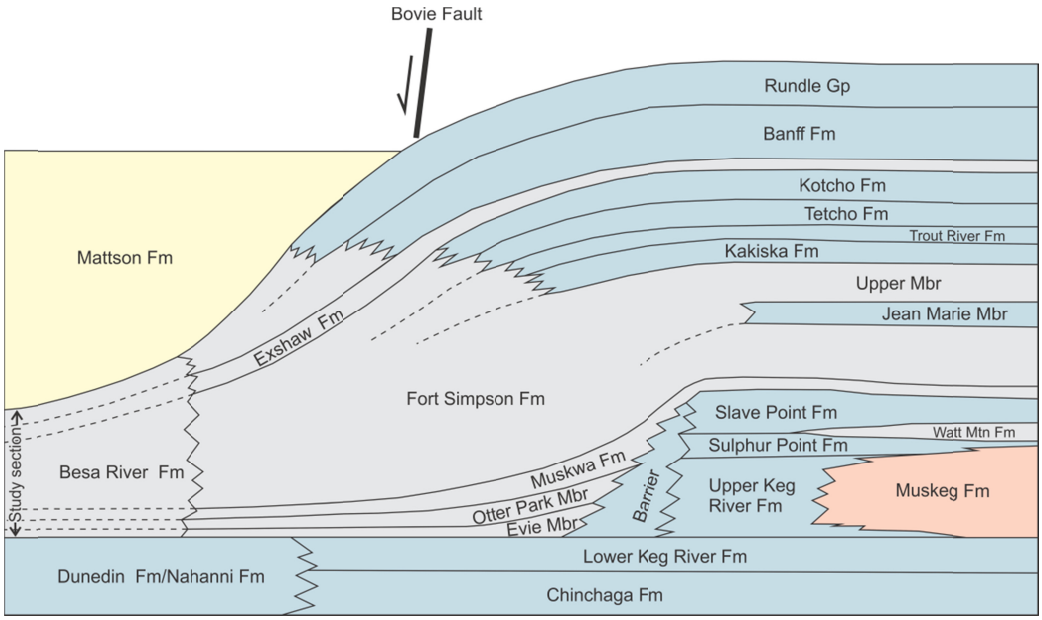

Figure 4. Schematic diagram showing relative thickness variations between mid to Upper Paleozoic shelf and off-shelf sequences depicted in Figure 5.

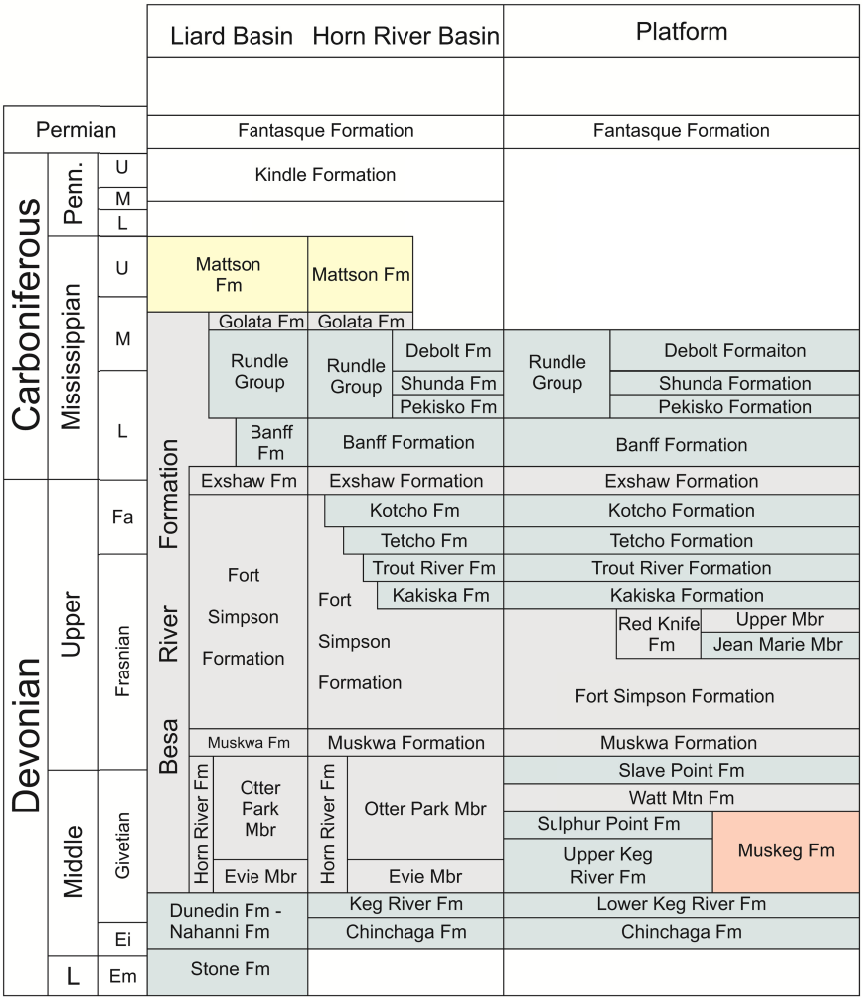

Figure 5. Time stratigraphic chart of the mid to Upper Paleozoic showing the main stratigraphic units along the northwestern part of the Western Canada Sedimentary Basin falling within northeastern British Columbia and the relationship between shelf and off-shelf sequences.

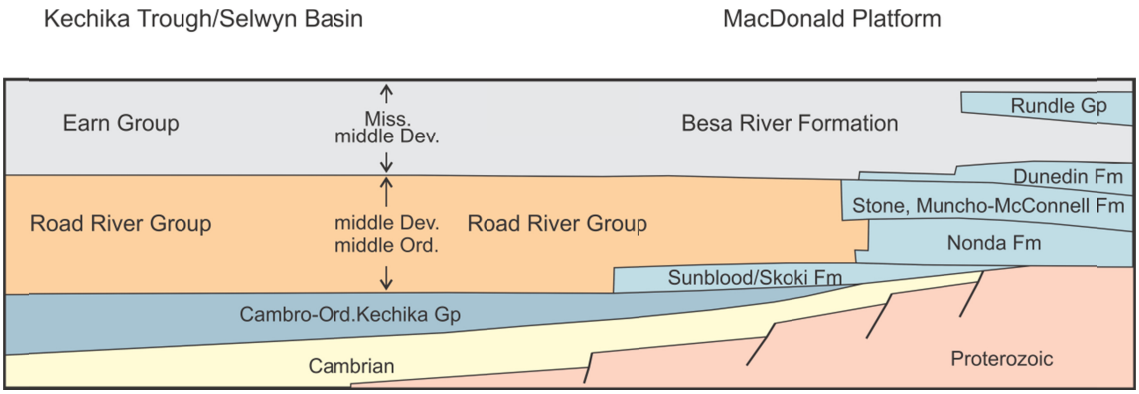

Figure 6. Schematic representation of westward shale-out of Lower Paleozoic carbonates into Road River siltstone and shales within the Kechika Trough and Selwyn Basin, and the relationship between the Besa River Formation and the Earn Group.

and Morrow, 2004). In addition, the westerly directed thrust associated with the Bovie fault structure, is probably related to compressional re-activation of this graben structure (McLay and Buchanan, 1992). This pre-existing fault allowed compressional structures to form outboard of major Laramide structures (Figure 3). MacLean and Morrow (2004), using seismic data, interpret Bovie fault as having Late Paleozoic and Mesozoic compressional tectonics followed by extension in the Cretaceous. Mattson clastics are part of a slope to delta plain and shallow marine sandstone succession that was sourced from the north (Bamber *et al.*, 1991). These rocks correlate with similar deposits of the Carboniferous Stoddart Group, deposited within the Late Paleozoic Dawson Creek graben complex (Barclay *et al.*, 1990). Deltaic deposits of the Mattson Formation disappear westward and are replaced by upper Earn Group siltstones and shales within the Kechika Trough.

To the west, within the Kechika Trough and Selwyn Basin, Besa River shales and siltstones correlate with the Middle Devonian to Early Mississippian Earn Group (Ferri *et al.*, 1999; MacIntyre, 1998; Paradis *et al.*, 1998). These deeper water siliciclastic strata overlie Middle Ordovician to Middle Devonian siltstone, shale and minor carbonate of the Road River Group, representing basinal equivalents of coeval carbonates of the MacDonald Platform (Figure 6).

The Kechika Trough and Selwyn Basin host widespread and locally significant sedimentary exhalative (SEDEX) Pb-Zn-Ba deposits within the Earn Group, including the Cirque, Driftpile Creek and Akie deposits of the Kechika Trough (Paradis *et al.*, 1998; MacIntyre, 1998) and the Tom and Jason deposits of the Selwyn Basin (Goodfellow and Lydon, 2007). Major sulphide mineralization is of Late Devonian age (Frasnian to Famennian), although barite mineralization with minor sulphides also occurs in Early Mississippian sections (Tournaisian; Paradis *et al.*, 1998; Irwin and Orchard, 1991).

Besa River rocks examined during the 2010 field season are located within the northern part of the Caribou Range, part of the southern Hyland Highlands and represent the southernmost extent of the Mackenzie Mountains (Mathews, 1986). The broad highland that constitute the Caribou Range is underlain by a westwardly directed thrust panel of gently, east dipping Paleozoic rocks (Figures 3, 7). These north to northeast-striking rocks follow the general trend of structures within the Mackenzie and Franklin mountains, and are at almost right angles to the northwest structural grain of the Rocky Mountains, resulting in the large bend in the trace of major structures across the Liard River (Figure 3). Furthermore, the southern portion of the Mackenzie and Franklin mountains represents a portion of the Foreland Belt dominated by west-verging structures, compared to overall northeast vergence (see Fallas *et al.*, 2004).

Rocks as old as Cambrian are mapped within the Caribou Range, although these can be traced northward into the Yukon where they assigned a Proterozoic age (Taylor and Stott, 1999; Fallas *et al.*, 2004). Cambrian siliciclastics are succeeded by shelf carbonates of the Nonda, Muncho-McConnell, Wokpash, Stone and Dunedin formations of broadly Silurian to Middle Devonian age (Figure 7). Generally, rocks of the Besa River Formation overlie the Dunedin Formation, although in the north, all of the Dunedin and parts of the upper Stone formations shale out into the Besa River Formation (Taylor and Stott, 1999; Figure 7).

In British Columbia, the regional geological data base in the vicinity of the section includes mapping within Toad River (Taylor and Stott, 1999), Tuchodi Lakes (Stott and Taylor, 1973) and Rabbit River (Gabrielse, 1963; Ferri *et al.*, 1999) map areas. In Yukon and Northwest Territories, La Biche River (095C) has been compiled at 1:50 000 (Fallas, 2001; Fallas and Evenchick, 2002) and 100 000 scales (Fallas *et al.*, 2004). The Besa River Formation was first defined by Kidd (1963) north of the Muskwa River, and Pelzer (1966) further described its mineralogy and broad stratigraphy. The organic petrography and thermal maturity of similar rocks in Yukon and Northwest Territories were described by Potter *et al.*, (1993) and Morrow *et al.* (1992). A recent sub-surface evaluation of Devono-Mississippian fine clastic sequences was published by Ross and Bustin

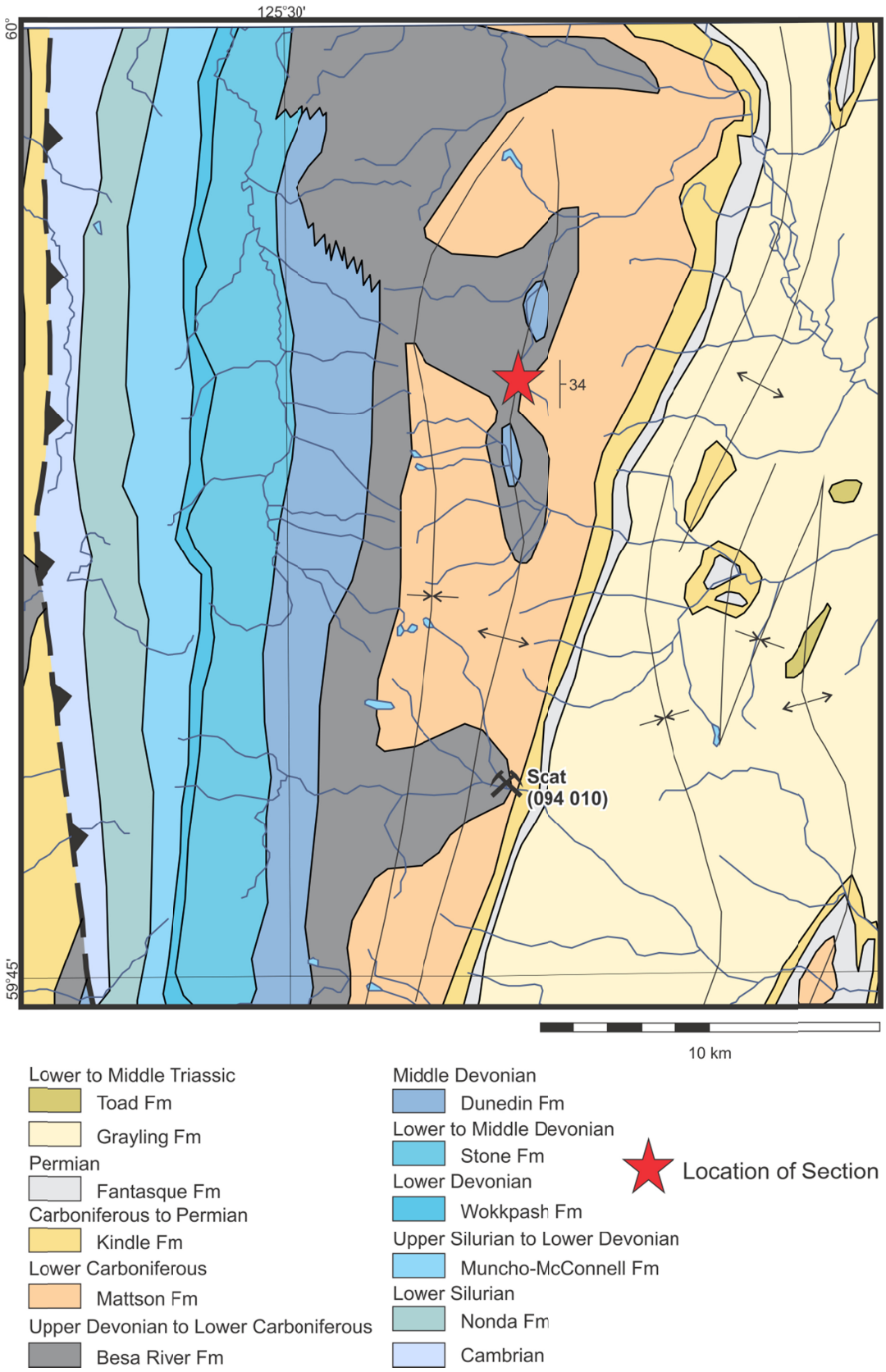

Figure 7. Geology of the Caribou Range, showing the location of the measured section. Geology from MapPlace.ca (URL: http://www.mapplace.ca/).

(2008) which included Besa River rocks within the Liard Basin area. An assessment of the conventional hydrocarbon resources of the Liard Basin was produced by Monahan (2000).

METHODOLOGY AND RESULTS

A nearly complete section of Besa River Formation was measured and described through use of a 1.5 m staff along a west-facing valley, approximately 22 km southwest of Beavercrow Mountain (base of section; UTM 367107E, 6643192N; Zone 10, NAD 83; Figure 7). Representative chip samples were acquired across 2 m intervals along the entire section. Samples were split, with one group being analysed for whole rock, trace and rare earth element abundances at Acme Analytical Laboratories in Vancouver, and a second group, at 4 m spacings, for Rock Eval analysis at Geological Survey of Canada (GSC) laboratories in Calgary. A smaller sub-set of these samples will also be analysed by x-ray diffraction (XRD) at GSC laboratories for semi-quantative determination of mineral abundances. Another subset will be processed for their potential to contain palynomorphs for biostratigraphy. Separate samples were collected for thermal maturity determination at GSC laboratories in Calgary through reflected light microscopy. In addition, a hand held gamma ray spectrometer (RS-230 by Radiation Solutions Inc.) was used to measured natural gamma radiation every 1 m over a 2 minute time interval allowing the calculation of K (%), U (ppm), Th (ppm) and total gamma ray count. Data were plotted against depth and variation in total natural radiation along the section is approximately equivalent to the subsurface gamma ray trace routinely collected in oil and gas wells. This assists in the correlation of the outcrop section with equivalent rocks in the subsurface.

Approximately 285 m of siltstone and shale belonging to the Besa River Formation were measured west of Beavercrow Mountain (Figure 8). The upper and lower parts of the Besa River Formation were not exposed, but examination of rocks to the north indicate approximately 15 m of missing Besa River rocks below the base of the Mattson Formation, and a structural section suggests some 25 m of covered rocks above the Dunedin Formation.

Generally, the Besa River Formation consists of dark grey to black, carbonaceous siltstone and shale (Figure 8). Besa River rocks along the measured section can be subdivided into 6 units consisting of, from the base (Figure 9); 1) Tan to orange-brown or beige weathering, dark grey to black carbonaceous siltstone to blocky siltstone with shale partings (34 m; Figure 10a); 2) 34 m of dark grey to beige weathering, dark grey to black, fissile to blocky carbonaceous siltstone; 3) Rusty to grey or dark grey weathering, dark grey to black carbonaceous blocky siltstone and shale (32 m; Figure 10b); 4) Rusty to light grey weathering, grey to light grey, blocky to platy

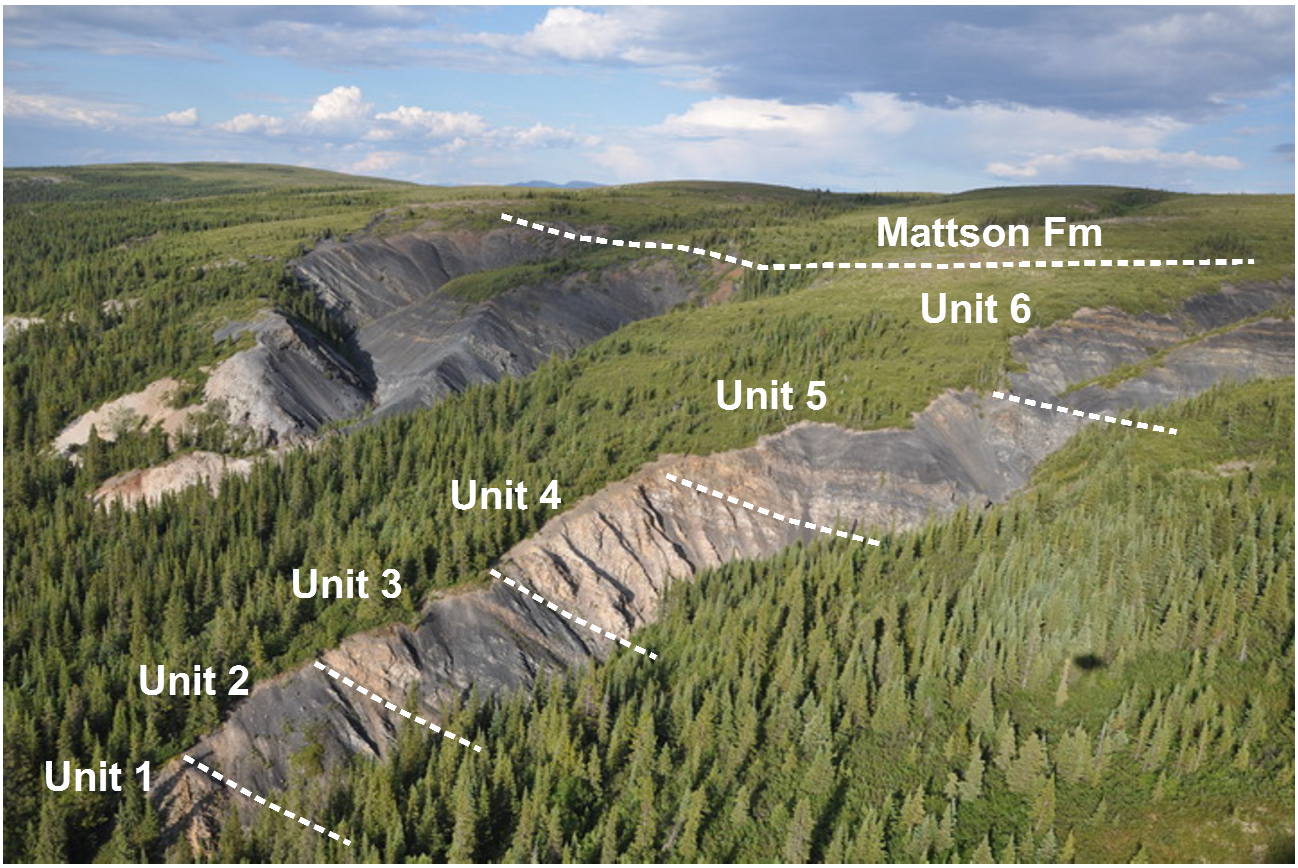

Figure 8. Aerial photograph of the measured section of Besa River Formation showing the character of exposed lithologies. The light coloured material is produced by the more siliceous siltstones of unit 4. Upper Besa River siltstones (unit 6) appear somewhat more recessive than the underlying siltstones of unit 5.

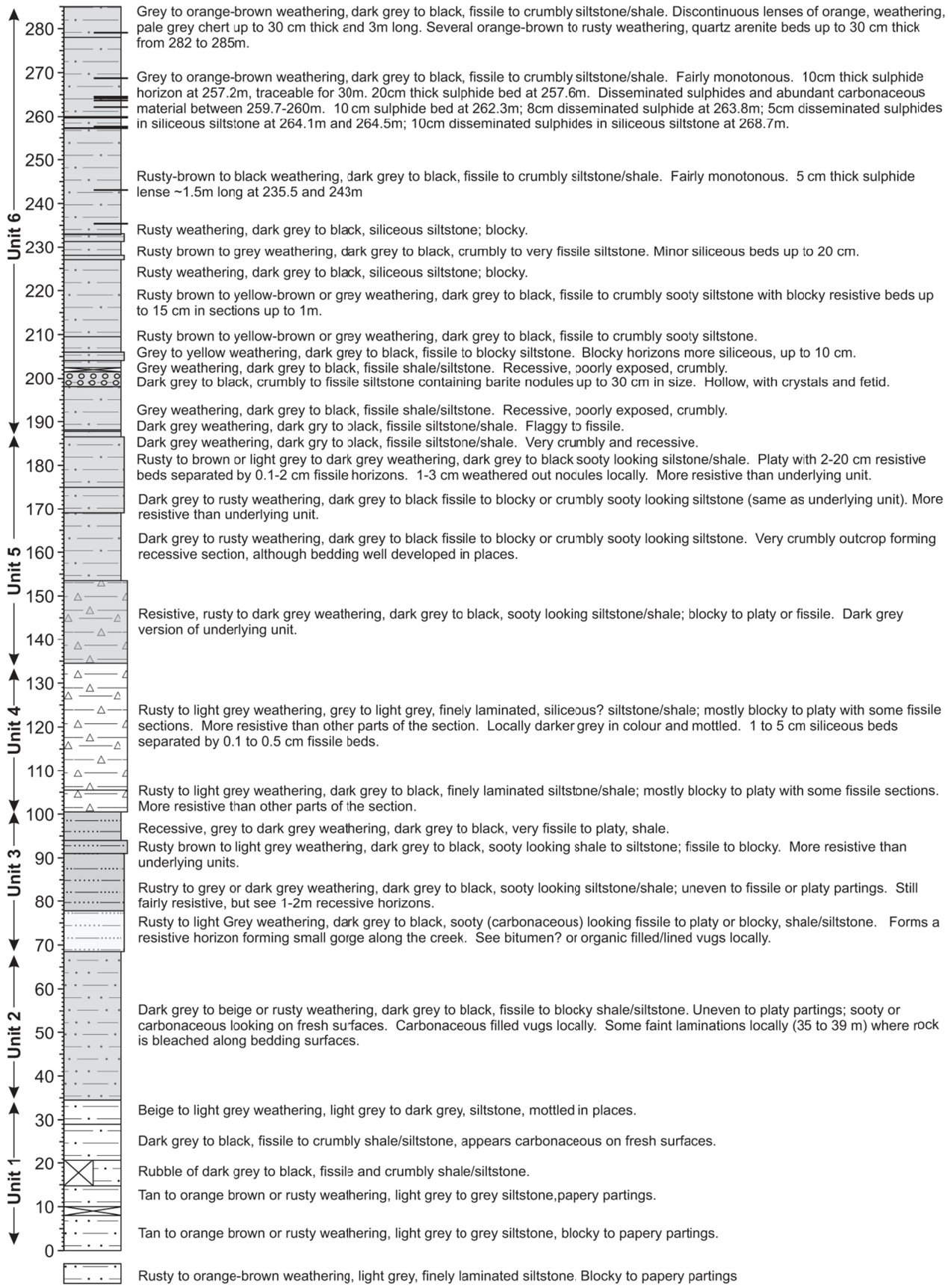

Figure 9. Lithologic section of Besa River Formation measured along the eastern part of the Caribou Range.

and laminated siliceous siltstone (34 m; Figure 10c); 5) Rusty to dark grey weathering, dark grey to black, blocky to platy and laminated, carbonaceous and siliceous siltstone (51 m; Figure 10d); 6) Dark grey to rusty weathering, dark grey to black crumbly siltstone to shale with uneven partings, with lesser blocky siltstone in the lower and middle parts (100 m; Figure 10e). Exposures of Besa River Formation in the Caribou Range displays the distinctive light grey weathering of unit 4 together with the recessive, crumbly nature of the upper part of unit 6 (Figures 8 and 10e). Distinctive rusty to ochre coloured run-off in channels emanating from exposures of unit 6 can also be observed within the central part of the Caribou Range.

Comparison of the broad lithologic composition, total gamma ray counts, K, Th and U concentrations and total organic carbon (TOC) contents along the section are shown in Figure 11. TOC levels are relatively high across several portions of the formation, nearing 5% by weight in some parts and consistently higher than 2% for the upper half of the section. There is a very good correlation between relative abundances of uranium and organic

Figure 10a. Rusty weathering siltstone of unit 1 at the 5 m level.

Figure 10b. General shot of grey to dark grey weathering siltstones of unit 3 at the 80 m level.

Figure 10c. Light grey and rusty weathering siltstone of unit 4, 116 m level.

Figure 10d. Dark grey and resistive siltstones with shaly partings within unit 5 at the 150 m level.

Figure 10e. Transition from more resistive ribs of siltstone in unit 5 into more recessive siltstones of unit 6.

Figure 10f. Barite nodules within unit 6 at the 198-200 m level.

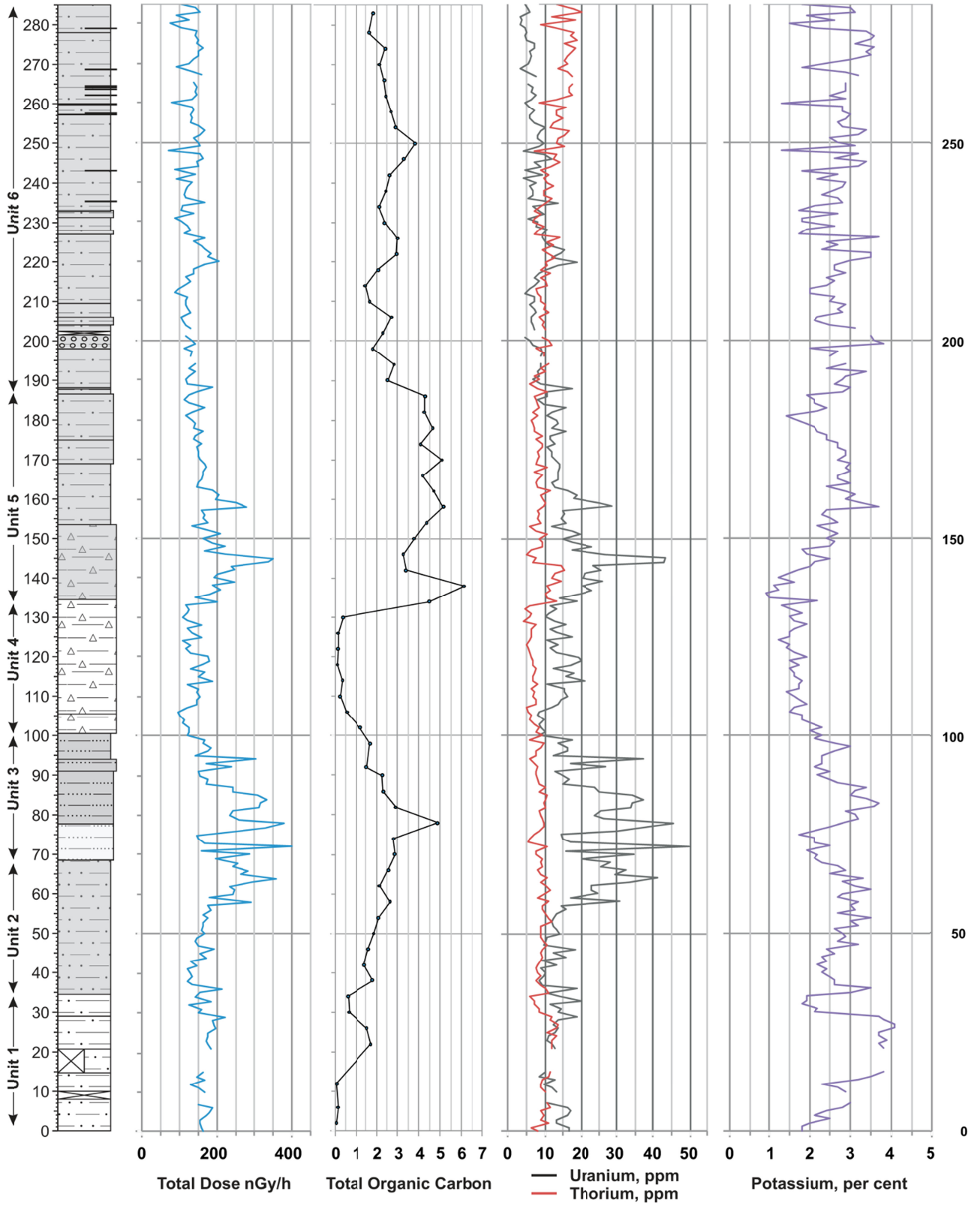

Figure 11. Comparison of main lithologic units of the measured Besa River Formation section with measured levels of total gamma ray counts, uranium, thorium, potassium and total organic carbon.

carbon content, suggesting precipitation of uranium either syngenetically during periods of higher anoxia or diagenetically within horizons rich in organic material. Although uranium concentrations appear to generally decrease towards the upper part of the section, thorium shows an increase in abundance. The concentration of potassium does not appear to correlate with the abundances of the other elements, and is probably tied to the mineralogy of the sediments being deposited.

The carbonaceous (*i.e.* organic-rich) nature of these sediments is a reflection of the reducing conditions present during deposition (Goodfellow and Lydon, 2007). These very low oxygen conditions did not permit aerobic organic activity and led to the preservation of organic matter (Fowler *et al.*, 2005). In these anoxic waters, bacteria that respire through reduction of sulphur became *abundant, producing a large amount of reduced sulphur* which could then be utilized in the precipitation of metal sulphides from any metalliferous brines being expelled on the sea floor (Goodfellow and Lydon, 2007). Even if these brines had sufficient reduced sulphur, this anoxic environment favoured the preservation of any precipitated sulphides. Oxygenated bottom waters, as in today's oceans, would have led to the oxidation of the sulphides in the water column or along the sea floor, shrinking the size of, or totally eliminating, any sulphide mineralization (Force *et al.*, 1983).

BARITE AND SULPHIDE MINERALIZATION

Barite and sulphide mineralization discovered in this section is located within the middle to upper part of unit 6 (Figures 10f, 12a, b). This new showing is named the MT occurrence (MINFILE 094N 012). It contains mineralization similar to that described within the Scat occurrence some 10 km to the south (MINFILE 094N 010; Burt, 1982).

At the MT showing, barite nodules over 30 cm in diameter are found between the 198 and 202 m level of the section, where they constitute up to 15% of the section (Figure 10f, 12a, b). The nodules vary in morphology from smooth or composite spheres to spheres or coatings displaying colloform texture (Figure 12a). Morphologically, many nodules have one flat surface devoid of colloform texture, suggesting growth on the sediment surface (Figure 12b). Other nodules are essentially coatings, also suggesting they grew along the sediment surface (Figure 12b). These observations imply precipitation of barite from ocean waters and would support a hydrothermal vent source for the barium, as opposed to diagenetic precipitation within the sediment. Many of the nodules contain vugs lined with fine, prismatic, needle-like crystals consistent with barite, although their composition has not been confirmed by x-ray diffraction. These vugs also give off a very strong fetid to petroliferous odour when broken.

Sulphide mineralization is found at ten levels between 235.5 and 279 m of the section and manifests as beds 5 to 20 cm in thickness. Most of the sulphide beds are thin, less than 10 cm thick and consist of disseminated pyrite forming discontinuous horizons traceable laterally for several metres, suggesting they may be diagenetic in origin (Figures 12c-f). Only two beds (at 257.2 m and 259.7 m) can be traced for over 30 m along strike (Figure 12c) and display textures indicative of sedimentary exhalative processes (*e.g.* laminations and graded sulphides beds). Sulphide mineralization at 257.2 m is 10 cm in thickness, contains up to 50% sulphides and displaying variation in sulphide contents suggesting settling from the water column (Figure 12e). A thicker sulphide bed (20 cm), with similar texture, occurs 20 cm above the first bed, but is only traceable for a few metres. The horizon at 259.7 m is 30 cm thick and traceable across the entire section (>50 m). This horizon consists of oxidized pyrite and abundant carbonaceous material containing remnant sulphides in the upper part (Figure 12f). This horizon is also visible in the next gulley, approximately 250 m to the north.

Chemical analysis of these beds (Table 1) suggests that pyrite constitutes the bulk of the sulphide mineralization. Interestingly, there are several horizons that are rich in Mn (0.2 to 0.4%), relatively poor in Ba, but elevated in Zn, Co and Ni. Although these horizons are rich in Fe, the highest horizons are comparatively poor in S, suggesting perhaps that the main iron-bearing mineral is a non-sulphide and likely a carbonate. This may be corroborated by the relatively higher Ca content of these horizons. These sulphur-poor horizons may reflect changing oxygen levels within the water column during deposition resulting in lower amounts of reduced sulphur. Mn, which is relatively soluble in anoxic waters, readily precipitates when the water column is oxygenated (Force *et al.*, 1983). Alternatively, these iron-rich horizons may be diagenetic in origin (*i.e.* nodules). Concentrations of elements presented here are comparable to pyritic shales of the Akie Formation, in the upper part of the Earn Group of the Kechika Trough and correlative with the upper Besa River Formation (MacIntyre, 1998).

DISCUSSION

SEDEX-style mineralization in the Caribou Range

Previous exploration, as part of the extensive exploration boom for SEDEX mineralization within the Selwyn and Kechika basins in the late 1970s to early 1980s, led to recognition of anomalous levels of Pb, Zn, together with Ba mineralization within Besa River rocks of the Caribou Range (Burt, 1982). This mineralization has been catalogued as the Scat mineral occurrence (MINFILE 094N 010) and is located within the upper Besa River Formation exposed along the Scatter River, approximately 10 km due south of the current mineralization (Burt, 1982). Lithologic units, geochemical

Figure 12a. Close-up of barite nodules. Sample on the left shows colloform encrustation of bedding surface; the nodule on the left also shows large and small colloform texture and flat bottom. The habit of barite mineralization shown here suggests growth at the seafloor.

Figure 12b. Prismatic barite crystals found within the vugs. Colloform text of barite growing along a bedding layer.

Figure 12c. Outcrop picture of Besa River rocks and the sulphide horizons at the 257 m level. The arrow points to exposed portions (with a nearby hammer for scale). The lower sulphide horizon can be traced for up to 30 m across the outcrop.

signatures and Ba mineralization in the vicinity of the Scat occurrence are very similar to those observed in the present study area, although the Besa River section is considerably thicker along the Scatter River. Burt (1982) noted that anomalous zinc values (0.3%) were found as fracture fillings within siliceous and pyritic nodules in the

Figure 12d. Photograph showing the sulphide horizon at the 257 m level.

Figure 12e. Close-up of fresh surface across the lower sulphide horizon at the 257 m level showing the bedded nature of the pyrite mineralization and the variation in its concentration which could be attributed to settling from the water column.

Figure 12f. Pyritiferous zone at the 260 m level of the Besa River section (above the hammer) showing the continuity of the horizon. This horizon was also noted on the next gulley to the north.

upper Besa River Formation. He attributed this to leaching of metals from the surrounding shales during diagenesis. These nodules have some similarities to the discontinuous pyrite bearing horizons described in the study area, suggesting they may have a common origin.

Burt (1982) noted that the barite nodules were likely of hydrothermal origin, but the relatively low concentrations and lack of any sulphide mineralization

Table 1. Geochemical analysis of several sulphide horizons from the upper part of the Besa River Formation, as measured within the study area.

		Sample	FF10-116	FF10-117	FF10-162	FF10-165	FF10-168	FF10-169	FF10-171	FF10-173	FF10-176	FF10-177	FF10-179	FF10-181
		Thickness	2 m	2 m	1 m	15 cm	10 cm	10 cm	30 cm	10 cm	8 cm	5 cm	20 cm	10 cm
		Elevation	198-200 m	200-202 m	225-226 m	243 m	257.2 m	257.5 m	259.7 m	262.3 m	263.8 m	264.1 m	268.7 m	279 m
Element	Accuracy	Detection Limit												
Au	ppb	0.5	<0.5	<0.5	<0.5	0.8	<0.5	0.6	<0.5	0.5	<0.5	<0.5	<0.5	<0.5
Mo	ppm	0.1	0.6	0.5	0.7	1.9	0.7	0.8	1.5	0.4	0.6	1	0.3	0.5
Cu	ppm	0.1	3	8.1	11.1	13.1	30.7	37.5	15.8	44.9	22	26.2	7.7	6.8
Pb	ppm	0.1	34	13.5	27.9	8.2	32.2	21.1	17.5	37	17.6	18.7	10.3	6.9
Zn	ppm	1	8	16	9	567	57	109	68	92	358	92	221	308
Ag	ppm	0.1	0.7	0.9	0.7	0.3	0.6	0.7	1	1.1	1.1	1.5	0.4	0.2
Ni	ppm	0.1	4.4	6.3	2.2	261.1	43.2	57.4	30.8	43.2	82	70	32.6	60.8
Co	ppm	0.2	0.7	0.6	0.2	41.7	7.5	9.4	3.5	5.2	8.8	8.7	4.9	16.6
Mn	ppm	1	28	65	30	3793	88	88	98	108	201	168	1973	2997
Fe	%	0.01	0.74	1.18	1.04	39.87	25.24	19.82	11.97	34.19	16.11	9.96	30.62	31.7
As	ppm	1	3	1	4	6	9	11	7	7	9	12	4	9
U	ppm	0.1	1.6	3.3	1.3	1.3	1.9	2.8	2.4	1.8	2	2.7	0.7	0.8
Au	ppm	0.1	<0.1	<0.1	<0.1	<0.1	<0.1	<0.1	<0.1	<0.1	<0.1	<0.1	<0.1	<0.1
Th	ppm	0.1	2.8	4.7	1	1.8	3.8	5.4	5.9	2.5	7	8.6	2.9	1.8
Sr	ppm	1	34	61	12	22	33	49	31	22	34	45	26	49
Cd	ppm	0.1	<0.1	0.2	<0.1	0.5	<0.1	0.2	<0.1	<0.1	0.4	<0.1	0.4	0.3
Sb	ppm	0.1	1.1	0.6	0.9	0.2	0.7	0.7	0.6	0.4	0.5	0.7	0.3	0.3
Bi	ppm	0.1	0.2	0.2	<0.1	<0.1	0.1	0.2	0.2	<0.1	0.2	0.2	<0.1	<0.1
V	ppm	1	236	229	21	59	139	204	190	70	179	218	69	91
Ca	%	0.01	0.02	0.05	0.01	0.36	0.12	0.1	0.02	0.28	0.05	0.03	0.57	1.17
P	%	0.001	0.011	0.037	0.016	0.042	0.072	0.066	0.031	0.178	0.026	0.031	0.037	0.162
La	ppm	0.1	3.7	16.2	4	16.2	26.7	35.5	23.8	16	25.6	28.9	13.4	18.6
Cr	ppm	1	99	101	14	37	59	86	73	38	90	99	34	27
Mg	%	0.01	0.41	0.32	0.02	0.75	1.53	1.67	2.01	0.88	2.44	1.99	5.6	4.75
Ba	ppm	1	5720	4014	845	64	137	236	36	12	99	138	159	284
Ti	%	0.001	0.408	0.245	0.058	0.059	0.145	0.196	0.201	0.089	0.26	0.29	0.103	0.086
Al	%	0.01	7.16	5.17	0.5	1.87	3.71	4.91	5.06	2.35	6.95	7.94	2.81	1.77
Na	%	0.001	0.195	0.13	0.017	0.016	0.01	0.03	0.017	0.006	0.053	0.13	0.014	0.011
K	%	0.01	3.03	2.02	0.12	0.18	0.04	0.4	0.14	0.03	0.4	0.96	0.03	0.02
W	ppm	0.1	1.4	0.9	0.3	0.2	0.5	0.7	0.7	0.4	0.7	0.9	0.4	0.4
Zr	ppm	0.1	87	62.7	16.4	24.2	43.3	61.9	61.9	27.8	61	71.2	33.2	38.9
Ce	ppm	1	10	38	8	26	64	79	50	31	51	61	26	37
Sn	ppm	0.1	2.4	1.4	0.3	0.7	1.1	1.5	1.1	1.1	1.7	2.2	0.8	0.5
Y	ppm	0.1	2.6	10.6	2.1	69.2	23.8	27.7	18.2	23.9	16.3	19.1	14.9	28.9
Nb	ppm	0.1	10.7	6.7	1.6	1.8	5	6	6.8	2.8	7	9	3.4	2.8
Ta	ppm	0.1	0.7	0.4	<0.1	0.1	0.2	0.3	0.4	0.2	0.4	0.5	0.2	0.1
Be	ppm	1	2	2	<1	<1	<1	<1	<1	<1	<1	<1	<1	<1
Sc	ppm	1	9	9	1	5	9	12	8	8	11	14	5	7
Li	ppm	0.1	18.7	12.3	14.2	30.2	59.4	69.4	70.4	30.6	135.7	132.4	40.8	40
S	%	0.1	0.3	0.1	0.2	4.2	>10.0	>10.0	2.6	>10.0	5.6	2.2	0.4	0.4
Rb	ppm	0.1	125.9	95.4	4.1	9.8	2.3	20.1	6.9	0.6	18.1	44.3	<0.1	0.1
Hf	ppm	0.1	2.3	1.6	0.4	0.4	0.8	1.3	1.3	0.6	1.5	1.8	0.7	0.5

Analysis performed at ACME Analytical Laboratories Ltd., Vancouver, BC.

Au; 0.5g sample leached in hot Aqua Regia and analyzed by ICP-MS.

All other elements; 0.25g processed by 4-acid digetstion (HNO_3-$HClO_4$-HF and HCL) analyzed by ICP-MS.

precluded any estimate on distance to the vent system. The presence of bedded sulphide mineralization associated with nodular barite in the current study area supports the inference that this is of hydrothermal origin and that it may be in a more proximal setting to the source of the mineralization.

REGIONAL CORRELATIONS AND METALLOGENY

Besa River rocks in the study area can be broadly correlated with the Earn Group of the Kechika Trough (Figure 6). Units 1 through 5 most likely correlate with cherty argillite, carbonaceous siliceous shale and lesser black carbonaceous siltstone and shale of the Middle to Late Devonian Gunsteel Formation (MacIntyre, 1998). The succeeding more recessive and crumbly siltstone and shales of unit 6 are probably correlative to recessive dark grey siltstone of the Akie Formation, postulated to be Late Devonian to Early Mississippian in age (MacIntyre, 1998).

Correlation of the outcropping Besa River Formation with subsurface formations to the east is suggested based on the total gamma ray trace across the measured section (Figures 13, 14). In the subsurface, as the Keg River reef and successive Devonian and Mississippian carbonate successions shale out westward into fine clastics of the Horn River, Fort Simpson and Besa River successions, the distinctive radioactive shales of the Evie, Muskwa and Exshaw formations can be traced across into the thick, monotonous siltstone sequence. The Exshaw Formation can be traced with confidence as it forms a regional marker horizon throughout a large part of the Western Canada Sedimentary Basin. The Evie shales above the Lower Keg River carbonates also define a distinctive package, and together with the succeeding Muskwa horizon define a recognizable sequence.

Suggested correlations for several wells west of the Liard River are depicted in Figure 14. The Exshaw Formation can be traced into the strongly radioactive central part of the Besa River section, and the lower most radioactive zone equates to the Muskwa Formation. Approximately 25 m of basal Besa River siltstones are covered; they are assumed to represent the Evie member of the Horn River Formation. The siltstones below Muskwa-equivalent rocks would be equivalent to the Otter Park siltstones, and those between the Muskwa and Exshaw horizons to the Fort Simpson Formation. These correlations also correspond broadly to the main lithologic units described previously: unit 1 corresponds to the Otter Park Member, units 2 and 3 to the Muskwa Formation, unit 4 to the Fort Simpson Formation, and unit 5 to the Exshaw Formation (Figure 14). Note that the distinctive light grey weathering panel within Besa River Formation exposures in the Caribou Range, which corresponds to the Fort Simpson equivalent horizon, is

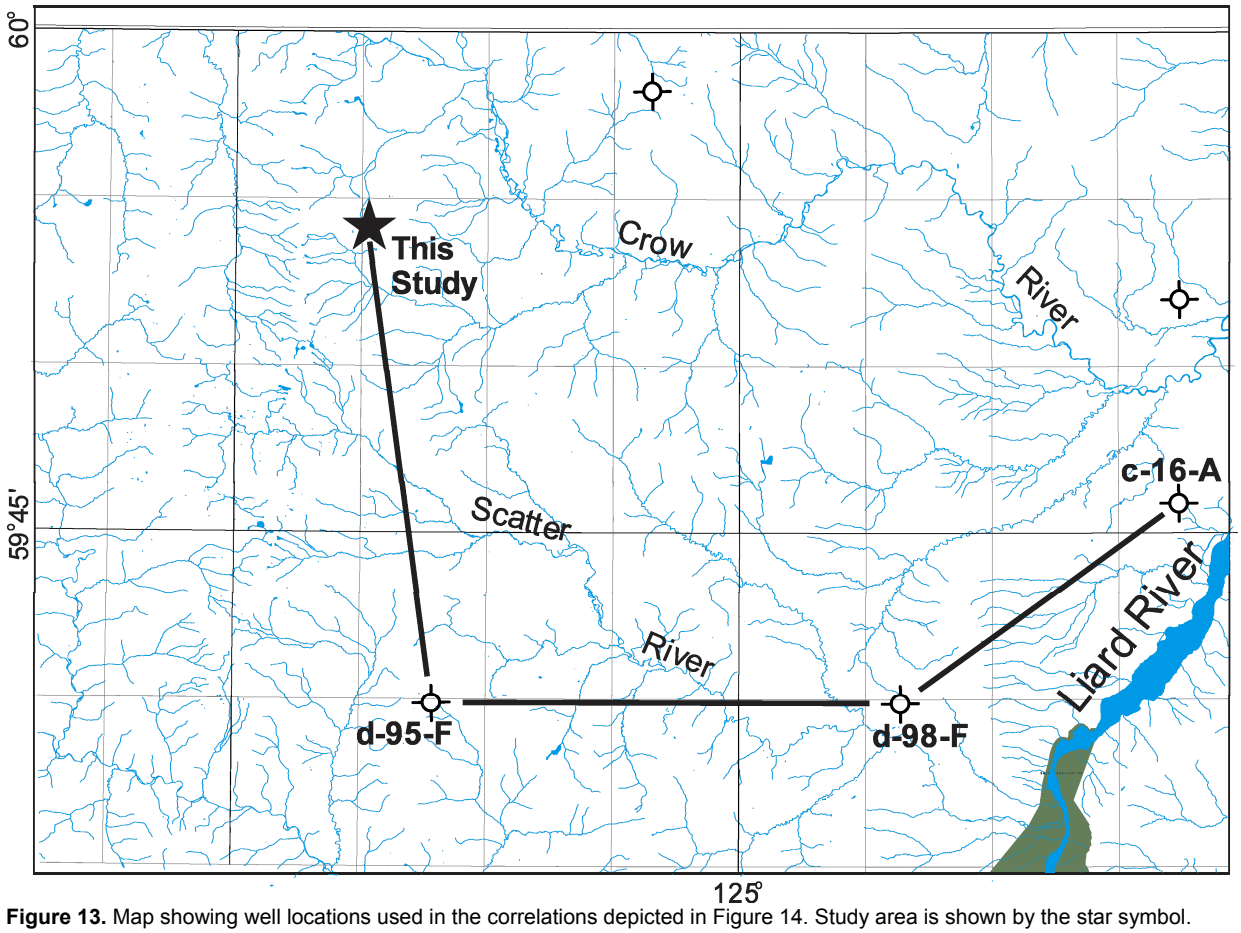

Figure 13. Map showing well locations used in the correlations depicted in Figure 14. Study area is shown by the star symbol.

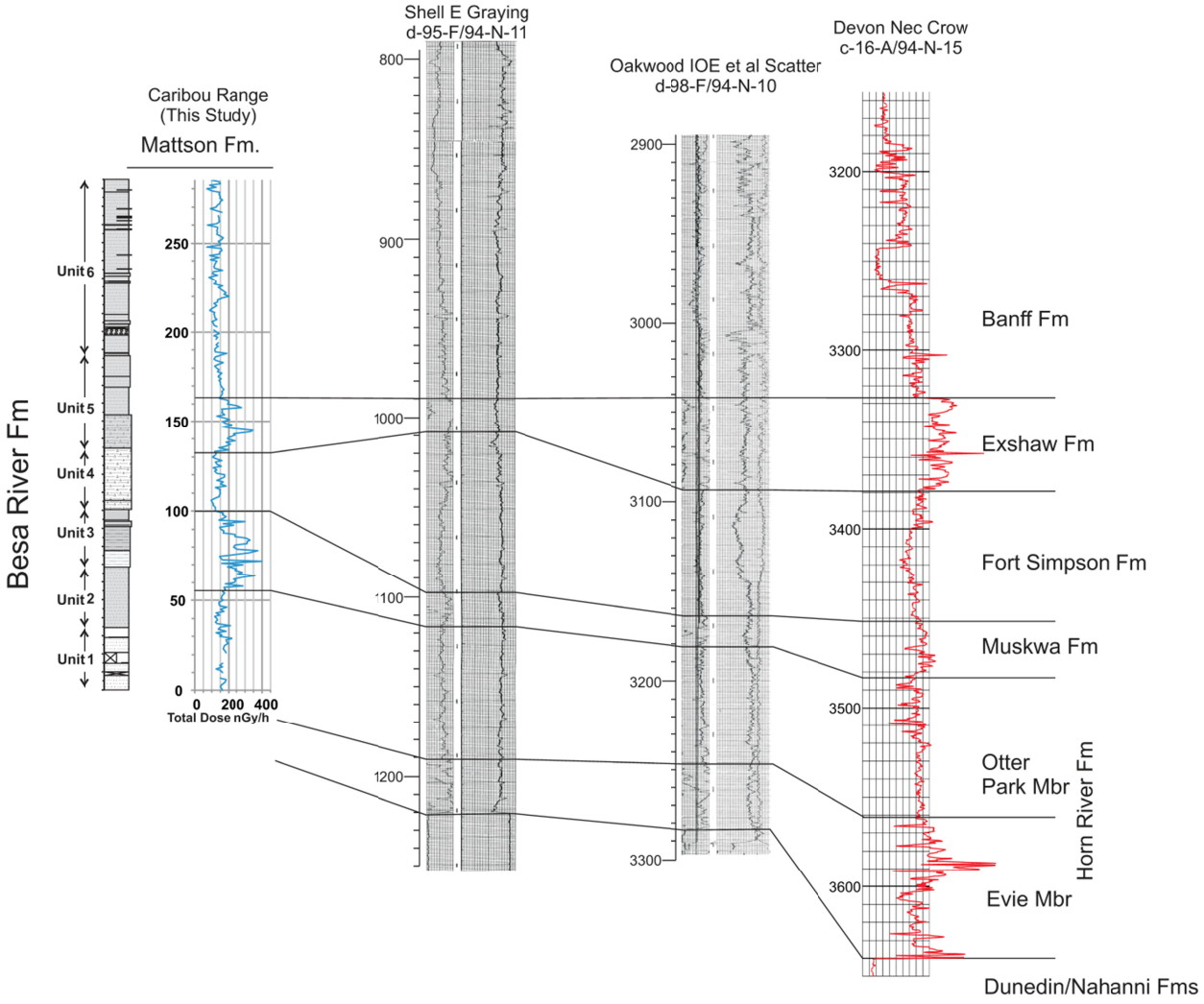

Figure 14. Correlation of measured Besa River section, using the trace of total gamma ray counts, with several subsurface sections, the location of which are shown in Figure 13. Only the gamma ray log is shown for the c-16-A well. Bulk density is shown for the d-98-F well and the acoustic log for the d-95-F well.

only some 25 to 35 m in thickness, attesting to the extremely condensed nature of this section. In outcrop, the succeeding section that correlates with the Exshaw Formation appears as siliceous as underlying Fort Simpson equivalent strata, but is considerably darker and more carbonaceous.

Although the overall trace of the gamma ray log across the outcrop is very similar to subsurface gamma ray logs, the unit boundaries defined by this methodology do not necessarily correspond to those defined within the lithologic log (Figures 11, 14). The relatively sharp contacts of unit 4 correlate with breaks in the gamma ray trace (Fort Simpson Formation equivalent, Figure 11). The upper boundary of the Exshaw marker, as defined by the gamma ray trace, falls within the upper part of unit 5. This unit is also defined by high organic contents and higher uranium concentrations than the base of unit 6 (Figure 11), suggesting this may be the upper contact of the Exshaw marker.

The contact between units 2 and 3 occurs within the lower part of the Muskwa marker. Furthermore, the contact between unit 1 and 2 is not very distinctive on the gamma ray trace, although total organic carbon contents are higher in unit 2 and potassium levels are higher in unit 1. Even though the overall organic content and uranium level are increasing within unit 2, the general lithologic character is not changing. This should be reflected in the lithogeochemistry.

This correlation technique is powerful in that it allows one to assign approximate stratigraphic ages to the various units within an otherwise monotonous sequence, based on the linkages to defined stratigraphy in other parts of the basin (Figure 14). A consequence of this is that the sulphide mineralization within the section is probably Tournaisian or Visean in age, based on its

position above the Exshaw marker within the section. In Kechika and Selwyn basins, major exhalative sulphide deposits are of Frasnian to Famennian age, with minor sulphide and barite mineralization within rocks as young as Early Mississippian (Paradis *et al.*, 1998; Irwin and Orchard, 1991). This younger sulphide mineralization is roughly coeval with major volcanogenic massive sulphide deposits within arc sequences that lay immediately outboard of the Selwyn Basin (Wolverine deposit; Piercey *et al.*, 2008 Paradis *et al.*, 1998).

CONCLUSIONS

- Approximately 285 m of the Besa River Formation outcrops along the western margin of the Liard Basin and consists of light grey to black weathering carbonaceous siltstone to siliceous siltstone. The lower 25 m of the unit was not exposed.
- The Besa River Formation has been subdivided into 6 informal units based on overall outcrop composition.
- Rock Eval analysis of representative samples on 4 m spacing across the outcrop indicate two zones of high organic carbon content, with levels reaching 6% by weight.
- A gamma ray spectroscopic log across the outcrop defines several zones of higher radiation which correlate to higher concentration of uranium and organic carbon.
- Correlation of the gamma ray trace with subsurface sections to the east suggests that the lower and upper radioactive zones in the outcrop correlate with the Muskwa and Exshaw markers, respectively.
- Nodular barite and bedded pyrite mineralization was discovered in the upper part of the Besar River section (MT showing, MINFILE 094N 012) which is similar to mineralization at the nearby Scat showing (MINFILE 094N 010).

ACKNOWLEDGMENTS

The authors would like to thank Lauren Wilson and Lisa Fodor for competent and cheerful assistance in the field. We would like to acknowledge Great Slave Helicopters, of Fort Liard, for the efforts in transporting us to our field localities. The senior author would like to thank Sarah Saad, at Geological Survey of Canada laboratories in Calgary, for her patience and knowledge in preparation and analysis of Rock Eval samples. We would also like to thank JoAnne Nelson of the British Columbia Geological Survey Branch for carefully reviewing an earlier version of this manuscript.

REFERENCES

Bamber, E.W., Henderson, C.M., Richards, B.C. and McGugan, A. (1991): Carboniferous and Permian stratigraphy of the Foreland Belt, Part A. Ancestral North America; in Upper Devonian to Middle Jurassic assemblages, Chapter 8 of Geology of the Cordilleran Orogen in Canada, H. Gabrielse and C.J. Yorath (ed.); *Geological Survey of Canada*, Geology of Canada, No. 4, pages 242-265.

Barclay, J.E., Krause, F.F.; Campbell R.I. and Utting, J. (1990): Dynamic casting and growth faulting; Dawson Creek graben complex, Carboniferous-Permian Peace River Embayment, Western Canada; *Bulletin of Canadian Petroleum Geology*, Vol. 38A, pages 115-145.

Burt, P. (1982): Geological and geochemical report on SCAT 1 – 20 claims, 59°50' north - 125°25' west, Liard Mining Division; *BC Ministry of Energy, Mines and Petroleum Resources*, Assessment Report 10810.

Fallas, K.M. and Evenchick, C.A. (2002): Preliminary geology, Mount Merrill, Yukon Territory - British Columbia; *Geological Survey of Canada*, Open File 4264.

Fallas, K.M.(2001): Preliminary geology, Mount Martin, Yukon Territory-British Columbia-Northwest Territories; *Geological Survey of Canada*, Open File 3402.

Fallas, K.M., Pigage, L.C., MacNaughton, R.B. (2004): Geology, La Biche River southwest (95 C/SW), Yukon Territory - British Columbia; *Geological Survey of Canada*, Open File 4664.

Ferri, F., Hickin, A. and Huntley, D. (2011): Besa River Formation, western Liard Basin, British Columbia; geochemistry and regional correlations; *BC Ministry of Energy*, Geoscience Reports 2011, pages.

Ferri, F., Rees, C., Nelson, J. and Legun, A. (1999): Geology and mineral deposits of the northern Kechika Trough between Gataga River and the 60th parallel, *BC Ministry of Energy, Mines and Petroleum Resources*, Bulletin 107, 122 pages.

Force, E., Cannon, W.F., Koski, R.A, Passmore, K.T. and Doe, B.R. (1983): Influences of ocean anoxic events on manganese deposition and ophiolite-hosted sulphide preservation; in T.M. Cronin, W.F. Cannon and R.Z. Poore (editors), Paleoclimate and mineral deposits; *US Geological Survey*, Circular 822, pages 26-29.

Fowler, M., Snowdon, L. And Stasiuk, V. (2005): Applying petroleum geochemistry to hydrocarbon exploration and exploitation; *American Association of Petroleum Geologists,* Annual Convention, Short Course Handbook; Calgary, AB.

Gabrielse, H. (1963): Geology, Rabbit River, British Columbia; *Geological Survey of Canada*, Preliminary Map 46-1962.

Gabrielse, H. (1967): Tectonic evolution of the northern Canadian Cordillera, *Canadian Journal of Earth Sciences*, Volume 4, pages 271-298.

Goodfellow, W.D. and Lydon, J.W. (2007): Sedimentary Exhalative (SEDEX) Deposits; in Mineral Deposits of Canada, Wayne D. Goodfellow (editor), *Geological Association of Canada*, Special Publication 5, pages 163-184.

Huntley, D.H. and Sidwell, C.F. (2010): Application of the GEM surficial geology data model to resource evaluation and geohazard assessment for the Maxhamish Lake map area (NTS 94O), British Columbia; *Geological Survey of Canada*, Open File 6553, 12 pages.

Huntley, D.H. Hickin, A.S. (2010): Surficial deposits, landforms, glacial history and potential for granular aggregate and frac sand: Maxhamish Lake map sheet (NTS 94O), British Columbia; *Geological Survey of Canada*, Open File 6430, 17 pages.

Irwin, S.E.B. and Orchard, M.J. (1991): Upper Devonian-Lower Carboniferous conodont biostratigraphy of the Earn Group and overlying units, northern Canadian Cordillera; in Ordovician to Triassic conodont paleontology of the Canadian Cordillera, Orchard, M.J. and McCracken, A.D. (editors), *Geological Survey of Canada*, Bulletin 417, pages 185-213.

Kidd, F.A. (1963): The Besa River Formation; *Bulletin of Canadian Petroleum Geology*, Volume 11, Issue 4, pages 369-372.

Leckie, D.A., Potocki, D.J. and Visser, K. (1991): The Lower Cretaceous Chinkeh Formation: A frontier-type play in the Liard Basin of Western Canada, *American Association of Petroleum Geologists Bulletin*, Volume 75, No. 8, pages 1324-1352.

MacIntyre, D.G. (1998): Geology, Geochemistry and Mineral Deposits of the Akie River Area, Northeast British Columbia (NTS 094F01, 02, 07, 10, 11); *BC Ministry of Energy, Mines and Petroleum Resources*, Bulletin 103, 99 pages.

MacLean, B. C. and Morrow, D. W. (2004): Bovie Structure; its evolution and regional context; *Bulletin of Canadian Petroleum Geology*, Vol. 52, Issue 4, Part 1, pages 302-324.

Mathews, W.H. (1986): Physiography of the Canadian Cordillera; *Geological Survey of Canada*, Map 1701A.

McClay, K.R. and Buchanan, P.G. (1992): Thrust faults in inverted extensional basins, in *Thrust Tectonics*, K.R. McClay (editor); Chapman and Hall, New York, pages 93-104.

Meijer Drees, N.C. (1994): Devonian Elk Point Group of the Western Canada Sedimentary Basin; in Geological Atlas of the Western Canada Sedimentary Basin, G.D. Mossop and I. Shetsen (comp.), *Canadian Society of Petroleum Geologists and Alberta Research Council*, Special Report 4, URL <http://www.ags.gov.ab.ca/publications/wcsb_atlas/atlas.html>, [2010].

Monahan, P. (2000): Liard Basin area; *BC Ministry of Energy*, special report; URL <http://www.empr.gov.bc.ca/OG/oilandgas/petroleumgeology/ConventionalOilAndGas/Pages/NortheasternBCBasin.aspx>, [2010].

Morrow, D. W., Potter, J. Richards, B. and Goodarzi, F. (1993): Paleozoic burial and organic maturation in the Liard Basin region, northern Canada; *Bulletin of Canadian Petroleum Geology*, Volume 41, Issue 1, pages 17-31.

Mossop, G.D., Wallace-Dudley, K.E., Smith, G.G. and Harrison, J.C. (comp.) (2004): Sedimentary basins of Canada; *Geological Survey of Canada*, Open File Map 4673.

Oldale, H.S. and Munday, R. J. (1994): Devonian Beaverhill Lake Group of the Western Canada Sedimentary Basin; in Geological Atlas of the Western Canada Sedimentary Basin, G.D. Mossop and I. Shetsen (comp.), *Canadian Society of Petroleum Geologists and Alberta Research Council*, Special Report 4, URL <http://www.ags.gov.ab.ca/publications/wcsb_atlas/atlas.html>, [2010].

Paradis, S., Nelson, J.L. and Irwin, Steve E. B. (1998): Age constraints on the Devonian shale-hosted Zn-Pb-Ba deposits, Gataga District, northeastern British Columbia, Canada; *Bulletin of the Society of Economic Geologists*, Volume 93, Issue 2, pages 184-200.

Pelzer, E.E. (1966): Mineralogy, geochemistry, and stratigraphy of Besa River Shale, British Columbia; *Bulletin of Canadian Petroleum Geology*, Volume 14, Issue 2, pages 273-321.

Piercey, S.J., Mortensen, J.K., Paradis, S, Murphy, D.C. and Tucker, T.L. (2008): Petrology and U-Pb geochronology of footwall porphyritic rhyolites from the Wolverine volcanogenic massive sulfide deposit, Yukon, Canada; implications for the genesis of massive sulfide deposits in continental margin environments; *Bulletin of the Society of Economic Geologists*, Volume 103, Issue 1, pages 5-33.

Potter, J., Richards, B. C. and Goodarzi, F. (1993): The organic petrology and thermal maturity of Lower Carboniferous and Upper Devonian source rocks in the Liard Basin, at Jackfish Gap-Yohin Ridge and North Beaver River, northern Canada; implications for hydrocarbon exploration, *Energy Sources*, Volume 15, Issue 2, pages 289-314.

Ross, D.J.K. and Bustin, R. (2008): Characterizing the shale gas resource potential of Devonian-Mississippian strata in the Western Canada Sedimentary Basin; application of an integrated formation evaluation; *American Association of Petroleum Geologists*, Bulletin, Volume 92, Issue 1, pages 87-125.

Stott, D.F. and Taylor, G.C. (1973): Tuchodi Lakes map area, British Columbia; *Geological Survey of Canada*, Memoir 373, 37 pages.

Switzer, S.B., Holland, W.G., Christie, D.S., Graf, G.C., Hedinger, A.S., McAuley, R.J., Wierzbicki, R.A. and Packard, J.J. (1994): Devonian Woodbend-Winterburn Strata of the Western Canada Sedimentary Basin; in Geological Atlas of the Western Canada Sedimentary Basin, G.D. Mossop and I. Shetsen (comp.), *Canadian Society of Petroleum Geologists and Alberta Research Council*, Special Report 4, URL <http://www.ags.gov.ab.ca/publications/wcsb_atlas/atlas.html>, [2010].

Taylor, G.C. and Stott, D.F. (1999): Geology, Toad River, British Columbia; *Geological Survey of Canada*, Map 1955A.

Wright, G.N., McMechan, M.E. and Potter, D.E.G. (1994): Structure and Architecture of the Western Canada Sedimentary Basin; in Geological Atlas of the Western Canada Sedimentary Basin, G.D. Mossop and I. Shetsen (comp.), *Canadian Society of Petroleum Geologists and Alberta Research Council*, Special Report 4, URL <http://www.ags.gov.ab.ca/publications/wcsb_atlas/atlas.html>, [2010].

Nickeliferous Minerals in the Cassiar Asbestos Deposit, Northern British Columbia (NTS 104P/05) - Relevance for Nickel Exploration

by Z.D. Hora[1], A. Langrová[2] and E. Pivec[3]

KEYWORDS: Cassiar deposit, MINFILE 104P 005, chrysotile asbestos, Cr-magnetite, magnetite, nickel, Ni, heazlewoodite, serpentinization products and nickel minerals, awaruite

INTRODUCTION

The discovery of nickel and cobalt bearing minerals in a rhodonite sample from the Bridge River Complex in 2006 (Hora *et al.*, 2007) raised our interest in nickel occurrences associated with the serpentinization of ultramafic rocks in British Columbia. A number of reports from sites in Quebec and Northwest Territories described occurrences of nickel sulphides and nickel-iron alloys as a co-product of serpentinization (Nickel, 1959; Chamberlain *et al.*, 1965; Chamberlain, 1966; Eckstrand, 1975). In British Columbia, there are a number of reports of possible similar nickel minerals. For example, previous workers identified "some nickeliferous sand" in alluvial gold from the Fraser River (Sutton, 1888), awaruite on Wheaton Creek in Cassiar District in the late 1800s (Holland, 1940; Ramdohr, 1950), Letain Creek (Krishnarao, 1964) and nickel-iron (possible awaruite Ni_3Fe) in the Blue River area north of Cassiar (Gabrielse, 1963; Wolfe, 1964). In the Cassiar asbestos deposit (MINFILE 104P 005), O`Hanley *et al.* (1992) identified pentlandite and heazlewoodite. However, the distribution of nickel at Cassiar did not receive any closer attention.

With all this in mind, the Cassiar mine tailings pile was sampled during the summer of 2008 and several fresh samples collected from the minesite ore zone in 1990 were selected for a preliminary study with specific attention given to minerals with nickel content (Figure 1).

[1] *British Columbia Geological Survey, Victoria, BC (retired)*

[2] *Institute of Geology, Academy of Sciences of the Czech Republic, Prague, Czech Republic*

[3] *Institute of Geology, Academy of Sciences of the Czech Republic, Prague, Czech Republic (retired)*

This publication is also available, free of charge, as colour digital files in Adobe Acrobat® PDF format from the BC Ministry of Forests, Mines and Lands website at http://www.empr.gov.bc.ca/Mining/Geoscience/PublicationsCatalogue/Fieldwork.

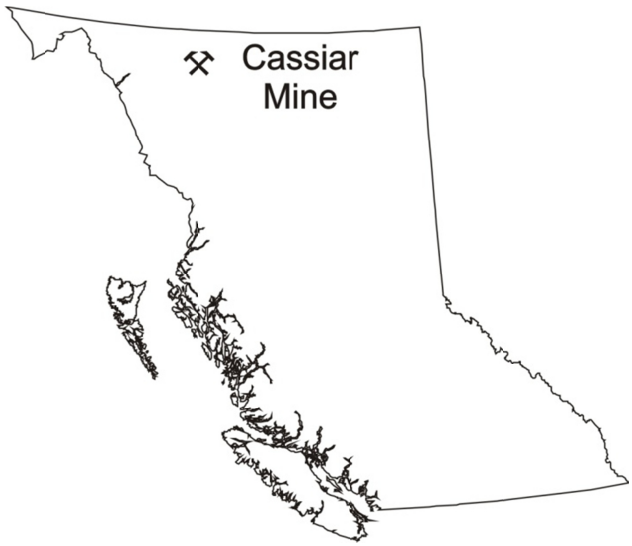

Figure 1. Location of study area, Cassiar, northern British Columbia.

Cassiar Mineralogy

Two samples of Cassiar mine tailings were collected directly from the tailings impoundment. The first sample (#001) represented a visually typical bulk tailings material. The second sample had the magnetic component separated in the field using a permanent magnet (#002). Previous work by Cassiar Asbestos Ltd. carried during 1986 over the period of several months identified that material dumped into Cassiar tailings contain in average by weight of approximately 9% of magnetite (Hancock, 1988). Laboratory results of 3131 ppm nickel in the magnetic sample (#002) and 2230.9 ppm nickel in the bulk sample (#001) shown in Table 1 encouraged the more detailed study. That involved XRD mineral identification in individual samples and analytical microprobe examination.

Identification of mineral phases was made by x-ray powder diffraction, using a Phillips X`Pert APD that employs CoKα radiation and secondary monochromator. Scanning speed was set to 1^0/min, generator voltage to 40 kV and current to 30 mA. Analytical microprobe examination used a CAMECA SX-100 electron microprobe using the wavelength dispersive technique. The beam diameter was 2μm with an accelerating potential of 15 kV. A beam current of 10 nA was

Table 1. Analytical results, Cassiar mine tailings samples, British Columbia.

Sample	Mo ppm	Cu ppm	Pb ppm	Zn ppm	Ag ppm	Ni ppm	Co ppm	Mn ppm	Fe %	As ppm	U ppm	Au ppb
CAS 001	0.3	2.6	1.9	17	<0.1	3131	207	921	18.24	1.3	<0.1	
CAS 002	0.2	0.9	1	14	<0.1	2230.9	84.3	562	5.21	<0.5	<0.1	<0.5

Th ppm	Sr ppm	Cd ppm	Sb ppm	Bi ppm	V ppm	Ca %	P ppm	La ppm	Cr ppm	Mg %	Ba ppm	Ti %
<0.1	1	<0.1	<0.1	0.5	38	0.11	<0.001	<1	1594	14.45	3	0.004
<0.1	2	<0.1	<0.1	<0.1	30	0.08	<0.001	<1	1372	21.48	4	0.004

B ppm	Al %	Na %	K %	W ppm	Hg ppm	Sc ppm	Tl ppm	S %	Ga ppm	Se ppm
<20	0.29	<0.001	<0.01	<0.1	0.02	7.7	<0.1	<0.05	<1	<0.5
32	0.38	<0.001	<0.01	<0.1	<0.01	13.3	<0.1	<0.05	<1	<0.5

ACME Analytical Laboratories Ltd.
Method 1DX

measured on a Faraday cup. The standards employed were synthetic and natural minerals. The data were reduced using the Merlot correction (φ).

Silicate minerals

Serpentinite mineral aggregates at Cassiar consist mainly of the mixture of chrysotile and antigorite (O`Hanley *et al.*, 1992). The XRD results of tailings samples confirmed the presence of these minerals, the chrysotile being both ortho and clinochrysotile. This study identified the presence of baumite $(Mg,Fe,Mn,Zn)_3Si_2O_5(OH)_4$, caryopilite $(Mg,Mn)_3Si_2O_5(OH)_4$ and jamborite $(Ni^{+2},Ni^{+3},Fe)(OH)_2(OH, S,H_2O)$. All these silicate minerals together with magnesite and stichtite $(Mg_6Cr_6(CO_3)(OH)_{16}.4H_2O)$ were reported previously (O`Hanley *et al.*,1992) and are serpentinization products. Other studies of the serpentinization on ore zone samples showed it was so pervasive, that no primary constituents like olivine or pyroxene have been preserved (Gabrielse, 1960, O`Hanley *et al.*, 1992).

Opaque minerals

Sample #002 was processed on magnetic separator for a further study. The resulting magnetic concentrate contained the Cr-magnetite $Fe(Fe,Cr)_2O_4$ and magnetite (Fe_3O_4) only. Because of increased Ni content in the analysis of the magnetic concentrate it was expected to find a presence of trevorite ($NiFe_2O_4$) component in magnetite or Ni-Fe alloys awaruite (Ni_3Fe) or taenite (NiFe). However, petrographic and x-ray analysis did not identify the presence of nickel minerals. A possible explanation for absence of awaruite may be its usual association with antigorite (Eckstrand, 1975). Antigorite is a higher alteration temperature mineral product then chrysotile.

MICROPROBE WORK

Microanalytical study was made on polished rock samples collected in 1990 from the ore zone as well as polished grains of magnetic concentrate. Nickel in these samples was found to be primarily in three main minerals–Cr-magnetite, magnetite and heazlewoodite. The chemical compositions are presented in Table 2.

Cr-magnetite and magnetite, both magnetic minerals, are the most common minerals in the samples with significant nickel contents. In magnetite, 9 out of 16 measurements show Ni contents between 0.03% and 0.6%, the remaining 7 between 0.87% and 1.57%. Similar values are reported for magnetite from a Western Australia serpentinized dunite (Donaldson, 1981). Nickel content in Cr-magnetite is of similar values. Out of ten measurements six average 0.24% and the remaining four average 1.07% nickel. As expected, Cr-magnetite contains Al, Mg and Mn, while these elements are low or practically absent in the magnetite.

The third nickeliferous mineral from Cassiar - heazlewoodite (Ni_3S_2) is considerably less common in studied rock samples and is present in grains of very small size around 25 to 100 μm. The chemical compositions of the opaque minerals are shown in Table 2.

As shown on the microphotographs (Figures 2a, b, e), Cr-magnetite predates the magnetite. Donaldson (1981) describes similar age relationship between magnetite and chromite from Archean dunites in Western Australia. Cr-magnetite is less resistant to alteration (Figures 2c, d), which can be particularly noticed where in contact with magnetite (Figures 2a, b, e).

Table 2. Representative opaque minerals, Cassiar mine.

	magnetite						Cr - magnetite			heazlewoodite			
Sample No.	3	6	7	13	14	15	4	8	10	1	5	9	12
%													
Fe	69.19	69.77	69.72	70.79	62.80	72.46	35.32	35.49	45.10	0.00	0.51	0.08	53.44
Ni	0.63	0.75	0.97	0.52	1.57	0.17	0.42	0.76	0.64	71.65	71.17	71.92	1.17
Al	0.00	0.00	0.02	0.1	0.00		1.28	1.54	0.75				0.02
S	0.00	0.00	0.00	0.00	0.00	0.00	0.00	0.00	0.00	27.40	27.35	27.88	0.00
Cr	1.79	1.21	1.02	1.02	5.55		18.08	17.83	16.83				13.09
Mn	0.36	0.20	0.23	0.00	0.65	0.00	3.59	3.79	3.09	0.00	0.00	0.02	2.67
Co	0.08	0.00	0.00	0.00	0.13	0.00	0.22	0.23	0.26	0.03	0.04	0.00	0.21
As	0.00	0.00	0.00		0.00	0.00	0.00	0.00	0.00	0.08	0.00	0.02	
0	21.28	21.08	21.12	20.41	21.40	20.80	23.69	23.89	23.65				22.87
Mg	0.52	0.44	0.52	0.31	0.31		4.37	4.18	1.77				0.56
Total %	93.85	93.39	92.45	93.15	92.39	93.43	86.96	87.7	92.06	99.16	99.07	99.92	94.03

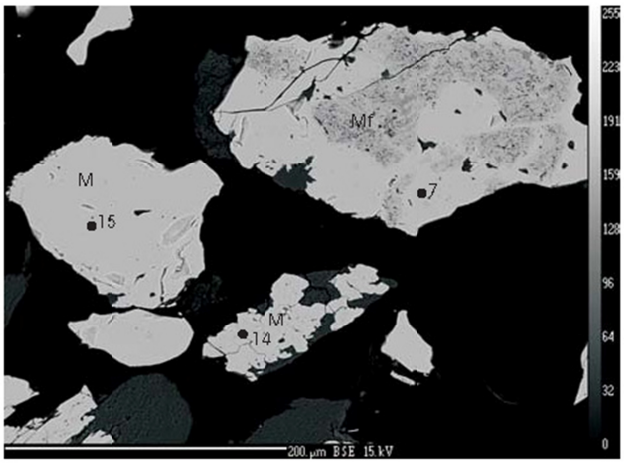

a

Figure 2a. Scanning electron microprobe (SEM) photomicrograph showing separated magnetite grains. White fields correspond to magnetite (M), dark and altered fields to Cr-magnetite (Mf); both with variable contents of Ni (analytical points 7, 14, 15); scale bar 200 µm.

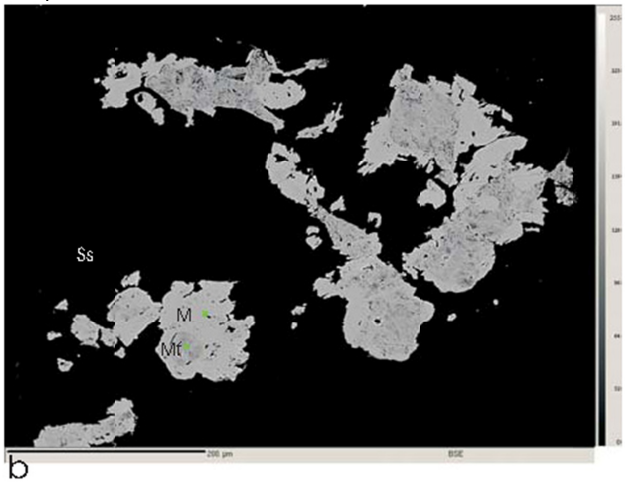

b

Figure 2b. Scanning electron microprobe (SEM) photomicrograph showing rock polished section of serpentinite (Ss) with grains of Cr-magnetite (Mf) altered to magnetite (M), (analytical points 4, 5); scale bar 200 µm.

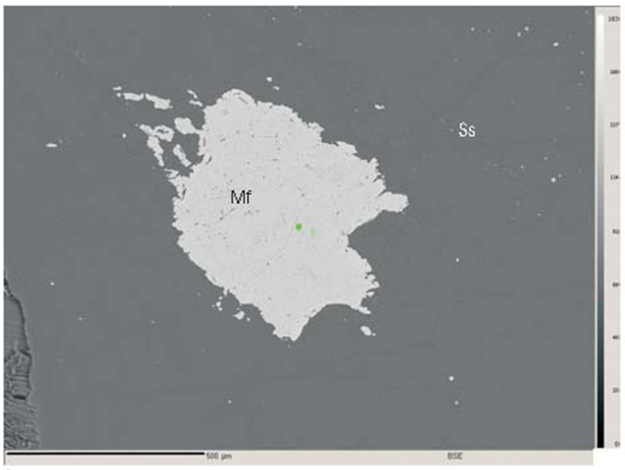

c

Figure 2c. Scanning electron microprobe (SEM) photomicrograph showing rock polished section, single grain of Cr-magnetite (Mf) in serpentinite (Ss); (analytical point 8); scale bar 100 µm.

d

Figure 2d. Scanning electron microprobe (SEM) photomicrograph showing rock polished section, grains of Cr-magnetite (Mf) partly crushed and weakly altered (analytical point 10); scale bar 1 mm.

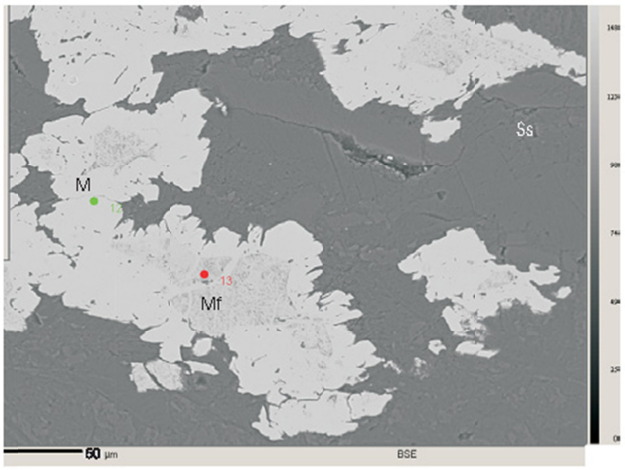

e

Figure 2e. Scanning electron microprobe (SEM) photomicrograph showing rock polished section, Cr-magnetite grains (Mf) completely surrounded by magnetite (analytical points 12, 13); scale bar 50 µm.

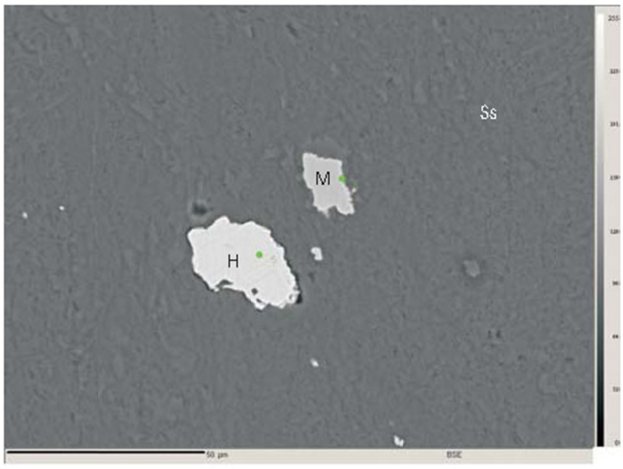

f

Figure 2f. Scanning electron microprobe (SEM) photomicrograph showing rock polished section, grains of magnetite (M) (analytical point 6) and heazlewoodite (H) (analytical point 5); scale bar 50 µm.

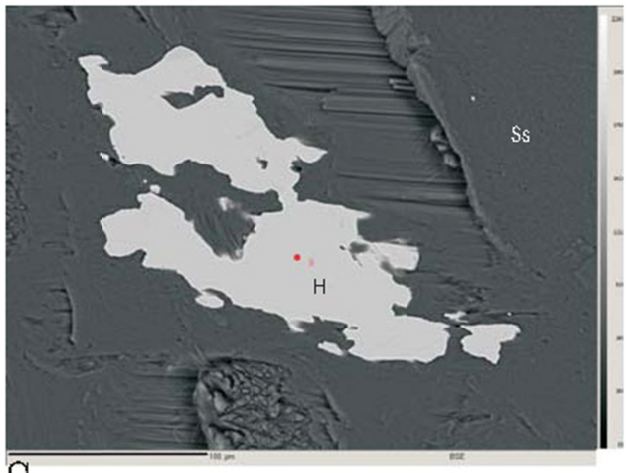

g

Figure 2g. Scanning electron microprobe (SEM) photomicrograph showing rock polished section, large grain of heazlewoodite (H) (analytical point 9); scale bar 150 µm.

Heazlewoodite is the only mineral with Ni as a main component identified in Cassiar samples. It is described as a typical component of serpentinites from many localities (Eckstrand, 1975; Frost, 1985; Ramdohr 1967) and it is particularly common in association with chrysotile asbestos. As shown on Figures 2f and 2g, in the Cassiar samples of this study it occurs in isolated, very small grains of irregular shape between 25 and 100 µm in diameter.

DISCUSSION

Opaque nickel minerals formed as a co-product of serpentinization of ultramafic rocks are a relatively common occurrence in Canada and worldwide. Ramdohr in 1950 was one of the early authors who realized the significance of this phenomenon, pointing out that the size of the grains is usually so minute that they often escape notice. Serpentinization is a highly reducing process and while only a small portion of the silicate FeO enters into the serpentine formula. The bulk of the iron forms magnetite and together with other minor metallic elements (namely S, As and Sb) forms alloys or occurs as native metals. If no free oxygen is available during the serpentinization process, it then gives the possibility for the occurrence of many, mostly extremely fine-grained minerals, like native metals and alloys of iron, nickel, cobalt and copper, sulphides with low sulphur, and similar arsenides and antimonides (Ramdohr, 1967). Such elements have under most conditions a very limited mobility and usually remain as interstitial grains at the place of their origin. Similar in situ nickel mineralization is described by Eckstrand (1975) from northern Quebec and by Chamberlain (1966) and Nickel (1959) from asbestos deposits in Quebec. Under some circumstances, such fine-grained mineralization may be mobilized to form coarser grained disseminations and higher grade accumulations (Frost, 1985), but the formation process is not yet fully understood. It has been suggested, that some originally low grade sulphide copper-nickel deposits were also enriched by a serpentinization process at a later stage (Donaldson, 1981). In his paper about nickel sulphide mineralization in Western Australia, Donaldson (1981) describes studies, where larger scale movement of nickel is considered possible in the presence of sulphur with chloride in solutions.

In British Columbia, recent discoveries of several coarser awaruite zones over large tracts of ultramafic rocks in the area between Fort St. James and Ogden Mountain suggest an economic potential of ultramafic belts for a possibility of bulk mineable nickel deposits (First Point Minerals, 2009). Awaruite is also reported from the Shulaps Range and Dease Lake area in northern British Columbia (Bradshaw, 2008).

CONCLUSIONS

- More attention should be paid to the potential for non-sulphide nickel minerals.
- Serpentinization has been documented to produce secondary sulphide and non-sulphide nickel minerals.
- British Columbia has considerable distribution of serpentinized ultramafics with a number of proven and suspected awaruite showings.
- Cassiar mine tailings have low grade nickel present in Cr-magnetite and magnetite.
- Cassiar tailings are a potential low cost source for heavy media suspension material that could be used for coal deposits, like the Groundhog.

ACKNOWLEDGMENTS

Several persons helped with preparing this report. Mitch Mihalynuk and Garry Payie provided moral support, numerous discussions, and Garry Payie collected the samples from Cassiar tailings. In course of laboratory work, V. Sedláček helped with magnetic separation and J. Dobrovolný with x-ray records. For the technical assistance with data collection and report preparation we thank J. Pávková and V. Šrein. Dave Lefebure provided constructive comments in improving the original manuscript.

REFERENCES

Anonymous (2009): Nickel-Iron Alloy Properties North America; First Point Minerals Corp., PowerPoint presentation, 26 pages.

Bradshaw, P.M.D. (2008): First Point Acquires Two More Large Nickel Properties in British Columbia; First Point Minerals press release, January 10, 2008, 2 pages.

Chamberlain, J.A. (1966): Heazlewoodite and Awaruite in Serpentinites of the Eastern Townships, Quebec; Canadian Mineralogist, Volume 8, pages 519-522.

Chamberlain, J.A., McLeod, C.R., Traill, R.J. and Lachance, G.E. (1965): Native Metals in the Muskox Intrusion; Canadian Journal of Earth Sciences, Volume 2, pages 188-215.

Donaldson, M.J. (1981): Redistribution of Ore Elements during Serpentinization and Talc-Carbonate Alteration of Some Archean Dunites, Western Australia; Economic Geology, Volume 76, pages 1698-1713.

Eckstrand, O.R. (1975): The Dumont Serpentinite: A Model for Control of Nickeliferous Opaque Mineral Assemblages by Alteration Reactions in Ultramafic Rocks; Economic Geology, Vol.70, pages 183-201.

Frost, B.R. (1985): On the Stability of Sulfides, Oxides, and Native Metals in Serpentinite; Journal of Petrology, Volume 26, pages 31-63.

Gabrielse, H. (1960): The Genesis of Chrysotile Asbestos in the Cassiar Asbestos Deposit, Northern British Columbia; Economic Geology, Volume 55, pages 327-337.

Gabrielse, H. (1963): McDame Map Area, Cassiar District, British Columbia; Geological Survey of Canada, Memoir 319, 138 pages.

Hancock, K.D. (1988): Magnetite Occurrences in British Columbia; B.C. Ministry of Energy, Mines and Petroleum Resources, Open File 1988-28, 153 pages.

Holland, S.S. (1940): Placer Gold Deposits, Wheaton (Boulder) Creek, Cassiar District, Northern British Columbia; British Columbia Department of Mines, Bulletin 2, 43 pages.

Hora, Z.D., Langrová, A. and Pivec, E. (2007): Rhodonite from the Bridge River Assemblage, Downton Creek (NTS 092J/09), Southwestern British Columbia; B.C. Ministry of Energy, Mines and Petroleum Resources, Paper 2007-1, pages 39-43.

Krishnarao, J.S.R. (1964): Native Nickel – Iron Alloy, its Mode of Occurrence, Distribution and Origine; Economic Geology, Volume 59, pages 443-448.

O`Hanley, D.S., Schandl, E.S. and Wicks, F.J. (1992): The Origin of Rodingites from Cassiar, British Columbia, and their use to Estimate T and P (H2O) During Serpentinization; Geochimica and Cosmochimica Acta, Volume 56, pages 97-108.

Nickel, E.H. (1959): The Occurrence of Native Nickel-iron in the Serpentine Rock of the Eastern Townships of Quebec Province; Canadian Mineralogist, Volume 6, pages 307-319.

Ramdohr, P. (1950): Űber Josephinit, Awaruit, Souesit, ihre Eigenschaften, Entstehung und Paragenesis; Mineralogical Magazine, Volume XXIX, Number 2112, pages 374-394.

Ramdohr, P. (1967): A Widespread Mineral Association, Connected with Serpentinization; Neues Jahrbuch fűr Mineralogie, Abhandlungen, Band 107, pages 241-265.

Sutton, W.J. (1888): Cobalt and Nickel; in Report by W.J. Sutton, Government Assayer, Annual Report of the Minister of Mines for the Year Ending 31st December 1888, Province of British Columbia, page 325.

Wolfe, W.J. (1964): The Blue River Ultramafic Intrusion, Cassiar District, British Columbia; Geological Survey of Canada, Paper 64-48, 15 pages.

Geology and Mineralization of the Hoodoo Mountain Area (NTS 104B/14E)

by M.G. Mihalynuk, J.M. Logan, A. Zagorevski[1] and N. Joyce[1]

KEYWORDS: Hoodoo Mountain, Andrei Icefield, volcanic-hosted massive sulphide, Rock and Roll, copper porphyry, Galore Creek, Stikine assemblage, Stuhini Group, Iskut River, Twin Glacier River, Bronson

INTRODUCTION

The Iskut River area of northwestern British Columbia is characterized by exceptional mineral endowment. A 20 km-wide corridor south of the Iskut River includes the Bronson Slope, Snip, Johnny Mountain, Eskay Creek and Rock and Roll deposits with past production or defined resources (Figure 1). These deposits formed in a surprisingly diverse set of environments ranging from intrusion hosted sulphide veins to shallow subaqueous hotspring settings. No deposits with past production or defined resources occur within a 20 km corridor immediately north of the Iskut River, yet those farther afield include Galore Creek, Copper Canyon and Schaft Creek deposits that are hosted by alkalic and calcalkalic porphyries. An obvious explanation for the dearth of deposits within the northern corridor is not forthcoming from existing geological maps; however, a significant part of the corridor has either never been systematically mapped or at least not since it was surveyed by Forrest Kerr in the 1920s. A working partnership was established between the British Columbia Ministry of Energy, Mines and Petroleum Resources, the Geological Survey of Canada (under the auspices of the Geoscience for Energy and Minerals Strategy: GEMS), Pacific North West Capital Corp., and the University of Victoria to address this lack of public geologic knowledge through systematic mapping. Supplementary goals were to provide a more accurate geological setting for the Rock and Roll deposit and to evaluate the potential for similar precious metal rich polymetallic massive sulphide mineralization within the Iskut and adjacent regions (Figure 1). Our work was mainly focused where published mapping was entirely lacking: the eastern half of the Hoodoo Mountain map

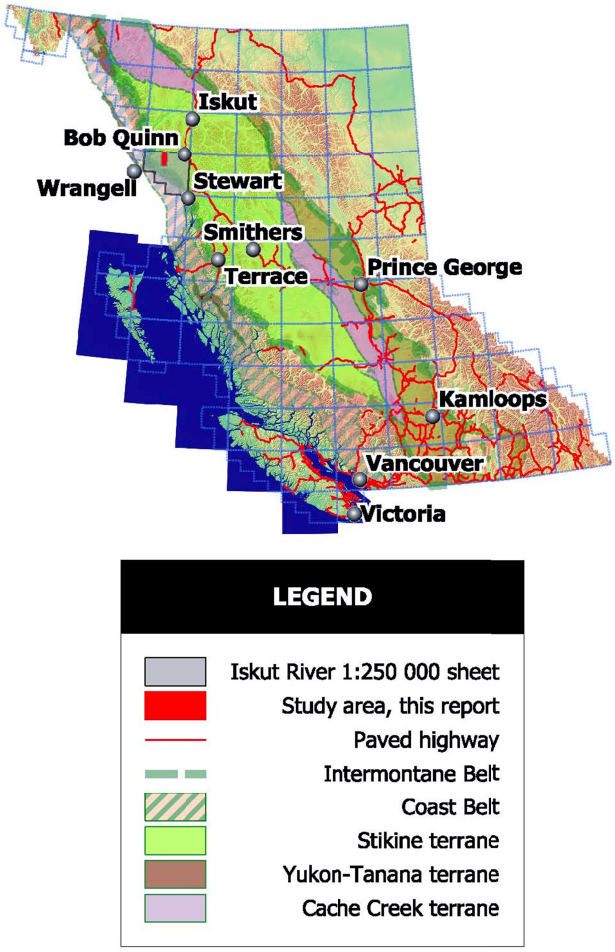

Figure 1. Location of the Iskut study area near the boundary of the Coast Belt and western Stikine terrane.

sheet (NTS 104B/14E, Figures 2 and 3). This map sheet is bordered to the north by the Galore Creek map sheet (104G/03; Figure 2) and to the east by Forrest Kerr map sheet (104B/15), both covered by relatively recent regional geological surveys (Logan and Koyanagi, 1994, 104G/03, 04; and Logan *et al.*, 2000, 104B/10, 15, 104G/02, 07W; Figure 2).

LOCATION AND ACCESS

Access to the Hoodoo Mountain map area (NTS 104B/14E) is via the Bronson airstrip, located along the Iskut River 300 km north-northwest of Terrace, 330 km northwest of Smithers, and 75 km east-northeast of

[1] *Geological Survey of Canada, Natural Resources Canada, Ottawa, ON*

This publication is also available, free of charge, as colour digital files in Adobe Acrobat® PDF format from the BC Ministry of Forests, Mines and Lands website at http://www.empr.gov.bc.ca/Mining/Geoscience/PublicationsCatalogue/Fieldwork.

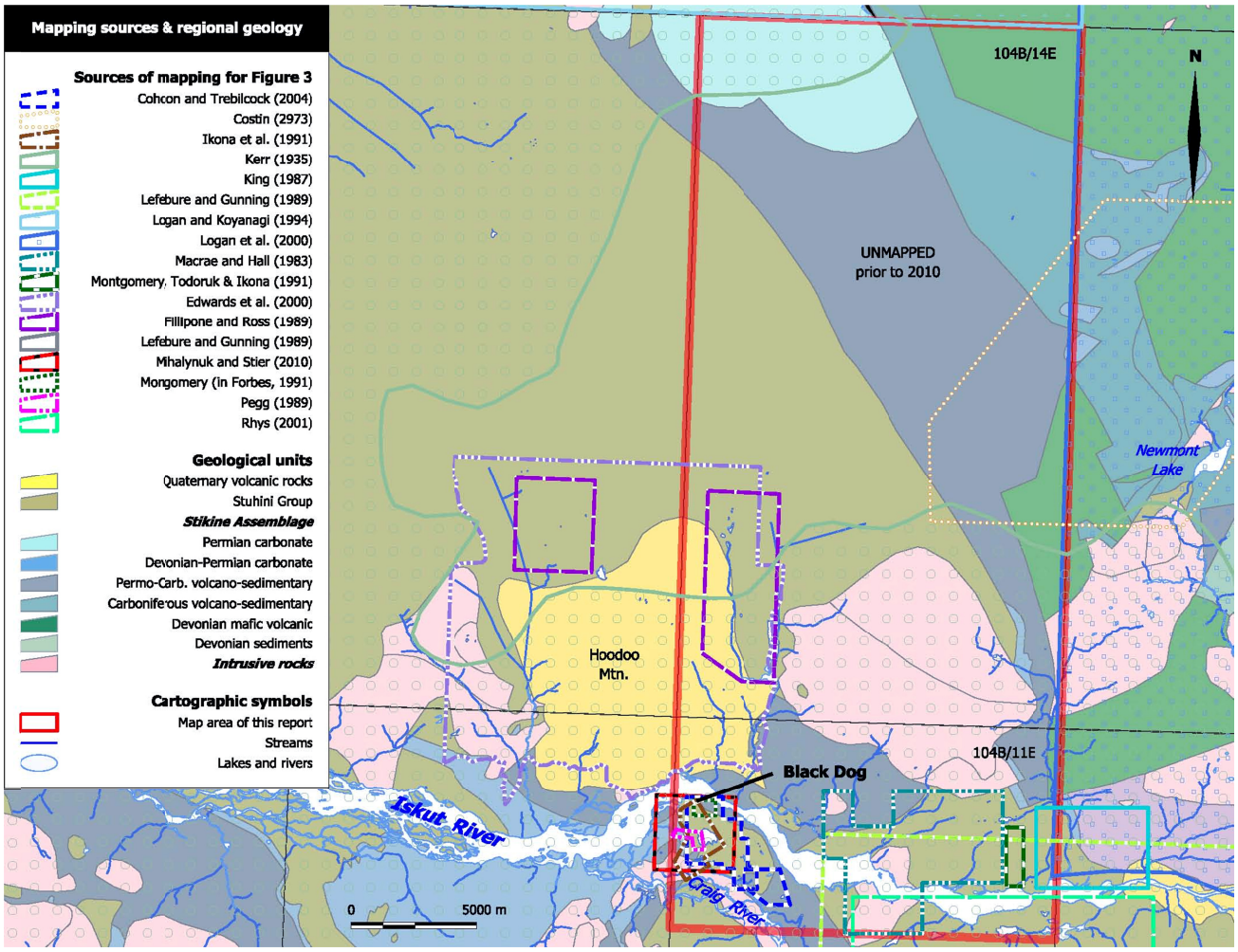

Figure 2. Sources of geological map information within the area between the Craig River and the eastern Hoodoo Mountain map sheet (NTS 104B/14W). Location of the Rock and Roll property (Black Dog surface showing) and important landmarks are also indicated. The regional geology portrayed within the study area (red rectangle) is largely after Kerr (1935) as compiled by (Massey *et al.*, 2005).

Wrangell, Alaska (Figure 1). Both Terrace and Smithers are serviced by scheduled commercial flights from Vancouver and both are approximately 400 km by road (~5 hour drive) from Bob Quinn airstrip. Bronson airstrip is a 60 km flight southwest from Bob Quinn, the nearest airstrip that is serviced by road access. Seasonal charter helicopter service is generally available from Bob Quinn. The nearest permanent charter helicopter base is in Stewart, approximately 110 km to the southeast. In 2010, two seasonal camps adjacent to the airstrip were in operation. Accommodations could be arranged at the Skyline Gold Corp. or the Kossey fishing camp on the Iskut River.

Iskut River occupies a U-shaped glacial valley with alpine glaciers draping many of the adjacent ridges and extending to well below treeline at ~1000 m elevation. Our fieldwork focused on the mountain slopes north of the Iskut River and nunataks of the Andrei Icefield and its distributary glaciers. (Note that herein we refer to the Andrei Icefield as the collective ice mass and high névé/accumulation zone from which the many large valley glaciers of the area emanate. The Andrei Glacier we refer to as the main, >2 km wide, outflow glacier in the northeast corner of 104B/14 (Figure 3) the terminus of which is 10.5 km north-northeast of Newmont Lake in 104B/15; Figure 2). Work in this typically rainy coastal region is commonly curtailed by low cloud and inability to fly; however, mid-August of 2010 was uncharacteristically warm and cloud-free. Our work was also facilitated by the well-appointed Skyline Gold Corp. base camp at Bronson airstrip and helicopter accompaniment of VIH Helicopters Ltd.

REGIONAL GEOLOGY AND PREVIOUS WORK

Most rocks north of the Iskut River within NTS 104B/14E have not been mapped as part of a systematic regional program. Topographical mapping by the International Boundary Commission with additions by Forrest Kerr between 1926 and 1929 (Kerr, 1948; Figure 2) covered the corridor along the Iskut River, but Kerr

Layered Rocks

Quaternary
- Hoodoo volcanic complex

Early Jurassic
- well-bedded green lapilli-ash tuff
- maroon ash tuff/tuffite, also in Late Triassic and Carboniferous
- hornblende-biotite ash flow ~187Ma

Late Triassic
- orange wacke ± biotite/K-feldspar
- well-bedded wacke ± chert clasts
- dacite ash flow ~220 Ma
- polymictic conglomerate
- feldspar pyroxene breccia ±pillowed

Middle-Late Triassic
- rusty graphitic argillite/siltstone

Paleozoic - Triassic
- quartz sandstone
- siltstone ±volcanic / laminated
- chert (also Carboniferous-Permian)
- carbonaceous siltstone
- tuffaceousPhyllite/wacke
- andesite breccia and lesser ash
- mafic volcanic - tuff and minor flow
- sericite schist
- undivided sediment/volcanic
- felsic tuff and minor flows
- ash flow in Carboniferous
- argillite > volcanic sediment/tuff turbiditic, also Carboniferous

Early Permian
- limestone -massive to well-bedded
- marble (± Carboniferous)

Carboniferous
- tuffite with chert/exhalite
- volcanic wacke/conglomerate
- limestone, commonly crinoidal
- basalt -pillowed and breccia

Intrusive Rocks

Eocene
- Early? Eocene granodiorite
- Jurassic-Eocene quartz diorite

Early to Middle Jurassic
- granodiorite, diorite, undivided

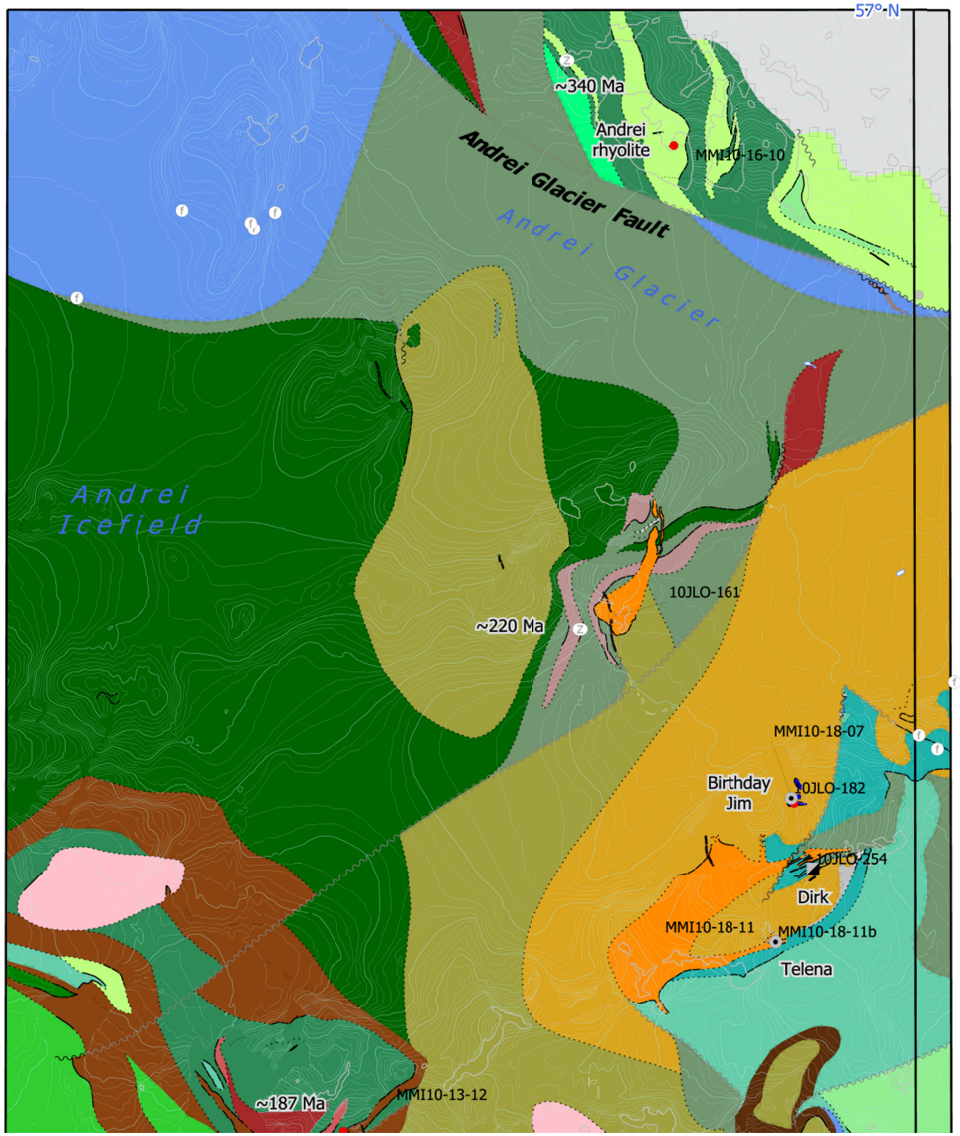

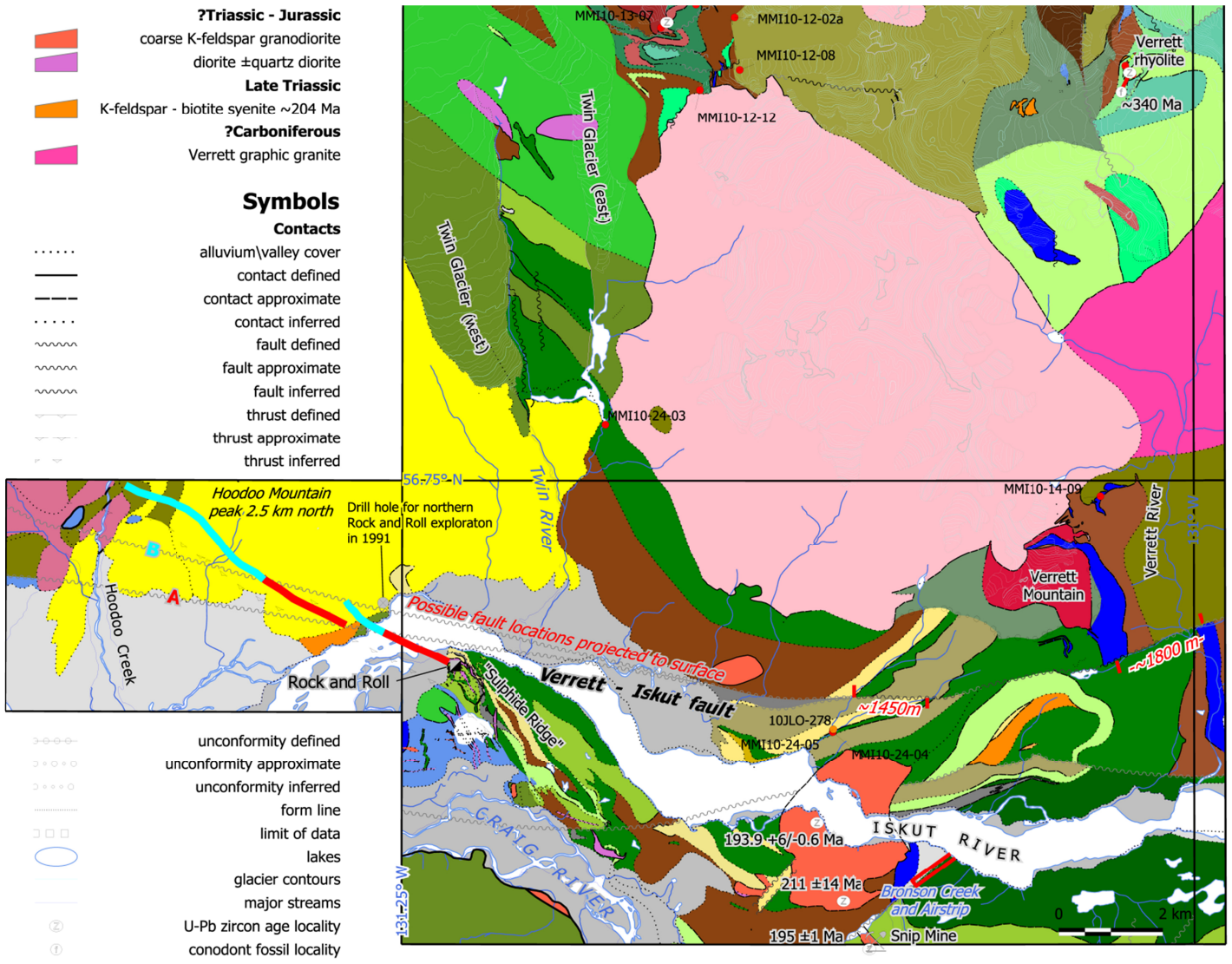

Figure 3. Geology of the Hoodoo Mountain – Iskut River area simplified after Mihalynuk *et al.* (2011a). Shown south of Hoodoo Mountain are possible western extensions of the Verrett-Iskut fault (A, B) and modelled range of sinistral offsets. These could offset the northern Rock and Roll host strata (schematically shown by thick red and blue lines -see text for caveats), and the possible eastern limit of the carbonate belt (projected thrust trace). For sources of data constraining the geology south of Mount Verrett see Mihalynuk *et al.* (2011a).

designated the area farther north as one "Large ice field with a few peaks rising above the ice level". Indeed, in the 1920s much more of the region was covered by ice than is today. A striking example of glacial retreat can be seen at Twin Glacier (Figure 4). When Kerr surveyed and mapped this area, two tongues of ice surrounded a 5 km long nunatak east of Hoodoo Mountain, re-joining and extending about 1 km south of the nunatak as shown on his 1:126 720 scale map. By the time aerial surveys were conducted in the mid 1970s for the National Topographic 1:50 000 scale Mapping program, the glacier had melted back to form two separate tongues with a kilometre of the eastern tongue replaced by a lake. Provincial aerial surveys in the late 1980s produced the base for the 1:20 000 scale Terrain Resource Information Management (TRIM) maps, at which time the lake had grown to 2 km in length, with the ice having melted back an additional 1 km. High resolution satellite imagery captured in October, 2010 show the terminus of the eastern tongue having retreated an additional 1.7 km. Thus, much of Kerr's "Large Ice fields..." terrain is now exposed and never-before-seen rock exposures are everywhere, including new outcrops with significant mineralization.

Subsequent mapping in the area covered the southwest corner of 104B/14E as part of a study of the Holocene Hoodoo Mountain volcanic rocks (Edwards *et al.*, 2000) and a structural study focused in part on the Twin Glacier nunatak (Fillipone and Ross, 1989). Many parts of the Iskut map area (1:250 000 scale, NTS 104B) were mapped as part of Geological Survey of Canada program under the direction of Anderson in 1991 (Anderson, 1993), but persistently inclement weather prevented systematic coverage in the area around the Andrei icefield in 104B/14E (Anderson, personal communication, 2010). Mihalynuk *et al.* (2010) provides an overview of other geological studies in the Iskut region, which is not repeated here.

Existing maps of 104B/14E separate the Mesozoic and older strata into two domains: an eastern domain underlain primarily by Paleozoic Stikine assemblage (Monger, 1977) and a western domain underlain by volcanic and derived sedimentary rocks of the Stuhini Group (Souther, 1971). Our work in 104B/14E extends the geological relationships most recently outlined by Logan *et al.* (2000) in the adjoining map sheets to the east and north. Preliminary interpretation of the geological data collected in 2010 indicates that the Late Triassic

Figure 4. A view to the south of the eastern lobe of the Twin Glacier showing drastic retreat since *ca.* 1920. The ridge on the west side of the photo formed an isolated nunatak in the 1920s. This photo was taken at the end of a heat wave in August of 2010.

Stuhini Group arc and basinal strata form a belt that broadens westward where it is overlain by Early Jurassic volcanic strata (Figure 3). Stuhini Group unconformably overlies a composite basement of deformed, Carboniferous (to Devonian (?)) and Late Paleozoic volcanic arc and carbonate bank deposits of the Stikine assemblage (Brown *et al.*, 1991).

East-directed thrust faults interleave and duplicate Paleozoic and Mesozoic strata. High angle faults dissect the thrust faulted terrain and have subsequently been cut by intrusions that are Mesozoic to Eocene in age. Two main periods of mineralization are recognized: Carboniferous, volcanogenic massive sulphide-style and probable Late Triassic age (Bernales *et al.*, 2008) intrusion-related vein, skarn and disseminated mineralization. Details of the stratigraphy, structural disruption, intrusion and mineralization follow.

STRATIGRAPHY

Stratigraphic assignments rely on the work in adjacent areas, particularly the work of Logan *et al.* (2000), which builds upon extensive fossil collections and isotopic age data. Three well dated and easily recognizable stratigraphic intervals form the framework for stratigraphic correlations within the Hoodoo Mountain area. Two of these intervals, Carboniferous and Permian, contain distinctive thick carbonate units. Carboniferous carbonate is characterized by abundant large crinoid columnals (Figure 5). Permian carbonate is recognized by the presence of large Rugosan horn corals (Figure 6a), and locally, by accumulations of giant foraminifera (Figure 6b). A third interval, dominated by brown and orange weathering, coarse biotite and K-feldspar-phyric tuff and volcanogenic conglomerate, is believed to be of Late Triassic age (see below). Other conglomerate units are less diagnostic and likely range from Devonian to Jurassic in age.

Figure 5. Packstone dominated by crinoid columns in the eastern Hoodoo Mountain area. Large crinoid columns are characteristic of the Carboniferous limestone strata.

Figure 6a. Characteristic Permian fossils within the Hoodoo Mountain area; Rugosan horn corals.

Figure 6b. Characteristic Permian fossils within the Hoodoo Mountain area; giant fusulinaceans (2 cm long) in a packstone.

Devonian

Lower to Middle Devonian strata are recognized in the Forrest Kerr area as "...penetratively deformed, intermediate to mafic metavolcanic tuff, flows, diorite and gabbro, recrystallized limestone, graphitic schist and quartz sericite schist..." (page 12, Logan *et al.*, 2000). Devonian rocks have not been positively identified within the eastern Hoodoo Mountain area; however, isolated outcrops of marble and mafic meta-igneous rocks immediately west of the Bronson airstrip may belong to this old rock package. In addition, an undated sequence of mafic to intermediate volcaniclastic rocks, tuff, graphitic phyllite, slate and limestone intruded by metagabbro

plugs and basic dikes underlie the Twin Glacier nunatak. The lithological associations, poly-phase deformation and metamorphism resemble those of Devonian strata elsewhere (Logan *et al.*, 2000). However, the lack of concrete age control for these rocks does not preclude the originally suggested Triassic age (Kerr, 1948).

Carboniferous

Strata of Carboniferous age are extensively exposed in the eastern Hoodoo Mountain area. They include bimodal mafic and felsic volcanic rocks and intervals of well-bedded carbonate, chert and wacke. Similar volcanic rocks in the Forrest Kerr area display primitive arc characteristics (Logan *et al.*, 2000) and are associated with VHMS Zn-Pb-Cu ±Ag-Au mineralization (Logan, 2004). Carbonate and other sediment-dominated strata overlie the Carboniferous volcanic sequence.

Mafic volcanic rocks

Carboniferous mafic volcanic rocks are typically bright green, aphyric to finely plagioclase-phyric pillow basalt and breccia. Calcite amygdaloidal pillows tend to be less than 0.5 m in long dimension and are commonly rimmed by bright red jasper, and/or occur with interpillow jasper (Figure 7). This unit is well exposed 7 km west-northwest of Newmont Lake where it is overlain by rubbly carbonate matrix to flow-top breccia fragments contains abundant large crinoids ossicles (Figure 5) and grades into thick-bedded carbonate containing basalt scoria. The carbonate locally forms crinoidal packstone.

The lower contact of the mafic volcanic unit is poorly defined. In northeast part of the area, the mafic volcanic rocks overly polymictic conglomerate and are intercalated with Viséan felsic volcanic rocks.

Felsic volcanic rocks

Carboniferous felsic volcanic rocks comprise white, pink and pale green weathering and aphyric to quartz-phyric tuff and rhyolitic to dacitic locally flow-banded effusive units. The upper part of the section is characterized by well bedded, decimetre-thick, normal-graded felsic ash flow tuff beds which may be underlain by coarse basal breccia (5-10 m) thick, and may grade upwards into thin cherty dust tuffs beds (Figure 8a).These units define separate eruptive cycles that preserve 2-300 m of felsic ejecta interbedded with the pillowed and hyaloclastite basalt (Figures 8b, c), particularly well-

Figure 7. Irregular flow top on Carboniferous pillow basalt is in-filled with carbonate containing abundant large fossil crinoids stems (*i.e.* few centimetres above fingers). Pillows are outlined, and in some cases veined, by red jasper. Flow-top breccias grades into well-bedded carbonate containing basalt scoria.

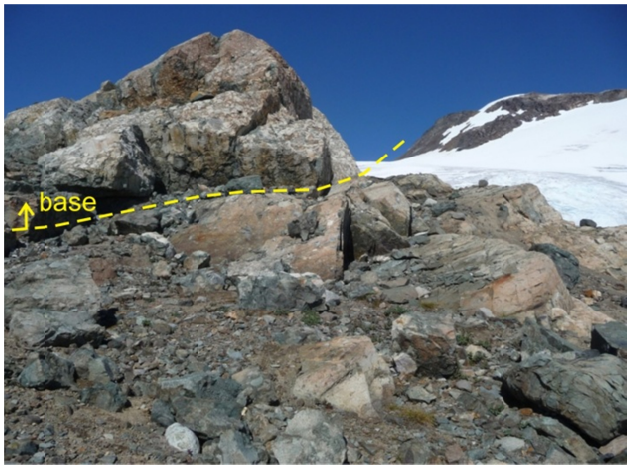

Figure 8a. Early Carboniferous felsic ash flow and block breccia. Contact line highlights the top of one eruptive unit and coarse base of the next.

Figure 8b. Early Carboniferous pillow breccia with hyaloclastite matrix.

Figure 8c. Early Carboniferous basaltic pillows and tubes.

displayed in the north and eastern portions of the map area. Pink weathering, quartz-phyric rhyolite dikes that commonly cut the section may be related to felsic volcanic rocks. Bedding tops suggest an upright facing volcanic section which projects beneath mid-Carboniferous (?) carbonate that is distinguished by the presence of large (>3.5 cm) crinoids ossicles. A preliminary isotopic age determination of ~340 Ma from a felsic tuff unit near the top of the succession confirms the Early Carboniferous (Viséan) age (N. Joyce, unpublished data).

Mid-Carboniferous carbonate

An approximately 190 m thick section of carbonate is dominated by thinly-bedded sets to massive metre-thick beds of crinoidal limestone (Figure 9a) with ossicles up to 4 cm diameter (Figure 5). Colonial coral heads more than a metre across are preserved. Bright green basalt clasts (Figure 9b), angular lapilli and reworked ash are of variable abundance, up to a maximum of ~15%. Volcanic content is sporadic, but generally decreases up section with pyroclastic debris all but absent more than ~40 m above the base of the unit. Planar chert beds are interlayered with crinoidal grainstone near the upper contact of the unit.

Coarse crinoidal packstone extends to the east where it has been extensively sampled for fossil age determination (Logan *et al.*, 2000). Faunas providing the most precise age control reveal a Serpukovian to Bashkirian age (~328-312 Ma), spanning the Lower Carboniferous (Mississippian) and Upper Carboniferous (Pennsylvanian) boundary.

Carboniferous chert-claystone

Parallel interbeds of grey to black chert and recessive light grey and yellow-weathering claystone form a distinctive unit above the Carboniferous carbonate. Chert beds 5 to 15 cm thick alternate (Figure 10) with recessive, poorly indurated claystone layers that are typically less than 5 cm thick. Rounded cloudy quartz grains ≤ 1 mm

Figure 9a. View to the north of a set of thin tuffaceous packstone beds flanked by more massive beds, each 1-1.5 m thick.

Figure 9b. Thickly bedded conglomeratic crinoidal packstone with scoraceous basalt clasts.

Figure 10. Very well bedded chert-siltstone-claystone unit contains distinctive grey and yellow weathering, recessive clay beds.

diameter within chert are interpreted as recrystallized radiolaria; although some white grains appear to have a cleavage and are likely reworked feldspar. Thus, the unit may be a distal turbidite and not strictly a biogenic pelagic ribbon chert succession.

Only a few exposures of this unit have been observed. It presumably grades into the underlying chert-bearing portions of Carboniferous carbonate, but a section that has not been structurally disrupted was not identified during the course of our mapping. Stratigraphic contacts with units of assumed Permian age are similarly disrupted or not exposed. Where best exposed, the unit is strongly deformed such that all that can be stated of the unit thickness is that it is more than ~10 m and probably less than 100 m.

Late Carboniferous (?)

Thickness of Upper Carboniferous mafic and felsic volcanic stratigraphy have been estimated as >1500 m north of the Scud River (Brown *et al.*, 1991; see their Figures 2-4) and in the Mess Creek area (Logan *et al.*, 2000) and are anticipated to crop out in the study area.

Varicoloured wacke, polylithic volcanic conglomerate and fine grained turbiditic sediments at least 900 m thick that underlie the northeast corner of the Hoodoo Mountain area might belong to this unit. However, we interpret them as belonging to the Late Triassic succession (see following). Arguments for an Upper Carboniferous assignment can be made along strike to the north and we cannot unequivocally rule out such arguments. For example: these rocks occupy a structural, as well as upright facing position above mid-Carboniferous limestone and further northwest, apparently dip beneath Early Permian limestone as shown by Logan and Koyanagi (1994). The maroon to dark green conglomerate locally contains limestone cobble-rich layers and large (10 m^2) olistoliths of Carboniferous limestone. Along strike to the north, the unit grades upward into maroon plagioclase phyric tuff which appears to conformably underlie limestone containing Late Carboniferous or Early Permian, Moscovian or younger corals and late Asselian to Sakmarian fusulinacean foraminifers, suggesting a conformable volcaniclastic sequence of probable Upper Carboniferous age.

Similar contact and faunal relationships have not been corroborated in the present study area where the varicoloured volcaniclastic section is interpreted to represent Upper Triassic deposition and cannibalism of older arc strata. Limestone granule conglomerate was collected for extraction of conodonts. If present, they will provide a maximum age for this unit.

Permian

Permian sections are comprised of massive to well-bedded carbonate and lesser chert. In most sections there is little or no evidence of volcanic debris. Although they are very diverse in detail, three mappable Permian units are separated herein: massive light grey carbonate, dark grey chert-carbonate, well bedded grey and cream carbonate. All of these units are correlative with the Permian Ambition Formation ~50 km to the north (Gunning *et al.*, 1994), where its thickness ranges between 500 and ~1100 m.

Well bedded grey and cream carbonate

Medium grey to cream-coloured carbonate is typically well bedded and fossiliferous. Large rugose corals, fenestrate and branching bryozoa, brachiopods, gastropods and giant fusulinaceans are common. Fossil debris may dominate some layers (Figure 6 and Figure 11) forming packstones. An Early to Middle Permian age is proposed for this unit on the basis of fossil age determinations from units along strike (Logan and Koyanagi, 1994; Brown *et al.*, 1996), where they range from Latest Carboniferous (Gzhelian) through Early Permian to Middle Permian (Roadian and Wordian). This is supported by the occurrence of giant fusulinaceans which are typically of Rhodian to Wordian age. (Brown *et al.,* 1996 and Logan *et al.,* 2000 used the Harland *et al.,* 1990 time scale which lacked a Middle Permian. As a consequence, they considered Roadian to be an Early Permian stage; both Roadian and Wordian stages are now included in the Middle Permian (Okulitch, 1999; Ogg *et al.*, 2008)).

Figure 11. Bryozoan packstone within Early to Middle Permian section. Silicified branching and fenestrate bryozoan fossils form layers up to 30 cm thick.

Dark grey chert and carbonate

Irregularly bedded dark grey chert and carbonate tends to be relatively impoverished in macrofossils. Bulbous to hackly, chert layers and nodules up to 30 cm thick are crudely stratiform and are generally less than half the thickness of adjacent micritic carbonate layers, which may be fetid. Chert is presumably secondary as sponge spicules that could provide a source of silica could not be identified in outcrop. This unit appears to be in abrupt contact with overlying massive carbonate.

Massive light grey carbonate

Medium to coarse crinoidal grainstone commonly forms massive, light grey outcrops that lack any obvious bedding. Most outcrops contain at least sparse horn coral fragments and they may be abundant is some layers, typically best preserved where replaced by silica. Fossil horn corals may exceed 10 cm diameter and 30 cm in length. Unlike Carboniferous carbonate, crinoid ossicles are generally less than 0.5 cm diameter (not several centimetres). In two localities near the eastern edge of the map area, this unit is overlain by strata interpreted as Middle to Late Triassic age.

Early to Middle Triassic

Strata interpreted to be of Early to Middle Triassic age comprise a condensed section of graphitic cherty argillite with thin, fetid limestone and wacke layers. This sediment-starved package displays a fault-modified contact with underlying massive Permian carbonate, elsewhere it may be entirely removed by subsequent Late Triassic erosion.

Triassic cherty argillite

Black and rust, well bedded volcanic chert and sooty argillite comprises a section that is rarely exposed, and has not been observed undeformed. The deformed section is estimated to have a true thickness of less than ~40 m (Figure 12). It is composed of 3-6 cm thick cherty volcanic layers with generally thinner sooty argillite interbeds. Cherty layers are comprised of a significant proportion (up to ~10%) of silt and sand-sized lithic grains that could be water lain tuff, although an immature volcanic silt/sand source cannot be ruled out.

Laminated carbonate

Light grey to black, poorly indurated marl occurs as well laminated layers up to 20 cm thick within the chert-argillite-dominated section. At one locality, at least two of the marl layers are packstones of paper-thin bivalves tentatively identified as *Daonella* or *Halobia* of Middle to Late Triassic age. Subequal hinge-parallel and -normal dimensions favour the latter identification. Unfortunately bedding-perpendicular cleavage typically results in slabby weathering and incomplete fossil preservation.

Late Triassic

Late Triassic strata are dominated by volcaniclastic units, particularly polymictic boulder conglomerate. Distinctive coarse biotite- and K-feldspar-bearing conglomerate occurs together with hypabyssal rocks from which they were derived. Augite-phyric flows, a hallmark of the Stuhini Group, are present, but are less abundant than clastic rocks. The conglomerate is variable, green, purple or maroon; dominantly matrix-supported in a poorly sorted chaotic groundmass of plagioclase and pyroxene crystal and lithic sand-sized grains. Horizons are often characterized by clasts of sedimentary units, particularly recrystallized and/or fossiliferous limestone. An interval of dacite ash-flow occurs near the top of the clastic section yields a preliminary U-Pb zircon age of ~220 Ma.

Turbiditic arkosic sediments

Well bedded turbiditic sediments are comprised mainly of graded volcanic sandstone- argillite couplets, but also include conglomerate. Blocky, cliff-forming outcrops of this unit weather olive brown. Graded turbidite couplets are typically 1 to 15 cm thick (Figure 13a). Basal scours and local development of ripple cross-stratification near bedding tops are features consistent with deposition from turbidity currents. Conglomerate beds contain subangular to rounded cobbles to small boulders of medium grained augite-porphyry (25% pyroxene and 20-25% fine to medium-grained plagioclase) and angular intraformational rip-up clasts (Figure 13b).

This unit rests unconformably on basinal strata of presumed Middle Triassic age. Olistostromal blocks metres across have been derived from the underlying chert and sooty argillite.

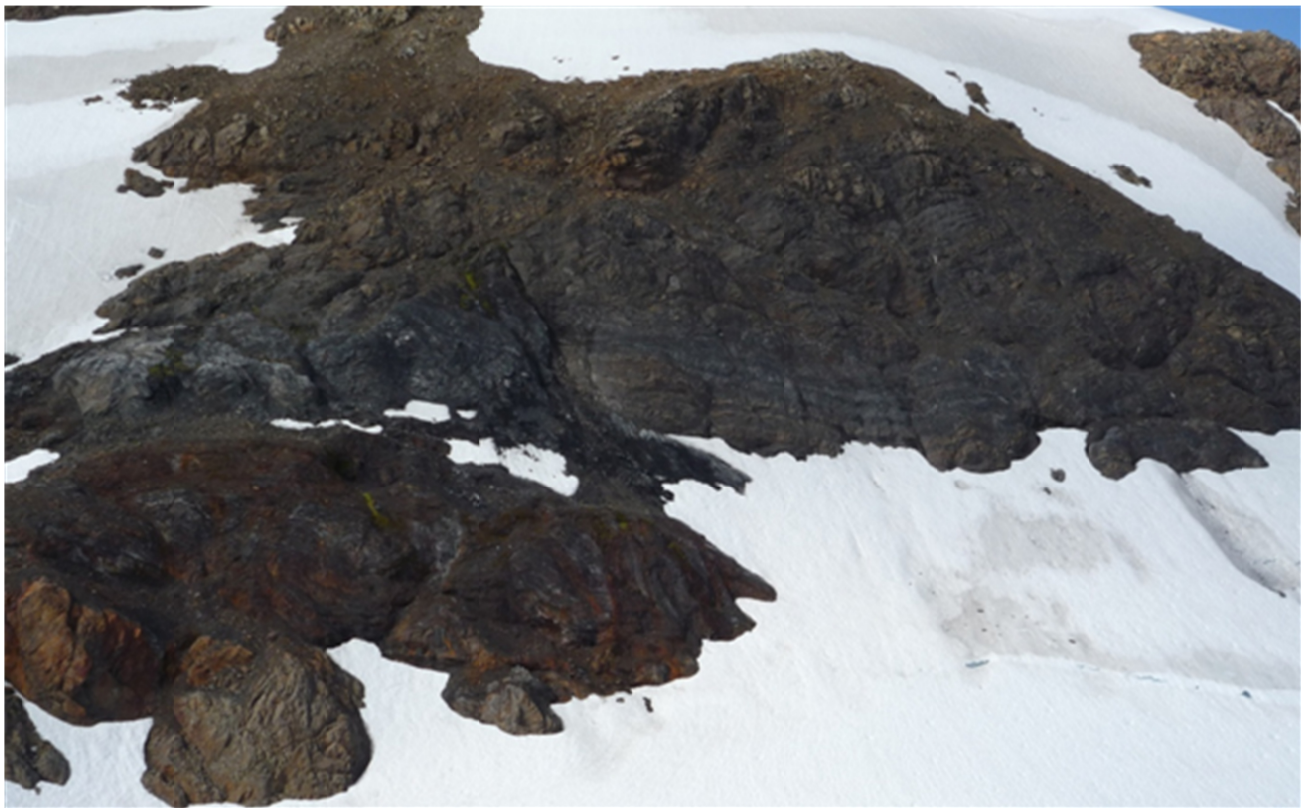

Figure 12. View to the north of rusty black chert, argillite and grey carbonate of interpreted Early to Late Triassic (?) age (fossil age determinations are pending). Blocky olive-brown rocks in the upper third of the section are conglomeratic volcanic wacke of presumed Late Triassic age. To the immediate east, the unit is underlain by massive grey limestone of presumed Permian age.

Figure 13a. Typical Late Triassic turbiditic sandstone-argillite couplets.

Figure 13b. Angular to rounded augite porphyry boulders and angular intraformational rip-up clasts.

Augite-phyric volcanic and epiclastic rocks

An apparently continuous section more than ~340m thick of coarse, crowded augite-phyric flows and breccia is exposed on nunataks north of Twin Glacier. Rocks of similar character extend to the west, outside of the mapped area, and could represent a section more than 1000 m thick. This unit is light olive green to brown and is blocky weathering. Conspicuous, euhedral, often zoned pyroxene comprises 15-30% of flows and breccia. Pillows are locally well developed with light grey and siliceous intrapillow laminated sediment. Vesicles commonly comprise a few per cent by volume and are infilled with calcite and sparse chalcedony. Well bedded maroon tuff layers up to several metres thick are interlayered with the flows.

Feldspar-phyric breccia and epiclastic rocks

Green to grey weathering, feldspar-phyric breccia and associated epiclastic rocks are extensively exposed in two areas: Upper Twin Glacier in east-central 104B/14E, and on south and east flanks of Verrett Mountain. Angular, coarse breccia, without significant epiclastic components, is particularly well displayed in the upper Twin Glacier area where it is associated with pillowed, augite- porphyritic basalt. Typical lithologies contain medium grained, tabular feldspar that may display trachytic alignment and comprise 5-35% of the rock. However, grain size ranges from fine to coarse and pyroxene commonly accompanies feldspar. Quartz, carbonate and chlorite-filled vesicles can comprise up to 5%, or rarely 15%, of the unit. Chlorite, carbonate and epidote alteration and veining is common. Clasts, which could have been derived from this or similar units, comprise the dominant clast type within the dark brown and orange-weathering conglomerate and parts of the polymictic conglomerate unit.

Polymictic boulder conglomerate

The most widespread unit of the Stuhini Group in 104B/14E is a conspicuous polymictic boulder conglomerate. It crops out in a northwest-trending belt across the northern half of the map area where it probably attains a thickness of at least 2000 m. It is maroon to brown weathering and forms rounded outcrops and cliffs in which boulders of contrasting lithology are beautifully highlighted. Conglomerates belonging to this unit may be clast-supported, but are more commonly supported by a matrix of maroon ash tuffite or tuffaceous wacke. In order of decreasing relative abundance, common clast types include: medium to fine grained tabular feldspar-phyric volcanic tuff, coarse to medium grained augite and augite-feldspar porphyry, fine grained to aphanitic green to brown basalt, grey to white limestone (commonly fossiliferous and of presumed Paleozoic age), hornblende quartz diorite, recycled conglomerate, coarsely bladed plagioclase ±K-feldspar porphyry, turbiditic wacke, pink medium- to coarse grained holocrystalline granodiorite, and in upper parts of the unit, dacite and picrite. The latter two clast types are recognized above a layer of ~220 Ma dacite tuff (Figure 14a).

Maroon tuff

Maroon to green water-lain tuff forms sections up to 200 m thick in the northeastern map area (along strike with Carboniferous strata PnSt, uCScg and uCSt on Logan and Koyanagi map) where it grades upwards into well indurated, coarse volcanic sandstone and then turbidites and carbonate-rich conglomerate with gastropods, crinoids and bivalves. Well bedded maroon, aphanitic to fine grained, lapilli and ash tuff to plagioclase tuffites occur close to the top of the section and these locally contain accretionary lapilli horizons. Planar, well-developed beds are typical.

Lithologies typical of this unit also occur as distinctive layers within several other units such as augite porphyry flows, turbidite and polymictic conglomerate within both Paleozoic and Mesozoic sections (see especially “Late Carboniferous (?)” above).

Dacitic ash flow

Crowded tabular feldspar and quartz-phyric dacite ash tuff comprise two layers near the top of the polymictic boulder conglomerate unit (Figure 14a). The thickest, upper layer attains a thicknesses of between ~80 m and ~130 m. It is a maroon and pinkish to grey and blocky weathering, resistant unit. Medium grained tabular plagioclase and lesser, coarser K-feldspar together comprise 35-40% of the unit with quartz eyes up to 0.5 cm diameter (Figure 14b) comprising ~5%, with lesser altered biotite (~3%) and sparse titanite. Some crystal-rich, flattened fragments may have been pumiceous and compacted during partial welding in an ash flow. Flow banding is conspicuous in some fragments. The uppermost 1-3 m of the unit is a tan weathering and slightly recessive probable airfall and reworked lithic lapilli crystal ash tuff. A preliminary isotopic age determination from a sample of this unit has returned a Late Triassic, ~220 Ma age (N. Joyce, unpublished).

K-feldspar megacrystic tuff, breccia and hypabyssal rocks

Texturally diverse tuffaceous, fragmental and hypabyssal rocks containing fragments of syenite and K-feldspar megacrysts are intermittently exposed over a broad region within east-central 104B/14E. This unit is characterized by abundant detrital biotite, comprising up to 25% of the rock.

Locally, the K-feldspar porphyritic and biotite rich fragmental rocks clearly exist as clastic dikes. Where such dikes cut contemporaneous strata, the distinction between intrusive, extrusive and immature epiclastic modes of occurrence is less obvious (Figure 15a). Hypabyssal units locally display delicate glomeroporphyritic K-feldspar "flowers" which are unlikely to have been preserved in an ash cloud or sedimentary environment. Some bombs of trachytic, crowded K-feldspar porphyry display a mantle of vesicular glass (*i.e.* chilled; Figure 15b). This same crowded K-feldspar porphyry comprises one of the several slight variants of K-feldspar megacrystic dikes in west-trending swarms, some of which display porphyry-style copper mineralization (see later section: "Intrusive Rocks").

Late Triassic to Early Jurassic

Dark brown and orange-weathering conglomerate, wacke and coal

Dark brown conglomerate is dominated by well-rounded, finely tabular feldspar-phyric clasts and conspicuous pink-orange syenite and coarse K-feldspar crystals derived from the unit described previously. In most places the unit is carbonate-altered and weathers orange. Clasts are typically supported by a distinctive matrix of immature sandstone containing as much as 5% detrital biotite up to 1.5 cm diameter. Locally the conglomerate passes laterally or vertically into well-bedded wacke (Figure 16a) and in places is tuffaceous

Figure 14a. Polymictic conglomerate (above ice axe) overlies light pink lithic lapilli crystal ash tuff (marking top of ash flow cooling unit). An unconformable contact is marked by a layer of tan weathering reworked tuff (at base of ice axe).

Figure 14b. Close-up of quartz-phyric dacite ash tuff.

with pink lapilli that include megacrystic K-feldspar crystals. Wacke layers commonly contain coaly plant fragments. One distinctive fossilized plant includes an

Figure 15a. Angular pink syenite fragments as well as K-feldspar crystals float within an orange-weathering matrix. Silvery glints are altered biotite crystals. Multiple generations of erosion or brecciation and milling have produced clasts of clastic material. Planar, dike-like bodies of the same clastic material (top and right side) appear to have cut the rock body.

Figure 15b. Boulder sized, trachytic, crowded K-feldspar porphyry clast, perhaps a bomb (?), is mantled by glassy vesicular material.

artichoke-like cone/flower with nested woody scales/petals, perhaps *Williamsonia,* a cycad common in the Jurassic (Figure 16b; extraction and identification of fossil pollen from a collected sample is pending).

Figure 16a. Orange-weathering conglomerate interbedded with graded arkosic sand and siltstone.

Figure 16b. Within coal-rich parts of the unit, wood fragments are common (bottom edge of photo) as are scales of an artichoke-like fossil (arrows).

Hornblende-feldspar ash flow and breccia

Resistant, blocky to rounded weathering, hornblende ±biotite dacite ash flow forms a distinctive unit about 100m thick. It is medium grained and light grey to light maroon or green where chlorite- and epidote-altered. Partly welded ash flow and flow top breccia textures are well displayed. Acicular, euhedral oxyhornblende comprise 5-10% of the unit and tabular feldspar commonly comprises 35-40% (Figure 17). Ash flow is in sharp contact with deep maroon ash tuff which may have been part of the same eruptive event. Brecciated zones may have a carbonate matrix and eruptive units are interbedded with limestone matrix-supported conglomerate beds typically less than a metre thick.

Preliminary age determination on a sample of hornblende-plagioclase ash flow breccia yielded a ~187 Ma age (N. Joyce, unpublished data) confirming Early Jurassic magmatism in the Hoodoo Mountain area. Britton *et al.* (1990) note that these Dacitic rocks are texturally similar to the "Premier Porphyry" unit that marks the top of the Unuk River Formation and base of the Betty Creek Formation. Representative isotopic age

Figure 17. Chlorite-altered hornblende ±biotite and feldspar crystal ash flow tuff.

determinations from the Betty Creek Formation are: 187.7 $^{+5.8}_{-1.5}$ Ma and 187.7 $^{+5.3}_{-4.4}$ Ma (U-Pb, abraided zircons; Lewis, 2001).

Hoodoo tuff

The youngest volcanic rocks identified within the eastern Hoodoo Mountain area are flows, un-lithified soil and wind-sorted scoria of the *ca.* 28 to 1800 Ka Hoodoo Mountain volcanic complex (Figure 18; Edwards *et al.*, 2000). Flows which have emanated from the extinct Hoodoo Mountain volcano are exceptionally well exposed near the toe of western Twin Glacier where they unconformably overly polydeformed rocks. Tan to brown aphanitic and scoriaceous lapilli and ash occupy hollows in the high ridges in the western part of the area and form relicts of a presumably once continuous blanket where it has not been removed by rain, wind or ice. Mapping the lower elevation extent of these relicts could provide limits for glacier extents at the time of eruption; however, our work did not include such mapping, as we have focused on rock packages of importance for mineral exploration.

Figure 18. Lapilli sized, pumiceous scoria, probably originating from the extinct Hoodoo Mountain volcano. These deposits and derived soils cap many of the ridges in western 104B/14E and restrict glacial ice extents at the time of eruption to an elevation of less than ~1240 m (less than 240 m above its current level).

Preliminary $^{40}Ar/^{39}Ar$ age determinations from volcanic samples collected at Hoodoo Mountain are reported by Edwards *et al.* (2000) as ranging from 28 to 1800 Ka (no error limits on personal communication from M. Villeneuve, 1998).

INTRUSIVE ROCKS

Three main intrusive units and several suites of dikes cut stratigraphy within the Hoodoo Mountain area. Of these, deformed granite exposed in the upper Verrett River valley and an undeformed pluton extending from the Verrett River to Twin River, are by far the most voluminous (Figure 3).

Verrett pluton - graphic granite

Graphic granite is exposed in the upper Verrett River valley. We follow the nomenclature of Logan *et al.* (2000) who called it the Verrett Pluton. Within the eastern Hoodoo Mountain map area, the Verrett pluton is white to tan and rust weathering, forming blocky to low, rounded outcrops. It is composed mainly of subequal amounts of intergrown quartz and K-feldspar (Figure 19). Feldspar is turbid due to alteration to white mica and carbonate. Anhedral pyrite grains locally comprise up to 3% of the rock. In places the body appears clastic, due to structural cataclasis. Contacts with adjacent units are both faulted and intrusive. Its northern contact crosscuts ?Carboniferous volcanic and sedimentary bedding at high angle and locally displays a narrow chilled margin adjacent to country rock. Verrett pluton was tentatively correlated with the Late Devonian Forrest Kerr plutonic suite (Logan *et al.*, 2000). It is undated, but if it intrudes Carboniferous volcanic rocks, as it appears to in the Hoodoo map area (Figure 3), it cannot be Devonian in age. If these contact relations are correctly interpreted, the Verrett Pluton must be at least as young as Carboniferous. An isotopic age determination from a sample of this unit is pending.

Figure 19. Verrett pluton graphic granite of interpreted Devonian age. Note clastic texture along left margin in this cross polarized light 4 mm field of view.

Biotite-rich diatreme

Dark grey-brown weathering dike-like bodies of clast- ±xenocryst-rich biotite syenite (Figures 20a, b, c) cut across Mesozoic and Paleozoic strata within central and eastern 104B/14E. Where weathered, rounded clasts may be plucked from rubbly debris, but fresh outcrops are blocky, highly compact, and difficult to break. Phenocrysts include: biotite ~25%, diopsidic (?) pyroxene 5%, K-feldspar 5% with minor aegirine and accessory apatite and opaque grains. Matrix mineralogy is 40% K-feldspar (±feldspathoids (?)) and up to 20% carbonate occurring as patches. Biotite occurs as three distinct modes: oldest are coarse grained dark brown to black pleochroic crystals altered by carbonate and having expanded basal plates with abundant opaque inclusions, second are medium grained, golden to green-tan pleochroic elongate and ragged crystals that are commonly kinked or warped, youngest are fine- to medium grained, zoned, dark brown to dark green pleochroic crystals that commonly occur as clusters of euhedral booklets. Pyroxene is bright green and occurs glomerocrysts, euhedral crystals and crystal fragments. Outsized, bright green pyroxene crystals are interpreted as chrome diopside xenocrysts; although no evidence of crystal disequilibrium is seen in thin section. Positive identification awaits microanalytical investigation. K-feldspar phenocrysts range up to 1.5 cm and may form Carlsbad twins or glomerocrysts. Xenoliths are dominantly pink syenite and may be highly spherical indicating significant milling during diatreme emplacement.

Figure 20a. Dense and compact biotite syenite containing a large xenocryst of bright green pyroxene, probably chrome diopside.

Figure 20b. Where weathered, milled clasts fall from the intrusive matrix.

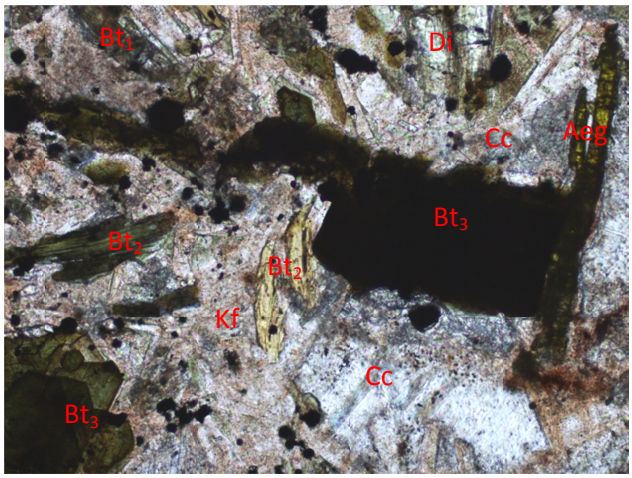

Figure 20c. Photomicrograph showing multiple generations of biotite ($Bt_{1, 2, 3}$), a matrix of K-feldspar (Kf) and carbonate (Cc), a phenocryst of aegirine (Aeg), and a xenocryst (?) fragment of diopside (Di). Plane polarized light view of ~2 mm field of view of sample MMI10-18-9.

Biotite-rich diatreme dikes are commonly spatially associated with K-feldspar megacrystic dikes or breccia dikes. These dikes probably occupied vents feeding pyroclastic eruptions as evidenced by the extrusive tuffaceous equivalents found in the K-feldspar megacrystic tuff and related rocks.

Mesozoic to Tertiary varitextured melano-granodiorite

Light to dark grey, blocky weathering hornblende melano-granodiorite forms an irregularly-shaped body that extends north from the southeast flank of Mount Verrett. Hornblende and plagioclase are randomly intergrown forming fine grained to pegmatitic zones or alternating hornblende and quartz-feldspar-rich layers (Figures 21a, b). Feldspar may be altered to white mica, and both hornblende and subordinate biotite are chlorite-altered. Fine miarolitic cavities may be lined with feldspar and quartz and infilled with chlorite. Secondary calcite commonly occurs near the margins of accessory titanite.

No age has been determined for the varitextured melano-granodiorite; however, it conforms to the eastern margin of the Twin River pluton and may be an earlier phase of the pluton which has been intruded by more leucocratic granodiorite. Previous maps show the Twin River pluton as Eocene in age. Youngest rocks cut by the melano-granodiorite are interpreted to be of Late Triassic age. A persistent set of several metre thick dikes is lithologically similar and cuts strata that may be as young as Early Jurassic.

Figure 21a. Textural variability in hornblende granodiorite: pegmatitic zone with intergrowths of K-feldspar plagioclase and hornblende within texturally diverse melano-granodiorite.

Figure 21b. Textural variability in hornblende granodiorite: compositional banding and including pegmatitic zones.

Eocene Twin River granodiorite

Light grey to white weathering, blocky, hornblende-biotite granodiorite forms a 50 km^2, northwest-elongated pluton; the largest in the map area. Herein called the Twin River pluton, it extends from Mount Verrett to Twin River. A compositionally similar, satellite stock is exposed 15 km farther to the northwest.

The most abundant phase is a medium grained, salt and pepper granodiorite that contains black and vitreous hornblende (5-10%, some with biotite in cores) and sub-euhedral biotite booklets (10-15%). Plagioclase is oscillatory reverse zoned with an average anorthite content of ~An_{27-30}. Composition of the body tends to be uniform with the exception of contorted hornblende-rich screens and contact zones, especially with melano-granodiorite, which may be xenoliths-rich (Figure 21c). Thermal metamorphism attributed to the Twin River pluton extends for several hundred metres from its mapped contacts. Schistose rocks south of the pluton are mineralized with chalcopyrite and possibly traces of native gold.

Figure 21c. Textural variability in hornblende granodiorite: contact zone with Twin River granodiorite (light matrix) is rich in xenoliths of hornblende granodiorite.

ECONOMIC GEOLOGY

Previous Exploration

Mineral claims were first recorded for the Iskut River area in the early 1900s followed shortly thereafter by a one ton shipment of Johnny Mountain ore that yielded 2.05 grams gold, 1.37 kilograms silver and 12.45% copper (Clothier, 1918). Subsequent exploration work focussing primarily south of the Iskut River began with discoveries of high grade auriferous massive sulphide mineralized float in 1954 by Hudson Bay Mining & Smelting Ltd. (Pickaxe). In 1969, R. Gifford restaked and vended the Inel property to Skyline Exploration Limited (Gifford, 1980) who explored and developed the Inel and Reg/Stonehouse properties. From 1988-90 and 1993, the Johnny Mountain Mine produced 4.34 million grams of silver, 2.81 million grams of gold and 1 008 000 kilograms of copper from steep dilatational quartz-pyrite veins at the Stonehouse deposit from 225 247 tonnes milled before shutting down due to low metal prices (BC MINFILE, 2010). At about the same time, Delaware Resources Corp. and Cominco Ltd. had delineated approximately a million tonnes of 27 g/t Au on the Snip property, about 5 km north of the Johnny Mountain Mine. Between 1991 and 1999, the Snip deposit produced 32.093 million grams of gold, 12.183 million grams of silver and 249 276 kilograms of copper from about 1.2 million tonnes of ore (BC MINFILE, 2010).

North of the Iskut River, a major exploration and geological mapping program was undertaken by Newmont Mining Corporation of Canada Ltd. (Newmont) in 1972. It was the era of copper porphyry exploration, and in this region efforts were directed towards copper-iron skarn mineralization associated with feldspar megacrystic syenite intrusions on the Dirk and Ken showings. Gulf International Minerals staked the McLymont claims south of Newmont Lake in 1986 to cover auriferous skarn mineralization. Recent work covering the Dirk and Newmont Lake areas has been

conducted by Romios Gold Resources (Ray, 2006; Bernales *et al.*, 2008; Chadwick and Close, 2009).

Late Triassic Copper Mountain Intrusive-Related

Copper, gold and silver mineralization at the Dirk, Telena and Birthday Jim prospects is related to a regionally extensive Latest Triassic alkaline magmatic event, the Copper Mountain Plutonic Suite (Woodsworth *et al.*, 1992). This magmatic event is causative to porphyry mineralization along the length of British Columbia. In the northwest, related mineralization is found at Galore Creek, Red Chris and GJ. In central and southern BC, related deposits include Mount Polley, Afton and Copper Mountain.

Dirk Showing (MINFILE 104B 114)

In 1972, Newmont carried out geological mapping, airborne and ground magnetometer surveys and drilled six holes totalling 93.87 m. Three holes were drilled at each of the Dirk and Ken claims using a Winkie drill and "A" drill string (the Ken zone is located 5.5 km east of the Dirk on NTS map sheet 104B/15, east of the study area that we report on here). It was concluded then that the Winkie drill was an ineffective tool for sampling these zones (Costin, 1973). In 2009, Romios Gold Resources conducted followed up geological investigations (Chadwick and Close, 2009) and sampling of the mineralization on two of the known mineral showings: the Dirk and Telena zones, which are separated by a kilometre-wide expanse of glacier.

The Dirk prospect occupies the eastern margin of an alkaline intrusive center more than 3 by 4 km in size. The intrusive centre is a swarm of easterly-trending sills and dikes as well as stock-like bodies of texturally variable, porphyritic and equigranular syenite containing orthoclase ±pseudoleucite. K-feldspar porphyry bodies are identical to the Late Triassic "rhomb porphyries" of the alkaline feldspar porphyry intrusive suites at Galore Creek, located 40 km to the northwest. Crystallization ages of the intrusions at Galore Creek range from 210.2 ±1.0 Ma (U/Pb, titanite; Mortensen *et al.*, 1995) for a syn-mineral dike to 208.8 ±0.8 Ma (U/Pb, zircon; Logan, unpublished) for a post-mineral dike. The Dirk intrusions, like those at Galore, are silica-under saturated, syenite and foid-bearing syenite characterized by centimetre-scale megacrysts of orthoclase and smaller phenocrysts of biotite, sodic pyroxene, hornblende, apatite, magnetite, and titanite. They are variably altered, containing assemblages of andradite garnet, epidote, clinozoisite, secondary biotite, chlorite, calcite and anhydrite (?). Diatreme bodies containing breccia fragments of distinctive porphyritic syenite and bright green pyroxene form part of this magmatic suite and are cut by younger syenite dikes containing coarse orthoclase crystals.

The main Dirk showing is an east trending eight metre wide skarn zone of patchy bornite, covellite and chalcopyrite ±pyrite mineralization replacing limestone adjacent to pink, potassium feldspar-phyric syenite dikes. Sulphides occupy millimetres thick veinlets and irregular patches locally with magnetite and/or andradite, epidote and albitic (?) alteration. Metal assemblages of economic interest include chalcopyrite ±gold. Alteration assemblages (*i.e.* magnetite, specular hematite, andradite and epidote) infer a highly oxidizing character of the main hydrothermal event. Late stage iron carbonate and barite veins are common at the Dirk and Telena zones. Eight, 1 m chip samples taken along a north-south traverse across the main Dirk showing returned 2.9% Cu and 0.64 g/t Au (Chadwick and Close, 2009). Additional copper-gold mineralization has been recognized 200 m southeast of the main zone and a 3.0 m chip sample from this mineralized section assayed 6.21% Cu and 0.57 g/t Au (Chadwick and Close, 2009). A sample collected during the course of our mapping contained >1% Cu, 5 ppm Ag, 0.6 ppm Au and 0.38% Zn (see sample 10JLO-254, Tables 1 and 2).

Telena Showing

Mineralization at the Telena showing is described as a 40 by 40 m cliff exposure of disseminated and vein chalcopyrite with intermittent bornite-bearing breccias within a syenite porphyry (Chadwick and Close, 2009). A reported grab sample from the Telena Zone assayed 2.07% Cu and 0.97 g/t Au. Two samples were collected during the course of our mapping. These are representative of the two ends of the spectrum of mineralized K-feldspar porphyritic rocks. One sample was collected from largest of many irregular patches and veins of semi-massive chalcopyrite (~0.25 by 1.1 m) within a strongly copper-stained, brecciated and skarnified coarse K-feldspar and calcite amygdaloidal porphyry. A second sample was collected from a relatively poorly mineralized dike at least 4 m thick, which cuts across the unit from which the first sample was collected. This dike contains medium to coarse K-feldspar phenocrysts. Notable results from analysis of these two samples are: Cu, >10 000 ppm, 1058 ppm; Au, 4.1 ppm, 0.1 ppm; Ag, 15.5 ppm, 0.7 ppm; Pd, 64 ppb, 27 ppb; Pt, 21 ppb, 3 ppb (samples MMI10-18-11 and MMI10-18-11b, Table 1).

About 650 m southwest of the Telena is a 2 km long, west-trending nunatak. It largely underlain by an east-northeast striking dike swarm of calc-potassic altered megacrystic potassium feldspar syenite dikes which abut against and intrude a large olistostromal block of thick bedded recrystallized limestone forming the eastern end of the nunatak. Brecciated, white orthoclase flooded syenite porphyries overprinted and replaced by brown or green euhedral zoned andradite garnet, anhydrite, traces of malachite and late carbonate attest to a vigorous magmatic/hydrothermal centre.

Table 1. Selected elements from Inductively Coupled Mass Spectrographic analyses (ICPMS) of samples collected in the Hoodoo Mountain area. For entire dataset see Mihalynuk *et al.* (2011b).

SampleNumber	Latitude	Longitude	Lab Number	Ag	As	Au	Ba	Bi	Cd	Ce	Co	Cs	Cu	Fe	Ga	Hg	K	Mn	Mo	Pb	Pd	Pt	S	Se	Te	Th	Y	Zn	Zr
			Detection Limit	2	0.1	0.2	0.5	0.02	0.01	0.1	0.1	0.02	0.01	0.01	0.1	5	0.01	1	0.01	0.01	10	2	0.02	0.1	0.02	0.1	0.01	0.1	0.1
			Measure unit	PPB	PPM	PPB	PPM	PPM	PPM	PPM	PPM	PPM	PPM	%	PPM	PPB	%	PPM	PPM	PPM	PPB	PPB	%	PPM	PPM	PPM	PPM	PPM	PPM
10JLO-161	56.9093	-131.0831	62121	260	37.1	27.9	50.1	1.97	1.41	31.7	17.1	0.36	69.37	4.3	7.1	90	0.16	879	0.66	16.3	<10	4	2.75	1.6	0.18	2.6	10	203.4	2.2
10JLO-161	56.9093	-131.0831	62121	276	36.6	24.7	50.2	2.05	1.38	31.5	17.1	0.4	69.59	4.38	7.1	70	0.15	894	0.61	17.28	<10	4	2.74	1.3	0.2	2.7	9.93	211.1	2.4
10JLO-182	56.8819	-131.0340	62122	3839	23.2	6403.5	22.4	0.26	0.08	5.4	12.1	0.04	5153.48	6.63	4.8	171	<0.01	1698	2.05	1.89	<10	4	0.23	0.3	0.05	0.6	7.94	33.1	5.4
10JLO-254	56.8713	-131.0280	62123	5049	208.7	625.3	11.5	0.48	10	2.9	602.5	0.11	>10000.00	23.36	3.9	29570	<0.01	2392	5.07	22.2	48	<2	0.04	2.3	0.26	0.2	2.02	3819.3	1.3
10JLO-278	56.7071	-131.1140	62124	23534	85.3	2113.9	55.5	53.39	1.68	1.8	10	2.04	381.68	14.78	6.5	55	0.98	335	9.3	516.24	<10	<2	5.05	33.4	18.08	0.2	3.05	219	0.3
MMI10-1-05	58.7571	-133.7057	62125	16	0.6	7.4	27	0.03	0.12	0.4	20.5	0.09	8.09	3.83	7	<5	0.03	1523	0.12	3.32	<10	<2	0.08	<0.1	<0.02	<0.1	5.06	37.3	<0.1
MMI10-12-08	56.8210	-131.1433	62126	7497	11.1	1754.8	61.9	1.87	3.34	5.7	20.4	5.28	1567.05	6.9	12.9	54	2.45	1019	1.3	6.38	<10	<2	1.88	1.6	0.45	0.7	8.86	184.3	0.9
MMI10-12-12	56.8175	-131.1558	62127	101	4.3	6.6	151.4	0.08	0.07	16.5	9.5	1.44	38.5	3.29	2.1	12	0.2	1007	3.41	2.73	<10	<2	0.33	<0.1	<0.02	2.5	10.39	60.1	0.3
MMI10-13-07	56.8281	-131.1684	62128	24	5.3	2.8	17.3	<0.02	0.31	3.8	0.9	<0.02	23.57	0.36	3.6	30	0.01	548	0.12	5.13	<10	<2	0.03	<0.1	<0.02	0.5	1.84	6	6.3
MMI10-13-12	56.8321	-131.1570	62129	168	3.1	2.1	61.6	0.12	0.03	1.6	27.9	0.5	29.56	2.81	0.5	636	0.19	7	0.88	0.77	<10	<2	2.96	0.1	<0.02	1	1.32	3.5	5.4
MMI10-14-09	56.7473	-131.0294	62130	1039	3.1	6.7	111.2	0.28	0.05	8.2	12.3	3.07	233.65	3.26	7.7	14	0.63	92	1.01	6.53	10	2	1.95	0.7	0.26	0.5	1.95	17.8	1.1
MMI10-16-10	56.9797	-131.0662	62131	5843	<0.1	5	717.6	0.38	14.01	16.3	6.4	0.14	1616.02	1.8	4.8	1557	0.06	147	0.47	33.34	<10	<2	0.04	2.4	<0.02	0.3	7.12	4044.1	1.4
MMI10-16-10b	56.9797	-131.0662	62132	5970	0.3	4.6	742	0.37	14.47	16.6	6.5	0.14	1668.12	1.84	4.9	1564	0.06	146	0.43	33.03	21	<2	0.04	2.3	<0.02	0.3	7.53	4168.1	1.3
MMI10-16-10b	56.9797	-131.0662	62132	6223	<0.1	4.5	761	0.39	14.62	17.1	6.6	0.16	1719.17	1.91	5.3	1644	0.06	153	0.48	34.81	38	<2	0.04	2.3	<0.02	0.4	7.69	4297.5	1.5
MMI10-18-07	56.8811	-131.0332	62133	417	8.2	153.1	112	0.4	0.04	6.7	25.1	0.09	4474.48	8.03	0.7	1497	0.03	633	3.75	1.64	<10	<2	0.75	0.5	0.08	<0.1	5.4	9.3	1.1
MMI10-18-11	56.8604	-131.0384	62134	15522	208.4	4110.6	55.3	2.08	0.23	30.1	377	0.37	>10000.00	15.92	11.2	469	<0.01	2349	22.65	15.89	64	21	1.57	28.6	1.13	0.5	15.92	120.2	2.5
MMI10-18-11b	56.8604	-131.0384	62135	737	10.5	136.8	13.7	0.55	0.18	60.4	74.8	1.16	1058	7.18	4.2	92	0.05	3213	2.12	12.4	27	3	2.27	5.8	0.33	1.4	33.68	54	3
MMI10-20-12	56.8201	-131.0190	62136	1654	16.9	80.8	145.3	2.41	0.18	4.5	36.7	1.22	584.01	4.98	2.2	144	0.34	1631	4.14	5.14	<10	3	1.31	1	1	0.2	7.46	42.8	0.9
MMI10-20-12b	56.8201	-131.0190	62137	15657	63.2	736.6	30.8	49.5	0.22	2.5	37.8	0.37	2490.92	11.72	8.4	137	0.17	418	24.97	9.33	<10	<2	5.94	7.3	28.47	0.4	3.61	77.9	1.3
MMI10-20-13	56.8208	-131.0201	62138	441	23.7	<0.2	46.1	0.41	0.08	6.6	6.9	0.61	1064.39	2.39	0.7	20	0.19	1713	1.48	5.1	<10	<2	0.53	0.7	0.05	0.2	9.17	15.1	0.4
MMI10-22-06	56.8216	-131.0214	62139	100	3.2	2.4	124.3	0.06	0.04	2	7.3	0.16	311.75	2.86	0.4	8	0.09	387	1.5	1.21	<10	<2	0.59	0.2	0.02	<0.1	1.73	6.3	0.3
MMI10-24-03	56.7598	-131.1858	62140	260	6	6.7	46.2	0.07	0.07	2.9	17.4	1.22	249.87	2.25	3.7	18	0.29	393	0.83	9.72	<10	4	0.61	0.3	0.03	0.3	4.07	23.6	1.3
MMI10-24-04	56.7067	-131.1142	62141	3079	0.2	368.5	128.3	2.43	0.05	5.2	31.1	8.08	2000.94	7.13	13.1	<5	2.76	701	88.16	1.81	13	<2	1.78	4.6	1.48	0.5	3.87	74.3	0.4
MMI10-24-05	56.7070	-131.1141	62142	7139	22.8	885.2	78.5	15.65	0.23	6.2	10.7	4.59	4151.72	4.16	6.9	18	1.57	454	25.01	2.3	<10	2	2.22	7.7	5.96	1.3	9.11	43.5	0.5
MMI10-24-06	56.6785	-131.0937	62143	5495	197.9	584.6	32	31.81	0.26	5.1	21.3	2.57	1528.42	14.86	8.7	22	0.99	426	138.42	10.84	11	2	>10.00	35.4	7.4	0.5	5.89	41.1	0.9
Reference Materials																													
Standard BCGS till			62144	1619	65.3	29.5	275.5	0.3	0.76	27.9	49.4	0.56	175.55	7.61	9.5	369	0.05	1604	0.92	236.26	<10	<2	<0.02	0.7	0.34	3.6	13.04	350.4	3.2
Standard DS7			STD DS7	1020	51.7	87.6	425.2	5.1	6.41	39.9	9.6	6.59	103.9	2.41	4.8	219	0.46	634	22.28	74	83	39	0.21	3.3	1.39	5	6.23	393	5.9
Blank			BLK	<2	<0.1	<0.2	<0.5	<0.02	<0.01	<0.1	<0.1	<0.02	<0.01	<0.01	<0.1	<5	<0.01	<1	<0.01	<0.01	<10	<2	<0.02	<0.1	<0.02	<0.1	<0.01	<0.1	<0.1

Table 2. Selected elements from Instrumental Neutron Activation Analysis (INAA) of samples collected in the Hoodoo Mountain area. For entire dataset see Mihalynuk *et al.* (2011b).

Sample Number	Latitude	Longitude	Lab Number	Au	Ag	As	Ba	Ca	Co	Cr	Cs	Fe	Hf	Hg	Mo	Na	Ni	Rb	Sb	Sc	Se	Th	U	W	Zn	La	Ce	Nd	Sm	Eu	Tb	Yb	Lu	Mass
			Detection Limit	ppb	ppm	ppm	ppm	%	ppm	ppm	ppm	%	ppm	ppm	ppm	%	ppm	ppm	ppm	ppm	ppm	ppm	ppm	ppm	ppm	ppm	ppm	ppm	ppm	ppm	ppm	ppm	ppm	ppm	g
			Measure unit	5	5	2	100	1	5	10	2	0.02	1	1	5	0.05	50	30	0.2	0.1	5	0.5	0.5	4	50	1	3	5	0.1	0.2	0.5	0.2	0.05	
10JLO-161	56.9093	-131.0831	62121	< 5	< 5	42	2000	< 1	14	50	< 2	4.41	< 1	< 1	13	2.32	< 50	140	2.7	11.3	< 5	5.3	< 0.5	< 4	290	18	40	< 5	2.5	< 0.2	< 0.5	1.5	0.32	35.2
10JLO-182	56.8819	-131.0340	62122	6810	< 5	35	700	12	14	70	< 2	14.4	< 1	< 1	< 5	0.05	< 50	< 30	2	5.8	< 5	< 0.5	< 0.5	139	70	6	< 3	< 5	1	< 0.2	< 0.5	1	0.14	36.3
10JLO-254	56.8713	-131.0280	62123	560	< 5	238	500	< 1	623	60	< 2	51.5	< 1	26	< 5	< 0.05	< 50	< 30	6.4	0.7	11	< 0.5	< 0.5	11	4520	4	< 3	< 5	0.3	< 0.2	< 0.5	< 0.2	< 0.05	45.2
10JLO-278	56.7071	-131.1140	62124	1980	25	90	1200	2	10	220	4	13.2	2	2	< 5	0.34	< 50	< 30	1.2	11.6	25	1.4	2.9	9	240	7	14	17	1.4	0.7	< 0.5	1.4	0.29	45.2
MM10-1-05	58.7571	-133.7057	62125	< 5	< 5	< 2	< 100	11	22	130	< 2	4.75	< 1	< 1	< 5	1.78	< 50	< 30	< 0.2	24.6	< 5	< 0.5	< 0.5	< 4	< 50	1	8	< 5	0.7	0.5	< 0.5	2	0.3	33.1
MM10-12-08	56.8210	-131.1433	62126	2400	9	18	1400	< 1	22	40	6	7.01	2	< 1	< 5	1.96	< 50	< 30	9.8	18.6	< 5	3.8	3	< 4	< 50	14	34	< 5	3.3	< 0.2	< 0.5	2.7	0.41	34.5
MM10-12-12	56.8175	-131.1558	62127	< 5	< 5	< 2	400	4	10	50	< 2	3.31	1	< 1	< 5	0.25	< 50	50	1.5	13.6	< 5	4.1	3.1	< 4	80	12	25	14	2.3	0.7	< 0.5	2.4	0.27	36.3
MM10-13-07	56.8281	-131.1684	62128	< 5	< 5	32	300	11	< 5	100	< 2	2.12	1	< 1	< 5	0.16	< 50	< 30	3	7.7	< 5	2.5	< 0.5	< 4	60	7	12	< 5	1	0.4	< 0.5	0.6	< 0.05	42.3
MM10-13-12	56.8321	-131.1570	62129	< 5	< 5	< 2	2200	< 1	28	100	3	3.75	2	< 1	< 5	0.27	< 50	130	1.4	24.2	< 5	2.9	5.9	< 4	< 50	6	12	16	1.1	< 0.2	< 0.5	3.1	0.5	26.9
MM10-14-09	56.7473	-131.0294	62130	< 5	< 5	< 2	4200	< 1	11	80	7	3.26	6	< 1	< 5	0.28	< 50	70	0.4	21.8	< 5	4.6	< 0.5	< 4	< 50	31	63	23	6.4	2.1	< 0.5	5.3	0.82	35.1
MM10-16-10	56.9797	-131.0662	62131	< 5	7	< 2	600	< 1	8	120	< 2	1.9	4	< 1	< 5	3.6	< 50	< 30	1.5	8.3	< 5	2.4	2.5	< 4	4040	9	17	< 5	2.8	1	< 0.5	4.4	0.67	34.7
MM10-16-10b	56.9797	-131.0662	62132	< 5	8	4	1200	3	8	140	< 2	1.9	3	< 1	< 5	3.7	< 50	< 30	1.6	8.4	< 5	2.4	< 0.5	< 4	4130	9	24	28	3.1	1	< 0.5	4	0.67	32
MM10-18-07	56.8811	-131.0332	62133	188	< 5	20	< 100	5	26	70	< 2	29.4	< 1	< 1	15	< 0.05	< 50	< 30	4.9	1.4	< 5	< 0.5	< 0.5	91	< 50	4	8	< 5	0.8	< 0.2	< 0.5	0.7	< 0.05	41.9
MM10-18-11	56.8604	-131.0384	62134	4260	17	200	< 100	6	366	40	< 2	14.8	< 1	< 1	22	< 0.05	230	< 30	9.1	14.4	27	< 0.5	< 0.5	21	150	23	29	25	2.8	0.9	< 0.5	3.8	0.64	37
MM10-18-11b	56.8604	-131.0384	62135	135	< 5	15	< 100	20	73	30	< 2	12.2	< 1	< 1	< 5	< 0.05	< 50	< 30	5.9	14.2	< 5	1.1	3.1	10	< 50	48	61	< 5	4.9	2.4	1	4.4	0.62	37.3
MM10-20-12	56.8201	-131.0190	62136	73	< 5	20	1000	7	35	480	3	5.32	< 1	< 1	< 5	0.05	< 50	50	6.6	34.6	< 5	< 0.5	< 0.5	< 4	80	4	< 3	6	1.2	0.5	< 0.5	1.4	0.06	36.6
MM10-20-12b	56.8201	-131.0190	62137	762	16	61	300	< 1	38	60	< 2	10.7	2	< 1	27	0.34	< 50	40	5	12.9	< 5	2.1	< 0.5	5	110	3	5	< 5	1.8	0.6	< 0.5	3.6	0.57	37.1
MM10-20-13	56.8208	-131.0201	62138	< 5	< 5	23	500	4	< 5	60	< 2	2.51	2	< 1	< 5	0.26	< 50	< 30	4.5	14.7	< 5	1.8	< 0.5	< 4	< 50	15	25	10	3.5	1.4	0.6	3.9	0.66	29.4
MM10-22-06	56.8216	-131.0214	62139	< 5	< 5	5	300	< 1	7	210	< 2	3.26	< 1	< 1	< 5	< 0.05	< 50	< 30	1.9	1.5	< 5	< 0.5	< 0.5	< 4	< 50	1	< 3	< 5	0.4	0.2	< 0.5	< 0.2	< 0.05	39.2
MM10-24-03	56.7598	-131.1858	62140	< 5	< 5	< 2	1200	10	32	430	3	6.13	1	< 1	< 5	0.87	< 50	50	2.9	35.8	< 5	1.2	< 0.5	< 4	100	7	12	< 5	1.7	0.8	< 0.5	1.8	0.3	40.5
MM10-24-04	56.7067	-131.1142	62141	413	< 5	< 2	1300	< 1	33	310	10	7.15	2	< 1	79	0.65	< 50	190	0.7	14.7	< 5	2	4.8	37	130	14	22	15	2.3	0.6	< 0.5	2	0.26	37.5
MM10-24-05	56.7070	-131.1141	62142	1260	8	24	500	< 1	13	90	5	4.22	2	< 1	29	2.49	< 50	140	1	10.7	< 5	3	< 0.5	17	160	6	16	< 5	2.3	0.7	< 0.5	2	0.32	33.3
MM10-24-06	56.6785	-131.0937	62143	675	8	206	1000	6	23	310	< 2	15.1	< 1	< 1	180	1	< 50	150	2.5	15.7	38	2.3	5.3	40	< 50	16	32	< 5	2.6	0.7	< 0.5	1.8	0.31	36.9
Reference Materials																																		
Standard BCGS till			62144	< 5	< 5	75	< 100	< 1	58	420	< 2	9.3	3	< 1	< 5	2	< 50	< 30	17.4	32.4	< 5	5.9	< 0.5	< 4	280	30	54	20	5.8	2.6	< 0.5	2.8	0.63	25
Standard Measured			DMMAS 111	1770		1470	1200		34	50		3.03				1.9				5.9			13.9			14	25		1.7					
Standard as certified			DMMAS 111	1670		1450	1140		34	52		2.79				1.87				5.8			14			14	19.3		1.9					
Blank			BLK	< 5	< 5	< 2	< 100	< 1	< 5	< 10	< 2	< 0.02	< 1	< 1	< 5	< 0.05	< 50	< 30	< 0.2	< 0.1	< 5	< 0.5	< 0.5	< 4	< 50	< 1	< 3	< 5	< 0.1	< 0.2	< 0.5	< 0.2	< 0.05	30

Birthday Jim Showing

The Birthday Jim showing is located approximately 1 km north of the Dirk. Specularite skarn mineralization has been known at this locality for nearly 40 years, and was recorded during property scale mapping which extended north from the Dirk prospect (Costin, 1973). Mineralization is set in a package of southwest-striking, north-dipping volcaniclastic rocks, including coarse polylithic volcanic conglomerate, sandstone and fine grained siltstone, cherty argillite and fossiliferous limestone. Intruding the bedded sequence are dikes and sills of fine grained pink weathering syenite and xenolith-rich biotite phyric syenite and a coarse potassium feldspar megacrystic syenite porphyry clast-dominated diatreme (units described previously). The syenite is locally flow laminated and displays chilled margins where it intrudes the diatreme, but where it intrudes limestone the contacts are more diffuse because the dike has assimilated limestone xenoliths and is overprinted by skarn alteration. Mineralization occurs as veins and patchy replacements of limestone xenoliths within the syenite or adjacent to the syenite contact, within limestone. Skarn mineralization is dominated by specular hematite, lesser magnetite, andradite garnet and epidote with chalcopyrite and malachite (Figures 22a, b). We collected two grab samples of specularite-chalcopyrite mineralization. Most notable of the analytical results were those obtained from sample 10JLO-182 (Table 1) which returned 0.5 % Cu, 3.8 ppm Ag and 6.4 ppm Au.

Early Carboniferous - VHMS

Verrett rhyolite

An unnamed east-flowing glacier is the northern source of Verrett River. North of this glacier is a volcano-sedimentary section comprised of well bedded rhyolite tuffite containing sulphide clasts (Figures 23a, b) and peperite sills that pass up section into rhyolite lapilli and breccia units. Preliminary U-Pb age determinations on

Figure 22a. Skarn mineralization at the Birthday Jim occurrence: photomicrograph of reflected light view of bladed specular hematite which is enclosed by late chalcopyrite. Accessory pyrite occurs outside the ~5 mm field of view.

Figure 22b. Skarn mineralization at the Birthday Jim occurrence: quartz and hematite replace colonial corals.

Figure 23a. Well bedded rhyolite tuffite with sulphide clasts.

zircons separated from this rhyolite indicate an age of ~340 Ma (the same preliminary age as determined for the rhyolite in the northeast corner of the map sheet). Sulphide veins are common within the overlying rhyolite, occurring as irregular pyrite-chalcopyrite veins in late breccia zones (Figure 23c) and as 1 to 5 cm thick, planar veins of chlorite-carbonate-euhedral pyrite ±chalcopyrite enveloped by decimetre wide carbonate alteration halos. On its western side, the succession shares a structurally modified contact with rust, tan and black turbiditic volcanic sediments. At this contact are fault-striated relicts of a barite-chalcopyrite layer up to ~5 cm thick

Figure 23b. Well bedded rhyolite tuffite is locally brecciated.

Figure 23c. Well bedded rhyolite tuffite with infillings of pyrite and lesser chalcopyrite.

(Figure 24a) at the structural base of the rhyolite tuff. Approximately 100 m above the contact with turbiditic strata the section becomes more tuffaceous with green and maroon tuffite containing magnetite-rich layers interbedded with irregular jasperoid layers (Figure 24b). Some jasperoid boulders contain stratiform layers of pyrite and chalcopyrite (Figure 24c), but chalcopyrite layers could not be found in place.

Barite, chalcopyrite, magnetite layers and jasper layers are all features of productive VMS environments. If the Fe-rich tuff – jasper layers are exhalative in origin, they represent active subaqueous hydrothermal environment in which chalcopyrite is accumulating, and significant mineral exploration target. Jasperoid layers within the stratigraphy about 1.5 km to the southeast may be related and, if so, represents a target with significant strike length.

Andrei rhyolite

Perhaps the most inconspicuous mineralization encountered during the 2010 mapping campaign shows no sign of having been looked at previously. Mineralization occurs in a section of felsic flows and tuff, pillowed mafic flows and hyaloclastite, and immature volcanic sediments

Figure 24a. The structurally modified contact between fine grained turbiditic sediments and coarse rhyolite tuff is a layer of baritic argillite with chalcopyrite (inset).

Figure 24b. Stratigraphically above the turbiditic section is well-bedded tuffite with magnetite-rich layers as well as jasperoid layers.

in the northeast part of the map area. An early Carboniferous age is indicated by extension of geology mapped by (Logan *et al.*, 2000) as well as a new preliminary isotopic age determination of ~340 Ma. Mineralization consists of finely disseminated chalcopyrite and millimetre to centimetre clots of covellite-bornite as intergrowths with mafic glomerocrysts or xenoliths (?) in a medium grained K-feldspar-phyric unit (Figures 25a, b). Millimetre-thick, black, irregular quartz veinlets locally cut the unit. Copper

Figure 24c. Boulders of jasper contain stratiform pyrite and, as seen here, chalcopyrite.

Figure 25a. Character of black veinlets cutting a typical exposure of the Andrei rhyolite. Metal content is related to disseminated sulphides as contents determined by analyses remain consistent regardless of the degree of veining.

staining is scarce. We interpret the unit as a rhyolite flow and flow breccia unit, but it could be a dike with highly irregular margins. Two samples of this unit were collected about 10 m apart, both contain appreciable Cu (1600 ppm), Zn (4000 ppm), Ag (5.8 ppm) and Cd (14 ppm; see Table 1 and note consistency of replicate analyses). In consideration of its potentially consistent but inconspicuous mineralization, this unit and others like it need to be systematically mapped and sampled.

Pink epidote veins

On the ridge east of Twin Glacier, pink veins composed of a resistant, hard silicate mineral cut the ~187 Ma hornblende ±biotite dacite ash flow / air fall tuff and breccia. Such veins may be of interest to mineral collectors and more than ten of these veins occur within a zone that extends at least 100 m and may be 30 m across. Individual veins attain thicknesses of 0.5 m but pinch and swell, such that 5-10 cm thickness is more typical (Figure 26). Petrographic analysis of one of the vein samples collected reveals a fine grained intergrowth of quartz with

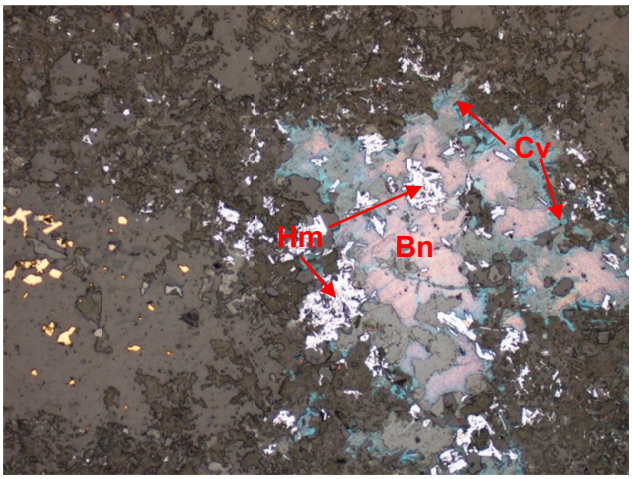

Figure 25b. Photomicrograph of mineralization within mafic clots in the felsic volcanic unit includes purple twinned bornite (Bn) rimmed by pleochroic blue covellite (Cv) and enclosing idiomorphic blue-white hematite (Hm). Disseminated chalcopyrite occurs outside the ~1.2 mm field of view. Disseminations of a yellow, highly reflective mineral at the left centre have a softer polishing hardness and higher reflectance than is typical of chalcopyrite (perhaps cubanite or eskebornite, $CuFeSe_2$). Sphalerite occurs as ~20-30 µ irregular blebs scattered around the margins of the bornite.

Figure 26. Veins of pink epidote cut feldspar-phyric volcanic rocks east of Twin Glacier.

minor carbonate and chlorite and a predominance of a strongly zoned, high relief, highly birefringent mineral (~0.035) with yellow-lime to pale pink pleochroism. Optical properties, confirmed by XRD analysis, indicate that the mineral is epidote, probably a Mn-bearing

pistacite, as opposed to the optically positive and strongly pleochroic (magenta to yellow) piedmontite, the Mn-rich member of the epidote family. Trace element analysis of the vein reveals only minor Mn-enrichment (which may impart the pale pink colour), but relatively high values of halfnium and zirconium (0.19 and 6.3 ppm, see Hf and Zr, sample MMI10-13-7, Table 1).

STRUCTURAL GEOLOGY

Zones of foliated, folded and faulted rocks have been identified at various scales throughout the map area. However, the strongest penetrative fabrics affecting areas of more than a square kilometre are generally restricted to the regions south and west of the Twin River pluton where two phases of folding are displayed.

Folds, foliation and schistosity

Partitioning of strain into elongate, foliated domains can be observed on the ridges east of Twin Glacier. Some of these domains can be explained by their position in the axial zones of mainly northwest-trending folds. Northeast-verging thrusts and duplex zones which are presumably syn-kinematic with northwest-trending folds, are interpreted to root beneath the foliated rocks.

On the nunatak between the Twin Glaciers, penetrative fabrics are developed in the volcano-sedimentary rocks. In these areas, the rocks are pervasively recrystallized to such an extent that they are locally schistose. Strong to moderately strong, steep S1 foliation is shallower than or sub-parallel to poorly preserved bedding indicating local upright isoclinals folding of the stratigraphy. S1 is commonly accompanied by development of strong to intense, steep to downdip stretching lineation, locally with L>S, forming L-tectonites. L-tectonites are spectacularly preserved in limestone-bearing conglomerates where the limestone clasts have aspect ratios of >>10:1. S1 is overprinted by open to tight recumbent F2 folds with minimal S2 development.

Timing and conditions leading to the formation of the schistosity have not been firmly established. North and east of the map area Logan and Koyanagi (1994) and Logan *et al.* (2000, Figure 2; 1994) record similar fabrics which affect pre-mid Carboniferous rocks; whereas the strata affected at Twin Glacier nunatak are suspected to be Triassic (Kerr, 1935; Fillipone and Ross, 1989). Age control for strata at the nunatak are lacking and interleaving of foliated and non-foliated strata by complex thrust faulting cannot be ruled out. Minimum age of D1 is constrained as pre-Eocene, the age of the Twin River pluton that appears to hornfels the S1-L1 tectonites. The age of S2 is not constrained as the hornfelsed Triassic strata do not appear to preserve F2.

Some schistose fabrics were developed in response to intrusion of the Twin River pluton, but these fabrics are restricted to a zone within ~500 m of the pluton contacts. Elsewhere, fabrics within regionally foliated rock outcrops are cut by the pluton and related dikes. At the map scale, regional foliation tends to wrap around the margin of the intrusion. Such relations suggest that pluton emplacement was in part accommodated by ductile flow of country rocks.

Folds and thrust belts

Thrust faults are best displayed within well bedded, relatively incompetent strata which presumably acted as glide horizons and décollements. This strain is particularly concentrated within two units: sooty and cherty strata of presumed Middle Triassic age and chert-claystone of presumed Carboniferous age. Nevertheless, well bedded calcareous wacke has also been deformed by thrust faulting; and thrust offsets within this unit must be appreciable as a several hundred metre-long zone of complex, thrust-related deformation has been developed ~3 km east of Twin Glacier (Figures 27a, b). Fold asymmetry within both the footwall and hangingwall, as well as the geometry of bedding cut-offs, suggest that thrusts mainly verged to the north and east.

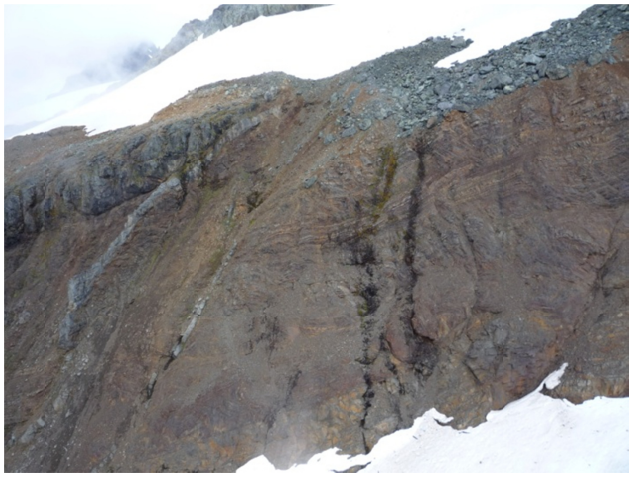

Figure 27a. A cliff face between the clouds east of Twin Glacier displays an incised thrust belt.

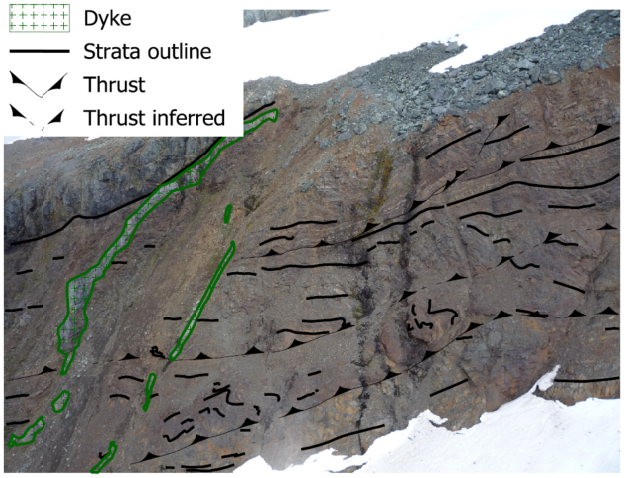

Figure 27b. An interpretation of the deformation displayed by the strata.

Late faults

Two major brittle-ductile faults have been mapped. The apparent offsets on these faults are inferred to exceed 1 km, and as such they impart a significant control on the continuation of stratigraphic units and mineralization. The faults are named after nearby geographic features: Andrei Glacier fault and the Verrett-Iskut Fault.

Andrei Glacier fault

Numerous fault strands that together comprise the Andrei Glacier Fault are exposed and oriented northwest, roughly parallel to the northeastern margin of the Andrei Glacier. This fault juxtaposes Middle Carboniferous carbonate (Logan *et al.*, 2000) to the northeast, with orange-weathering conglomerate of presumed Late Triassic age to the southwest. Orange, strongly carbonate-altered, 1 to 2 m thick dikes have intruded along the fault zone where they display ghosted, coarse phenocrysts that are probably relicts of orthoclase. Similar dikes are observed cutting Triassic strata to the south and are interpreted to be of Late Triassic age.

Several sets of minor structures have been identified within the fault zone including two sets slickensides indicating components of subhorizontal-dextral as well as south-side-down-normal motion. We acknowledge that the slickensides are minor features that may have formed at any time, even in response to glacial rebound. However, the downdip slickensides are superimposed on fault flutings with ~10 cm of relief and may represent significant fault motion. The entire Upper Carboniferous and most of the Late Triassic section appears to be offset across the fault, perhaps as much as 3 km of apparent vertical displacement. Actual offset could be much less depending upon how much section was removed during a sub-Late Triassic erosional event.

The opposite sense of relative offset is displayed by the inferred northwest extensions of the Andrei Glacier fault where polymictic conglomerate of presumed Upper Triassic age that lay northeast of the fault is juxtaposed with Early Permian strata southwest of the fault. Thus, motion on the fault may have been either scissor-like or the fault displaced previously deformed strata (*e.g.*, folded strata). Southeast extensions of the Andrei Fault are orthogonal to the northeast-trending McLymont fault and other faults bounding the Newmont Lake graben (Logan *et al.*, 2000), suggesting that the Andrei Glacier Fault predates the Newmont Lake Graben.

Verrett-Iskut fault

The Verrett-Iskut fault (V-I fault) is a discrete, high angle fault with a gently arcuate ~east-trending trace. On the southeast flank of Mount Verrett, the V-I fault cuts off a Paleozoic marble unit that is ~200 to ~450 m thick. One kilometre north of the fault, relict layering within the marble dips moderately west. Nearer the fault, layering steepens. Based upon its map pattern, the marble is nearly vertical where intersected by the VI fault. South of the fault and to the east in 104B/15 (Logan *et al.*, 2000), a band of marble outcrops can be extrapolated to intersect the fault at a point which would indicate ~1800 m of sinistral offset. If the marble is vertical where cut by the fault, the 1800 m of apparent sinistral offset is likely close to the true horizontal component of offset.

Farther east, the VI fault juxtaposes Late Devonian biotite granite and Devono-Mississippian tuffaceous rocks in 104B/15 (Logan *et al.,* 2000). To the west, the V-I fault appears to follow a well-defined, glacially scoured lineament trending ~250°, until it is lost at elevations below 1200 m. In this area, adjacent units of "quartz sandstone" and mafic tuff with a combined thickness of 300-500 m and enveloped by argillite are also offset by the fault (see Figure 2 and Mihalynuk *et al.* 2011 for data sources). Amount of offset cannot be precisely constrained because the unit contacts are not exposed, but about 1450 m of apparent sinistral motion is indicated.

WHERE DOES THE WESTERN V-I FAULT GO (?)

West of its intersection with the Iskut River valley bottom, the VI fault is masked by the vegetation and Quaternary sediments. However, the VI fault is unlikely to trend directly west across the Iskut River because it does not offset a belt of limestone between the Craig and Iskut rivers (see Figure 3). Instead, it is interpreted to deflect northwest-ward towards the "Sulphide Ridge" and the Rock and Roll deposit (Figure 3). Farther west, the most likely fault trace beyond its point of re-emergence from the river gravels is obscured by Quaternary to Recent lava flows of Hoodoo Mountain, or by the Hoodoo River alluvial fan deposits. Strong magnetic susceptibility of the flows and clay-rich layers in the gravels obscure both aeromagnetic and airborne electromagnetic responses on geophysical surveys reported by Jones (2009), Walcott, (2009) and Dvorak (1991). However, a

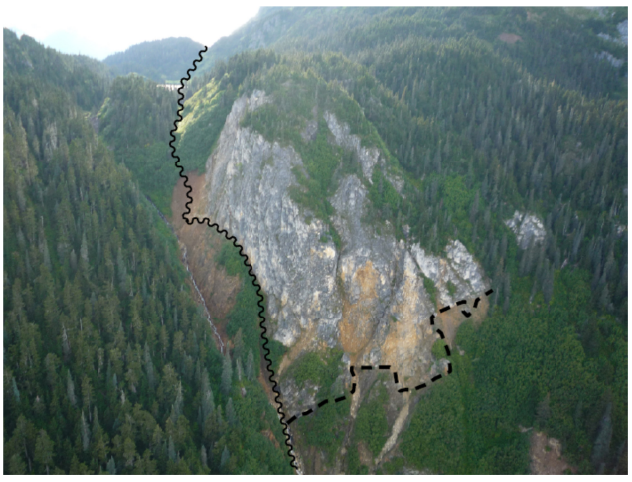

Figure 28. A view to the west along the Verrett-Iskut fault on the southeast flank of Mount Verrett (photo taken from above Verrett River). Following the V-I fault is a strong topographic lineament. A highly irregular trace of the eastern marble contact (highlighted by dashed line) is interpreted as due to intersection of a subvertical contact surface with the steep topography. In the upper right corner of the photo is the northern continuation of the marble band.

break in the aeromagnetic responses in the survey reported by Jones (2009) may respond to a fault trace B on Figure 3 that is deflected slightly to the north. Minimal deflection of the fault is shown by the fault trace A option.

HOW MUCH OFFSET ON V-I FAULT (?)

The displacements of marble bands and quartzose sandstone indicate an average sinistral offset of ~1600 m in the eastern part of the Iskut River valley. Alternatively, decreasing sinistral offset along the fault to the west, as could be inferred from the data, may result in westward decrease of apparent motion by as much as 350 m per 5 km. Hence, the northern continuation of the "Sulphide ridge" stratigraphy could intersect the fault about 10 km west of the offset quartz-rich sandstone. At this point ~750 m of apparent sinistral offset might be inferred. Constraints on the vertical component of motion on the fault are lacking.

WHERE IS THE NORTHERN ROCK AND ROLL (?)

Modelled offsets and locations of the western V-I fault extension have significant implications for identification of a northern continuation of the strata that host the Rock and Roll deposit. Before speculating on the continuation of the Rock and Roll host strata north of the Iskut River Valley, it is necessary to consider several caveats:

1) The mineralization at the Rock and Roll deposit may not have a northern extension. Although the Rock and Roll deposit appears to be stratiform, a syngenetic origin has yet to be unequivocally established (*e.g.* Mihalynuk *et al.*, 2010). Even if the mineralization is stratiform, it may not have had sufficient lateral continuity to outcrop to the north.
2) A northwestern extension of Rock and Roll, if it ever existed, may have been located above the present erosional surface unless the folds that deform the prospective stratigraphy remain approximately horizontal on average or plunge northwestward.
3) Units on "Sulphide Ridge" while complexly folded, display relatively simple bounding surfaces and intersection of these bounding surfaces with present day topography have a relatively consistent northwest trend. In this analysis it is assumed that this trend persists beyond the V-I fault extension.

In the simplest case scenario, barring any of the complication noted above, a potential extension to the Rock and Roll mineralization could be somewhere between the two localities marked by the thick blue and red lines on Figure 3. This supposition needs to be tested by constraining the location of carbonate belt north of the VI fault, particularly because the axis of mineralization along "Sulphide ridge" is consistently between 350 and 450 m northeast of this contact.

SUMMARY

Parts of the southern Hoodoo Mountain sheet were first mapped at a reconnaissance scale by Forrest Kerr between 1926 and 1929. Yet, despite the high mineral potential of the adjacent areas, the northern 2/3 of the sheet was never systematically mapped prior to the work presented here. This report is a synopsis of 2.5 weeks of intensive field investigation that established a geological framework for the eastern Hoodoo Mountain sheet, and extended that framework southwards into the Iskut River valley, where a wealth of geological data exists in industry reports.

Our mapping revealed that the regional geological contacts formerly extrapolated through the Hoodoo Mountain area (Massey *et al.*, 2005) inadequately represent its geological complexity and high mineral potential. As a result, significant mineral prospects, such as the Dirk, which has been recognized since at least 1972, lacked regional geological framework around which a district exploration program could be established.

Even though our mapping was limited by budgetary constraints, it provides enough detail for first order predictive metallogeny, and directions for future mineral exploration work. For example:

- Modelled offset on the V-I fault provides an exploration target for the northern extension of strata that host the Rock and Roll deposit. Future work should include detailed structural analyses aimed at constraining the displacement on units in the western Hoodoo Mountain area, including the vertical component of motion on the V-I fault.
- Recognition of a corridor of alkalic intrusive/volcanic "centres" permits us to pose the question of how extensive are mineralizing systems within the corridor? Alkalic rocks hosting mineralization at the Dirk are analogous to mineralizing intrusions at the Galore Creek deposit. Future work should address characteristics specific to mineralizing intrusions and their extents within the corridor.
- Our work outlines a bimodal submarine volcanic succession of Carboniferous age that contains indications of an active VMS mineralizing system of regional extent. Future exploration work will need to evaluate the significance and distribution of newly discovered primary Cu-Ag-Zn mineralization in both the Andrei rhyolite and the Verrett Creek rhyolite separated by ~20 km.

We will attempt to address some of these questions with targeted laboratory work, but others await the future work of explorationists and regional mappers in the eastern Hoodoo Mountain area. Some answers may lie in

the western Hoodoo Mountain area, parts of which STILL lack regional geological mapping.

ACKNOWLEDGMENTS

This project would not have been possible without the financial assistance of our project partners: Pacific Northwest Capital, the Geological Survey of Canada GEM initiative, and the University of Victoria (British Columbia Ministry of Energy, Mines and Resources Partnership Fund). This project is also funded in part by an NSERC Discovery grant to Stephen T. Johnston. Safe and courteous helicopter support was provided by Jim Beise of VIH Helicopters Ltd. Renaud Soucy la Roche ably assisted with field work. Comfortable accommodations were arranged by David Jensen and others of Skyline Gold Corp. We are especially grateful for the excellent camp cuisine and maintenance all attributable to Esther Nagli of Rugged Edge Holdings Ltd.

REFERENCES

Anderson, R.G. (1993): A Mesozoic stratigraphic and plutonic framework for northwestern Stikinia (Iskut River area), northwestern British Columbia, Canada; *in* Mesozoic Paleogeography of the Western United States - II, Dunne, G. and McDougall, K. (Editors), *Society of Economic Paleontologists and Mineralogists, Pacific Section*, 71, pages 477-494.

BC MINFILE (2010): British Columbia mineral inventory database; *BC Ministry of Energy, Mines and Petroleum Resources*, online database, http://www.empr.gov.bc.ca/MINING/GEOSCIENCE/MINFILE/Pages/default.aspx [November, 2010].

Bernales, S., Chadwick, P. And Guszowaty, E. (2008): 2008 exploration activities on the Romios Gold Resources, Inc. Newmont project, prepared for Romios Gold Resources; *B.C. Ministry of Energy, Mines and Petroleum Resources*, Assessment Report 30449, 59 pages plus 12 appendices**.**

Britton, J.M., Fletcher, B.A. and Alldrick, D.J. (1990): Snippaker map area (104B/6E, 10W, 11E); *in* Geological Fieldwork 1989, *BC Ministry of Energy, Mines and Petroleum Resources*, Paper 1990-1, pages 115-125.

Brown, D.A., Gunning, M.H. and Greig, C.J. (1996): The Stikine Project: Geology of western Telegraph Creek map area, northwestern British Columbia (NTS 104G/5,6,11W, 12 and 13); *BC Ministry of Employment and Investment*, Bulletin 95, 175 pages**.**

Brown, D.A., Logan, J.M., Gunning, M.H., Orchard, M.1. and Bamber, W.E. (1991): Stratigraphic evolution of the Paleozoic Stikine assemblage in the Stikine and lskut Rivers area, northwestern British Columbia; *Canadian Journal of Earth Sciences*, Volume 28, pages 958-972.

Chadwick, P. and Close, S. (2009): Geological and geochemical report on the Dirk property, prepared for Romios Gold Resources; *B.C. Ministry of Energy, Mines and Petroleum Resources*, Assessment Report 31250, 31 pages plus appendices**.**

Clothier (1918): The Stikine Mining Division-Iskut Mining camp; *BC Minister of Mines*, Annual Report of the Minister of Mines for 1917, pages 73-74.

Cohoon, G.A. and Trebilcock, D.A. (2004a): Phiz Property geology and geochemistry surveys; *BC Ministry of Energy, Mines and Petroleum Resources*, Assessment Report 27555, 73 pages plus appendices and maps.

Cohoon, G.A. and Trebilcock, D.A. (2004b): Rock and Roll Project, Geology and Geochemical Surveys; *BC Ministry of Energy, Mines and Petroleum Resources*, Assessment Report 27582, 84 pages plus maps.

Costin, C.P. (1973): Report of geological, geophysical, and physical work, Dirk claim group; *BC Ministry of Energy, Mines and Petroleum Resources*, Assessment Report 4150, 15 pages plus maps**.**

Dvorak, Z. (1991): Geophysical Report on the Hard Place Project; *BC Ministry of Energy, Mines and Petroleum Resources*, Assessment Report 21681, 27 pages**.**

Edwards, B.R., Anderson, R.G., Russell, J.K., Hastings, N.L. and Guo, Y.T. (2000): The Quaternary Hoodoo Mountain Volcanic Complex and Paleozoic and Mesozoic basement rocks, parts of Hoodoo Mountain (NTS 104B/14) and Craig River (NTS 104B/11) map areas, northwestern British Columbia, *Geological Survey of Canada,* Open File 3721, scale 1:20 000.

Fillipone, J.A. and Ross, J.V. (1989): Stratigraphy and structure in the Twin Glacier-Hoodoo Mountain area, northwestern British Columbia (104B/ 14); *in* Geological fieldwork 1988, Smyth (Editor), *BC Ministry of Energy, Mines and Petroleum Resources*, 1989-1, pages 285-292.

Gifford, R.G. (1980): Geological report – Inel mineral claims; *BC Ministry of Energy, Mines and Petroleum Resources*, Assessment Report 8997, 10 pages, 3 appendices and 4 maps**.**

Gunning, M.H., Bamber, E.W., Brown, D.A., Rui, L., Mamet, B.L. and Orchard, M.J. (1994): The Permian Ambition Formation of northwestern Stikinia, British Columbia; *in* Pangaea; global environments and resources, Embry, F, Beauchamp, B and Glass (Editors), *Canadian Society of Petroleum Geologists*, 17, pages 589-619.

Harland, W.B., Armstrong, R.L., Cox, A.V., Craig, L.E., Smith, A.G. and Smith, D.G. (1990): A Geological Time Scale 1989; Cambridge, Cambridge University Press.

Jones, M. (2009): 2009 Geophysical Report on the Rock and Roll Property; *BC Ministry of Energy, Mines and Petroleum Resources*, Assessment Report 31158, 59 plus geophysical maps pages.

Kerr, F A. (1935): Stikine River Area, South Sheet, Cassiar District, British Columbia; *Geological Survey of Canada*, Map 311A, 1:126 720 scale.

Kerr, F.A. (1948): Lower Stikine and western Iskut River areas, British Columbia; *Geological Survey of Canada*, Memoir 246, 94 pages**.**

King, G.R. (1987): Geological and geochemical report on the Ian 1 to 4 claims, Iskut River area, Liard mining division, B.C. *B.C. Ministry of Energy, Mines and Petroleum Resources,* Assessment Report 16953, 19 pages plus 6 appendices and 4 maps.

Lefebure, D.V. and Gunning, M.H. (1989): Geology of the Bronson Creek area, NTS 104B/10W, 11E [in part]; *BC Ministry of Energy, Mines and Petroleum Resources*, Open File 1989-28, 2 sheets, 1:25 000 scale.

Lewis, P.D., Mortensen, J.K., Childe, F., Friedman, R.M., Gabites, J., Ghosh, D. and Bevier, M.L. (2001): Geochronology data set; Metallogenesis of the Iskut River area, northwestern BC, *Mineral Deposits Research Unit*, Miscellaneous Report, pages 89-96.

Logan, J.M. (2004): Preliminary lithogeochemistry and polymetallic VHMS mineralization in Early Devonian and (?) Early Carboniferous volcanic rocks, Foremore property; *in* Geological fieldwork 2003, *BC Ministry of Energy, Mines and Petroleum Resources*, Paper 2004-1, pages 105-124.

Logan, J.M. and Koyanagi, V.M. (1994): Geology and mineral deposits of the Galore Creek area (104G/3, 4); *BC Ministry of Energy, Mines and Petroleum Resources*, Bulletin 92, 96 pages**.**

Logan, J.M., Drobe, J.R. and McClelland, W.C. (2000): Geology of the Forrest Kerr-Mess Creek Area, Northwestern British Columbia (NTS 104B/10, 15 & 104G/2 & 7W); *BC Ministry of Energy, Mines and Petroleum Resources*, Bulletin 104, 163 pages**.**

Macrae, R., and Hall, B.V. (1983): Geological and geochemical report on the Hemlo west and Aurum claim group, Iskut River area, Liard Mining Division*, BC Ministry of Energy, Mines and Petroleum Resources*, Assessment Report 11320, 24 pages plus 4 appendices and 9 maps.

Massey, N.W.D., MacIntyre, D.G., Desjardins, P.J. and Cooney, R.T. (2005): Digital Geology Map of British Columbia: Whole Province, *BC Ministry of Energy, Mines and Petroleum Resources*, Geofile 2005-1.

Mihalynuk, M.G., Stier, T.J., Jones, M.I. and Johnston, S.T. (2010): Stratigraphic and structural setting of the Rock and Roll deposit, northwestern British Columbia; *in* Geological Fieldwork 2009, *BC Ministry of Energy, Mines and Petroleum Resources*, Paper 2010-1, pages 7-18.

Mihalynuk, M.G., Logan, J.M. and Zagorevski, A. (2011a): East Hoodoo Mountain - Iskut River Geology (NTS 104B/14E, 11NE); *BC Ministry of Energy, Mines and Petroleum Resources*, Open File 2011-4, 1:50 000 scale map.

Mihalynuk, M.G., Logan, J.M. and Zagorevski, A. (2011b): Tabulated digital geochemical results from samples collected in the East Hoodoo – Iskut River area (NTS 104B/14E, 11NE); *BC Ministry of Energy, Mines and Petroleum Resources*, Geofile 2011-1, on-line.

Monger, J.W.H. (1977): Upper Paleozoic rocks of the western Canadian Cordillera and their bearing on Cordilleran evolution; *Canadian Journal of Earth Sciences*, Volume 14, pages 1832-1859.

Montgomery, A.T., Todoruk, S.L. and Ikona, C.K. (1991a): Assessment Report on the Rock and Roll Project; *BC Ministry of Energy, Mines and Petroleum Resources*, Assessment Report 20884, 18 pages plus figures, appendices and maps.

Montgomery, A.T., Todoruk, S.L. and Ikona, C.K. (1991b): 1990 Summary geological and geochemical report on the STU 8 & 9 mineral claims, Liard Mining Division; *BC Ministry of Energy, Mines and Petroleum Resources*, Assessment Report 21051, 15 pages plus figures, 8 appendices and 5 maps.

Mortensen, J.K., Gosh, D. and Ferri, F. (1995): U-Pb geochronology of intrusive rocks associated with Cu-Au porphyry deposits in the Canadian Cordillera; *in* Porphyry deposits of the northwestern Cordillera of North America, *in* Schroeter, T. G. (Editor), *Canadian Institute of Mining and Metallurgy*, Special Volume 46, pages 142-158.

Okulitch, A.V. (1999): Geological time scale, 1999; *Geological Survey of Canada*, National Earth Science Series, Geological Atlas, Open File 3040, wall chart**.**

Pegg, R. (1989): Geological and Geochemical Report on the 1989 Exploration Program of the Rock and Roll property; *BC Ministry of Energy, Mines and Petroleum Resources*, Assessment Report 19566, 8 pages plus 8 appendices and 5 maps.

Ray, G.E. (2006): Geology, mineral potential & 2005 work completed at the Romios Gold Resources property, McLymont Creek Forrest Kerr area, NW British Columbia; *BC Ministry of Energy, Mines and Petroleum Resources*, Assessment Report 29085, 189 pages.

Rhys, D.A. (2000): Geology and metallogeny of the Johnny Mountain area; *in* Metallogenesis of the Iskut River area, northwestern B.C., *Mineral Deposit Research Unit*, Special Publication Number 1, pages 300-324.

Souther, J.G. (1971): Geology and mineral deposits of Tulsequah map-area, British Columbia; *Geological Survey of Canada*, Memoir, 362, 84 pages**.**

Walcott, P.E. (2009): Geophysical Interpretation Report on the Grizz and Zip Properties, Assessment Report 30936, 86 pages plus maps.

Woodsworth, G.J., Anderson, R.G., Armstrong, R.L., Struik, L.C. and Van der Heyden, P. (1992): Plutonic regimes; *in* Geology of the Cordilleran Orogen in Canada, Gabrielse, H. and Yorath, C. J. (Editors), *Geological Survey of Canada*, Geology of Canada, No. 4, pages 493-531.

Atlin Placer Gold Nuggets Containing Mineral and Rock Matter: Implications for Lode Gold Exploration

by M.G. Mihalynuk, T.K. Ambrose[1], F.A.M. Devine[2] and S.T. Johnston[1]

KEYWORDS: placer gold, intrusive-related gold, Atlin, Yellow Jacket, gold deposit, listwanite, quartz-carbonate-mariposite alteration, Surprise Lake batholith, Boulder Creek, Otter Creek, Snake Creek, Quartz Creek, Ruby Creek, Pine Creek, Feather Creek, anthropogenic gold nuggets

INTRODUCTION

Placer gold deposits are derived from lode gold bedrock sources. Thus, gold placers are a first-order exploration vector for lode gold deposits. In many placer camps lode gold sources remain elusive as past attempts to trace placer mineralization upstream to the lode source have not met with success. However, an oft-overlooked and effective means for establishing a geological context for the lode gold source is to look for diagnostic mineral matter that is intergrown with the placer gold. Non-quartz mineral or rock matter is of most use as quartz is ubiquitous. In the Atlin placer camp of northwestern British Columbia (Figure 1), this methodology was applied to the juvenile placer deposits of Feather Creek (Sack and Mihalynuk, 2004) and diagnostic mineral intergrowths of gold with thorite and cassiterite were identified. These minerals provide an unambiguous genetic linkage to the U, Th and Sn-enriched Surprise Lake batholith (Figure 2). Such a relationship is not surprising given that most of the productive placer streams in the Atlin camp have at their headwaters the Surprise Lake batholith or its thermal metamorphic halo (Figures 2, 3). However past exploration efforts in the Atlin placer camp have followed the ultramafic-associated lode gold deposit model, focusing on the widely distributed altered ultramafic rocks. Indeed, within the entire Atlin camp, the only significant lode gold production is from altered mafic-ultramafic rocks at the Yellow Jacket deposit.

As a test for the utility of searching for more subtle intrusive-related lode gold sources of gold, this project looked for intrusive-related mineral matter intergrown with gold in nuggets recovered from five established placer streams in the Atlin camp. So far, we have been unable to repeat the results of Sack and Mihalynuk (2004) in any other placer stream. We find no clear signal of an intrusive-related source for the placer gold, nor do we see evidence of a listwanite lode gold source. In at least one placer stream, gold is intergrown with graphitic argillite in the stream bed.

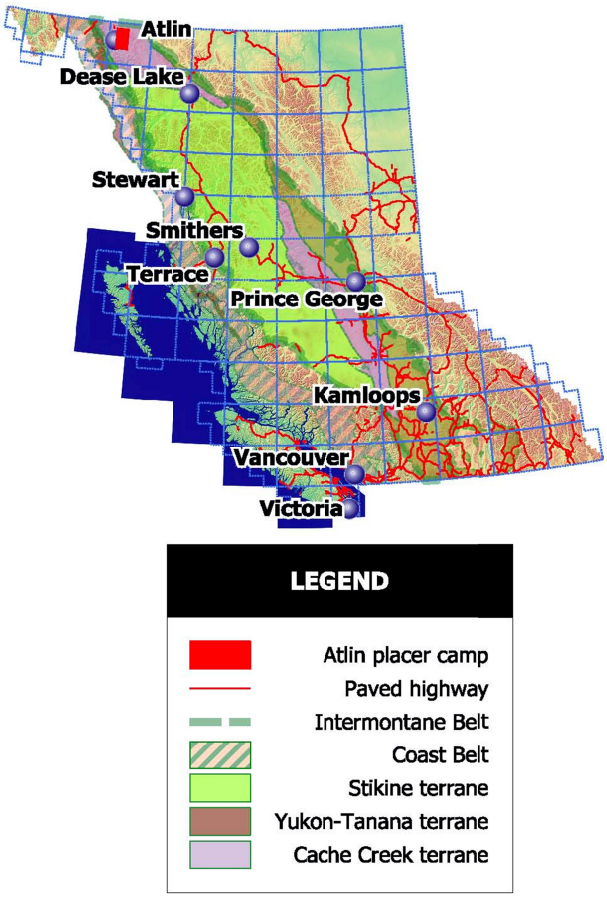

Figure 1. Location of the Atlin placer camp in northwestern British Columbia.

LODE GOLD EXPLORATION

Persistent exploration efforts in placer camps can succeed in revealing lode gold sources. One recent success story is at the margin of the historic Klondike district (Lowey, 2006), where a resurgence of lode gold

[1] *University of Victoria, Victoria, BC*

[2] *Merlin Geosciences Inc., Atlin, BC*

This publication is also available, free of charge, as colour digital files in Adobe Acrobat® PDF format from the BC Ministry of Forests, Mines and Lands website at http://www.empr.gov.bc.ca/Mining/Geoscience/PublicationsCatalogue/Fieldwork.

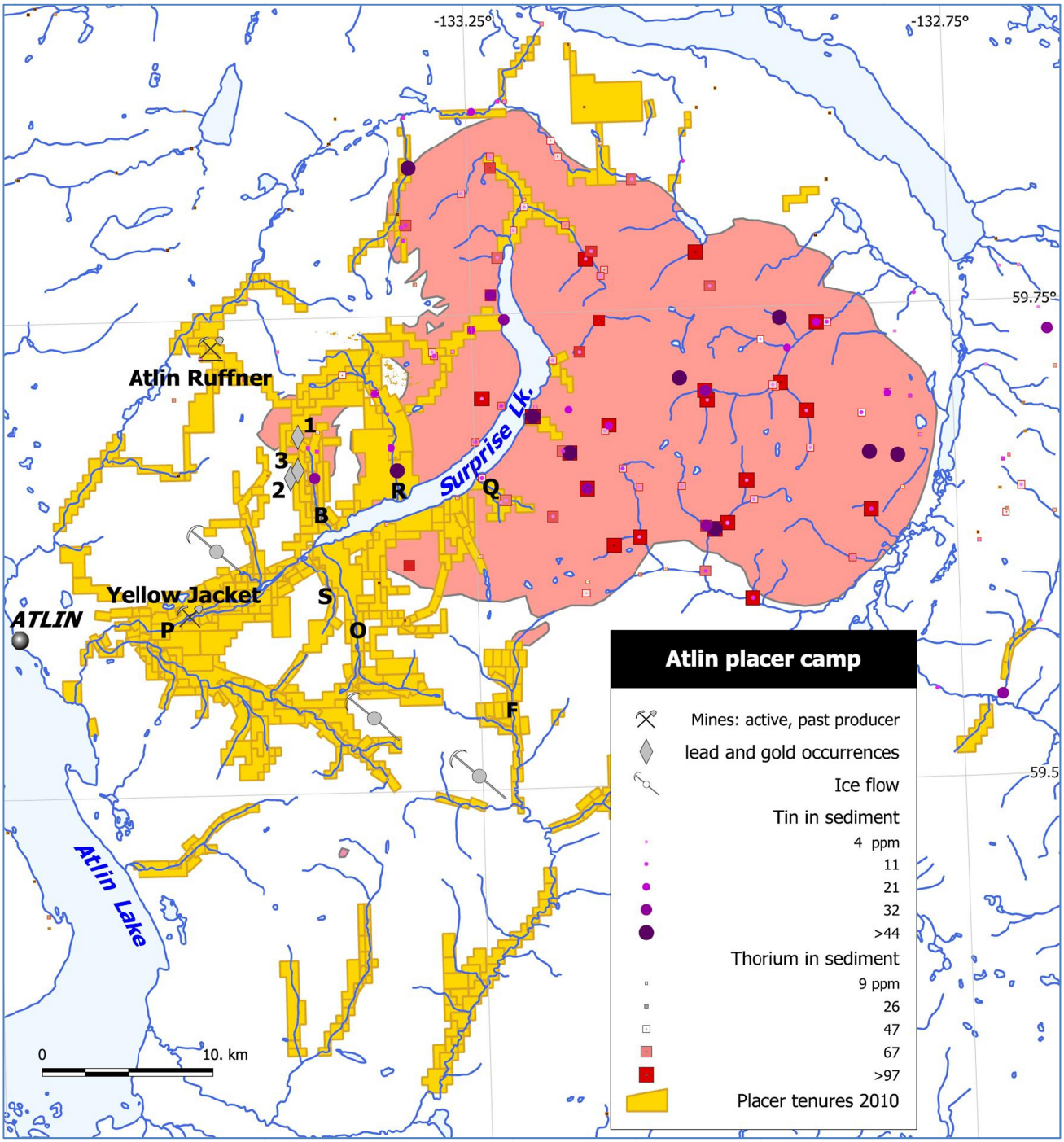

Figure 2. Map of the Atlin camp showing placer tenures (yellow) as of November, 2010. Almost all of the placer streams have the Surprise Lake batholith (pink) or its thermal metamorphic halo in their headwaters. There is a direct spatial relationship of regional stream sediment geochemical survey results for thorium (squares in shades of red) and tin (circles in shades of purple) with the areas underlain by the Surprise Lake batholith, showing that these elements are derived from the batholith. Creeks discussed in the text are denoted by the letters: B = Boulder, F = Feather, O = Otter, P = Pine, Q = Quartz, R = Ruby, S = Snake.

Figure 3. A view to the north over the placer operation on Snake Creek. In the middle background are disturbed white gravels of Boulder Creek which are largely derived from the underlying Surprise Lake batholith. Light-coloured slopes on the horizon are underlain by the Surprise Lake batholith.

exploration has followed discovery of the White Gold deposit in 2008 (Burke and Lewis, 2010). About 450 km to the south, lode gold exploration on the outskirts of Atlin has been on-going for more than a century. It was not until 2008, however, that viable lode gold production was demonstrated by Prize Mining Corporation (then Muskox Minerals Corp.) with the liberation of 18.63 kg of gold (doré with unspecified fineness) from a 2880 tonne bulk sample of the Yellow Jacket deposit (Figure 2; Dandy and Price, 2010).

Yellow Jacket deposit

The Yellow Jacket deposit has a historical resource estimate of 453 500 tonnes at 10.26 g/t Au (non-NI43-101 compliant; Schroeter and Pinsent, 2000). Lode gold is hosted in a faulted and altered mafic-ultramafite rock package beneath the Pine Creek valley floor, near the location of the first claims staked within the placer camp in 1898[1]. Ash (1994) recognized the quartz-carbonate-mariposite (chrome mica)-gold association and was successful in extracting mariposite from which undisturbed radiogenic argon release spectra could be obtained[2]. These release spectra provided ages of ~165-175 Ma, consistent with cooling following tectonic emplacement of the Atlin ophiolite and accretionary complex and intrusion of the Fourth of July batholith which cuts and immediately postdates emplacement fabrics (Mihalynuk *et al.*, 2004). Thus, Ash (2001) concluded that gold deposition was genetically related to ophiolite emplacement and that "The placers are considered to be derived from quartz lodes previously contained within the ophiolitic crustal rocks" (page 25).

More recent work at the Yellow Jacket deposit has shown that the highest gold grades are associated with a dark green, fine-grained andesite (Dandy and Price, 2010). This unit is described by Dandy and Price (2010) as forming irregular pods and slivers and containing 10-15% quartz phenocrysts along with hornblende±biotite and/or plagioclase. These authors attributed the concentration of auriferous vein material to the competency contrast between the andesite and the enclosing altered ultramafite. The brittle andesite "shattered" and the spaces thus formed between the fragments were then flooded with carbonate and auriferous quartz. Dandy and Price (2010) also believe that the Yellow Jacket gold mineralization to be related to the Pine Creek fault which cuts the ophiolite emplacement fabrics of Ash (1994). Gold mineralization and the associated alteration and veining assemblages that occur along the Pine Creek fault are, therefore, related to a younger mineralizing event, of as-yet undetermined age. Late-stage mariposite, which is spatially related to gold mineralization along the Pine Creek fault zone, could display reset ages or could record the age of the mineralizing event. Further analysis of mariposite in the area needs to be undertaken to confirm the timing relationships of local gold mineralization and alteration events. It is possible that there are multiple stages of mariposite-forming alteration within ultramafic rocks in the region, related to different structural and intrusive events.

If gold mineralization at the Yellow Jacket is typical of lode gold sources for most of the placer gold in the Atlin camp, then quartz, carbonate, pyrite and mariposite should occur as intergrowths with some of the impure gold nuggets. In our investigation of nuggets from five placer creeks we have observed quartz, carbonate and evidence of weathered pyrite and other minerals/alloys, but so far, no mariposite.

COMPOSITION OF IMPURE NUGGETS

Results of our study of impure nuggets are grouped according to the composition of the impurity. Here we present observations of rock matter, carbonate, pyrite and mercury. Nuggets that are an intergrowth of gold and rock were obtained from Otter, Snake and Boulder Creeks. At this point in the study, compositional analyses have been attempted only for the rock within the Otter Creek nuggets.

[1] *Placer workings that were about 50 years old were reported by the early placer miners ca. 1898. These old workings were probably of Russian origin, and indicate that low-grade placers were known in the Atlin camp by ca. 1850, prior to discovery of the rich placer deposits on Pine Creek (Bilsland, W.W. (1952): Atlin, 1898-1910: The story of a gold boom; British Columbia Historical Quarterly, Volume 16, Numbers 3 and 4; Reprinted in 1971 by the Atlin Centennial Committee, 63 pages with pictorial supplement) University of Victoria, Victoria, BC.*

[2] *Subsequent attempts (by MGM) to acquire undisturbed spectra from mariposite collected from altered ultramafic rocks elsewhere in the Atlin region have not been successful.*

Analytical Methods

All elemental analyses reported here are semi-quantitative. They have been obtained using the University of Victoria Advanced Microscopy Facility Hitachi S-4800 scanning electron microscope (SEM) fitted with a Bruker Quantax energy-dispersive x-ray spectroscopy (EDX) system. Operating conditions were optimized for EDX analysis of both points and fields on the grains. Working distance was set to approximately 15mm with a beam voltage of 20kV. Samples were mounted to aluminum or carbon stubs with either carbon tape or carbon paste. One sample from upper Otter Creek required a carbon coating as it was not sufficiently conductive.

Otter Creek nuggets

Rock matter intergrown with gold in nuggets recovered from the upper portions of Otter and Snake creeks appears to be of local derivation. In both cases the hostrock is fine-grained sediment that has been recrystallized. Like most placer workings, the Zogas operation on upper Otter Creek recovers gold from both pay gravels and regolith (Figure 4). Processing of regolith is primarily for detrital gold that has worked its way down into cracks within the fractured and weathered bedrock. Rock scraped from the placer pit in 2010 was black, graphitic and phyllitic argillite, commonly with quartz veins less than 1 cm thick. We know of two recently recovered nuggets with pieces of the graphitic argillite attached. The smaller of these, donated to us for analysis, is shown in Figure 5. Scanning Electron Microscope and Energy Dispersive Spectral analysis revealed nothing unexpected. The mineral matter is mainly quartz, with some Mg-Fe-bearing mineral, probably chlorite, and graphite(?); however, because it was necessary to coat the nugget with conductive carbon, carbon analyses are meaningless.

Snake Creek nuggets

Near the top end of Snake Creek, a small dredging operation has recovered nuggets of gold intergrown with rock (Figure 6). The rock matter appears to be recrystallized fine grained siliceous sediment. Unfortunately we were unable to obtain a sample for analysis. Outcrops of thermally altered cherty argillite and argillaceous chert located within the drainage basin at an elevation above the dredging operation represent the bedrock from which the gold was likely derived.

Boulder Creek nugget

A nugget of gold intergrown with very dark green to black rock was obtained from Boulder Creek. No elemental analysis of the rock has yet been performed. It appears monomineralic, has a hardness of ~3 (Figure 7), and is probably chlorite or serpentine.

Figure 4. Aerial overview of the Zogas' operation on upper Otter Creek. The deep part of the pit at right is excavated down to bedrock.

Figure 5. Gold intergrown with graphitic phyllite like that of the local creek bedrock (about 1.5 cm across).

Figure 6. Nugget from Snake Creek is gold intergrown with rock which is like thermally-altered argillaceous chert comprising the bedrock upstream. Scale divisions are millimetres.

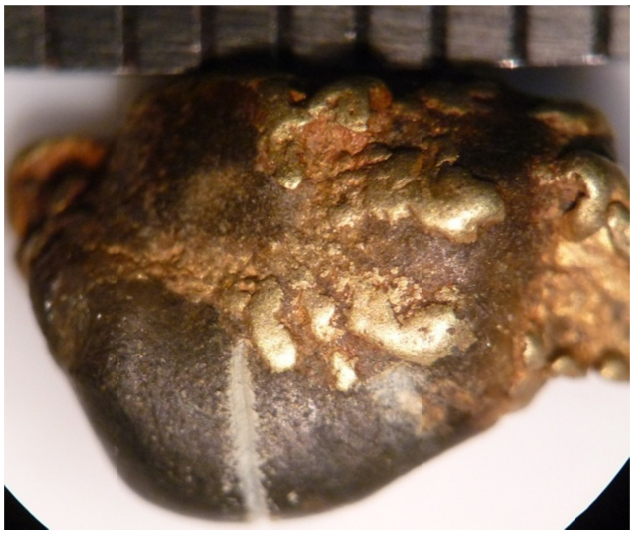

Figure 7. Photomicrograph of intergrown gold and rock nugget from Boulder Creek. The homogeneous rock matter was easily scratched to produce the furrow. Scale markings are millimetres.

Gold with mercury

Gold nuggets with conspicuous light silver patches were recovered from Quartz and Boulder creeks, and are common in placer gold recovered from Pine Creek. This patchy silver colouration is known as "mercury staining" (Figures 8a, b, c). SEM-EDX analyses of the silver patches confirmed that they are mixtures of mercury and gold. While the silver patches are distinct, they have diffuse margins. At high magnification, the surface of the gold appears fissured (Figure 8b) as a result of amalgam removed following attack by mercury.

Figure 8a. Nuggets from Quartz Creek with silver patches. Width of top nugget is about 1.5 mm.

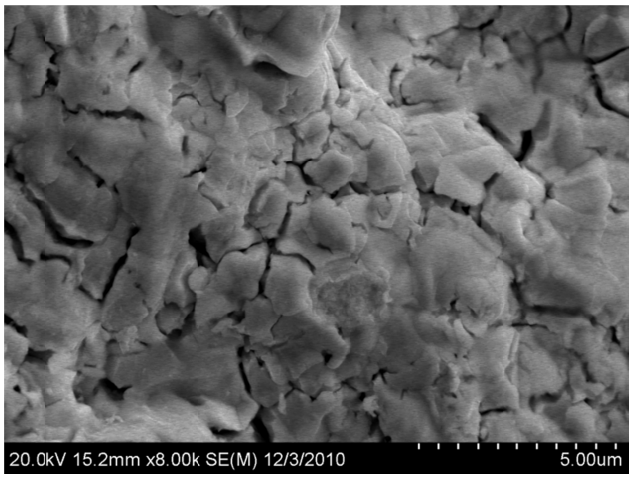

Figure 8b. SEM photomicrograph of sponge-like fissures created by mercury attack of a Boulder Creek nugget.

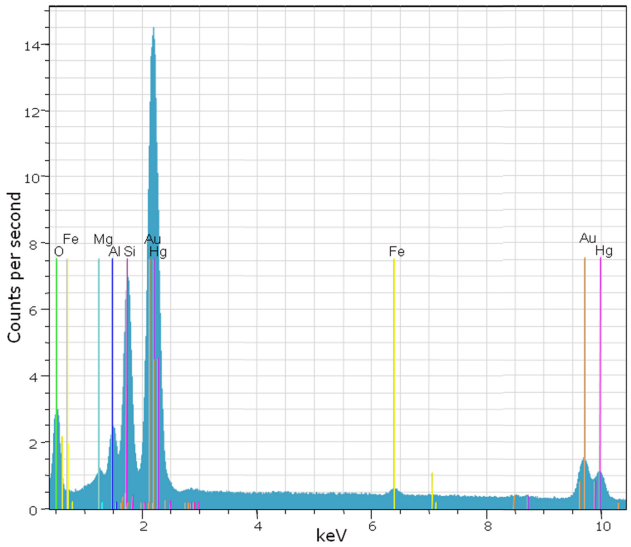

Figure 8c. EDX analysis of a broader field of view includes quartz and Fe-Mg mineral, probably chlorite.

Mercury was commonly used in most old placer camps to aid in recovery of fine gold from heavy separates, and staining from introduced sources of mercury is well known in Pine Creek, especially near the old Discovery showing. Modern knowledge of the cumulative toxicity of mercury in humans and the environment has resulted in severe curtailment of its use in all but the least regulated of nations. Naturally occurring native mercury is also common in most placer camps and we argue below that the mercury etching seen on nuggets from Boulder Creek could be a natural phenomenon rather than anthropogenic.

PSEUDO-BIOGENIC GOLD

One gold nugget from Boulder Creek was analyzed at high magnification to reveal a network of ovoid and filiform morphologies which resemble bacteria (Figure 9). Although evidence for gold mobility in biofilms has

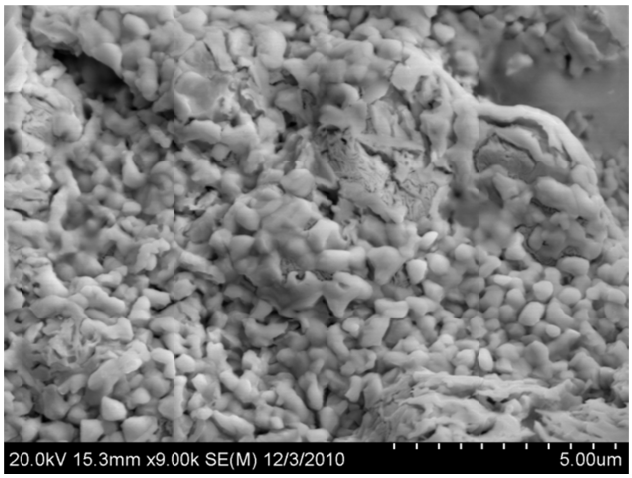

Figure 9. Pseudo-biogenic features on the surface of a gold nugget from Boulder Creek. EDX analysis shows the field of view to be Au with minor Ag.

recently been demonstrated for gold nuggets in Australia (Reith *et al.*, 2010), the textures that we observed are probably artefacts. Identical textures were discovered by John Watterson of the US Geological Survey during an SEM study of acid-cleaned gold nuggets from Lillian Creek in Alaska. These textures were found to be widespread in Alaskan placer deposits prompting the suggestion that bacteria was widely implicated in Alaskan gold nugget formation (Watterson, 1992). Watterson later retracted this hypothesis after he was able to reproduce the pseudo-biogenic structures with a combination of amalgam attack and nitric acid leaching (Watterson, 1994). Treatment of nuggets with nitric acid is a common practice in many placer camps and is specifically used to remove mercury staining.

We suspect that the Boulder Creek nuggets have NOT been subjected to nitric acid etching because such treatment leaves the gold bright and shiny; whereas the Boulder Creek nuggets are dull and partly Fe-oxide stained. These nuggets may have been subjected to low pH fluids formed naturally through the aqueous oxidation of pyrite which generates sulphuric acid. Cubic pits within some of the gold nuggets imaged suggest that pyrite, once intimately intergrown, has been removed by oxidation or mechanical action. Nevertheless, it is difficult to rule out the possibility that acid cleaned nuggets were subsequently stained. Such staining can occur in a few days if nuggets are left in waterlogged sluice concentrates together with rusting magnetite and pyrite.

MINERAL INCLUSIONS IN GOLD

Mineral inclusions within gold nuggets of the Atlin placer camp have been identified on the basis of crystal morphology and composition as determined by semi-quantitative EDX analyses. Identified minerals include: chlorite, Mg-calcite or dolomite, cerussite ($PbCO_3$), a range of Fe-oxides/hydroxides and quartz. Except for cerussite, these minerals are ubiquitous within the veins and country rocks of the Atlin camp. Cerussite is a common alteration product of galena and its occurrence in gold nuggets may indicate that gold streaks occur within sulphide veins. Auriferous polymetallic veins at the old Atlin Ruffner mine, located 5 km northwest of Boulder Creek headwaters (Figure 2), are associated with carbonate-altered lamprophyre dikes which cut the Fourth of July batholith and are, in turn, cut by the Surprise Lake batholith. Ore produced from 1916 to 1981 from the Ruffner had an average grade of 5% combined lead and zinc, 600 grams silver and 0.42 grams gold (MINFILE, 2006). Quaternary ice-flow direction is to the northwest (Levson and Blyth, 1993) and opposite to that required to carry ice-scoured materials from the Atlin Ruffner deposit to the Boulder Creek drainage. However, skarn mineralization at the South and Silver Diamond prospects (MINFILE, 2006), located at the margin of the Surprise Lake batholith in the Boulder Creek drainage (Figure 2, locations 1 and 2), is reported to contain galena. Gold is not reported as a commodity in these prospects, but the intervening Sunbeam occurrence (Figure 2, location 3) purportedly returned high gold assays (MINFILE, 2006).

Anthropogenic nuggets

For more than 100 years placer miners have been living and working along the placer streams of the Atlin camp. During much of this time waste materials were discarded into the bush or burned. Trash burning remains the most common form of garbage disposal. In the mid-1900s plastics would have been introduced to burning barrels and in the last few decades, electronic circuitry might have been added.

Some of the samples that we analyzed are likely "burning barrel nuggets". One nugget from Boulder Creek is primarily composed of lead, probably originally part of a lead acid battery. Another Boulder Creek nugget is a mixture of plastic and gold, perhaps the product of a smelting mishap, an accidental cabin fire, or a melted electronics component. A nugget from Snake Creek is relatively pure gold with a "splattered droplet" of lead-tin-zinc alloy (Figure 10) of the type used in the electronics industry prior to widespread replacement of lead-based solders with tin-silver-copper±antimony alloys. It is likely the product of a melted circuit board.

SUMMARY

Analysis of intergrown rock and gold nuggets in Otter and Snake creeks show that in each case the rock matter can be explained by a local bedrock source. In Otter Creek at least, a local source is consistent with angular, gold rich colluvium within the pay gravels (Levson, 1992). A rock-gold nugget from Boulder Creek could be the product of altered lamprophyre dike, but this hypothesis needs to be tested with further analyses. If so, it might have been sourced from mineralization similar to that of the nearby Atlin Ruffner mine where auriferous

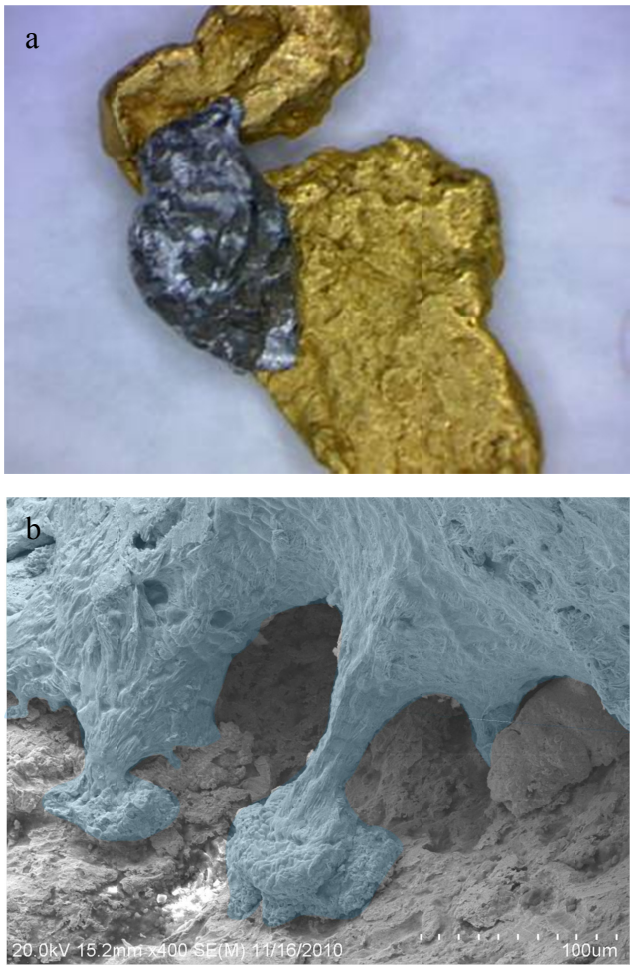

Figure 10. (a) Soft blue-grey metal attached to gold nugget (~0.5 cm long in photo) is shown to be a lead-tin-zinc alloy by analysis with SEM-EDX. It displays a morphology (b) interpreted as arising from a formerly molten drop (coloured blue) adhering to a gold substrate. It is probably the product of a melted circuit board.

lead-zinc ore was associated with lamprophyre dikes and may also be the source of cerussite intergrown with another Boulder Creek nugget.

In no nuggets did we find intergrown listwanitic alteration assemblage characterized by mariposite, as is found at the Yellow Jacket deposit (*e.g.* Dandy and Price, 2010), nor did we find cassiterite and thorite intergrown with gold as has been reported by Sack and Mihalynuk (2004). Multiple bedrock sources for the Atlin placer gold seems most likely, and the Surprise Lake batholith is still the most likely candidate for the ultimate source of gold. However, proving or disproving its role will require further study, including isotopic age determinations from both stages of mariposite growth at the Yellow Jacket, age of mineralization at the Atlin Ruffner, and age of thermal metamorphism of fine-grained sediment with gold-quartz veins in the Otter and Snake creek drainages. Future work also needs to focus on the composition of placer nugget impurities in the outlying creeks within the Atlin placer camp. Workers who study attached mineral matter need to be aware of the possibilities of anthropogenic contamination of gold nuggets.

An unequivocal underlying cause for the concentration of gold in the Atlin camp remains to be discerned.

ACKNOWLEDGMENTS

John Zogas generously provided samples of gold-rich placer clean-ups and impure nuggets from Otter Creek. Norm Graham liberally loaned nuggets from Quartz and Boulder creeks. Larry McKay shared his knowledge of placers in Snake Creek. SEM-EDX results presented here arise from the B.Sc. thesis work of T.K. Ambrose. SEM-EDX work at the Advanced Microscope Facility benefitted from the sage advice of Dr. Elaine Humphrey and Adam Schuetze. This research has been made possible by a NSERC Discovery grant to S.T. Johnston.

REFERENCES

Ash, C.H. (1994): Origin and tectonic setting of ophiolitic ultramafic and related rocks in the Atlin area, British Columbia (NTS 104N); *B.C. Ministry of Energy, Mines and Petroleum Resources*, Bulletin, 94, 48 pages.

Ash, C.H. (2001): Ophiolite related gold quartz veins in the North American Cordillera; *BC Ministry of Energy and Mines*, Bulletin 108, 140 pages.

Bilsland, W.W. (1952): Atlin, 1898-1910: The story of a gold boom; *British Columbia Historical Quarterly*, Volume 16, Numbers 3 and 4 (Reprinted in 1971 by the Atlin Centennial Committee, 63 pages with pictorial supplement).

Burke, M. and Lewis, L.L. (2010): Yukon hardrock mining, development and exploration overview 2009; *in* Yukon Exploration and Geology Overview 2009, MacFarlane, K. E., Weston, L. H. and Blackburn, L. R. (Editors), *Yukon Geological Survey*, 2010, pages 17-58.

Dandy, L. and Price, B.J. (2010): Yellowjacket Gold Project; *National Instrument 43-101 Technical Report*, 92 pages.

Levson, V.M. (1992): Quaternary geology of the Atlin area (104N/11W, 12E); *in* Geological Fieldwork 1991, *BC Ministry of Energy, Mines and Petroleum Resources*, Paper 1992-1, pages 375-390.

Levson, V.M. and Blyth, H. (1993): Applications of Quaternary geology to placer deposit investigations in glaciated areas; a case study, Atlin, British Columbia; *in* Applied Quaternary research., Bobrowsky, Peter, T ; Liverman and David (Editors), *Pergamon*, 20, pages 93-105.

Lowey, G.W. (2006): The origin and evolution of the Klondike goldfields, Yukon, Canada; *Ore Geology Reviews*, Volume 28, pages 431-450.

Mihalynuk, M.G., Erdmer, P., Ghent, E.D., Cordey, F., Archibald, D.A., Friedman, R.M. and Johannson, G.G. (2004): Coherent French Range blueschist: Subduction to exhumation in <2.5 Ma?; *Geological Society of America Bulletin*, Volume 116, pages 910-922.

MINFILE (2006): MINFILE/pc database; *BC Ministry of Energy and Mines*, www.em.gov.bc.ca/Mining/Geolsurv/Minfile/minfpc.htm, [November 22, 2005].

Reith, F., Fairbrother, L., Nolze, G., Wilhelmi, O., Clode, P.L., Gregg, A., Parsons, J.E., Wakelin, S.A., Pring, A., Hough, R., Southam, G. and Brugger, J. (2010):

Nanoparticle factories: Biofilms hold the key to gold dispersion and nugget formation; *Geology*, Volume 38, pages 843-846.

Sack, P.J. and Mihalynuk, M.G. (2004): Proximal gold-cassiterite nuggets and composition of the Feather Creek placer gravels: clues to a lode source near Atlin, B.C.; *in* Geological Fieldwork 2003, *BC Ministry of Energy, Mines and Petroleum Resources*, Paper 2004-1, pages 147-161.

Schroeter, T.G. and Pinsent, R.H. (2000): Gold production, resources and total inventories in British Columbia (1858-1998); *BC Ministry of Energy, Mines and Petroleum Resources*, Open File 2000-2, 96 pages**.**

Watterson, J.R. (1992): Preliminary evidence for the involvement of budding bacteria in the origin of Alaskan placer gold; *Geology*, Volume 20, pages 315-318.

Watterson, J.R. (1994): Artifacts resembling budding bacteria produced in placer-gold amalgams by nitric acid leaching; *Geology*, Volume 22, pages 1144-1146.

Geology and Mineral Potential of the Southern Alexander Terrane and western Coast Plutonic Complex near Klemtu, Northwestern British Columbia

by J.L. Nelson, L.J. Diakow, S. Karl[1], J.B. Mahoney[2], G.E. Gehrels[3], M. Pecha[3] and C. van Staal[4]

KEYWORDS: Alexander terrane, Grenville Channel fault, Coast Mountains, Coast Plutonic Complex

INTRODUCTION

Although the northern coastal area of British Columbia contains a significant number of tracts with high mineral potential assessments (Categories 1 and 2 out of 10; BC Mineral Potential Assessment Program; Kilby, 1995; see also Mineral Resources Assessment – Mineral Potential, on Mapplace.ca), mineral exploration has been at low levels, as indicated by the small number of assessment reports and recorded mineral showings. Just as it has received comparatively little exploration interest, this area also has not seen systematic public geological mapping since the original Geological Survey of Canada work in the 1960s (Roddick, 1970; Hutchison, 1982).

This report covers the second of a planned 3-year program study of the bedrock geology and mineral potential of the British Columbia North Coast area (Figure 1). The North Coast bedrock mapping and mineral deposit study is part of a cooperative, Natural Resources Canada (NRCan)-led endeavour, the *Edges Multiple Metals – NW Canadian Cordillera (British Columbia and Yukon) Project*. The Edges Project aims to increase our understanding of the far travelled lithotectonic terranes that make up the outer, accreted margin of the Canadian Cordillera and assess their metallic mineral potential (for a detailed project description see http://gsc.nrcan.gc.ca/gem/min/edges_e.php). Edges is a contribution to the GEM Program (Geo-mapping for Energy and Mineral), a federal program that was initiated in 2008, to enhance public geoscience knowledge of northern Canada in order to stimulate economic activity in the energy and mineral sectors. The Edges project is a collaboration between the Geological Survey of Canada, British Columbia Geological Survey, and Yukon Geological Survey and involves the United States Geological Survey and Canadian and American academic contributors.

The northern coastal area of British Columbia is underlain in part by rocks of the southern Alexander terrane, a large composite crustal fragment that underlies most of southeastern Alaska and extends farther north into part of the St. Elias Range on the Yukon-Alaskan border, (Figure 1; Wheeler *et al.*, 1991). The Alexander terrane as a whole has attracted considerable exploration interest because of the volcanogenic massive sulphide deposits that it hosts, including Niblack and others on southern Prince of Wales Island, just north of the British Columbia-Alaska border, as well as a trend of Triassic deposits, notably Windy Craggy and the Greens Creek mine (Figure 1). In 2009, the first year of the North Coast project, geological mapping began on and near Porcher Island, at the northern end of Alexander terrane rocks along the north coast, in order to take advantage of proximity to the much better known stratigraphy in southeastern Alaska, and to nearby volcanogenic mineral deposits. Mapping in 2010 focused on the southern end of the terrane near Klemtu. In 2011, sparse exposures of pre-plutonic stratified rocks in the intervening region will be documented.

PREVIOUS WORK

The northern coastal region of British Columbia was first mapped systematically as part of Geological Survey of Canada regional coverage of the entire Coast Mountains batholith and enclosed metamorphic rocks. The Porcher Island – Grenville Channel area was covered as part of the Prince Rupert – Skeena sheet (Hutchison, 1982) and the Douglas Channel – Hecate Strait sheet (Roddick, 1970), and the area around Klemtu as part of the Laredo Sound sheet (Baer, 1973), all at a scale of 1:250 000. The focus of these studies was on the plutonic rather than supracrustal rocks; in addition, modern tools for the analysis of metamorphosed volcanic and sedimentary sequences, including uranium-lead geochronology and trace element geochemistry, were not available at that time. Recent geological work in the northern coastal region of British Columbia has focused on understanding the structural and igneous history of the

[1] *United States Geological Survey, Anchorage, AK*

[2] *University of Wisconsin at Eau Claire, WI*

[3] *University of Arizona, Tucson, AZ*

[4] *Geological Survey of Canada, Vancouver, BC*

This publication is also available, free of charge, as colour digital files in Adobe Acrobat® PDF format from the BC Ministry of Forests, Mines and Lands website at http://www.empr.gov.bc.ca/Mining/Geoscience/PublicationsCatalogue/Fieldwork.

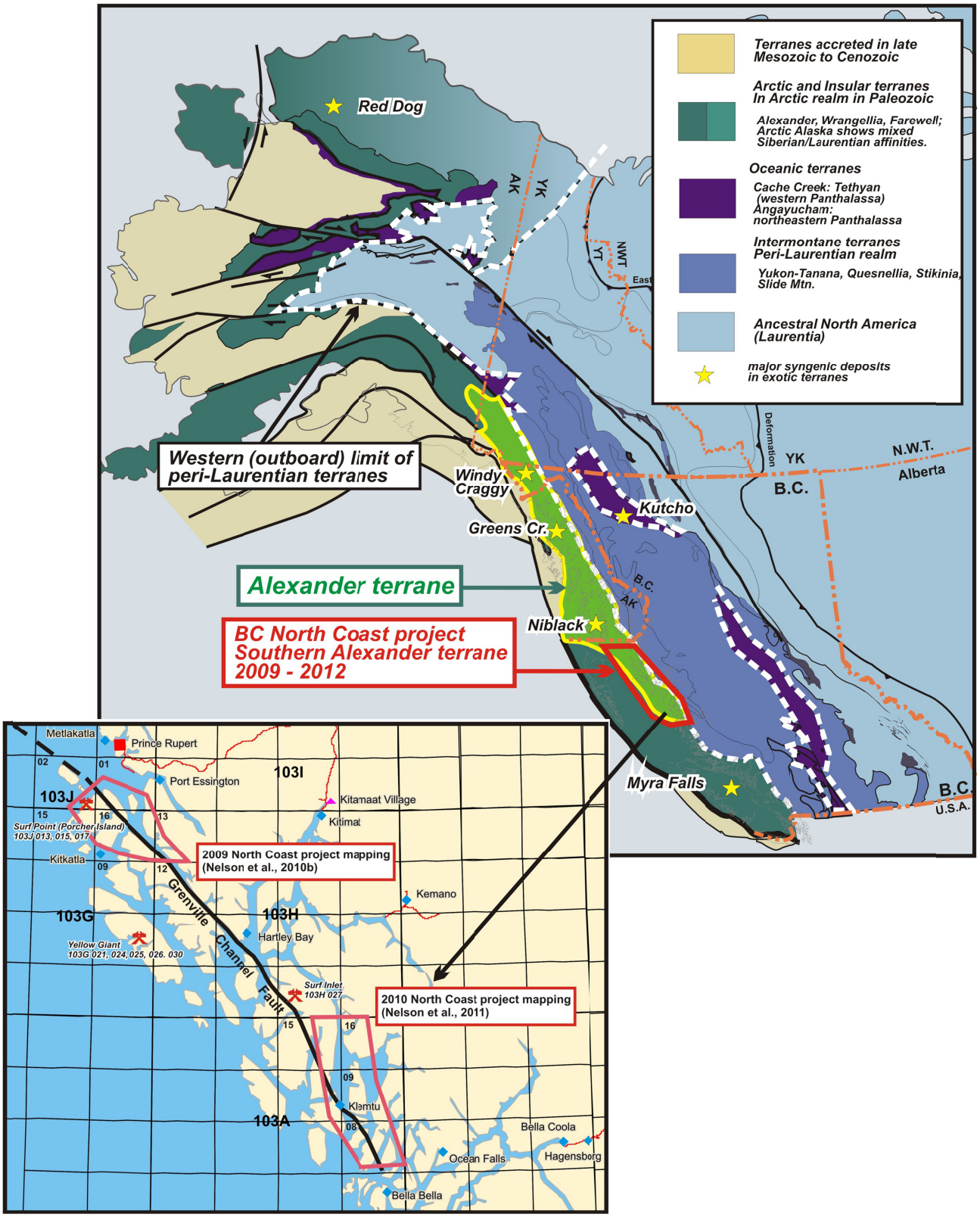

Figure 1. Location of the North Coast project in the context of northern Cordilleran terranes and in terms of local geography. Inset shows 2009 and 2010 field map footprints. Also shown on inset: trace of Grenville Channel fault, and location of major gold deposits.

Coast Mountains orogen. Within the North Coast project area, Porcher Island and Grenville Channel have been visited by researchers in the course of much broader structural studies and plutonic syntheses (Chardon *et al.*, 1999; Chardon, 2003; Butler *et al.*, 2006; Gehrels *et al.*, 2009). Detailed geology, in particular the pre-batholithic stratified rocks of the Alexander terrane, have not been thoroughly investigated. The sole exception to this is the ongoing, mostly unpublished, regional geologic work of George Gehrels, part of which is summarized in Gehrels (2001) and Gehrels and Boghossian (2000).

REGIONAL GEOLOGICAL SETTING

The Alexander terrane (Wheeler *et al.*, 1991), which forms the principal focus of this project, is flanked by variably metamorphosed and deformed metasedimentary-metavolcanic rock units that comprise the Banks Island assemblage to the west, and the Gravina belt and the Yukon-Tanana terrane to the east (Figure 2). With the exception of the Banks Island assemblage, which has only been recognized along the outer coast of northern British Columbia, these terranes continue northward into adjacent portions of southeastern Alaska, where equivalents have been described by Gehrels and Saleeby (1987; 1996), Rubin and Saleeby (1992), Saleeby (2000), and Gehrels (2001).

Alexander terrane

The Alexander terrane in southeastern Alaska and northern coastal British Columbia consists of a broad range of volcanic, sedimentary, and plutonic rocks and their metamorphic equivalents that are primarily of early Paleozoic age, overlain in places by thin younger sequences (Figure 3). In southeastern Alaska, these rocks have undergone limited post-Paleozoic metamorphism, deformation, and plutonism. Farther to the southeast, in northern coastal British Columbia, Cretaceous plutons become more widespread and the degree of Mesozoic deformation and metamorphism increases. In spite of these younger overprinting events, it is possible to correlate geologic units of southeastern Alaska with those of northwestern coastal British Columbia, and as such we use the nomenclature established in southeastern Alaska wherever possible. The following unit descriptions are taken from the well-preserved portion of the Alexander terrane in southern southeastern Alaska as decribed in Eberlein *et al.* (1983), Gehrels and Saleeby (1987) and Gehrels *et al.* (1996).

The oldest rocks recognized in the Alexander terrane consist of Late Proterozoic to Cambrian metavolcanic and metasedimenary assemblages of the Wales Group (Figure 3; Gehrels and Saleeby, 1987). Metavolcanic components range from mafic to felsic in composition, with lithic units ranging from metres to hundreds of metres in thickness. Relict textures indicate that protoliths of these rocks were pillowed flows, flow breccias, tuffaceous breccias, and tuffs. Metasedimentary units, similar in abundance to the metavolcanic rocks, consist of volcanic clast-rich metagreywacke, pelitc phyllite or schist, and marble. These assemblages are intruded by bodies of complexly interlayered gabbro, diorite, tonalite, and granodiorite, with layering commonly on a metre to decimetre scale. All rocks of the Wales Group have a strong foliation and lineation that are deformed by outcrop-scale open folds. Metamorphism ranges from greenschist facies (actinolite-chlorite-epidote assemblages) to amphibolite facies (amphibole-biotite-muscovite and rare garnet).

Rocks of the Wales Group in southeastern Alaska are overlain by a less deformed, Early Ordovician to Late Silurian suite of greenschist or lower metamorphic grade volcanic and sedimentary rocks referred to as the Descon Formation. Protoliths of these rocks are similar to those in the Wales Group. Dioritic to granitic plutons that are coeval (and probably cogenetic) with volcanic rocks of the Descon Formation are widespread.

Lower Paleozoic strata are overlain unconformably by a variety of Devonian strata that commonly include a basal clastic sequence (conglomerates and sandstones, including redbeds) of the Karheen Formation, mafic volcanic rocks of the Coronados Volcanics and St. Joseph Islands Volcanics, and limestones of the Wadlegh Formation (Eberlein and Churkin, 1970). The basal conglomerate is interpreted to represent a major phase of uplift and erosion, the Klakas orogeny, as it overlies and contains clasts of a wide variety of older rocks (Gehrels and Saleeby, 1987). Younger, local unconformities are represented by conglomerates in the Late Devonian Port Refugio Formation. The Port Refugio Formation also includes fossiliferous and locally dolomitic limestone, radiolarian chert, mafic and felsic volcanic rocks, and volcaniclastic turbidites. The variability of facies and the presence of locally-derived conglomerates and bimodal volcanic sequences in these formations suggest that they were deposited in rift basins.

Younger strata in the Alexander terrane include fine to medium grained clastic rocks, carbonate, minor basalt of Carboniferous and Permian age, and Triassic basal conglomerate overlain by bimodal volcanic rocks, carbonate, and volcaniclastic strata. The Upper Jurassic to Upper Cretaceous Gravina belt, described separately below, overlies the Alexander terrane.

VMS potential of the Alexander terrane

The Niblack prospect on southern Prince of Wales Island (Figure 1) is a copper-zinc-gold-silver-rich Kuroko-type volcanogenic massive sulphide deposit, with 2.6 million tonnes of indicated mineral resource grading 1.18 per cent copper, 2.33 grams per tonne gold, 2.19 per cent zinc and 33.18 grams per tonne silver; and 1.7 million tonnes of inferred mineral resource grading 1.55 per cent copper, 2.08 grams per tonne gold, 3.17 per cent zinc and 32.56 grams per tonne silver, as of July 2009 (http://www.heatherdaleresources.com/hdr/Projects.asp).

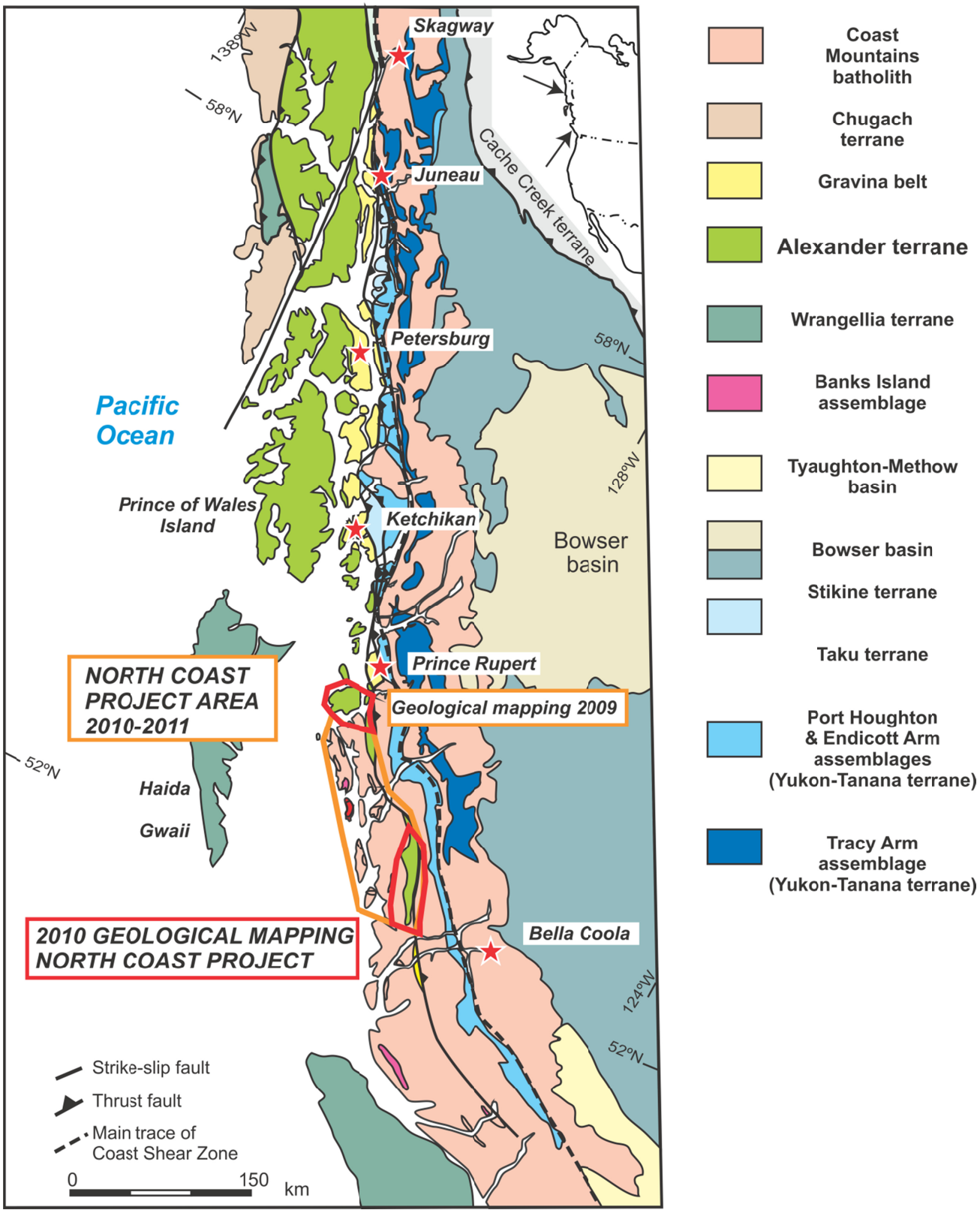

Figure 2. Regional geology and terrane map of northern coastal British Columbia and southeastern Alaska; G.E. Gehrels, 2009.

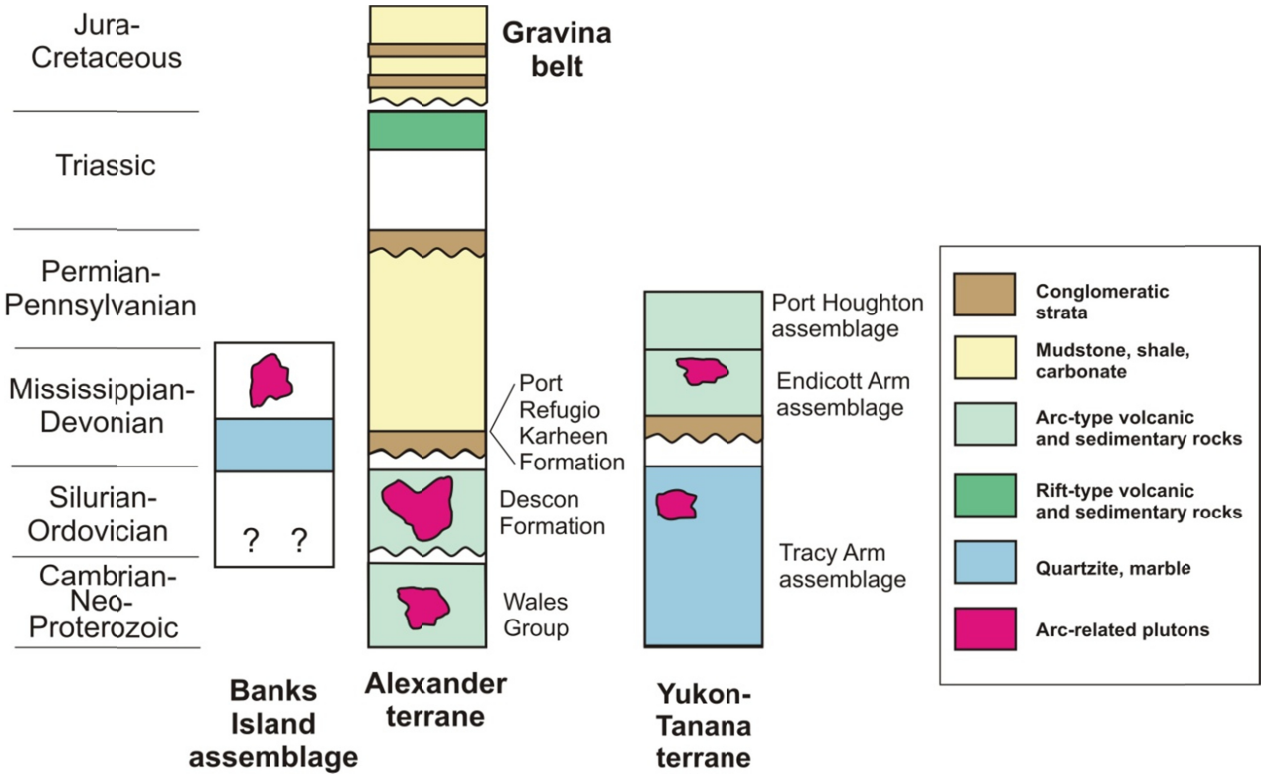

Figure 3. Stratigraphic columns for major terranes of southeastern Alaska and coastal northwestern British Columbia.

It is currently optioned by Heatherdale Resources Inc., an affiliate of Hunter Dickinson Inc., from Niblack Mineral Development Inc. It is located within a tightly folded pyroclastic rhyolite unit, the Lookout rhyolite, that lies above a mixed felsic to mafic volcanic sequence and below a section of mafic volcanic rocks, all of which have been assigned to the informal Moira Sound unit by Ayuso *et al.* (2005) and Slack *et al.* (2005). Although it has been regarded as hosted by the Wales Group (Gehrels *et al.*, 1996), a recent Ordovician U-Pb zircon date of *ca.* 478 Ma has been obtained from the Lookout rhyolite (Karl *et al.*, 2009). Ayuso *et al.* (2005) and Slack *et al.* (2005), as well as Gehrels *et al.* (1983), point out that volcanogenic deposits are known both in this unit and within the Wales Group and that both Neoproterozoic and Ordovician volcanic sequences are prospective for syngenetic base metal mineralization.

Other terranes and assemblages

Banks Island assemblage

The Banks Island assemblage (Figures 2, 3) has been recognized as a distinct unit of possible continental margin affinity, based on the predominance of interlayered quartzites (meta-quartz arenites) and marbles, which are rare in the generally more primitive Paleozoic arc-related assemblages of the Alexander terrane (Gehrels and Boghossian, 2000). These rocks are exposed on the southern shore of Banks Island, on western Porcher Island, and on the outer islands as far south as Klemtu. The dominant lithic components are strongly deformed and regionally metamorphosed metaclastic quartzites that commonly occur in centimetre-scale bands (Figure 4), marble layers with thicknesses of several centimetres to several tens of metres, and pelitic phyllite/schist. These rocks everywhere have a well-developed foliation and display outcrop-scale isoclinal folds. Pelitic components have been metamorphosed to biotite phyllite or schist, and garnet is present in some regions.

Figure 4. Banks Island assemblage on southern Digby Island, showing typical lithology of quartz siltstone laminae in carbonate.

The age of the Banks Island assemblage is constrained by the following relationships:

1) detrital zircons recovered from two quartzites are as young as ~415 Ma (Silurian-Devonian boundary; G. Gehrels, unpublished data),
2) an orthogneiss on Aristazabal Island that has undergone the regional deformation and amphibolite-facies metamorphism along with the adjacent marble and metabasite has yielded a U-Pb age of 357 Ma (Early Mississippian), and
3) plutons of Late Jurassic age are emplaced into these rocks (Gehrels *et al.*, 2009) and at least locally intrude across the regional foliation and folds.

These constraints suggest that at least some portions of the Banks Island assemblage accumulated during mid-Paleozoic time.

Yukon-Tanana terrane

East of the Alexander terrane are metavolcanic and metasedimentary rocks of the Yukon-Tanana terrane that underlie the western margin of the Coast Mountains, along the length of southeastern Alaska and northern coastal British Columbia (Figure 2). In general, these rocks form a panel that dips eastward and youngs westward, suggesting an overall inverted stratigraphy. Using the nomenclature defined in southeastern Alaska (Gehrels *et al.*, 1992), the Yukon-Tanana terrane includes the following units (Figure 3):

1) Tracy Arm assemblage: This package contains marbles, quartzites, pelitic schists, and orthogneisses, which are commonly high in metamorphic grade and migmatitic. The age of this unit is constrained as Devonian or older based on ages from the overlying Endicott Arm assemblage.
2) Endicott Arm assemblage: This unit has a distinctive basal conglomerate containing clasts derived from the Tracy Arm assemblage. Overlying strata include greenschist to amphibolite facies felsic to mafic metavolcanic rocks, pelitic schists, and minor marble. Available faunal and U-Pb geochronologic constraints suggest that most strata are Devonian-Mississippian in age.
3) Port Houghton assemblage: These strata gradationally overlie the Endicott Arm assemblage and consist of greenschist to amphibolite facies metaturbidites, pelitic schist, and metabasalt. Available faunal constraints suggest that most strata are late Paleozoic in age.

In northwestern British Columbia, the Ecstall belt (Alldrick, 2001; Alldrick *et al.*, 2001; see also Gareau and Woodsworth, 2000) with its enclosed Devonian volcanogenic deposits, is also assigned to the Yukon-Tanana terrane. The host units are equivalent to the middle, Endicott Arm assemblage of southeastern Alaska.

Gravina belt

Rocks of the Alexander terrane are overlain by Upper Jurassic to Upper Cretaceous (Oxfordian to Cenomanian) turbidites and subordinate mafic volcanic rocks of the Gravina belt. These rocks can be traced, generally along the inboard margin of the Alexander terrane, for the length of southeastern Alaska (Berg *et al.*, 1972) and into northern coastal British Columbia (Figure 2). On Tongass Island in southeastern Alaska, and on the mainland east of Port Simpson (Lax Kw'alaams) rocks assigned to the Gravina belt also overlie a sequence of metavolcanic and metasedimentary rocks that have been assigned to the Yukon-Tanana terrane (Gehrels, 2001).

Plutons of the western Coast Plutonic Complex

Tonalitic to granodioritic plutons of the Coast Plutonic Complex, or Coast Mountains batholith, occur as isolated bodies in northern and western portions of northern coastal British Columbia, and increase in extent southeastward to form huge continuous bodies of plutonic rock (Gehrels *et al.*, 2009; Figure 2). Compositionally, most are tonalite and granodiorite, with subordinate diorite and minor gabbro and leucogranodiorite. A large majority of plutons have hornblende abundances exceeding those of biotite, are rich in titanite, and some plutonic suites contain euhedral epidote that is interpreted to be magmatic in origin.

According to a recent comprehensive geochronological summary (Gehrels *et al.*, 2009), plutonic U-Pb ages record a history of eastward migration of emplacement across the Coast Mountains. The westernmost plutons are 160-140 Ma (Late Jurassic) tonalites and granodiorites. Early Cretaceous (120-100 Ma) tonalites and granodiorites occur directly east of the Late Jurassic bodies. A nearly continuous band of 100-85 Ma plutons (*e.g.* Ecstall pluton of Hutchison, 1982) underlies the western margin of the Coast Mountains, succeeded eastward by mainly tonalitic sills of *ca.* 70-60 Ma (latest Cretaceous-earliest Tertiary) age, and the central and eastern portions of the Coast Mountains are underlain by huge 60-50 Ma (Eocene) granodiorite bodies.

The emplacement depth of plutons also increases eastward across the Coast Mountains as shown by hornblende barometric studies conducted by Butler *et al.* (2001). This work suggests that westernmost Late Jurassic bodies were emplaced at depths of ~15 km, whereas Early Cretaceous plutons were slightly deeper, ~20 km, and farther east, mid-Cretaceous plutons of the Ecstall belt were emplaced at significantly greater depths, perhaps 25-30 km. This increase in depth of emplacement correlates well with the eastward increase in metamorphic grade.

SUMMARY OF PORCHER ISLAND – NORTHERN GRENVILLE CHANNEL GEOLOGY

The 2009 map area, comprising the vicinity of Porcher Island, northwestern Pitt Island and Grenville Channel, is underlain by metamorphosed supracrustal and plutonic rocks, intruded by late synkinematic Cretaceous plutons and cut by an array of northwest-striking sinistral faults that divide the geology of Porcher Island into a series of panels (Nelson *et al.*, 2010a, b). Some faults mark major lithologic breaks, whereas others repeat similar sequences. The Grenville Channel fault (GCF) is the master fault; from it the Salt Lagoon and Useless fault splays cross Porcher Island. The northern continuation of GCF in Telegraph Passage may be an older, dextral structure (J. Angen, personal communication, 2010).

Detailed field mapping, supported by U-Pb geochronology (Gehrels and Boghossian, 2000; Butler *et al.*, 2006; J.B. Mahoney, unpublished data, 2010; G. Gehrels, unpublished data, 2010) has allowed positive identification of many units in the mapped area, and tentative assignment of others. Because they are based on more complete geochronological data, unit ages and assignments shown on the open file map of the area (Nelson *et al.*, 2010b) supercede those in Nelson *et al.* (2010a). Most important, field identification in 2009 of possible Wales Group equivalents on Porcher Island (Nelson *et al.,* 2010a) was refuted by subsequent Ordovician U-Pb ages. The main metavolcanic sequence, which comprises most of the Alexander terrane in this area, is correlated with the Ordovician Descon Formation (*s.l.*) of southeast Alaska. In particular, it resembles the rhyolite-bearing Moira Sound unit, which hosts the Niblack volcanogenic massive sulphide deposit. Clastic rocks on Kennedy Island and near Baron Point on the mainland are correlated with the Early Devonian Karheen Formation.

Pre-Cretaceous plutonic bodies include the Ordovician McMicking and Hunt Inlet plutons, the Early Mississippian (?) Swede Point pluton, and a Devonian pluton in Porcher Inlet. Southwest of the metamorphosed supracrustal units, two metamorphosed igneous complexes, the Ogden Channel and Billy Bay complexes, are recognised. The Billy Bay complex is an intrusive equivalent of the Descon volcanic sequence. At this point, no conclusive age determination on the Ogden Channel complex has been made.

LOCAL GEOLOGY – 2010 MAPPING NEAR KLEMTU

The 2010 map area is located 100 km southeast of the 2009 map area, in eastern Laredo Sound (103A) map sheet. It extends from Return Channel in the south to Graham Reach, on the eastern side of Princess Royal Island, in the north (Figure 1). As shown in Figure 5, most of this area is underlain by large plutons, with deformed and metamorphosed older stratified rocks of the Alexander terrane exposed in narrow pendants between them. The southern projection of the Grenville Channel fault passes through Klemtu Pass at Klemtu, then crosses Finlayson Channel and continues south through Jackson and Oscar passages and into southern Mathieson Channel.

Because of difficult access to the island interiors and extensive forest cover, most of the observations that form the basis of our mapping were made along shorelines. These were supplemented with logging road traverses, helicopter spot checking and limited traverses, together with image analysis of 5-metre resolution SPOT-5 satellite data captured between 2004 and 2006.

The geology in Figure 5 is based on a 1:50 000-scale open file map in preparation that will be available in early 2011 (Nelson *et al.*, 2011).

Stratified Units

Mathieson Channel Formation

Strong lithologic similarities between layered metasedimentary and metavolcanic pendants in the Alexander terrane scattered throughout the 2010 map area have led to their inclusion within a single map unit, herein named the Mathieson Channel Formation. Because the original depositional relationships and stratigraphic continuity of units is disrupted by strike-slip faults, several generations of intrusive rocks and repeated by isoclinal folding, no simple stratigraphic section can be constructed, and true thicknesses of the stratigraphic layers are uncertain due to folding and structural repetition. However, overall stratigraphy of the Mathieson Channel Formation is based on consistent internal lithologic features and contact relationships that are documented in the layered units throughout the area. Figure 6 shows an interpretive stratigraphic section of the formation, measured along the eastern shoreline of Pooley Island. It includes the following provisional stratigraphic members:

1) Clastic-carbonate member
   Calcareous siliciclastic rocks and calcarenite make up the most widespread and abundant map unit.
2) Marble member
   Clastic-poor carbonates grade into the main clastic-carbonate member. They form mappable bodies in the Graham Reach area.
3) Conglomerate-greywacke member
   Coarse clastic units are locally important on eastern Pooley Island where they are interlayered with the clastic-carbonate member. They also occur at a few other sites in the area.
4) Andesite-gabbro member
   Andesite sills and flows (?) are restricted to part of the eastern shore of Graham Reach.

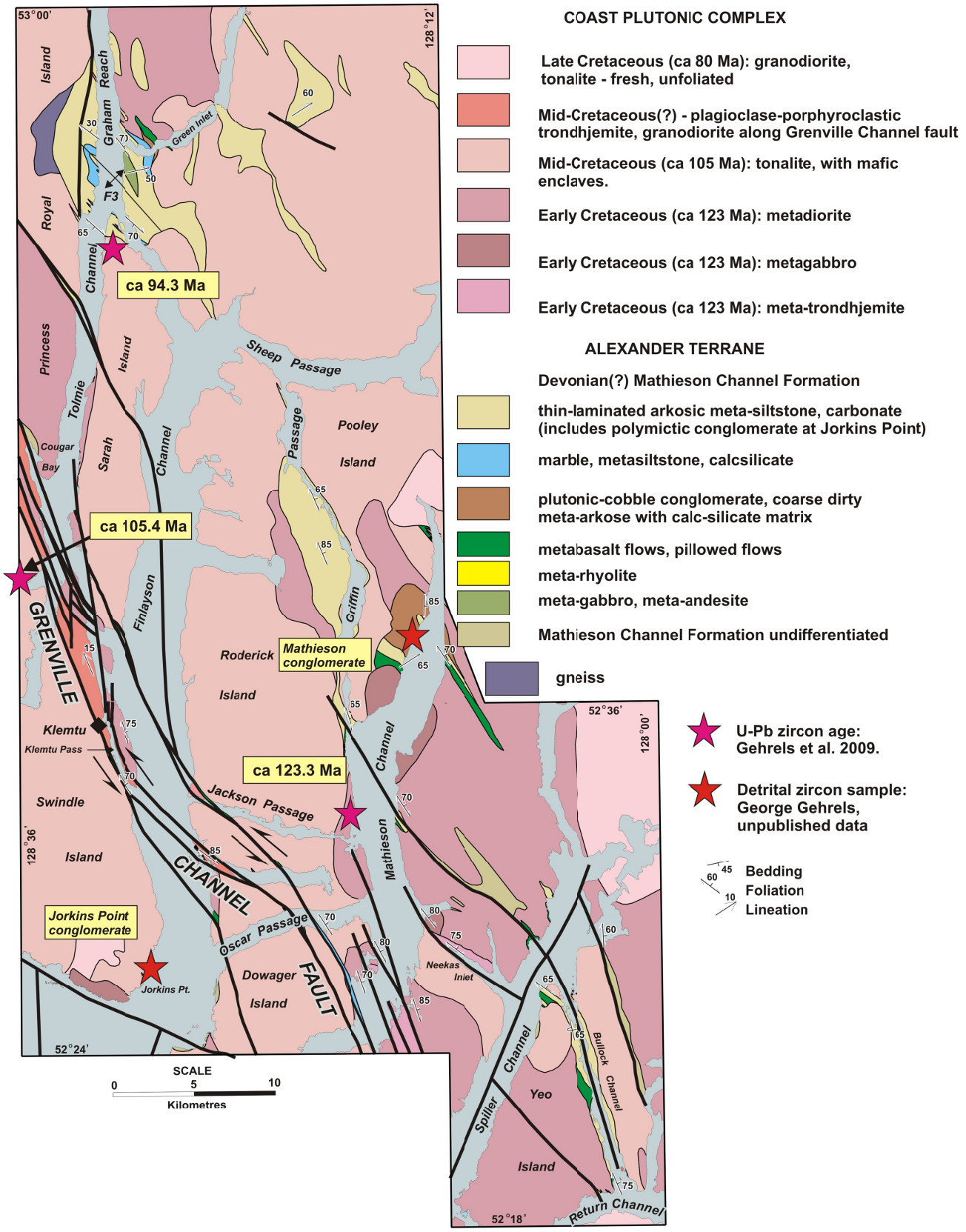

Figure 5. Geology of northeastern Laredo Sound map area (103A). Geological mapping 2010 (J. Nelson, L. Diakow, S. Karl, J.B. Mahoney, G.E. Gehrels, M. Pecha and C. van Staal. Some contacts from Baer, 1973).

5) Volcanic member: Dominated by basalts and volumetrically minor rhyolites, this sequence tends to occur west of, and possibly stratigraphically beneath, the clastic and carbonate members.

Interfingering and transitional relationships are observed between all of these units; thus the Mathieson Channel Formation is inferred to represent the varied fill of a single basin. Observations that support inferred depositional relationships between the various units are described below.

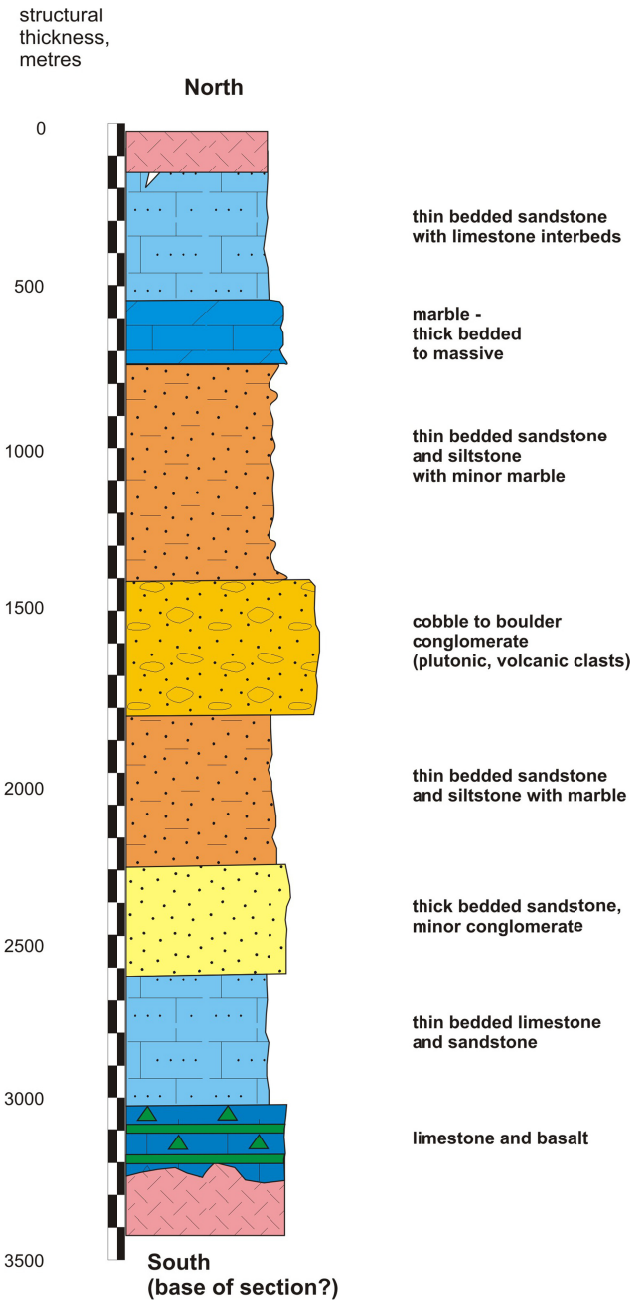

Figure 6. Structural-stratigraphic section of Mathieson Channel Formation on east shoreline of Pooley Island.

Clastic-carbonate member

This unit typifies exposures in of the Alexander terrane in the map area. It comprises metasiltstones and lesser metasandstones and metagreywackes, which in places alternate on a millimetre to decimetre scale with impure carbonates and calcsilicates. The regular, thin parallel layering and lamination in this unit are distinctive (Figure 7a). The main clastic components, as determined petrographically, are quartz and plagioclase, with significant orthoclase in some samples. Grains are equant, and form polygonal, fine-grained aggregates. In the metasiltstones, quartzofeldspathic laminae of millimetre to centimetre thickness have biotite-rich partings. Trace detrital minerals include titanite, apatite and zircon. Metagreywacke alternates with "purer", less biotite-rich clastic intervals. Some of the thicker bedded sandy sequences are distinguished by rusty orange weathering, and pinkish or reddish colours in outcrops (Figure 7b). The quartz-feldspar metasiltstone layers contain abundant, finely distributed reddish brown (Fe^{+3}-rich) biotite and pyrite or pyrrhotite. These phases formed in equilibrium

Figure 7a. Clastic-carbonate member of the Mathieson Channel Formation. Thinly layered metasiltstone in impure marble (meta-calcarenite), characteristic of finer grained facies of Mathieson Channel Formation (10JN07-01; 543688E, 5871816N).

Figure 7b. Clastic-carbonate member of the Mathieson Channel Formation. Redbeds, Sarah Head (10JN05-10; 533126E, 5859204N).

with calcic plagioclase, hornblende, and diopside in amphibolite facies metamorphism. They indicate original Fe-rich composition of the otherwise well-sorted arkosic protolith. We consider it likely that these were redbeds that contained authigenic matrix hematite. Inferred arkosic protoliths, supported by a sample from the mountains east of Graham Reach that contains fine laminae of pure granular apatite, suggest a plutonic provenance for the clastic-carbonate member.

Although sedimentary structures are rarely preserved in this unit, graded beds were observed in relatively coarse, thick-bedded sandstones in Bullock and along Spiller channels (Figure 7c). Possible siltstone cross-laminations were also noted in carbonate at several localities, including Sarah Head at the northern tip of Sarah Island (Figure 7d). Given the degree of deformation, these delicate laminations may not be primary depositional features.

Carbonate layers are generally impure, ranging from calcite-rich meta-calcarenite to pale green, diopside-rich

Figure 7c. Clastic-carbonate member of the Mathieson Channel Formation. Sandstone sequence in Bullock Channel. Thickest bed shows grading, and contains grit-size plutonic clasts (10JN12-05; 564040E, 5801153N).

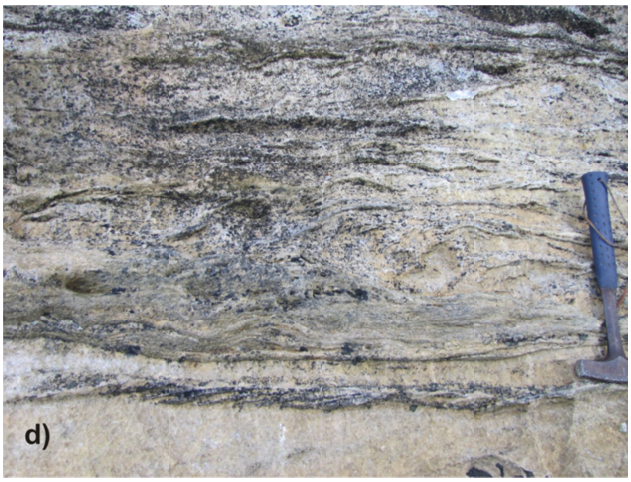

Figure 7d. Clastic-carbonate member of the Mathieson Channel Formation. Delicate crossbeds of quartz-feldspar in impure marble, Sarah Head (10JN05-10; 533126E, 5859204N).

calcsilicate. Very dirty marbles, dense with tiny irregular clasts, may have contained fossil hash; but deformation and recrystallization prevent a positive identification of any possible biogenic material in them.

Dark meta-argillites form a relatively minor component of the unit, found mainly along Bullock Channel near the southern terminus of the Alexander terrane. In general, argillaceous rocks appear to increase relative to pure carbonates toward the southern end of the belt, which may represent the deepest part of the basin.

Conglomerate-greywacke member

A sequence of thick-bedded conglomerate and greywacke is exposed for over 2 km along the eastern shore of Pooley Island next to Mathieson Channel. The true thickness of this unit is difficult to determine because deformation has produced variable bedding attitudes (Figure 6). The conglomerate beds consist of elongate, rounded, but poorly sorted plutonic and subordinate volcanic clasts (Figures 8a, b), and vary from matrix to clast-supported deposits. Individual clasts range in size from 1 to over 40 cm in diameter; average size is in the 10 cm range. Grading and erosive bases of beds are seen in some places (Figure 8a). Elsewhere in this exposure, conglomerates take the form of trains of clasts concentrated in a poorly sorted matrix composed of angular, sand-size lithic and mineral grains.

The intrusive clasts are medium grained equigranular to porphyritic in texture, consistent with fairly shallow depths of emplacement. None contain a foliation developed prior to incorporation in the clastic deposit. Most were deformed after lithification and exhibit varying degrees of flattening. Clast compositions include tonalites and also plagioclase-phyric granodiorites. The volcanic clasts are mostly basalt, less commonly dacite and/or rhyolite. Abundant diopside in the conglomerate matrix attests to an original micritic matrix.

Conglomerates at Pooley Island extend eastward across Mathieson Channel to a locality where multiple thin beds are intercalated with clastic-carbonate layers. Elsewhere, the northern extent of the conglomerate member includes minor occurrences in Griffin Passage and Green Inlet.

Transitional contacts are observed between the conglomerate-greywacke member and the overall finer-grained and more thinly layered clastic-carbonate member. On eastern Pooley Island, the two members are interbedded on a metre scale, and in one case a granitoid cobble lies within carbonate. In Griffin Passage, intrusive clasts occur in a carbonate matrix, in a metre-thick bed interlayered with more typical carbonate and in sandstone-siltstone (Figure 8c). The extreme size and compositional contrast between igneous clasts and calcarenitic matrix suggest these could be lag deposits. These observations document that the coarse, high-energy conglomerate-greywacke unit is integral to the Mathieson Channel Formation. It does not rest unconformably upon

Figure 8a. Conglomerate-greywacke member. East Pooley Island conglomerate with erosive base (10JN11-04; 552198E, 5832156N).

Figure 8b. Conglomerate-greywacke member. Granitoid and dark green mafic volcanic clasts (10SK04-2; 553101E, 5833771N).

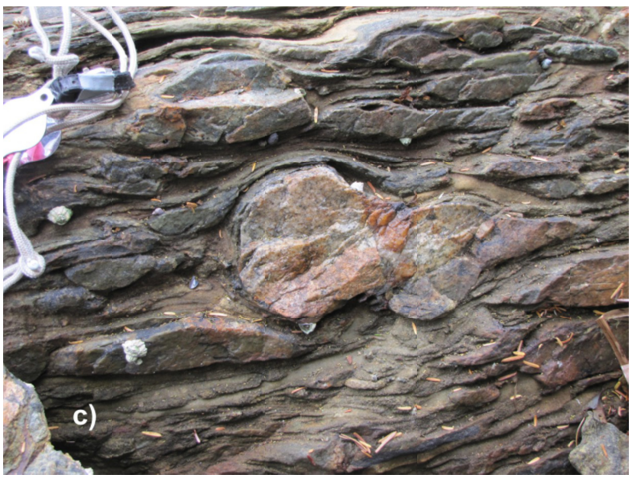

Figure 8c. Conglomerate-greywacke member. Conglomerate clasts in carbonate matrix, Griffin Passage (10JN18-01; 544781E, 5842872N).

it, and thus does not represent a basal conglomerate.

Marble member

Pure or nearly pure marble forms mappable layers in the Mathieson Channel Formation. Intervals of pure bedded marbles, thickest along Graham Reach, pass gradationally into more clastic-rich variants. Thin, discontinuous marble units also occur along faults that transect Jackson and Oscar passages. Marble layers vary considerably in thickness, due in part to plastic flow during deformation that produced tight folds. They weather buff yellow-tan with white coarsely crystalline fresh surfaces One of them, at Quarry Point (MINFILE 103A 007), was previously mined for use at the Swanson Bay pulp mill, 11 km to the north.

Andesite-gabbro member

Dark green meta-igneous rocks occur along the east shore of Graham Reach south of Green Inlet. Some appear to be metamorphosed dikes and/or sills of andesitic composition with fine to coarse-grained textures. Locally there are fragmental or pseudofragmental textures, and some intrusives contain coarse grained gabbro clasts in a highly deformed matrix. This unit may be entirely intrusive and thus not part of the supracrustal succession.

Volcanic member

Mappable bodies of metabasalt, in places containing carbonate pods, occur in southwestern Bullock Channel, along Spiller Channel, in Mathieson Channel, on the south end of Sarah Island, in northern Graham Reach and in Green Inlet. There are also metabasic mylonites along the Grenville Channel fault and its splays. In the least deformed exposures, pillows and pillow breccias are distinguishable (Figure 9a), as well as layers of angular scoria in carbonate matrix. Microscopically, some of the otherwise mafic (hornblende-calcic plagioclase-rich) metabasalts also contain biotite and/or potassium feldspar. These minerals suggest unusually potassium-rich, alkalic compositions.

Small occurrences of metarhyolite accompany the basalt at a few localities, at both ends of the Bullock Channel exposures, and along Spiller Channel. In Return Channel and into the south end of Bullock Channel, off-white weathered, coherent rhyolite shows delicate flow-banding (Figure 9b). At the north end of Bullock Channel and in one outcrop along Spiller Channel, rhyolite breccias occur, consisting of angular white fragments in darker matrix.

Along Bullock Channel, there are gradational contacts between the volcanic and clastic-carbonate members of the Mathieson Channel Formation. The base of the clastic member there contains fine grained tuffaceous layers; and some siltstones are anomalously rich in orthoclase compared to siltstones elsewhere. It is likely that the abundant potassium feldspar is locally derived from rhyolitic sources, as may be the case at the southern end of Bullock Channel. This volcanic to fine

Figure 9a. Volcanic member. Pillow basalt, Spiller Channel; note preservation of protolith features in amphibolite grade metamorphism (10SK02-8; 560835E, 5814316N).

Figure 9b. Volcanic member. Flow-banded metarhyolite (10JN12-01; 564086E, 5796866N).

volcaniclastic to clastic transition appears to young northeastward. Overall, volcanic rocks are most abundant in the more westerly exposures of the Mathieson Channel Formation. For this reason, we tentatively regard it as a northeast-facing sequence, with a volcanic-rich base succeeded by clastic and carbonate members in the upper section.

The rhyolite flow in Return Channel is presumed to occupy a low stratigraphic position within the Mathieson Channel Formation and was sampled for U-Pb zircon geochronology to determine its eruptive age which would place a lower stratigraphic age constraint on the formation.

DEPOSITIONAL ENVIRONMENT, AGE, DETRITAL ZIRCON CHARACTER AND POSSIBLE CORRELATIONS

The Mathieson Channel Formation was deposited in marine conditions, as shown by the prevalence of limestone. Its along-strike homogeneity and interlayered and gradational contact relationships between all of the members suggest deposition within a single marine basin. Depths did not generally exceed the carbonate compensation depth. Possible redbed protoliths within the sequence are also an indication of shallow-water deposition. Conglomerates are most abundant in the type area on Pooley Island and nearby; overall conglomerate forms less than 5 per cent of an overall sequence of arenaceous clastics interlayered with carbonates. The local occurrences of coarse, poorly sorted conglomerate and more widespread but thin intervals of greywacke indicate periodic mass flow deposition, perhaps related to basin-margin faulting. Their restricted occurrence argues against deposition in a large-scale submarine fan, as does the inferred general shallow depth of water. The presence of small-scale bimodal volcanism is consistent with a rift origin for the basin. Overall, a rifted, epeiric sea in a subtropical, arid setting, into which ephemeral streams locally discharged high loads of coarse sediment is envisaged. Sandy and silty fractions may have been re-deposited by tidal currents or storm surges that alternated with background carbonate deposition.

In some regards, the Mathieson Channel Formation resembles the sandstone-conglomerate unit on Kennedy Island in northern Grenville Channel (Nelson *et al.*, 2010a) which, in turn, has been correlated with the Karheen Formation of southeastern Alaska. The Karheen Formation was named for a succession of conglomerate, sandstone, siltstone, shale and minor limestone exposed on Prince of Wales Island (Eberlein and Churkin, 1970, Gehrels and Saleeby, 1987). Conodont and brachiopod biostratigraphy indicate the formation is middle Early Devonian (Pragian) in age. The formation overlies Silurian and older rocks, and is interpreted as part of a subaerial to shallow marine clastic wedge that coarsens and thickens to the southeast (Eberlein and Churkin, 1970; Gehrels and Saleeby, 1987). Detrital zircon geochronology from the Karheen Formation includes a *ca.* 420-450 Ma dominant population, apparently derived from Late Ordovician and Silurian plutonic rocks of the southern Alexander terrane, and a diverse, much less abundant Middle Proterozoic to Late Archean population of unknown cratonic derivation (Gehrels *et al.*, 1996).

Like the Karheen Formation, the cobble population from conglomerate in the Mathieson Channel Formation is dominated by shallowly emplaced (unfoliated, medium grained to porphyritic) granitoids, and sandstone compositions are similarly arkosic with disseminated biotite. However, the great thickness and extent of boulder-rich facies and large-scale crossbedding that characterize the Karheen Formation are not present in the Mathieson Channel Formation. Instead, the fairly minor, local conglomerates in the latter are interpreted as mass-flow deposits, some with erosive bases. Further, the Karheen Formation does not contain regular intervals of carbonate or the monotonously thin-bedded siltstones that are so common in this unit. Overall, the Mathieson Channel Formation is finer grained and more calcareous

than the Karheen Formation, features that may reflect smaller scale uplift in a less active basin.

At present, a single detrital zircon sample has been analysed from the conglomerate-sandstone member of the Mathieson Channel Formation on Pooley Island ; it shows a unimodal peak at about 420 Ma (Gehrels and Boghossian, 2000; Gehrels, unpublished data, 2010). This is somewhat younger than typical Ordovician-Silurian populations in the Karheen Formation of southeast Alaska (Gehrels and Boghossian, 2000) and gives an earliest Devonian maximum age for the unit. Like the Karheen, the signature reflects a plutonic source terrane younger than the mainly Ordovician volcanism of the Descon Formation.

Given the probable Devonian age of the Mathieson Channel Formation and its mode of origin in a shallow, marine basin bounded in part by local scarps, it could represent a separate basin analogous to the rift basins in which the Karheen Formation probably accumulated. Another possible correlative in the Alexander terrane of southeast Alaska is the Late Devonian Port Refugio Formation, defined by Eberlein and Churkin (1970). It consists of greywacke, conglomerate, thinly-bedded siltstone and shale, limestone, basalt in the form of lava flows, both pillowed and brecciated, and tuff and minor rhyolite.

Jorkins Point conglomerate

An unusual quartzite-cobble conglomerate outcrops on the headland 2 km northeast of Jorkins Point on southern Swindle Island. It is described separately here because it represents a pericontinental source completely unlike the plutonic-volcanic sources of the Mathieson Channel Formation. At its southernmost exposure, it is poorly sorted and immature, consisting of angular centimetre to decimetre-size fragments of impure quartzite, along with a few clasts of metasiltstone and diopside-rich, carbonate-altered metavolcanics in a dirty, diopsidic calcsilicate matrix (Figure 10a) Farther north along the shoreline, the conglomerate becomes more polymictic with increasing quantities of volcanic and siltstone clasts, and better sorted; cobbles are more rounded (Figure 10b). The most southerly exposure has the aspect of a nearly single-sourced fanglomerate, while its continuation to the north indicates farther transport and mixing of lithologic types. Texturally, the local occurrence of conglomerate and the abrupt variation in degree of maturity resemble base-of-scarp deposits in rift basins, for instance along the Eskay rift in northwestern British Columbia (Alldrick *et al.*, 2005). The next exposure to the south of the conglomerate, across a septum of tonalite and diorite, is a thin-layered calcsilicate-metasiltstone unit that resembles the quartz-plagioclase (±orthoclase) arenitic siltstones in the Mathieson Channel Formation.

Microscopically, the quartzite clasts are dominated by coarse grained, interlocking quartz, but they also

Figure 10a. Jorkins Point conglomerate. Chaotic, poorly sorted conglomerate of mostly quartzite clasts in calcsilicate matrix (10JN02-01; 535273E, 5810889N).

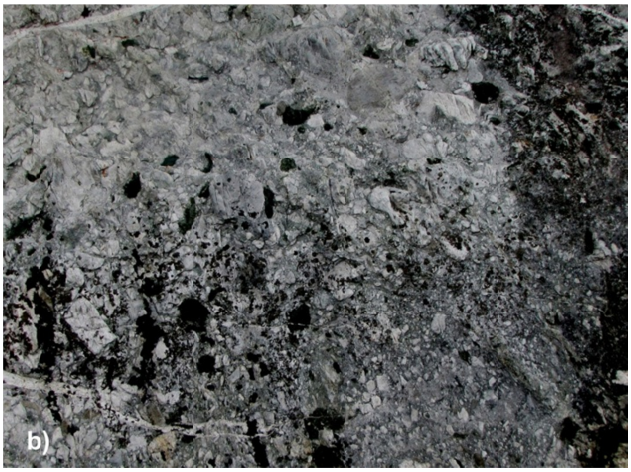

Figure 10b. Jorkins Point conglomerate. Polymictic conglomerate with more clast rounding and sorting. FOV 2 metres. (10JN02-01a; 535255E, 5811050N).

contain minor quantities of plagioclase, orthoclase, diopside, titanite, hornblende and tiny zircon grains.

Siltstone clasts are finely laminated and contain varying proportions of fine grained quartz, plagioclase, and orthoclase, and mafic laminations in which hornblende, titanite and diopside dominate. These have a strong resemblance to siltstones that are widespread in the Mathieson Channel Formation. The presence of orthoclase in them is particularly noteworthy, in that it is of somewhat restricted occurrence within the Mathieson Channel Formation.

A detrital zircon sample of quartzite clasts from the conglomerate shows a very broad Precambrian peak between about 900 and 2000 Ma, with lesser peaks to 2600 Ma; no Paleozoic grains were identified (George Gehrels, unpublished data, 2010). The cratonal signature of the Jorkins Point quartzites contrasts markedly with signatures of both autochthonous northwestern North America (Gehrels *et al.*, 1995) or the more inboard, pericratonic Yukon-Tanana terrane (Gehrels and Kapp, 1998; Nelson and Gehrels, 2007). It suggests an exotic

origin. However, the resemblance of siltstone clasts to the Mathieson Channel Formation may provide a sedimentological link between the two units. In this case, pericontinental rocks possibly formed part of the basement to the Mathieson Channel basin, and the Jorkins Point conglomerate could have formed along a western scarp. Gehrels *et al.* (1996) argued that the Silurian-Devonian Klakas orogeny involved interaction between the Alexander terrane and an outboard (present coordinates) continental fragment, such as is represented by the Banks Island assemblage (Gehrels and Boghossian, 2000; Figure 2, this paper). The Jorkins Point conglomerate may represent a "missing link" between the two. Ongoing detrital zircon studies (J.B. Mahoney, 2010-11) may shed light on this important potential correlation.

Intrusive units

As shown on Figure 2, over 90 per cent of the project area is underlain by Cretaceous intrusive rocks of the western Coast Plutonic Complex. In the original mapping of the Laredo Sound area (Baer, 1973), the granitoids were given unit assignments based on composition and degree of foliation. This study benefited from the use of uranium-lead zircon dates from representative sites in the area (Gehrels *et al.*, 2009), as well as an enhanced appreciation for styles of deformation of the plutonic bodies. This has resulted in significant changes in the location of plutonic contacts and interpreted contact relationships.

Uranium-lead ages reported by Gehrels *et al.* (2009) were important in the definition of three main plutonic suites in the study area (Figure 5). The oldest plutonic suite is based on an age of *ca.* 123 Ma from a site north of the east end of Jackson Passage (Figure 5), obtained from a penetratively deformed, amphibolite grade diorite-pyroxenite-gabbro complex. In our mapping, this metaplutonic complex corresponds to most of Baer's unit 2 and some of his unit 3; several small bodies of trondhjemite, shown on his map as unit 5, are also part of the complex. The second plutonic suite ranges in age from *ca.* 104 to *ca.* 94 Ma and is dominated by large homogenous tonalite bodies that comprise much of Sarah and Roderick islands, adjacent to Finlayson Channel. These plutons range from comparatively leucocratic and unfoliated cores (Baer's unit 5) to darker and more foliated margins (Baer's unit 3). The youngest plutonic suite, designated as unit 14a in Baer (1973), have several ages of approximately 82 Ma. One small intrusion was mapped near James Bay, along the western shoreline of Mathieson Channel. This body continues southeast across the channel where a coeval age indicates that it also includes a body previously mapped as Baer's unit 5. These significant changes emphasise the importance of new detailed mapping in concert with U-Pb dating as necessary to the understanding of the Coast Plutonic Complex.

Early Cretaceous (ca. 123 Ma) mafic intrusive complex

A deformed and metamorphosed, generally mafic plutonic suite outcrops extensively along both sides of Mathieson Channel. Similar bodies also occur northwest of Klemtu and north of Green Inlet. Diorite is the dominant phase, although variants from ultramafite to trondhjemite are present. Where large enough, the gabbro-ultramafite and trondhjemite bodies have been mapped separately from the main, undivided, dominantly dioritic bodies. It should be noted, however, that this suite shows strong variability even at outcrop scale (Figure 11a).

Diorites, which are most abundant throughout these complexes, are typically penetratively foliated to protomylonitic with asymmetric fabrics (Figure 11b). The foliation involves fine grained metamorphic hornblende, accompanied by quartz, calcic plagioclase, and titanite. Primary igneous minerals survive as pseudomorphs and porphyroclasts. Gabbro bodies contain areas of ultramafic cumulates, for instance near the eastern entrance of Jackson Passage. Ultramafites are metamorphosed to coarse grained tremolite/actinolite-clinochlore-biotite assemblages, in one case with bright green picotite (?) grains. Trondhjemites south of southern Mathieson Channel are highly foliated to protomylonitic, with a strong biotite fabric (Figure 11c).

No relationships with angular discordance were observed between phases of this complex and the Mathieson Channel Formation. Foliation involving amphibolite-facies assemblages is strongly developed in both, parallel to their contacts.

A U-Pb age of 123.3 ± 1.4 Ma was reported by Gehrels *et al.* (2009) from this suite, at a location 1.5 km north of the eastern end of Jackson Passage. The sample is from a medium-grained diorite with moderate foliation, which grades compositionally into gabbro and tonalite. The latest phase at this outcrop is a highly foliated trondhjemite/pegmatite dike (Figure 11a).

An unusual body of partly protomylonitic granodiorite in Neekas Inlet is tentatively assigned to this suite, based on its occurrences as a northwest-aligned sliver, and its degree of deformation. In it, coarse igneous microcline grew in equilibrium with plagioclase, and large brown allanite grains are rimmed with epidote. Subsolidus mylonitic fabrics include wispy biotite trains partly overgrown by late muscovite and chlorite, quartz ribboning and extensive development of trains of small neoblasts. Well-formed epidote grains grow across biotite. This body will form part of a U-Pb geochronological study by M. Pecha, aimed at constraining ages of deformation (2010-11).

Figure 11a. *Ca.* 123 Ma intrusive complex. U-Pb site north of Jackson Passage; outcrop-scale intrusive complex. Note wall-parallel foliation in crosscutting trondhjemite dike. FOV 1.5 metres.

Figure 11b. *Ca.* 123 Ma intrusive complex. Well-foliated metadiorite (10JN20-02; 549391E, 5816174N).

Figure 11c. *Ca.* 123 Ma intrusive complex. Protomylonitic trondhjemite (10JN25-06; 551404E, 5808794N).

Mid-Cretaceous (ca. 94-105 Ma) tonalite and quartz diorite

Bodies of tonalite transitional to quartz diorite compositions underlie most of the islands adjacent to Finlayson Channel, forming part of a batholithic mass that dominates the Laredo Sound map area. Baer (1973) designated these rocks as units 3 and 5; however, only relatively minor internal compositional and textural variability are recognized and hence these units are now combined (Figure 5). Distinguishing features of these plutons include uniform off-white color that approaches greyish shades with increasing mafic mineral content, ubiquitous mafic enclaves, and comparatively weak to moderate strain manifested by aligned mafic minerals and enclaves (Figures 12a, b).

Internally, the large tonalite bodies are medium grained, equigranular and have consistent mineralogy dominated by zoned plagioclase, euhedral hornblende and interstial quartz. Aligned biotite aggregates define foliation. Titanite is sparse but ubiquitous. The presence of mafic enclaves distinguishes these tonalite bodies. They typically make up less than 3 per cent of the rock, but particularly in border phases they may constitute more than 40 per cent. Composed of plagioclase and mafic minerals, they are amphibolites with fine- to medium-grained texture, and variably strained. Depending on strain intensity, the enclaves vary from ovoid to lenticular in shape.

Tonalite in Meyers Channel, west of Klemtu has several U-Pb ages averaging about 104 ± 1.5 Ma, and a single age of 94.3 ± 1.4 Ma was obtained at the northern end of the tonalite body on Sarah Island (Gehrels, 2009).

Figure 12a. Mid-Cretaceous (94-105 Ma) tonalite suite. Typical tonalite from the mid-Cretaceous suite displays elongate mafic enclaves.

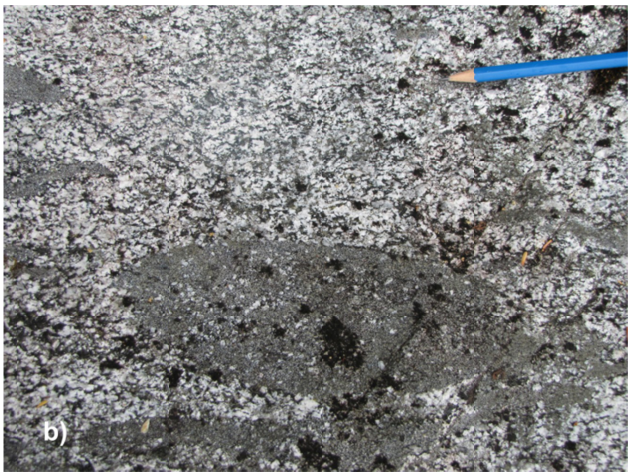

Figure 12b. Mid-Cretaceous (94-105 Ma) tonalite suite. Detail of foliated tonalite with mafic enclaves – note plagioclase porphyroblasts in the enclaves, which are compositionally identical to igneous plagioclase in the tonalite (10JN21-01; 534258E, 5820134N).

Figure 12c. Mid-Cretaceous (94-105 Ma) tonalite suite. Mid-Cretaceous tonalite with enclaves, showing moderate igneous foliation, cuts and surrounds *ca.* 123 Ma amphibolite facies metadiorite (10JN25-02; 552821E, 5814165N).

Contacts between tonalite and rocks from the older mafic complex and Mathieson Channel Formation are exposed on shorelines of Sarah Island in Tolmie Channel, and in southern Mathieson Channel. Most contacts are sharp breaks, presumed to be steep faults; however, in a few localities clear crosscutting relationships can be observed, in which phases of the tonalite suite cut across the transposition foliation in the metamorphic rocks, and the amphibolite fabric in the *ca.* 123 Ma plutons. Tonalite dikes intrude rocks of the older mafic complex and at one locality tonalite engulfs rounded, milled blocks of foliated metadiorite and pyroxenite at its contact with the mafic complex. In southern Mathieson Channel, a weakly foliated, mafic enclave-rich border phase of a large tonalite pluton contains large inclusions of amphibolite-facies metadiorite (Figure 12c).

Late Cretaceous (ca. 80 Ma) tonalite

A tonalite stock north of James Bay, western Mathieson Channel represents the youngest pluton in the study area. This small body comprises the western lobe of a larger pluton, unit 14a, that Baer (1973) extends southeastward across the channel and beyond the study area. Apophyses of the pluton cut obliquely across the general northwest regional structural fabric, and contacts are sharp and intrusive into rocks of the Mathieson Channel Formation and Early Cretaceous plutonic suite. Near the margin of the pluton on the south side of James Bay, angular inclusions with internal foliation occur in undeformed tonalite matrix. Shoreline exposures typically are white; and bold cliffs with sparse jointing pass at higher elevation into clusters of steep-sided knobs supporting only sparse tree cover.

The tonalite body near James Bay overall resembles those comprising the mid-Cretaceous suite; however, mafic enclaves are not present and the pluton lacks features due to regional metamorphism or deformation, unlike parts of the older suite. Internally, the James Bay tonalite is homogeneous and consists of medium-size grains of equigranular plagioclase and quartz, in addition to 10-15 per cent combined mafic minerals (biotite and lesser hornblende). Except for incipient replacement of zoned plagioclase by fine opaques, all minerals are pristine and unstrained. Prismatic titanite is abundant.

The timing for emplacement of these undeformed tonalitic intrusions is inferred from U-Pb dating at the eastern extension of the body that straddles Mathieson Channel, which is 81.7 ± 1.2 Ma (Gehrels *et al.*, 2009). An equivalent U-Pb date was also obtained immediately north from a circular pluton originally assigned to Baer's (1973) unit 5. Elsewhere in the study area, however, because of distinguishing lithologic features and in absence of supporting geochronology, we have reassigned other unit 5 tonalitic plutons to the mid-Cretaceous suite.

White pegmatite and aplite dikes occur regionally, cross-cutting all other rock units. They are probably related to the mid- and Late Cretaceous intrusive suites. Pegmatitic boudins in the Mathieson Channel Formation show that deformation continued during Cretaceous intrusion.

STRUCTURAL GEOLOGY AND METAMORPHISM

Structural styles and metamorphic grades in the map area are specific to the major rock units. Both the Mathieson Channel Formation and the older (*ca.* 123 Ma) Cretaceous intrusive suite are characterized by penetrative deformation at amphibolite grade: this is characterized by polyphase folding within the layered metamorphic rocks and penetrative foliations in the plutons (Figure 13a). Planar fabrics in the map area strike northwest and deep steeply to the east, an orientation that is common throughout the western Coast Mountains (Rusmore *et al.*,

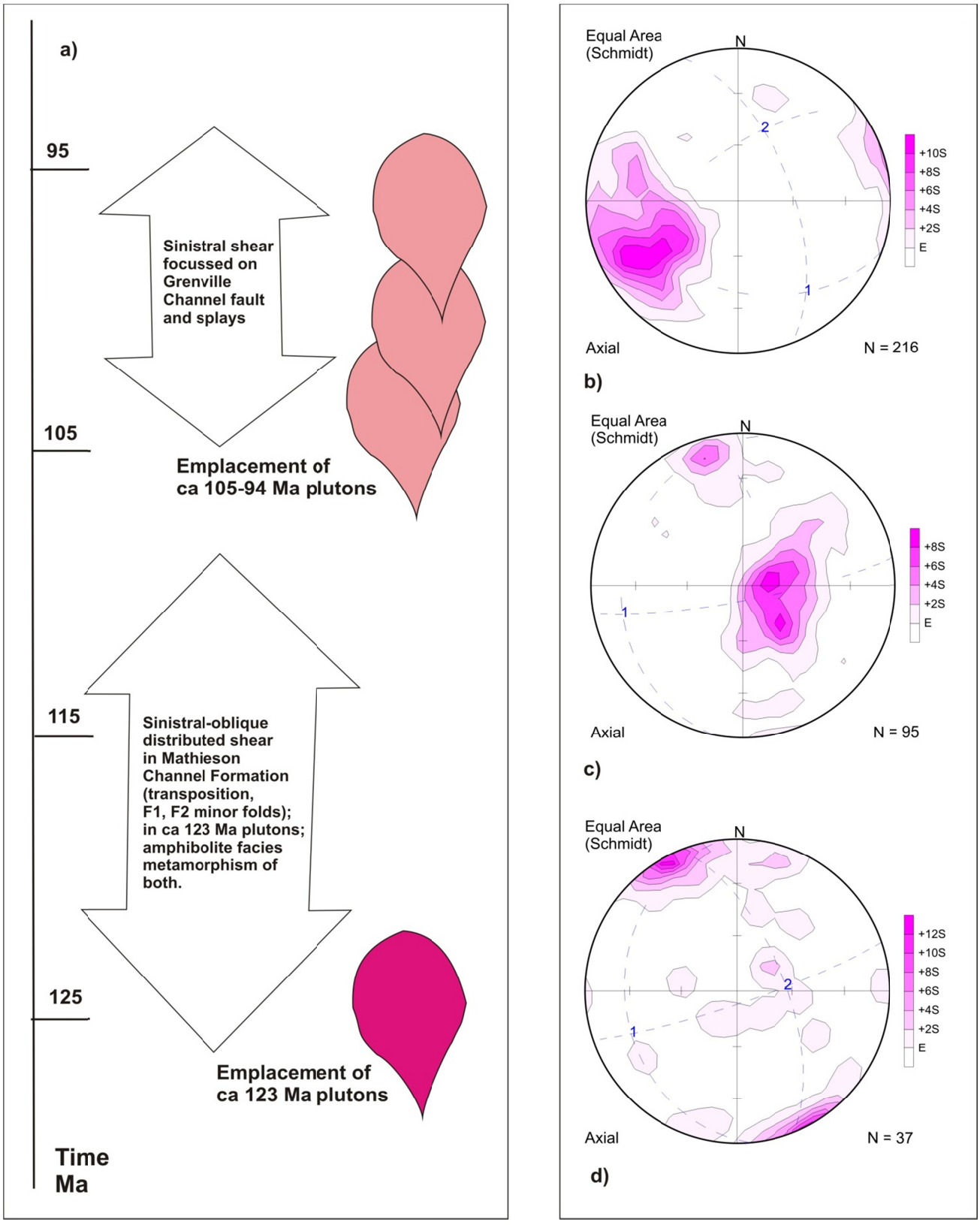

Figure 13. a) Cartoon Cretaceous structural history of eastern Laredo Sound map area. b-d) Stereo plots of minor structures in the northeastern Laredo Sound map area; b) Poles to planar structures (bedding, transposition fabrics) in Mathieson Channel Formation; c) Linear minor structures (F1 and F2 rootless and isoclines - L1 and L2 mineral lineations) in Mathieson Channel Formation; d) Linear minor structures (mineral, stretching and mylonitic lineations) in Cretaceous intrusions.

2005; Crawford *et al.*, 2000) as well as on Porcher Island and along northern Grenville Channel (Nelson *et al.*, 2010a). Within the map area, the intensity of deformation increases towards the northeast.

Plutons of the mid-Cretaceous suite are not penetratively deformed, except for local mylonitic fabrics along major fault strands. The northwest-striking Grenville Channel fault passes through the western and south-central part of the map area (Figure 5). Measured kinematic indicators show sinistral displacement, affecting all rock units including the mid-Cretaceous plutons and also younger leucocratic dike phases that were emplaced along fault strands. North-striking faults with minor dextral displacements join the Grenville Channel fault array in southern Tolmie Passage and northern Swindle Island.

Mathieson Channel Formation

Regional fabric orientations in the Mathieson Channel Formation strike northwesterly, and dip steeply to the northeast (Figure 13b). Transposition fabrics are prevalent throughout the unit. The exceptions to this reflect lithologic control; the thick-bedded conglomerate and sandstone on eastern Pooley Island are deformed into open folds with an axial planar cleavage, and metavolcanic sections devoid of carbonate show preservation of original textures and few outcrop-scale folds. Because of its thinly layered nature and high proportion of marble layers in the Mathieson Channel Formation, small-scale isoclinal folds and rootless isoclines are well-developed within it, recording polyphase folding during progressive deformation (Figure 14a). F1 minor folds are intrafolial and do not appear to refold the transposition fabric, whereas F2 folds clearly involve both layering and fabric. Isoclinal fold axes - both F1 and F2, which are generally coaxial - and also mineral lineations, vary in plunge from gentle to steep and downdip. Steep plunges in the southeastern quadrant are more common than in the northeast (Figure 13c). On ridges southeast of Green Inlet, sheath folds in metasiltstones attest to the large amount of strain accommodated by this unit, particularly in its northeastern extent (Figure 14b).

Sinistral asymmetries are observed in "tails" on conglomerate clasts and boudins throughout the area (Figure 14c). Rootless isoclines show sinistral asymmetry in many cases. Strain in these rocks appears to have been dominantly pure shear, with northeast-southwest shortening and overall southwesterly vergence. In addition, a sinistral reverse component of motion is shown by the predominantly southeast-plunging linear features developed on northeast-dipping layering (Figure 13b).

Open to closed F3 folds on hundred metre scale are seen west of Graham Reach, in Griffin Passage, and affect the conglomerate-sandstone member on eastern Pooley Island. F3 fold axes trend either north or northwest. These

Figure 14a. Deformational features in Mathieson Channel Formation. Thin siltstone layers in marble, showing tight to isoclinal F2 minor folds refolding the transposition foliation (10JN11-05; 551556E, 5830550N).

Figure 14b. Deformational features in Mathieson Channel Formation. Sheath folds in siltstone-calcsilicate, east of Green Inlet (10JN07-02; 546439E, 5865759N).

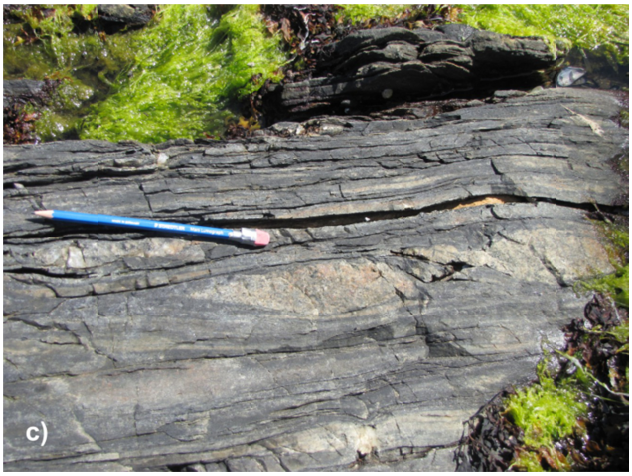

Figure 14c. Deformational features in Mathieson Channel Formation. Sinistrally asymmetric pressure shadows on conglomerate clasts (10JN17-03; 554736E, 5830695N).

folds appear to be local accommodation features. There is insufficient lithologic variation or sedimentary top

indicators in the Mathieson Channel Formation to establish the degree of large-scale folding or internal thrust repetition that it may have experienced.

Deformation in the Mathieson Channel Formation occurred during amphibolite-facies metamorphism, as indicated by assemblages in the metabasalts that consist of trains of well-oriented subidioblastic hornblende, accompanied by polygonal aggregates of calcic plagioclase; quartz, diopside, biotite and titanite. Metasiltstones comprise laminations and thin layers of polygonal quartz, plagioclase, and in some cases orthoclase, alternating with biotite or diopside-rich layers. Strong biotite alignment parallel to compositional layering defines the transposition fabric. It is assumed that the F1 isoclines formed during the transposition event. Individual biotite platelets within the quartzofeldspathic laminations are also well aligned parallel to compositional layering. Tight to isoclinal F2 folds refold the biotite fabric, with some regrowth of biotite in axial planar cleavage.

One metatuff from Bullock Channel and a greywacke from Hiekish Narrows contain post-kinematic cordierite, probably of contact metamorphic origin. Garnet and muscovite are very rare, attesting to the alumina-poor composition of the siliciclastic protolith. Diopside is the most common calcsilicate mineral in the Mathieson Channel Formation, occurring as discrete laminations in the siltstones and marbles, and forming matrix to conglomerates and sandstones. It is accompanied by subordinate amphibole–tremolite/actinolite to hornblende, depending on rock composition, as well as clinozoisite and epidote. A few of the purer marbles contain garnet and/or phlogopite and/or forsterite. One sandstone-calcsilicate sample from eastern Pooley Island contains probable scapolite.

EARLY CRETACEOUS PLUTONIC SUITE – METAMORPHISM AND DEFORMATION

The oldest of the three Cretaceous plutonic suites is distinguished by its degree of metamorphism and deformation. Phases in the suite are highly variable in composition, ranging from gabbros and ultramafites, through diorites to trondhjemites. Diorite is the most common phase. In the gabbro and diorite, original clinopyroxene is pseudomorphed by Mg-rich, pale-pleochroic hornblende, and original igneous hornblendes are overgrown by metamorphic aggregates, with darker hornblende along with secondary calcic plagioclase in the matrix. Ultramafites are converted to spectacular sprays of clinochlore, biotite, and amphibole. Both the trondhjemites and the Neekas granodiorite show strong metamorphic biotite fabrics.

Widespread development of subsolidus, metamorphic and mylonitic fabrics in this suite indicates that it was emplaced synkinematically during ongoing regional sinistral deformation. Contacts between diorite and trondhjemite phases are steep, northwest-striking zones of shearing. At the *ca.* 123 Ma U-Pb sample locality north of Jackson Passage, a leucotrondhjemite dike cuts across fabric in metadiorite, but itself displays a strongly lineated mylonitic fabric parallel to its walls, which provides evidence that the cooling felsic body localized shearing (Figure 11a). Outside of discrete fault zones, shear fabrics such as asymmetric pressure shadows around plagioclase porphyroclasts are developed in the metadiorites (Figure 15). Both steeply and gently plunging streaky to mylonitic lineations are seen.

THE GRENVILLE CHANNEL FAULT AND MID-CRETACEOUS SINISTRAL SHEARING

Regionally, the Grenville Channel fault can be traced as a prominent topographic linear feature from northern Grenville Channel, south through the channel north of Gil Island, where a small offset or deflection places it in the strong northwesterly topographic linear that transects Princess Royal Island (inset, Figure 1). It continues southeast across Laredo Inlet and into the present map area. There, it emerges on the southeastern end of Princess Royal Island in several strands under and near Cougar Bay and continues to the southeast (Figure 5). The fault cuts across plutons of the *ca.* 105-94 Ma tonalite suite. On Swindle Island and north towards Cougar Bay, a gradual transition can be traced from unfoliated tonalite to the west, to a zone in which considerable flattening has accompanied late stages of magmatic recrystallization nearer to the Grenville Channel fault. Along the fault itself, the mafic enclave-rich tonalite of the mid-Cretaceous suite has been affected by protomylonitization, with quartz ribboning, trains of neoblasts, and subsolidus biotite recrystallization. The gradual transitions from unfoliated cores into broad zones of igneous fabrics, to narrow mylonites along the fault suggest that these plutons may have been emplaced during motion on the fault.

Figure 15. Detail, sinistral sense of shear in *ca.* 123 Ma metagabbro, southern Mathieson Channel north of Neekas Inlet (10JN25-01; 552934E, 5814518N).

From Cougar Bay through Klemtu Pass and across Jackson and Oscar passages, dikes of plagioclase-phyric tonalite and granodiorite occupy strands of the Grenville Channel fault. These late bodies are themselves strongly protomylonitized, with pervasive porphyroclastic textures and quartz ribboning (Figure 16). Unlike the 123 Ma plutons, they were deformed in greenschist facies, as shown by stable biotite, chlorite and epidote, and igneous plagioclase overprinted by heavy saussurite. Sinistral asymmetric shear indicators such as pressure shadows and rotated porphyroclasts characterize these rocks. Plunges of mylonitic lineations are generally very shallow, indicating nearly pure translation on the Grenville Channel fault (Figure 13d). One significant exception to this is the presence of more steeply plunging lineations in the complex zone of intersecting faults at the northern end of Swindle Island. These steep faults may represent accommodation structures. On northern Swindle Island, and north along Tolmie Channel, faults with minor dextral displacement offset the main sinistral strands. The most prominent of these is a mylonite zone that strikes due north along the east side of Tolmie Channel. Its northward projection does not appear to significantly offset the sinistral fault that cuts across Sarah Island (Figure 5). Although it is possible that the dextral faults represent a separate, later transcurrent event, their intimate association with the main Grenville Channel fault array and the possibility that some of them may terminate against sinistral faults both favour the idea that they form northerly-oriented conjugate structures in a single system.

A presumed splay of the Grenville Channel fault corresponds with the northwest alignment of spaced high strain zones that are developed within various rock units in southern Sarah Island. At the northern exposed end of this structure on the island, the tonalite is protomylonitic, displaying porphyroclastic texture with feldspar augen. Farther south along this structure is an important locality where several probable hypabyssal intrusive phases,

Figure 16. Deformation adjacent to and within Grenville Channel fault zone: mylonitized granodiorite, Klemtu shear zone. Shows sinistral rotation of plagioclase porphyroclast (10JN21-05; 534542E, 5822824N).

including potassium feldspar-rich aplite and plagioclase porphyry, are in parallel and vertical juxtaposition within a high strain zone that in turn is crosscut by comparatively weakly strained tonalite. Uranium-lead dating of each intrusive phase is part of a geochronological study by M. Pecha (2010-11). The southern extension of the fault on Sarah Island is marked by metabasite from the Mathieson Channel Formation, exposed at Pering Point. These metabasalts are at amphibolite grade and alternate with marble layers that are crosscut by tonalite dikes projecting east off the main body. Tonalite dikes also occupy another Grenville Channel fault strand striking northerly at Keen Point south of Klemtu. Here tonalite dikes form boudins paralleling a steep penetrative foliation developed in metabasalts. Sampling of these tonalite dikes for a U-Pb zircon date is intended to partly constrain timing for motion on Grenville Channel fault.

STRUCTURAL HISTORY

The intense development of amphibolite-facies regional metamorphic fabrics and sinistral-oblique shear deformation in the *ca.* 123 Ma plutonic suite provides a new, important constraint on timing of this event. In northwestern British Columbia, several studies have documented that *ca.* 110-90 Ma plutons were emplaced at a late stage in the sinistral shearing (Chardon *et al.*, 1999; Chardon, 2003; Bulter *et al.*, 2006; Nelson *et al.*, 2010a), but no maximum age for this event has been established. In this area, Early Cretaceous plutons were emplaced into deeply buried Alexander terrane supracrustal rocks and shared sinistral-reverse deformation and exhumation (Figure 13a). In common with the Mathieson Channel Formation, this intrusive suite experienced amphibolite-grade dynamothermal metamorphism and distributed sinistral sense of shear associated with steeply plunging lineations. Earlier faults and shear zones may exist in the map area, but they are not required to explain the tectonic features that we observe.

By 105 Ma, the north coastal region was uplifted and exhumed to the point of quenching the amphibolite-facies assemblages. At this time a renewed pulse of intrusive activity delivered large bodies of tonalitic magma . The reverse (compressional) strain component dwindled, and the mid-Cretaceous plutonic suite was emplaced in a regime of nearly pure strike-slip motion (Figure 13a). Sinistral shear progressively focussed into a single fault zone, the Grenville Channel fault.

The tectonic cycle of burial, metamorphism, plutonism, and sinistral-orthogonal contraction described above for the western Coast Mountains predates the main Late Cretaceous contractional event in the central Coast Mountains to the east (Rusmore *et al.*, 2005) by more than 10 million years. These two events reflect changes in plate vectors and larger scale interplate relative motions. The sinistral component is unique to the Early Cretaceous event. The Late Cretaceous event was characterized by orthogonal shortening that evolved to dextral-reverse and then dextral-normal by Eocene time. Also, the Late

Cretaceous event involved much greater degrees of crustal thickening and subsequent uplift. However, both tectonic regimes involved southwest-vergent structures, and both probably probably formed in response to coupling between the overriding North American plate and subducting plates in the Pacific ocean realm. In each case the deformation was concentrated in the axial region of the arc (which migrated east between 110 and 80 Ma), and involved interplay between tectonics and emplacement of voluminous magmas over a 40 million year interval of Early and Late Cretaceous time.

AU MINERAL POTENTIAL OF THE CENTRAL COAST

The Surf Inlet mine (MINFILE 103H 027) is located on northern Princess Royal Island 45 km north of the present map area (inset, Figure 1). A past producing gold mine with considerable remaining underground resources, its genesis represents an important aspect of the metallogeny of the central British Columbia coast. The following account is based on a brief field visit in 2010, along with detailed geological mapping available from von Einsiedel (2001), and descriptions of the property in the MINFILE database.

Surf Inlet is a classic mesothermal (orogenic) gold-quartz vein system that formed in a series of third order structures, along a second-order splay of the Grenville Channel fault. There are two separate orebodies, the Surf and Pugley mines, both located within 2 km of the main fault, which underlies Bear Lake (Figure 17). The second order fault that controls the orebodies diverges northward from the main fault, curving to the northeast. The two mines are located within the north striking, middle section of the fault trajectory. Here, the fault zone consists of several shear zones with average dips of 45° to the west. The hostrock, a deformed and protomylonitic diorite-tonalite body, has yielded a U-Pb zircon age of 106 Ma (J. Mortensen and R. Friedman in Gehrels *et al.*, 2009). Quartz veins occupy late-stage, brittle structures and typically have alteration selvages composed of sheared chlorite, sericite, carbonate and epidote. In the veins, coarse quartz contains very coarse clots of pyrite and chalcopyrite, with lesser chalcocite, bornite, covellite and molybdenite (Figure 18).

Production from the mine was carried out intermittently by several companies between 1917 and 1946. In total, nearly 1 million tonnes was produced from the two mines averaging 13.0 grams per tonne gold, 6.8 grams per tonne silver and 0.31 per cent copper (BC MINFILE). The property is currently held by Rupert Resources Ltd. Economic potential is recognized for downdip extensions of the mined ore zones.

The host pluton to the Surf Inlet mine bears strong similarities to mid-Cretaceous plutons elsewhere. It is unmetamorphosed, so emplacement post-dated the amphibolite-facies event that affected the older Cretaceous plutons. Igneous foliation manifested by

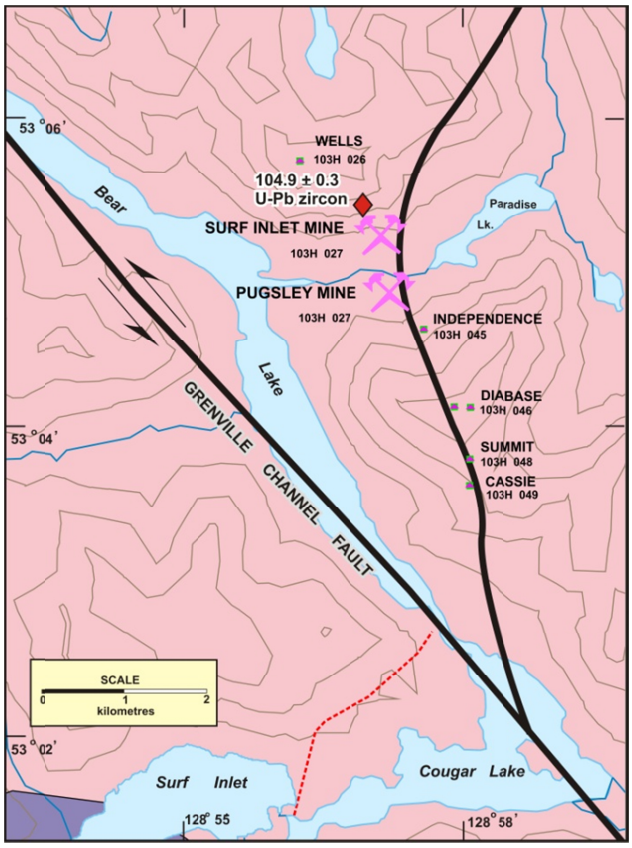

Figure 17. Detailed map of Surf Inlet mine and its surroundings. Pink = Cretaceous granitoids; purple = metamorphic rocks.

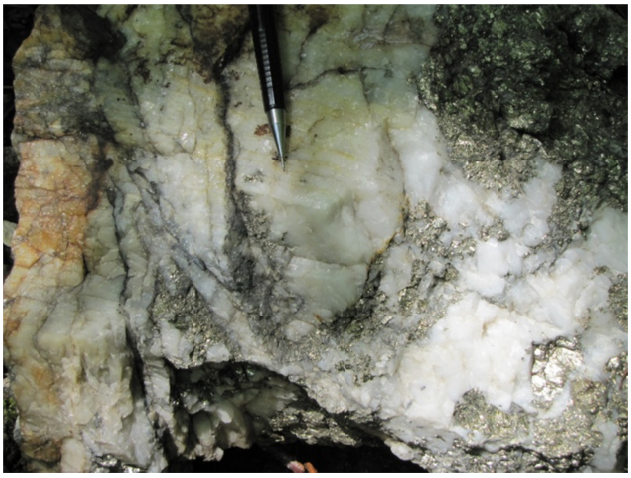

Figure 18. Surf Inlet ore, from creekbed in tallings dump (507636E, 5881725N).

alignment of coarse biotites with subordinate, late, cross-cutting plates is identical to textures in the ca 105 Ma pluton west of Klemtu. The protomylonitic overprint occurred at low temperatures, with high H_2O and CO_2 contents. This deposit is similar in type and structural setting to the Surf Point (Edye Pass) gold-quartz system on northwestern Porcher Island (inset, Figure 1; Nelson *et al.*, 2010a). Surf Point is also located on second and third order shears related to the Grenville Channel fault. The repeated association of significant mesothermal gold-quartz veins with structures related to the later, brittle

phases of sinistral motion on the Grenville Channel and related faults demonstrates an important mid-Cretaceous metallotect in coastal British Columbia.

DISCUSSION

The southern Alexander Terrane in coastal British Columbia

In 2009 and 2010, detailed mapping was completed for the Alexander terrane near both ends of its extent south of Alaska. The two areas are underlain by stratigraphically different units. At the northern end of the Alexander terrane, Ordovician volcanogenic and related plutonic rocks are widespread on Porcher Island and northern Pitt Island. By contrast, the southern end of the Alexander terrane consists of a siliclastic, carbonate and bimodal volcanic unit named herein the Mathieson Channel Formation and speculated to be of Devonian age. Broadly similar clastic rocks are limited to a few locales in the north. Regionally, the oldest exposed Alexander terrane rocks progress in age from Precambrian-Cambrian Wales Group on southern Prince of Wales Island, through Ordovician rocks along the northern Inside Passage, to possible Devonian clastic rocks in the far south, in the Laredo Sound map area.

Volcanogenic base metal mineral potential in the Alexander terrane is primarily associated with Ordovician arc sequences, notably the Moira Sound unit of Karl *et al.* (2009), which hosts the Niblack deposit on southern Prince of Wales Island. Thus the Mathieson Channel Formation in the current map area is considered unprospective for syngenetic volcanogenic deposits. The bimodal volcanic rocks in it erupted into a shallow basin, probably under oxidizing conditions as indicated by the possible presence of redbeds.

The Mathieson Channel Formation and the quartzite-siltstone-volcanic conglomerate at Jorkins Point are significant indicators of the tectonic history of the Alexander terrane. They reflect patterns of tectonics and sedimentation in the aftermath of the earliest Devonian Klakas orogeny. The Mathieson Channel Formation, with its dominant fine-grained siliciclastics and carbonates, its narrow intervals of bimodal and potentially alkalic volcanics, and its sporadic local influxes of very coarse clastic debris, is inferred to represent a rift basin fill.

In the Alexander terrane of southeastern Alaska, the slightly older Silurian Heceta conglomerates have been speculated to be equivalent to late Caledonian rift basin sequences (Soja and Krutikov, 2008). A similar correlation will be possible for the Mathieson Channel Formation, if suspected Devonian ages are confirmed by detrital U-Pb geochronology of possible rift-related clastic rocks.

The Jorkins Point conglomerate may have been deposited in or near the Mathieson Channel basin. The presence of Mathieson-like siltstone clasts supports this idea; although its depositional age is not yet known. The prominence of quartzite clasts in Jorkins Point conglomerate certainly demonstrates recycling of continentally derived debris, possibly due to arc-continent sliver amalgamation events such as the Early Devonian Klakas orogeny.

Early to mid-Cretaceous sinistral tectonics, the Grenville Channel fault, and mesothermal gold mineralization

In 2010 mapping, we have recognized the southern Grenville Channel fault near Klemtu as a locus of mid-Cretaceous sinistral shearing, and also documented a somewhat older Early Cretaceous event of distributed shear during amphibolite facies metamorphism. Magmatic ages constrain the timing of the distributed sinistral shear event between 123 and 105 Ma, the age of the synkinematic versus postkinematic plutons. These observations provide an important dimension to the mid-Cretaceous sinistral shear history of the northern Grenville Channel fault and its splays. Intense fabric development in the *ca.* 123 Ma plutonic suite indicates that this deformation is entirely Early Cretaceous, rather than a continuation of the mid-Jurassic accretion kinematics of Alexander and Yukon-Tanana terranes.

The Early to mid-Cretaceous sinistral-oblique shear system, as recorded in exposed rocks, evolved from deep-crustal, sinistral-reverse motion, to upper crustal, nearly pure transcurrent motion on the Grenville Channel fault, in which the latest synkinematic phases record greenschist facies metamorphism at high fluid pressures as shown by the presence of abundant chlorite, sericite and carbonate. Tectonically, regimes of partitioned transcurrent motion during exhumation from amphibolite to greenschist facies are recognized worldwide as highly favourable to the emplacement of mesothermal (orogenic) gold-quartz vein systems. Therefore it is no surprise that two significant ex-producing gold mines of this type lie proximal to the Grenville Channel fault, controlled by second and third order fault arrays. Another promising gold-quartz vein system, Yellow Giant (MINFILE 103G 021, 24, 25, 26, 30), is located on Banks Island. It is currently held by Imperial Metals, who hope to begin an exploration program there in 2011 (Jim Miller-Tait, personal communication, November 2010).

FUTURE RESEARCH DIRECTIONS AND MAPPING PLANS

The third and final field season of the North Coast Project is planned for 2011. It will have the following key goals:

1) Revisit and resample for geochronology parts of the areas previously mapped, in which present structural, lithologic and geochronometric data indicate unsolved problems. Examples of this include a) the Devonian pluton in Porcher Inlet, which cuts an older orthogneiss complex that so far has only yielded an apparent Jurassic U-Pb

Laserchron age displaying complex systematics (J.B. Mahoney, unpublished data, 2010); b) the Swede Point pluton on Porcher Island, which may be Mississippian or, alternatively, Mesozoic with inherited cores and c) Kumealon Inlet, where a structural contact between Alexander terrane and Yukon-Tanana terrane has been inferred (Nelson *et al.*, 2010b), but detrital zircon data are conflicting, and where U-Pb dating of the metavolcanic rocks has yet to be done.

2) Collaborate with Joel Angen, who is studying the fault systems on Porcher Island and along northern Grenville Channel as an M.Sc. thesis at the University of Waterloo. His work is sponsored by the Geological Survey of Canada as a contribution to the Edges project.

3) Visit key mineral occurrences in the area, particularly the Yellow Giant mesothermal Au deposit and the Pitt volcanogenic prospect, in order to place them in regional context.

4) Complete field investigation of the Alexander terrane between Grenville Channel and northern Princess Royal Island, targeting a full update of this part of the BC Geological Map in 2012.

SUMMARY AND CONCLUSIONS

In this second year of operation, the North Coast project can list the following accomplishments:

Completion of geological map coverage of an area of 30 by 50 km, covering the channels and islands between Return Channel and northern Princess Royal Island, in eastern Laredo Sound map area (103A). This map will be released as a British Columbia Geological Survey open file in early 2011 (Nelson *et al.*, 2011).

Rock units of the Alexander terrane of southeastern Alaska can be traced into northwestern British Columbia (Porcher and Pitt islands), including those that are known to host Ordovician volcanogenic massive sulphide mineralization. Farther south, in the current map area, the Alexander terrane is represented by younger, probably Devonian, clastic-carbonate strata.

The Grenville Channel fault is a mid-Cretaceous sinistral fault of regional extent (>150 km). It and its splays form the tectonic framework for mesothermal gold-quartz vein systems including Surf Point on Porcher Island, Surf Inlet on Princess Royal Island, and probably Yellow Giant on Banks Island. This is an important new metallotect on the coast of British Columbia.

ACKNOWLEDGMENTS

We once again acknowledge the key role of our captain, Don Willson and his boat, the Phoebe, in providing a convenient logistical base of operations and safe coordination of our daily zodiac traverses. The senior author (Nelson) wishes to thank all the members of the project team for their strong contributions to our task, deterred by neither metamorphism nor voluminous intrusion nor polyphase deformation from reconstructing original depositional environments and establishing the regional framework of faults. We were also fortunate to have two excellent, hard-working student assistants from the University of Wisconsin, Brennan Kadulski and Julia Potter. The North Coast Project is part of Edges (Multiple Metals – NW Canadian Cordillera (Yukon, British Columbia); financial and logistical support from the Geological Survey of Canada made it all possible. Moreover, the conduct of this project within the larger framework of Edges, with its focus on understanding the exotic terranes, their accretion and interaction with the continent margin, gives it more meaning than if it stood alone. Fil Ferri's careful review improved the accuracy and clarity of the manuscript.

REFERENCES

Alldrick, D.J. (2001): Geology and mineral deposits of the Ecstall belt, northwest B.C.: *in* Geological Fieldwork 1999, *B.C. Ministry of Energy and Mines*, Paper 2000-1, pages 279-306.

Alldrick, D.J., Friedman, R.M. and Childe, F.C. (2001): Age and geologic history of the Ecstall greenstone belt, northwest B.C: *in* Geological Fieldwork 1999, *B.C. Ministry of Energy and Mines*, Paper 2000-1, pages 269-278.

Alldrick, D.J., Nelson, J.L. and Barresi, T. (2005): The geology and mineral deposits of the upper Iskut River area: Tracking the Eskay rift through northern British Columbia (104G/1,2; 104B/9,10,15,16) *in* Geological Fieldwork 2004, *B.C. Ministry of Energy and Mines*, Paper 2005-1, pages 1-30.

Ayuso, R.A., Karl, S.M., Slack, J.F., Haeussler, P.J., Bittenbender, P.E., Wandless, G.A. and Colvin, A.S. (2005): Oceanic Pb-isotopic sources of Proterozoic and Paleozoic volcanogenic massive sulphide deposits on Prince of Wales Island and vicinity, southeastern Alaska: *in* Studies by the U.S. Geological Survey in Alaska 2005, *U.S. Geological Survey,* Professional Paper 1732-E, pages 1-20.

Baer, A.J., 1973: Bella Coola – Laredo Sound map-areas, British Columbia; *Geological Survey of Canada*, Memoir 372, 122 pages, 1:250 000 geological maps.

Berg, H.C., Jones, D.L. and Richter, D.H. (1972): Gravina-Nutzotin belt – tectonic significance of an upper Mesozoic sedimentary and volcanic sequence in southern and southeastern Alaska; *U.S. Geological Survey,* Professional Paper 800-D, pages D1-D24.

Butler, R.F., Gehrels, G.E., Hart, W., Davidson, C., and Crawford, M.L. (2006): Paleomagnetism of Late Jurassic to mid-Cretaceous plutons near Prince Rupert, British Columbia, *in* Haggart, J.W., Enkin, R.J., and Monger, J.W.H., eds., Paleogeography of the North American Cordillera: Evidence for and against large-scale displacements: *Geological Association of Canada*, Special Paper 46, pages 171-200.

Chardon, D. (2003): Strain partitioning and batholith emplacement at the root of a transpressive magmatic arc; *Journal of Structural Geology*, Volume 25, pages 91-108.

Chardon, D., Andronicos, C.L., and Hollister, L.S. (1999): Large-scale transpressive shear zone patterns and displacements within magmatic arcs: the Coast Plutonic Complex, British Columbia; *Tectonics*, Volume 18, pages 278-292.

Crawford, M.L., Crawford, W.A. and Gehrels, G.E. (2000): Terrane assembly and structural relationships in the eastern Prince Rupert quadrangle, British Columbia; *in* Stowell, H.H. and McClelland, W.C., editors., Tectonics of the Coast Mountains, southeastern Alaska and British Columbia; *Geological Society of America,* Special Paper 343, pages 1-22.

Eberlein, G.D., and Churkin, M. Jr. (1970): Paleozoic stratigraphy in the northwest coastal area of Prince of Wales Island, southeastern Alaska: *U.S. Geological Survey* Bulletin 1284, 67 pages, 2 sheets, 1:125 000 scale.

Eberlein, G.D., Churkin, M. Jr., Carter, C., Berg, H.C. and Ovenshine, A.T. (1983): Geology of the Craig quadrangle, Alaska: *U.S. Geological Survey* Open-File Report 83-91, 28 pages, 1:250 000 scale.

Gareau, S.A. and Woodsworth, G.J. (2000): Yukon-Tanana terrane in the Scotia-Quaal belt, Coast Plutonic Complex, central-western British Columbia, *in* Stowell, H.H. and McClelland, W.C., editors., Tectonics of the Coast Mountains, southeastern Alaska and British Columbia, *Geological Society of America*, Special Paper 343, pages 23-44.

Gehrels, G.E. (2001): Geology of the Chatham Sound region, southeast Alaska and coastal British Columbia: C*anadian Journal of Earth Sciences*, Volume 38, pages 1579-1599.

Gehrels, G.E. and Boghossian, N.D. (2000): Reconnaissance geology and U-Pb geochronology of the west flank of the Coast Mountains between Bella Coola and Prince Rupert, coastal British Columbia; *in* Stowell, H.H. and McClelland, W.C., editors., Tectonics of the Coast Mountains, southeastern Alaska and British Columbia; *Geological Society of America,* Special Paper 343, pages 61-76.

Gehrels, G.E. and Kapp, P.A. (1998): Detrital zircon geochronology and regional correlation of metasedimentary rocks in the Coast Mountains, southeastern Alaska; *Canadian Journal of Earth Sciences*, Volume 3, pages 269-279.

Gehrels, G. E. & Saleeby, J. B. (1987): Geologic framework, tectonic evolution and displacement history of the Alexander terrane, *Tectonics*, Volume 6, pages 151-174.

Gehrels, G.E., Berg, H.C., and Saleeby, J.B. (1983): Ordovician-Silurian volcanogenic massive sulfide deposits on southern Prince of Wales Island and the Barrier Islands, southeastern Alaska; *US Geological Survey*, Open File Report 83-318, 11 pages.

Gehrels, G.E., McClelland, W.C., Samson, S.D., Patchett, J.P. and Orchard, M.J. (1992): Geology of the western flank of the Coast Mountains between Cape Fanshaw and Taku Inlet, southeastern Alaska; *Tectonics*, Volume 11, pages 567-585.

Gehrels, G.E., Dickinson, W.R., Ross, G.M., Stewart, J.H. and Howell, D.G. (1995): Detrital zircon reference for Cambrian to Triassic miogeoclinal strata of western North America.; *Geology*, Volume 23, pages 831-834.

Gehrels, G. E., Butler, R. F. and Bazard, D. R. (1996): Detrital zircon geochronology of the Alexander terrane, southeastern Alaska, *Geological Society of America Bulletin*, Volume 108, pages 722-734.

Gehrels, G. , Rusmore, M. , Woodsworth, G. , Crawford, M. , Andronicos, C. , Hollister, L. , Patchett, J. , Ducea, M. , Butler, R. , Klepeis, K. , Davidson, C. , Friedman, R. , Haggart, J. , Mahoney, B. , Crawford, W., Pearson D. and Girardi, J. (2009): U-Th-Pb geochronology of the Coast Mountains batholith in north-coastal British Columbia: Constraints on age and tectonic evolution; *Geological Society of America Bulletin*, Volume 121, pages 1341-1361.

Hutchison, W.W. (1982): Geology of the Prince Rupert – Skeena map area, British Columbia; *Geological Survey of Canada* Memoir 394, 115 pages, with 1:250 000 scale geological map GSC Map 1427A.

Karl, S.M., Ayuso, R.A. , Slack, J.F. and Friedman, R.M. (2009): Neoproterozoic to Triassic rift-associated VMS deposits in the Alexander composite oceanic arc terrane, southeast Alaska; *in* Morris, H., editor, Mining: Modern Mine Reclamation: *Alaska Miners Association* 2009 Annual Convention, Abstracts, page 9.

Kilby, W. E., (1995): Mineral Potential Project - Overview; *in* Geological Fieldwork 1994, Grant, B. and Newell, J.M., Editors, *B.C. Ministry of Energy, Mines and Petroleum Resources*, Paper 1995-1, pages 411-416.

Nelson, J.L. and Gehrels, G.E. (2007): Detrital zircon geochronology and provenance of the southeastern Yukon-Tanana terrane; *Canadian Journal of Earth Sciences*, Volume 44, pages 297-316.

Nelson, J.L., Mahoney, J.B., Gehrels, G.E., van Staal, C. and Potter, J.J. (2010a): Geology and mineral potential of Porcher Island, northern Grenville Channel and vicinity, northwestern British Columbia; *B.C. Ministry of Energy and Mines*, Geological Fieldwork 2009, pages 19-42.

Nelson, J.L., Mahoney, J.B. and Gehrels, G.E. (2010b): Geology and mineral potential of the Porcher Island – Grenville Channel area, northwestern British Columbia; *B.C. Ministry of Energy and Mines*, Open-File 2010-03 (also, *Geological Survey of Canada*, Open File 6654, 1:50 000 scale.

Nelson, J.L., Diakow, L.J., Karl, S., Mahoney, J.B. , Gehrels G.E. , Pecha, M. , and van Staal, C. (2011): Geology of the mid-coast region of BC near Klemtu, parts of 103A/08, A09, A/15 and A/16; *B.C. Ministry of Energy and Mines*, Open-File 2011-3, 1:100 000 scale.

Roddick, J.A. (1970): Douglas Channel – Hecate Strait map-area, British Columbia; *Geological Survey of Canada*, Paper 70-41; 70 pages, with 1:250 000 scale geological map, GSC Map 23-1970.

Rubin, C.M. and Saleeby, J.B. (1992) Tectonic history of the eastern edge of the Alexander terrane, southeast Alaska; *Tectonics*, Volume 11, pages 586-602.

Rusmore, M.E., Woodsworth, G.J. and Gehrels, G.E. (2005): Two-stage exhumation of midcrustal arc rocks, Coast Mountains, British Columbia; *Tectonics*, Volume 24, Oct. 2005, Paper TC5013, doi:10.1029/2004TC001750, 25 pages.

Saleeby, J.B. (2000): Geochronologic investigations along the Alexander-Taku terrane boundary, southern Revillagigedo Island to Cape Fox areas, southeast Alaska; *in* Stowell, H.H. and McClelland, W.C., editors, Tectonics of the Coast Mountains, southeastern Alaska

and British Columbia; *Geological Society of America* Special Paper 343, pages 107-143.

Slack, J.F., Shanks, W.C., Karl, S.M., Gemery, P.A., Bittenbender, P.E. and Ridley, W.I. (2005): Geochemical and sulphur-isotopic signatures of volcanogenic massive sulphide deposits on Prince of Wales Island and vicinity, southeastern Alaska: *in* Studies by the U.S. Geological Survey in Alaska 2005, *U.S. Geological Survey* Professional Paper 1732-C, 37 pages.

Soja, C.M. and Krutikov, L. (2008): Provenance, depositional setting, and tectonic implications of Silurian polymictic conglomerates in Alaska's Alexander terrane; *in* Blodgett, R.B. and Stanley, G.D. Jr., The terrane puzzle: new perspectives on paleontology and stratigraphy from the North American Cordillera; *Geological Society of America* Special Paper 442, pages 63-75.

von Einsiedel, C. (2001): Underground drilling report, Surf mine 900 level, Surf Inlet Project. B.C Ministry of Energy, Mines and Petroleum Resources, Assessment Report 26704, 31 pages.

Wheeler, J.O., Brookfield, A.J., Gabrielse, H., Monger, J.W.H., Tipper, H.W. and Woodsworth, G.J. (1991): Terrane map of the Canadian Cordillera: *Geological Survey of Canada* Map 1713A, 1:2 000 000 scale.

Geology of the Kutcho assemblage between Kutcho Creek and the Tucho River, northern British Columbia (NTS 104I/01)

by P. Schiarizza

KEYWORDS: Kutcho assemblage, Cache Creek terrane, King Salmon fault, Nahlin fault, Kutcho fault, Kutcho Creek volcanogenic massive sulphide deposit

INTRODUCTION

The Kutcho project is a two-year bedrock mapping program initiated by the British Columbia Geological Survey Branch in 2010. The aim of the project is to gain a better understanding of, and provide more detailed geological maps for, the Permo-Triassic Kutcho assemblage, which hosts the Kutcho Creek volcanogenic massive sulphide deposit. The study is part of the Edges (Multiple Metals-Northwest Canadian Cordillera (Yukon, British Columbia)) project, which is a contribution to the GEM (Geomapping for Energy and Minerals) program. This program was initiated by the Federal Government in 2008 to enhance public geoscience knowledge in northern Canada, in order to stimulate economic activity in the energy and mineral sectors.

This report summarizes preliminary results from the first year's fieldwork on the Kutcho project. Fieldwork was conducted over seven weeks (July 2-28; August 12 - September 2) by a single traverse team comprising the author and student assistant Scott Caldwell (University of Victoria). Work was conducted from Kutcho Copper Corporation's exploration camp on Kutcho Creek. Operating funds were provided by the British Columbia Geological Survey, a private-public partnership agreement with Kutcho Copper Corporation, the Geological Survey of Canada (Edges project) and a partnership agreement with the University of Victoria.

The 2010 map area covers about 200 square kilometres and encompasses the main exposure belt of the Kutcho assemblage, between Kutcho Creek and the Tucho River, including the Kutcho Creek Cu-Zn volcanogenic massive sulphide occurrence (MINFILE 104I 060). It is located in the southeast corner of NTS map sheet 104I (Cry Lake) and encompasses the transition between the Stikine Ranges of the Cassiar Mountains to the north and the Spatsizi Plateau to the south. The nearest community is Dease Lake, located on Highway 37, 100 km west-northwest of the Kutcho Creek deposit. A poor tote road connects the map area to Dease Lake, but the most efficient access is by air, facilitated by a gravel airstrip at the exploration camp on the west side of Kutcho Creek.

This publication is also available, free of charge, as colour digital files in Adobe Acrobat® PDF format from the BC Ministry of Forests, Mines and Lands website at http://www.empr.gov.bc.ca/Mining/Geoscience/PublicationsCatalogue/Fieldwork.

PREVIOUS WORK

Geological studies by the Geological Survey of Canada in the Cry Lake and Dease Lake map areas, carried out intermittently from 1956 to 1991, are summarized in the report and 1:250 000-scale geological maps of Gabrielse (1998). This work incorporates regional studies of the Kutcho assemblage by Monger (1977), Monger and Thorstad (1978), Thorstad (1979, 1984) and Thorstad and Gabrielse (1986), as well as studies carried out in the immediate vicinity of Kutcho Creek deposit by provincial government geologists from 1974 to 1977 (Panteleyev, 1975, 1978; Pearson and Panteleyev, 1976; Panteleyev and Pearson, 1977a, b).

The Kutcho Creek massive sulphide deposit, discovered in 1973, was described by Bridge *et al.* (1986) after more than a decade of exploration, including 292 drillholes, by Esso Minerals Canada and Sumitomo Metal Mining Co. More recently, the deposit and host rocks were described by Barrett *et al.* (1996), who document details of primary and alteration geochemistry. A concurrent study by Childe and Thompson (1997) presents U-Pb radiometric dates and radiogenic isotope characteristics of the Kutcho assemblage.

REGIONAL GEOLOGICAL SETTING

The geological setting of the Kutcho Creek – Tucho River map area is shown on Figure 1. The map area is located at the east end of the King Salmon allochthon, a relatively narrow structural/stratigraphic belt that has been traced several hundred kilometres to the west-northwest, and separates the main exposures of the oceanic Cache Creek terrane to the north from those of the Stikine arc terrane to the south. The allochthon itself consists mainly of Early to Middle Jurassic clastic sedimentary rocks of the Inklin Formation, which forms the main exposure belt of the Whitehorse trough in northern British Columbia. Older rocks that are preserved locally in the eastern part of the allochthon include bimodal volcanic and volcaniclastic rocks of the Kutcho assemblage, as well as narrow lenses of oceanic rock (basalt, chert, serpentinite)

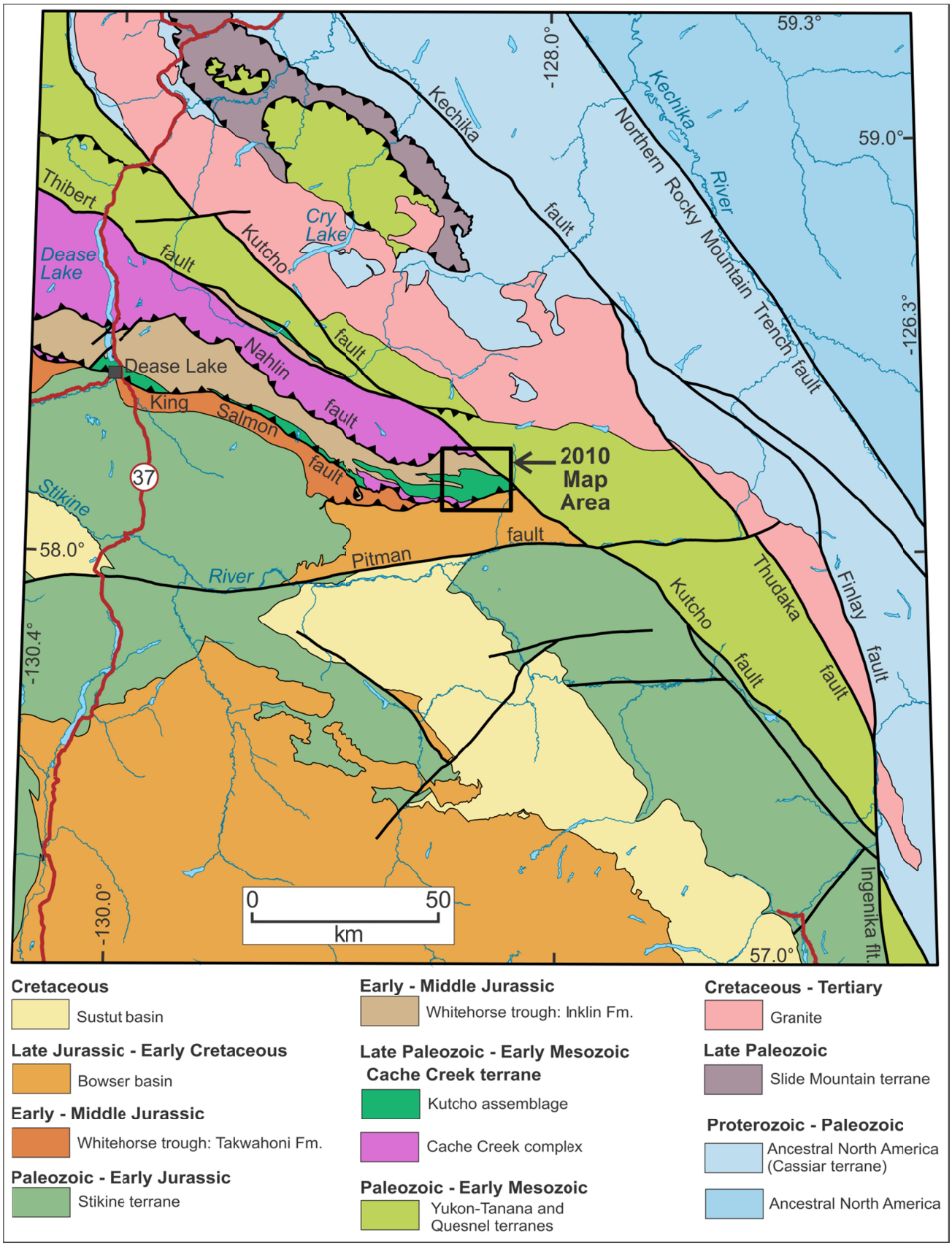

Figure 1. Regional geological setting of the 2010 map area, after Massey *et al.* (2005).

that have been included in Cache Creek terrane (Gabrielse, 1998). The King Salmon allochthon is bounded by the King Salmon and Nahlin faults, which are interpreted as northerly dipping thrust faults that were active in early Middle Jurassic time.

The King Salmon allochthon, together with adjacent Cache Creek and Stikine terranes, is truncated to the northeast by a system of northwest-striking faults that record significant dextral strike-slip displacement of Cretaceous and Tertiary age (Gabrielse, 1985, 1998; Gabrielse *et al.*, 2006). The fault panels directly northeast of the Cache Creek – King Salmon – Stikine belts include mid-Paleozoic, late Paleozoic and Mesozoic arc sequences that are part of Yukon-Tanana and Quesnel terranes (Gabrielse, 1991; Nelson and Friedman, 2004). Farther northeast, these rocks are faulted against, and intruded by, a major belt of granitic rocks that includes the Cretaceous Cassiar Batholith. The rocks northeast of this granitic belt consist mainly of Proterozoic through Paleozoic sedimentary rocks of North American affinity, locally overlain by thrust slices of oceanic Slide Mountain terrane, Quesnel terrane and Yukon-Tanana terrane, which together comprise the Sylvester allochthon (Gabrielse, 1991; Nelson and Friedman, 2004).

GEOLOGICAL UNITS

The distribution of the main geological units within the 2010 map area is shown on Figure 2, and a schematic vertical cross-section through the western part of the area is shown on Figure 3. Most units are part of the King Salmon allochthon, which includes the Permo-Triassic Kutcho assemblage, together with a structurally underlying unit of mainly metabasalt and serpentinite assigned to the Cache Creek Complex, and a Triassic-Jurassic metasedimentary succession that overlies the Kutcho assemblage across an erosional unconformity. The latter succession includes a local conglomerate unit containing clasts derived from the Kutcho assemblage, and overlying limestone, slate, siltstone and sandstone correlated with the regionally extensive Late Triassic Sinwa and Early to Middle Jurassic Inklin formations. All map units within the allochthon are deformed by south-verging folds, with an associated axial planar cleavage defined by greenschist facies mineral assemblages. The allochthon is bounded to the south by the north dipping King Salmon thrust fault, and to the north by the Nahlin fault. Jurassic chert-pebble conglomerate of the Bowser Lake Group occurs in the footwall of the King Salmon fault, and serpentinized ultramafic rocks of the Cache Creek terrane crop out on the north side of the Nahlin fault. The northwest striking Kutcho fault truncates the King Salmon allochthon near the northeast edge of the map area, and juxtaposes it against undated plutonic rocks, mainly granodiorite and quartz diorite, which are part of the Quesnel terrane. The youngest unit mapped in the area is a small post-metamorphic plug of diorite that cuts the Kutcho assemblage in the southwest part of the map area. This plug, and abundant sills and dikes of hornblende-pyroxene-plagioclase porphyry that are too small to be shown on Figure 2, are probably Eocene in age.

Cache Creek Complex within the King Salmon allochthon

Metabasalt and related rocks that occur at the base of the King Salmon allochthon in the southwest part of the map area are assigned to the Cache Creek Complex. These rocks rest structurally above the Bowser Lake Group across the King Salmon fault, and are in turn overlain by the basal part of the Kutcho assemblage across a suspected fault contact. They pinch out to the east, within the current map area, but have been traced as a continuous belt for 25 km to the west of the area (Gabrielse, 1998).

The Cache Creek Complex in the southwestern part of the map area is dominated by metabasalt, but also includes minor amounts of bedded chert, limestone and gabbro, and includes substantial amounts of serpentinite along the structural base and top of the succession. The fine-grained metabasalt is medium to pale green, weakly to strongly schistose, and typically forms monotonous greenish brown to rusty brown weathered exposures that show little or no indication of original mineralogy or texture. Vague pillow outlines occur locally, and fragmental schist, containing light greenish grey epidote altered feldspathic fragments and dark green chloritic fragments, was noted in one area about 2 km south-southeast of peak 2075. Thin sections of typical metabasalt reveal a foliated metamorphic assemblage of mainly actinolite, chlorite and epidote, with partial preservation of an original groundmass comprising intergrown clinopyroxene and plagioclase, as well as rare clinopyroxene microphenocrysts.

Fine and medium grained chlorite-epidote-plagioclase semischists, derived from diabasic and gabbroic rocks, respectively, were noted at two widely-spaced locations within the southern Cache Creek Complex, and may represent sills or dikes within the compositionally similar metabasalt. Medium grey to brownish grey bedded chert, comprising chert beds 1-4 cm thick separated by chloritic partings, forms an interval about 10 m thick that is intercalated with metabasalt just west of peak 1667. Similar chert, and light grey weathered limestone, occur as lenses between the metabasalt and structurally underlying serpentinite, about 300 m southwest of the peak. The serpentinite forms the structural base of the Cache Creek Complex, and rests above chert-pebble conglomerate of the Bowser Lake Group across the unexposed trace of the King Salmon fault. Serpentinite also occurs at the structural top of the Cache Creek Complex, directly beneath unit KS1 of the Kutcho assemblage, and commonly encloses lenses of silicified metabasalt and chert.

The rocks described above are readily included in the Cache Creek Complex on the basis of lithology. They are

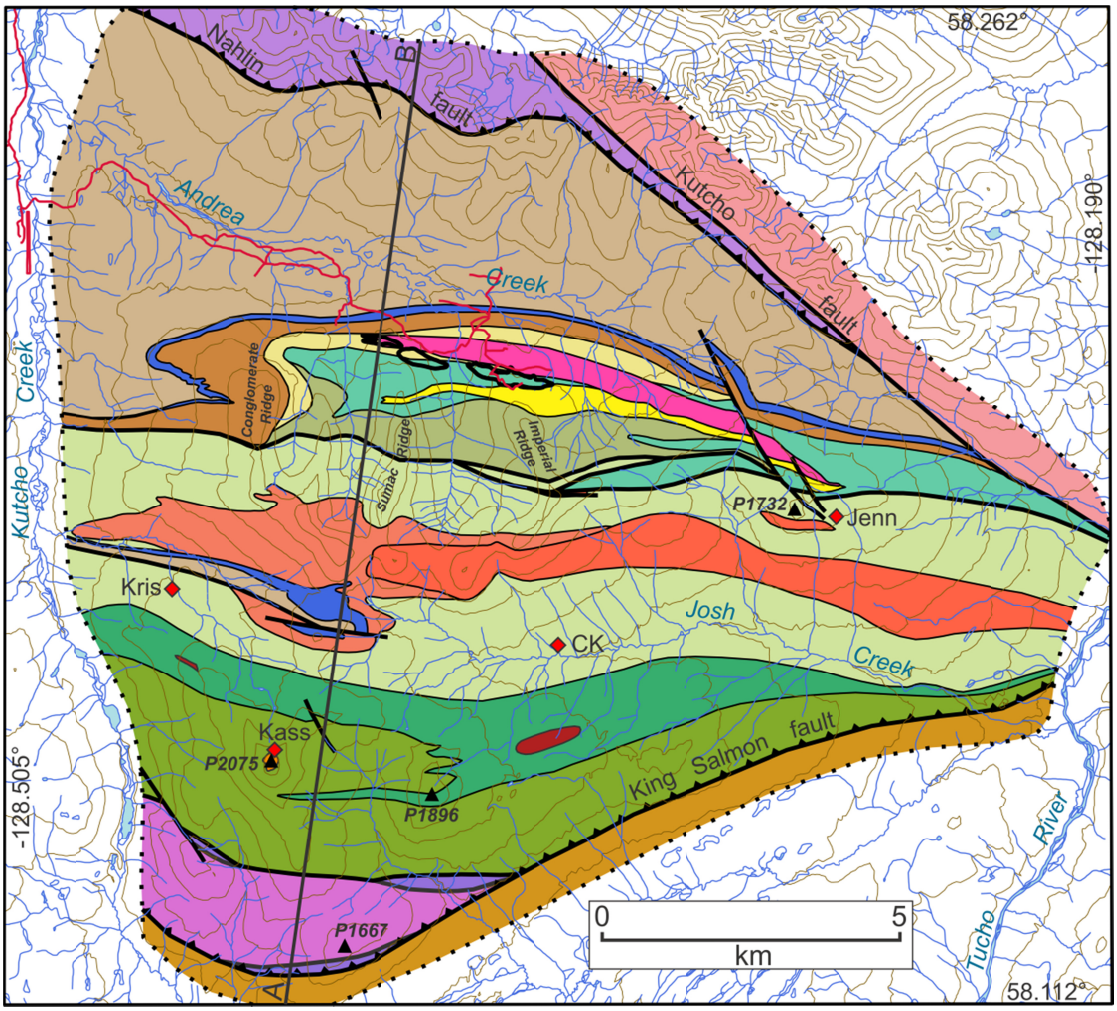

Cache Creek Terrane
Kutcho assemblage
Late Permian - Early Triassic
Northern division
- Gabbro
- KN4: phyllite, siltstone, sandstone, gabbro
- KN3: coarse quartz-eye chlorite-sericite schist; locally includes coarse breccia
- KN2: pyritic quartz-sericite schist; fragmental schist; rhyolite
- KN1: feldspathic sericite-chlorite schist

Central division
- Tonalite
- Rhyolite; epidote-chlorite schist; felsic fragmental schist; sandstone, phyllite, chert
- Rhyolite

Southern division
- KS2: Epidote-chlorite schist derived from mafic volcanic rocks
- Diorite
- KS1: sandstone, phyllite; felsic fragmental schist

Cache Creek complex
Late Paleozoic - Early Mesozoic
- Basalt, chert, limestone
- Serpentinite, serpentinite melange

Eocene
- Diorite

Bowser Basin
Late Jurassic - Early Cretaceous
- Chert-pebble conglomerate; sandstone, slate

Quesnel Terrane
Early Jurassic
- Quartz diorite, quartz monzodiorite, granodiorite

Whitehorse Trough
Early - Middle Jurassic
- Inklin Formation: slate, siltstone, sandstone

Late Triassic
- Sinwa Formation: limestone, marble

Late Triassic ?
- Conglomerate; clasts derived from Kutcho assemblage

Cache Creek Terrane
Late Paleozoic
- Harzburgite, dunite, serpentinite, listwanite

- Kutcho Creek deposit: volcanogenic massive sulphide lens (projected vertically to surface)
- Minor mineral occurrence
- P2075 ▲ Mountain peak (elevation in metres) referred to in text

Figure 2. Generalized geology of the Kutcho Creek – Tucho River map area, based mainly on 2010 fieldwork.

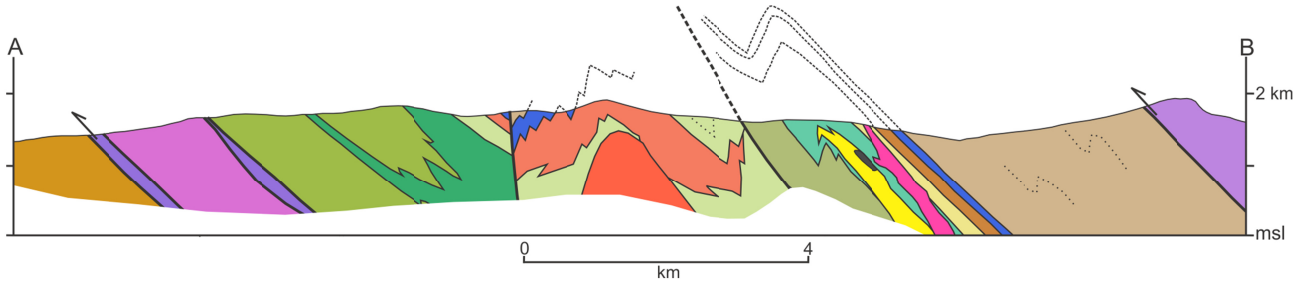

Figure 3. Schematic vertical cross-section along line A-B in Figure 2. See Figure 2 for legend.

not dated, but chert and limestone samples collected during the 2010 field season are currently being processed for microfossils.

Kutcho assemblage

The Kutcho assemblage is a heterogeneous package of schists derived from felsic and mafic volcanic and volcaniclastic rocks and associated felsic and mafic intrusions. The widest belt of exposures, and the informal type area for the assemblage, is within the current map area (Thorstad and Gabrielse, 1986). This belt continues for about 25 km to the west of Kutcho Creek, and the assemblage is also represented by several smaller lenses that have been mapped within the King Salmon allochthon as far west as Dease Lake (Gabrielse, 1998).

Gabrielse (1962) included rocks presently assigned to the Kutcho assemblage in a diverse map unit, of Devono-Mississippian and possibly younger age, that also contained adjacent rocks currently assigned to the Cache Creek Complex. Rocks of the Kutcho assemblage caught the attention of exploration and government geologists with the discovery of the Kutcho Creek Cu-Zn volcanogenic massive sulphide deposit in 1973. The rocks in the vicinity of the deposit were described by Panteleyev (1975) and Pearson and Panteleyev (1976), and were correlated with the Late Paleozoic Asitka Group of the Stikine terrane by Panteleyev and Pearson (1977b) and Monger (1977), on the basis of lithologic similarity and an Early Permian Rb-Sr isochron date of 275 ±15 Ma. Monger and Thorstad (1978) referred to these rocks as the Kutcho sequence and, together with Panteleyev (1978), suggested that they might be Triassic, based on the apparent intercalation of Kutcho felsic schists with Triassic limestone assigned to the Sinwa Formation on the west side of Kutcho Creek. Thorstad (1979, 1984) and Thorstad and Gabrielse (1986) referred to these rocks as the Kutcho Formation, and assigned them a Late Triassic age, based in part on a Rb-Sr isochron date of 210 ±10 Ma that was considered to be more robust than the Early Permian date quoted by Panteleyev and Pearson (1977b).

Childe and Thompson (1997) introduced the term assemblage, rather than formation, for the Kutcho rocks, and presented U-Pb zircon radiometric dates that established an Early Triassic age for the upper part of the assemblage. They obtained a date of 242 ±1 Ma from rocks directly above the Kutcho Creek deposit, a date of 246 +7/-5 Ma from rocks in the footwall of the deposit, and a date of 244 ±6 Ma from a quartz-plagioclase porphyry dike to the south of the deposit. Childe and Thompson (1997) also obtained primitive Nd isotopic signatures from Kutcho volcanic rocks and primitive Pb isotopic signatures from the syngenetic mineralization of the Kutcho Creek volcanogenic massive sulphide deposit. These data, together with geochemical data presented by Barrett *et al.* (1996), showing that mafic and felsic volcanic rocks from the Kutcho assemblage have a tholeiitic affinity, with depleted high field-strength elements and flat to LREE-depleted REE patterns, indicate that the Kutcho assemblage formed in an intra-oceanic arc environment.

The Kutcho assemblage within the 2010 map area is subdivided into 3 divisions referred to as southern, central and northern. Although there are local fold repetitions, the assemblage generally dips and faces to the north, such that the southern division includes the structural base of the assemblage and the northern division includes the highest stratigraphic units within the assemblage. However, the structural relationship between the central and northern divisions is not well understood, and they may in part be laterally equivalent.

SOUTHERN DIVISION

The southern division of the Kutcho assemblage comprises two mappable units. Unit KS1 includes phyllite, siltstone and sandstone that form the base of the assemblage, together with overlying schists derived mainly from felsic volcaniclastic rocks. Unit KS2 overlies and interfingers with unit KS1, and consists of schists derived mainly from mafic volcanic rocks.

Unit KS1

The basal part of unit KS1 comprises up to a few tens of metres of dark grey phyllite and calcareous phyllite, intercalated with intervals of laminated siltstone and phyllitic limestone, and thin to medium beds of schisty sandstone and gritty sandstone (Figure 4). The gritty sandstone contains plagioclase, quartz and pale grey felsic lithic fragments, within a recrystallized matrix of fine grained, foliated sericite, chlorite, quartz and plagioclase, locally with significant amounts of calcite and epidote. It becomes predominant in the upper part of the basal

Figure 4. Thin-bedded sandstone, siltstone and phyllite, basal part of unit KS1, southwestern part of the map area.

Figure 6. Graded gritty sandstone bed, unit KS1, 700 m southeast of peak 1896.

section, and passes upwards into a thick interval of fragmental schists that form the dominant rock type within unit KS1. These fragmental schists are typically medium to dark green, and weather to a pale brownish green colour. They comprise flattened, commonly epidote altered lithic fragments and plagioclase grains within a well-foliated matrix that contains variable proportions of chlorite, sericite, quartz, plagioclase, calcite and epidote, and locally actinolite or stilpnomelane (Figure 5). The lithic fragments are typically a few millimetres to a few centimetres in size, but coarser units, with lithic clasts up to 10 cm in longest dimension, occur locally. The fragments are dominated by aphanitic to very fine grained felsite, locally with small feldspar and/or quartz phenocrysts. Fragments composed of fine grained, equigranular intergrowths of feldspar and quartz are also present, and one exposure, 1.5 km east of peak 1896, includes a substantial number of medium grained quartz monzonite clasts. The fragmental schists commonly display a crude stratification, and in places occur as distinct thin to thick beds, some of which are graded (Figure 6). The stratification is enhanced locally by intercalations of thin bedded medium green chlorite-sericite schist with relict sand-size grains of quartz and plagioclase, or medium to dark grey laminated phyllite and siltstone.

Figure 5. Felsic fragmental schist, unit KS1, 1 km south of peak 2075.

In the western part of the map area, the uppermost part of unit KS1 is dominated by relatively fine grained, commonly thin bedded to laminated schists comprised of well-foliated quartz, plagioclase, sericite, chlorite, epidote and calcite, locally with biotite or stilpnomelane, commonly containing relict silt to sand-size grains of quartz and plagioclase. These rocks, derived from felsic tuffs and/or epiclastic rocks, are intercalated with compositionally similar schists and semischists derived from coherent felsic volcanic rocks, with porphyritic textures defined by scattered phenocrysts of plagioclase±quartz.

A sill of medium grained melanocratic hornblende-pyroxene gabbro cuts fragmental schists of unit KS1 about 1 km east of peak 1896. The sill locally displays a weak foliation and is suspected to be broadly related to the Kutcho assemblage. It may be part of a magmatic system that fed overlying mafic metavolcanic rocks of unit KS2.

Unit KS2

Unit KS2 consists mainly of chlorite-epidote schist derived from mafic volcanic and volcaniclastic rocks. The mafic schists overlie, and interfinger with, the felsic schists of unit KS1, and locally include narrow units of similar felsic schist, as well as units of chlorite-epidote-feldspar schist derived from dioritic intrusive rocks.

The predominant rock type of unit KS2 is medium to dark green, greenish brown weathered, calcareous epidote-chlorite schist that commonly has a laminated appearance due to the segregation of metamorphic minerals into alternating chlorite-rich and calcite-epidote-rich layers (Figure 7). Relict feldspar grains are conspicuous in many exposures, and blebs of dark green chlorite, 2-4 mm across, that may have been derived from pyroxene phenocrysts were observed in an exposure 500 m north of peak 1896. This exposure also features small vesicles, suggesting that these schists were derived from

Figure 7. Plagioclase-epidote-chlorite schist, unit KS2, 2 km northwest of peak 2075.

weakly vesicular flows. Elsewhere, protolith textures are obscure, although fragmental schist, with epidote-altered fragments several centimetres in size, occurs locally, and may have been derived from pillow or flow breccia. Thin sections of typical schist comprise thoroughly recrystallized calcite-epidote-chlorite-plagioclase, with traces of quartz and sericite.

Dioritic rocks, with a relict medium grained, equigranular texture of intergrown plagioclase and altered mafic minerals, were noted at several localities within unit KS2, and locally form sill-like bodies up to several tens of metres wide. A thin section from one of these metadiorite units comprises relict plagioclase grains interspersed with a metamorphic assemblage dominated by epidote, actinolite, chlorite and calcite.

Quartz-plagioclase-sericite schists, derived from felsic volcanic and volcaniclastic rocks, are scattered throughout unit KS2, but are a relatively minor component and typically form narrow units less than 10 m wide. Some are porphyritic rocks, derived from flows, sills or dikes, which contain relict phenocrysts of plagioclase and/or quartz. Others are derived from tuffs or epiclastic rocks, and contain small felsic lithic fragments as well as relict crystals of quartz and plagioclase. One felsic dike that cuts mafic schists 500 m north of peak 1896 comprises fine grained, equigranular hornblende-biotite tonalite.

CENTRAL DIVISION

The central division of the Kutcho assemblage is a heterogeneous succession that includes large amounts of coherent metarhyolite, as well as epidote-chlorite schists derived from mafic volcanic rocks, fragmental schists derived from felsic volcaniclastic rocks, and bedded metasedimentary intervals that include sandstone, siltstone, phyllite and chert. Metarhyolite forms a large mappable unit in the west-central part of the unit, but most of the components are intercalated on too fine a scale to be separated out on Figure 2. Tonalite forms a large sill-like intrusion in the central part of the division, and two smaller bodies farther north. Small bodies of metadiorite are also present, but are not sufficiently large to be shown on Figure 2.

Mafic metavolcanic rocks form dark green, brownish-weathered units that range from a few metres to several tens of metres thick. They consist of variably calcareous actinolite-epidote-chlorite-plagioclase schists that display little of their original mineralogy or texture, although epidote-rich amygdules are preserved locally, and hints of pillows were noted in a few exposures. Small bodies of metadiorite are associated with the mafic metavolcanic rocks locally, and are recognized by a relict medium grained, equigranular texture of plagioclase intergrown with mafic grains that are now altered to actinolite, epidote and chlorite.

Metarhyolite units range from a few metres to several hundreds of metres thick, and probably include flows, sills and dikes. They are typically light grey to greenish grey, weakly foliated rocks that display conspicuous phenocrysts, 1-4 mm in size, of quartz and plagioclase, within a very fine-grained groundmass of quartz, plagioclase and scattered flakes of sericite (Figure 8). Relict flow banding was noted at a few localities, and breccia zones comprising metarhyolite fragments within a similar metarhyolite matrix, occur locally. Some narrow units, and the margins of some thicker units, are strongly foliated quartz-sericite schists with flattened phenocrysts. Metarhyolite typically forms tabular concordant units intercalated with all other major components of the central division. Locally, however, it occurs as irregular dikes that crosscut some mafic metavolcanic units. The large mappable metarhyolite body is probably a composite flow-dome unit. It displays considerable variation with respect to amounts, proportions and size of quartz and feldspar phenocrysts, and several internal breccia zones, but does not include significant intercalations of mafic metavolcanic or metasedimentary rocks.

Fragmental schists within the central division consist of flattened, pale grey to green felsic volcanic clasts, and

Figure 8. Quartz-feldspar phyric metarhyolite, central division of the Kutcho assemblage, Sumac ridge.

grains of plagioclase and quartz, within a foliated matrix of fine-grained chlorite, sericite, plagioclase and quartz (Figure 9). These occur as poorly stratified units that were probably derived from felsic tuffs or mass-flow deposits, as well as thick beds intercalated with finer grained metasedimentary rocks. Locally, fragmental schists are derived from the brecciated margins of coherent metarhyolite units.

Intervals of well bedded metasedimentary rocks, from a few metres to several tens of metres thick, are fairly common within the central division of the Kutcho assemblage, particularly within the northern, stratigraphically higher parts of the division. The metasedimentary rocks are commonly represented by narrow intervals of thin bedded, dark grey to greenish grey phyllite, siliceous phyllite, chert and siltstone (Figure 10). Thicker sections include thin to thick beds of fine to coarse-grained sandstone and granule conglomerate that contain feldspar, quartz and felsic lithic fragments. Pale grey to greenish grey bedded chert, comprising thin chert beds separated by thinner interbeds and partings of siliceous phyllite, locally dominates intervals up to 20 m thick. Chert also occurs as massive to vaguely laminated

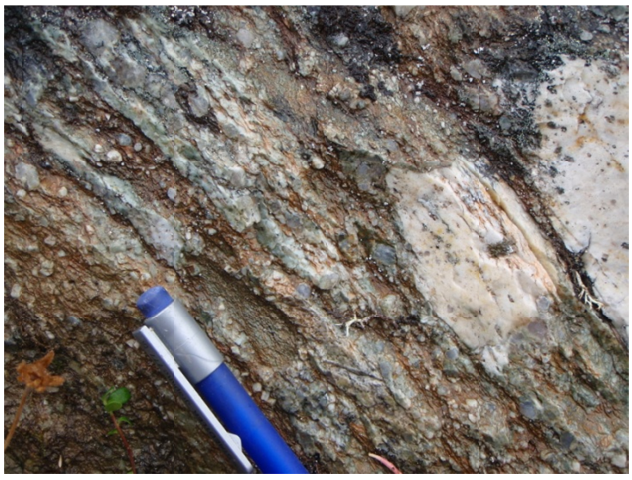

Figure 9. Felsic fragmental schist, central division of the Kutcho assemblage, south end of Conglomerate ridge.

Figure 10. Thin-bedded phyllite, siliceous phyllite and chert, central division of the Kutcho assemblage, Sumac ridge.

layers up to several metres thick that may have been derived from siliceous exhalites.

Tonalite

Tonalite forms a large elongate pluton, up to 1 km wide and more than 10 km long, within the central part of the central division of the Kutcho assemblage. Two smaller tonalite bodies are mapped to the north of the main body, and narrow dikes or sills of tonalite were noted at a few localities elsewhere in the division. The tonalite typically forms blocky, light grey-weathered exposures. It is characterized by a medium grained, equigranular texture of intergrown quartz and plagioclase, but some sections are coarse grained, with quartz grains and aggregates more than 1 cm in size (Figure 11). Primary mafic minerals are not preserved, but clots of chlorite-epidote comprise 5 to 20% of the rock. A weak to moderate foliation is displayed locally, and is defined by anastomosing seams of sericite and chlorite that enclose partially shredded grains of relict quartz and feldspar and, locally, small titanite grains.

NORTHERN DIVISION

The northern division of the Kutcho assemblage consists mainly of chlorite-sericite schists that contain variable proportions of quartz and feldspar crystals and felsic lithic fragments. These rocks were derived from felsic tuffs, flows and related epiclastic deposits. They are subdivided into 3 units, KN1, KN2 and KN3, on the basis of the types and proportions of the crystal and lithic fragments they contain. The uppermost unit within the division, KN4, consists mainly of thin bedded volcanic sandstone, siltstone and phyllite. A thick gabbroic sill is mappable within the northern division, and dikes and sills of similar composition are common within unit KN4.

Unit KN1

Unit KN1 comprises feldspar and quartz-bearing schists derived mainly from crystal-rich tuffs. It forms the base of the northern Kutcho division in the area south of

Figure 11. Tonalite, from main tonalite body that cuts the central division of the Kutcho assemblage, 800 m south of peak 1732.

the Kutcho Creek deposit, where it underlies unit KN2, which hosts the massive sulphide lenses. It thins to the east, where it becomes stratigraphically or structurally interleaved with a belt of rocks assigned to unit KN3, and was not recognized in the area northwest of peak 1732.

The schists of unit KN1 are medium green on fresh surfaces and typically weather to a grey-green or brownish green colour. They are characterized by conspicuous grains of plagioclase, typically 1-4 mm in size, which are invariably accompanied by quartz grains of similar or smaller size, and locally by quartzofeldspathic and/or epidote altered lithic grains, 2-10 mm in size (Figure 12). The plagioclase typically forms whole or broken crystals with subhedral shapes. The quartz crystals commonly display embayed margins, and locally include granophyric intergrowths of plagioclase. The relict mineral and lithic grains typically form more than 50% of the rock, and are enclosed in a fine grained, well-foliated matrix of chlorite, sericite, quartz and plagioclase, locally with significant amounts of epidote and carbonate. The schists are for the most part not conspicuously stratified, but locally they are intercalated with narrow intervals of thin-bedded schist of similar composition but finer grain size.

Unit KN2

Unit KN2 comprises fissile, variably pyritic quartz-sericite schists and fragmental schists that comprise the hydrothermally altered footwall to the Kutcho Creek massive sulphide lenses. The unit is referred to as the footwall lapilli tuff by Bridge *et al.* (1986) and Barrett *et al.* (1996). It has been traced about 5 km eastward from the Kutcho Creek deposit, to the area north of peak 1732.

Unit KN2 consists mainly of pale grey to greenish grey, very fissile quartz-sericite schist that commonly weathers rusty due to the presence of disseminated pyrite and flattened porphyroblasts of Fe-Mg carbonate (Figure 13). Small grains of quartz are common, as are flattened lithic fragments, up to a few centimetres long, of pale grey siliceous felsite, with or without small phenocrysts of quartz. Narrow lenses of quartz-plagioclase phyric metarhyolite, derived from flows, sills or dikes, were noted locally. They comprise about 25% quartz and plagioclase phenocrysts, 2-4 mm in size, within a very fine grained, weakly foliated groundmass of quartz, plagioclase and sericite.

Unit KN3

Unit KN3 is a distinctive unit characterized by coarse quartz grains. It occurs stratigraphically above the Kutcho Creek massive sulphide lenses, where it is referred to as hangingwall quartz-feldspar crystal tuff (QFCT) by Bridge *et al.* (1986), and QFCT rhyolite by Barrett *et al.* (1996). This belt can be traced into the eastern part of the map area, but is partially obscured by the gabbro sill. A belt of similar rocks forms the south margin of the northern division east of Imperial ridge. It is suspected that this belt is a fault bounded repetition of the

Figure 12. Sericite-chlorite schist with plagioclase and quartz grains, unit KN1, Imperial ridge.

Figure 13. Rusty weathered quartz-sericite schist, unit KN2, 3 km northwest of peak 1732.

hangingwall belt, although there appears to be some stratigraphic interfingering with unit KN1. The northern and southern belts of unit KN3 apparently merge farther to the east, to form a single wide belt that forms most or all of the northern Kutcho division in the eastern part of the map area. If the southern belt is, in fact, largely fault bounded, then this wide belt northeast of peak 1732 probably includes one or more fault repetitions.

Unit KN3 consists primarily of medium to pale green or silvery green schists that contain abundant glassy quartz eyes, typically 2-10 mm in size, but locally to 1.5 cm, as well as smaller plagioclase grains, typically 1-5 mm in size (Figure 14). The quartz crystals are highly strained and commonly have embayed margins. The plagioclase grains are variably altered to sericite and/or epidote, and commonly have subhedral or euhedral outlines. In a few exposures the crystal grains are accompanied by sparse quartzofeldspathic lithic fragments, up to 3 cm in size. The large crystal grains commonly form 20-40% of the rock, and are enveloped by a matrix that consists mainly of fine grained, well-foliated quartz, plagioclase sericite and chlorite. There is little evidence for stratification or internal contacts within

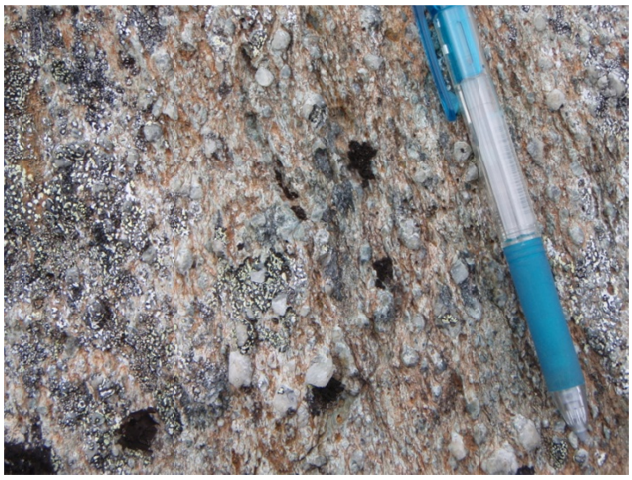

Figure 14. Coarse quartz-eye schist, unit KN3, north end of Imperial ridge.

the unit, despite the fact that there is considerable variation in the abundance and proportions of crystal grains, as well as sericite versus chlorite content of the foliated matrix. However, Bridge *et al.* (1986) report that drillholes in the vicinity of the Esso massive sulphide lens have intersected thick graded beds in the upper part of the unit.

A lens of coarse matrix-supported breccia, at least several tens of metres wide, is exposed within the upper part of unit KN3 at the north end of Sumac ridge. The matrix consists of coarse quartz-eye schist typical of the unit, and the vast majority of the clasts, which range up to 30 cm in size, are the same rock type (Figure 15). The clast population also includes a minor proportion of fine to medium grained equigranular quartzofeldspathic rock, and rare mafic clasts of calcareous epidote-chlorite schist. Parts of the breccia unit display hints of a crude stratification, and lenses of laminated coarse grained quartz-feldspar sandstone are intercalated with coarse breccia units locally (Barrett *et al.*, 1996).

The schists of unit KN3 are clearly derived from rhyolitic volcanic or volcaniclastic rocks, but it is not generally obvious whether the protolith was coherent

Figure 15. Breccia, unit KN3, north end of Sumac ridge.

porphyritic flows, tuffs or epiclastic rocks. Barrett *et al.* (1996) suggest that the unit is derived mainly from crystal rich pyroclastic flows with lesser block and ash flows, locally reworked as high density debris flows.

Unit KN4

Unit KN4, comprising siltstone, sandstone and phyllite, is the uppermost unit of the Kutcho assemblage within the map area. It is underlain mainly by coarse quartz-eye schists of unit KN3, and is overlain by the conglomerate unit. Unit KN4 is cut by the main gabbro sill, and includes numerous thinner sills and dikes of gabbro.

Unit KN4 is equivalent to the tuff-argillite unit of Bridge *et al.* (1986) and Childe and Thompson (1997), and the argillite-siltstone unit of Barrett *et al.* (1996). It is not well exposed, and a large proportion of the few available outcrops are dominated by gabbroic sills and dikes that intrude the metasedimentary rocks of the unit. Where exposed, the metasedimentary succession includes grey, brownish grey weathered, well bedded schisty sandstone, vaguely laminated grey-green phyllitic siltstone to fine-grained sandstone, and grey phyllite to silty phyllite. The schisty sandstone ranges from coarse to fine grained and occurs as thin to medium, locally graded beds (Figure 16). Detrital grains are mainly feldspar and quartz, but coarse sandstone and gritty sandstone beds also contain flattened chips of quartz-feldspar-sericite phyllite, probably derived from felsic lithic grains, and blebs of biotite-chlorite that may have been derived from mafic mineral or lithic grains. A thin section from a fine-grained sandstone unit consists of well-foliated quartz-plagioclase-sericite-biotite, with minor chlorite and calcite, which preserves little of its original clastic texture.

Gabbro

Gabbro forms a thick body, up to 500 m wide in map-view, which has been traced for about 8 km within the northern division of the Kutcho assemblage. Although its three-dimensional orientation and true thickness are

Figure 16. Graded sandstone beds, unit KN4, northeast of Kutcho Creek massive sulphide deposits.

not well constrained, it has the appearance of a transgressive sill that gradually cuts upsection from east to west. Similar gabbro is common as dikes and sills within unit KN4, and has also been reported as narrow dikes in felsic schists lower in the section (Childe and Thompson, 1997).

The gabbro is dark green on fresh surfaces and typically forms blocky, grey-green or brownish green weathered exposures. Relict crystals of randomly-oriented plagioclase, commonly up to 1 cm, and locally to several centimetres in size, are conspicuous in most exposures. Relict hornblende grains may also be present, but the mafic component has largely been replaced by a weakly to moderately foliated metamorphic assemblage dominated by epidote, biotite, actinolite, chlorite and calcite. Sericite is also common, typically as an alteration mineral within the relict plagioclase grains, and minor amounts of apatite occur as small relict grains.

The gabbro unit cuts the uppermost part of the northern Kutcho division, including post-volcanic sedimentary rocks of unit KN4, and it has a chemical signature that is distinct from mafic metavolcanic rocks elsewhere within the Kutcho assemblage (Barrett *et al.*, 1996; Childe and Thompson, 1997). It may, therefore, be unrelated to the volcanic and plutonic rocks of the Kutcho assemblage. However, Childe and Thompson (1997) suggest that the gabbro is not significantly younger, because gabbro units display peperitic textures where they contact metasedimentary rocks of unit KN4, and interaction zones where they contact underlying felsic metavolcanic rocks, suggesting that these units had not been completely lithified when they were intruded by the gabbro.

Conglomerate unit

The conglomerate unit forms a single belt that has been traced across the north-central part of the map area, where it is underlain by the Kutcho assemblage and overlain by the Sinwa Formation. It has long been recognized as a distinct map unit, but has been variably interpreted as either part of the Kutcho assemblage (Bridge *et al.*, 1986; Thorstad and Gabrielse, 1986) or part of the stratigraphic succession that overlies the Kutcho assemblage (Panteleyev and Pearson, 1977b; Childe and Thompson, 1997). Here, it is included in the succession that overlies the Kutcho assemblage, possibly across a significant disconformity. This interpretation is based on the abrupt lower contact of the conglomerate unit, a provenance that is dominated by a variety of lithologic units within the underlying Kutcho assemblage, and a gradational contact with the overlying Sinwa Formation. The conglomerate may have a limited lateral extent, because it is not present in the syncline south of its exposure belt, where the Sinwa Formation rests directly above the central division of the Kutcho assemblage.

The conglomerate unit generally weathers to a light greenish grey to brownish grey colour, and consists of flattened pebbles and cobbles within a schistose matrix of chlorite, sericite and sand-size grains of quartz and feldspar (Figure 17). The clast population is dominated by a variety of pale grey felsic rock types, including aphanitic felsite, quartz±plagioclase-phyric felsite, quartz-sericite schist and fine to coarse grained equigranular tonalite. Less common clast types include sericite-chlorite schist, medium to dark green chlorite schist, feldspathic chlorite schist and limestone. Foliation within the schistose clasts is parallel to, and continuous with, the matrix schistosity. The conglomerate is typically unstratified, poorly size-sorted and matrix supported. Some sections, however, consist of moderately sorted pebble conglomerate that occurs in poorly defined thick beds. Locally the conglomerate is intercalated with thin to medium beds of finer grained rocks, including schistose sandstone, pebbly sandstone and grey phyllite. Lenses of limestone, up to 1.5 m wide and several tens of metres long, also occur, and some of these enclose smaller lenses of schistose granule conglomerate that contains quartz, feldspar and small felsic lithic fragments. In a fairly well-exposed section northeast of the Kutcho Creek VMS deposit, limestone lenses become gradually more abundant in the upper part of the conglomerate unit, where associated pebble conglomerate units commonly have a limestone matrix.

The conglomerate unit is not dated, but is suspected to be Late Triassic on the basis of its gradational contact with limestone correlated with the latest Triassic Sinwa Formation. It is on the order of 150 m thick along most of its exposure belt, but appears to thicken where it is folded through an anticline-syncline pair west of the Kutcho Creek VMS deposit, although the effects of internal folding on this apparent thickness are unknown. However, assuming that some of this apparent thickening is primary, it suggests that the conglomerate unit thickens to the south or southwest, toward the contact with the central Kutcho division. In contrast to this apparent southward thickening, the conglomerate unit is not even present 2 to 3 km farther south, where the Sinwa Formation rests directly above metarhyolite of the central division. This pattern suggests that the basin in which the conglomerate

Figure 17. Conglomerate of the conglomerate unit, Conglomerate ridge.

was deposited may have been controlled by a down-to-the-north growth fault located near the present contact between central and northern divisions of the Kutcho assemblage.

Sinwa Formation

The Sinwa Formation is a limestone unit that has been traced across most of the width of north-central part of the map area, where it occupies a stratigraphic position between the underlying conglomerate unit and the overlying Inklin Formation. The Sinwa Formation is also exposed farther south, in the west-central part of the map area, where it outlines a faulted syncline cored by the Inklin Formation. The conglomerate unit is not present in this area, and the Sinwa limestone rests directly above metarhyolite of the central division of the Kutcho assemblage. The width of the Sinwa Formation in map-view suggests that it has a stratigraphic thickness ranging from a few tens of metres to almost 100 m in the north-central part of the map area, although the apparent thickness may be modified by internal folding, as it appears be in the large area of limestone exposures on the north limb of the syncline in the west-central part of the map area.

The Sinwa Formation consists almost entirely of grey and white, weakly to moderately foliated, recrystallized limestone that weathers to a uniform light grey to medium brownish grey colour (Figure 18). Intervals of dark grey, fine-grained limestone and slaty limestone occur locally. The basal contact with underlying conglomerate in the northern belt appears to be gradational, as suggested by the common occurrence of limestone lenses in the upper part of the conglomerate unit, and local intercalations of calcareous, schistose conglomerate, compositionally similar to the underlying unit, within the basal part of the Sinwa. The contact between Sinwa limestone and underlying Kutcho metarhyolite in the west-central part of the map area was not observed, but it is well constrained locally, and appears to be sharp and probably disconformable.

The type area of the Sinwa Formation is at Sinwa Mountain in the Tulsequah map area (NTS 104K), almost 300 km west-northwest of Kutcho Creek (Souther, 1971). There, the formation comprises late Upper Triassic (Norian) limestone that occurs in the hangingwall of the King Salmon thrust fault, and is stratigraphically overlain by the Lower Jurassic Inklin Formation. Exposures of Sinwa Formation are intermittent between the type area and the current map area (Gabrielse, 1998), but the correlation is reasonable, given the commonality of stratigraphic position directly beneath the Inklin Formation and structural setting within the King Salmon allochthon. The Sinwa Formation is not dated in the current map area, but fossils collected from correlative limestone west of Kutcho Creek include schleractinian corals, consistent with a Late Triassic age (Panteleyev and Pearson, 1977b; Monger, 1977). Samples collected from the map area in 2010 are currently being processed for conodonts.

Figure 18. Limestone, Sinwa Formation, 2 km north of peak 1732.

Inklin Formation

Clastic metasedimentary rocks assigned to the Lower to Middle Jurassic Inklin Formation form a wide belt that crosses the northern part of the map area. They are in stratigraphic contact with the underlying Sinwa Formation to the south, and are juxtaposed against ultramafic rocks of the Cache Creek terrane across the Nahlin fault to the north. The Inklin Formation is not well exposed in much of this belt, but good exposures occur on ridges south of the Nahlin fault, and along parts of Andrea Creek. The formation is also represented by a narrow belt of scattered exposures in the west-central part of the map area, where it occurs above the Sinwa Formation in the core of a faulted syncline.

The Inklin Formation consists mainly of dark to medium grey slate that typically contains small porphyroblasts of rusty Fe-Mg carbonate. Bedding is commonly defined by laminations and thin interbeds of siltstone and slaty siltstone (Figure 19). Sandstone, containing detrital quartz and feldspar, is less common, but dominates some parts of the formation. It typically occurs as thin to thick, locally graded beds intercalated

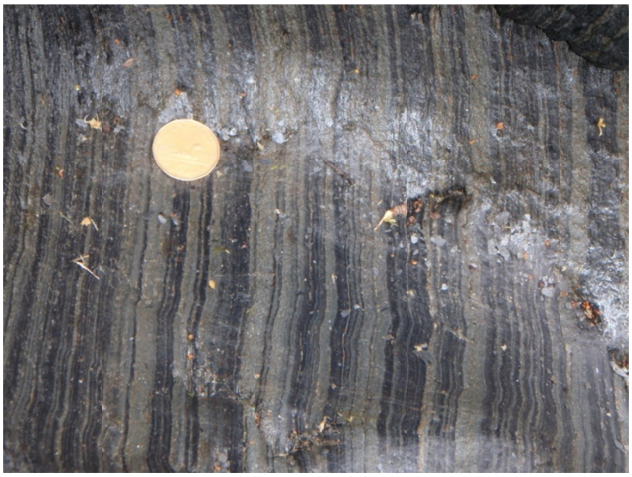

Figure 19. Laminated slate and siltstone, Inklin Formation, Andrea Creek.

with thinner interbeds of slaty siltstone. Limestone and brown weathered calcareous sandstone form thin to medium beds and lenses in the basal part of the formation, giving the impression of a gradational contact with the underlying Sinwa Formation.

The Inklin exposures within the current map area have been traced westward through the Cry Lake and Dease Lake map areas (Gabrielse, 1998) into the type area of the Inklin Formation in the Tulsequah map area (Souther, 1971). The formation is not well dated anywhere along this belt (Gabrielse, 1998), but fossil data from contiguous strata still farther to the northwest, in the Atlin Lake and Tagish Lake areas, indicate an Early Jurassic, Sinemurian to Toarcian age (Johannson *et al.*, 1997; Mihalynuk, 1999). Correlative strata farther north, in the Yukon, range from Lower to Middle Jurassic (Bajocian) (Pálfy and Hart, 1995).

Ultramafic rocks of Cache Creek terrane north of the Nahlin fault

Ultramafic rocks of the Cache Creek terrane crop out along the north margin of the study area. They are juxtaposed against the Inklin Formation across the Nahlin fault, and are truncated to the east by the Kutcho fault. They are part of a widespread ophiolitic assemblage that forms a major part of the Cache Creek terrane of northern British Columbia (Monger, 1975; Terry, 1977; Ash, 2001; English *et al.*, 2010).

The ultramafic rocks for the first 100 to 200 m north of the Nahlin fault comprise irregularly foliated and fractured serpentinite that weathers to shades of light to dark green and grey. The serpentinization is less pervasive farther north, where the protolith is largely harzburgite with local patches of dunite. The harzburgite weathers to a rusty brown colour, with an irregular surface that is the result of resistant grains of orthopyroxene, 4 to 12 mm in size, standing in relief against a recessive background inferred to be mainly serpentinized olivine. Dunite, consisting mainly of serpentinized olivine, is characterized by weathered surfaces that are relatively smooth and a lighter reddish tan colour. Lenses of chlorite schist occur locally within serpentinized ultramafite and might be tectonic inclusions or altered mafic dikes. A lens of dark grey slaty siltstone that was traced for about 150 m in a west-northwest direction, 600 m north of the trace of the Nahlin fault, is probably a fault-bound sliver derived from the Inklin Formation.

Ultramafic rocks along the Kutcho fault are altered to orange weathered listwanite which forms a conspicuous band up to 200 m wide. Listwanite was also noted along a minor north-striking fault within the main part of the ultramafic unit, several kilometres west of the Kutcho fault. The listwanite consists of finely crystalline magnesite, locally with scattered small grains of mariposite, cut by variably oriented veins of quartz and magnesite.

Plutonic rocks of Quesnel terrane

Granitic rocks that crop out on the northeast side of the Kutcho fault are part of an unnamed and undated pluton within Quesnel terrane. The pluton cuts Late Triassic volcanic and sedimentary rocks of the Shonektaw Formation to the east and northeast of the map area (Gabrielse, 1998). Exposures examined in the northern and central parts of the current study area comprise a heterogeneous mixture of hornblende diorite to quartz diorite and hornblende-biotite tonalite, with numerous patches of dark grey hornfels and fine grained dioritic rock that probably represent screens of country rock and/or older phases of the pluton. Exposures in the southern part of the area are more homogeneous, consisting of grey-green, medium grained, equigranular hornblende granodiorite.

Bowser Lake Group

Rocks assigned to the Bowser Lake Group form the southernmost unit mapped within the study area, where they occur in the footwall of the King Salmon thrust fault. They were examined in several exposures along lower Josh Creek near the eastern edge of the map area, and in a small exposure in the southwestern part of the area, on the wooded slopes near the southern limit of mapping. Pebble conglomerate forms the latter exposure, and is the dominant lithology in the Josh Creek exposures. It weathers brown to rusty brown, and contains subangular to subrounded clasts ranging from a few millimetres to 5 cm in size. The clasts are dominated by chert, in shades of light to dark grey and light to medium green, but fragments of mafic volcanic rock, siliceous argillite and quartz are also present. The small size fraction grades into a sandy matrix dominated by grains of chert and quartz.

Brown weathered, fine to coarse-grained sandstone, composed mainly of chert and quartz, occurs as single or multiple thin to medium beds intercalated with conglomerate in the Josh Creek exposures. Some beds are graded, and overlying conglomerate forms a channel cutting into the top of one sandstone bed.

The Bowser Lake Group along Josh Creek also includes exposures of dark grey slate that were not seen in stratigraphic contact with the dominant conglomerate. The slate is highly folded and faulted, and contains cleavage-parallel veins and lenses of rusty weathered Fe-Mg carbonate.

The Bowser Lake Group ranges from Middle Jurassic to Early Cretaceous in age (Tipper and Richards, 1976; Evenchick, 1991). The panel of rocks in the current map area probably represents part of the lower, Middle Jurassic, portion of the group (Gabrielse, 1998); it has yielded Bajocian fossils 30 km west of the map area, and is cut by a late Middle Jurassic pluton 15 km southeast of the map area.

Eocene intrusions

Small, intermediate to mafic, post-metamorphic intrusions are scattered sparsely through much of the map area, and are common within the Kutcho assemblage and Cache Creek Complex in the southwestern part of the area. Most of the intrusions are porphyritic sills and dikes, ranging from a few metres to a few tens of metres wide, comprising phenocrysts of feldspar, hornblende and locally pyroxene, within a grey to brown, massive to platy, aphanitic to very fine grained feldspathic groundmass. Medium grained, equigranular diorite that might be part of the same plutonic suite forms a small stock, 300 m in diameter, that underlies peak 2075, and also a north-northeast striking dike, 6 to 8 m wide, that cuts schists of unit KN3 about 1 km northeast of peak 1732. The diorite contains approximately equal proportions of plagioclase and mafic minerals, the latter comprising clinopyroxene, hornblende and biotite.

The intrusive suite described above is inferred to be Eocene, on the basis of a radiometric date obtained from a dike that crops out 1 km northeast of peak 2075. Stevens *et al.* (1982) report that a hornblende separate, containing about 10% biotite, from this dike yielded a K/Ar date of 55.4 ±3.0 Ma.

STRUCTURE

Mesoscopic structure

All map units within the King Salmon allochthon are characterized by a penetrative cleavage or schistosity defined by the preferred orientation of greenschist facies metamorphic mineral assemblages and, in coarse-grained units, variably flattened primary crystal and lithic fragments. The schistosity typically dips at moderate to steep angles to the north, and is axial planar to mesoscopic folds of bedding which were observed sporadically within well-bedded units. The folds plunge gently to the west or west-northwest, and typically verge to the south. Lineations defined by bedding/cleavage intersections and, rarely, the elongation of mineral and lithic fragments, are parallel to the fold axes. A younger crenulation cleavage, which dips more gently to the north, was observed to cut the schistosity at a few locations scattered across the map area. It is best developed in the Inklin Formation within the core of the syncline 2.5 km north-northeast of peak 2075. There, the crenulation cleavage dips 30 to 40 degrees to the north, and is axial planar to open folds of the main slaty cleavage that plunge gently to the west-northwest. The main schistosity is also deformed by another, more common set of mesoscopic folds and kinks with axes that plunge steeply to the north or northeast. Axial surfaces are typically steep and do not have an associated cleavage.

Macroscopic structure of the King Salmon allochthon

The macroscopic structure of the King Salmon allochthon comprises predominantly north dipping and facing map units that are locally deformed by south-verging asymmetric folds and(?) north dipping thrust faults (Figure 3). The folds formed at the same time as the penetrative schistosity displayed by all units within the allochthon. The bounding King Salmon and Nahlin thrust faults, as well as the inferred north dipping thrust faults within the allochthon, probably formed during the same deformational event, but in detail may be slightly younger. A variety of constraints beyond the current map area suggest that this deformation occurred in early Middle Jurassic time (Tipper, 1978; Mihalynuk *et al.*, 1992, 2004).

The Cache Creek rocks that form the base of the allochthon in the southwest part of the map area are inferred to underlie the Kutcho assemblage across a north dipping thrust fault that appears to merge with the King Salmon fault. The overlying southern division of the Kutcho assemblage forms a panel that mainly dips and faces to the north. The sinuous contact between units KS1 and KS2 is suspected to be the result of stratigraphic interfingering, but might indicate the presence of an east-plunging south-verging fold pair.

The central division of the Kutcho assemblage structurally overlies the southern division with no apparent discordance. The contact is interpreted to be stratigraphic, but is not well enough exposed to preclude the presence of significant layer-parallel faults. A west-plunging syncline in the southwestern part of the division is defined by infolded Sinwa and Inklin formations, and a poorly defined complimentary anticline to the north is apparently cored by metarhyolite and tonalite. The northern part of the central division occupies the north limb of this anticline, and is deformed by numerous mesoscopic and medium-scale folds that show southward vergence, as defined by long moderately north-dipping backlimbs and short, steeply-dipping forelimbs.

The northern part of the King Salmon allochthon, including the northern division of the Kutcho assemblage and overlying sedimentary units, forms a predominantly north dipping and facing succession that is deformed by a west-plunging, south-verging anticline/syncline pair that is well defined by the conglomerate unit and overlying Sinwa Formation. The Inklin Formation displays considerable internal folding and might encompass additional folds of similar magnitude, but was not examined in sufficient detail to determine if this is the case. The structure of the southern part of this panel, including the contact between the northern and central divisions of the Kutcho assemblage, is not well understood. It is suspected that the boundary between the two divisions is a system of faults, in part because there is an apparent truncation of medium-scale folds in the central division along this contact in the western part of

the map area. Farther east, there is a structural(?) interleaving of central and northern division lithologies across recessive contacts that are suspected, but not proven, to be faults. This system of inferred faults may have accommodated south-directed thrust movement, congruent with other major structures within and bounding the King Salmon allochthon. However, as discussed previously, these faults may, in part, have originated at an earlier time, as down-to-the-north growth faults that localised deposition of the conglomerate unit.

The youngest structures mapped within the King Salmon allochthon are steeply dipping, northwest-striking faults that correspond to local offsets of the predominantly east trending lithologic contacts and structures. These late structures display both dextral and sinistral apparent offsets, but the actual sense of movement was not established.

King Salmon thrust fault

The King Salmon fault is an important regional structure that forms the structural base of the King Salmon allochthon. It has been traced about 300 km west-northwest from the current map area, where it apparently merges with the long-lived, northwest trending Llewellyn fault zone (Mihalynuk, 1999). Where exposed, the King Salmon fault dips at low to moderate angles to the north, and displays deformation fabrics and map relationships consistent with south-directed thrust motion (Souther, 1971; Thorstad and Gabrielse, 1986; Gabrielse, 1998).

The King Salmon thrust fault crosses the southern part of the map area, but its position is well constrained only in the southwest corner of the area, southwest of peak 1667, and along the lower reaches of Josh Creek in the southeast part of the area. In the southwest, the fault separates the Cache Creek Complex from the Bowser Lake Group. It is constrained by exposures of Cache Creek serpentinite and Bowser Lake chert-pebble conglomerate about 200 m apart, but no structures or fabrics related to the fault were observed.

The fault is more tightly constrained along Josh Creek, where it is defined by exposures of Kutcho assemblage and Bowser Lake Group about 30 m apart. The Kutcho rocks directly above the fault are part of unit KS1, and consist mainly of dark grey phyllite that locally contains thin to medium graded sandstone beds that dip and face 45º to the north-northwest. The grey phyllite is commonly altered to pale green, rusty weathered ankerite-sericite schist, and the phyllitic cleavage is contorted by folds with highly variable orientations. Folds within altered ankerite-sericite schist near the structural base of the exposure, however, generally plunge gently to the east or west, and, where asymmetric, verge to the south. Exposures of footwall Bowser Lake Group most proximal to the fault trace consist of chert pebble conglomerate with local graded sandstone interbeds that are vertical and face to the north-northeast. These rocks are cut by brittle faults that dip at moderate to steep angles to the north, and locally display downdip striations. Farther to the southeast, an isolated exposure displays a minor thrust(?) fault that dips 45º to the north and places massive chert-pebble conglomerate above contorted magnesite-altered slate that is also part of the Bowser Lake Group. Similar magnesite-altered slate forms a larger exposure farther downstream, but still within 100 m of the King Salmon fault trace. In this exposure the slaty cleavage is folded by northeast-plunging folds that are cut by younger faults that dip at moderate to steep angles to the east-northeast.

Nahlin fault

The Nahlin fault has been traced from the current map area more than 350 km west-northwest to the Atlin Lake area (Souther, 1971; Mihalynuk *et al.*, 1992; Gabrielse, 1998). It forms the northeast boundary of the King Salmon allochthon, and juxtaposes the Inklin Formation, on the southwest side of the fault, with rocks of the Cache Creek terrane to the northeast. The fault is generally interpreted as a northeast-dipping thrust, although some segments dip steeply and may have a component of dextral strike-slip movement (Gabrielse, 1998).

The trace of the Nahlin fault trends east-southeast across the northern part of the map area, and bends sharply to the southeast as it is truncated by the Kutcho fault. It juxtaposes ultramafic rocks of the Cache Creek terrane to the north and northeast against the Inklin Formation to the south and southwest. The fault is easily identified where it crosses alpine ridges and juxtaposes green serpentinite against grey metasedimentary rocks, but it was not studied in enough detail to establish its orientation or kinematic history. A notable feature, however, is the common presence of lenses of rock along the fault trace that are not derived from either the Cache Creek ultramafic unit or the Inklin Formation. These lenses include limestone, sericite-quartz schist (metarhyolite?), silicified chlorite-sericite schist and actinolite-epidote-chlorite schist. They resemble rocks that are common in the Sinwa Formation and the Kutcho assemblage, and may have been derived from these units as the fault ramped through them into the overlying Inklin Formation.

Kutcho fault

The Kutcho fault is a prominent northwest striking regional structure that truncates the east end of the King Salmon allochthon. It is part of a network of orogen-parallel dextral strike-slip faults, of Cretaceous to Eocene age, with a combined displacement of several hundred kilometres (Gabrielse, 1985; Gabrielse *et al.*, 2006). The Kutcho fault displays mylonitic fabrics with dextral kinematic indicators where it cuts the Cassiar Batholith to the northwest of the current map area (Gabrielse, 1998). Right-lateral displacement of about 100 km is indicated by offset of the Hottah and Klinkit faults, which are truncated by the Kutcho fault 15 and 115 km northwest of the present map area (Gabrielse, 1985). Restoration of an additional 200 km of displacement, distributed along

other faults of the network (Thibert, Thudaka, Finlay, Ingenika, Takla), matches the King Salmon allochthon with correlative units included in the Sitlika assemblage of central British Columbia (Monger *et al.*, 1978; Gabrielse, 1985).

The Kutcho fault transects the northeast corner of the Kutcho-Tucho map area, where it truncates the Kutcho assemblage and overlying units, and juxtaposes them against granitic rocks of Quesnel terrane. The fault is easily defined by the contrasting rock packages it separates, and its trace is highly visible through much of the area because ultramafic rocks directly southeast of the fault are altered to orange weathered listwanite. Granitic rocks directly northeast of the fault are highly fractured and altered with chlorite, epidote and carbonate. The deflection of the Nahlin fault into the younger structure is consistent with dextral movement along the Kutcho fault.

MINERAL OCCURRENCES

The Kutcho Creek Cu-Zn volcanogenic massive sulphide deposit occurs within the upper part of the Kutcho assemblage about 6 km east of Kutcho Creek. Known mineralization elsewhere within the map area is restricted to a few minor occurrences of disseminated chalcopyrite and sphalerite. Some of these, however, are associated with extensive zones of pyrite-sericite-quartz alteration, indicating that there is potential for future discoveries within the Kutcho assemblage.

Kutcho Creek (MINFILE 104I 060)

The Kutcho Creek volcanogenic massive sulphide deposit is hosted by the northern division of the Kutcho assemblage on the south side of Andrea Creek. The deposit comprises three lenses of massive sulphide that form a linear, west-northwest trending belt about 3.5 km long. These lenses were originally named, from east to west, the Kutcho, Sumac West and Esso West deposits (Bridge *et al.*, 1986), but are currently referred to as the Main, Sumac and Esso deposits (Makarenko *et al.*, 2010). The deposit was not examined during the current study, and the summary presented here is based mainly on the published reports of Bridge *et al.* (1986) and Barrett *et al.* (1996), as well as a preliminary economic assessment prepared for Kutcho Copper Corporation by JDS Energy and Mining Inc. in July 2010 (Makarenko *et al.*, 2010).

The Kutcho Creek deposit was detected in 1967 by anomalous values for Cu and Zn in a stream sediment sample collected during a joint-venture regional geochemical survey operated by Imperial Oil Ltd. Subsequent prospecting in 1968 identified pyritic quartz-sericite schists, and claims were staked over the not-yet-discovered Main lens. These claims were allowed to lapse, but Imperial Oil Ltd. returned to restake the area in 1972. However, Sumac Mines Ltd. had staked claims in the same area earlier that year, after locating disseminated pyrite-chalcopyrite mineralization during follow-up exploration of a Cu-Zn stream sediment anomaly in a creek west of the Imperial Oil anomaly. The staking by Imperial Oil (later to become Esso Minerals Canada Ltd.) in 1972, and additional staking in the following years, generated a large claim block that surrounded the Sumac claims. Subsequent exploration by both companies, including about 60 000 m of diamond drilling carried out between 1974 and 1982, outlined the 3 massive sulphide lenses, with the western part of the Main lens and the Sumac lens located within the claim block held by Sumac Mines Ltd., and the eastern part of the Main lens and the Esso lens located on claims held by Esso Minerals Canada Ltd. A partnership agreement to conduct engineering and development work was signed by the two companies in 1983, and a prefeasibility study was completed in 1985, but the project was then put on hold pending further exploration results.

Homestake Canada Ltd. bought most of Esso's mining assets in 1989. Some regional and deposit-scale work was carried out on the Kutcho property in 1990 and 1992 under option agreements with American Reserve Mining Corp. and Teck Cominco Ltd. Homestake was purchased by Barrick Gold Corp. in 2003, and Western Keltic Mines Inc. purchased the Kutcho property from Barrick and Sumitomo in 2004. Western Keltic carried out drill programs on the Kutcho deposit in 2004, 2005 and 2006, and completed a pre-feasibility study in 2007. In May 2008 Sherwood Copper Corp. acquired Western Keltic Mines Ltd., and amalgamated it with a wholly owned subsidiary to create the Kutcho Copper Corporation. Later that same year, Sherwood merged with Capstone Mining Corp., such that Kutcho Copper Corporation, owner of the Kutcho property, became a wholly owned subsidiary of Capstone Mining Corp. Major drilling programs were carried out by Kutcho Copper Corporation in 2008 and 2010. The company released a preliminary economic assessment in September 2009, and a revised preliminary economic assessment in July 2010.

The three massive sulphide lenses that comprise the Kutcho Creek deposit occur at about the same stratigraphic level, at the top of unit KN2, and define a west-northwest plunging linear array, 3.5 km long, that probably defines the intersection of a fracture or fault system with the seafloor at the time of their accumulation. The individual lenses are elongate parallel to this trend, and approximately conformable with the enclosing stratigraphy. The east end of the Main lens intersects the topographic surface, and the Esso lens occurs at depths of 400-500 m below the surface. Drillholes have intersected several additional small massive sulphide pods up to 450 m west of the Esso lens, along the same linear trend. The Main lens is the largest and best defined, and measures about 1500 m long by 260 m wide, with a maximum thickness of 36 m. The Esso lens is smaller but higher grade, and was the main target of the 2010 diamond-drill program by Kutcho Copper Corporation. The intervening Sumac lens is fairly large but remains poorly defined because of relatively low grades. In detail, individual

lenses comprise multiple layers of massive to disseminated sulphide, dominated by pyrite, sphalerite, chalcopyrite and bornite, interspersed with carbonate-quartz-sericite schist and massive to laminated dolomite. The sulphide lenses are underlain by pyritic quartz-sericite-carbonate schists with foliation parallel quartz-pyrite veins that may represent tectonically transposed stockwork veins. Sulphide content decreases sharply across the upper contacts of the massive sulphide lenses, but chemical alteration effects that extend at least 100 m into the footwall, mainly Na depletion and variable additions of Mg, Ca, Si and Fe, also continue for 10 to 20 m into the hangingwall.

Capstone Mining Corp. (now Kutcho Copper Corporation) announced results of an independent NI43-101 compliant mineral resource estimate for the Kutcho Creek deposits in February 2009 (Capstone Mining Corp., 2009). The estimate was completed by Garth Kirkham, P.Geo., of Kirkham Geosystems Ltd., and was based on all drillholes completed prior to that time, including those from a 2008 program designed to better define the mineralization within the Main deposit. Using a 1.5% Cu cut-off, the Main deposit has a measured resource of 5 421 296 t grading 2.15% Cu, 2.86% Zn, 31.45 g/t Ag and 0.34 g/t Au; an indicated resource of 4 042 659 t grading 2.04% Cu, 2.54% Zn 31.15 g/t Ag and 0.35 g/t Au; and an inferred resource of 464 457 t grading 1.84% Cu, 2.83% Zn, 31.55 g/t Ag and 0.43 g/t Au. The Sumac deposit has an inferred resource of 625 577 t grading 1.67% Cu, 1.46% Zn, 30.12 g/t Ag and 0.29 g/t Au. The 2009 resource estimate for the Esso deposit has recently been updated, following a 2010 infill drill program that demonstrated continuity of high grade mineralization over significant distances. Using a 1.5% Cu cut-off, the Esso deposit now has an indicated resource of 1 816 200 t grading 2.69% Cu, 6.18% Zn, 64.8 g/t Ag and 0.66 g/t Au (Capstone Mining Corp., 2010).

Eastern extension of the Kutcho horizon

The Kutcho Creek massive sulphide deposits occur at the top of unit KN2. This unit has been traced more than 5 km eastward from the Kutcho Creek deposits, to the area north and northeast of peak 1732. It is not well exposed, but is characterized by fissile quartz-sericite schists that commonly contain substantial amounts of disseminated pyrite. Drill tests that have been conducted at several localities along this trend confirm that the unit hosts substantial intervals of pyrite-sericite-quartz alteration, locally with anomalous copper and zinc concentrations (Bridge, 1978; Holbek, 1990; Weiss *et al.*, 2006). One of these drillholes, 1100 m north of peak 1732, intersected a thin massive sulphide (mainly pyrite) zone that yielded 0.03% Cu, 0.02% Zn, 0.03% Pb, 6.17 ppm Ag and 0.07 ppm Au over 0.5 m (Bridge, 1978, hole 78).

Jenn

The Jenn occurrence is hosted by schists in the upper part of the central Kutcho division, about 700 m east of peak 1732. It comprises scattered narrow intervals of disseminated to semimassive pyrite, locally with traces of chalcopyrite and sphalerite, which were intersected in drillholes bored by Esso Minerals Canada between 1974 and 1983 (Oddy and Neilans, 1974, 1975; Bridge, 1983). The sulphide intervals are hosted mainly by quartz-sericite schists derived from felsic volcaniclastic rocks, but the host succession also includes, metarhyolite, chlorite schist, siltstone and phyllite.

CK (MINFILE 104I 075) and Kris occurrences

The CK occurrence is hosted by a broad zone of pyritic sericite-quartz altered rocks within the lower part of the central Kutcho division along Josh Creek (Figure 20). Belik (1978) notes that traces of chalcopyrite and sphalerite occur in tabular to lenticular zones of heavily disseminated pyrite hosted by quartz-sericite schist that contains relict quartz eyes. The altered rocks were tested with several diamond-drill holes in 1990, which intersected narrow zones of semimassive to massive pyrite that are enriched in copper and zinc (Holbek, 1990).

Pyritic quartz-sericite schists are common within the lower part of the central Kutcho division within a belt that extends at least 7 km west from the CK occurrence, to the slopes east of Kutcho Creek. The pyritic zones occur mainly in altered felsic volcanic and volcaniclastic rocks, but some comprise narrow zones of pyritic cherty rock that are interpreted as exhalites, and these occur within both felsic and mafic schists of the central division, and also in mafic schists of unit KS2 of the underlying southern division (Holbek, 1990; Alldrick *et al.*, 2009b). The Kris occurrence, in the northern part of this belt, comprises minor amounts of chalcopyrite that occur in several different pyritic zones, within felsic volcaniclastic rocks, that were intersected in a diamond-drill hole cored by Homestake in 1990 (Holbek, 1990; Alldrick *et al.*, 2009a).

Kass (MINFILE 104I 095)

The Kass showing occurs in the southwest part of the

Figure 20. Pyrite-sericite-quartz schist, CK occurrence, Josh Creek.

map area, within schists of unit KS1 just north of the small diorite plug that forms peak 2075. The schists enclose several lenses of pyrrhotite, with minor amounts of chalcopyrite and sphalerite, which were discovered in 1982, and further evaluated in 1983, during exploration programs by Canamax Resources Inc. (Fleming and Roth, 1983). The pyrrhotite lenses range from 0.5 to 1 m in width, and vary from laminated to brecciated. Grab samples returned up to 1100 ppm Cu, 1700 ppm Zn and 6.17 ppm Ag (Fleming and Roth, 1983). The mineralized lenses have been documented in only a very small area, and have apparently received little attention since their initial discovery.

ACKNOWLEDGMENTS

I thank Scott Caldwell for his capable and enthusiastic assistance during fieldwork. I am grateful for the logistical and financial support provided by Kutcho Copper Corporation, the Geological Survey of Canada (Edges Project) and the University of Victoria, which made the field program possible. I particularly thank Dani Alldrick for his efforts in arranging the partnership agreement with Kutcho, and for sharing many ideas on the geology of the area. Jim Logan reviewed an earlier version of the manuscript and suggested improvements.

REFERENCES

Alldrick, D., Willett, B. and Wilson, R.G. (2009a): Geological assessment report on the Kutcho project, north central British Columbia; *BC Ministry of Energy, Mines and Petroleum Resources*, Assessment Report 31029, 77 pages.

Alldrick, D., Willett, B. and Wilson, R.G. (2009b): Geological assessment report on the Kutcho project, north central British Columbia; *BC Ministry of Energy, Mines and Petroleum Resources*, Assessment Report 31032, 167 pages.

Ash, C.H. (2001): Ophiolite related gold quartz veins in the North American Cordillera; *BC Ministry of Energy, Mines and Petroleum Resources*, Bulletin 108, 140 pages.

Barrett, T.J., Thompson, J.F.H. and Sherlock, R.L. (1996): Stratigraphic, lithogeochemical and tectonic setting of the Kutcho Creek massive sulphide deposit, northern British Columbia; *Exploration and Mining Geology*, Volume 5, pages 309-338.

Belik, G. (1978): Geophysical report on the CK mineral claims; *BC Ministry of Energy, Mines and Petroleum Resources*, Assessment Report 6630, 21 pages.

Bridge, D.A. (1978): Diamond-drill hole report for Group XIII, 14 and XI, on Jeff 37-40, 90-92, 94, Andrea, Svea and Stu; Lin 11, 39, 40, Kris 1-9, 11-16 and Cgl 1, 2; and Jeff 63, 64, 101-116, 135-138 and Moe 1 mineral claims; *BC Ministry of Energy, Mines and Petroleum Resources*, Assessment Report 7914, 290 pages.

Bridge, D. (1983): Diamond drilling assessment report, Kutcho Creek property, Group Kutcho 83, 83A and ungrouped claims; *BC Ministry of Energy, Mines and Petroleum Resources*, Assessment Report 11323, 232 pages.

Bridge, D.A., Marr, J.M., Hashimoto, K., Obara, M. and Suzuki, R. (1986): Geology of the Kutcho Creek volcanogenic massive sulphide deposits, northern British Columbia; *in* Mineral Deposits of Northern Cordillera, Morin, J.A., Editor, *The Canadian Institute of Mining and Metallurgy*, Special Volume 37, pages 115-128.

Capstone Mining Corp. (2009): Capstone announces robust mineral resource update for high grade Kutcho Copper project; Capstone Mining Corp., news release, February 9, 2009.

Capstone Mining Corp. (2010): Capstone reports significant increase in grade and classification of Esso mineral resource at Kutcho; Capstone Mining Corp., news release, December 6, 2010.

Childe, F.C. and Thompson, J.F.H. (1997): Geological setting, U-Pb geochronology, and radiogenic isotopic characteristics of the Permo-Triassic Kutcho assemblage, north-central British Columbia; *Canadian Journal of Earth Sciences*, Volume 34, pages 1310-1324.

English, J.M., Mihalynuk, M.G. and Johnston, S.T. (2010): Geochemistry of the northern Cache Creek terrane and implications for accretionary processes in the Canadian Cordillera; *Canadian Journal of Earth Sciences*, Volume 47, pages 13-34.

Evenchick, C.A. (1991): Geometry, evolution, and tectonic framework of the Skeena fold belt, north central British Columbia; *Tectonics*, Volume 10, pages 527-546.

Fleming, D.B. and Roth, J. (1983): 1983 geological, geochemical and geophysical assessment report, Kutcho property, Kass 1-8 claims; *BC Ministry of Energy, Mines and Petroleum Resources*, Assessment Report 11314, 76 pages.

Gabrielse, H. (1962): Geology, Cry Lake, British Columbia; *Geological Survey of Canada*, Map 29-1962, 1:253 440 scale.

Gabrielse, H. (1985): Major dextral transcurrent displacements along the northern Rocky Mountain Trench and related lineaments in north-central British Columbia; *Geological Society of America Bulletin*, Volume 96, pages 1-14.

Gabrielse, H. (1991): Late Paleozoic and Mesozoic terrane interactions in north-central British Columbia; *Canadian Journal of Earth Sciences*, Volume 28, pages 947-957.

Gabrielse, H. (1998): Geology of Cry Lake and Dease Lake map areas, north-central British Columbia; *Geological Survey of Canada*, Bulletin 504, 147 pages.

Gabrielse, H., Murphy, D.C. and Mortensen, J.K. (2006): Cretaceous and Cenozoic dextral orogen-parallel displacements, magmatism and paleogeography, north-central Canadian Cordillera; *in* Paleogeography of the North American Cordillera: evidence for and against large-scale displacements, Haggart, J.W., Enkin, R.J. and Monger, J.W.H., Editors, *Geological Association of Canada*, Special Paper 46, pages 255-276.

Holbek, P. (1990): 1990 diamond drilling report on the Kutcho claim groups, Kutcho Creek area, northwestern B.C.; *BC Ministry of Energy, Mines and Petroleum Resources*, Assessment Report 20636, 194 pages.

Johannson, G.G., Smith, P.L. and Gordey, S.P. (1997): Early Jurassic evolution of the northern Stikinian arc: evidence from the Laberge Group, northwestern British Columbia; *Canadian Journal of Earth Sciences*, Volume 234, pages 1030-1057.

Makarenko, M., Sheykholeslami, A., Kirkham, G., Hendriks, D., Mercer, B. and Craig, D. (2010): Preliminary economic assessment, revised underground mining option, Kutcho Project, British Columbia; *Report prepared for Kutcho Copper Corporation by JDS Energy and Mining Inc.*, 293 pages.

Massey, N.W.D., MacIntyre, D.G., Desjardins, P.J. and Cooney, R.T. (2005): Digital geology map of British Columbia: whole province; *BC Ministry of Energy, Mines and Petroleum Resources*, GeoFile 2005-1.

Mihalynuk, M.G. (1999): Geology and mineral resources of the Tagish Lake area, northwestern British Columbia (NTS 104M/8, 9, 10E, 15; 104N/12W); *BC Ministry of Energy, Mines and Petroleum Resources*, Bulletin 105, 217 pages.

Mihalynuk, M.G., Smith, M.T., Gabites, J.E., Runkle, D. and Lefebure, D. (1992): Age of emplacement and basement character of the Cache Creek terrane as constrained by new isotopic and geochemical data; *Canadian Journal of Earth Sciences*, Volume 29, pages 2463-2477.

Mihalynuk, M.G., Erdmer, P., Ghent, E.D., Cordey, F., Archibald, D.A., Friedman, R.M. and Johannson, G.G. (2004): Coherent French Range blueschist: Subduction to exhumation in <2.5 Ma?; *Geological Society of America Bulletin*, Volume 116, pages 910-922.

Monger, J.W.H. (1975): Upper Paleozoic rocks of the Atlin Terrane, northwestern British Columbia and south-central Yukon; *Geological Survey of Canada*, Paper 74-47, 63 pages.

Monger, J.W.H. (1977): Upper Paleozoic rocks of northwestern British Columbia; *in* Report of Activities, Part A, *Geological Survey of Canada*, Paper 77-1A, pages 255-262.

Monger, J.W.H. and Thorstad, L. (1978): Lower Mesozoic stratigraphy, Cry Lake and Spatsizi map-areas, British Columbia; *in* Current Research, Part A, *Geological Survey of Canada*, Paper 78-1A, pages 21-24.

Monger, J.W.H., Richards, T.A. and Paterson, I.A. (1978): The hinterland belt of the Canadian Cordillera: new data from northern and central British Columbia; *Canadian Journal of Earth Sciences*, Volume 15, pages 823-830.

Nelson, J. and Friedman, R. (2004): Superimposed Quesnel (late Paleozoic-Jurassic) and Yukon-Tanana (Devonian-Mississippian) arc assemblages, Cassiar Mountains, northern British Columbia: field, U-Pb, and igneous petrochemical evidence; *Canadian Journal of Earth Sciences*, Volume 41, pages 1201-1235.

Oddy, R. and Neilans, J. (1974): Diamond drilling report on groups IV, V, VI, VII, Kutcho Creek area; *BC Ministry of Energy, Mines and Petroleum Resources*, Assessment Report 5138, 30 pages.

Oddy, R. and Neilans, J. (1975): Diamond drilling report on the Jeff and Jenn claim groups, Kutcho Creek area; *BC Ministry of Energy, Mines and Petroleum Resources*, Assessment Report 5641, 42 pages.

Pálfy, J. And Hart, C.J.R. (1995): Biostratigraphy of the Lower to Middle Jurassic Laberge Group, Whitehorse map area (105D), southern Yukon; *in* Yukon Exploration and Geology 1994, *Exploration and Geological Services Division, Yukon, Indian and Northern Affairs Canada*, pages 73-86.

Panteleyev, A. (1975): Jeff (104I-61): *in* Geology, Exploration and Mining in British Columbia 1974; *BC Ministry of Energy, Mines and Petroleum Resources*, pages 343-348.

Panteleyev, A. (1978): Kutcho Creek map-area (104I/1W); *in* Geological Fieldwork 1977, *BC Ministry of Energy, Mines and Petroleum Resources*, Paper 1978-1, page 43.

Panteleyev, A. and Pearson, D.E. (1977a): Kutcho Creek map-area (104I/1W); *in* Geology in British Columbia 1975; *BC Ministry of Energy, Mines and Petroleum Resources*, pages G87-G93.

Panteleyev, A. and Pearson, D.E. (1977b): Kutcho Creek map-area (104I/1W); *in* Geological Fieldwork 1976; *BC Ministry of Energy, Mines and Petroleum Resources*, Paper 1977-1, pages 74-76.

Pearson, D.E. and Panteleyev, A. (1976): Cupriferous iron sulphide deposits, Kutcho Creek map-area (104I/1W); *in* Geological Fieldwork 1975; *BC Ministry of Energy, Mines and Petroleum Resources*, Paper 1976-1, pages 86-92.

Souther, J.G. (1971): Geology and mineral deposits of Tulsequah map-area, British Columbia; *Geological Survey of Canada*, Memoir 362, 84 pages.

Stevens, R.D., Delabio, R.N. and Lachance, G.R. (1982): Age determinations and geological studies, K-Ar isotopic ages, report 15; *Geological Survey of Canada*, Paper 81-2, 56 pages.

Terry, J. (1977): Geology of the Nahlin ultramafic body, Atlin and Tulsequah map-areas, northwestern British Columbia; *in* Report of Activities, Part A, *Geological Survey of Canada*, Paper 77-1A, pages 263-266.

Thorstad, L.E. (1979): The lower Mesozoic King Salmon assemblage – Cry Lake map area, British Columbia; *in* Current Research, Part A, *Geological Survey of Canada*, Paper 79-1A, pages 21-24.

Thorstad, L.E. (1984): The Upper Triassic Kutcho Formation, Cassiar Mountains, north-central British Columbia; M.Sc. thesis, *The University of British Columbia*, 271 pages.

Thorstad, L.E. and Gabrielse, H. (1986): The Upper Triassic Kutcho Formation, Cassiar Mountains, north-central British Columbia; *Geological Survey of Canada*, Paper 86-16, 53 pages.

Tipper, H.W. (1978): Jurassic biostratigraphy, Cry Lake map-area, British Columbia; *in* Current Research, Part A, *Geological Survey of Canada*, Paper 78-1A, pages 25-27.

Tipper, H.W. and Richards, T.A. (1976): Jurassic stratigraphy and history of north-central British Columbia; *Geological Survey of Canada*, Bulletin 270, 73 pages.

Weiss, A., Holbek, P.M. and Wilson, R.G. (2006): Diamond drilling assessment report on the Kutcho Creek project, north central British Columbia; *BC Ministry of Energy, Mines and Petroleum Resources*, Assessment Report 28701, 249 pages.

Quaternary Geology and Till Geochemistry of the Colleymount Map Area (NTS 093L/01), West-Central British Columbia

by T. Ferbey

KEYWORDS: Nechako Plateau, Quaternary geology, surficial mapping, till geochemistry, heavy minerals, gold grain counts, porphyry Cu-Mo, polymetallic vein, volcanogenic massive sulphide

INTRODUCTION

The Tahtsa Lake district, and surrounding area, has high potential to host undiscovered porphyry Cu±Mo and polymetallic vein-style (including Au) mineralization. Centred on Tahtsa Lake (approximately 100 km south of Houston, British Columbia; Figure 1) this district, and areas immediately adjacent to it, have a rich mineral exploration history and at present host a producing porphyry Cu-Mo mine (Huckleberry mine) and numerous developed Cu±Mo prospects (*e.g.* Berg, Lucky Ship, Whiting Creek; Figure 2). This district also hosts epithermal vein and perhaps volcanogenic massive sulphide (VMS) style mineralization, as suggested by past producers such as Equity Silver, Emerald Glacier, and Silver Queen (MacIntyre, 1985; MacIntyre *et al.*, 2004; Alldrick *et al.*, 2007; Figure 2).

A two-year Quaternary geology and till geochemistry program is currently underway within the northern portion of the Tahtsa Lake district, within NTS map areas 093E/15, 16, and 093L/01, 02 (Figure 2). Presented here are observations made, and details on till samples collected, during the 2010 field season within Colleymount map area (NTS 093L/01). This is the second and final year of this program and builds on previous Quaternary geology and till geochemistry work by Ferbey (2010a, b) conducted immediately to the southwest in NTS 093E/15.

The Colleymount map area is ideally suited for Quaternary geology studies and till geochemical exploration as much of the map area is covered with glacial drift and continuously exposed bedrock outcrop is limited. Till geochemical surveys are an effective method for assessing the metallic mineral potential of areas covered with glacial drift (Levson, 2001a) and can be used to follow-up airborne geophysical data acquired over drift covered areas.

This publication is also available, free of charge, as colour digital files in Adobe Acrobat® PDF format from the BC Ministry of Forests, Mines and Lands website at http://www.empr.gov.bc.ca/Mining/Geoscience/PublicationsCatalogue/Fieldwork.

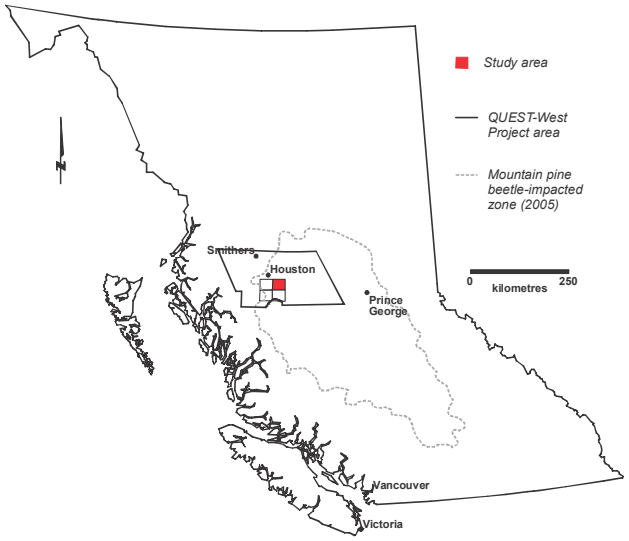

Figure 1. Location of study area in west-central British Columbia.

The objectives of this two-year Quaternary geology and till geochemistry program are to:

1) characterize and delineate the Quaternary materials that occur in the study area and reconstruct the region's glacial and ice-flow history; and

2) assess the economic potential of covered bedrock (subcrop) by conducting till geochemistry surveys.

The study area falls within the mountain pine beetle impacted zone and Geoscience BC's QUEST-West Project area. The goal of the project discussed here is to provide the mineral exploration community with high quality, regional scale, geochemical data that will help guide exploration efforts. In addition to geochemical and geophysical data recently collected by Geoscience BC, historic regional bedrock mapping and geochemical data have been published by the British Columbia Geological Survey (BCGS) and the Geological Survey of Canada (GSC) (Hanson *et al.* ,1942; Tipper, 1976; Church and Barakso, 1990; Alldrick, 2007a, b). The BCGS has also made significant contributions towards an understanding of the region's metallogeny (*e.g.* Carter, 1981; MacIntyre, 1985, 2001; MacIntyre *et al.*, 2004; Alldrick, 2007a, b; Alldrick *et al.*, 2007). New discoveries, and new insights into known mineral occurrences, will likely be realized through the integration of these new and existing datasets.

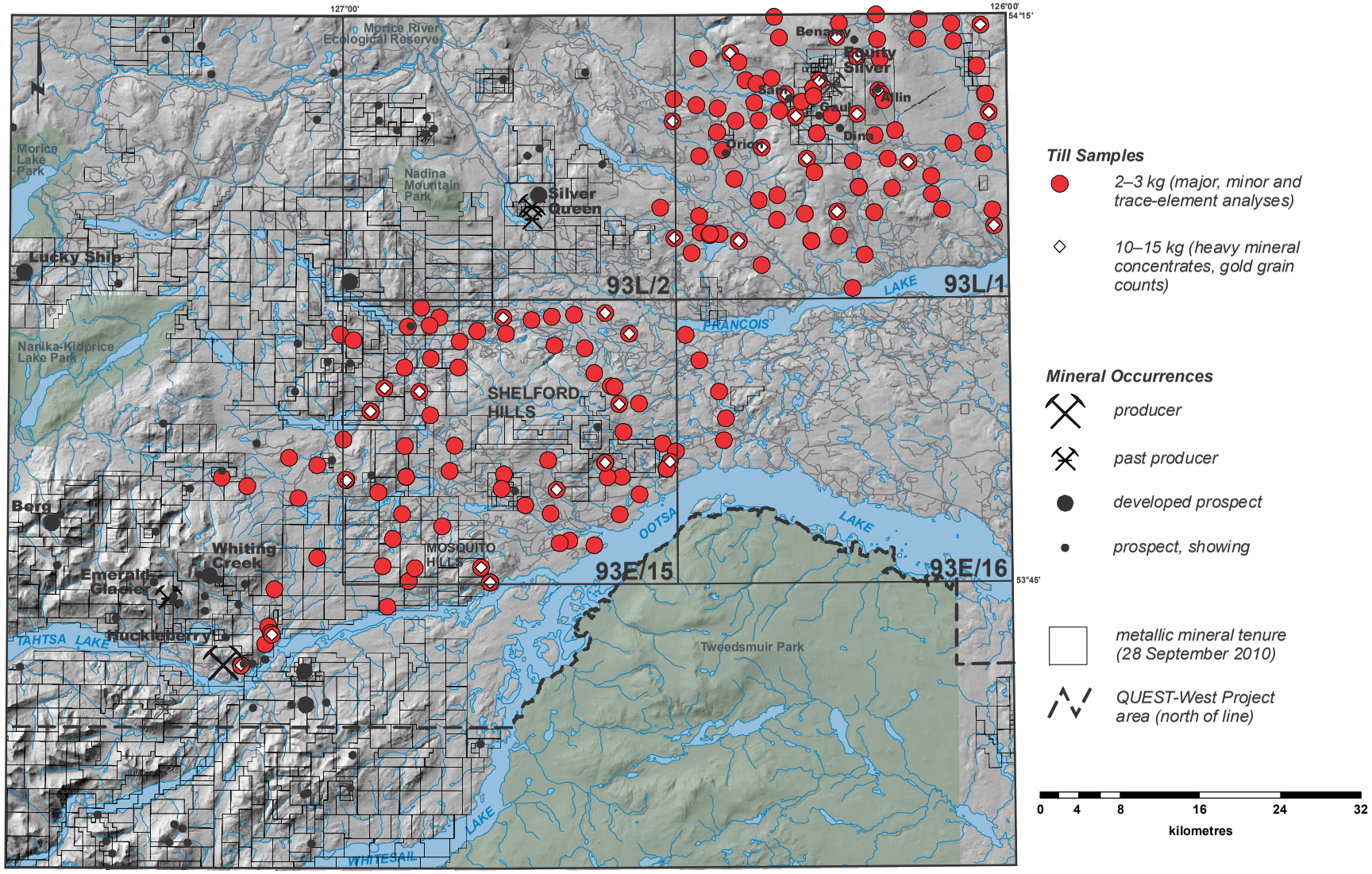

Figure 2. Study area including locations of mineral occurrences. Also shown are locations of till samples collected during the 2009 and 2010 field seasons within NTS 093E/15 and 093L/01, respectively.

STUDY AREA

The study area is located in west-central British Columbia, approximately 65 km southeast of Houston (Figures 1, 2), and is accessible by Forest Service, mine, and mineral exploration roads. Quaternary sediments were studied in detail within 093L/01 while a regional scale glacial history and ice-flow study was conducted within NTS 093L/01, 02 and 08. The primary objective of the 2010 till geochemistry survey is to assess the mineral potential of NTS 093L/01. To do this, additional infill till samples were collected within the most eastern portions of NTS 093L/02, to cover a lack of appropriate sample material within NTS 093L/01 (Figure 2).

The study area is situated in the Nechako Plateau, a subdivision of the Interior Plateau (Holland, 1976). The Nechako Plateau is an area of low relief with flat or gently rolling topography and near continuous forest cover (Figure 3). Elevations within the study area range from 715 to 1624 m asl. Although glacial sediments are ubiquitous, bedrock outcrop can be found along lake shorelines (at elevations above 715 m asl) on the flanks of steep terrain, and on local small scale erosional remnants that stand above Quaternary sediment at lower elevations. Small lakes and low discharge streams are common within the study area. The largest lake within the study area is Francois Lake which is fed at its west end by Nadina River and drained at its east end into Stellako River.

Figure 3. Subdued topography of the study area.

BEDROCK GEOLOGY

The bedrock geology of the study area was first described and mapped by Hanson *et al.* (1942). More detailed mapping has since been completed by Tipper (1976), Church and Barakso (1990), and Alldrick (2007a, b). The following is a summary of the main geological subdivisions found in the study area from this more recent work.

The study area lies within the Stikine terrane, just east of the Coast Crystalline Belt (Monger *et al.*, 1991). The oldest rocks include calcalkaline volcanic rocks belonging to the Telkwa Formation of the Early Jurassic Hazelton Group (Figure 4). Unconformably overlying these rocks are coarse clastic marine sedimentary and volcanic rocks belonging to the Lower Cretaceous Skeena Group. The Lower Cretaceous volcanic succession is significant from a mineral exploration perspective as a pyroclastic unit within it (a distal dacitic dust tuff) hosts Ag-Cu-Au mineralization at the past-producing Equity Silver Mine (Alldrick, 2007a, b; MacIntyre and Villeneuve, 2007). These rocks are in turn unconformably overlain by volcanic rocks of the Upper Cretaceous Kasalka Group and Eocene Ootsa Lake and Endako groups. Andesite and basalt flows belonging to the Buck Creek Formation, and trachyte to basalt flows of the Goosly Lake Formation (both of the Endako Group), are the most areally extensive bedrock units exposed at surface in the study area (Figure 4).

Small to medium-sized stocks of Late Cretaceous to Early Tertiary age intrude these Jurassic and Cretaceous volcanic and sedimentary units (Figure 4). Here, as in elsewhere in the region, there is an association between the location of intrusive lithologies (in particular porphyritic intrusions like those of the Late Cretaceous Bulkley suite) and the locations of Cu, Mo, Ag, Pb, Zn, and/or Au mineralization (Carter, 1981; MacIntyre, 1985).

Significant contributions towards understanding the metallogenesis of the region's porphyry Cu-Mo deposits has been made from Carter (1981) and MacIntyre (1985). More recently MacIntyre (2001), MacIntyre *et al.* (2004), Alldrick (2007a, b) and Alldrick *et al.* (2007) have investigated the mineral potential of the Skeena Group.

Mineral Occurrences

There are seven documented metallic mineral occurrences within the study area (Figure 4). With the exception of Orion showing (MINFILE 093L 330; Ag, Zn), for which a mineral deposit type has not yet been assigned, all metallic mineral showings and prospects within the study area are considered to be transitional, intrusion-related stockworks and veins (Panteleyev, 1995). Minimal exploration work has been conducted on Sam (MINFILE 093L 260; Ag, Zn;), Dina (MINFILE 093L 313; Cu, Ag), and Benamy (MINFILE 093L 331; Ag) showings while prospecting and mapping, geochemical, geophysical, and diamond drill programs have been conducted on Gaul (MINFILE 093L 256; Ag, Cu, Zn) and Allin (MINFILE 093L 293; Cu, Ag, Zn, Pb, Mo) prospects.

Equity Silver (MINFILE 093L 001; Ag, Cu, Au), located in the north-central part of the study area, is a past-producing Ag-Cu-Au mine. While in operation from 1980 to 1994 it was British Columbia's largest silver mine and produced 33.8 million tonnes of ore grading 64.9 g/t Ag, 0.4% Cu, and 0.46 g/t Au (MINFILE, 2010). Since its discovery, there has been some debate over the style of mineralization at Equity Silver and the relationship, if any, between the orebodies and a Paleocene quartz

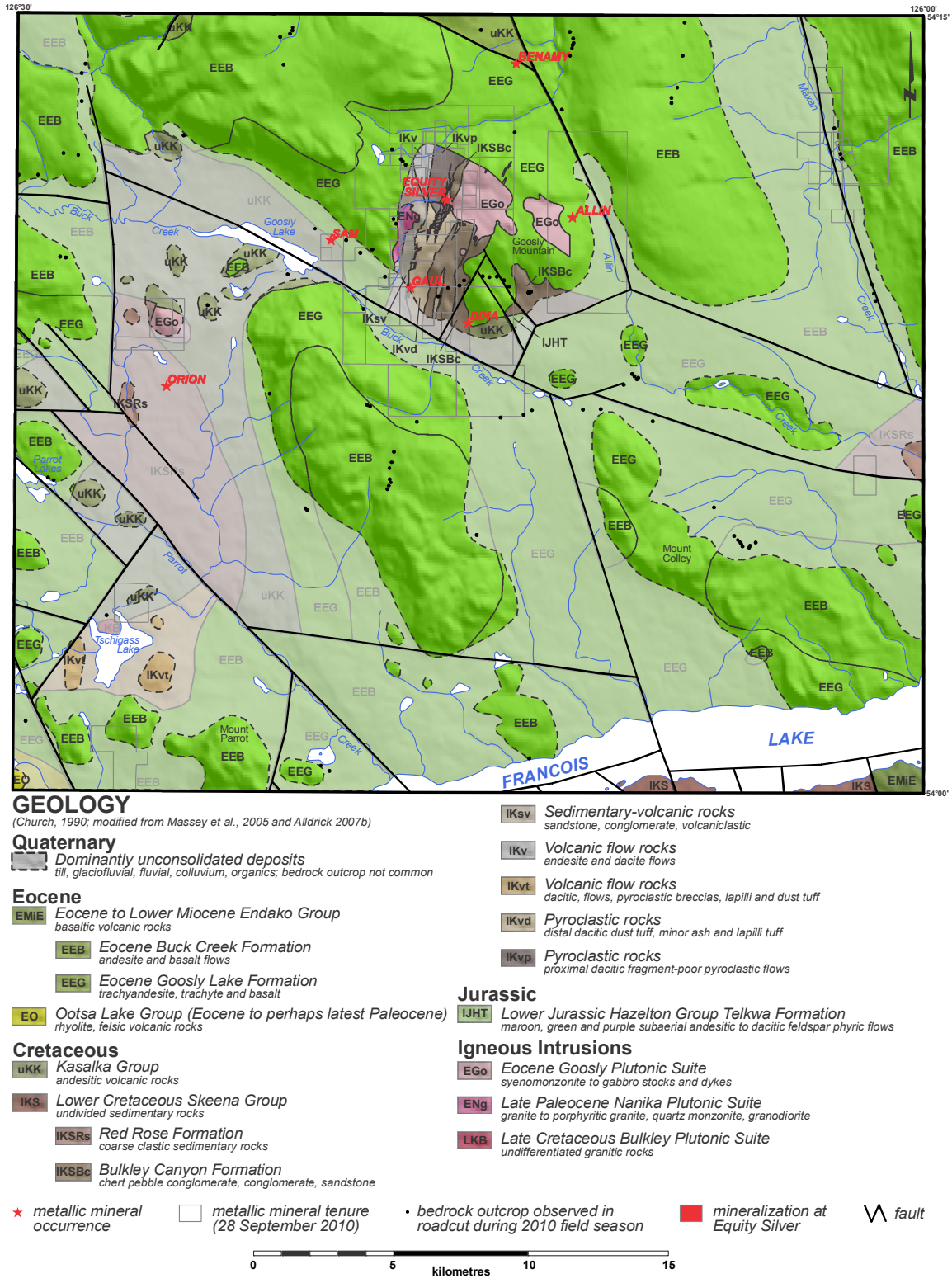

GEOLOGY

(Church, 1990; modified from Massey et al., 2005 and Alldrick 2007b)

Quaternary

- Dominantly unconsolidated deposits — till, glaciofluvial, fluvial, colluvium, organics; bedrock outcrop not common

Eocene

- EMiE — Eocene to Lower Miocene Endako Group — basaltic volcanic rocks
- EEB — Eocene Buck Creek Formation — andesite and basalt flows
- EEG — Eocene Goosly Lake Formation — trachyandesite, trachyte and basalt
- EO — Ootsa Lake Group (Eocene to perhaps latest Paleocene) — rhyolite, felsic volcanic rocks

Cretaceous

- uKK — Kasalka Group — andesitic volcanic rocks
- IKS — Lower Cretaceous Skeena Group — undivided sedimentary rocks
- IKSRs — Red Rose Formation — coarse clastic sedimentary rocks
- IKSBc — Bulkley Canyon Formation — chert pebble conglomerate, conglomerate, sandstone
- IKSv — Sedimentary-volcanic rocks — sandstone, conglomerate, volcaniclastic
- IKv — Volcanic flow rocks — andesite and dacite flows
- IKvt — Volcanic flow rocks — dacitic, flows, pyroclastic breccias, lapilli and dust tuff
- IKvd — Pyroclastic rocks — distal dacitic dust tuff, minor ash and lapilli tuff
- IKvp — Pyroclastic rocks — proximal dacitic fragment-poor pyroclastic flows

Jurassic

- IJHT — Lower Jurassic Hazelton Group Telkwa Formation — maroon, green and purple subaerial andesitic to dacitic feldspar phyric flows

Igneous Intrusions

- EGo — Eocene Goosly Plutonic Suite — syenomonzonite to gabbro stocks and dykes
- ENg — Late Paleocene Nanika Plutonic Suite — granite to porphyritic granite, quartz monzonite, granodiorite
- LKB — Late Cretaceous Bulkley Plutonic Suite — undifferentiated granitic rocks

★ metallic mineral occurrence

metallic mineral tenure (28 September 2010)

• bedrock outcrop observed in roadcut during 2010 field season

mineralization at Equity Silver

fault

Figure 4. Bedrock geology of the study area. Quaternary sediment cover is approximated by the light grey transparent overlay and black dashed line.

monzonite stock to the west and an Eocene gabbro-monzonite stock to the east. The five genetic models that have been proposed for mineralization at Equity Silver, summarized from Alldrick *et al.* (2007), are:

1) Early Cretaceous syngenetic exhalative mineralization with later remobilization resulting from emplacement of the eastern Eocene stock (Ney *et al.*, 1972; MacIntyre, 2006);
2) Early Cretaceous epithermal mineralization with later remobilization resulting from emplacement of the eastern Eocene stock (Wojdak and Sinclair, 1984);
3) Early Cretaceous porphyry-epithermal (transitional) mineralization with later remobilization resulting from emplacement of the eastern Eocene stock (Panteleyev, 1995);
4) epigenetic mineralization related to emplacement of the western Paleocene stock (Cyr *et al.*, 1984); and
5) epigenetic mineralization related to emplacement of the eastern Eocene stock (Church and Barakso, 1990).

A U-Pb zircon radiometric age of 113.5 +4.5/-7.2 Ma, reported by MacIntyre and Villeneuve (2007), confirms that the volcanic hostrock at Equity Silver is Early Cretaceous (Alldrick, 2007a, b; Alldrick *et al.*, 2007). Galena Pb isotope studies by Godwin *et al.* (1988) and Alldrick (1993) indicate that Pb was introduced into the ore zones during the Early Cretaceous, and may have been contemporaneous with the deposition of the dacitic dust tuff that hosts these mineralized zones (Alldrick *et al.*, 2007). Of the five genetic models proposed the first three fit this geochronological control best. Understanding the timing and style of mineralization at Equity Silver, and the bedrock lithologies that host this mineralization, is important for the success of future exploration programs in the region.

QUATERNARY GEOLOGY

Previous Quaternary geology work conducted within the study area is limited to soils and terrain mapping. Researchers with the British Columbia Ministry of Environment were the first to map the area, producing a 1:50 000-scale soil and landform map (BC Ministry of Environment, Lands, and Parks, 1976). Singh (1998) has completed the most recent mapping within the study area, a terrain classification map completed at 1:20 000-scale.

Quaternary geological studies have been conducted in adjacent areas. To the north and northwest, Clague (1984), Tipper (1994), Levson (2001a), and Levson (2002) discuss the Quaternary geology and geomorphic features of portions of NTS 093L, M and 103I, P. To the northeast, Plouffe (1996a, b) mapped the surficial deposits and described the Quaternary stratigraphy of the west half of NTS 093K. Mate (2000) conducted a similar study to the southeast in NTS 093F/12 while Ferbey and Levson (2001a, b, 2003), and Ferbey (2004) conducted a detailed study of the Quaternary geology and till geochemistry of the Huckleberry mine region. Included in this work was surficial geology mapping and detailed sedimentological descriptions for Quaternary sediments in the vicinity of Huckleberry mine and an investigation into the region's ice-flow history. Most recently Ferbey (2010a, b) presents data and interpretations on the Quaternary geology and till geochemistry of NTS 093E/15, located immediately to the southwest of the study area.

Surficial Geology

During the 2010 field season surficial materials were described at 141 sites within the study area. Observations were made at roadcuts and streamcuts, in hand-dug pits, and at discontinuous exposures along Francois Lake. Data collected at each site included map unit, topographic position, slope aspect and angle, and sedimentological characteristics such as texture, structure, lateral and vertical variability, lower contacts, and relationships with adjacent sediment units.

The dominant surficial material found in the study area is an overconsolidated, light brown coloured diamicton with a clayey silt to silt-rich matrix, similar to that described by Ferbey (2010a, b) for areas to the southwest. It is typically massive and matrix supported, and often exhibits vertical jointing and subhorizontal fissility giving it a blocky appearance (Figure 5). Matrix proportion varies from 65 to 75% and modal clast size is small pebble but can include boulder-sized material. Clast shape is typically subangular to subrounded. This diamicton generally conforms to underlying bedrock topography. Unlike areas to the south and southeast, however, streamlined or drumlinized and fluted terrain is relatively uncommon in 093L/01 (*cf.* Ferbey, 2010a, b). Nevertheless, this overconsolidated, silt and clay-rich diamicton is thought to be a subglacially derived diamicton (Dreimanis, 1989) and is interpreted as a basal

Figure 5. Clayey silt to silt rich, overconsolidated diamicton, interpreted as a basal till. Well developed vertical jointing and subhorizontal fissility give this basal till a blocky appearance. Pick for scale (65 cm).

till; the ideal sample medium for a till geochemistry survey.

Other glacial sediments occur within the study area. Glaciofluvial sands and gravels can be found along the south end of Parrott Lakes and extend southeast through Parrot Creek (locally known as Trout Creek) in a late-glacial to de-glacial drainage system. Other similar, but smaller-scale systems occur in south flowing creeks that drain into Francois Lake. Sandy, cobble-sized gravels occur in outwash plains and fan-deltas where these creeks approach Francois Lake. Another de-glacial drainage system occurs within the Allin and Buck creek valleys east of Goosly Lake. Glaciofluvial hummocks in this system are up to 425 m long, 225 m across, and 20 m high, and are composed of sandy pebble to cobble-sized gravels.

Glaciolacustrine and lacustrine sediments appear to be rare within the study area, even along the shore of Francois Lake. This, and the almost exclusive occurrence of sands and gravels immediately adjacent to the larger physiographic features (such as the Francois and Goosly lake valleys), suggest that during deglaciation they were conduits for meltwater drainage rather than basins for meltwater ponding.

Surficial geology mapping is currently in progress for NTS 093E/15 and 093L/01. This mapping is being conducted at 1:50 000-scale using aerial photographs (1:40 000-scale black and white), digital orthophotographs, and other available remotely-sensed imagery (*e.g.* Landsat). An integral part of this mapping, and of field data collection, is the reconstruction of the region's glacial and ice-flow history.

Ice-Flow History

During the 2010 field season ice-flow data were observed and recorded at 33 field stations. These data supplement 153 field stations and 207 moderately well to well preserved streamlined landforms presented by Ferbey and Levson (2001a, b) and Ferbey (2004, 2010a, b) that summarize the ice-flow history of the region. The majority of ice-flow indicators recorded during the 2010 field season were outcrop-scale features such as striations, grooves and rat tails (Benn and Evans, 1998). These features are typically found on the lower flanks of hill slopes where relatively unweathered bedrock has been exposed in road cuts. In some cases, these features are remarkably well developed and preserved (Figure 6).

Orientations of the ice-flow indicators show there are two dominant ice-flow directions in the study area, 062°-092° and 252°-288°. These values are in agreement with those presented by Stumpf *et al.* (2000), Ferbey and Levson (2001a, b) and Ferbey (2004, 2010a, b) and confirm that an ice-flow reversal occurred within the study area during the Late Wisconsinan. During the onset of glaciation, ice flowed radially from accumulation centres such as the Coast Mountains towards central-

Figure 6. Photograph of well preserved rat tails on an outcrop of Goosly Lake Formation trachyandesite. The outcrop is located 3 km southeast of the Equity Silver minesite, on a southeastern aspect slope. Orientations of these rat tails indicate ice flow towards 272°. Pen for scale (14 cm).

British Columbia and the coast. Sometime during the glacial maximum the ice divide migrated from the Coast Mountains east into central British Columbia. Ice was now flowing radially from central British Columbia resulting in a reversal of ice flow over the study area. Glaciers that were once flowing east were now flowing west across some parts of the western Nechako Plateau, over the Coast Mountains and towards the Pacific Ocean. Eastward ice flow resumed within the study area once the ice divide migrated back over the axis of the Coast Mountains, and continued until the close of the Late Wisconsinan glaciation.

TILL GEOCHEMISTRY SURVEY

Till geochemical surveys are well suited for assessing the mineral potential of areas covered by glacial drift (Levson *et al.*, 1994; Cook *et al.*, 1995; Levson, 2002; Lett *et al.*, 2006). Basal till, the sample medium used in these surveys, is ideal for these assessments as, in most cases, it has a relatively simple transport history, is deposited directly down-ice of its source, and glacial processes that erode and distribute sediment produce a geochemical signature that is areally more extensive than the bedrock source from which it was derived and therefore, at a regional scale, can be more easily detected (Levson, 2001a).

Approximately 60 km southwest of the study area, Ferbey and Levson (2001a) and Ferbey (2004) conducted a detailed till geochemical survey of the Huckleberry mine region. These studies demonstrate a clear relationship between till samples elevated in Cu, Mo, Au, Ag, and Zn and Cu-Mo ore zones at Huckleberry mine and smaller scale polymetallic vein occurrences on the mine property. Lateral and vertical variability in trace element concentrations in till at Huckleberry mine provide further evidence for the ice-flow reversal mentioned above, that occurred during the Late Wisconsinan glacial maximum (Ferbey and Levson, 2007). Results from another case study conducted by

Ferbey and Levson (2010) near the Copper Star Cu±Mo±Au occurrence, approximately 50 km west-northwest of the study area, also provide geochemical evidence for an ice-flow reversal. These results suggest that interpreting trace element geochemical data from tills or soils in this region, in particular transport direction, can be complex.

Ney *et al.* (1972) recognized this ice-flow reversal during the early stages of exploration on the Sam Goosly deposit (eventually to become Equity Silver mine) when exploratory trenching and drilling of Ag anomalies in soils was initially unsuccessful. The eventual recognition of westward transport of glacial sediments (resulting from studies of ice-flow indicators on bedrock outcrop and in aerial photographs) led to drilling up-ice or northeast of the Ag anomalies in soils. This resulted in the delineation of a mineralized zone.

Plouffe and Ballantyne (1993), Plouffe (1995), Plouffe *et al.* (2001), and Levson and Mate (2002) have also conducted till geochemistry surveys to the east of the study area, in NTS 093F and K. Using percentile plots of precious metal, base metal, and pathfinder element concentrations, and/or gold grain counts, each of these surveys identifies prospective ground where there were no previously reported mineral occurrences.

Sample Media

During the 2010 field season, 2-3 kg till samples were collected at 85 sample sites for major, minor, and trace element geochemical analyses (Figure 2). An additional 18 till samples, each weighing 10-15 kg, were collected for heavy mineral separation and gold grain counts (Figure 2). These larger samples were collected at sites where there was an adequate exposure of sample material. Till sample density for this survey is one sample per 10.5 km^2. Most samples were collected from unweathered till typically 1 m below surface.

Till samples collected for major, minor, and trace element analyses were sieved, decanted and centrifuged, to produce a silt plus clay sized (<0.063 mm) and clay-sized (<0.002 mm) fraction. This sample preparation was conducted at Acme Analytical Laboratories Ltd. (Vancouver, British Columbia). Heavy mineral samples were sent to Overburden Drilling Management (Nepean, ON), where heavy mineral (0.25 to 2.0 mm) and gold grain (<2.0 mm) concentrates were produced using a combination of gravity tabling and heavy liquids.

On the 2-3 kg samples, minor and trace element analyses (37 elements) were conducted on splits of the silt plus clay and clay-sized fractions, respectively, by inductively coupled plasma mass spectrometry (ICP-MS), following an aqua regia digestion. Major element analyses were conducted on a split of the silt plus clay-sized fraction only using inductively coupled plasma emission spectrometry (ICP-ES), following a lithium metaborate/tetraborate fusion and dilute nitric acid digestion. This analytical work was conducted at Acme Analytical Laboratories Ltd. (Vancouver, British Columbia).

Also as part of this project, a split of the silt plus clay-sized fraction (<0.063 mm) was analyzed for 35 elements by instrumental neutron activation analysis (INAA) at Becquerel Laboratories Inc. (Mississauga, ON). Instrumental neutron activation analyses for elements such as Au, Ba and Cr complement those produced by an aqua regia digestion followed ICP-MS as they are considered to be a near-total determination and hence more representative of rock forming and economic mineral geochemistry. Additionally, INAA determinations will be conducted on bulk heavy mineral concentrates produced from the 10-15 kg samples.

Quality Control

Quality control measures for analytical determinations include the use of field duplicates, analytical duplicates, and reference standards. For each block of 20 samples submitted for analysis, one field duplicate (taken at a randomly selected sample site), one analytical duplicate (a sample split after sample preparation but before analysis), and one reference standard is included in INAA and ICP-MS (following an aqua regia digestion) analyses. Reference standards used are a combination of certified Canada Centre for Mineral and Energy Technology (CANMET) and in-house BCGS geochemical reference materials. Duplicate samples are used to measure sampling and analytical variability, whereas reference standards are used to measure the accuracy and precision of the analytical methods.

SUMMARY

During the 2010 field season 85 basal till samples were collected for major, minor, and trace element geochemical analyses, while an additional 18 till samples were collected for separation and analysis of heavy mineral concentrates and gold grain counts. The goal of this till geochemical survey is to assess the mineral potential of the Colleymount map area (NTS 093L/01). Mineral exploration of this area will benefit from a regional till geochemistry program as much of the map area is covered with glacial drift and continuous bedrock outcrop is limited. Ongoing surficial geology mapping at 1:50 000-scale and a regional ice-flow study will complement this till geochemical survey. Delineating and characterizing surficial materials of the study area and quantifying the net transport direction of basal tills are integral to the interpretation of resultant till geochemical data and will be useful to mineral exploration companies conducting their own surficial sediment geochemistry surveys in the area.

The 2010 field season saw the completion of field work for the second and last year of a Quaternary geology program designed to assess the mineral potential of the northern portion of the Tahtsa Lake district, and adjacent areas (NTS 093E/15, 16, and 093L/01, 02). This study

area falls within Geoscience BC's QUEST-West Project area where additional geochemical data have recently been compiled and collected, mineral occurrence data have been updated (*i.e.* MINFILE, 2010), and helicopter-borne time domain electromagnetic and gravity data have been acquired. These new data in combination with the previous data published by the BCGS and GSC, makes the Colleymount map area an attractive area to explore.

Till geochemical data for the Colleymount map area (NTS 093L/01) will be the topic of a combined BCGS Open File and Geoscience BC Report to be released in late spring 2011.

ACKNOWLEDGMENTS

The author would like to thank L.J. Diakow and S.M. Rowins for discussions on, and their insight into, local bedrock lithologies. The Touronds (Nanika Guiding Limited) and Slots (Wild Rose Camp) are thanked for their hospitality during the 2010 field season and sharing their local knowledge on the region's mineral exploration history. L. Howarth is thanked for her assistance in the field. T.E. Demchuk, P. Schiarizza, and A.S. Hickin are thanked for their review of an earlier version of this manuscript.

REFERENCES

Alldrick, D.J. (1993): Geology and metallogeny of the Stewart mining camp, northwestern BC; British Columbia Ministry of Energy, Mines, and Petroleum Resources, Bulletin 85, 105 pages.

Alldrick, D.J. (2007a): Geology of the Skeena Group, central British Columbia (NTS 93E, 93F, 93K, 93L, 93M, 103I, 103P); British Columbia Ministry of Energy, Mines, and Petroleum Resources, Open File 2007-8, scale 1:250 000.

Alldrick, D.J. (2007b): Geology of the Equity Silver mine area; British Columbia Ministry of Energy, Mines, and Petroleum Resources, Open File 2007-9, scale 1:10 000.

Alldrick, D.J., MacIntyre, D.G. and Villeneuve, M.E. (2007): Geology, mineral deposits, and exploration potential of the Skeena Group (NTS 093E, L, M; 103I), central British Columbia; in Geological Fieldwork 2006, British Columbia Ministry of Energy, Mines, and Petroleum Resources, Paper 2007-1, pages 1-17.

Benn, D.I. and Evans, D.J.A (1998): Glaciers and glaciation; *Arnold*, London, 734 pages.

BC Ministry of Environment, Lands, and Parks (1976): Landforms 93L/1; Department of Lands and Forests, 1:50 000 scale map.

Carter, N.C. (1981): Porphyry copper and molybdenum deposits, west-central British Columbia; British Columbia Ministry of Energy, Mines and Petroleum Resources, Bulletin 64, 150 pages.

Church, B.N. and Barakso, J.J. (1990): Geology, lithogeochemistry and mineralization in the Buck Creek area, British Columbia; British Columbia Ministry of Energy, Mines and Petroleum Resources, Paper 1990-2, 95 pages.

Clague, J.J. (1984): Quaternary geology and geomorphology, Smithers-Terrace-Prince Rupert Area, British Columbia; Geological Survey of Canada, Memoir 413, 71 pages.

Cook, S.J., Levson, V.M., Giles, T.R. and Jackaman, W. (1995): A comparison of regional lake sediment and till geochemistry surveys: a case study from the Fawnie Creek area, central British Columbia; Exploration Mining Geology, v. 4, pages 93-101.

Cyr, J.B., Pease, R.B. and Schroeter, T.G. (1984): Geology and mineralization at Equity Silver mine; Economic Geology, v. 29, pages 947-968.

Dreimanis, A. (1989): Tills: their genetic terminology and classification; in Genetic Classification of Glacigenic Deposits, Goldthwait, R.P. and Matsch, C.L., Editors, A.A. Balkema, Rotterdam, pages17–83.

Ferbey, T. (2004): Quaternary geology, ice-flow history and till geochemistry of the Huckleberry mine region, west-central British Columbia; M.Sc. Thesis, Earth and Ocean Sciences, University of Victoria, British Columbia, Canada, 301 pages.

Ferbey, T. (2010a): Quaternary geology and till geochemistry of the Nadina River map area (NTS 093E/15), west-Central British Columbia; in Geological Fieldwork 2009, British Columbia Ministry of Energy, Mines, and Petroleum Resources, Paper 2010-1, pages 43-54.

Ferbey, T. (2010b): Till Geochemistry of the Nadina River map area (093E/15), west-central British Columbia; British Columbia Ministry of Energy, Mines, and Petroleum Resources, Open File 2010-7, Geoscience BC, Report 2010-10, 56 pages.

Ferbey, T. and Levson, V.M. (2001a): Quaternary geology and till geochemistry of the Huckleberry mine area; in Geological Fieldwork 2000, British Columbia Ministry of Energy, Mines, and Petroleum Resources, Paper 2001-1, pages 397-410.

Ferbey, T. and Levson, V.M. (2001b). Ice-flow history of the Tahtsa Lake – Ootsa Lake region; British Columbia Ministry of Energy, Mines, and Petroleum Resources, Open File 2001-8, scale 1:110 000.

Ferbey, T. and Levson, V.M. (2003): Surficial geology of the Huckleberry mine area; British Columbia Ministry of Energy, Mines, and Petroleum Resources, Open File 2003-2, scale 1:15 000.

Ferbey, T. and Levson, V.M. (2007): The influence of ice-flow reversals on the vertical and horizontal distribution of trace elements in tills, Huckleberry mine area, west-central British Columbia; in Application of Till and Stream Sediment Heavy Mineral and Geochemical Methods to Mineral Exploration in Western and Northern Canada; Paulen, R.C. and McMartin, I., Editors, Geological Association of Canada, Short Course Notes 18, pages 145-151.

Ferbey, T. and Levson, V.M. (2010): Evidence of westward glacial dispersal along a till geochemical transect of the Copper Star Cu±Mo±Au occurrence, west-central British Columbia; British Columbia Ministry of Energy, Mines, and Petroleum Resources, Open File 2010-04, 21 pages.

Hanson, G., Pehmister, T.C. and Lang, A.H. (1942): Houston, Coast District, British Columbia; Geological Survey of Canada, Map 671A, scale 1:253 440.

Godwin, C.I., Gabites, J.E. and Andrew, A. (1988): Leadtable – a galena lead isotope database for the Canadian Cordillera; British Columbia Ministry of Energy and

Mines, and Petroleum Resources, Paper 1988-4, 188 pages.

Holland, S.S. (1976): Landforms of British Columbia: a physiographic outline; British Columbia Ministry of Energy and Mines, and Petroleum Resources, Bulletin 48, 138 pages.

Lett, R.E., Cook, S.J. and Levson, V.M. (2006): Till geochemistry of the Chilanko Forks, Chezacut, Clusko, and Toil Mountain map areas, British Columbia (NTS 93C/1, 8, 9, and 16); British Columbia Ministry of Energy, Mines, and Petroleum Resources, GeoFile 2006-1, 272 pages.

Levson, V.M. (2001a): Regional till geochemical surveys in the Canadian Cordillera: sample media, methods, and anomaly evaluation; in Drift Exploration in Glaciated Terrain; McClenaghan, M.B., Bobrowsky, P.T., Hall, G.E.M. and Cook, S.J., Editors, Geological Society, Special Publication, No. 185, pages 45-68.

Levson, V.M. (2001b): Quaternary geology of the Babine Porphyry Copper District: implications for geochemical exploration; Canadian Journal of Earth Sciences, Volume 38, pages 733-749.

Levson, V.M. (2002): Quaternary geology and till geochemistry of the Babine Porphyry Copper Belt, British Columbia (NTS 93 L/9,16, M/1, 2, 7, 8); British Columbia Ministry of Energy, Mines, and Petroleum Resources, Bulletin 110, 278 pages.

Levson, V.M. and Mate, D.J. (2002): Till geochemistry of the Tetachuck Lake and Marilla map areas (NTS 93F/5 and F/12); British Columbia Ministry of Energy and Mines, and Petroleum Resources, Open File 2002-11, 180 pages.

Levson, V.M., Giles, T.R., Cook, S.J. and Jackaman, W. (1994): Till geochemistry of the Fawnie Creek area (93F/03); British Columbia Ministry of Energy, Mines and Petroleum Resources, Open File 1994-18, 40 pages.

MacIntyre, D.G. (1985): Geology and mineral deposits of the Tahtsa Lake District, west-central British Columbia; British Columbia Ministry of Energy, Mines and Petroleum Resources, Bulletin 75, 82 pages.

MacIntyre, D.G. (2001): The mid-Cretaceous Rocky Ridge Formation – a new target for subaqueous hot-spring deposits (Eskay Creek type) in central British Columbia; in Geological Field work 2000, British Columbia Ministry of Energy, Mines and Petroleum Resources, Paper 2001-1, pages 253–268.

MacIntyre, D.G. (2006): Geology and mineral deposits of the Skeena Arch – a new target for subaqueous hot-spring deposits (Eskay Creek type) in central British Columbia; in Geological Fieldwork 2005, British Columbia Ministry of Energy, Mines and Petroleum Resources, Paper 2006-1, pages 303-312.

MacIntyre, D.G. and Villeneuve, M.E. (2007): Geochronology of the Rocky ridge volcanics, Skeena Group, British Columbia; British Columbia Ministry of Energy, Mines, and Petroleum Resources, GeoFile 2007-4.

MacIntyre, D.G., McMillan, R.H. and Villeneuve, M.E. (2004): The mid-Cretaceous Rocky Ridge Formation – important hostrocks for VMS and related deposits in central British Columbia; in Geological Field work 2003, British Columbia Ministry of Energy, Mines, and Petroleum Resources, Paper 2004-1, pages 231-247.

Mate, D.J. (2000): Quaternary geology, stratigraphy and applied geomorphology in southern Nechako Plateau, central British Columbia; unpublished MSc thesis, University of Victoria, 253 pages.

MINFILE (2010): MINFILE BC mineral deposits database; British Columbia Ministry of Energy, Mines and Petroleum Resources, URL <http://minfile.ca> [October 2010].

Monger, J.W.H., Wheeler, J.O., Tipper, H.W., Gabrielse, H., Harms, T., Struik, L.C., Campbell, R.B., Dodds, C.J., Gehrels, G.E. and O'Brien, J. (1991): Cordilleran terranes (Chapter 8: Upper Devonian to Middle Jurassic assemblages); in Geology of the Cordilleran Orogen in Canada, Gabrielse, H. and Yorath, C.J., Editors, Geological Survey of Canada, Geology of Canada Series Number 4, pages 281-327.

Ney, C.S., Anderson, J.M. and Panteleyev, A. (1972): Discovery, geological setting and style of mineralization, Sam Goosly deposit, British Columbia; Canadian Institute of Mining and Metallurgy Bulletin, v. 65, pages 53-64.

Panteleyev, A. (1995): Subvolcanic Cu-Au-Ag (As-Sb); in Selected British Columbia Mineral Deposit Profiles, Volume 1 - Metallics and Coal, Lefebure, D.V. and Ray, G.E., Editors, British Columbia Ministry of Energy of Employment and Investment, Open File 1995-20, pages 79-82.

Plouffe, A. (1995): Geochemistry, lithology, mineralogy, and visible gold grain content of till in the Manson River and Fort Fraser map areas, central British Columbia (NTS 93K and N); Geological Survey of Canada, Open File 3194, 119 pages.

Plouffe, A. (1996a): Surficial geology, Cunningham Lake, British Columbia (NTS 93K/NW); Geological Survey of Canada, Open File 3183, scale 1:50 000.

Plouffe, A. (1996b): Surficial geology, Burns Lake, British Columbia (NTS 93K/SW); Geological Survey of Canada, Open File 3184, scale 1:50 000.

Plouffe, A. and Ballantyne, S.B. (1993): Regional till geochemistry, Manson River and Fort Fraser area, British Columbia (93K, 93N), silt plus clay and clay size fractions; Geological Survey of Canada, Open File 2593, 210 pages.

Plouffe, A., Levson, V.M. and Mate, D.J. (2001): Till geochemistry of the Nechako River map area (NTS 93F), central British Columbia; Geological Survey of Canada, Open File 4166, 66 pages.

Singh, N. (1998): Terrain classification map phase 3, 93L.008, 009, 018, 019, 028, 029; British Columbia Ministry of Forests, scale 1:20 000.

Stumpf, A.J., Broster, B.E. and Levson, V.M. (2000): Multiphase flow of the Late Wisconsinan Cordilleran Ice Sheet in western Canada; Geological Society of America Bulletin, v. 112, pages 1850-1863.

Tipper, H.W. (1994): Preliminary interpretations of glacial and geomorphic features of Smithers map area (93L), British Columbia; Geological Survey of Canada, Open File 2837, 7 pages.

Tipper, H.W. (1976): Bedrock geology, Smithers, B.C., 93L; Geological Survey of Canada, Open File 351, scale 1:250 000.

Wojdak, P.J. and Sinclair, A.J. (1984): Equity Silver silver-copper-gold deposit – alteration and fluid inclusion studies, Economic Geology, v. 79, pages 969-990.

Age Constraints of Mineralization at the Brenda and Woodjam Cu-Mo±Au Porphyry Deposits – An Early Jurassic Calcalkaline Event, South-Central British Columbia

by J.M. Logan, M.G. Mihalynuk, R.M. Friedman[1] and R.A. Creaser[2]

KEYWORDS: Brenda mine, Woodjam, calcalkaline porphyry, copper-molybdenum-gold deposit, Early Jurassic mineralization, alteration, geochronology, isotopic age, U/Pb zircon, Re/Os molybdenum, $^{40}Ar/^{39}Ar$, Quesnel arc

INTRODUCTION

British Columbia is well endowed with porphyry deposits, including calcalkaline Cu-Mo±Au and alkaline Cu-Au±Ag porphyry deposits. Most of the well-known deposits display geological characteristics consistent with formation in an island-arc setting, primarily in the Mesozoic arc successions. As a result, exploring for British Columbia Cordilleran porphyry deposits has traditionally focussed in the Mesozoic arc terranes, Stikine and Quesnel, of the Intermontane Belt (Figure 1).

Within this extensive area, explorationists have historically been constrained by "commodity" and/or "deposit model" driven exploration often resulting in missed opportunities for discovery or left large areas under-explored and requiring re-evaluation when "new models" appear. For example, calcalkaline Cu-Mo±Au deposits not only have different alteration/mineralization footprints than alkaline Cu-Au±Ag porphyry deposits, they are associated with different plutonic suites and may form either along and/or orthogonal to the arc axis. Therefore knowledge of the paleo-architecture and the age and type of porphyry target is important when planning an exploration strategy or interpreting the regional and/or property scale geophysical, geochemical and mineral assemblage data. In addition, large areas of Stikine and Quesnel terranes are mantled by younger basalts and overburden. Exploration is particularly difficult and expensive in these areas, necessitating highly focused programs that rely on subtle techniques for recognition and evaluation of mineral/alteration vectors that characterize different styles of porphyry deposits.

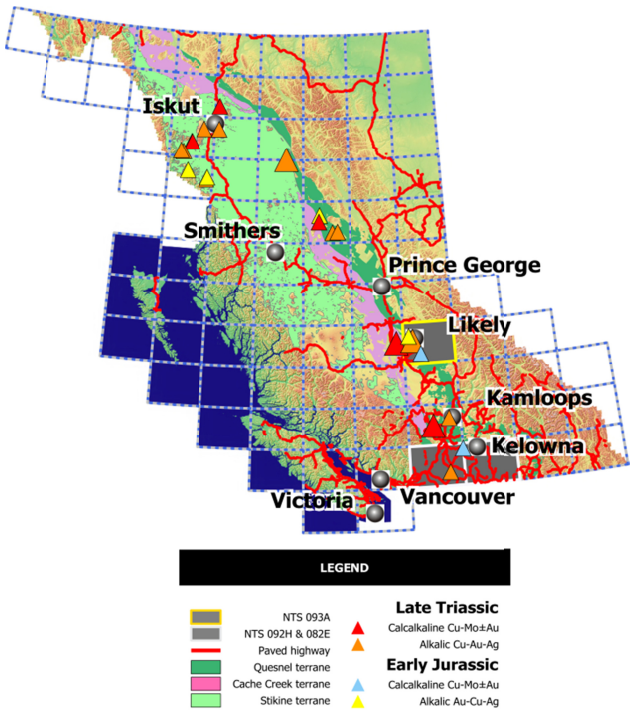

Figure 1. Location of Woodjam (southwest of Likely) and Brenda mine (west of Kelowna) areas, south-central British Columbia. The areas covered by Figure 2 and 3 are shown on the respective NTS map sheets as blue triangles. Also shown are pre-185 Ma calcalkaline Cu-Mo±Au (red), alkaline Cu-Au±Ag (orange) and Au-Cu±Ag (yellow) porphyry deposits in Quesnel and Stikine terranes (after Wheeler and McFeely, 1991).

Southern Quesnel contains at least three main Mesozoic magmatic suites that display copper porphyry mineralization. The Guichon and Copper Mountain suites are well known and relatively well explored in the exposed parts of Quesnel (Woodsworth *et al.*, 1991). The youngest suite, the Takomkane/Wildhorse is not.

Calcalkaline plutons in Southern BC that were emplaced in the middle to late parts of the Early Jurassic (Takomkane/Wildhorse suites, Breitsprecher *et al.*, 2010) have historically been ignored or designated as "poorly mineralized" (*e.g.* Breitsprecher *et al.,* 2010). Herein we show that plutons of this age can be significant Cu-Mo-Au producers. Geochronological evidence is presented that shows Cu-Mo±Au mineralizing events at Brenda

[1] *Pacific Centre for Isotope and Geochemical Research, The University of British Columbia, Vancouver, BC*

[2] *Earth and Atmospheric Sciences, University of Alberta, Edmonton, AB*

This publication is also available, free of charge, as colour digital files in Adobe Acrobat® PDF format from the BC Ministry of Forests, Mines and Lands website at http://www.empr.gov.bc.ca/Mining/Geoscience/PublicationsCatalogue/Fieldwork.

(Pennask batholith) and Woodjam-Southeast zone (Takomkane batholith) to be essentially synchronous. We assert that the Takomkane/Wildhorse magmatic belt is not an exploration dud, but rather is highly prospective along its length – currently known to extend 375 km.

This report aims to briefly outline the geological setting, age, mineralization and alteration within the Takomkane/Wildhorse magmatic belt as displayed at two deposits, the past producing Brenda mine, and the actively developing Woodjam prospect.

LOCATION & GEOLOGICAL SETTING

The Brenda mine and the Woodjam property are located within the Quesnel terrane (Figure 1), a stack of Paleozoic and Mesozoic arcs that nucleated on a crustal ribbon that lay adjacent to ancestral North America (ANA). Subduction of ancient Pacific Ocean crust to form the proto-Quesnel and conjoined Stikine arcs is believed to have begun in the Devonian (*e.g.* Logan *et al.*, 2000; Beatty *et al.*, 2006). Arc growth continued sporadically with a significant pulse in the Late Triassic–Early Jurassic (212-192 Ma). Na-and K-rich volcanic arc magmatism evolved during this 20 Ma epoch with the emplacement into the arc of three main Cordilleran-wide plutonic suites: the Late Triassic Guichon batholith (212-208 Ma), Latest Triassic Copper Mountain (206-200 Ma) and Early Jurassic Takomkane/Wildhorse (197-193 Ma) suites (Woodsworth *et al.* 1991; Logan and Mihalynuk , in review) and their associated porphyry mineralizing events. In southern British Columbia these respective mineralizing events produced Highland Valley and Gibraltar; Copper Mountain, Afton and Mountain Polley; and Brenda and Woodjam. Normal arc subduction beneath the composite Quesnel terrane ceased following its accretion to ANA in Early Jurassic time (~186 Ma, Nixon *et al.*, 1993; herein we use the Jurassic time scale of Palfy *et al.*, 2000).

Brenda mine (MINFILE 092HNE047)

The Brenda copper-molybdenum deposit is hosted within the "Brenda stock", an informal subdivision of the much larger, polyphase granodiorite and quartz diorite of the Early Jurassic Pennask batholith. It is located about 22 km west of Peachland. Carr (1967) mapped five, northerly-trending textural phases of quartz diorite, in the vicinity of the Brenda mine distinguished by slight variations in grain size and modal mineralogy. Progressing eastward from the hornfelsed contact with Nicola Group volcaniclastic rocks, the five phases are:

1) medium quartz diorite,
2) speckled quartz diorite,
3) uniform quartz diorite,
4) porphyritic quartz diorite, and
5) fine quartz diorite (Figure 2).

Typical mineral contents average: quartz (25%), plagioclase (50%), potassium feldspar (5-20%), hornblende (5-7%) and biotite (5-7%). Later work by Soregaroli and Whitford (1976) simplified the geology to only two units. Unit 1, is a marginal phase with more abundant mafic minerals (hornblende>biotite) and angular quartz grains, that embraces most of Carr's phases 1, 2, and 3. Unit 2 is characterised by fewer mafic minerals (biotite>hornblende), euhedral biotite phenocrysts and subhedral quartz grains, that include Carr's phases 4 and 5 (Figure 2). The contact between the two units is described as typically diffuse, but where sharp, Unit 2 is chilled against Unit 1(Soregaroli and Whitford, 1976). Several ages and compositions of pre and post-ore dikes cut the stock. The deposit is approximately 390 m from the contact with Nicola Group rocks to the west (Figure 2).

Mineralization is confined almost entirely to veins which cut relatively unaltered quartz diorite. Vein walls can be sharp and/or diffuse where gangue and sulphides have variably infiltrated and replaced the wall rock. Vein density within the Brenda Mines orebody is not uniform. It ranges from less than 9 veins per metre near the periphery of the orebody to 63 per metre and locally 90 per metre near the centre (Oriel, 1972). Potassic alteration forms narrow potash feldspar or biotite alteration envelopes related to sulphide mineralization, where as propylitic alteration predates and accompanies some of the late-stage veining events. Soregaroli (1968) and Oriel (1972) studied the mineralogy, geometry and crosscutting relationships of veins at Brenda and developed the following paragenesis:

Stage 1. Biotite-chalcopyrite

Stage 2. Quartz-potassium feldspar-sulphide. These veins form the bulk of the mineralization. They are composed of quartz and potassium feldspar, with variable quantities of chalcopyrite, molybdenite and pyrite (Figure 3).

Stage 3. Quartz-molybdenite-pyrite

Stage 4. Epidote-sulphide-magnetite

Stage 5. Biotite; calcite; quartz.

Production at the mine began in early 1970 and officially ceased June 08, 1990 after milling 181.7 Mt of ore grading 0.22% Cu and 0.064% Mo (mill head grades; Weeks *et al.*, 1995). Production totalled 0.27 Mt of copper, 0.068 Mt Mo and 2.28 t Au (MINFILE).

Woodjam (MINFILE 093A 078)

The Woodjam property is located 35 km southeast of the Mount Polley copper-gold mine. It is underlain by hornfelsed Late Triassic Nicola Group volcanic and related sedimentary rocks within the contact metamorphic aureole of the Late Triassic to Early Jurassic Takomkane batholith (~202-193 Ma); a composite, quartz-saturated calcalkaline intrusion composed of hornblende monzodiorite to hornblende-biotite monzogranite (Figure 4). Intrusive rocks dominate the eastern portion of the

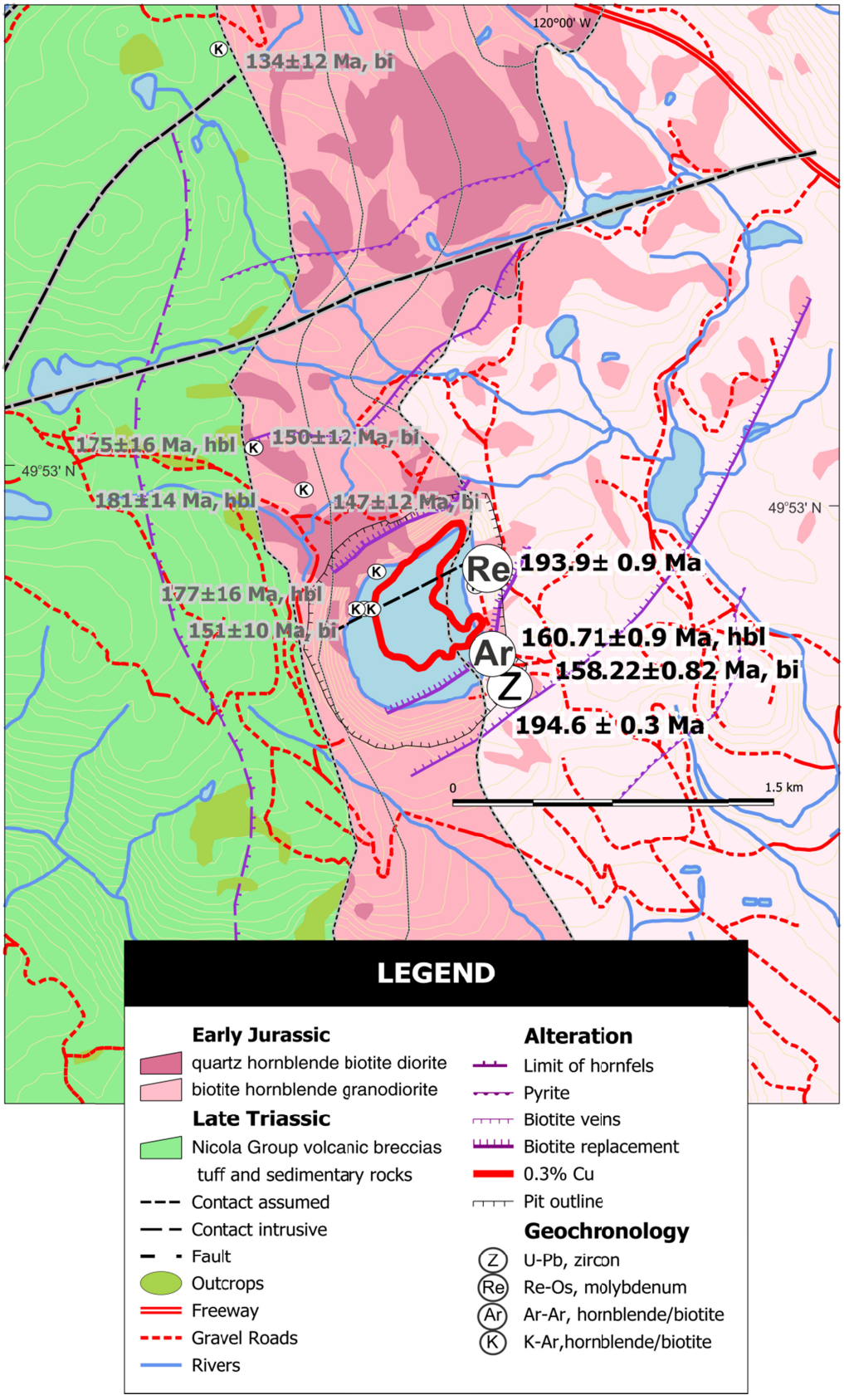

Figure 2. Local geology of the Brenda mine area showing location of geochronological samples collected as part of this study (large symbols) and those collected previously by other authors (smaller symbols) as reported by Breitsprecher and Mortensen (2004). Geological contacts adapted from Carr (1967), Soregaroli and Whitford (1976) and Dawson and Ray (1988).

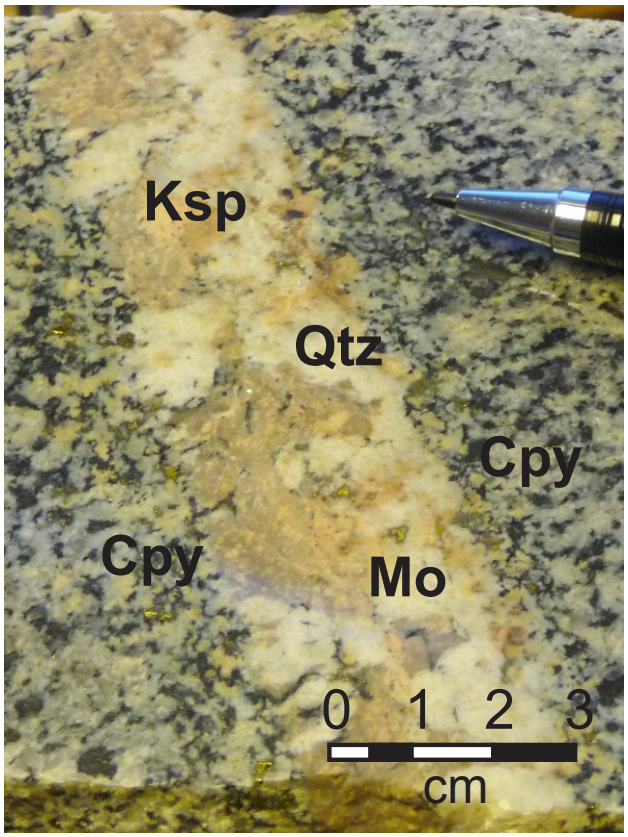

Figure 3. Stage 2 quartz-potassium feldspar-sulphide vein cutting hornblende±biotite granodiorite of the Brenda stock - Pennask batholith. Note diffuse vein boundary with chalcopyrite (Cpy) >>pyrite replacement peripheral to vein as well as chalcopyrite and molybdenite (Mo) interstitial to potassium feldspar (Ksp) and quartz (Qtz) vein gangue.

property. To the west, Miocene to Pleistocene alkali olivine flood basalts of the Chilcotin Group overlie Nicola Group volcanic rocks (Wetherup, 2000; Schiarizza *et al.*, 2009a). Cu-Mo±Au mineralization is hosted within the intrusion (Southeast zone) and Cu-Au±Mo mineralized quartz stockwork and breccias (Megabuck, Deerhorn, Spellbound and Takom zones) are hosted in the volcanic and volcaniclastic country rock up to 1.5 km west of the north-trending contact with the batholith (Logan *et al.*, 2007).

Mineralization at Megabuck crosscuts upper volcaniclastic units of the Nicola Group and consists of an early quartz-magnetite-chalcopyrite±gold stockwork system overprinted by carbonate±chalcopyrite-pyrite veinlets. A pyritic halo surrounds the mineralized stockwork. Analogy with the alkalic porphyry mineralization at Mount Polley mine has been suggested, but the alkaline Cu-Au porphyries are typically quartz undersaturated. In addition, the alkalic porphyries are not characterized by quartz stockwork, and they are Late Triassic in age (Logan and Bath, 2006).

The Southeast zone is a blind deposit that was discovered in 2007 by drilling a well-defined (>1500 m wide), overburden-covered IP chargeability anomaly. Three widely spaced vertical diamond-drill holes completed during the 2007 program were mineralized from top to bottom (each hole reaching ~300 m depth). The best grades came from hole WJ-07-79, which intersected 203.55 m grading 0.34% Cu and 0.014% Mo (Fjordland Exploration Inc., 2008). Follow-up drilling to date totals 18 holes and indicates that the pyrite, chalcopyrite and molybdenite mineralization is vertically zoned from copper-gold mineralization (1.01% Cu, 0.44 g/t Au over 200.8 m) to copper- molybdenum (0.24% Cu, 0.014% Mo over 60.0 m) mineralization with increasing depth (Peters, 2009; Fjordland website). Mineralization in the Southeast zone consists of pyrite, chalcopyrite, molybdenite and trace bornite, which occur along fractures, in quartz veinlets and as disseminations (Figure 5). It is hosted entirely in quartz monzonite and granodiorite of the Takomkane batholith.

PREVIOUS AGE DATING

Isotopic age determinations for mineralized rock assemblages sampled in the vicinity of the Brenda deposit have been reported by various authors (Figures 2, 6). Parrish and Monger (1992) reported U/Pb dates for zircons and titanite separates. White *et al.* (1968) and Oriel (1972) report a number of K-Ar dates from whole rock, hornblende and biotite samples. A sample collected 13 km north of the Brenda pit returned an Early Jurassic U-Pb crystallization age from zircon, and a sample collected 13 km southwest of the pit yielded cooling ages between 150 and 140 Ma for titanite (Parrish and Monger, 1992). The titanite corroborates similar age brackets for K/Ar, biotite cooling ages at Brenda mine. The historical K/Ar data from biotite and hornblende separates for the Brenda mine suggested a ~176 Ma age for primary (?) hornblende and a ~146 Ma age for secondary, hydrothermal (?) biotite, with an interpretation that the pluton that hosts the deposit is older and not the causative phase assuming that the secondary biotite is dating the mineralizing event (Soregaroli and Whitford, 1976). To test this hypothesis we collected three samples from the vicinity of Brenda pit; one for U-Pb analyses, one for Ar-Ar and a mineralized vein sample for Re-Os age modelling.

Age dating in the vicinity of the Woodjam Property includes U-Pb, zircon constraints on the crystallization age of a number of phases of the Takomkane batholith and cooling ages established by Ar-Ar step heating of hornblende and feldspar mineral separates (Logan *et al.*, 2007; Schiarizza *et al.*, 2009a&b). Schiarizza (personal communication) has provided unpublished zircon ages of 196.84 ±0.22 Ma for the Woodjam Creek phase of the Takomkane batholith and a rough age estimate of *ca.* 204 Ma for an unnamed coarse plagioclase porphyry stock; both are shown on Figure 4. In addition a drill core sample (WJ04-37) of quartz-feldspar-biotite porphyry dike that cuts mineralization in the Megabuck Cu-Au zone returned an undisturbed biotite cooling age of 163.67 ±0.83 Ma, providing an upper age limit for the Cu-Au±Mo mineralization (Logan *et al.*, 2007).

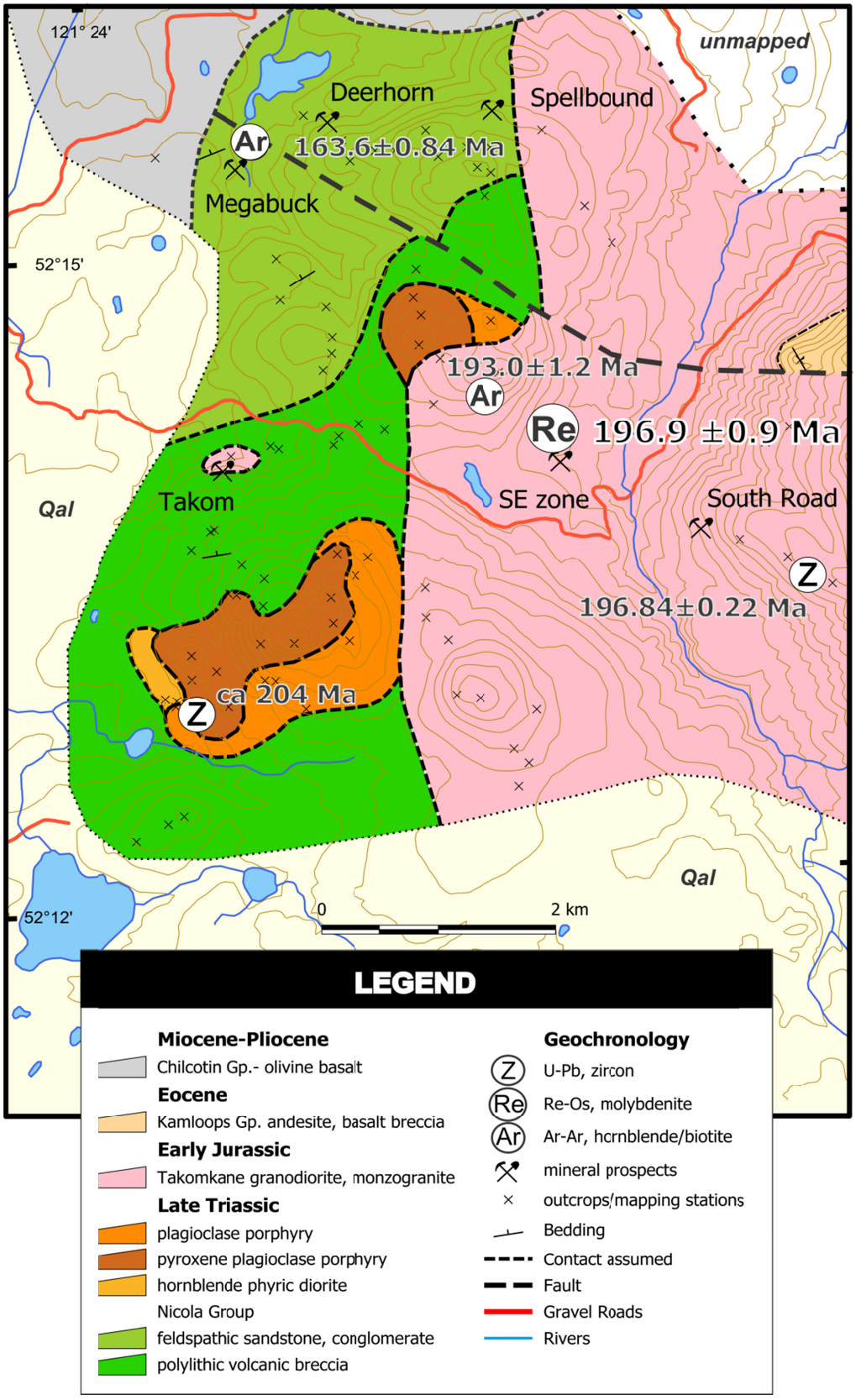

Figure 4. Local geology of the Woodjam property showing location of geochronological sample collected as part of this study (large symbol) and those collected previously by other authors (smaller symbols) as reported by Logan *et al.* (2007) and Schiarizza (personal communication, 2010). Geological contacts from Schiarizza *et al.* (2009b).

Figure 5. High-grade molybdenite (Mo) – chalcopyrite (Cpy) mineralized fracture cutting weakly altered hornblende quartz granodiorite of Takomkane batholith. Drill core from Southeast zone, drillhole WJ07-79.

SAMPLES FOR AGE DETERMINATION

To better understand the temporal relationships between the magmatic, hydrothermal and cooling history of the Brenda stock; U-Pb, Re-Os and Ar-Ar dating techniques were employed on zircon, molybdenite, and hornblende and biotite mineral separates respectively (Figure 2). Three samples were selected for isotopic age determination. Two samples of the weakly altered and mineralized hornblende-biotite-quartz diorite were collected and submitted to the Pacific Centre for Isotopic and Geochemical Research (PCIGR) at the Department of Earth and Ocean Sciences, The University of British Columbia. A third sample of mineralized quartz vein that contained medium-grained pyrite, chalcopyrite and coarse platelets of molybdenite was collected and analysed at the Radiogenic Isotope Facility at the University of Alberta.

Brenda

Hornblende±biotite granodiorite

A 20 kg sample (07JLO32-225) of hornblende-biotite granodiorite was collected from an upper bench outcropping at the southeast end of the pit (Zn 10, UTM 715234E, 5529257N). The granodiorite, a mesocratic, medium grained intrusive is comprised of equigranular intergrowths of plagioclase (40%) and potassium feldspar (25%), sub-rounded quartz (20%), chloritic hornblende and vitreous euhedral biotite (5-15%, total mafics) with sparse poikilitic potassium feldspar megacrysts. Accessory titanite, apatite and variable amounts of interstitial magnetite comprise noticeable but minor disseminated grains.

Zircon, hornblende and biotite were separated from the granodiorite and analysed separately to constrain the cooling history of the pluton, and its alteration and mineralizing system.

Chalcopyrite-molybdenum-pyrite bearing quartz veins

The molybdenite sample (07JLO32-226) submitted

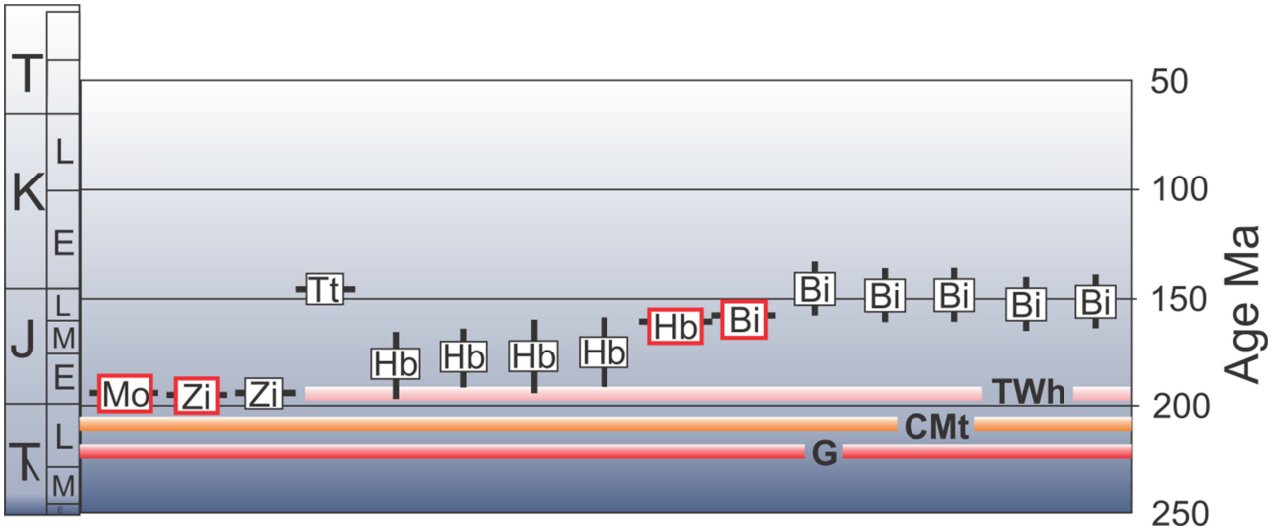

Figure 6. Age's plot of Re/Os (Mo), U/Pb (Zi & Tt), K/Ar (Hb), Ar/Ar (Hb & Bi) and K/Ar (Bi) analyses of samples from the area around the Brenda mine. Red squares are samples from this study, black squares compiled from White, Harakal and Carter (1968), Oriel (1972) and Parrish and Monger (1992). The zircon and molybdenite dates are interpreted to be crystallization and mineralization ages, titanite, hornblende and biotite show consistently younger ages that reflect a complicated cooling and/or resetting history that is evident with both K/Ar and Ar/Ar analyses. 2 σ error bars for each analysis are shown. Age spans for the Guichon (G), Copper Mountain (CMt) and Takomkane-Wildhorse (TWh) plutonic suites also shown.

for Re-Os dating was collected from the northeast corner of the Brenda pit (Zone 10, UTM 715279E, 5529449N) from a 35 cm wide, steeply dipping northeast trending bullish quartz vein mineralized with chalcopyrite, disseminated pyrite and fracture-filling molybdenite (Figure 7). The mineralogy, orientation and its' crosscutting relationship with pegmatitic feldspar-quartz veins suggest that the molybdenite sampled comes from a Stage 3 vein (Soregaroli and Whitford, 1976).

Woodjam - Southeast zone

Hornblende±biotite quartz monzonite

A well-mineralized interval of Takomkane batholith quartz monzonite containing molybdenum was sampled from an 8 cm long sample of split drillcore (provided by B. Laird, of Mincord Exploration Consultants Ltd.) from 317 m below the collar of diamond-drill hole WJ07-79 (Zn 10, 613104E, 5788240N). Molybdenite and chalcopyrite occupy millimetre-wide quartz veins and fractures cutting weak potassium-altered and silicified medium-grained hornblende quartz monzonite. Molybdenite was separated from the quartz monzonite and analysed to obtain a model age for mineralization.

U-PB AND ^{40}AR/^{39}AR GEOCHRONOLOGY METHODS

Sample preparation and analytical work for both the U-Pb and the ^{40}Ar/^{39}Ar isotopic ages presented herein was conducted at the Pacific Centre for Isotopic and Geochemical Research (PCIGR) at the Department of Earth and Ocean Sciences, The University of British Columbia.

Zircon was separated from the "Brenda stock" sample JLO07-32-225 using standard mineral separation techniques (crushing, grinding, Wilfley (wet shaker) table, heavy liquids and magnetic separation), followed by hand picking. Details of the separation techniques can be found in Logan *et al.* (2007). Air abraded single zircon grains were analysed with results listed in Table 1 and plotted in Figure 8a. U-Pb isotopic age determinations were obtained by Thermal Ionization Mass Spectroscopy (U-Pb ID-TIMS). Details of the both the mineral separation and analytical techniques are presented in (Logan *et al.*, 2007).

^{40}Ar/^{39}Ar isotopic age determinations were obtained by the laser-induced step-heating technique. Details of the analytical techniques are presented in (Logan *et al.*, 2007). Hornblende and biotite were separated from a granodiorite phase of the Brenda stock and analysed separately to constrain its cooling history.

U-Pb geochronology results

U-Pb analyses of five zircon grains separated from the Brenda granodiorite were determined by thermal ionization mass spectrometry (TIMS) technique.

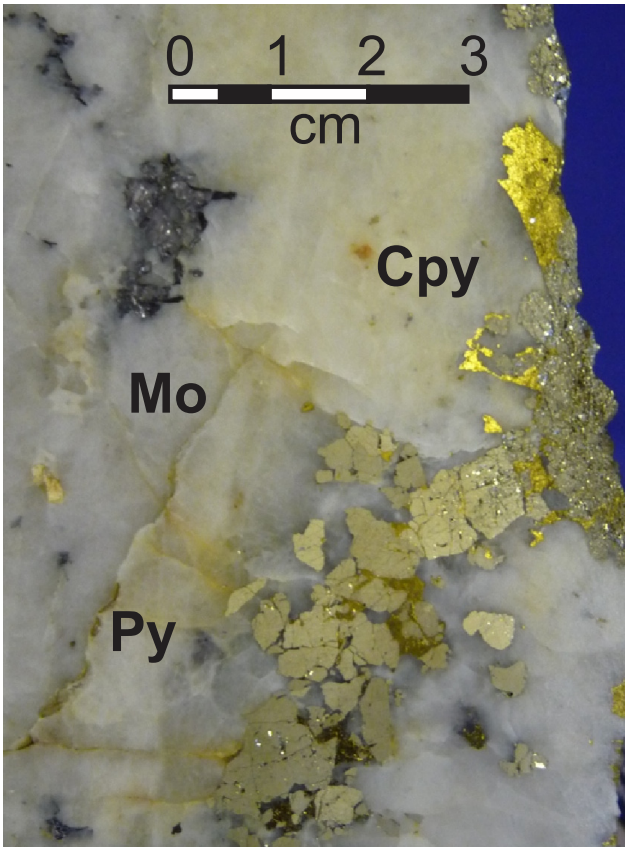

Figure 7. Stage 3 quartz vein mineralized with disseminated pyrite (Py), coarse blebby chalcopyrite (Cpy) and fracture-filling molybdenite (Mo). Re/Os sample JLO07-226.

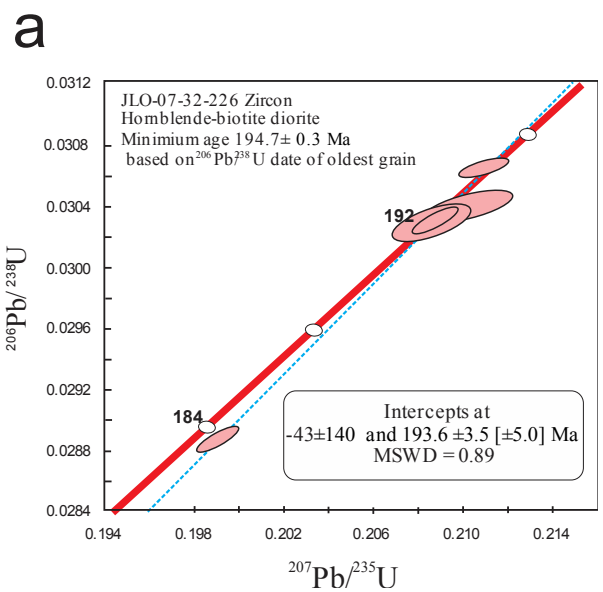

Figure 8a. Concordia plot for U/Pb TIMS data for sample JLO07-32-226. 2 σ error ellipses for individual analytical fractions are red. Minimum age 194.7 ±0.3 Ma based on ^{206}Pb/^{238}U date of oldest grain. Concordia bands include 2 σ errors on U decay constants.

Analysed mineral fractions and results are presented in Table 1, and the data are illustrated in Figure 8a.

Of the five grains dated, four overlap Concordia at the 2 σ confidence level between about 192-195 Ma and

Table1. U-Pb Thermal Ionization Mass Spectrometry analytical data for zircon from hornblende, biotite quartz diorite of the Brenda stock, sample JLO07-32-225.

		Compositional Parameters							Radiogenic Isotope Ratios										Isotopic Ages						
Sample	Wt. mg	U ppm	Th/U	Pb ppm	$^{206}Pb^*$ x10^{-13} mol	mol % $^{206}Pb^*$	Pb^*/Pb_c	Pb_c (pg)	$^{206}Pb/^{204}Pb$	$^{208}Pb/^{206}Pb$	$^{207}Pb/^{206}Pb$	% err	$^{207}Pb/^{235}U$	% err	$^{206}Pb/^{238}U$	% err	corr. coef.	$^{207}Pb/^{206}Pb$	±	$^{207}Pb/^{235}U$	±	$^{206}Pb/^{238}U$	±	% disc
	(a)	(b)	(c)	(d)	(c)	(e)	(e)	(e)	(e)	(f)	(g)	(g)	(h)	(g)	(h)	(g)	(h)		(i)	(h)	(i)	(h)	(i)	(h)	
JLO-07-32-225																									
A	0.013	202	0.351	6.2	3.3605	99.55%	65	1.24	4142	0.112	0.050188	0.590	0.210449	0.690	0.030412	0.264	0.545	203.69	13.68	193.93	1.22	193.13	0.50	5.19
B	0.009	251	0.376	7.8	2.9461	99.58%	70	1.01	4452	0.120	0.049979	0.239	0.208895	0.367	0.030314	0.229	0.773	194.00	5.56	192.62	0.64	192.51	0.43	0.77
C	0.008	368	0.375	10.9	3.3267	99.56%	67	1.21	4212	0.120	0.050012	0.239	0.199138	0.372	0.028879	0.240	0.778	195.53	5.56	184.40	0.63	183.53	0.43	6.14
D	0.007	448	0.376	13.8	3.6796	99.76%	122	0.73	7699	0.120	0.049945	0.553	0.208626	0.683	0.030295	0.328	0.598	192.42	12.87	192.40	1.20	192.40	0.62	0.01
E	0.006	113	0.357	3.6	0.9137	99.28%	40	0.54	2586	0.113	0.049906	0.340	0.210936	0.422	0.030655	0.169	0.637	190.60	7.92	194.34	0.75	194.65	0.32	-2.12

(a) A, B etc. are labels for abraded single zircon grains.
(b) Fraction masses determined on Sartorious SE2 ultramicrobalance to +/- 1 microgram.
(c) Nominal U and total Pb concentrations subject to uncertainty in fraction masses.
(d) Model Th/U ratio calculated from radiogenic 208Pb/206Pb ratio and 207Pb/235U age.
(e) Pb* and Pbc represent radiogenic and common Pb, respectively; mol % $^{206}Pb^*$ with respect to radiogenic, blank and initial common Pb.
(f) Measured ratio corrected for spike and fractionation only. Mass discrimination of 0.23% +/- 0.05%/amu +/- 1s, absolute, based on analysis of NBS-982; all Daly analyses.
(g) Corrected for fractionation, spike, and common Pb; up to 1 pg of common Pb was assumed to be procedural blank: 206Pb/204Pb = 18.50 ± 1.0%; 207Pb/204Pb = 15.50 ± 1.0%; 208Pb/204Pb = 38.40 ± 1.0% (all uncertainties 1-sigma). Excess over blank was assigned to initial common Pb with Stacey and Kramers (1975) model Pb composition at 195 Ma.
(h) Errors are 2-sigma, propagated using the algorithms of Schmitz and Schoene (2007) and Crowley et al. (2007).
(i) Isotopic dates are calculated using the decay constants l238=1.55125E-10 and l235=9.8485E-10 (Jaffey et al., 1971). 206Pb/238U and 207Pb/206Pb ages corrected for initial disequilibrium in 230Th/238U using Th/U [magma] = 3.
(j) Corrected for fractionation, spike, and blank Pb only.

one is normally discordant, lying slightly off Concordia at about 184 Ma. This data array is likely the result of Pb loss from at least four of the five analysed grains (Figure 8a, Table 1). The $^{206}Pb/^{238}U$ date for the oldest grain, at 194.7 Ma, is taken as a minimum age of crystallization for the rock, which assumes that none of the analysed grains contain older inherited zircon.

$^{40}Ar/^{39}Ar$ cooling age

Hornblende separated from the Brenda stock yields a complicated argon release spectra with older apparent ages in the low-temperature steps (1-5) indicating probable excess argon. The five-step plateau age of 160.7 ±0.9 Ma is calculated from the final 40.8% of the total ^{39}Ar (Figure 8b). Gas measurements obtained during each of the heating steps are presented in Table 2.

Biotite from the same sample Brenda stock granodiorite gave a well-defined plateau age of 158.22 ±0.82 Ma, represented by 83.7% of the total ^{39}Ar released (Figure 8c). Gas measurements obtained during each of the heating steps are presented in Table 3. The inverse isochron results in 11 points which define a poor quality isochron with an age of 158.7 ±1.1 Ma, an initial $^{40}Ar/^{36}Ar$ of 211 ±160 Ma, and a MSWD of 1.07.

RE-OS GEOCHRONOLOGY METHODS

Molybdenite was separated from the rock samples by metal-free crushing and milling, and concentrated using gravity and magnetic methods following Selby and Creaser (2004). The Re content was established for each molybdenite separate, to determine optimal spiking for the subsequent measurement of Re and Os by isotope dilution using a mixed double spike solution containing isotopically enriched ^{185}Re and isotopically enriched ^{188}Os and ^{190}Os.

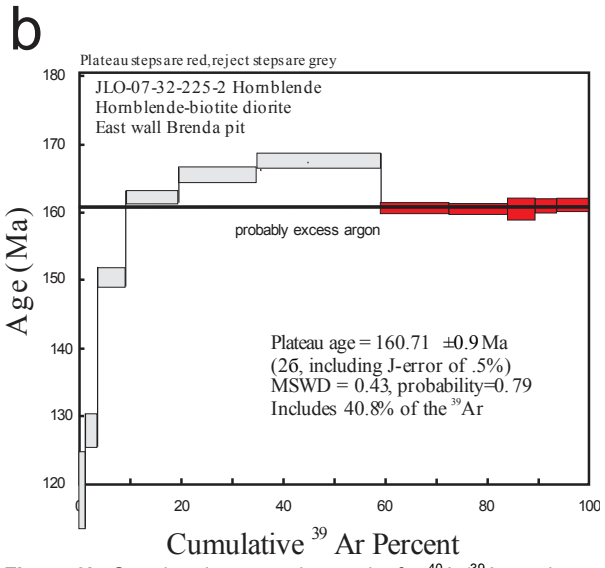

Figure 8b. Step-heating gas release plot for $^{40}Ar/^{39}Ar$ analyses for hornblende sample JLO07-32-225-2 hornblende.

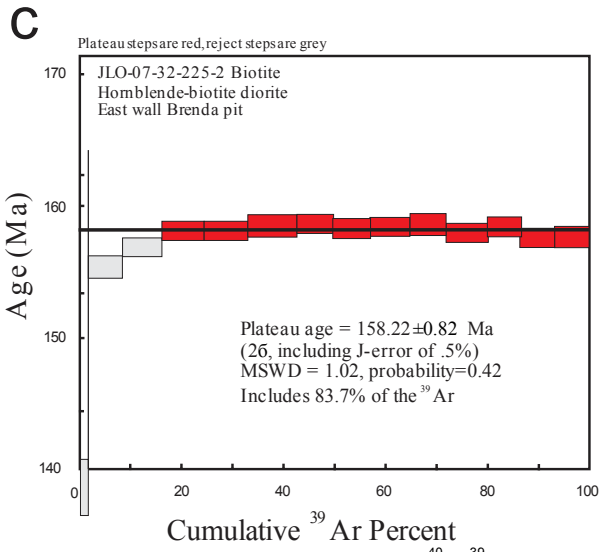

Figure 8c. Step-heating gas release plot for $^{40}Ar/^{39}Ar$ analyses for biotite sample JLO07-32-225-2.

Table 2. $^{40}Ar/^{39}Ar$ step heating gas release data from sample JLO07-32-225-2 hornblende.

07JLO32-225-2	Hornblende									
Laser	Isotope Ratios									
Power(%)	$^{40}Ar/^{39}Ar$	$^{38}Ar/^{39}Ar$	$^{37}Ar/^{39}Ar$	$^{36}Ar/^{39}Ar$	Ca/K	Cl/K	$\%^{40}Ar$ atm	f ^{39}Ar	$^{40}Ar^*/^{39}ArK$	Age
2	195.8500±0.0417	0.4150±0.0670	-0.1166±18.0450	0.5249±0.0583	0	0.073	79.32	0.08	38.143±7.094	327.07±55.63
2.3	42.6956 0.0149	0.0992 0.0827	0.1174 1.5399	0.0994 0.0257	0.461	0.016	68.72	1.25	13.071 0.662	118.88 5.83
2.6	20.6180 0.0096	0.0360 0.1174	0.0945 0.9724	0.0218 0.0404	0.371	0.004	30.16	2.34	14.070 0.291	127.65 2.55
2.9	19.5351 0.0060	0.0374 0.0371	0.2265 0.2086	0.0095 0.0440	0.888	0.005	13.6	5.6	16.689 0.160	150.44 1.39
3.2	19.1815 0.0054	0.0962 0.0197	0.7585 0.0195	0.0041 0.0559	2.974	0.019	5.27	10.34	18.055 0.121	162.22 1.04
3.5	19.3676 0.0067	0.1537 0.0176	1.1309 0.0233	0.0037 0.0396	4.436	0.032	4.41	15.4	18.438 0.134	165.50 1.15
3.8	19.4876 0.0067	0.1589 0.0159	1.7967 0.0159	0.0038 0.0217	7.055	0.033	4.01	24.23	18.670 0.130	167.50 1.12
4.1	18.3525 0.0046	0.0745 0.0187	0.5371 0.0386	0.0018 0.0499	2.105	0.014	2.03	13.31	17.876 0.088	160.68 0.75
4.3	18.1525 0.0042	0.0709 0.0260	0.5589 0.0422	0.0012 0.0934	2.191	0.013	1.05	11.66	17.848 0.084	160.44 0.72
4.5	18.2846 0.0076	0.0573 0.0786	0.4295 0.1939	0.0015 0.2607	1.684	0.01	1.16	5.15	17.851 0.179	160.47 1.54
4.8	18.3992 0.0058	0.0636 0.0563	0.5870 0.0847	0.0018 0.1195	2.301	0.011	1.37	4.46	17.902 0.124	160.91 1.07
5.4	18.3739 0.0053	0.0691 0.0469	0.6906 0.0970	0.0017 0.0886	2.708	0.013	1.42	6.19	17.930 0.107	161.15 0.92
Total/Average	19.2832±0.0011	0.1050±0.0042	1.9943±0.0031	0.0050±0.0067	3.655	0.02		100	17.974±0.025	

J-error = 0.005211±0.000008

Volume ^{39}ArK = 385.12

Integrated Date = 161.53±0.49

Volumes are $1x10^{-13}$ cm^3 NPT

Neutron flux monitors: 28.02 Ma FCs (Renne et al., 1998)

Isotope production ratios: ($^{40}Ar/^{39}Ar$)K=0.0302±0.00006, ($^{37}Ar/^{39}Ar$)Ca=1416.4±0.5, ($^{36}Ar/^{39}Ar$)Ca=0.3952±0.0004, Ca/K=1.83±0.01($^{37}ArCa/^{39}ArK$).

Table 3. $^{40}Ar/^{39}Ar$ step heating gas release data from sample JLO07-32-225-2 biotite.

07JLO32-225-2	Biotite									
Laser	Isotope Ratios									
Power(%)	$^{40}Ar/^{39}Ar$	$^{38}Ar/^{39}Ar$	$^{37}Ar/^{39}Ar$	$^{36}Ar/^{39}Ar$	Ca/K	Cl/K	$\%^{40}Ar$ atm	f ^{39}Ar	$^{40}Ar^*/^{39}ArK$	Age
2	123.5134±0.0287	0.1456±0.1915	0.2985±0.0827	0.3857±0.0491	1.168	0.016	93.21	0.04	7.862±4.704	72.34±42.42
2.3	31.9991 0.0076	0.0549 0.1191	0.1600 0.0343	0.0745 0.0372	0.621	0.006	68.65	0.46	9.776 0.811	89.52 7.25
2.6	19.1244 0.0045	0.0334 0.0473	0.0606 0.0411	0.0182 0.0427	0.235	0.004	27.4	1.21	13.648 0.240	123.79 2.10
2.9	19.4652 0.0043	0.0322 0.0154	0.0258 0.0282	0.0072 0.0286	0.1	0.004	10.77	6.75	17.280 0.098	155.35 0.85
3.1	18.6313 0.0044	0.0320 0.0250	0.0179 0.0572	0.0038 0.0209	0.069	0.004	5.85	7.8	17.456 0.082	156.86 0.70
3.3	17.9873 0.0044	0.0307 0.0211	0.0200 0.0375	0.0011 0.0619	0.078	0.004	1.67	8.35	17.602 0.081	158.12 0.70
3.5	17.8601 0.0043	0.0314 0.0353	0.0194 0.0238	0.0007 0.0881	0.075	0.004	0.97	8.5	17.602 0.080	158.12 0.69
3.7	17.8887 0.0051	0.0312 0.0381	0.0278 0.0272	0.0007 0.0609	0.108	0.004	0.9	9.56	17.648 0.093	158.51 0.80
3.8	17.9001 0.0045	0.0314 0.0240	0.0218 0.0351	0.0006 0.1005	0.084	0.004	0.78	6.98	17.669 0.083	158.69 0.71
4	17.8708 0.0049	0.0340 0.0403	0.0580 0.0244	0.0007 0.0854	0.223	0.005	0.88	7.36	17.625 0.089	158.32 0.77
4.2	17.8661 0.0044	0.0313 0.0206	0.0367 0.0297	0.0006 0.0865	0.141	0.004	0.77	7.79	17.642 0.081	158.47 0.69
4.4	17.9249 0.0048	0.0318 0.0451	0.0406 0.0221	0.0007 0.1042	0.156	0.004	0.96	7.27	17.663 0.089	158.64 0.77
4.6	17.8118 0.0045	0.0315 0.0207	0.0448 0.0265	0.0006 0.0916	0.172	0.004	0.81	7.99	17.582 0.082	157.95 0.71
4.8	17.9181 0.0046	0.0322 0.0244	0.0488 0.0290	0.0008 0.0685	0.187	0.004	1.06	6.5	17.634 0.085	158.40 0.73
5	17.8185 0.0046	0.0317 0.0181	0.0783 0.0235	0.0008 0.0954	0.301	0.004	1.05	6.54	17.538 0.086	157.57 0.74
5.3	17.8425 0.0047	0.0318 0.0274	0.1172 0.0152	0.0009 0.0434	0.45	0.004	1.13	6.88	17.552 0.085	157.69 0.73
Total/Average	18.1053±0.0006	0.0320±0.0041	0.0890±0.0018	0.0020±0.0068	0.163	0.005		100	17.491±0.014	

J-error = 0.005204±0.000008

Volume ^{39}ArK = 1149.1

Integrated Date = 157.17±0.34

Volumes are $1x10^{-13}$ cm^3 NPT

Neutron flux monitors: 28.02 Ma FCs (Renne et al., 1998)

Isotope production ratios: ($^{40}Ar/^{39}Ar$)K=0.0302±0.00006, ($^{37}Ar/^{39}Ar$)Ca=1416.4±0.5, ($^{36}Ar/^{39}Ar$)Ca=0.3952±0.0004, Ca/K=1.83±0.01($^{37}ArCa/^{39}ArK$).

The Carius-tube method was used in this study for the dissolution of molybdenite and equilibration of sample and tracer Re and Os. Molybdenite samples were dissolved and equilibrated with a known amount of tracer in reverse aqua regia (2:1 16 N HNO_3 and 12N HCl, 3 ml) at 240°C for 24 h then cooled and refrigerated prior to Os and Re separation. Extraction of OsO_4 from the acid-sample mix was achieved using modified solvent extraction and microdistillation techniques. Mo was removed by solvent extraction from the acid-sample mixture after Os separation. Rhenium was then purified by HNO_3 + HCl-based anion exchange chromatography using standard techniques. Total procedural blanks for Re and Os are less than 2 picograms and 0.5 picograms, respectively. These procedural blanks are insignificant in comparison to the Re and Os concentrations in the molybdenite analysed here. The purified Re and Os was analysed by Negative Thermal Ion Mass Spectrometry (N-TIMS), and abundances of ^{187}Re and ^{187}Os calculated.

Typically, 20 mg of molybdenite was used for the full Re-Os analysis, and all data are presented in Table 4. An overview of the Re-Os method of dating molybdenite can be found in Stein *et al.* (2001).

Model ages are calculated from the simplified isotope equation: $t = \ln(^{187}Os/^{187}Re + 1)/\lambda$, where λ is the ^{187}Re decay constant ($1.666 \pm 0.005 \times 10^{-11}$ a-1; Smoliar *et al.*, 1996), which contains a ±0.31% uncertainty in the value of λ (Selby *et al.*, 2007) and assumes that molybdenite crystallizes with only Re and no Os. The 2σ age uncertainty quoted above (Table 4) reflects all known sources of analytical error, fully propagated to arrive at the quoted age uncertainty.

Re-Os Geochronology Results

The Re-Os model ages for molybdenite from the Brenda mine and Southeast zone of the Woodjam South property are early Jurassic, 193.9 ±0.9 Ma and 196.9 ±0.9 Ma respectively (Table 4). These are considered good quality data that accurately reflect the age of molybdenite crystallization.

DISCUSSION OF AGE DETERMINATIONS

Typical porphyry systems are characterized by multiple intrusive and hydrothermal phases that overprint and reset metal and alteration zonations and isotopic-signatures (Gustafson and Hunt, 1975). So too has copper-molybdenum mineralization at the Brenda deposit formed during multiple stages, as evidenced by crosscutting mineralized vein assemblages. To unravel the relationships between the magmatic (*i.e.* crystallization age) and mineralization and later cooling history of the Brenda stock; we utilized three different techniques: U-Pb zircon for magmatic crystallization, Re-Os isotope system for hydrothermal mineralization, and $^{40}Ar/^{39}Ar$ dating of two mineral systems for the age and rate of cooling. Zircon closure temperatures are generally taken to be > 900°C in a magmatic environment (Mezger, 1990).The Re-Os geochronometer is remarkably resilient to both hydrothermal metamorphism (Selby and Creaser, 2001) and granulite-facies metamorphism (Bingen and Stein, 2002) and should reliably date crystallization of molybdenite, not later disturbance events. Hornblende and biotite have Ar retention closure temperatures of 570-465°C and 360-280°C (Reiners and Brandon, 2006) respectively. The $^{40}Ar/^{39}Ar$ dating techniques is more robust than the K-Ar biotite technique used in the past and provides more information about the rate of cooling.

Brenda

Historical potassium-argon dates of samples from the Brenda mine area produced a mean age (n=4) for hornblende of 178.5 ±15.5 Ma and a mean age of 148 ±9.2 Ma (n=5) for apparent co-existing biotite (Figure 6). Interpretation of these results suggested that the Brenda stock crystallized about *ca.* 178 Ma and the148 Ma biotite date from the pit area was interpreted to be the age of mineralization (White *et al.*, 1968). In addition, it was postulated that the Cu and Mo could have been emplaced at different times due in part to their independent concentration within separate structural trends. Copper is distributed along northeast-trends and the molybdenite on northwest-trending structures. To test this scenario the molybedenite mineralization dated was collected from one of the younger vein sets (Stage 3 vein). However, it has an Early Jurassic Re-Os model age identical, within error, to the crystallization age of the batholith.

Our $^{40}Ar/^{39}Ar$ results for hornblende indicate excessive radiogenic argon and a plateau age defined by only 40% of ^{39}Ar and a biotite cooling age that is identical, within error, to the hornblende data ca 159 Ma. This age is intermediate to the historic K/Ar clusters for

Table 4. Re/Os isotopic results and age determinations of molybdenite for samples JLO07-226 and WJ-07-79.

Sample	Re (ppm)	^{187}Re (ppm)	^{187}Os (ppb)	Common Os (pg)	Age ± 2σ (Ma)
WJ07-79	403.2 ± 1.3	253.4 ± 0.8	832.6 ± 0.6	1.6	196.9 ± 0.9
JLO07-32-226	68.45 ± 0.23	43.02 ± 0.14	139.2 ± 0.2	<0.5	193.9 ± 0.9

ppm = parts per million by weight, ppb = parts per billion by weight, pg = picograms (10^{-12} g)

hornblende and biotite (Figure 6) and has no clear cause inherent to the Brenda stock. However, a ~167 Ma titanite cooling age (Parrish and Monger, 1992; Figure 6) is reported for a sample of the Pennask batholith collected ~2 km north of its southern contact with the Osprey Lake batholith (166 ±1 Ma) and less than a kilometre away from a suite of north-trending Early Tertiary (62 ±2 Ma) potassium feldspar porphyry dikes and plugs (Parrish and Monger, 1992). In addition, historic K/Ar, Ar/Ar and Rb/Sr dates from around the mine range down to 135 Ma (Figure 6; Breitsprecher and Mortensen, 2004) and probably reflect partial re-setting of original cooling ages by younger magmatic suites in the area including; Middle Jurassic (Osprey Lake batholith), mid-Cretaceous (Okanagan batholith) and Early Tertiary (Nicola batholith) granitic bodies.

Our U/Pb results for zircon separated from the granodiorite hosting mineralization at the mine: ~194.7 ±0.3 Ma is identical, within error, to the 194 ±1Ma crystallization age reported for Pennask batholith biotite granodiorite by Parrish and Monger (1992). The Re-Os model age for molybdenite mineralization is 193.9 ±0.9 Ma also synchronous within error (Figure 6).

Woodjam - Southeast zone

The Re/Os model age for Southeast zone molybdenite mineralization at ~196.9 ±0.9 Ma is identical to the U/Pb, zircon crystallization ages (196.84 ±0.22 Ma, P. Schiarizza, personal communication, 2010) and is compatible with the Ar/Ar, biotite and feldspar cooling ages (193.0 ±1.2 Ma and 192.2 ±1.1 Ma, Logan *et al.*, 2007) for the Woodjam Creek phase of the Takomkane batholith (Schiarizza *et al.*, 2009b). The ore mineralogy, style and age indicate that Southeast zone formed in response to Early Jurassic calcalkaline magmatism. It is *ca.* 10 to 15 Ma younger than mineralization at Gibraltar (Oliver *et al.*, 2009) and *ca.* 8 Ma younger than mineralization associated with alkaline magmatism at Mount Polley.

If there is any systematic difference in the ages of intrusion and mineralization, its measurement is beyond the resolution of the geochronometers available to us. This contemporaneity of intrusion and hypogene mineralization is consistent with the results of similarly robust datasets elsewhere within the Cordilleran belt for alkalic porphyry deposits (*e.g.* Iron Mask and Mt. Polley (Logan *et al.*, 2007), and results from other porphyry systems globally (McInnes *et al.*, 2005). Our new data provide a tight integration with the ~195 Ma calcalkaline Cu-Mo±Au porphyry event that is exposed along the length of Quesnellia and may have implications for similar aged Cu-Au-Mo metallogenic systems in Stikinia (*i.e.* Kerr, Sulphurets and Premier (?)) and northern Cordillera.

MESOZOIC QUESNEL

Spatial and temporal relationships between magmatic cycles in arcs and porphyry copper formation has long been recognized (Sillitoe, 1972; Clark *et al.*, 1976; Sillitoe and Perrelló, 2005) and is well displayed in southern Quesnel terrane, where three subparallel, linear, Cu-Mo, Cu-Au and Cu-Mo±Au porphyry belts occur within the 20 Ma epoch considered here (Figure 9). In southern Quesnellia, migration of Late Triassic to Early Jurassic magmatism across southern British Columbia is indicated by linear belts of temporal plutons reflecting 50 Ma of arc evolution above an east-dipping subduction zone (Mortimer, 1987; Parrish and Monger 1992; Ghosh, 1995). Quesnel arc magmatism and associated porphyry mineralization migrated eastward with time, beginning in the west, *ca.* 210-215 Ma with emplacement of plutons and development of calcalkaline Cu-Mo±Au deposits at Highland Valley and Gibraltar. New data suggests multiple stages of mineralization at Highland Valley; that post-dates intrusion of the Guichon batholith by up to 4 Ma (Ash *et al.*, 2007). In the central axis of the arc are slightly younger alkaline intrusions and 205 Ma, Cu-Au mineralization at Mount Polley (Logan *et al.*, 2007) and Copper Mountain (Mihalynuk *et al.*, 2008), part of the chain of similar deposits that extends the length of the Intermontane Belt (Barr *et al.*, 1976; Figure 1).

Early Jurassic calcalkaline magmatism and Cu-Mo±Au mineralization was initiated following an approximate 3-5 Ma hiatus. In southern QN the roots of this arc are defined by a 375 km long arcuate belt of 197-193 Ma granodiorite plutons (Takomkane/Wildhorse suite) and in the north by the Hogem batholith. In central QN, it is under represented, probably because of the thick glacial cover in this region. Late Early Jurassic alkaline magmatism and porphyry Cu-Au formation at Mt Milligan closely followed emplacement of the Quesnel arc onto Ancestral North American (ANA) margin at ~186 Ma (Nixon *et al.*, 1993). A second pulse of alkaline magmatism at ~178 Ma in northern QN at Lorraine (Logan and Mihalynuk, in review) and >156 Ma in southern QN at Sappho (Nixon and Laflamme, 2002) are probable post-subduction partial melts of subduction-modified arc-lithosphere (Richards, 2009).

CONCLUSIONS

Copper-molybdenum±gold mineralization at the Brenda deposit formed during several stages, as evidenced by mineralogically different and crosscutting vein assemblages. Our isotopic age dating results show that the time span between magma crystallization and the final stages of mineralization is too small to be measured by the geochronometers employed. It is most likely less than a million years. It formed from the same evolving magmatic/mineralizing episode responsible for emplacement and crystallization of the Early Jurassic Pennask batholith. The same relationship between mineralization and magmatism is evident on the

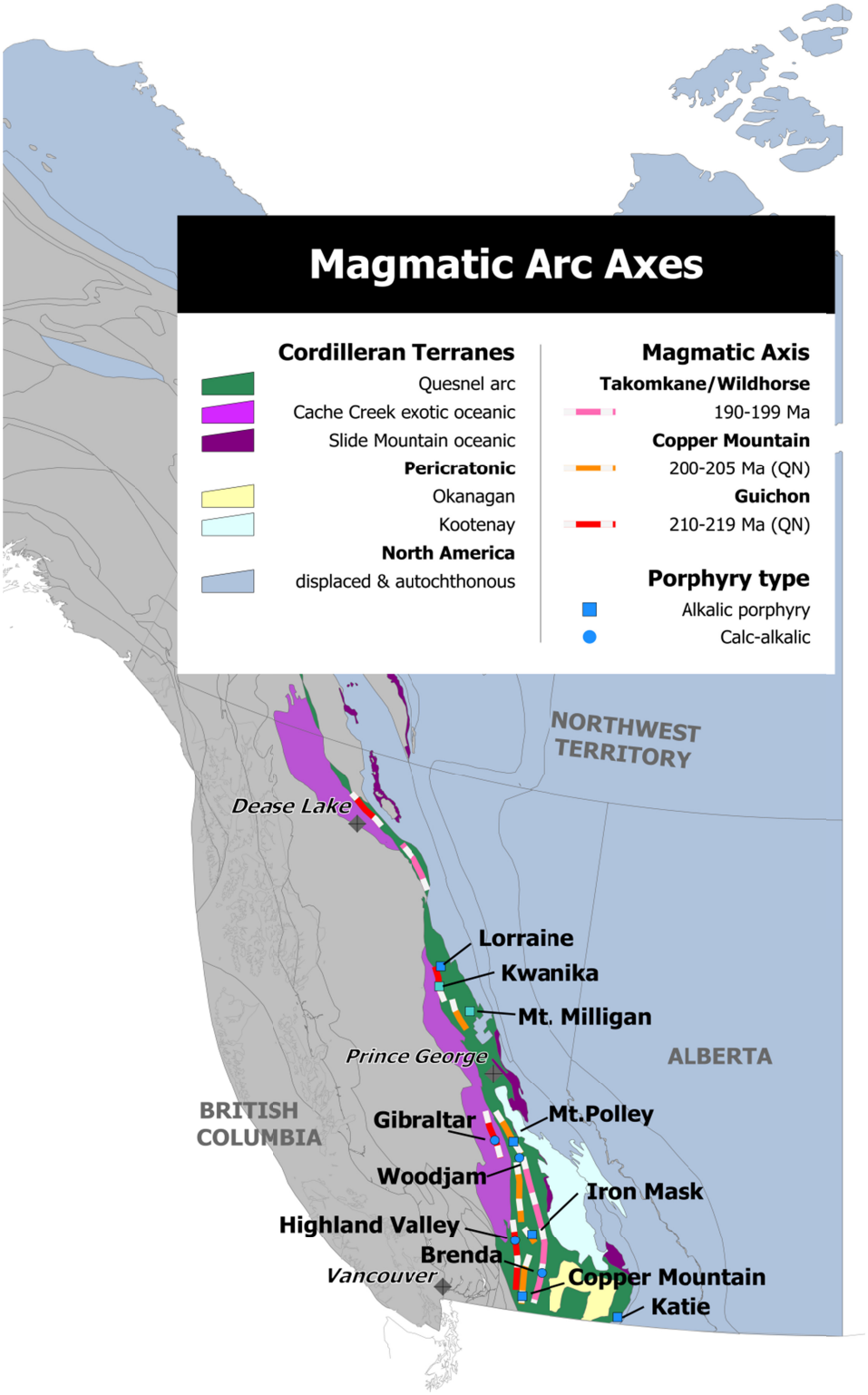

Figure 9. Linear traces of Late Triassic and Early Jurassic arc plutons define discrete north trending, eastward progressing axis of magmatism along the length of Quesnel.

Woodjam property 280 km to the north, where molybdenum from the Southeast zone has a Re-Os model age for mineralization that overlaps the Early Jurassic crystallization age of the host Takomkane batholith.

Early Jurassic mineralization at Brenda and Woodjam-Southeast is hosted in large, medium to coarse-grained, equigranular calcalkaline intrusives. In both cases Cu-Mo±Au mineralization occurs very close to the margins of these upper crustal batholith-sized intrusions. These are important exploration criteria that incorporate the type of porphyry deposit and degree of uplift and erosion affecting these parts of the porphyry belt. In contrast, the Late Triassic Cu-Au±Ag alkalic systems are small, high level complex intrusions which intrude coeval and cogenetic? volcanic rocks. Mineral and alteration assemblages are unique to each type of porphyry deposit (Sillitoe, 2002; McMillan, 2005). As a result, geochemical and geophysical responses dictate different techniques to delineate alkaline (eTh/K lows located on flanks of magnetic highs; Shives *et al.*, 1997) *vs.* calcalkaline (conductive I.P. geophysical response related to sulphide halo) porphyry deposits. It follows then, to ensure successful exploration along the Quesnel arc it is critical to understand where and in which magmatic/metallogenic belt you are and which potential targets you should expect.

It is anticipated from the exploration successes at Woodjam property by Fjordland Exploration Inc, Cariboo Rose Resources and Gold Fields Horsefly Exploration Corp., that the recognition of this Early Jurassic Cu-Mo±Au porphyry belt will help to focus more exploration on this 375 km long prospective belt of calcalkaline intrusions in south-central British Columbia. If so, new discoveries are certain to be realized.

ACKNOWLEDGMENTS

Paul Schiarizza is gratefully acknowledged for sharing his geological expertise of Quesnel terrane geology and for providing unpublished geochronology data for the Woodjam Creek area. Thomas Ullrich provided and interpreted the $^{40}Ar/^{39}Ar$ analyses. Access to the pit at the Brenda mine was kindly granted by Georges Guilleminot of Xstrata Copper Canada, Brenda Mines Division.

REFERENCES

Ash, C.H., Reynolds, P.H., Creaser, R.A. and Mihalynuk, M.G. (2007): ^{40}Ar-^{39}Ar and Re-O isotopic ages for hydrothermal alteration and related mineralization in the Highland Valley Cu-Mo deposit, SW BC; in Geological Fieldwork 2006, *BC Ministry of Energy, Mines and Petroleum Resources*, Paper 2007-1, pages 19-24.

Barr, D.A., Fox, P.E., Northcote, K.E. and Preto, V.A. (1976): The Alkaline Suite Porphyry Deposits: A Summary; in Porphyry Deposits of the Canadian Cordillera, Sutherland Brown, A., Editor, *Canadian Institute of Mining and Metallurgy*, Special Volume 15, pages 359-367.

Beatty, T. W., Orchard, M. J., and Mustard, P. S. (2006): Geology and tectonic history of the Quesnel terrane in the area of Kamloops, British Columbia; Colpron, M., and Nelson, J., Editors, *in* Paleozoic evolution of pericratonic terranes at the ancient pacific margin of North America, Canadian and Alaskan Cordillera, Special Paper 45, *Geological Association of Canada*, pages 483-504.

Bingen, B. and Stein, H.J. (2002): Molybdenite Re-Os dating of biotite dehydration melting: the Rogaland granulites, S Norway; 12th Annual V.M. Goldschimdt conference Davos, Switzerland, A78.

Breitsprecher, K. and Mortensen, J.K. (2004): BC Age 2004A-1: A database of isotopic age determinations for rock units from British Columbia; *B.C. Ministry of Energy, Mines and Petroleum Resource*, Open File 2004-03.

Breitsprecher, K., Weis, D., Scoates, J.S. and Anderson, R.G. (2010): Targeting mineralized Late Triassic to Early Jurassic plutons in the Nicola arc, southern Quesnel terrane, Canadian Cordillera; *in* Geological Association of Canada, Targeted Geoscience Initiative 3 Workshop, Vancouver, URL accessed November, 2010, http://www.gac-cs.ca/workshops/TGI3/abstracts/13_GAC_TGI3_Breitsprecher_mineralizd_plutons.pdf

Carr, J.M., (1967): Geology of the Brenda Lake Area; *British Columbia Minister of Mines and Petroleum Resources*, Annual Report, 1967, pages 183-212.

Clark, A. H., Farrar, E., Caelles, J. C., Haynes, S. J., Lortie, R. B., McBride, S. L., Quirt, G. S., Robertson, R. C. R., and Zentilli, M. (1976): Longitudinal variations in the metallogenetic evolution of the Central Andes: A progress report; *Geological Association of Canada,* 14, pages 23-58.

Cooke, D. R., Hollings, P., and Walshe, J. L. (2005): Giant Porphyry Deposits: Characteristics, Distribution, and Tectonic Controls; *Economic Geology and the Bulletin of the Society of Economic Geologists*, v. 100, pages 801-818.

Crowley, J.L., Schoene, B. and Bowring, S.A., (2007): U-Pb dating of zircon in the Bishop Tuff at the millennial scale; *Geology*, vol. 35, no. 12, pages 1123-1126.

Dawson, G.L. and Ray, G.E., (1988): Geology of the Pennask Mountain Area, 92H/16, *B.C. Ministry of Energy, Mines & Petroleum Resources* Open File Map 1988-7, scale 1:25 000.

Fjordland Exploration Inc. (2008a): Woodjam's Southeast zone returns 0.40% copper and 0.014% molybdenum over 113.8 metres; Fjordland Exploration Inc., news release, January 18, 2008.

Ghosh, D. K., (1995): Nd-Sr isotopic constraints on the interactions of the Intermontane Superterrane with the western edge of North America in the southern Canadian Cordillera, *Canadian Journal of Earth Sciences*, vol 32, pages 1740-1758.

Gustafson, L.B. and Hunt, J.P. (1975): The Porphyry copper deposit at El Salvador, Chile: *Economic Geology and the Bulletin of the Society of Economic Geologists*, v. 70, pages 857-912.

Jaffey, A.H., Flynn, K.F., Glendenin, L.E., Bentley, W.C., Essling, A.M., (1971): Precision measurement of half-lives and specific activities of ^{235}U and ^{238}U, Phys. Rev. C4, pages 1889–1906.

Logan, J.M. and Bath, A.B. (2006): Geochemistry of Nicola Group Basalt from the Central Quesnel Trough at the

Latitude of Mount Polley (NTS 093A/5, 6, 11, 12), Central British Columbia; *in* Geological Fieldwork 2005, *BC Ministry of Energy, Mines and Petroleum Resources*, Paper 2006-1, pages 83-98.

Logan, J.M. and Mihalynuk, M.G. (in review): Tectonic controls on Early Mesozoic paired alkaline porphyry deposit belts (Cu-Au ±Ag-Pt-Pd-Mo) within the Canadian Cordillera, Economic Geology.

Logan, J.M., Mihalynuk, M.G., Ullrich, T. and Friedman, R.M. (2007): U-Pb ages of intrusive rocks and 40Ar/39Ar plateau ages of copper-gold-silver mineralization associated with alkaline intrusive centres at Mount Polley and the Iron Mask batholith, southern and central British Columbia; *in* Geological Fieldwork 2006, *BC Ministry of Energy, Mines and Petroleum Resources*, Paper 2007-1, pages 93-116.

Massey, N.W.D., MacIntyre, D.G., Desjardins, P.J. and Cooney, R.T. (2005): Digital geology map of British Columbia: whole province; *BC Ministry of Energy, Mines and Petroleum Resources*, Geofile 2005-1, scale 1:250 000, URL <http://www.empr.gov.bc.ca/Mining/Geoscience/PublicationsCatalogue/GeoFiles/Pages/2005-1.aspx> [December 2010].

McInnes, B.I.A., Evans, N.J., Fu, F.Q. and Garwin, S. (2005): Application of thermochronology to hydrothermal ore deposits; *Reviews in Mineralogy and Geochemistry*, v. 58, pages 467-498.

McMillan, W.J. (2005): Porphyry Cu-Mo Deposits of the Highland Valley District, Guichon Creek batholith, British Columbia, Canada; Porter, T.M. Editor, in Super Porphyry Copper & Gold Deposits: A Global Perspective; PGC Publishing, Adelaide, v. 1, pages 259-274.

Mezger, K. (1990): Geochronology in granulites, in Granulites and Crustal Evolution, D. Vielzeuf and Ph. Vidal, eds. pp. 45 l-470, Kluwer, Dordrecht, The Netherlands.

Mihalynuk, M.G., Logan, J.M., Friedman R.M. and Preto V.A. (2010): Age of Mineralization and 'Mine Dykes' at Copper Mountain Alkaline Copper-Gold-Silver Porphyry Deposit (NTS 092H/07), South-Central British Columbia; *in* Geological Fieldwork 2009, *BC Ministry of Energy, Mines and Petroleum Resources*, Paper 2010-1, pages 163-172.

Minfile Number 92HNE047, Brenda Mine, *BC Ministry of Energy, Mines and Petroleum Resources*, online document, <http://minfile.gov.bc.ca/Summary.aspx?minfilno=092HNE047 >[December 2010].

Mortensen, J.K., Ghosh, D.K. and Ferri, F. (1995): U-Pb geochronology of intrusive rocks associated with copper-gold porphyry deposits in the Canadian Cordillera; in Porphyry deposits of the Northwestern Cordillera of North America, *Canadian Institute of Mining and Metallurgy,* Special Volume 46, pages 142-158.

Mortimer, N. (1987): The Nicola Group: Late Triassic and Early Jurassic Subduction-related Volcanism in British Columbia; Canadian Journal of Earth Sciences, Volume 24, pages 2521-2536.

Mortimer, N., Van, d. H. P., Armstrong, R. L., and Harakal, J., (1990): U-Pb and K-Ar dates related to the timing of magmatism and deformation in the Cache Creek terrane and Quesnellia, southern British Columbia: *Canadian Journal of Earth Science*, v. 27, pages 117-123.

Nixon, G.T., Archibald, D.A. and Heaman, L.M. (1993): 40Ar-39Ar and U-Pb geochronometry of the Polaris Alaskan-type complex, British Columbia; precise timing of Quesnellia-North America interaction, *in* Geological Association of Canada; Mineralogical Association of Canada; annual meeting; program with abstracts, Joint Annual Meeting: Waterloo, ON, Canada, Geological Association of Canada, page 76.

Nixon, G.T. and Laflamme, J.H.G. (2002): Cu-PGE mineralization in alkaline plutonic complexes, *BC Ministry of Energy, Mines and Petroleum Resources*, GeoFile 2002-2.

Oliver, J. L., Crozier, J., Kamionko, M., and Fleming, J. (2009): The Gibraltar Mine, British Columbia. A billion tonne deep copper-molybdenum porphyry system: structural style, patterns of mineralization and rock alteration; Roundup 2009 Program with abstracts: Vancouver, BC, *Association for Mineral Exploration British Columbia*, pages 35-36.

Oriel, W.M., (1972): Detailed bedrock geology of the Brenda copper-molybdenum mine, Peachland, British Columbia, *Unpublished* M.Sc. thesis, *University of British Columbia*, Vancouver, BC, 94 pages.

Palfy, J., Smith, P.L. and Mortensen, J.K. (2000): A U-Pb and 40Ar-39Ar time scale for the Jurassic; *Canadian Journal of Earth Sciences*, volume 37, pages 923–944.

Parrish, R., Roddick, J.C., Loveridge, W.D., and Sullivan, R.W. (1987): Uranium lead analytical techniques at the geochronology laboratory, Geological Survey of Canada; in Radiogenic Age and Isotopic Studies, Report 1, *Geological Survey of Canada*, Paper 87-2, pages 3-7.

Parrish, R. R., and Monger, J. W. H. (1992): New U-Pb dates from southwestern British Columbia, Radiogenic age and isotopic studies, Report 5, *Geological Survey of Canada*, pages 87-108.

Peters, L.J. (2005): Summary technical report on the Woodjam claims, Cariboo Mining District; unpublished report, Fjordland Exploration Inc., 115 pages.

Reiners, P.W and Brandon, M.T. (2006): Using thermochronology to understand orogenic erosion; Annual Review Earth and Planetary Science, volume 34, pages 410-466.

Renne, P.R., C.Swisher, C.C., III, Deino, A.L., Karner, D.B., Owens, T. and DePaolo, D.J., (1998): Intercalibration of standards, absolute ages and uncertainties in 40Ar/39Ar dating; Chemical Geolology, Volume 145(1-2), pages 117-152.

Richards, J.P. (2003): Tectono-magmatic precursors for porphyry Cu-(Mo-Au) deposit formation: *Economic Geology and the Bulletin of the Society of Economic Geologists*, v. 98, pages 1515-1533.

Richards, J.P. (2009): Postsubduction porphyry Cu-Au and epithermal Au deposits: Products of remelting of subduction-modified lithosphere; *Geology*, v. 37, pages 247-250.

Schiarizza, P., Bell, K., and Bayliss, S. (2009a): Geology and mineral occurrences of the Murphy Lake area, south-central British Columbia (93A/03); *in* Geological Fieldwork 2008, *BC Ministry of Energy, Mines and Petroleum Resources*, Paper 2009-1, pages 169-188.

Schiarizza, P., Bell, K., and Bayliss, S. (2009b): Geology of the Murphy Lake area, NTS 93A/03; *BC Ministry of Energy,*

Mines and Petroleum Resources, Open File 2009-03, 1:50 000 scale.

Selby, D. and Creaser, R.A. (2001): Re-Os geochronology and systematics in molybdenite from the Endako porphyry molybdenum deposit, British Columbia, Canada. ; *Economic Geology*, Volume 96, pages 197-204.

Schmitz, M. D., and Schoene, B., (2007): Derivation of isotope ratios, errors, and error correlations for U-Pb geochronology using ^{205}Pb-^{235}U-(^{233}U)-spiked isotope dilution thermal ionization mass spectrometric data; Geochem. Geophys. Geosyst., v.8, 20 pages.

Selby, D., and Creaser, R.A., (2004): Macroscale NTIMS and microscale LA-MC-ICP-MS Re-Os isotopic analysis of molybdenite: Testing spatial restrictions for reliable Re-Os age determinations, and implications for the decoupling of Re and Os within molybdenite; Geochimica et Cosmochimica Acta, 68, pages 3897-3908.

Selby, D., Creaser, R.A., Stein, H.J., Markey R.J., and Hannah, J.L., (2007): Assessment of the ^{187}Re decay constant by cross calibration of the ^{187}Re-^{187}Os molybdenite and U-Pb zircon chronometers; Geochimica *et* Cosmochimica Acta, 71, pages 1999-2013.

Shives, R.B.K., Charbonneau, B.W., and Ford, K.L. (1997): The detection of potassic alteration by gamma ray spectrometry - recognition of alteration related to mineralization; *in* "Geophysics and Geochemistry at the Millenium", Proceedings of the Fourth Decennial International Conference on Mineral Exploration (Exploration 97), 1100 pages, Toronto, Ontario, Canada, September 1997.

Sillitoe, R. H. (1972): Relation of metal provinces in western Americas to subduction of oceanic lithosphere; *Geological Society of America*, Bulletin, v. 83, pages 813–818.

Sillitoe, R. H. (2002): Some metallogenic features of gold and copper deposits related to alkaline rocks and consequences for exploration; *Mineraliun Deposita*, 37, pages 4-13.

Sillitoe, R.H. and Perrelló, J. (2005): Andean copper province: Tectonomagmatic settings, deposit types, metallogeny, exploration and discovery; *Economic Geology,* 100th Anniversary Volume, pages 845-890.

Soregaroli, A.E. (1968): preliminary report on geological studies at the Brenda Mine; unpublished report for Noranda Exploration Company, Limited.

Soregaroli, A.E. and Whitford, D.F., (1976): Brenda; Sutherland Brown, A., Editor, *in* Porphyry Deposits of the Canadian Cordillera, *Canadian Institute of Mining and Metallurgy*, Special Volume 15, pages 186-194.

Smoliar, M.I., Walker, R.J. and Morgan, J.W. (1996): Re-Os ages of Group IIA, IIIA, IVA, and IVB iron meteorites. *Science* 271, pages 1099-1102.

Stacey, J.S. and Kramer, J.D., (1975): Approximation of terrestrial lead isotope evolution by a two-stage model: Earth and Planetary Science Letters, v. 26, pages 207-221.

Stein, H.J., Markey, R.J., Morgan, J.W., Hannah, J.W., and Schersten, A. (2001): The remarkable Re-Os chronometer in molybdenite: how and why it works. Terra Nova, 13, pages 479-486.

Weeks, R.M., Bradburn, R.G., Flintoff, B.C., Harris, G.R., and Malcolm, G. (1995): The Brenda mine: The life of a low-cost porphyry copper-molybdenum producer (1970-1990), southern British Columbia, Schroeter, T., Editor, *in* Porphyry deposits of the Northwestern Cordillera of North America, *Canadian Institute of Mining and Metallurgy,* Special Volume 46, pages 192-200.

Wetherup, S. (2000): Diamond drilling report on the Woodjam Property; *BC Ministry of Energy, Mines and Petroleum Resources,* Assessment Report 26242, 40 pages.

Wheeler, J. O., and McFeely, P. (1991): Tectonic assemblage map of the Canadian Cordillera and adjacent parts of the United States of America, "A" series Map, *Geological Survey of Canada*, p. 1 sheet.

White, W.H., Harakal, J.E. and Carter, N.C. (1968): Potassium argon ages of some ore deposits in British Columbia; Canadian Institute of Mining and Metallurgy Bulletin, Volume 61, pages 1326–1334.

Woodsworth, G.J., Anderson, R.G. and Armstrong, R.L. (1991): Plutonic Regimes; Chapter 15, in Geology of the Cordilleran Orogen in Canada, Gabrielse, H. and Yorath, C.J., Editors, *Geological Association of Canada*, Geology of Canada, Volume 4, pages 491-531.

Southern Nicola Project: Geochemistry of Volcanic Rocks of the Nicola Group West of the Boundary Fault (Parts of NTS 092H/02, 07 and 10)

by N.W.D. Massey

KEYWORDS: Quesnellia, Nicola Group, volcanic geochemistry, calcalkaline, Western Belt

INTRODUCTION

The Southern Nicola Project area covers about 850 km^2 of southern British Columbia, south and west of the town of Princeton (Figure 1). The project area stretches from the Copper Mountain and Wolfe Creek area southwest to the boundary of Manning Park and northwest to the Tulameen River. Tectonically, the project area lies at the western edge of Quesnellia – just east of the bounding Pasayten fault, and includes the southernmost exposures of the Late Triassic Nicola Group. Mapping by Rice (1947), Preto (1972), Monger (1989) and Massey *et al.* (2010) has outlined the essential distribution of Late Triassic Nicola Group strata in the Princeton area (92HSE) and their relationships to younger intrusive and volcano-sedimentary sequences.

The bulk of Princeton Group volcanic and sedimentary units in the central part of the project area accumulated within a half-graben bounded on its eastern side by the Boundary fault (Figure 1). This subvertical, east-side down fault was first identified by Preto (1972), and confirmed by Read (1987), to the north. Present mapping continues the trace of the fault to the south where it curves into the valley of Placer Creek. Although active during the Eocene, the Boundary fault is part of a larger system, mapped mainly to the north, suspected by Preto (1979) to have been established early in the geological history of the region, controlling facies distributions and pluton emplacement within the Nicola Arc.

The Nicola Group in southern British Columbia has been subdivided into a western calcalkaline belt and central and eastern alkaline (shoshonitic) belts (Preto, 1979; Mortimer, 1987) Within the project area, rocks of the Nicola Group east of the Boundary fault display an alkalic affinity and have been assigned to the "Eastern Belt" (Preto, 1979). They host the important porphyry and skarn deposits of the Copper Mountain area (Preto, 1972).

This publication is also available, free of charge, as colour digital files in Adobe Acrobat® PDF format from the BC Ministry of Forests, Mines and Lands website at http://www.empr.gov.bc.ca/Mining/Geoscience/PublicationsCatalogue/Fieldwork.

However, prior to the present study, the designation of Nicola Group rocks west of the Boundary fault was uncertain. Mortimer (1987) suggested they may belong to the calcalkaline "Western Belt", though no geochemical data were presented from the area, while Monger (1989) referred to them as "undifferentiated". The "Central Belt" terminates north of Princeton (Preto, 1979) and does not extend into the project area.

This paper focuses on the results of geochemical analyses of samples of Nicola Group volcanic and volcaniclastic rocks collected in 2008 and 2009. These results confirm correlation of the Nicola Group rocks west of the Boundary fault with the "Western Belt" as suggested by Mortimer (1989).

GEOLOGY OF THE NICOLA GROUP WEST OF THE BOUNDARY FAULT

Rocks of the Nicola Group southwest of Princeton are divided into two informal lithologic units, a clastic sedimentary unit and a volcanic unit. These are lithologically similar to units to the east, but differ in details of the stratigraphic succession (Preto, 1972; Massey *et al.*, 2009; Massey and Oliver, 2010).

Clastic Sedimentary Unit

The clastic sedimentary unit is dominated by black argillite interbedded with grey to green-grey siltstone and sandstone and polymictic conglomerate. Finer grained beds are massive to laminated and may have a limy or siliceous matrix. Coarser beds can be massive, graded or laminated. Beds vary from millimetres to several centimetres thick. Layers of matrix supported, polymictic granule to pebble conglomerate are intercalated with the finer sedimentary rocks. The clasts are dominantly clastic sedimentary, but locally include limestone and volcanic material. The sedimentary rocks in the northwest corner of the map area are strongly metamorphosed in the aureole of the Eagle Plutonic Complex to produce a sequence of quartz ±feldspar-rich schists with variable proportions of biotite, actinolite, garnet, muscovite and magnetite. Chlorite and epidote may occur as secondary alteration minerals. Calcareous beds are recrystallized to buff weathering, medium to coarse grained white marble. The marbles are usually massive, but can display a weak foliation delineated by quartz, chlorite or minor calcsilicate minerals.

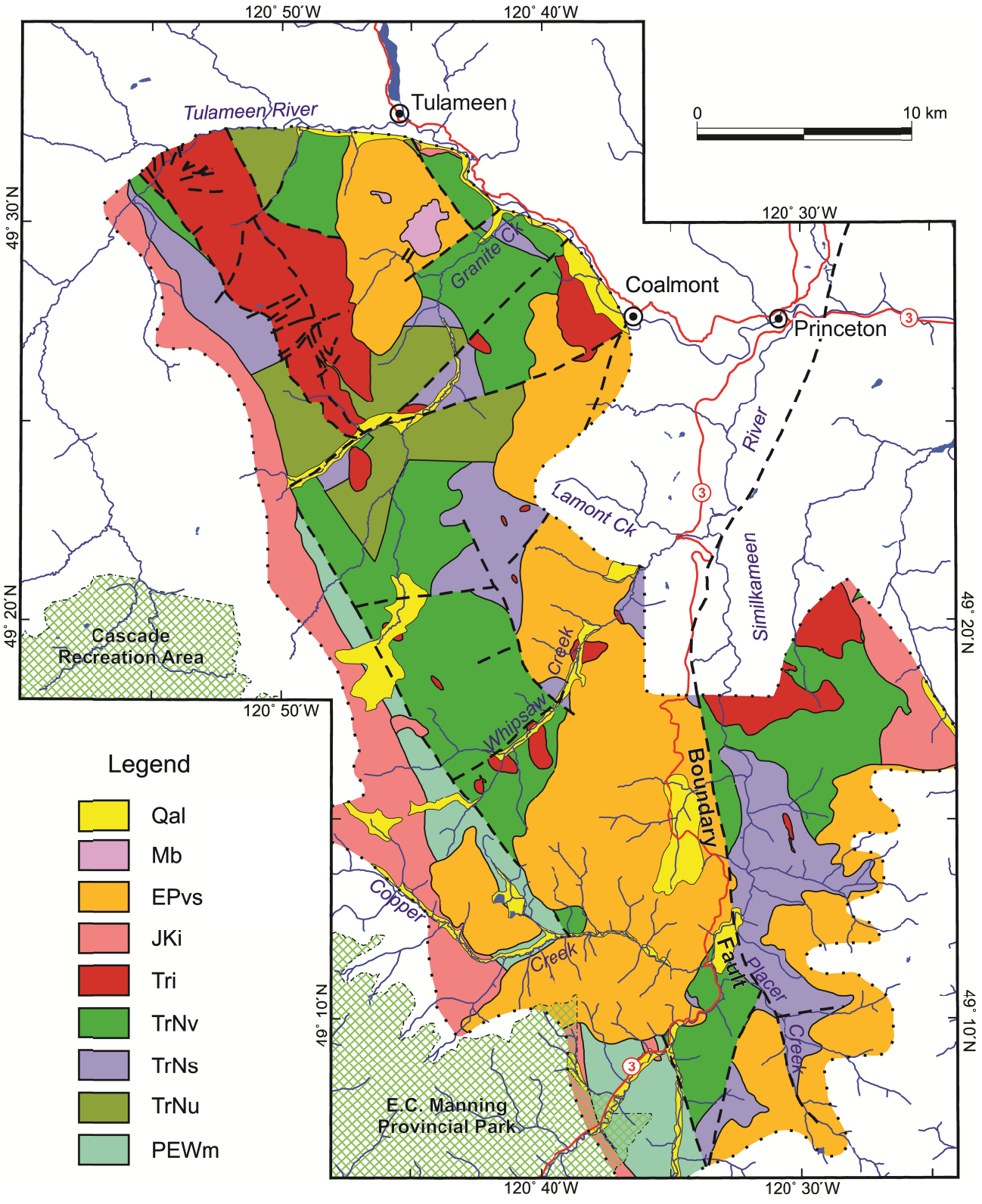

Figure 1. Simplified geology of the Southern Nicola Project area. Geology after Massey *et al.* (2010); extension of the Boundary fault outside the map area from Preto (1972) and Read (1987). Qal: Quaternary alluvium; Mb: Miocene basalt (?Chilcotin Group); EPvs: Eocene Princeton Group volcanic and sedimentary rocks; JKi Jurassic and Cretaceous felsic intrusions (including EP: the Eagle pluton , VC: Verde Creek pluton, and W: Whipsaw stock); Tri: Late Triassic ultramafite to diorite and syenite (including Tu: the Tulameen Complex, CM: Copper Mountain stock, V: Voigt stock, and R: Rice stock); TrNv: Nicola Group volcanic rocks; TrNs: Nicola Group sedimentary rocks, minor feldspathic volcaniclastic rocks; TrNu: undivided Nicola Group; PEWm: Permian Eastgate-Whipsaw metamorphic belt.

In the Lamont Main area, clastic sedimentary rocks are intercalated with feldspathic tuff, tuff breccia, tuffaceous sandstone, pebbly sandstone and fine grained cherty siltstone. Pyroxene is rare to absent in these beds. The clastic sediment and feldspathic volcaniclastic unit passes westwards, and probably upwards, into typical Nicola pyroxene-feldspar tuffs, lapilli tuffs and breccias of the volcanic unit.

Volcanic Unit

The volcanic unit includes interbedded pyroxene-feldspar tuffs, lapilli tuffs, breccias, agglomerates and tuffaceous sedimentary. They are light grey in colour, weathering to green-grey with orange stained fracture surfaces. Lithic clasts vary from angular to subrounded and are typically 3-5 cm across, ranging up to 20-25 cm in breccias and agglomerates. They are dominantly pyroxene feldspar porphyritic basalts and basaltic andesites, showing a wide variation in proportions and sizes of phenocrysts. Fragments of aphyric basalt are also present. The clasts are usually matrix supported. The matrix is medium to coarse sand sized, containing feldspar and pyroxene crystals as well as small lithic clasts. Epidote, chlorite and calcite occur as alteration minerals in clasts and matrix, and also in veins. Quartz veins are also common.

A sequence of massive feldspar phyric basalt flows occurs in the area southeast of the Granite Creek campsite. These are massive, fine grained, medium grey to green in colour. Feldspar phenocrysts are lath shaped, 1 to 3 millimetres in size and comprise 5 to 10% of the rock. One flow also contained subhedral pyroxene phenocrysts, 2 to 3 millimetres in size, with distinct blue-green feldspars in a bluish grey groundmass. Epidote and chlorite alteration is common, both in the matrix and in veins.

The volcanic rocks become progressively schistose from east to west. The tuffs and lapilli tuffs look massive in outcrop but display a weak foliation on broken surfaces. This foliation becomes progressively more penetrative to the west. Finer grained tuffs produce bluish green-grey chlorite schists. Relict pyroxenes are chloritized and vary from euhedral shapes to smeared blebs along the schistosity. Clasts in lapilli tuffs and breccias are undeformed to slightly flattened. Chloritic rims may develop around the clasts with feathering of their terminations along the foliation. Actinolite and biotite are developed in metavolcanic rocks in the aureole of the Eagle Plutonic Complex.

GEOCHEMISTRY OF THE VOLCANIC ROCKS

Thirty eight samples from the Nicola Group were analyzed for whole rock major, minor and trace elements. These are predominantly volcaniclastic rocks and some massive flows of the volcanic unit, but include three samples of volcaniclastic rocks interbedded with the clastic sediments. Results are summarized in Table 1. Samples range in composition from basalt to andesite (Figures 2 and 3). They show some mobility of alkalis but generally all preserve a subalkalic, medium-K calcalkaline character (Figures 2-5). They compare closely with the type 2 calcalkaline lavas of Mortimer (1987), which he collected from the Nicola Group in the "Western Belt" in the Merritt area and to the west of the Guichon batholith. They differ significantly from the shoshonitic type 1 lavas that are characteristic of the "Central" and "Eastern" belts (Mortimer, 1987; Preto, 1979).

Extended trace element spidergrams show typical calcalkaline patterns with the negative Nb-Ta anomaly characteristic of volcanic arcs (Figure 6). Minor and trace element petrotectonic discrimination diagrams are primarily designed for use with aphyric basaltic flows rather than porphyritic or volcaniclastic rocks. However, these plots support the formation of the Nicola Group volcanic rocks in an arc environment, though not all diagrams successfully discriminate them as calcalkaline (Figures 7-10). A few massive flows have higher P_2O_5 (>0.4 %), Zr (150 – 200 ppm) and Ti/V ratios (10 – 50), that compare with Mortimer's type 3 lavas. These latter are intermediate between arc and intra-plate character and occur in all three belts.

REGIONAL CORRELATIONS

The lithogeochemical data presented here support the correlation of Nicola Group volcanic rocks in the project area, west of the Boundary fault, with the "Western Belt" to the north, as originally proposed by Mortimer (1987). However, dacitic to rhyolitic rocks which are fairly common in the "Western Belt" to the north, are apparently absent within the project area. No paleontological or geochronological data are available on these rocks within the project area. Scattered fossil ages to the north are mainly late Carnian to early Norian (Monger and McMillan, 1989; Preto, 1979) and felsic volcanic rocks in the Merritt area yield late Triassic (Carnian) ages of 224.6 ±0.9 Ma and 224.5 ±0.3 Ma (Diakow and Barrios, 2009).

Correlation with the "Western Belt" may have implications for mineralization in the project area. Felsic volcanic rocks in the "Western Belt" are potential hosts to volcanic-hosted massive sulphide deposits. However, felsic volcanic rocks have not yet been identified in the project area.

Conversely, alkalic porphyry-copper deposits, like that at Copper Mountain, are hosted within, and probably consanguineous with, the shoshonitic "Eastern Belt" of the Nicola Group. Such mineralization is less likely to occur within the calcalkaline Western Belt. However, there are no geochemical or geochronological data from the diorite-pyroxenite stocks and minor intrusions of the project area, *e.g.* the Rice stock, which may test this.

Table 1. Whole rock chemical analyses for Nicola Group volcanic rocks. Major elements and Rb, Sr, Ba, Y, Zr, Nb, V, Ni, Cr determined by XRF (majors on fused disc, traces on pressed powder pellet) by Teck (Global Discovery) Labs. REEs, Th, Ta, Hf determined by peroxide fusion-ICPMS by Memorial University of Newfoundland. Dashes indicate element determinations below detection limit; blank values indicate element not analyzed. Map unit is as on Massey *et al.* (2010).

Sample	09SOL02-04	09SOL02-05-02	08NMA35-10	08NMA21-03	09NMA14-13	09NMA14-14	09NMA14-03	09NMA14-04	09NMA18-10
Lithology	px relics in act-qz-fsp-bio-chl-epid schist	px-phyric chl-act-bio-musc schist	fsp tuffs massive, some small lapilli	px-fsp porphyry, massive	fsp basalt, strong epidote alteration	blue-green fsp-px basalt, massive	massive vesicuar basalt	fsp basalt	massive aphyric basalt, sparse vesicles
Map Unit	TrNs	TrNs	TrNsv	TrNv	TrNvm	TrNvm	TrNv	TrNv	TrNv
SiO_2	49.61	49.21	57.17	46.68	48.41	47.28	45.49	54.47	54.20
TiO_2	0.79	0.62	0.64	0.65	1.72	1.13	1.11	1.34	1.34
Al_2O_3	17.38	13.37	17.44	14.60	15.56	17.99	16.24	16.31	14.34
Fe_2O_3t	10.03	10.23	7.39	10.10	11.99	9.73	9.74	7.14	10.86
MnO	0.17	0.17	0.14	0.15	0.17	0.17	0.16	0.11	0.15
MgO	5.43	10.73	3.25	8.77	4.50	4.91	9.80	3.25	3.53
CaO	9.83	11.38	5.94	13.00	7.41	10.13	8.25	5.74	6.00
Na_2O	4.18	1.90	3.56	1.46	4.37	3.07	1.52	4.47	3.68
K_2O	0.79	0.82	0.79	0.46	1.16	1.78	2.66	1.89	2.77
P_2O_5	0.15	0.11	0.23	0.13	0.47	0.30	0.58	0.38	0.51
BaO	0.02	0.02	0.03	0.01	0.03	0.03	0.08	0.04	0.07
LOI	1.30	1.40	2.66	3.92	3.70	3.20	4.40	3.20	2.00
Total	99.68	99.95	99.24	99.93	99.51	99.77	99.96	98.30	99.41
Ba	175	243	293	109	345	346	791	368	674
Rb	21	17	13	14	25	32	54	38	58
Sr	287	417	155	397	688	330	348	585	460
Y	16	16	27	18	24	23	26	26	42
Nb	-3	-3	16	7	4	4	9	8	5
Zr	34	30	104	52	69	116	166	192	180
V	279	251	133	257	236	287	144	320	255
Ni	43	129	-3	122	31	12	16	-3	34
Co			18	52					
Cr			18	351					
La			20.703			13.153	34.449		
Ce			34.497			28.624	70.060		
Pr			4.236			3.888	8.607		
Nd			16.432			17.235	34.722		
Sm			3.421			4.369	6.939		
Eu			1.245			1.243	2.043		
Gd			3.455			4.524	5.908		
Tb			0.579			0.709	0.847		
Dy			3.485			4.473	4.649		
Ho			0.731			0.883	0.806		
Er			1.993			2.415	2.116		
Tm			0.315			0.354	0.296		
Yb			2.359			1.975	1.739		
Lu			0.338			0.275	0.245		
Hf			2.446			1.714	3.505		
Ta			0.238			0.329	0.502		
Th			5.218			1.834	6.746		
Latitude (N)	49.493688	49.497555	49.391573	49.155825	49.493416	49.497105	49.491525	49.491832	49.443818
Longitude(W)	120.905837	120.906923	120.710806	120.586382	120.668382	120.668910	120.694723	120.693914	120.682400
Zone	10	10	10	10	10	10	10	10	10
Northing	5484447	5484874	5473506	5447582	5484922	5485331	5484653	5484689	5479377
Easting	651648	651557	666115	675980	668842	668791	666941	666999	667997

Table 1. (continued)

09NMA10-05	09NMA13-10	08NMA26-01-02	08SOL25-04	08SOL25-05	08NMA31-02-01	08NMA31-02-02	08JVI29-03	08JVI29-04	08JVI29-14
vesicular basalt	px-fsp basalt	green-grey tuffaceous sandstone, silt	px meta lapilli tuff,	px meta tuff,	px-fsp tuff, lap tuff; w eak foliation	px-fsp lap tuff; moderate foliation	massive tuffaceous sandstone and px crystal tuff	tuffaceous sandstone	tuffaceous sandstone
TrNv	TrNv	TrNv	TrNv	TrNv	TrNv	TrNv	TrNv	TrNv	TrNv
48.295	47.92	46.41	50.37	49.54	47.92	50.34	51.55	48.73	48.96
0.81	0.97	0.79	0.69	0.67	0.65	0.65	0.80	0.84	0.78
17.085	18.79	15.22	14.28	12.94	14.78	15.20	16.46	18.04	15.80
10.96	10.08	10.52	9.54	9.70	9.85	9.28	8.38	9.32	9.96
0.15	0.16	0.14	0.12	0.14	0.13	0.09	0.12	0.14	0.16
6.22	4.72	14.29	9.42	13.48	11.17	9.07	6.65	6.83	8.07
8.795	10.25	3.50	9.29	5.26	7.24	8.86	11.51	9.54	9.96
3.81	1.76	3.26	1.55	2.56	2.29	1.48	1.17	1.91	2.65
0.065	1.82	0.41	1.06	1.38	1.59	0.98	0.61	0.95	0.78
0.15	0.28	0.07	0.28	0.19	0.26	0.15	0.29	0.37	0.23
0.01	0.02	0.01	0.06	0.03	0.06	0.03	0.02	0.04	0.01
3.4	3.20	5.00	2.90	3.80	3.80	3.67	2.26	2.91	2.56
99.735	100.00	99.66	99.60	99.68	99.74	99.81	99.82	99.62	99.92
71.5	244	130	588	337	600	351	165	416	129
9	36	9	25	18	33	25	13	26	17
253	640	90	443	103	332	505	294	380	343
11	18	13	17	13	22	16	24	24	24
-3	6	-3	-3	-3	8	5	10	11	5
33.5	59	62	77	52	87	60	144	123	70
292.5	208	270	224	233	270	249	238	306	255
24	32	136	156	189	186	115	75	43	96
					47		32	30	46
					436		177	98	259
3.083					25.783		39.949	34.495	8.822
7.871					51.091		80.436	72.890	19.641
1.295					6.348		9.750	9.114	2.719
6.614					25.324		38.717	38.133	12.443
2.075					4.771		6.897	6.926	3.285
0.777					1.447		1.866	2.016	1.071
2.475					3.831		4.963	5.826	3.656
0.443					0.540		0.612	0.768	0.552
2.736					2.954		3.336	4.142	3.445
0.567					0.524		0.620	0.822	0.670
1.686					1.494		1.795	2.250	1.937
0.266					0.203		0.254	0.312	0.269
1.496					1.420		1.708	2.096	1.952
0.203					0.238		0.242	0.335	0.286
0.899					1.818		3.409	2.979	1.623
0.073					0.082		0.116	0.136	0.038
0.475					4.310		8.277	5.835	1.436
49.522734	49.473473	49.296624	49.279527	49.296584	49.323464	49.324289	49.365568	49.364846	49.381870
120.810926	120.687642	120.657719	120.678707	120.658002	120.692235	120.691125	120.748600	120.732478	120.746621
10	10	10	10	10	10	10	10	10	10
5487871	5482662	5463070	5461122	5463065	5465976	5466070	5470533	5470488	5472350
658426	667516	670295	668827	670274	667694	667772	663458	664631	663548

Table 1. (continued)

09NMA10-01	09NMA13-13	08NMA31-08	08NMA28-13-01	08NMA28-13-02	08NMA28-14	08NMA29-04	08NMA29-11	08NMA34-09	08SOL25-01
fsp-px lithic tuff	px-fsp crystal lapilli tuff	medium-coarse grained, px-fsp tuff	fsp-phyric chloritic meta-tuff	fine grained chloritic meta-tuff	px-fsp chlorite schist	px-phyric, chlorite schist	px-fsp chlorite schist	px chlorite schist	px-fsp phyric meta-tuff
TrNv	TrNv	TrNv'	TrNv'	TrNv'	TrNv'	TrNv'	TrNv'	TrNv'	TrNv'
46.81	42.45	46.14	48.95	50.63	46.58	47.29	47.65	44.17	48.01
1.26	0.81	0.77	0.85	0.98	0.69	0.66	0.63	0.66	0.57
16.96	16.62	16.57	20.23	18.33	14.67	15.35	14.51	15.99	11.71
10.32	10.31	9.50	10.25	8.93	9.18	8.71	8.78	9.59	9.87
0.14	0.15	0.13	0.15	0.18	0.14	0.14	0.09	0.13	0.16
3.13	7.76	8.86	3.94	2.98	9.64	10.14	6.84	9.37	12.87
8.56	11.01	8.70	8.40	9.51	10.75	8.94	7.79	8.18	11.81
4.90	2.40	2.79	3.04	3.00	2.26	2.53	3.20	1.54	1.17
1.04	1.46	0.92	0.65	0.91	0.68	1.01	0.51	0.71	0.69
0.40	0.13	0.33	0.10	0.12	0.17	0.19	0.18	0.18	0.12
0.03	0.03	0.03	0.02	0.02	0.02	0.05	0.02	0.03	0.02
6.00	6.80	4.78	3.30	4.00	4.90	4.80	9.70	9.10	2.80
99.53	99.94	99.52	99.91	99.62	100	99.79	99.93	99.59	99.79
308	302	336	168	161	157	472	230	289	197
27	19	21	18	19	17	25	16	22	16
458	350	601	173	175	387	473	426	636	369
27	15	20	16	23	17	15	17	18	18
9	-3	6	-3	-3	-3	-3	-3	-3	-3
138	36	106	36	49	32	46	61	55	25
284	222	285	250	200	235	213	242	248	206
16	111	72	6	6	147	181	90	111	199
		39							
		161							
34.821	8.043	28.230							
74.539	17.356	56.949							
9.386	2.411	7.033							
36.888	10.791	29.179							
7.045	2.752	5.524							
2.094	0.921	1.746							
6.383	3.060	4.540							
0.843	0.465	0.650							
4.959	2.929	3.835							
0.935	0.583	0.721							
2.528	1.700	1.954							
0.346	0.229	0.293							
2.063	1.420	1.937							
0.290	0.209	0.298							
2.430	0.886	2.376							
0.465	0.150	0.088							
3.862	1.461	4.535							
49.523798	49.481554	49.319200	49.280177	49.280177	49.288021	49.303283	49.301167	49.339825	49.296099
120.799553	120.704556	120.693300	120.736689	120.736689	120.736050	120.690157	120.683841	120.722864	120.739422
10	10	10	10	10	10	10	10	10	10
5488013	5483523	5465500	5461067	5461067	5461940	5463737	5463516	5467727	5462830
659246	666263	667631	664609	664609	664629	667914	668380	665414	664357

Table 1. (continued)

08SOL25-03	09NMA08-13	09NMA02-03	09NMA02-04	09NMA03-03-01	09SOL01-12	09SOL02-07	09NMA01-09-03	09NMA07-01
px meta-tuff	feldspathic tuffs with minor px	px-act schist; minor calcite	schistose px-phyric lapilli tuffs (act-chlor)	px-act-chlor schist	fsp-chlor schist, epidote	px-phyric chl-bio-act schist	chlor-bio-act schist (relict px)	chlor mafic meta-tuffs, fsp xst tuff
TrNv'	TrNv'	TrNv'	TrNv'	TrNv'	TrNv'	TrNv'	TrNv'	TrNv'
49.25	47.66	47.30	48.33	48.29	47.98	47.64	49.38	48.14
0.67	0.92	0.65	0.60	0.69	0.63	0.58	0.58	0.77
14.42	18.55	13.78	12.16	14.89	19.80	11.65	12.54	16.32
9.51	8.63	9.90	9.68	9.74	9.96	10.07	9.58	9.27
0.15	0.16	0.17	0.17	0.14	0.16	0.16	0.16	0.15
8.77	5.59	11.41	12.53	10.52	5.68	12.94	11.69	9.03
10.89	9.72	11.00	13.25	10.37	9.69	11.38	11.75	7.63
2.69	3.61	2.51	1.49	1.97	2.62	1.81	1.78	3.61
0.42	0.96	0.44	0.23	1.18	0.49	0.47	0.73	0.97
0.13	0.21	0.15	0.13	0.17	0.07	0.11	0.12	0.20
0.01	0.02	-0.01	-0.01	0.02	0.02	0.01	0.02	0.02
2.60	3.80	2.60	1.30	1.90	2.80	3.00	1.50	3.90
99.48	99.81	99.94	99.85	99.86	99.88	99.84	99.81	99.96
117	164	37	12	216	164	110	167	158
13	22	14	10	27	15	15	15	22
499	379	273	335	433	359	210	283	354
20	15	14	16	12	9	10	17	14
-3	-3	-3	-3	-3	-3	4	-3	-3
28	33	48	41	39	33	38	44	60
218	245	233	230	265	217	223	225	233
88	27	176	182	145	16	203	153	66
49.245159	49.474289	49.370972	49.372289	49.380612	49.494517	49.505620	49.512924	49.410049
120.695089	120.740078	120.806183	120.808296	120.815929	120.898125	120.910815	120.922770	120.780393
10	10	10	10	10	10	10	10	10
5457265	5482637	5471011	5471153	5472062	5484554	5485763	5486551	5475409
667752	663715	659260	659103	658522	652203	651250	650362	661005

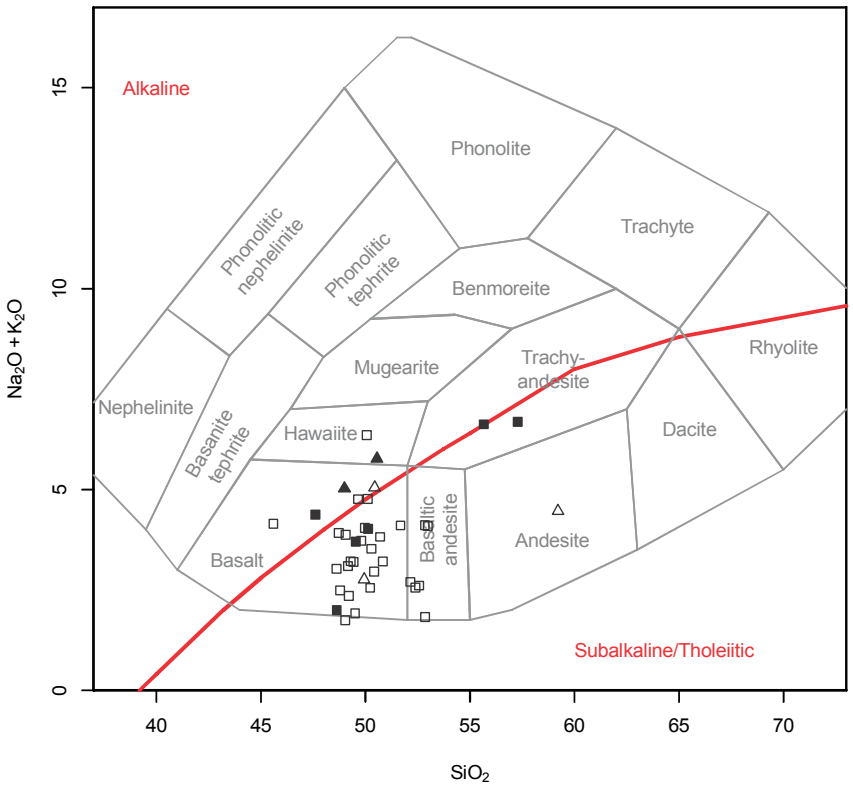

Figure 2. Total alkali vs SiO_2 (anhydrous weight %) plot for Nicola Group volcanic rocks. Classification fields and nomenclature after Cox *et al.* (1979). The alkaline-subalkaline dividing line after Irvine and Baragar (1971). Massive flows: closed symbols (squares: interbedded with volcaniclastic rocks; triangles: from massive subunit SE of Granite Creek); volcaniclastic rocks: open symbols (squares: from volcanic unit; triangles from sedimentary unit).

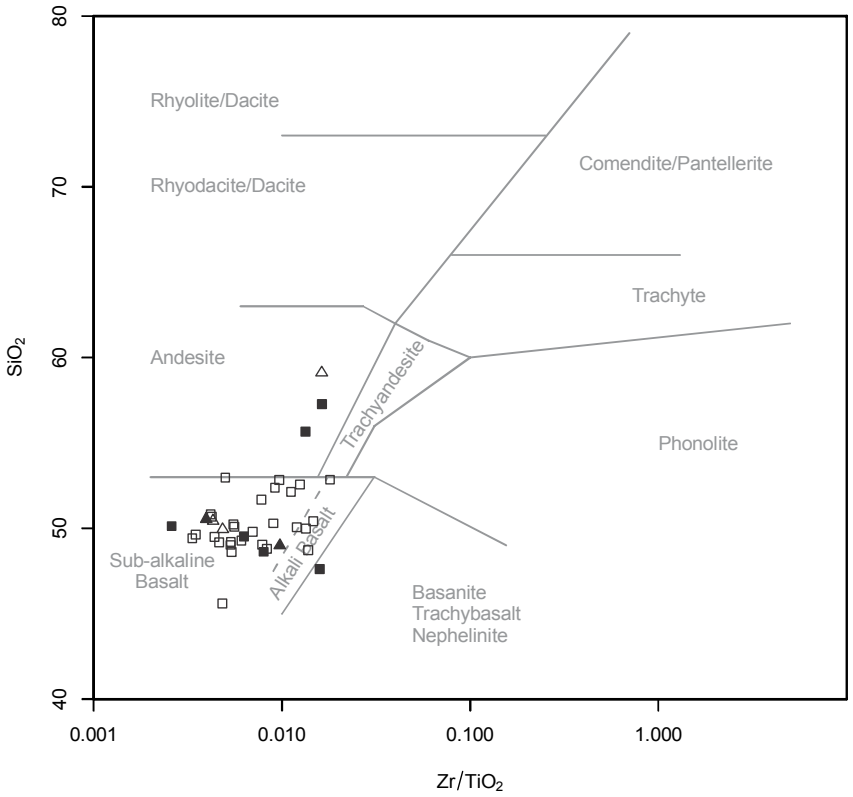

Figure 3. Zr/TiO_2 vs SiO_2 (anhydrous weight %) plot for Nicola Group volcanic rocks. Classification fields and nomenclature after Winchester and Floyd (1977). Symbols as in Figure 2.

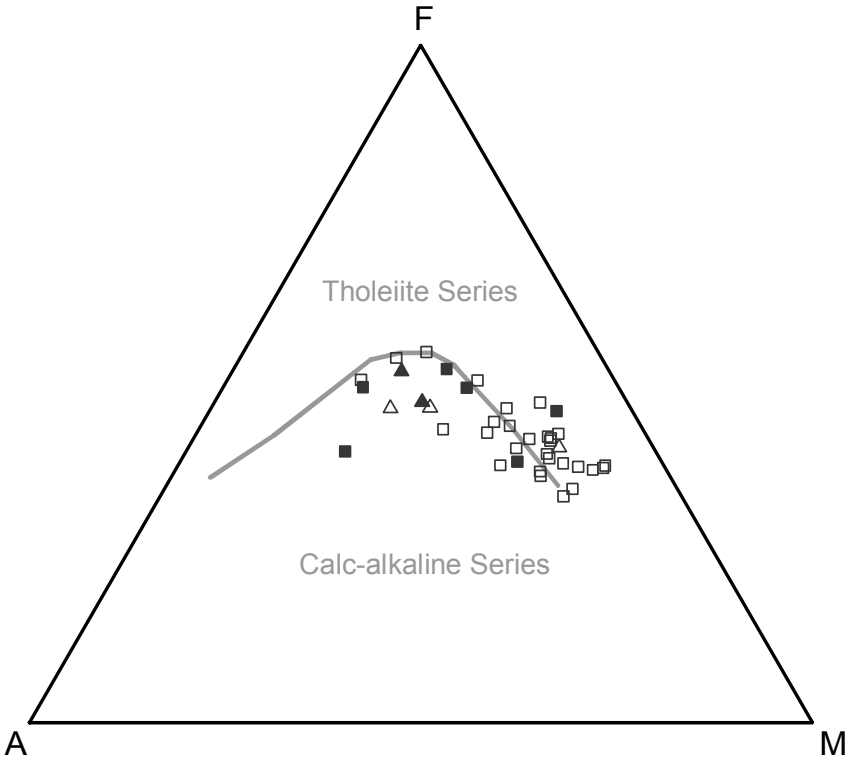

Figure 4. AFM diagram for Nicola Group volcanic rocks after Irvine and Baragar (1971). A = $Na_2O + K_2O$; F = FeO_{total}; M = MgO, all as anhydrous weight percents. Symbols are as in Figure 2.

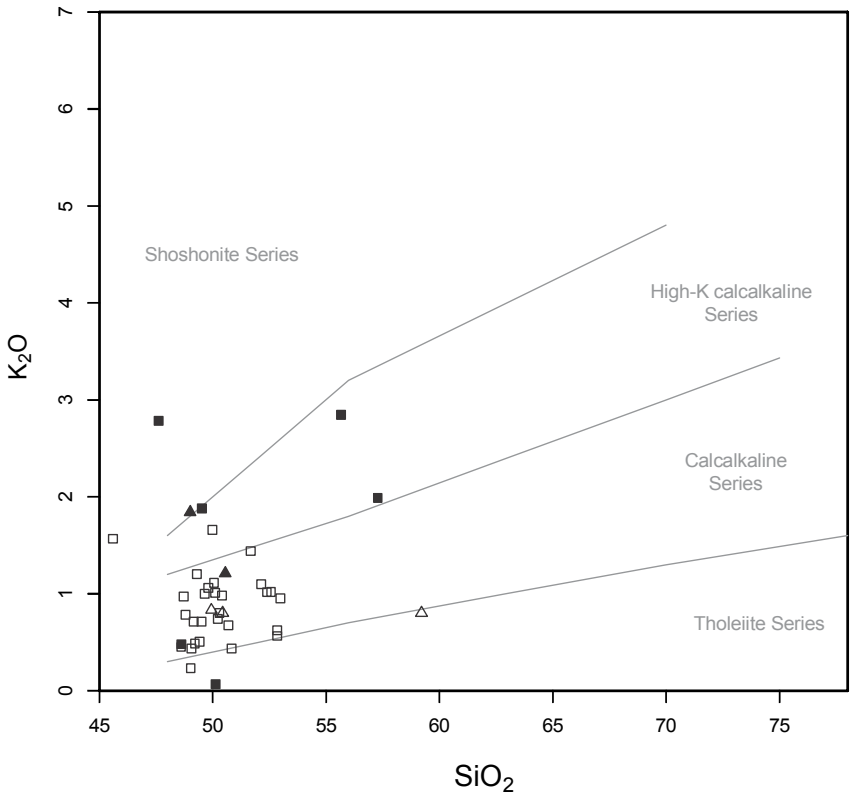

Figure 5. K_2O vs SiO_2 (anhydrous weight %) plot for Nicola Group volcanic rocks. Classification fields and nomenclature after Peccerillo and Taylor (1976). Symbols as in Figure 2.

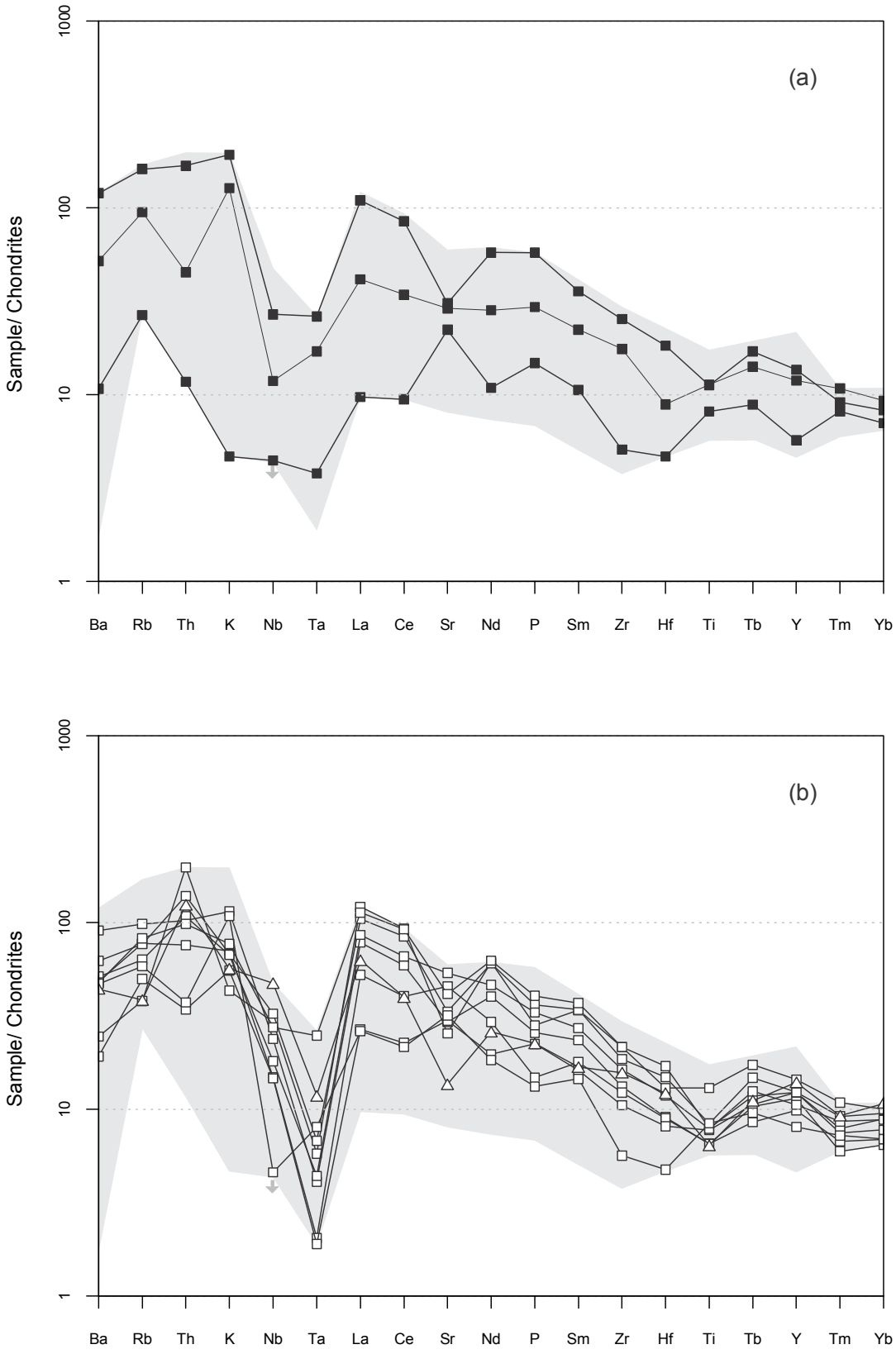

Figure 6. Trace element concentrations normalized to chondrite, after Thompson (1982). a) massive flows; b) volcaniclastic rocks. Symbols as in Figure 2. Only samples with the complete range of determined elements are plotted. The shaded field shows the range for all samples; arrow indicates that many samples have Nb values below the detection limit (3 ppm).

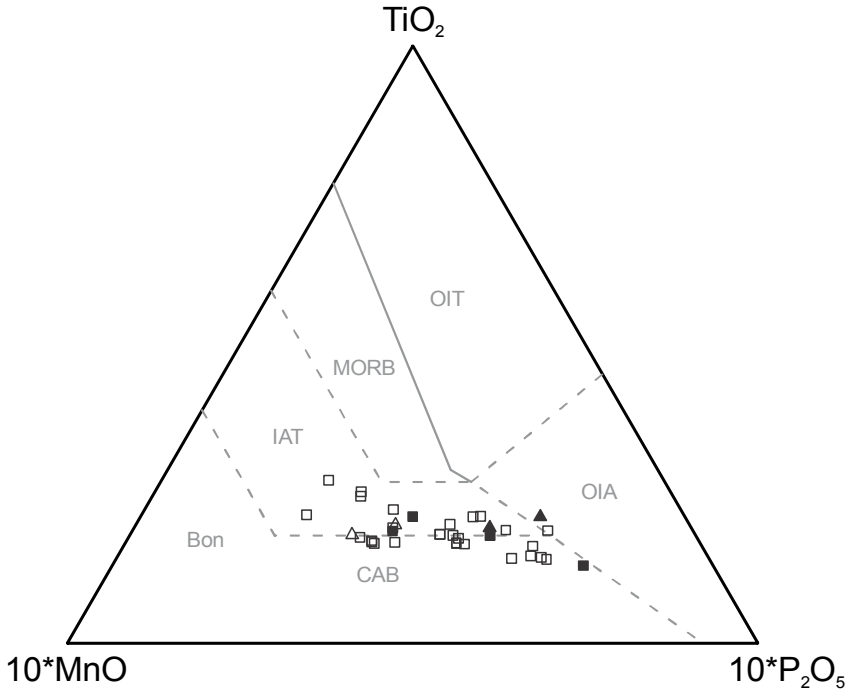

Figure 7. MnO-TiO_2-P_2O_5 (anhydrous weight %) discrimination diagram for Nicola Group volcanic rocks after Mullen (1983). OIT: ocean-island tholeiite; OIA: ocean-island alkali basalt; MORB: mid-ocean ridge basalt; IAT: island-arc tholeiite; CAB: calcalkaline basalt; Bon: boninite. Symbols are as in Figure 2. Only samples with 45<SiO_2<54 are shown.

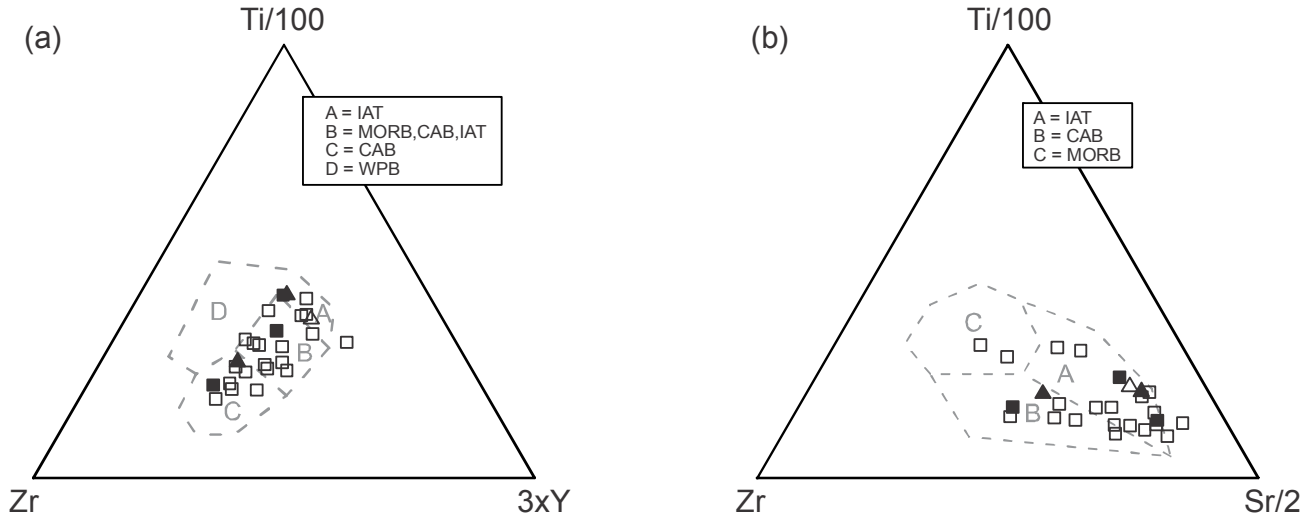

Figure 8. Trace element discrimination diagrams for Nicola Group volcanic rocks after Pearce and Cann (1973). a) Ti-Zr-Y diagram, A: island-arc tholeiites; B: mid-ocean ridge basalts, island-arc tholeiites and calcalkaline basalts; C: calcalkaline basalts; D within-plate basalts. b) Ti-Zr-Sr diagram, A: island-arc tholeiites; B: calcalkaline basalts; C: mid-ocean ridge basalts. Symbols are as in Figure 2. Only basaltic samples with 12<CaO + MgO<20 are shown.

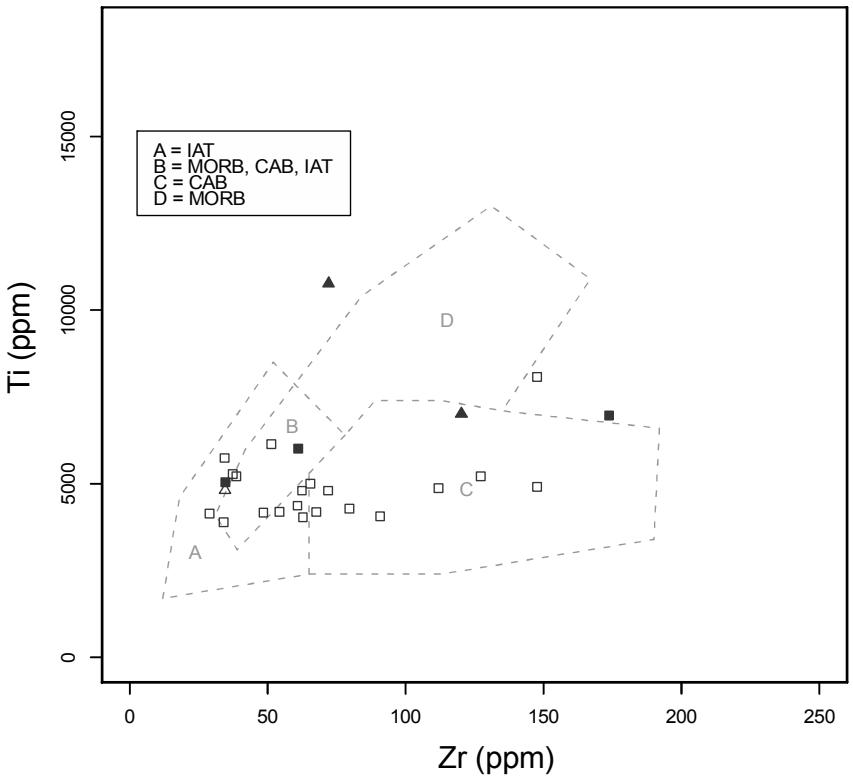

Figure 9. Ti-Zr (anhydrous parts per million) discrimination diagram for Nicola Group volcanic rocks after Pearce and Cann (1973). A: island-arc tholeiites; B: mid-ocean ridge basalts, island-arc tholeiites, calcalkaline basalts; C: calcalkaline basalts; D: within-plate basalts. Symbols are as in Figure 2. Only basaltic samples with 12<CaO + MgO<20 are shown.

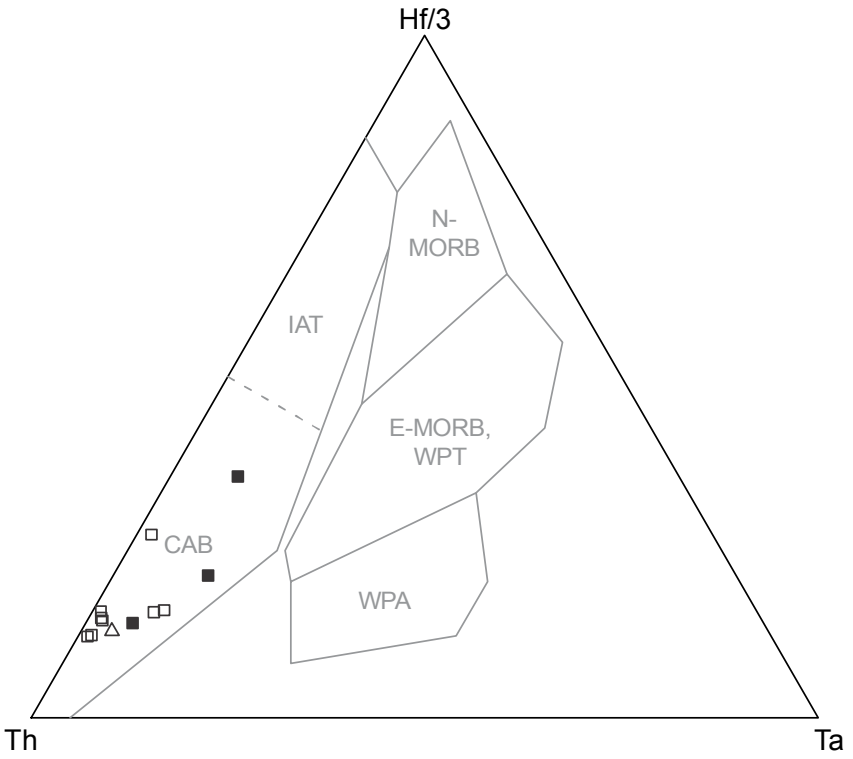

Figure 10. Th-Hf-Ta discrimination diagram for Nicola Group volcanic rocks after Wood (1980). IAT: island-arc tholeiite; CAB: calcalkaline basalt; N-MORB: normal-type mid-ocean ridge basalts; E-MORB: enriched-type mid-ocean ridge basalts; WPT: within-plate tholeiite; WPA: within-plate alkali basalt. Symbols are as in Figure 2.

ACKNOWLEDGMENTS

The author is much indebted to Rob Marshall, Weyerhaeuser Co. Ltd. (Princeton); Todd Chamberlain, Stuwix Resources (Merritt); and Dean Jaeger, Tolko Industries Ltd. (Merritt), for all their invaluable help and advice during the planning stages of this project. The incomparable assistance of Julie Vineham, Shelley Oliver and Scott Jaschenko during the field seasons of 2008 and 2009 made the whole project possible. Paul Schiarizza offered valuable comments on an earlier of draft of this manuscript.

REFERENCES

Cox, K.G., Bell, J.D. and Pankhurst, R.J. (1979): The interpretation of igneous rocks; George, Allen and Unwin, London.

Diakow, L.J. and Barrios, A. (2009): Geology and mineral occurrences of the mid-Cretaceous Spences Bridge Group near Merritt, southern British Columbia (parts of NTS 092H/14, 15; 092I/02, 03); *in* Geological Fieldwork 2008, *B.C. Ministry of Energy, Mines and Petroleum Resources*, Paper 2009-1, pages 63-80.

Irvine, T.N. (1974): Petrology of the Duke Island Ultramafic Complex, southeastern Alaska; *Geological Society of America*, Memoir 138, 240 pages.

Irvine, T.N. and Baragar, W.R.A. (1971): A guide to the chemical classification of the common volcanic rocks; *Canadian Journal of Earth Sciences*, volume 8, pages 523-548.

Massey, N.W.D. and Oliver, S.L. (2010): Southern Nicola Project: Granite Creek area (parts of 92H/07 and 92H/10); *in* Geological Fieldwork 2009, *B.C. Ministry of Energy, Mines and Petroleum Resources*, Paper 2010-1, pages 113-126.

Massey, N.W.D., Vineham, J.M.S. and Oliver, S.L. (2009): Southern Nicola Project: Whipsaw Creek-Eastgate-Wolfe Creek area (92H/01W, 92H/02E, 92H/07E and 92H/08W); *in* Geological Fieldwork 2008, *B.C. Ministry of Energy, Mines and Petroleum Resources*, Paper 2009-1, pages 189-204.

Massey, N.W.D., Vineham, J.M.S. and Oliver, S.L. (2010): Geology of the area south and west of Princeton, British Columbia, (parts of NTS 92H/01; 02; 07; 08 and 10); *B.C. Ministry of Energy, Mines and Petroleum Resources*, Geoscience Map 2010-4, scale 1:50 000.

Monger, J.W.H. (1989): Geology, Hope, British Columbia; *Geological Survey of Canada*, Map 41-1989, scale 1:250 000.

Monger, J.W.H. and McMillan, W.J. (1989): Geology, Ashcroft, British Columbia; *Geological Survey of Canada*, Map 42-1989, scale 1:250 000.

Mortimer, N. (1987): The Nicola Group: Late Triassic and Early Jurassic subduction-related volcanism in British Columbia; *Canadian Journal of Earth Sciences*, volume 24, pages 2521-2536.

Mullen, E.D. (1983): $MnO/TiO_2/P_2O_5$: a minor element discriminant for basaltic rocks of oceanic environments and its implication for petrogenesis; *Earth and Planetary Science Letters*, volume 62, pages 53-62.

Nakamura, N. (1974): Determination of REE, Ba, Fe, Mg, Na and K in carbonaceous and ordinary chondrites; *Geochimica et Cosmochimica Acta*, volume 38, pages 757-775.

Nixon, G.T. (1988): Geology of the Tulameen Ultramafic Complex; *B.C. Ministry of Energy, Mines and Petroleum Resources*, Open File 1988-25, scale 1:25 000.

Nixon, G.T., Hammack, J.L., Ash, C.A., Cabri, L.J., Case, G., Connelly, J.N., Heaman, L.M., Laflamme, J.H.G., Nuttall, C.N., Paterson, W.P.E., and Wong, R.H. (1997): Geology and platinum-group-element mineralization of Alaskan-type ultramafic-mafic complexes in British Columbia; *B.C. Ministry of Energy, Mines and Petroleum Resources*, Bulletin 93, 142 pages.

Pearce, J.A. and Cann, J.R. (1973): Tectonic setting of basic volcanic rocks determined using trace element analyses; *Earth and Planetary Science Letters*, volume 19, pages 290-300.

Peccerillo, A. & Taylor, S. R. (1976): Geochemistry of Eocene calc-alkaline volcanic rocks from the Kastamonu area, northern Turkey; *Contributions to Mineralogy and Petrology,* volume 58, pages 63-81.

Preto, V.A. (1972): Geology of Copper Mountain; *B.C. Ministry of Energy, Mines and Petroleum Resources*, Bulletin 59, 87 pages.

Preto, V.A. (1979): Geology of the Nicola Group between Merritt and Princeton; *B.C. Ministry of Energy, Mines and Petroleum Resources*, Bulletin 69, 90 pages.

Read, P.B. (1987): Tertiary stratigraphy and Industrial Minerals, Princeton and Tulameen Basins, British Columbia; *B.C. Ministry of Energy, Mines and Petroleum Resources*, Open File 1987-19, scale 1:25 000.

Rice, H.M.A. (1947): Geology and mineral deposits of the Princeton map-area, British Columbia; *Geological Survey of Canada*, Memoir 243, 136 pages.

Rubble, V.J. (1994): Chemical petrology, mineralogy and structure of the Tulameen Complex, Princeton Area, British Columbia; unpublished M.Sc. thesis, *University of Ottawa*, 183 pages.

Rubble, V.J. and Parrish, R.R. (1990): Chemistry, chronology and tectonic significance of the Tulameen Complex, south-western British Columbia: *Geological Association of Canada – Mineralogical Association of Canada*, Abstracts with Programs, volume 15, page A114.

Thompson, R.N. (1982): British Tertiary volcanic province; *Scottish Journal of Geology*, volume 18, pages 49 – 107.

Winchester, J.A. and Floyd, P.A. (1977): Geochemical discrimination of different magma series and their differentiation products using immobile elements; *Chemical Geology*, volume 20, pages 325-343.

Wood, D.A. (1980): The application of a Th-Hf-Ta diagram to problems of tectonomagmatic classification and to establishing the nature of crustal contamination of basaltic lavas of the British Tertiary volcanic province; *Earth and Planetary Science Letters*, volume 50, pages 11-30.

Improving the Efficiency in the Maintenance of the Provincial Geological Database

by Y. Cui

KEYWORDS: geological map, spatial database, maintenance, update, GIS, MapPlace, best practices

INTRODUCTION

This paper describes some of the best practices that are promoted by the British Columbia Geological Survey (BCGS) to improve the efficiency in maintaining geological maps. The main focus is to leverage interoperable (including freely available) spatial database technology to reduce the redundancy and efforts in map compilation and data integration while enhancing the data quality.

BCGS is responsible for producing and publishing province-wide geological maps through MapPlace (http://www.empr.gov.bc.ca/Mining/Geoscience/MapPlace/Pages/default.aspx) to mineral exploration, mining, land planning and other users. BCGS recognizes the value of a corporate database management environment for a seamless digital data flow from outcrop to dynamic maps on the web.

The most recent province-wide geological map was published at a scale of 1:250 000 scale in 2005 (Massey *et al.*, 2005). The map compilation was made in support of the Mineral Potential Project (1992-96), with updates in 2003 and 2004. The province-wide geological map has not been updated since 2005, except certain focused areas such as QUEST (Logan *et al.*, 2009).

Currently, new map compilation and updating are carried out by BCGS staff members using Manifold® System and MapInfo® desktop GIS tools. Data files are distributed across different file servers and desktop workstations of the mapping geologists. When a mapping project is completed, a version of the data is converted to the appropriate format and made available to the public through MapPlace. In addition to publications such as Geological Fieldwork, Open File, GeoFile and Geoscience Maps, geological maps are also available online as PDF files and GIS formats for download from MapPlace.

The GIS software tools (*e.g.*, Manifold® and MapInfo®) are sufficient in map compilation and analysis when working with a relatively small dataset and a limited number of data layers. However, this environment has a number of challenges and limitations, including:

- difficult to apply common data standards among the mapping geologists;
- unable to manage and apply data quality rules;
- difficult to share consistent legend and map styles;
- difficult to manage multiple versions of the same map at varying stages of editing and correction;
- slow performance in loading and incremental saving of edits for a large map; potential risk of losing un-saved work when the system crashes (more frequent on workstations with certain operating systems);
- limitation on accessing and loading a large volume of data, *e.g.*, province-wide topographic base map which is required to node the geological features;
- unable or difficult to collaborate amongst staff members on compiling adjacent mapping areas, resulting in discrepancies along the map boundaries and inconsistencies between mapping areas;
- unable to automatically create derived products (*e.g.*, different scales and customization) from the source geoscience data;
- difficult to manage multiple versions of the same map at different scales and customization;
- no automation in detecting and correcting defects or inconsistencies in the geoscience data; and
- difficult or unable to discover and access datasets from different sources, in different formats and projections, and stored on different locations, including staff's workstations.

The geology operational database environment (GODE) is proposed as part of a solution to address some of these issues at BCGS. This paper briefly describes the architecture of GODE, with a focus on the recommended best practices to maintain the operational database.

Typically, when organizations change operational environment, they should consider not only the specific

This publication is also available, free of charge, as colour digital files in Adobe Acrobat® PDF format from the BC Ministry of Forests, Mines and Lands website at http://www.empr.gov.bc.ca/Mining/Geoscience/PublicationsCatalogue/Fieldwork.

business drivers and user requirements, but also the existing processes, tools and most importantly the culture and human aspect in adopting changes. At BCGS, the following requirements are addressed in order to document a high level view of the GODE system architecture and design:

- full context of relevant map layers is available and not constrained by the volume of data: base maps, existing geological maps, new updates from other mapping projects, archived and retired or historical maps;
- base maps that are readily available and at the appropriate scales with consistent styles for new map compilation or updating, to provide the geographic context and geo-referencing in some cases;
- adopting consistent data model that can be enforced by schema validation and schema mapping;
- a custom user interface to Manifold® and MapInfo® for data capture and manual data entry to improve efficiency and to reduce errors;
- a workspace where the province-wide geoscience data, including other project geologists' maps, is readily accessible for data quality assurance and integrations (*e.g.*, boundary issues, connectivity, currency);
- an environment to support versioned map compilation and data archiving;
- reduced inconsistency in data through database triggers and constraints based on data access policies and data quality rules;
- shared legends and styles: if a new rock type and associated styles are defined, they become available instantly to all the users the moment they are implemented in the database;
- ability to carry out province-wide statistical and spatial analyses: *e.g.*, spatial overlay of bedrocks, faults, geochemical results, geophysical survey results;
- ability to create derived products through province-wide data processing;
- ability to provide up-to-date information through MapPlace directly served up from a database; and
- provision of dynamic provincial geological map as GeoWeb services such as WMS, WFS and KML.

DEVELOPMENT OF OPERATIONAL ENVIRONMENT

Guiding Principles

The development of GODE and the recommended best practices follow a set of guiding principles that are common in service-oriented architecture:

- **Interoperable**: GODE will be designed and developed based on ISO and open standards and specifications to ensure meaningful interoperability with other systems and services.
- **Scalable**: GODE will be designed to manage cumulative new map compilations and versioning of the integrated province-wide geological map.
- **Encapsulated**: Map maintenance users should be able to access all the relevant data and use the tools within GODE without the need to be exposed to the complexities of the underlying technology and information infrastructure.
- **Collaborative**: GODE will be developed with a "locking" mechanism and user profiles to facilitate collaborative map updating, especially at map boundaries of adjacent project areas.
- **Efficient**: Data quality and validation rules will be formally specified and automatically applied wherever possible to eliminate simple defects in the data and reduce repeated efforts, to sustain long-term maintainability.

Business Drivers

The requirements of GODE are largely driven by the business needs and processing cycles at BCGS. The collection and management of geoscience data are logically related to three service components and can be functionally grouped and deployed on a common Spatial Data Infrastructure (Figure 1):

1) Mapping Services: geological field mapping, mineral potential assessment, geochemical survey, and geophysical survey;
2) Data Management Services: map compilation, data quality assurance, data integration, and production; and
3) Publication and Access Services: MapPlace and other third party GeoWeb services.

Publication and Access Services are the front end where products and services are provided to clients. Access Services are positioned to collect and communicate user needs, which are documented as updated requirements and specifications of products and services. This would drive Mapping Services with mapping projects to address the new and changing business needs. Updates and new mapping results are available to Data Management Services to produce

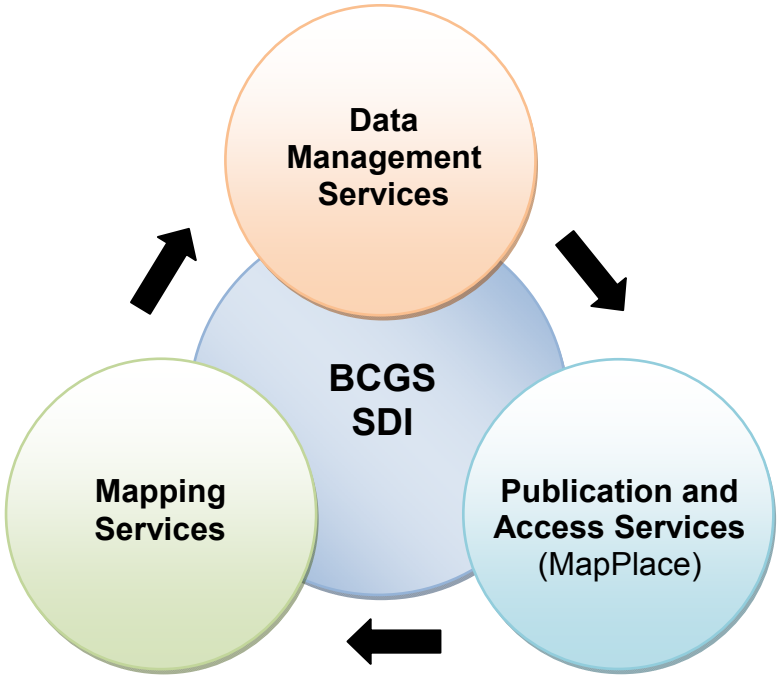

products and services that Publication and Access Services rely on.

System Context

GODE forms part of the Spatial Data Infrastructure (SDI) at BCGS to facilitate the management and provision of geoscience data. The SDI provides a suite of client-facing GeoWeb services enabled by standards, spatial database, and software components. Figure 2 shows the high-level context view of BCGS GeoWeb services and how the components or services interact with each other. The modelling and system architecture of the SDI at BCGS loosely follow ISO/ITU standard 10746-3 on Reference Model for Open Distributed Processing (*e.g.*, Farooqui *et al.*, 1996; ISO, 1998; ISO, 2010) and some of the recent work on modelling SDI (*e.g.*, Brodeur, 2011; Cooper, 2007; Hjelmager, 2005; Hjelmager, 2008).

System Architecture

To briefly describe the system architecture of GODE at a high-level, graphical depictions of a few selected viewpoints are presented here to illustrate the system domains, components in each domain, actors and interfaces. The enterprise viewpoint describes the purpose, scope and policies of the SDI. Figure 3 shows the actors (GODE Operator), domains (*e.g.*, Data Sources, GODE, and Geology Application Database Environment), and components in each domain in the context of this enterpriser viewpoint. The information viewpoint consists of BCGS geological data models enhanced with additional metadata to manage versioning and keep track of the various stages of initial field observation, quality assurance, integration, archiving and production. Due to its large volume, details of the information viewpoint are not included in this paper. The computational viewpoint (Figure 4) depicts the decomposed database components and interfaces that are required for the GODE to function. The engineering viewpoint (Figure 5) shows how the components used in the system are distributed across the various servers.

The technology viewpoint describes the hardware, software versions and other technologies used in the system. The feasibility study and prototyping of GODE rely heavily on free and open source software, including PostgreSQL/PostGIS as spatial database, OpenJUMP as desktop GIS, JEQL as a query and batch Web processing engine, and Apache PHP running on Windows Server® 2003 and Windows XP® and Vista® on workstations. The test deployment also includes Microsoft® SQL Server® 2008 R2 running on Windows Server® 2008 R2 64-bit, and Manifold® System as desktop GIS running on Windows Vista® 32-bit workstations.

Open distributed processing amongst the various system components and servers that are part of or related to GODE, is shown in Figure 5. These are supported by the adoption of Open Geospatial Consortium (OGC) standards, including the OGC Simple Features Specification for SQL (OGC, 1999). Spatial data, encoded as GEOMTRY or GEOGRAPHY data types on the database side, can be exposed as well-known text (WKT) or well-known binary (WKB) (OGC, 2001; OGC, 2010), to desktop clients and web services. This ensures

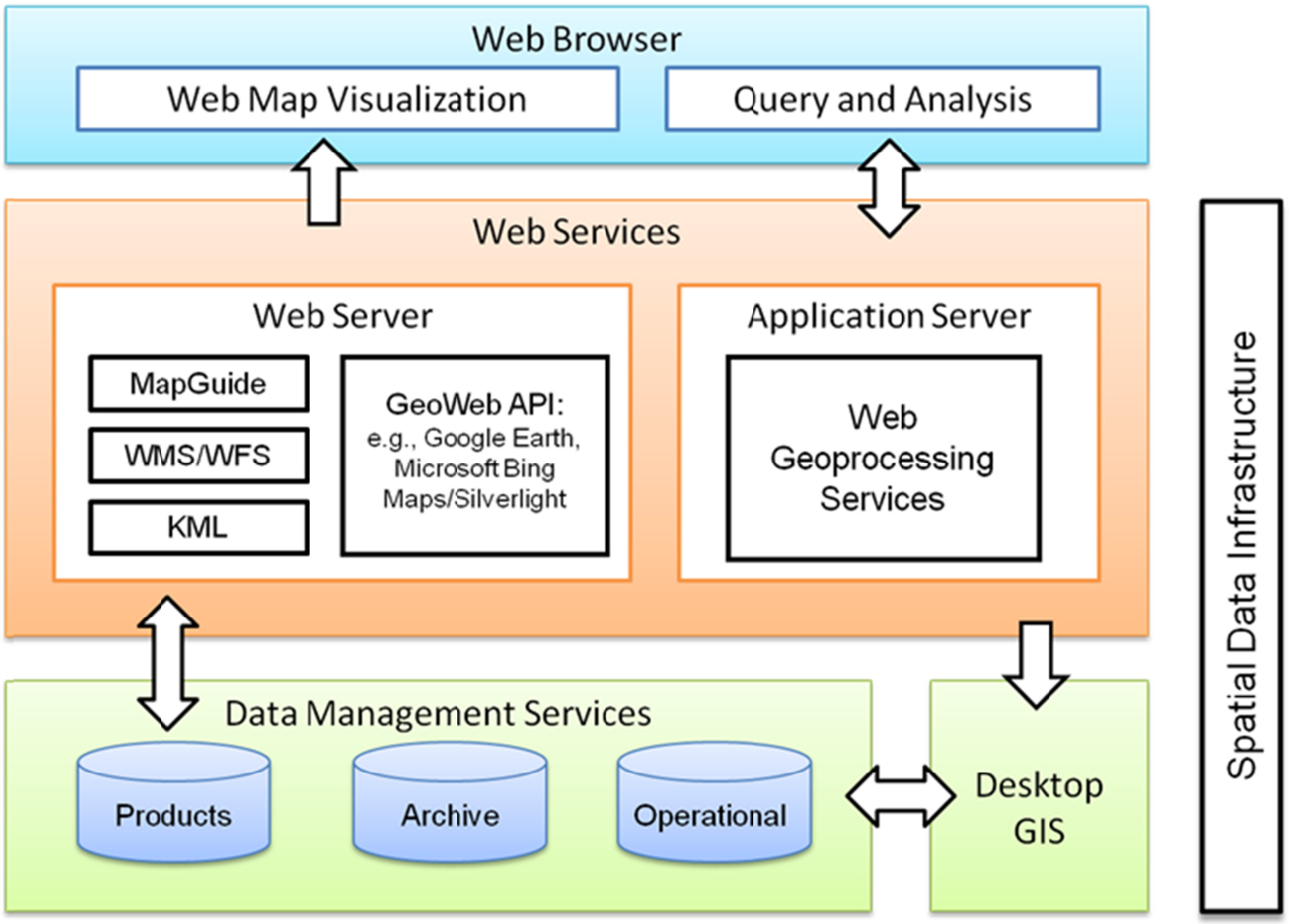

Figure 2. High level context view of BCGS GeoWeb services.

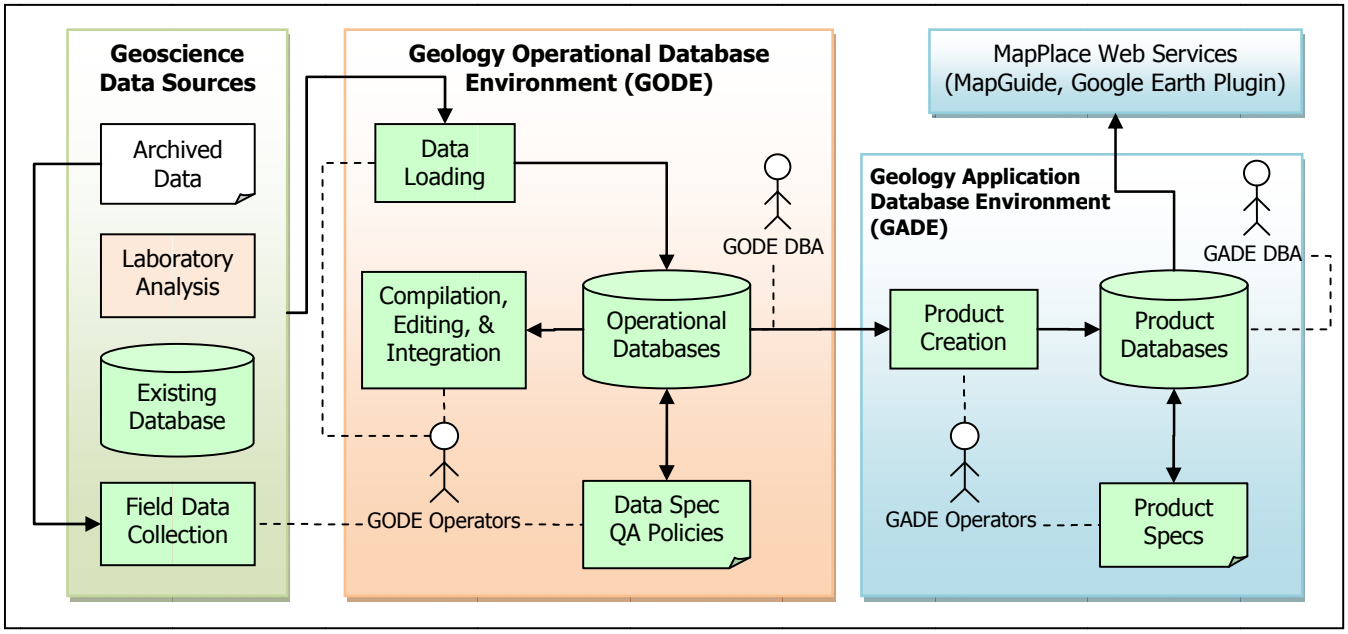

Figure 3. Enterprise viewpoint of GODE within the BCGS Spatial Data Infrastructure (SDI).

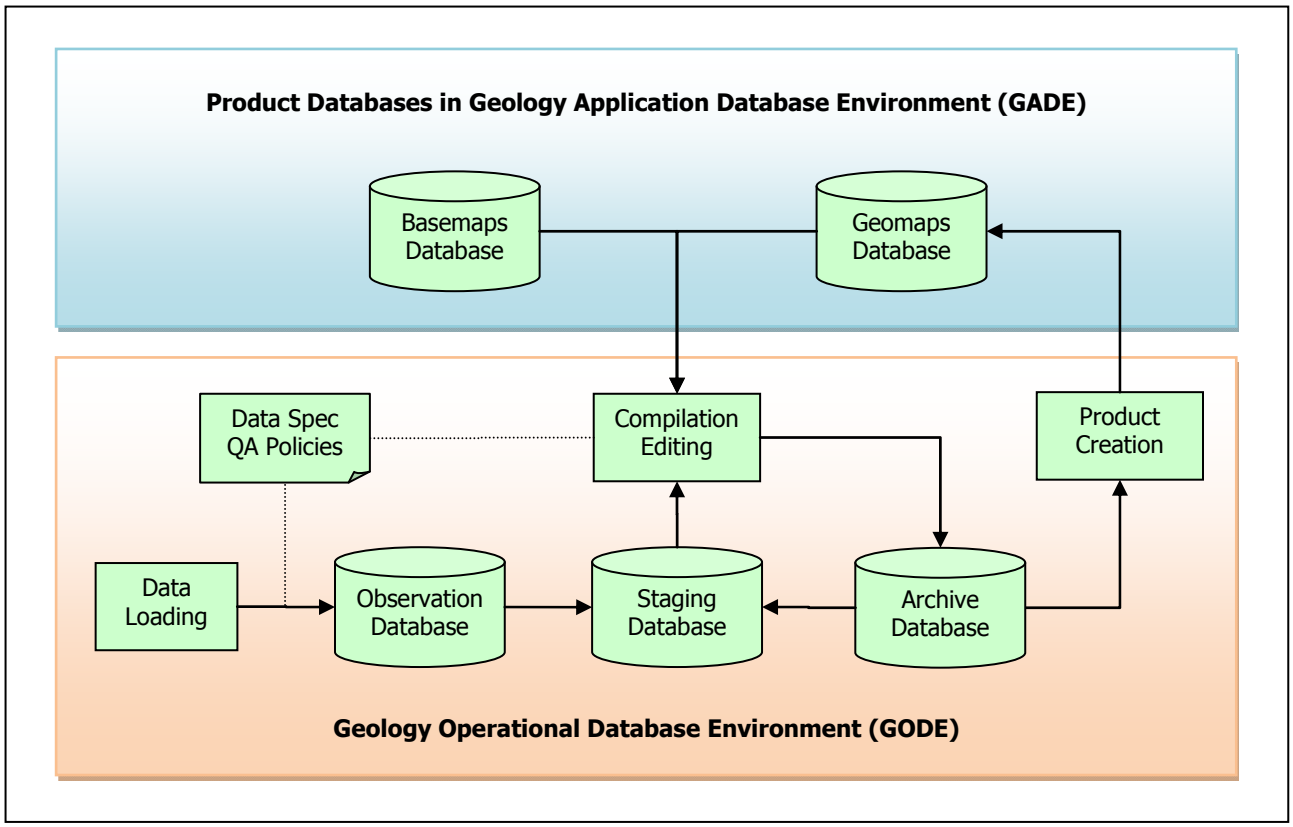

Figure 4. GODE database components.

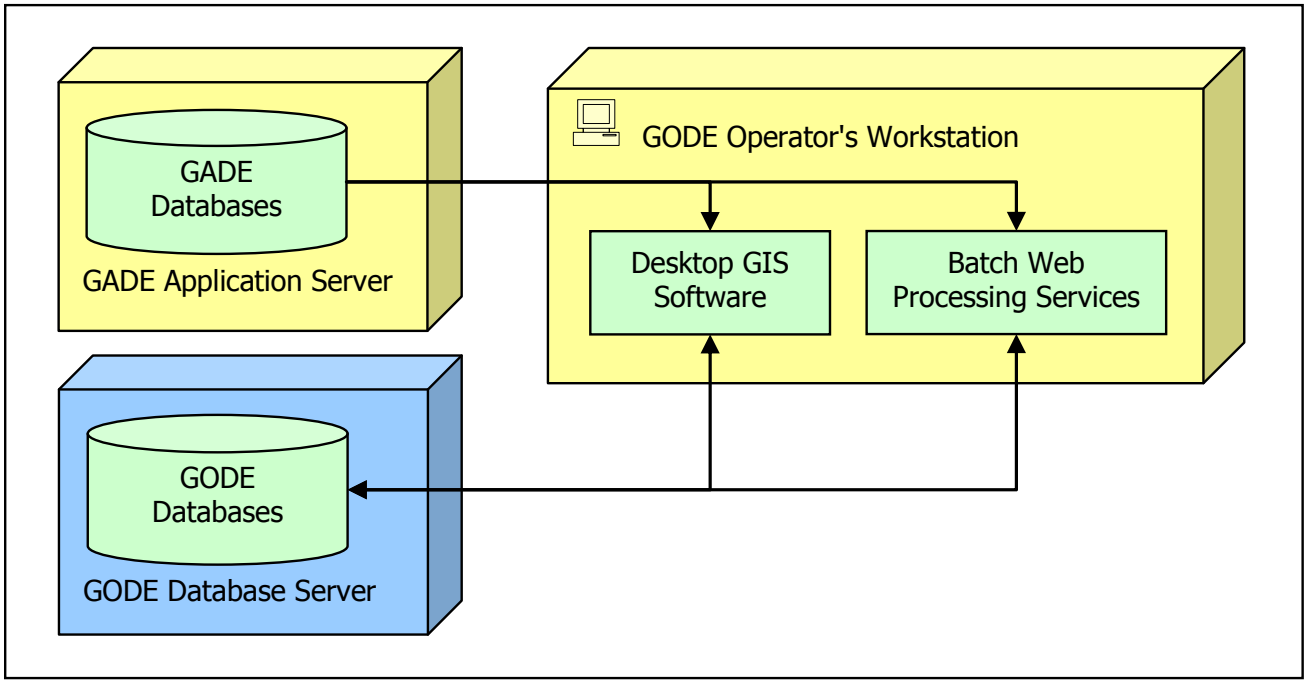

Figure 5. GODE engineering viewpoint.

interoperability at a more primitive and practical level without the need to parse a markup language with a complex schema and overloaded with redundancy.

BEST PRACTICES

Data Quality Assurance Rules and Policies

Geological mapping has multiple stages, from field survey, map compilation, cartographic enhancement, to final production. In addition to rigorous training and years of practical experience by the seasoned mapping geologists, there is also abundant literature on the geological mapping specifications and techniques for the various map producing stages, including the BC RIC standard (RIC, 1997), Ontario Digital Line Standards (Muir *et al.*, 2000), unpublished guide and manuals at BCGS, and over a decade of "Digital Mapping Techniques" workshop proceedings from the Association of American State Geologists and USGS (http://ngmdb.usgs.gov/Info/standards/datacapt/datacaptureWG.html).

The recommended best practices are derived from these established and well-adopted standards and guidelines with an emphasis on achieving efficiency in the configuration of map compilation environment and the specification and applications of data quality rules, such as:

- size of features: minimum area size of polygonal features, minimum length of linear features;
- density of coordinates: too many coordinates or too few coordinates; and
- geometric irregularity: duplicates, kick-backs, sharp angles between two lines, overlaps, overshoots, undershoots and gaps.

Map Projection

At different stages of geological mapping, a specific map projection is preferred to meet the requirements. In the initial map compilation, it is essential to ensure the proper positioning of the field observations with referencing to the most detailed topographic map, to preserve measurements of angles and orientation of directed linear features (*e.g.*, thrust fault traces). As an example, the choice of projection is conformal while the use of UTM is preferred by many geologists because orientation data works better with the orthogonal grid. At the stage of province-wide map integration and map production for applications such as statistical analysis, the choice of projection is equal-area based. In British Columbia, the preferred projection is BC Albers.

It is well known in the geospatial user community that coordinates can drift and shapes can change after map projection and round-trips of re-projections (*e.g.*, from geographic coordinate system WGS84, to BC Albers, to UTM and then back to WGS84). While it is impossible to avoid projections, there are measures that can be taken to reduce the coordinate drifting, including proper use of explicit unit of precision, coordinates densification for large features that do not have enough coordinates along straight and long edges, and avoiding clip or cookie-cut of contact lines when checking out the features for a mapping project area (more in the section of "Checking-out" Existing Geological Maps).

For maps published in a non-conformal projection, orientation is distorted in areas not at the central meridian. Certain orientation data (*e.g.*, the strike of a bedding) can be stored in a database as true north and displayed as symbols. This stored orientation data should be projected so that it is displayed consistently with the "distorted" orientation of other geological features.

Awareness of Varying Mapping Scales

Traditional systematic geological mapping at a fixed scale for a map sheet has been replaced by mapping at varying scales designed to answer specific geological questions or targeting economic mineral potential. At BCGS, project-based mapping can be carried out at a scale of 1:10 000 to 1:50 000, and the publication at regional or provincial extent might be generalized at a scale of 1:250 000 to 1:2 000 000.

It is worthwhile to include the mapping scale in the metadata and adjust the data capturing with positional accuracy, unit of precision (see next section), and level of details appropriate to the map scale. Digital mapping provides a perfect breeding ground for imperfect mixing of data captured at different scales in the same area or maps at different scales adjacent to each other. Data processing with scale awareness can treat the data at finer granularity while performing data validation and data quality assurance.

Explicit Unit of Precision

Most GIS and database systems can store coordinates and perform computation at a unit of precision below microscopic resolution. It is perfectly fine to use the highest precision that a system supports for computation. However, it can cause data quality issues with an excessively finer precision or different units of precision for data stored in different systems or formats, for mapping at a scale of 1:50 000 or smaller.

In GODE, map compilation is to be carried out at decimetre precision (or 7 floating points in decimal degrees), and the data is maintained at metre precision (or 6 floating points in decimal degrees) on the database side.

Common Topographic Base Maps

Topographic base maps are essential components for geological mapping, as background and cartographic enhancement to the final publication, as one of the sources for georeferencing or checking positional uncertainty, and also as noding bases to close off certain

geological boundaries to the topographical boundaries such as lake shores, river banks and coastal lines.

Corporate spatial database makes it possible to store a very large volume of the most detailed topographic base maps and to retrieve any given map sheets easily.

Another major advantage is that the styles applied to the base maps can be stored on the database side and shared by every user. This approach not only saves time on discovering, retrieving and styling base maps, it also provides visually consistent base map layers to the final publications.

Provincial orthophotography and other digital images at high resolution are available as WMS layers or image files to validate the accuracy of important geological features.

"Checking-out" Existing Geological Maps

Geological map updating can start during field surveys, which would require the "checking-out" of the existing geological map from the corporate database for the project or target area. A common practice is to use map sheet or project area neatlines as a cookie-cutter to clip out only the portion of the map in the area. It has been proven that this practice can cause lot of data issues by the time the updates are to be integrated to the corporate database.

It is highly recommended that the project area neatlines are used to intersect all the polygonal features (*e.g.*, bedrock polygons) in their entirety and then use the polygons to extract all linear geological contacts and faults that either form or intersect these polygons. When the updating is completed, the integration process should only involve accepting features marked as one of the following:

- no change,
- new compilation,
- revised with updates: geometries, attributes, both geometries and attributes, or due to integration), and
- retired (*e.g.*, replaced by updates).

Attribution through Standard Lexicon Templates

It is a challenge to standardize the nomenclature of geological units for an area as large as British Columbia with diverse geology and mapping contributions, primarily by BCGS, but also by federal government agencies, universities and mining industry. Nevertheless, an attempt is to derive a standard template by reconciling the differences between the Canadian Geoscience Knowledge Network (CGKN) lexicon entries for British Columbia and the ones existed in the current Geological Map of British Columbia database.

In order to accommodate more detailed mapping and subdivision of existing major geological units, a template for sub-units is also created.

During initial map compilation, the geological unit code mapped to the standardized lexicon in the template should be used to simplify the population of the attribution. Whereas the geological units are subdivisions of an existing major unit, then a template for the sub-units can be used or new sub-units can be created.

Map Neatline (Knowledge Boundaries)

A province-wide geological database could contain project-based mapping updates at multiple scales and different stages of completion. This would leave inconsistency, lost connectivity and other issues at map boundaries. While it is possible to produce a product at the smallest scale as a common denominator, the inconsistency and boundary issues will remain to be resolved at the observation level and has to be managed properly. One recommendation is to introduce a new contact type, "neatline", to separate areas of different mapping scales or stages of updating. In that sense, neatline is also the knowledge boundary, meaning a lack of knowledge occurs beyond the neatline, at the level of detail that a recent mapping project has taken place. The neatline is removed only when knowledge becomes available to resolve the inconsistency, connectivity and other data issues at the map boundary.

Treatment of Small Geological Units

There are bedrock units that are geologically or economically important, as determined by the mapping geologist, but they are small in size or spatial extent. These features should be kept in a separate map layer or a separate table in a spatial database. While most of them are mapped as polygons, some of them are best digitized as points or lines such that they can be properly symbolized or styled for display.

Mapping Mineralization

Mineralization or mineral occurrences can be mapped as points, lines and polygons. In most cases they are captured in a separate map layer or maintained in a separate table in a spatial database. In some cases the mineralization can be annotated through the use of a modifier code on the geological unit designation, preferably as a sub-unit, with explanation in the description.

There are also situations where the mineralization is significant both in importance and geographic extent and the hostrock or original rock types cannot be reliably traced through the zone of modification. In this case, it is acceptable that a new geological unit is created.

DATA UPDATING AND INTEGRATION

Data Loading

When a project-based map is available for updating the province-wide geological database, the contact lines (including regular contacts, faulted contacts and faults) and bedrock polygons are loaded into the observation database after schema mapping and validating projections, scales, and geo-referencing. The data remains in its original state without any changes or fixing.

A mandatory column in the data is a lexicon-based geological unit or unit code which must exist and can be matched to the lexicon major unit or sub-unit templates. If it is a new unit or subunit, full attribution must be provided.

Noding and Polygonization

A copy of the contact lines and existing province-wide geological contact lines are loaded into the staging database (Figure 4) for detecting changes, adding new features, replacing or retiring updated features, and noding contact lines. The resulting contact lines are used to form bedrock polygons.

Both the noding and polygonization can be carried out on the staging database side, through desktop GIS or batched processing services. At BCGS, most of the work is carried out in Manifold® System with linked in maps (or database tables) from the staging database.

Data Quality Assurance

During or after the noding and polygonization processes, a number of data quality assurance (QA) procedures are repeated to check and fix some of the potential data quality issues against the data quality rules. The QA rules and policies can be specified and stored on the database side to ensure the QA rules are not only enforced but also applied consistently. Another benefit is the potential to apply the QA rules automatically through the development of database side triggers, constraints, SQL scripts or other means accessing the same QA rules and policies stored on the database side.

At BCGS, the current QA work is carried out in a hybrid approach, depending on the functions, strength and performance on the spatial database side, desktop GIS and batched processing services. There is some success in a batched processing service enabled by JEQL scripts developed in-house to deal with certain QA tasks that are less efficient by the off-the-shelf software tools.

Population Attributes

After QA work is completed and a final version of polygons is formed, a centroid is generated for each of the polygons. A centroid must be guaranteed inside the intended polygon, *e.g.*, using ST_PointOnSurface, not ST_Centroid in PostGIS; using Centroid (Inner) in Manifold® System.

Through a spatial overlay of the centroids and the update source bedrock polygon table stored in the observation database, the geological unit or unit code is transferred from the polygon table to the centroids stored in the staging database. The geological unit or unit code and other attributes associated with each of the centroids are then transferred to the new and updated polygons.

The final population and QA checking of the attributes for the updated bedrock polygons are carried out by applying the lexicon major and sub-unit templates stored on the database. With a database, this is a process that can be fully automated with SQL scripts.

Consistent map styles and themes are applied to the updated maps and new styles for new geological units or sub-units are added to the metadata table and shared by any users connecting to the same database.

Archiving

Both the newly updated area and the province-wide bedrock maps and contact lines are versioned with time stamps and loaded to the archive database. The maps are consistent and complete within a given mapping area at a time or stage of progression. Data stored in the archive is considered as the BCGS authoritative source.

Production

Products are derived from the authoritative data source maintained by the archive database. Production is carried out by processes designed according to either product specifications or requirements for applications, such as a map at a specific scale or with a specific mineral focus, for visualization or high performance query, etc. The production can be automated with database side triggers or GeoRSS on updates, a topic beyond the scope of this discussion.

CONCLUSIONS

Efficiency in maintaining geological maps can be achieved by leveraging recent advancement in interoperable (and also freely available) spatial database and geospatial tool, and distilling a set of best practices by harvesting available knowledge and expertise in geological mapping.

British Columbia Geological Survey has shown success in prototyping a geology operational database environment (GODE) at a time of limited resources in information technology support and staffing. In-house expertise and the use of free and open source software, including PostgreSQL/PostGIS, JEQL and OpenJUMP, provide a cost effective solution to the GODE prototype.

BCGS is promoting the best practices of map compilation among the staff mapping geologists and some early adoption has helped to refine and expand the list of best practices. Using a phased approach to implement GODE on corporate infrastructure, BCGS builds a fully functional system component into the system architecture

before working on the next component. Currently Microsoft® SQL Server® 2008 R2 has been deployed as the back-end corporate spatial database, accessible from desktop GIS Manifold® System and batched data processing engine JEQL. It is already in heavy use for on-going data quality assurance and data integration. The next step is to implement the data quality assurance policies and applications, and to populate the database with required data layers such as the topographic base maps.

ACKNOWLEDGMENTS

Ward Kilby, Larry Jones and Pat Desjardins are thanked for providing insightful comments and carefully editing the manuscript. A portion of this paper is extracted from a technical document on the architecture specifications for the geology operational database environment that was completed by Yao Cui with the support of British Columbia Geological Survey, especially Larry Jones, director of Resource Information Section at BCGS. JoAnne Nelson helped with testing and improving some of the recommended best practices. The development of the system architecture for the geology operational database environment and the compilation of best practices benefited from the QUEST bedrock geology compilation and many discussions with BCGS geologists.

REFERENCES

Brodeur, J. (2011): Geosemantic interoperability and geospatial semantic web; in Handbook of Geographic Information, Kresse, W., Danko, D.M., Editors, *Springer*, in press.

Cooper, A.K., Moellering, H., Delgado, T., Düren, U., Hjelmager, J., Huet, M., Rapant, P., Rajabifard, A., Laurent, D., Iwaniak, A., Abad, P., and Martynenko, A. (2007): An initial model for the computation viewpoint of a spatial data infrastructure; *23rd International Cartographic Conference*, Moscow, Russia.

Farooqui, K., Logrippo, L., and de Meer, J. (1995): The ISO reference model for open distributed processing: an introduction; Computer Networks and ISDN Systems; *Special issue on ISO reference model for open distributed processing*, Volume 27, Issue 8, July 1995.

Hjelmager, J., Delgado, T., Moellering, H., Cooper, A.K., Danko, D., Huet, M., Aalders, H.J.G.L. and Martynenko, A. (2005): Developing a modeling for the Spatial Data Infrastructure; *Proceedings of the 22nd International Cartographic Conference*, A Coruña, Spain.

Hjelmager, J., Moellering, H., Delgado, T., Cooper, A.K., Rajabifard, A., Rapant, P., Danko, D., Huet, M., Laurent, D., Aalders, H.J.G.L., Iwaniak, A., Abad, P., Düren, U. and Martynenko, A. (2008): An initial formal model for Spatial Data Infrastructures; Taylor & Francis, Inc., *International Journal of Geographic Information Science*, Vol 22, No 11, pages 1295-1309.

ISO (1998): ISO/IEC 10746-1:1998-Information technology-Open Distributed Processing-Reference model: Overview.

ISO (2010): ISO/IEC 10746-3 Information Technology-Open Distributed Processing-Reference Model-Architecture.

Logan, J.M. Schiarizza, P., Struik, L.C., Barnett, C., Nelson, J.L., Kowalczyk, P., Ferri, F., Mihalynuk, M.G., Thomas, M.D., Gammon, P., Lett, R., Jackaman W. and Ferbey, T. (2010): Bedrock Geology of the QUEST map area, central British Columbia; *BC Ministry of Energy and Mines*, British Columbia Geological Survey, Geoscience Map 2010-1.

Massey, N.W.D., MacIntyre, D.G., Desjardins, P.J. and Cooney, R.T. (2005): Digital Geology Map of British Columbia: Whole Province; *BC Ministry of Energy and Mines*, British Columbia Geological Survey, GeoFile 2005-1.

Muir T.L., Watkins, T.W. and Berdusco, B.J. (2000): A library of digital line standards; *Ontario Geological Survey*, Open File Report 6026, 208 pages.

North American Geologic Map Data Model Steering Committee (2004): NADM Conceptual Model 1.0 - A conceptual model for geologic map information; *U.S. Geological Survey*, Open-File Report 2004-1334, 58 pages.

OGC (1999): OpenGIS® Simple Features Specification for SQL, Revision 1.1; *Open Geospatial Consortium, Inc.* OpenGIS® Project Document 99-049, Release May 5, 1999, 78 pages.

OGC (2001): OpenGIS® Implementation Specification: Coordinate Transformation Services; *Open Geospatial Consortium, Inc.* OpenGIS® Project Document 01-009, Revision 1.00, Release Date: 12 January 2001, 117 pages.

OGC (2010): OpenGIS® Implementation Standard for Geographic information - Simple feature access - Part 1: Common architecture; *Open Geospatial Consortium Inc.*, OGC 06-103r4, Version: 1.2.1, 93 pages.

RIC (1997): Specifications and guidelines for bedrock mapping in British Columbia; Resources Inventory Committee, *British Columbia Geological Survey*, Information Circular 1997-3, 185 pages.

Regional Geochemical Survey: Validation and Refitting of Stream Sample Locations

by Y. Cui

KEYWORDS: spatial data quality, regional geochemical survey, RGS, sample locations, refitting, catchment basins

INTRODUCTION

It is a common and challenging task to refit or adjust spatial data collected and geo-referenced on vintage hard copy topographic base maps at smaller scales, to more accurate digital topographic base maps at a much larger scale, in order to add value and advance the application of the spatial data.

A prerequisite of this task often involves the assessment or validation of the spatial data quality, and the need to manage and reduce the effects of uncertainty and error propagation. While spatial data quality is a topic that has been widely researched and published (*e.g.*, Goodchild, 1989; Guptill and Morrison, 1995; Shi *et al.*, 2002), it remains to be an issue to organizations that collect, integrate, disseminate and publish spatial data.

This paper summarizes recent work at the British Columbia Geological Survey (BCGS) in data quality assurance, data refitting and the results of the refitted Regional Geochemical Survey (RGS) stream sample sites in the province of British Columbia. The goal of the exercise is to develop an automated, practical and re-usable methodology based on a set of criteria and algorithms that computation can be performed within a spatial database environment. Highly uncertain sites will still require manual verification using high resolution imagery, large scale topographic maps and scanned paper maps. A brief summary is also provided on the preliminary results of adjusting the RGS stream sample sites from the streams on the original paper based National Topographic System (NTS) maps, to their equivalent or matching 1:20 000 scale streams from Terrain Resource Information Management (TRIM). The methodology and cases presented in this paper can be used as a guide to future efforts in validation of RGS stream sample sites.

This publication is also available, free of charge, as colour digital files in Adobe Acrobat® PDF format from the BC Ministry of Forests, Mines and Lands website at http://www.empr.gov.bc.ca/Mining/Geoscience/PublicationsCatalogue/Fieldwork.

The RGS program started in the 1970s and represents an investment of over $20 million in collecting and analysing over 60 000 stream sediment, moss, and lake sediment and water samples covering approximately 75% of British Columbia. The published RGS datasets contain analytical determinations for up to 50 elements, field observations and sample location information, which have been widely used in mineral exploration, land use planning, public health, and many other areas.

While the sample site location criteria are recognized as some of the most important aspects for the success of the RGS program (Ballantyne, 1991), the positional accuracy or data quality for the RGS sample locations has not been formally established or specified, partially due to the fact that the RGS program started as a geochemical survey of stream sediments at a reconnaissance scale to identify regions with a high mineral potential. As such positional accuracy of stream sample sites was not deemed as a concern.

The requirements of validating RGS data quality, especially positional accuracy of the stream sample locations, are largely driven by the applications of the RGS geochemical results in mineral exploration, through more detailed geochemical modelling and levelling.

Catchment basins of stream geochemical survey sites are recognized as being more effective to advance the levelling, interpretation, application and presentation of the geochemical results (*e.g.*, Bonham-Carter and Goodfellow, 1986; Bonham-Carter *et al.*, 1987; Hawkes, 1976; Jackaman and Matysek, 1995; Matysek and Jackaman,1995; Matysek and Jackaman, 1996; Sibbick, 1994; Sleath and Fletcher, 1982). BCGS has developed a fully automated algorithm to delineate catchment basins with high performance (Cui *et al.*, 2009). In order to use the most recent and detailed heights of land as the base of the catchment basins, it is required that RGS stream sample sites are validated and adjusted (or refitted) to the streams from the TRIM topographic base maps at a scale of 1:20 000. The confidence level of the RGS stream sample locations not only help to delineate catchment basins properly, but they also help to constrain the interpretation of the geochemical anomalies based on catchment basin analysis.

DATA SOURCES

Regional Geochemical Survey Sample Location Data

The RGS data includes more than 60 000 sample locations, field observations and analytical results for up to 50 elements for water, stream and lake sediment samples collected over a period of 30 years. Of the RGS samples, more than 52 000 were stream sediment and water sample sites.

The locations of the stream sample sites were measured on NTS paper-based maps at a scale of 1:250 000 and later more commonly at a scale of 1:50 000. The NTS maps were based on the NAD27 datum and have not been updated since publication. In recent years, the sample sites have been located with the aid of handheld GPS devices.

The selection method of RGS stream sample sites was based on Garrett *et al.* (1980), Ballantyne (1991) and refined by BCGS (Lett and Jackaman, 2004; Lett, 2005), which includes some of the following criteria:

- a regional survey with an average sample density of 1 sample per 13 square kilometres (km^2);
- active flowing first or second order streams that have a drainage basin area between 2 and 15 km^2 (first order streams will only generally be sampled for more detailed surveys, *e.g.*, 1 sample/5 km^2);
- within the active stream channel (subject to annual flooding);
- approximately 60 metres upstream from sources of possible contamination;
- approximately 60 metres upstream from a confluence;
- approximately 60 metres upstream from a high tide mark;
- upstream from lakes, ponds and marshes;
- prefer streams containing abundant fine-grained sediment (silts and clays) that have clean flowing water; and
- avoid very high or very low energy sites if possible.

The NTS paper maps at a scale of 1:50 000 are used as the Master Sample Location Maps to plan the traverse of the survey area, for identifying proposed sample collection sites. The sample collection crews use field copies of the paper maps as the Traverse Field Maps to record the actual sample sites, which may be different from the proposed location. The locations are transferred to the Master Sample Location Maps at the end of each day.

Further to potential uncertainty in identifying and marking the sample locations properly on the paper maps, the validation of the sample locations is also pertinent due to uncertainties from changes of geo-referencing sources and datum over the last 30 years and potential errors introduced from data transcription and transformation.

1:50 000 NTS Maps

While 1:250 000 NTS paper maps were used to locate some of RGS samples, the majority of the RGS samples were located on the 1:50 000 NTS maps. In addition to the available hard copy of paper based maps, a digital representation of the 1:50 000 NTS stream layer is used in this project. This dataset is also known as the "blueline" streams. In total, there are over 1 million stream network edges. Non-geometric attributes for this stream network include a hydrographical feature code, stream order, stream magnitude and a new watershed code which cross-references hydrographical features between the streams based on TRIM at a scale of 1:20 000 and the NTS 1:50 000 streams.

1:20 000 TRIM I Stream Data

For this project, the stream network and watersheds derived from the 1:20 000 scale TRIM I topographic base are considered as the provincial standard hydrographical base. The stream network has full connectivity by adding 'skeleton' network edges or connectors through water bodies such as lakes, rivers and canals digitized as polygons. In total, there are approximately 5 million stream network edges and over 3 million watershed polygons. Stream data collected through TRIM II and updates from the TRIM data exchange program are not included.

The stream network's non-geometric attributes are identical to the 50k stream attributes, except that they include a hierarchical key that was introduced to enable upstream and downstream queries in a non-spatial manner. The hierarchical keys were computed as the proportional distance along a stream where a child stream flows into its parent.

There is a stream cross-reference table (XREF_20K_50K_STREAMS) that lists the 50k stream edges and their equivalent or matching TRIM I stream edges. This table is used both in locating the matching TRIM I streams and in assessing data quality.

External Data Sources

For manual verification and visual inspection, high resolution imagery (*e.g.*, orthophotography) and more detailed topographic base map (*e.g.*, TRIM II streams) from external web services are accessed as WMS layers.

METHODOLOGY

Principles

This exercise is to develop a practical and re-usable methodology with the goal of validating the source data

and reducing the uncertainty in the positional accuracy of the sample locations. The procedures based on this methodology will also be used to refit or adjust the sample locations to the matching TRIM streams.

Throughout the process, the positional uncertainty of the original sample locations is assessed, leading to the ranking and the development of confidence levels that can be assigned to each of the sites after the adjustment to TRIM I streams is completed.

Processing Environment

To ensure re-usability of the procedure, the prototyping, data analysis and processing are carried out in a fully interoperable environment consisting of desktop GIS, GeoWeb and Web-based batch processing services connecting to spatial databases that support Open Geospatial Consortium (OGC) Simple Features Specification.

Microsoft SQL Server® 2008 and PostgreSQL/PostGIS are used to store and query RGS and hydrographic data.

To visualize and edit specific sample sites in the context of the 50k NTS streams and 20k TRIM streams anywhere in the province, all data has to be served up dynamically by a bounding box to handle the huge data volume (over 9 million of hydrographic data alone). Two free and open source desktop GIS packages, OpenJUMP and Quantum GIS, are used to directly query and visualize the over 9 million records of 50k NTS streams, 20k TRIM I streams and watersheds stored in a Postgres/PostGIS database. This high performance visualization is achieved through the use of the viewing and panning screen as a bounding box to dynamically and efficiently load the spatial data from a PostGIS databases.

Web-based batch processing services are enabled by JEQL, a query tool with enhancement to SQL and full access to spatial functions available from JTS Topology Suite.

Google Earth® and OpenJUMP are used to access imagery and detailed topographic base maps served up as WMS layers.

PROCEDURES

Through prototyping and testing, the refitting procedure is developed and refined with three major steps. A simplified view of the procedure is depicted in a flow-chart (Figure 1).

During the test period, a set of criteria is developed to determine and assign confidence level to the refitting results (Table 1).

Step 1: Selecting 50k Streams Nearest to the RGS Sample Sites

This step is taken to determine if a given RGS sample site can be located on an NTS 50k stream within a reasonable distance or tolerance, as a way to assess the positional uncertainty.

The "nearest" algorithm is used to calculate the distances between a given RGS sample site and the 50k streams within a given tolerance. The nearest stream is selected with the shortest distance and constrained by stream code and stream orders. The constraint on stream code is to avoid selecting stream edges that are part of the stream network but not appropriate as sample locations, *e.g.*, a construction line through a lake. The constraint on stream orders is to ensure that the selected 50k stream is appropriate with a stream order specified by the RGS sampling guide (*i.e.*, first or second order), and matching the actual stream order recorded in the RGS field data.

A tolerance of 300 metres is used arbitrarily after consideration of uncertainties in estimating coordinates from a paper map at a scale of 1:50 000, potential positional drift due to a conversion between NAD27 to NAD83, and rounding errors. To put it in perspective, the size of a pencil circle marked as a sample site on the 50k paper maps is 150 metres. The tolerance can and should be adjusted so a practical number of sites deemed as highly uncertain can be manually inspected.

Step 2: Selecting TRIM I Streams Nearest to the RGS Sample Sites

This step consists of three different passes to select the matching or nearest TRIM I stream for a given RGS sample site.

In the first pass, the 50k streams identified for the RGS sample sites from Step 1 are used to select their equivalent or matching TRIM I streams through the stream cross-reference table (XREF_20K_50K_ STREAMS).

In the second pass, a query is executed to select the TRIM I streams for the stream sample sites that are on or near the 50k streams as identified from Step 1 but they do not have matching or equivalent TRIM I streams based on the cross-reference table (XREF_20K_50K_STREAMS).

In the third pass, a query is performed to locate TRIM I streams within a radius of 150 metres and the nearest stream is selected for the stream sample sites not near any 50k streams within 300 metres.

Visual inspection is required for stream sample sites that are not near any 50k stream within 300 metres or near any TRIM I stream within 150 metres. Visual inspection is carried out on 50k paper maps (if available), TRIM II stream and orthophotography as WMS layers.

In the above three passes, the selection of TRIM I streams is constrained by the TRIM I stream order and the stream order recorded in the RGS field data. The TRIM I stream order must be the same or slightly higher than the matched 50k stream orders or the stream orders recorded in the RGS field data, due to the differences between mapping at scales of 1:20 000 and 1:50 000. Manual review is required if the stream orders are not equivalent

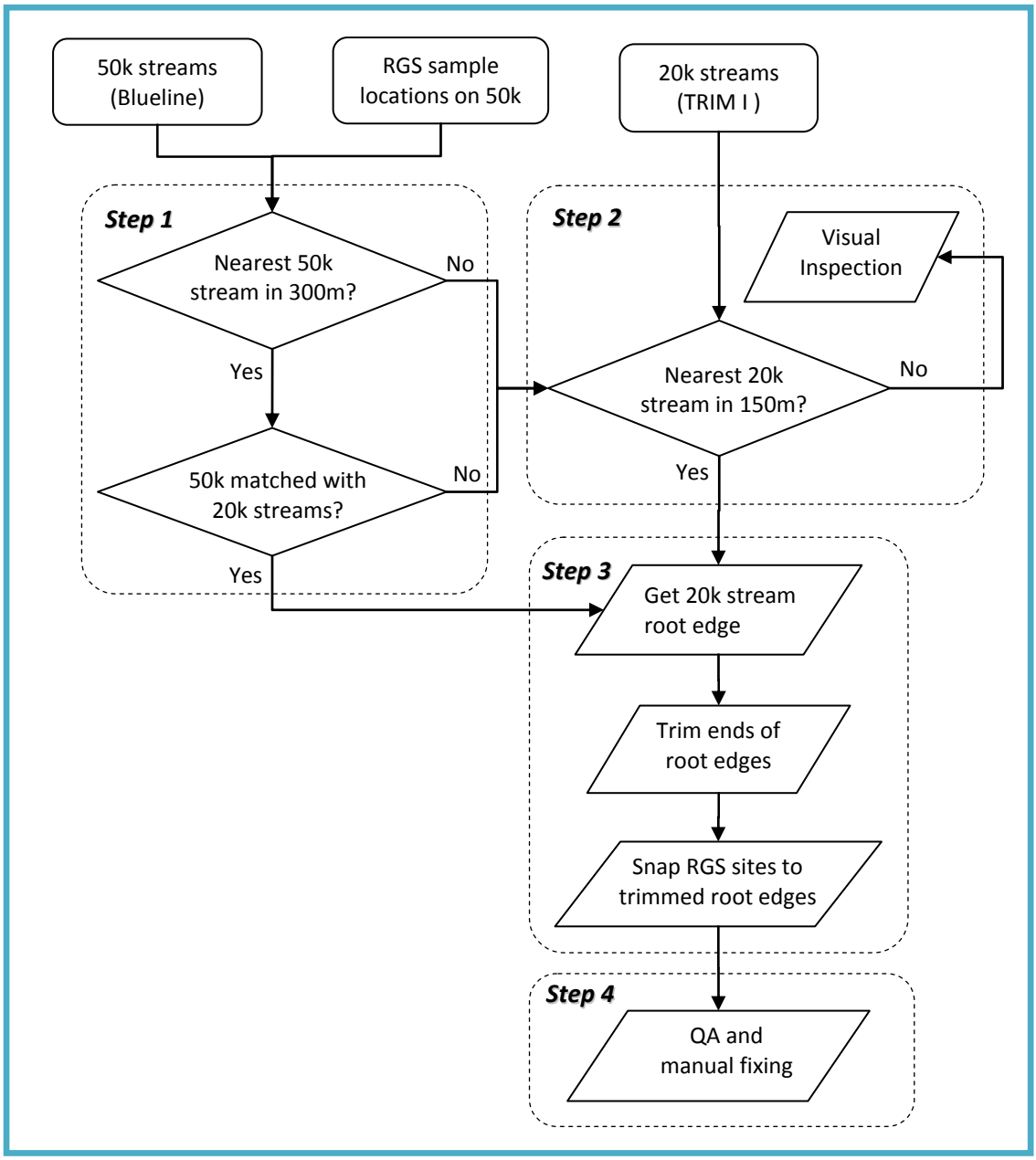

Figure 1. A simplified flow-chart of validation and refitting process.

between the selected TRIM I streams and the 50k streams or the RGS field data.

Some other constraints are placed on the TRIM I stream data to avoid selecting stream edges that are deemed not appropriate as the sample locations, *e.g.*, a construction line linking the main flow to a side channel. This is achieved by filtering them out based on spatial and non-spatial attributes.

The positional uncertainty of a site is assessed based on its distances to the nearest 50k stream and TRIM stream, if there is a match between the nearest 50k stream and nearest TRIM stream, and if the TRIM stream order matches the stream order recorded in the RGS field data.

The selected TRIM I streams are tested if they are located in the same 20k watersheds derived from TRIM I that contain the original RGS stream sample sites. This is carried out by spatial overlay between the 20k watershed polygons and the original RGS stream sample sites as points and the matched TRIM I streams as drainage lineStrings.

For a given sample site if there is no matching TRIM I stream, it is visually reviewed on the NTS 50k paper maps that were used in the field (if available) and then verified with the aid of TRIM II streams and high resolution images.

Table 1. Criteria for confidence level of validation and refitting results.

Confidence Level	Criteria
5	• Located on or near a 50k stream within 150 metres • A match between the nearest 50k and TRIM stream • Adjusted to the nearest TRIM stream within 150 metres with an equivalent stream order as the one from the RGS field data • Same resulting catchment basin after the adjustment of sample location
4	• Located on or near a 50k stream within 200 metres • A match between the nearest 50k stream and TRIM stream • Adjusted to a TRIM stream that is not the nearest but still within 200 metres with an equivalent stream order as the one from the RGS field data • Same resulting catchment basin after the adjustment of sample location or different catchment basin but the adjustment distance is less than 150 metres.
3	• Located on or near a 50k stream within 300 metres • No match between the nearest 50k stream and TRIM stream • Adjusted to a TRIM stream that may not be the nearest but still within 150 metres with the same stream order as or slightly higher than the stream order from the RGS field data • Different resulting catchment basin after the adjustment of sample location
2	• Located on or near a 50k stream over 300 metres • Not matched between the nearest 50k stream and TRIM stream • Adjusted to a TRIM stream over 150 metres • Different resulting catchment basin after the adjustment of the sample location to TRIM stream
1	• Location highly uncertain even after review and verification on other data sources • Adjustment distance is greater than 300 metres • Different resulting catchment basin after the adjustment of sample location
0	• No 50k or TRIM streams within 300 metres • Manual inspection unable to resolve a reasonable location • Adjustment is not applied: site left at its original location

Step 3: Adjusting RGS Sample Sites to the Matched TRIM Streams

The automated process to adjust or "snap" the original locations of the RGS stream sample sites to their matched TRIM I streams is carried out in a spatial database. When a matched TRIM I stream is identified as the best candidate for a given stream sample site, the stream is selected from the database. The lineString of the selected stream is trimmed for 1 metre at the ends, to prevent potentially snapping a sample site to a confluence with multiple up stream edges, thus ambiguity in upstream query and in conflict with the RGS guide of selecting sample sites 60 metres above a confluence. The adjustment of the stream sample sites to the trimmed TRIM I streams is carried out with the nearest algorithm that is executed in a spatial database.

Manual adjustment is carried out in a desktop GIS for stream sample sites that are located on TRIM II streams as identified by visual inspection or manual checking in Step 2.

Step 4: Quality Assurance and Manual Fixing

The final step is to sort the results based on their confidence level and manually check the results with the assistance of TRIM II streams, digital elevation models, high resolution orthophotography and other sources of information. Manual inspection and correction are carried out where results are considered incorrect or at a low confidence level.

DISCUSSIONS OF RESULTS

Summary of the Original RGS Stream Sample Sites

Stream order for a sample site is useful in resolving

the ambiguity of a sample location (*e.g.*, a sample site between two streams of different stream orders), in conjunction with other data collected in the field such as stream width and depth.

In the RGS field data, stream orders are unknown for 8% of the stream sample sites that were mostly collected in 1976.

For the sample sites that stream orders were identified in the field, 53% of them are located on first or second order streams, 16% are on third order streams and 23% are on fourth order streams, and one of the sample sites is on a fifth order stream. Contradictory to what was stated in the RGS stream sample guide, 39% of the stream samples were collected on streams with streams order 3 and 4.

It is also discovered that even though the 50k NTS paper maps were used in the planning of sample site selection and locating of the actual sample sites in the field, there are sample sites that were collected at locations where streams were not mapped on the 50k NTS maps (Figure 2). Occasionally, streams were sketched by pencil on the paper maps.

Summary of Adjustment Results for Recent QUEST South Stream Sample Sites

The application of a simplified validation and refitting procedure yielded results with high confidence (Cui, 2010) to the recent infill stream samples from the QUEST South regional geochemical studies in 2009 (Jackaman, 2010). Out of the 785 sample sites, over 95% of them are automatically adjusted to the matching TRIM streams with high confidence after extensive manual review of the sites initially deemed as low confidence. Less than 5% of the sites are not near any TRIM streams and they are left at their original locations after review by Steve Reichheld who conducted the field survey.

The success is also partially attributed to the use of handheld GPS devices to locate the sample sites. For 36 samples sites with locations not near streams mapped on 50k NTS, or TRIM, or visible on orthophotography, the followings are the possible explanations (S. Reichheld, personal communication):

1) streams are small, usually under one metre in width;
2) meandering streams which have widened or changed courses since they were mapped;
3) samples were taken from small tributary off a main stream that likely didn't exist or were not mapped; and
4) samples were taken further upstream in the drainage than the 50k line shows.

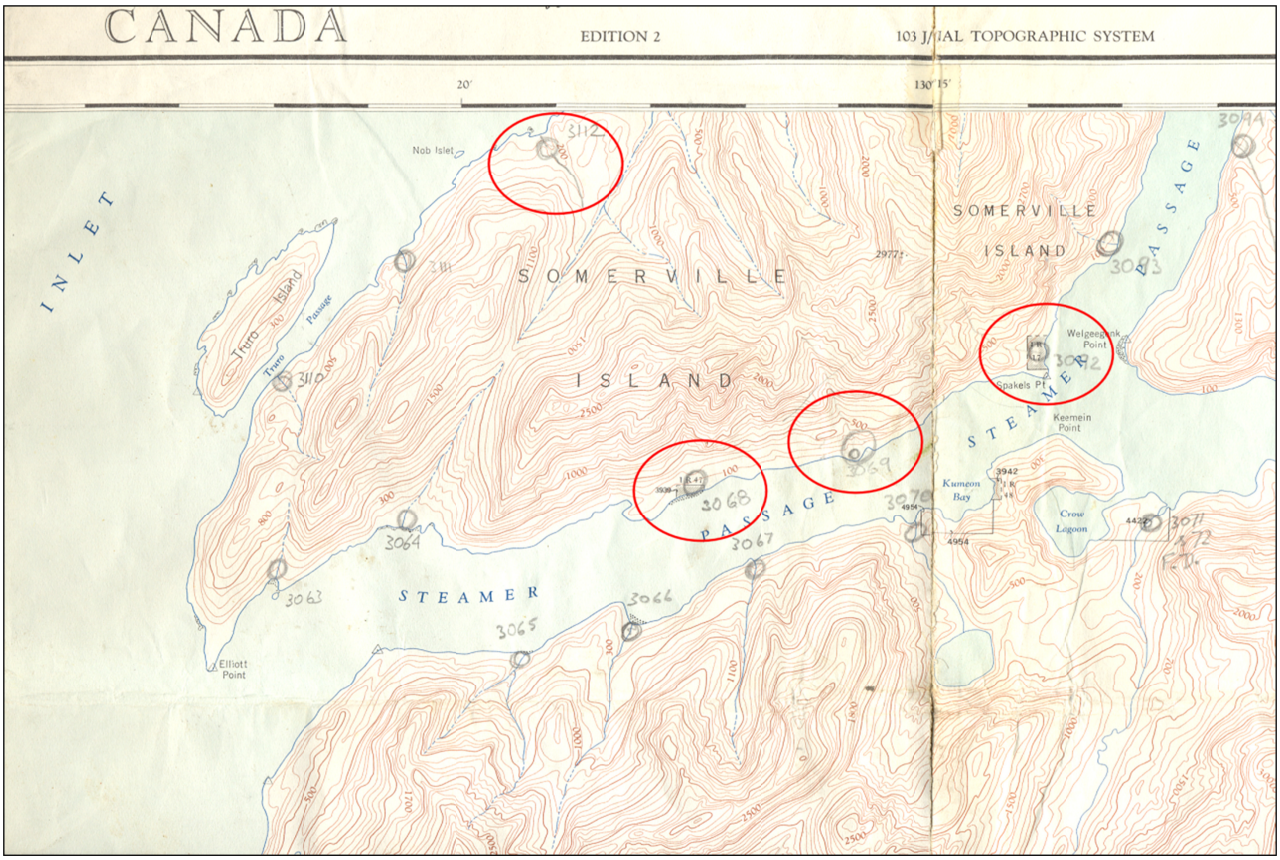

Figure 2. Examples of RGS stream samples collected on sites (in red circles) where 50k streams were not mapped on the 50 NTS paper map.

Summary of Adjustment Results for Stream Sample Sites Surveyed prior to 2008

The validation and refitting methodology has been applied to the RGS stream sample sites that were surveyed before 2008. A summary of the results follows the major steps in Figure 1, highlighting only the most common cases.

Sample sites located on 50k streams with matching TRIM streams

Among the RGS stream sample sites, 96% of them are located on or near 50k streams within a tolerance of 300 metres and 97% of the 50k streams for these sample sites have matching or equivalent TRIM streams. The automated adjustment of sample locations from the 50k streams to the TRIM streams is within 150 metres for 92% of the stream sample sites (Figure 3). However, 7% of the sites adjusted over 150 metres to the nearest matching TRIM streams. The cases assessed as highly uncertain (*e.g.*, over 200 metres) are visually inspected and manually adjusted if required, to ensure a high confidence level of the results (Figure 4).

The constraint on matching streams and equivalent stream orders is effective, as shown on Figure 5. Sample 92I813136 is closer to a third order TRIM stream flowing from the north which matches a first order 50k stream. However, the RGS field data indicates that this sample is collected on a fourth order stream, equivalent to the nearest third order 50k stream which matches the TRIM main stem (flowing from east) with a stream order of 5. With the constraints, this sample site is adjusted to the TRIM main stem with high confidence. In another case (Figure 6), the sample site (92H811428) is on a second order TRIM stream. The constraint on stream orders causes this sample site to be adjusted to a fourth order TRIM stream with acceptable confidence, because this sample was collected on a fourth order stream as recorded in the RGS field data.

The constraint on matching 50k streams and TIRM streams is also effective through the use of the cross-reference table (XREF_20K_50K_STREAMS) in resolving some of the ambiguities where a sample location can be adjusted to more than one TRIM stream. As shown on Figure 7, the 50k stream is closer to a TRIM stream to the west near the sample location (sample site 92G895273). The cross-reference table provides a match between the 50k stream and the TRIM stream to the east, causing the automated adjustment of the sample location to the TRIM stream on the east. However, it is worth pointing out that the cross-reference table should be treated as a reference source. If there is any concern on the result, the site should be visually inspected.

Sample sites located on 50k streams without matching TRIM streams

For the stream sample sites that are on or near 50k streams within a tolerance of 300 metres, 3% of the 50k

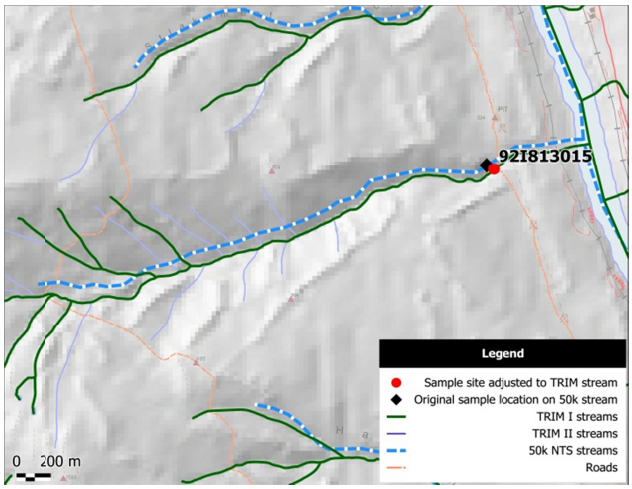

Figure 3. A case of high confidence on the sample location and adjustment result where a stream sample site (sample 92I813015) is located on a 50k stream within the tolerance and matched by a TRIM stream.

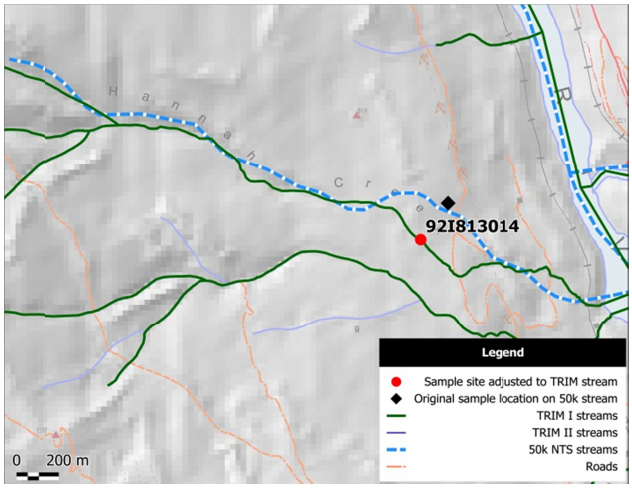

Figure 4. A case of acceptable confidence on the sample location and adjustment result where a stream sample site (sample 92I813014) is adjusted to a TRIM stream matching the 50k stream.

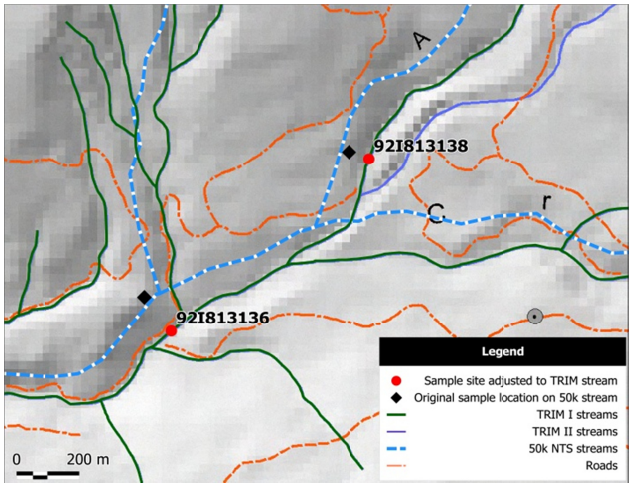

Figure 5. A case to show the effect of constraint on matching stream orders with high confidence.

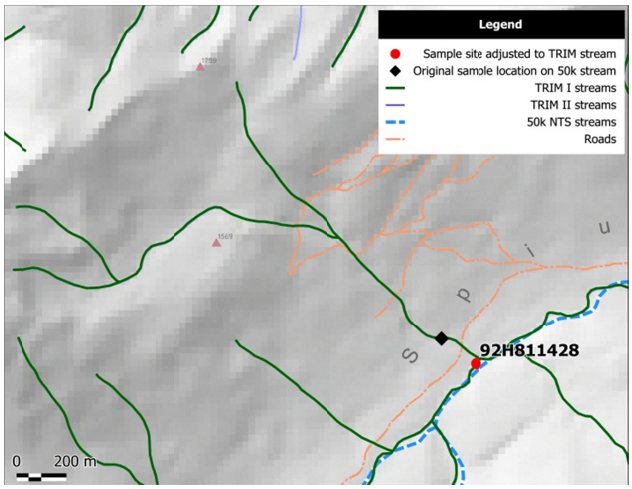

Figure 6. A case to show the effect of constraint on matching stream orders with acceptable confidence.

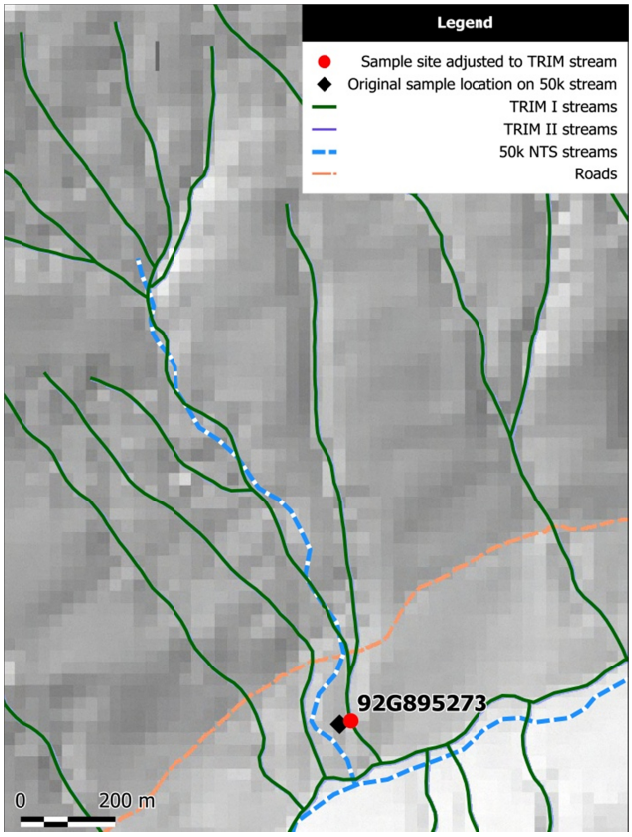

Figure 7. A case to show the effect of constraint on matching 50k streams with TRIM streams.

streams appear having no matching or equivalent TRIM streams using the cross-reference table XREF_20K_50K_STREAMS. In most cases, there are TRIM I streams within 150 metres of the stream sample sites. A 50k stream and a TRIM I stream are not matched usually because they have different upstream patterns (Figure 8). It is difficult to assign a confidence level to this kind of cases even after visual inspection.

When there is no TRIM I stream within 150 metres, the case should be inspected with the aid of the original 50k NTS paper maps, TRIM II streams and orthophotography. Some cases can be resolved by adjusting the sites to the nearest TRIM II streams with reasonable confidence (Figure 9). In other cases, the sites should be left at their original locations or adjusted to the nearest TRIM II streams with low confidence (Figure 10).

Sample sites not near 50k streams

For the 4% of the RGS stream sample sites that are not near any 50k stream within a tolerance of 300 metres, most of them are near TRIM I streams within 150 metres with an acceptable confidence level, typically as the case shown on Figure 11. A small number of stream sample sites are located on TRIM II streams (Figure 12).

In some cases there are TRIM streams near the sample sites but the results may not be acceptable. As shown in Figure 13, the field data indicates that sample 92J813009 was collected on a fourth order stream. However, the nearest TRIM II stream is order 1 and there is no fourth order stream within a reasonable distance.

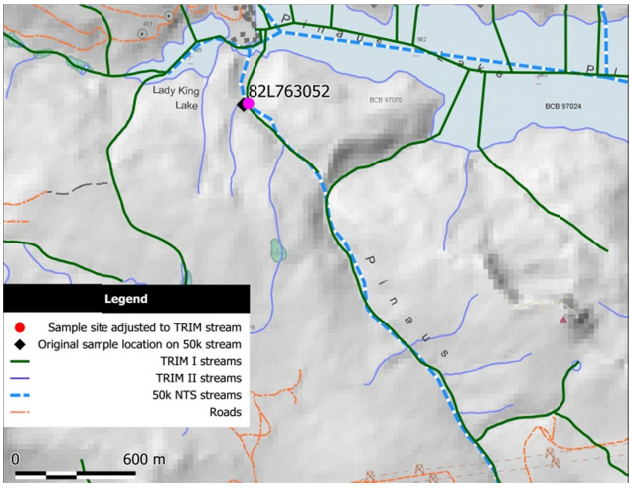

Figure 8. A case to show a stream sample site (82L763052) on a 50k stream that does not match the nearest TRIM I stream due to different upstream patterns.

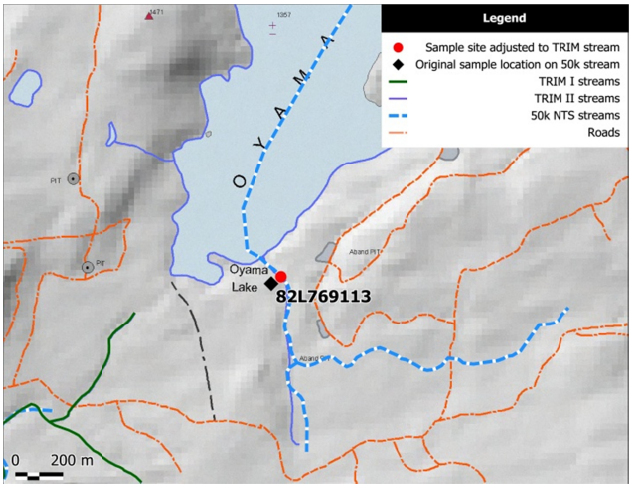

Figure 9. A case to show a stream sample site (82L769113) on a 50k stream that has no matching TRIM I stream mapped. This case is resolved by adjusting the site to a TRIM II stream.

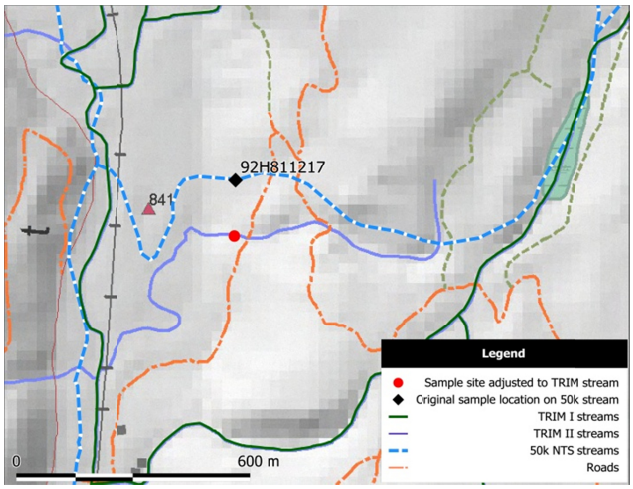

Figure 10. A case to show a stream sample site (92H811217) on a 50k stream that has no matching TRIM streams.

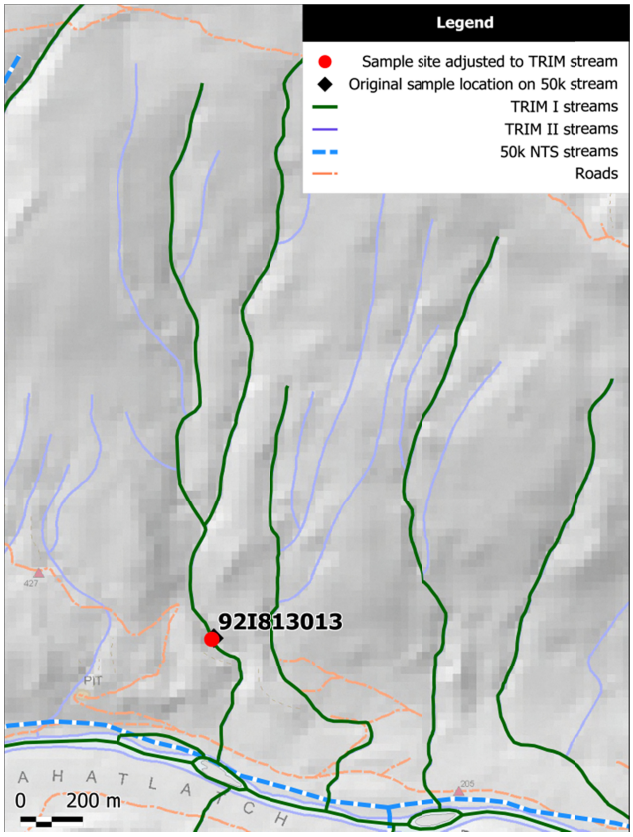

Figure 11. A case to show a stream sample site (92I813013) that is not near a 50k stream but is on a TRIM stream with acceptable confidence.

Only a small number of sites (1% of all the stream sample sites) are not near any streams. Some of the highly uncertain cases are shown on Figures 14 and 15.

One of the worst cases of location discrepancy is illustrated on Figures 16 and 17. Sample 92P793353 was collected on a fourth order stream based on the RGS field data (Figure 16). However, it is not near any 50k or TRIM stream with an order 4 or higher (Figure 16). An inspection of the hard copy 50k NTS map (Figure 16) indicates that the pencil sketch of the stream on the 50k NTS map for the sample site

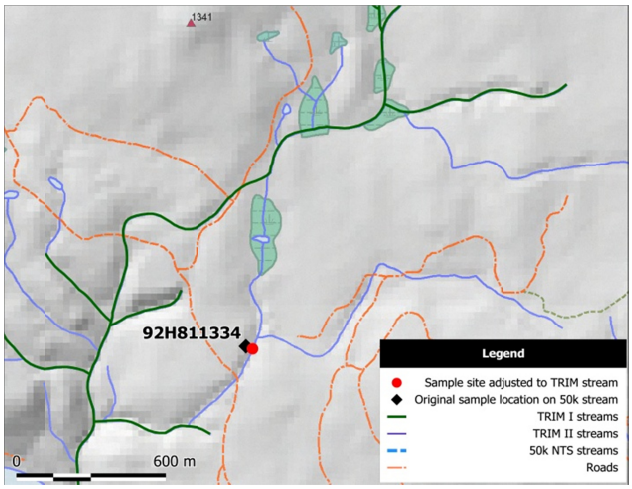

Figure 12. A case to show a stream sample site (92H811334) that is not near a 50k stream but is on a TRIM II stream with acceptable confidence.

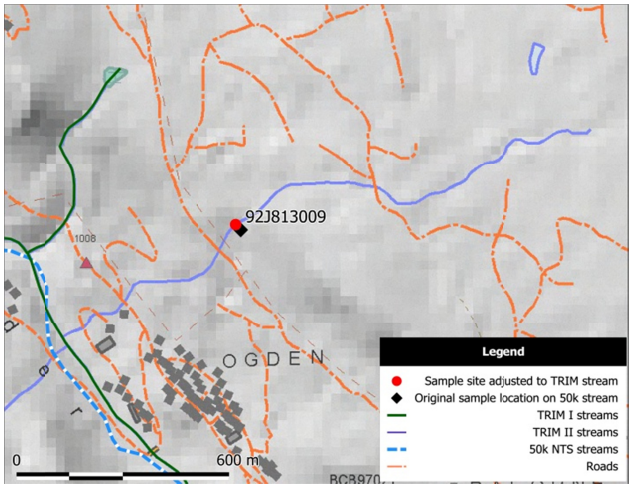

Figure 13. A case to show a stream sample site (92J813009) that is not near a 50k stream but is on a TRIM II stream with low confidence due to different stream orders between the TRIM II stream and the RGS field data.

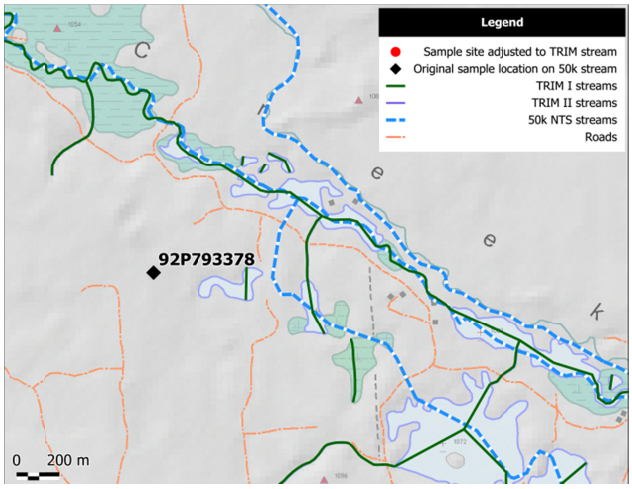

Figure 14. A case to show a stream sample site (92P793378) not near any streams.

matches a TRIM stream to the northeast of the sample site. If the location is adjusted to the matching TRIM stream (as shown by the red arrow), it represents a distance of over 680 metres. It is hoped that such case is an anomaly. Nevertheless it demonstrates that the location of the sample site could be off by over 600 metres.

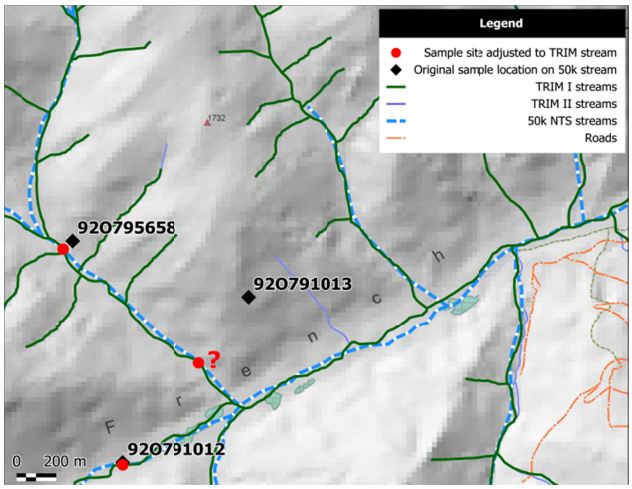

Figure 15. A case to show a stream sample site (92O791013) not near any streams.

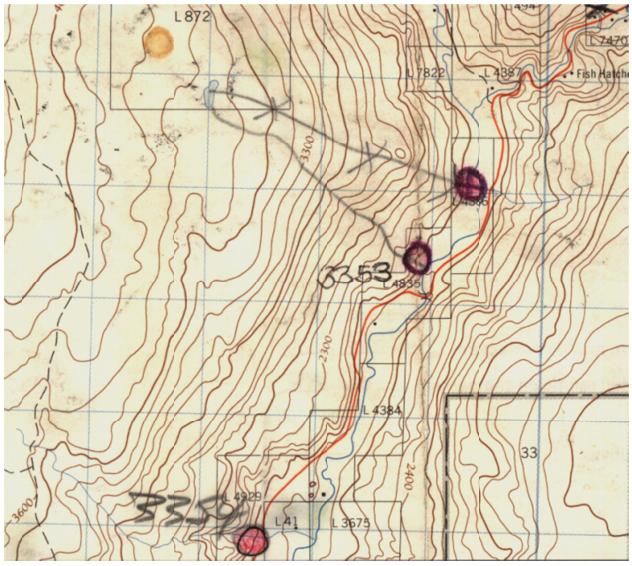

Figure 16. A stream sample site (3353) on a fourth order stream shown on the original 50k NTS paper map.

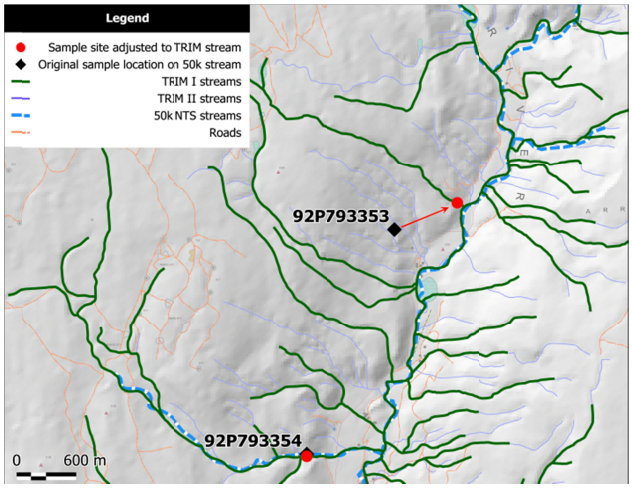

Figure 17. A stream sample site (92P793353, same as 3353 on Figure 16) that its location is off by over 600 metres from its original location as shown on Figure 16. The red arrow points to its original location.

Sources of Uncertainties

An attempt was made to document the sources of uncertainties. While an arbitrary confidence level can be assigned to a stream sample site based on the data quality criteria specified, the sources of uncertainties are not always obvious. As the case shown on Figures 16 and 17, it is difficult to speculate on the causes of the digital location off by over 600 metres away from the marked location on the paper map (Figure 16).

The validation on QUEST South stream sample sites and the cases documented so far for the pre-2008 stream sample sites shed some lights on the following sources of uncertainties:

- meandering streams which have widened or changed courses since they were mapped;
- samples were taken from small tributary off a main stream that were not mapped in 50k NTS or TRIM;
- different stream patterns between 50k streams and TRIM streams; and
- different definitions and field observations of stream orders in 50k streams, TRIM streams and RGS field data.

The following sources of uncertainties are possible but remain as a speculation pending further work:

- Data conversion between NAD27 and NAD83: difference up to 190 metres; and
- Errors in locations due to transcribing, conversion, or rounding.

Application of Results

The original locations of the RGS stream sample sites are suitable for geochemical modelling at a regional scale.

For more detailed analysis and geochemical modelling at finer granularity, the RGS stream sample sites should be validated and adjusted to the most detailed streams (*i.e.*, TRIM streams). This can be accomplished if the area is small enough by following and extending the methodology described in this paper.

Work is underway for future publication of a database of refitted RGS stream sample sites and updated catchment basins. Visual tools are also being developed for display in applications such as Google Earth.

ACKNOWLEDGMENTS

Ray Lett is thanked for sharing his knowledge and background information on the Regional Geochemical Survey program. Hailey Eckstrand assisted earlier effort on developing and testing the methodology. Aaron Chaput helped testing and inspecting some of the stream sample sites. Sophie Alexander from ioGlobal and Steve Reichheld reviewed some of the new stream sample sites in QUEST South. Discussions with Steve Reichheld are helpful on understanding the recent field survey. This manuscript benefited from a thorough review by Larry Jones and Pat Desjardins.

REFERENCES

Ballantyne, S.B. (1991): Stream geochemistry in the Canadian Cordillera: conventional and future applications for exploration; *in* Exploration Geochemistry Workshop, *Geological Survey of Canada*, Open File 2390, pages 6.1-6.74.

Bonham-Carter, G.F. and Goodfellow, W.D. (1986): Background correction to stream geochemical data using digitized drainage and geological maps: application to Selwyn Basin, Yukon and Northwest Territories; *Journal of Geochemical Exploration*, Volume 25, pages 139-155.

Bonham-Carter, G.F., Rogers, P.J. and Ellwood, D.J. (1987): Catchment basin analysis applied to surficial geochemical data, Cobequid Highlands, Nova Scotia; *Journal of Geochemical Exploration*, Volume 29, pages 259-278.

Cui, Y. (2010): QUEST South Regional Geochemical Survey: catchment basins for 2009 stream sample sites; *British Columbia Geological Survey* Geofile 2010-14, 4 pages.

Cui, Y., Eckstrand, H. and Lett, R. (2009): Regional Geochemical Survey: delineation of catchment basins for sample sites in British Columbia; *in* Geological Fieldwork 2008, *BC Ministry of Energy Mines and Petroleum Resources*, Paper 2009-1, pages 231-238.

Devillers, R. and Jeansoulin, R. (eds) (2006): Fundamentals of Spatial Data Quality; *Wiley-ISTE*, 309 pages.

Ehlschlaeger, C.R., Shortridge, A.M. and Goodchild, M.F. (1997): Visualizing spatial data uncertainty using animation; *Computers & Geosciences*, Volume 23, Issue 4, May 1997, pages 387-395.

Garrett, R.G., Kane, V.E. and Zeigler, R.K. (1980): The management and analysis of regional geochemical data. Journal of Geochemical Exploration, Volume 13, Numbers 2/3, pages 115-152.

Goodchild, M.F. and Gopal, S. (eds) (1989): Accuracy of Spatial Database; *Taylor and Francis*, Landon.

Guptill, S.C. and Morrison, J.L. (eds) (1995): Elements of spatial data quality (The International Cartographic Association); *Elsevier Science*, Oxford and Tarrytown NY, 202 pages.

Hawkes, H.E. (1976): The downstream dilution of stream sediment anomalies; *Journal of Geochemical Exploration*, Volume 6, pages 345-358.

Jackaman, W. (2010): QUEST South geochemical data, Southern British Columbia; *Geoscience BC* Report 2010-13, 153 pages.

Jackaman, W. and Balfour, J.S. (2007): QUEST project geochemistry: field surveys and data re-analysis (parts of NTS 093A, B, G, H, J, K, N, O), central British Columbia; *in* Geological Fieldwork 2006, *Geoscience BC,* Report 2007-1, pages 311-314.

Jackaman, W. and Matysek, P.F. (1995): British Columbia Regional Geochemical Survey – Nass River (NTS 103O/P); *BC Ministry of Energy, Mines and Petroleum Resources*, BC RGS 43.

Leggo, M.D. (1977): Contrasting geochemical expression of copper mineralization at Namosi, Fiji; *Journal of Geochemical Exploration*, Volume 8, pages 431-456.

Lett, R.E. (2005): The regional geochemical survey database on CD; *British Columbia Geological Survey* Geofile 2005-17; 8 pages.

Lett, R.E. and Jackaman, W. (2004): Stream geochemical survey guide; *British Columbia Geological Survey* Geofile 2004-07, 15 pages.

Massey, N.W.D. (1995): Geology and mineral resources of the Alberni – Nanaimo Lakes sheet, Vancouver Island, 92 F/1W, 92 F/2E and part of 92 F/7E; *BC Ministry of Energy, Mines and Petroleum Resources*, Paper 1992-2, 132 pages.

Matysek, P.F. and Jackaman, W. (1995): British Columbia Regional Geochemical Survey – Prince Rupert/Terrace (NTS 103I/J); *BC Ministry of Energy, Mines and Petroleum Resources*, BC RGS 42.

Matysek, P. and Jackaman, W. (1996): B.C. regional geochemical survey anomaly recognition, an example using catchment basin analysis (103I, 103J); *in* Geological Fieldwork 1995, *BC Ministry of Energy, Mines and Petroleum Resources*, Paper 1996-1, pages 185-190.

Shi, W.Z., Fisher, P.F. and Goodchild, M.F. (eds) (2002): Spatial Data Quality; *Taylor & Francis Group / CRC Press*, 2002, London and New York, 313 pages.

Shmoto, H. and Rye, R.O. (1979): Isotopes of sulfur and carbon; in Geochemistry of Hydrothermal Ore Deposits (Second Edition), Barnes, H.L., Editor, *John Wiley and Sons*, New York, pages 509-567.

Sibbick, S.J. (1994): Preliminary report on the application of catchment basin analysis to regional geochemical survey data, northern Vancouver Island (NTS 092L/03,04,05 and 06); *in* Geological Fieldwork 1993, *BC Ministry of Energy Mines and Petroleum Resources*, Paper 1994-1, pages 111-117.

Sleath, A.W. and Fletcher, W.K. (1982): Geochemical dispersion in a glacier melt-water stream, Purcell Mountains, B.C.; *in* Prospecting in areas of glaciated terrain 1982, *Canadian Institute Mining Metallurgy*, pages 195-203.

A Comparison of Several Commercially Available Methods for the Geochemical Analysis of Rare Earth, Rare Metal and High Field Strength Elements in Geological Samples

by R.E. Lett and K. Paterson[1]

KEYWORDS: REE, RM, HFES, geochemical analysis, gold deposits

INTRODUCTION

Rare earth elements (REE: La, Ce, Pr, Nd, Sm, Eu, Gd, Tb, Dy, Ho, Er, Tm, Yb, Lu), rare metals (RM: Sc, Nb, Ta) and high field strength elements (HFSE: Y, Zr, Hf) are important components in a wide range of industries such as the manufacture of computers, wind turbines and hybrid cars. They are also used extensively in geoscience research as a geochemical tool for discriminating different rock types or petrotectonic environment. Industry and geoscience research need an accurate estimation of REE, RM and HFSE content of rock and ore samples to satisfy both economic and scientific credibility. Fortunately, today, there are a number of analytical methods that satisfy this requirement. Some of the techniques, such as x-ray fluorescence (XRF) described by Potts and Webb, 1992, and instrumental neutron activation (INAA) described by Hoffman, 1992, and El-Taher, 2006 are non-destructive and are considered to produce an accurate determination of REE, RM and HFSE values. Other methods such as a fusion, sinter or acid digestion (Longerich *et al.*, 1990; Hall and Pelchat, 1990, Bayon *et al.*, 2009) are, by contrast, destructive and generate elemental values that range from near total to a partial estimate depending on the ability of the fusion or the digestion technique to completely release an element from rock-forming minerals in the sample. A reliable estimation of a rare earth-rare metal concentration before an economic resource requires a method to be accurate and precise, but not necessarily to be particularly sensitive because economic grades greatly exceed detection limits. However, high accuracy, good precision and low detection limits are all desirable criteria for a technique that will be used for lithogeochemical research.

Hall and Plant (1992) carried out a comprehensive and detailed study of the accuracy and precision of RE and HFS elements obtainable from XRF, INAA, lithium metaborate fusion - inductively coupled plasma mass spectrometry (ICPMS), and 4 acid (hydrofluoric-nitric-perchloric-hydrochloric) digestion-ICPMS analysis of bedrock samples and 8 reference standards. The aim of their study was to assess the reliability of REE and HFSE data produced by commercial laboratories. This paper describes a similar study using commercial laboratory analysis of bedrock samples from the Spanish Mountain Au deposit and the Galore Creek porphyry Cu-Au deposit in British Columbia and a reference standard, for REE, RM and HFSE elements by INAA, sodium peroxide sinter and inductively coupled plasma mass spectrometry (sinter-ICPMS), lithium metaborate-tetraborate fusion–inductively coupled plasma mass spectrometry (LMB–ICPMS), 4 acid digestion-ICPMS, XRF and AR (hydrochloric-nitric acid) digestion–ICPMS.

ANALYTICAL METHODS

All samples were jaw crushed in a Rhino TM™ jaw crusher, split into a subsample with a Jones splitter and a 100-150 gram subsample milled to 95 percent – 150 mesh in a Rocklabs™ ring and puck mill in the laboratory of the British Columbia Geological Survey, Victoria. Milled subsamples and quality control samples (sample duplicates, milled quartz blanks, a CANMET reference standard) were analyzed for REE, HFSE and RM at several laboratories by the following methods:

1) XRF analysis: La, Y, Nb and Zr were determined by x-ray fluorescence using a lithium metaborate-tetraborate pressed pellet (1 g sample: 5 g lithium metaborate-tetraborate) and Siemens model 3000 x-ray fluorescence spectrometer at Global Discovery Laboratories (now Acme Analytical Laboratories), Vancouver British Columbia.
2) INAA analysis: La, Ce, Nd, Sm, Eu, Tb, Yb, Lu, Sc, Ta, Cs were determined by irradiating 1-2 g of the milled rock sample for 20 minutes in a neutron flux (10^{11} neutrons/cm^2/second) and then, after a decay period of approximately 1 week, measuring the gamma-ray emissions from the sample with a gamma-ray spectrometer

[1] *Artisanal Gold Council, Victoria, BC*

This publication is also available, free of charge, as colour digital files in Adobe Acrobat® PDF format from the BC Ministry of Forests, Mines and Lands website at http://www.empr.gov.bc.ca/Mining/Geoscience/PublicationsCatalogue/Fieldwork.

equipped with a high resolution, coaxial germanium detector (Hoffman, 1992).

3) Sinter-ICPMS analysis: La, Ce, Pr, Nd, Sm, Eu, Gd, Tb, Dy, Ho, Er, Tm, Yb, Lu, Y, Nb, Zr, Ta and Hf were determined by sintering 0.2 g of milled rock with 0.8 g of sodium peroxide for 1 hour at 480°C in a closed nickel crucible (Longerich *et al.*, 1990). After dissolution of the sinter cake in 8M nitric acid the solution was analyzed for elements using an HP 4500 plus ICPMS at the Department of Earth Sciences, Memorial University, Newfoundland.

4) LMB-ICPMS analysis: La, Ce, Pr, Nd, Sm, Eu, Gd, Tb, Dy, Ho, Er, Tm, Yb, Lu, Cs, Y, Sc, Ta, Nb, Zr were determined by fusing 0.2 g of milled rock with lithium metaborate-lithium tetraborate flux at 980°C in a graphite crucible, dissolving the fused bead with weak hydrofluoric and hydrochloric acids and analyzing the solution by ICPMS at Acme Analytical Laboratories, Vancouver.

5) 4 acid digestion-ICPMS: La, Ce, Y, Hf, Nb, Zr, Ta, Sc were determined by digesting 0.5 g of milled sample in Teflon test tubes with HF-$HClO_4$-HNO_3-HCl acids and ICPMS analysis of the solutions at Acme Analytical Laboratories, Vancouver, British Columbia.

6) AR-ICPMS: La, Sc, were determined by digestion in HNO_3-HCl-H_2O and ICPMS analysis at Acme Analytical Laboratories, Vancouver, British Columbia.

Table 1 lists elements determined by methods 1 to 6 and detection limits reported by the laboratories for each element.

ORIGIN OF THE SAMPLES

Two groups of samples were used in the study. One group of 60 bedrock samples and diamond drill core samples were collected from the Spanish Mountain Au deposit and analysed as part of a University of Victoria B.Sc. Honours Thesis project (Paterson, 2009). Results of the project are also described by Paterson *et al.* (2009). All of the samples from Spanish Mountain were analysed for major, minor and trace elements by INAA, 4-acid - ICPMS, AR-ICPMS and by XRF. Selected samples were also analyzed for REEs by sinter-ICPMS and by LMB-ICPMS. Figure 1 shows the location of the Spanish Mountain and Galore Creek deposits and Figure 2 shows the distribution of mainly argillite and greywacke samples collected from the Spanish Mountain property. A second group of 27 volcanic and mineralized intrusive bedrock samples were collected by Logan, 2005, during a previous study of Galore Creek Cu-Au deposit.

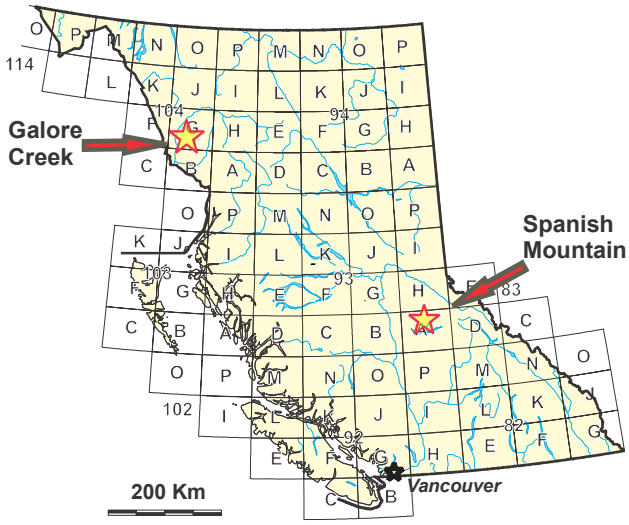

Figure 1. Locations of the Spanish Mountain Au and Galore Creek Cu-Au deposits.

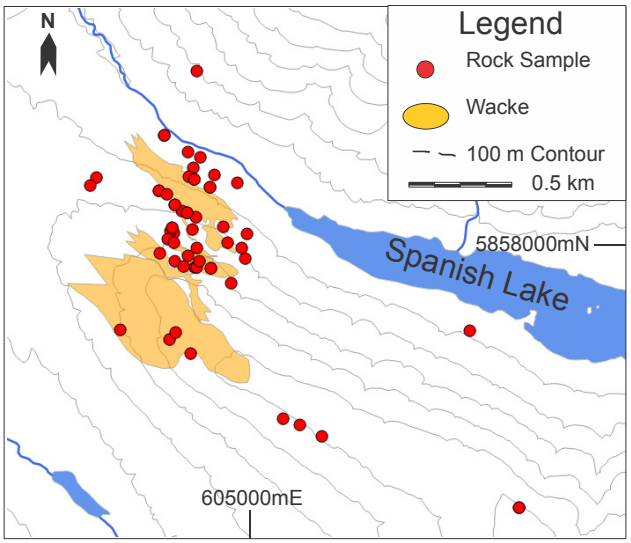

Figure 2. Location of bedrock and diamond-drill core samples collected by Paterson (2009), from the Spanish Mountain property.

ACCURACY AND PRECISION

As part of the British Columbia Geological Survey quality control program, the CANMET diorite gneiss standard SY4 (Bowman, 1995) is analysed routinely for REE, RM and HFSE by XRF, INAA, sinter-ICPMS, LMB-ICPMS and 4 acid-ICPMS. While the number of SY4 repeat determinations by each method is small (4-6 analyses), the analytical results allow a direct comparison of accuracy and precision for elements by different methods. For example, SY4 is analysed for La, Ce, Hf and Ta by all methods except AR – ICPMS. Figure 3 compares the mean value for La in SY4 by sinter-ICPMS, INAA, LMB-ICPMS and 4 acid-ICPMS, and the ±2 standard deviation (2 σ) range from multiple analyses, with the La content in SY4 (58 ppm) recommended by Bowman (1995). Mean La values by sinter-ICPMS, LMB-ICPMS

Table 1. Instrumental detection limits for elements described in this study by XRF, INAA, sinter-ICPMS, LMB-ICPMS, 4 acid-iCPMS and AR-ICPMS. Elements are grouped into REE, RM and HFSE.

Element	XRF	AR ICPMS	4 ACID ICPMS	INAA	Sinter-ICPMS	LMB-ICPMS
Units	ppm	ppm	ppm	ppm	ppm	ppm
REE						
La	3	0.5	0.1	0.5	0.03	0.1
Ce			1	3	0.14	0.1
Pr					0.02	0.02
Nd				5	0.03	0.3
Sm				0.1	0.8	0.05
Eu				0.2	0.04	0.02
Gd					0.07	0.05
Tb				0.2	0.01	0.01
Dy					0.06	0.05
Ho					0.01	0.02
Er					0.06	0.03
Tm					0.01	0.01
Yb				0.2	0.08	0.05
Lu				0.05	0.01	0.01
RM						
Cs				1		0.1
Sc		0.1	1	0.1		
Ta			0.1	0.5	0.08	0.1
HFSE						
Hf			0.1	1	0.09	0.1
Nb	3		0.1		0.08	0.1
Y	3		0.1		0.04	0.1
Zr	3		0.1		0.07	0.1

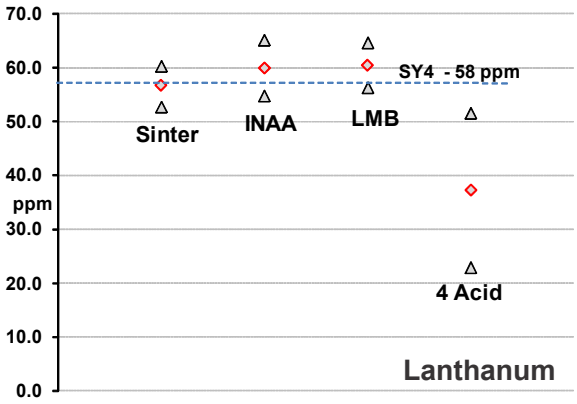

Figure 3. Determinations of La in SY4 by sinter-ICPMS, INAA, LMB-ICPMS and 4 acid - ICPMS. The mean value is indicated by a diamond symbol. The ±2 standard deviation range from the repeat analyses is shown by the triangle symbols and the recommended average La content (58 ppm) in SY4 (Bowman, 1995) is a broken line.

and INAA are within ±3 ppm of the recommended value and the ±2 standard deviation range is 4.5 ppm. However, the mean La value by 4 acid-ICPMS is 20 ppm lower than the recommended value and the ±2 standard deviation range is 14 ppm indicating that not all of the La is recovered by acid digestion from the standard matrix and there is a greater variation in values.

Figure 4 similarly compares the mean Ce value ±2 standard deviations in CANMET SY4 by the same four analytical methods with the recommended value for Ce in SY4 (122 ppm; Bowman, 1995). Cerium by sinter-ICPMS, INAA and LMB-ICPMS is within ±13 ppm of the recommended values for SY4 (122 ppm) with the INAA Ce having the largest variation. The Ce mean by 4 acid digestion ICPMS is much lower than by the other methods. In general, the precision estimate from the mean ±2 standard deviation range decreases in order from sinter-ICPMS > INAA> LMB-ICPMS => 4 acid digestion ICPMS.

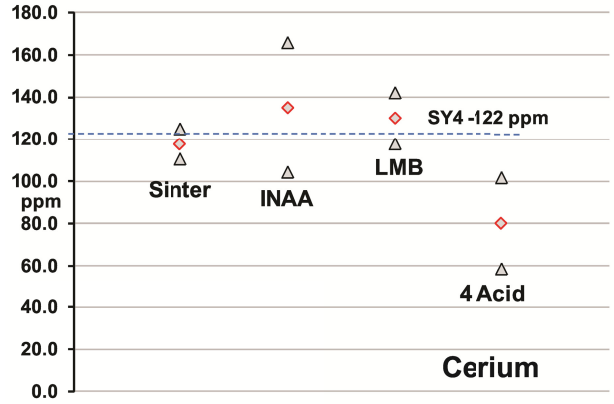

Figure 4. Determinations of Ce in SY4 by sinter-ICPMS, INAA, LMB-ICPMS 4 acid-ICPMS. symbols are the same as Figure 3. the recommended average Ce content (122 ppm) in SY4 (Bowman, 1995) is a broken line.

Precision and accuracy for Hf, Zr, Nb and Y from analyses of SY4 by multiple methods are compared in Figures 5, 6, 7 and 8. Only Hf is determined by INAA, whereas Zr, Y and Nb are measured by XRF. Mean Hf values are within 1.2 ppm of the CANMET recommended value (10.6 ppm) and the departure of the mean values from the standard are in the order INAA < sinter-ICPMS < LMB-ICPMS < 4 acid-ICPMS Hf. The Hf content in SY4 by LMB-ICPMS is clearly higher than the recommended value and the 4 acid-ICPMS Hf value is much lower (Figure 5). Hafnium precision estimated from the +/- 2 standard deviation range is in the order sinter-ICPMS> LMB> INAA> 4 acid-ICPMS.

Zirconium precision and accuracy from the analysis of SY4 is similar to Hf except that XRF replaces INAA as the non destructive method of analysis (Figure 6). From a comparison of the mean Zr value by XRF (513 ppm) to the recommended value (517 ppm) this is clearly the most precise and accurate of the four analytical methods. The Zr mean by sinter-ICPMS is 69 ppm above the recommended value whereas the Zr mean by LMB-ICPMS is 42 ppm higher than the recommended value. By contrast to LMB-ICPMS and sinter-ICPMS analysis, the 4 acid digest-ICPMS only recovers 48 ppm Zr from the standard. Although XRF is most accurate of the methods for Zr at a concentration similar to the standard the analytical error may be larger close to the XRF 3 ppm detection limit. Sinter-ICPMS and LMB-ICPMS have an advantage over XRF in that they can detect Zr to a lower detection limit (0.1 ppm) and consequently, have a higher accuracy at a lower concentration.

Unlike other REEs and HFSEs, the Nb content in SY 4 determined by XRF, LMB and 4 acid-ICPMS is very similar and is within 1 ppm of 13 ppm (Figure 7). However, the sinter-ICPMS Nb mean is more than 3 ppm higher than the recommended value. The larger ±2 standard deviation range for Nb by XRF, compared to the other methods, most likely reflects a value close to the 3 ppm Nb-XRF detection limit. Among common rock forming minerals zircon is known to be a host for Nb, but

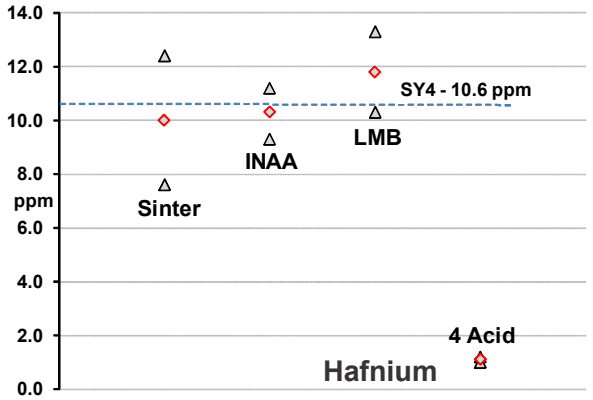

Figure 5. Determinations of Hf in SY4 by sinter-ICPMS, INAA, LMB-ICPMS and 4 acid digestion-ICPMS. Symbols are the same as Figure 3. The recommended average Hf content (10.6 ppm) in SY4 (Bowman, 1995) is a broken line.

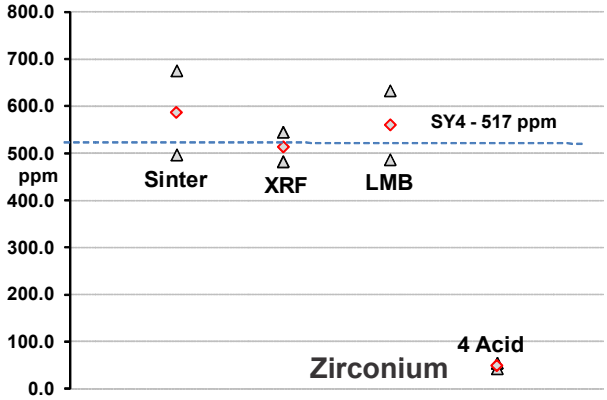

Figure 6. Determinations of Zr in SY4 by sinter-ICPMS, XRF, LMB-ICPMS and 4 acid digestion-ICPMS. Symbols are the same as Figure 3. The recommended average Zr (517 ppm) content in SY4 (Bowman, 1995) is a broken line.

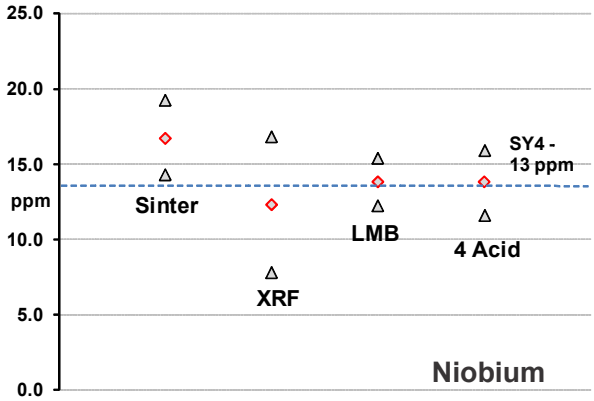

Figure 7. Determinations of Nb in SY4 by sinter-ICPMS, XRF, LMB-ICPMS and 4 acid digestion-ICPMS. Symbols are the same as Figure 3. The recommended average Nb content (13 ppm) in SY4 (Bowman, 1995) is a broken line.

the similar Nb mean by 4 acid-ICPMS compared to a much lower Zr mean suggests other rock forming mineral (*e.g.* Fe-Ti oxides) hosts the Nb. Figure 8 shows that the accuracy and precision for Y in SY4 follows the order of XRF> LMB-ICPMS> sinter-ICPMS> 4 acid-ICPMS.

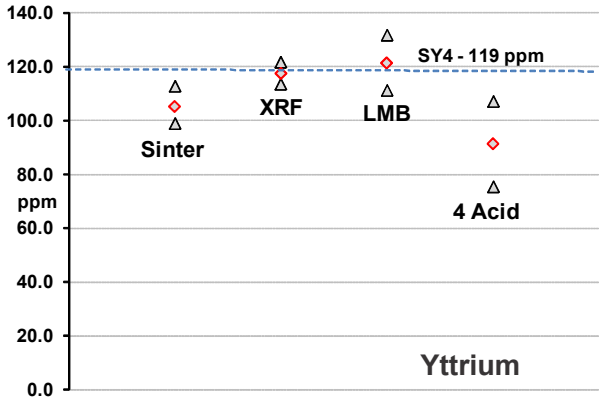

Figure 8. Determinations of Y in SY4 by sinter-ICPMS, XRF, LMB-ICPMS and 4 acid digestion-ICPMs. Symbols are the same as Figure 3. The recommended average Y content (119 ppm) in SY4 (Bowman, 1995) is a broken line.

Mean values and ±2 standard deviation ranges of Eu and Lu (typical of the heavier REEs) in SY4 by sinter-ICPMS, INAA and LMB-ICPMS are shown in Figures 9 and 10. Both elements display similar patterns

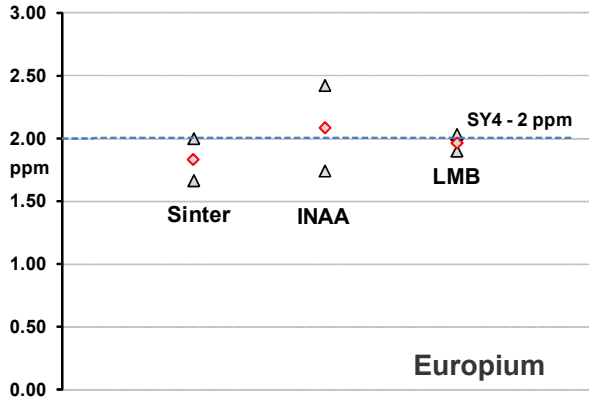

Figure 9. Determinations of Eu in SY4 by sinter-ICPMS, INAA and LMB-ICPMS. Symbols are the same as Figure 3. The recommended average Eu content (2 ppm) in SY4 (Bowman, 1995) is a broken line.

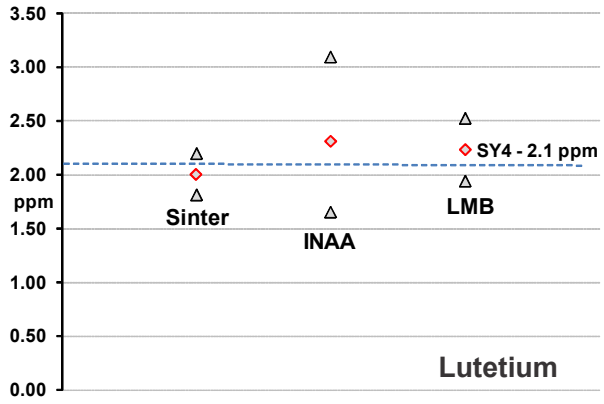

Figure 10. Determinations of Lu in SY4 by sinter-ICPMS, INAA and LMB-ICPMS. Symbols are the same as Figure 3. The recommended average Lu content (2.1 ppm) in SY4 (Bowman, 1995) is a broken line.

with mean values close to those recommended (Eu = 2 ppm, Lu = 2.1 ppm). The wider +/- 2 standard deviation range for INAA Eu and Lu could reflect values closer to the INAA detection limit compared to the sinter and LMB-ICPMS detection limits.

COMPARISON OF PARTIAL AND NEAR TOTAL METHODS FOR ANALYSIS

Aqua regia (HCl-HNO_3) or a similar mineral acid reagent (*e.g.* HCl-HNO_3-H_2O) is commonly used to dissolve soil, drainage sediment and rock samples before analysis by ICPMS for a range of ore indicator, mineralization pathfinder and other trace elements. Rare-earth element analyses produced by such acid digestions can be useful for outlining areas of mineralized bedrock. However, the determinations must be used cautiously if REE data are applied to geological research because accurate element values are essential for a confident interpretation of lithogeochemical results. There is often only a partial REE recovery by the acid digest from the different rock-forming minerals in the sample, limiting the usefulness of the results. An example of variable REE release is illustrated in Figure 11 by a scatter graph of La determined by AR-ICPMS (partial recovery) plotted against La determined by INAA (near-total estimate) from analyses of the rock samples from Spanish Mountain. A poor correlation between AR-ICPMS La and INAA La (correlation coefficient, R^2 = 0.422) and the analyses are scattered along a trend line of increasing La concentration. The scatter of values and the 0.3326 regression coefficient suggest that a varying, partial amount of the INAA determined La is liberated from individual samples by the AR-ICPMS acid digestion.

The stronger 4 acid digestion improves the La recovery from rock samples. For example, in Figure 12, La determined by the 4 acid digestion is plotted against La determined by INAA for the same samples. The values are more closely grouped along a common trend and the

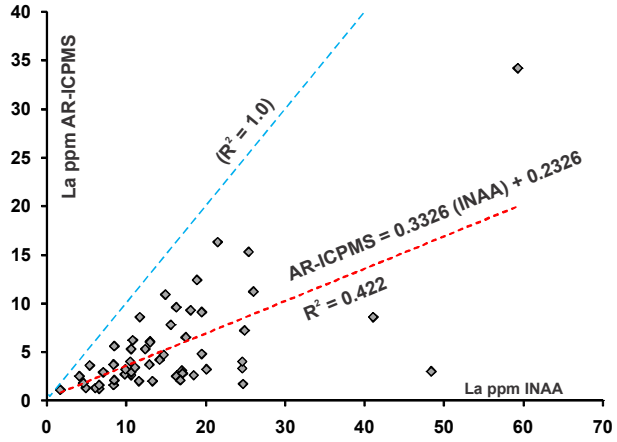

Figure 11. Scatter plot for La determined by AR-ICPMS and INAA in rock samples from Spanish Mountain. A least mean squares trend line, a regression equation and the correlation coefficient are shown on the graph and the trend line for a 1:1 correlation.

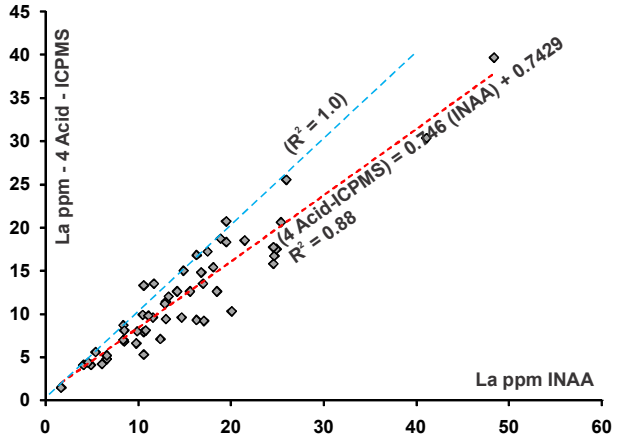

Figure 12. Scatter plot for La determined by 4 acid - ICPMS and INAA in rock samples from Spanish Mountain. A least mean squares trend line, a regression equation and the correlation coefficient are shown on the graph and the trend line for a 1:1 correlation.

correlation coefficient for the two populations is now R^2 = 0.88. However, the coefficient of 0.746 for the La-INAA – La 4 acid-ICPMS regression equation suggests that the acid still fails to release all of the La from samples. Although there are only 9 samples from Spanish Mountain analysed for La by INAA and LMB-ICPMS the correlation between the two populations is high (coefficient of R^2 = 0.996) with negligible scatter along the regression line (Figure 13). The coefficient of 0.9668 for the La-LMB-La-INAA regression equation indicates that virtually all of the La is determined by the two methods from the same samples.

While the rock samples from Galore Creek have only been analysed for REE elements by sinter-ICPMS and LMB-ICPMS the larger number of samples (29) allows comparison of results by the two methods over a different concentration range and in different rock types. Scatter graphs for La by sinter-ICPMS vs. La by LMB-ICPMS; Eu by sinter-ICPMS vs. Eu by LMB-ICPMS and for Lu by sinter-ICPMS vs. Lu by LMB-ICPMS in Figures 14, 15 and 16 all show that values cluster close to a trend line. Correlation coefficients are close to 1 and, similarly, the coefficients for the LMB-ICPMS – sinter-ICPMS equation are also close to 1.

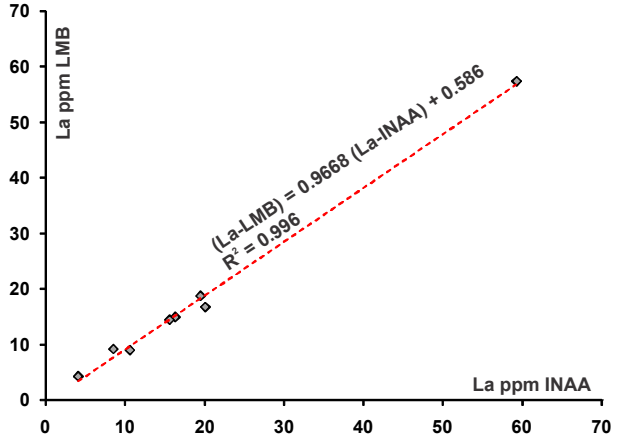

Figure 13. Scatter plot for La determined by LMB-ICPMS and INAA in the 9 rock samples from Spanish Mountain. A least mean squares trend line, a regression equation and the correlation coefficient are shown on the graph and the trend line for a 1:1 correlation.

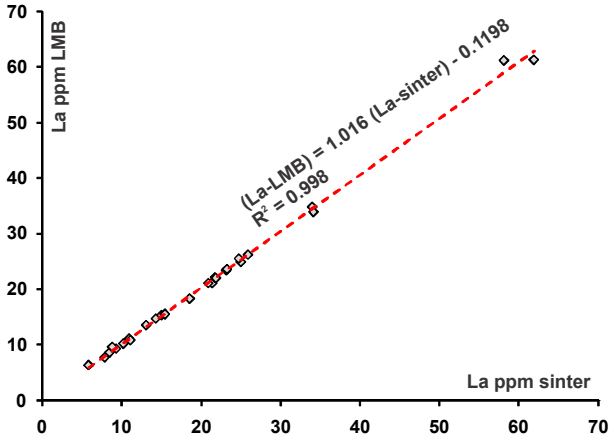

Figure 14. Scatter plot of La by LMB-ICPMS and by sinter-ICPMS in 29 rock samples from Galore Creek.

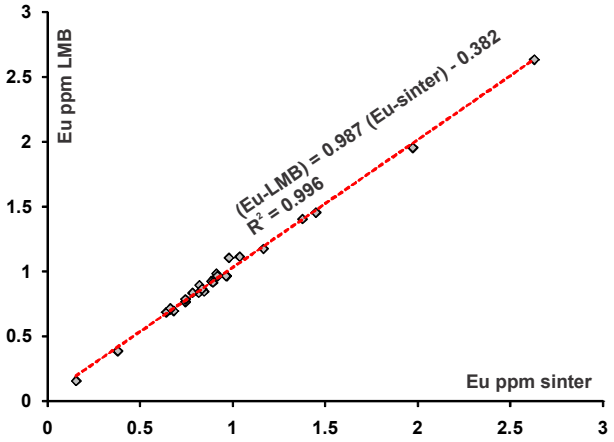

Figure 15. Scatter plot of Eu by LMB-ICPMS and by sinter-ICPMS in 29 rock samples from Galore Creek.

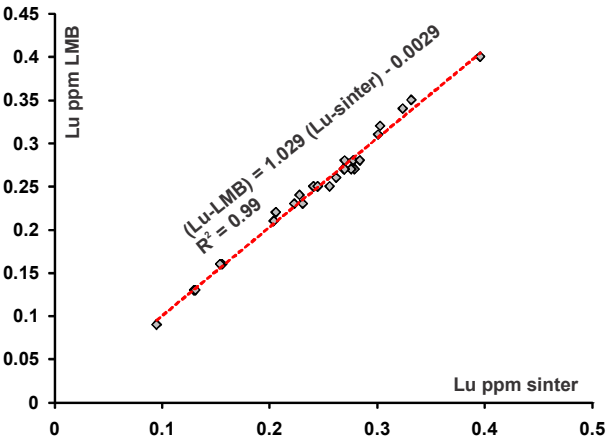

Figure 16. Scatter plot of Lu by LMB-ICPMS and by sinter-ICPMS in 29 rock samples from Galore Creek.

A practical application of comparing REE analyses using different digestions and sinter-ICPMS/fusion-ICPMS methods is to select the most suitable technique in terms of sensitivity, accuracy and economy for producing the data needed to create chondrite-normalized and other discrimination diagrams. Figure 17 is an example of a REE diagram from two argillite samples from the Spanish Mountain suite analysed by LMB-ICPMS and INAA. The only obvious divergence along the common REE plot for Argillite 1 is for Ce where the chondrite-normalized INAA Ce value is noticeably higher than LMB-ICPMS Ce value. Argillite 2 has much lower REE content and there is a greater difference between the INAA and LMB-ICPMS plots largely due to the Eu and Tb levels below the INAA detection limit. This emphasizes a requirement that an REE analytical method must have a detection limit able to cover a concentration range anticipated in all rock types.

A second comparison of chondrite-normalized values for a wacke and argillite from Spanish Mountain is shown in Figure 18. Plots for argillite and a wacke samples by sinter-ICPMS and LMB-ICPMS show a marked difference in the REE signature of the two rock types that

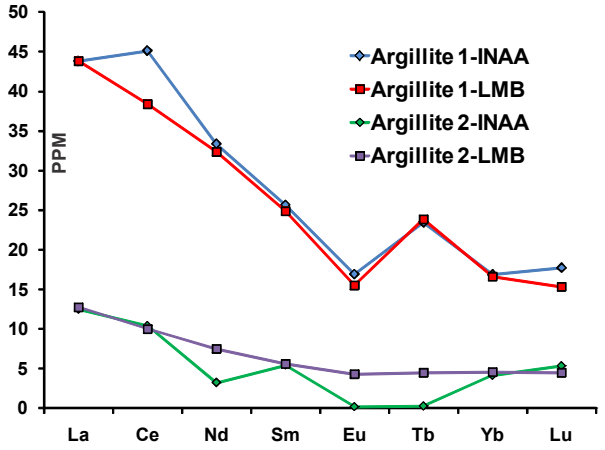

Figure 17. Chondrite-normalized (Nakamura, 1974) REE plot of two argillite samples from Spanish Mountain analysed by LMB fusion-ICPMS and INAA.

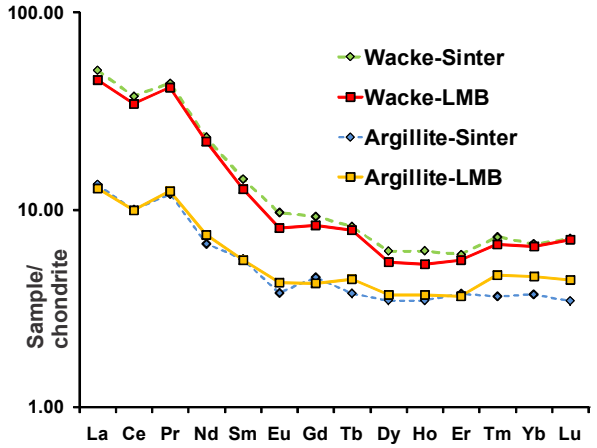

Figure 18. Log transformed chondrite-normalized (Nakamura, 1974) REE plot of argillite and wacke samples from Spanish Mountain analysed by LMB fusion-ICPMS and sinter-ICPMS.

possibly reflects a difference in the geochemistry of continental derive sediment (wacke) and island arc derived sediment (argillite). However, the two methods do produce very similar REE plots for each rock type. The only significant difference between the plots is for the heavier REEs, (Tm, Yb, Lu) in the argillite sample. A third example of sinter-ICPMS and LMB-ICPMS REE analysis (Figure 19) shows chondrite-normalized diagrams for three rock samples from Galore Creek. The two biotite-monzonite dikes show increasing light REE enrichment compared to the basalt and the only noticeable difference between the plots for the heavier REEs in the dike samples.

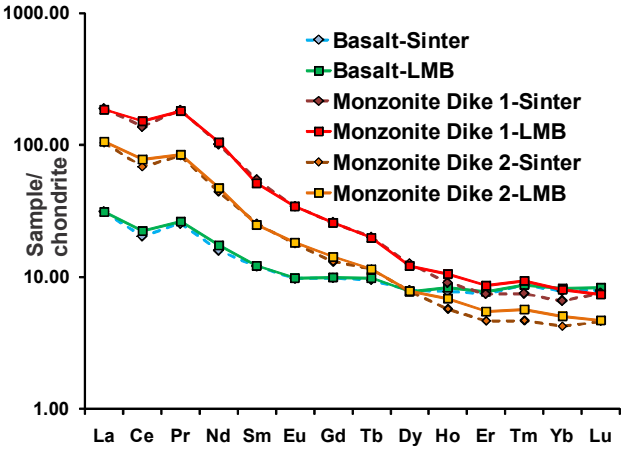

Figure 19. Log transformed chondrite-normalized (Nakamura, 1974) REE plot of a basalt and two bioite-monzonite dike samples from Galore Creek analysed by LMB fusion-ICPMS and sinter-ICPMS.

CONCLUSIONS

A study of La, Ce, Pr, Nd, Sm, Eu, Gd, Tb, Dy, Ho, Er, Tm, Yb, Lu, Nb, Ta, Y, Zr, Hf accuracy and precision determined by the analysis of the CANMET diorite gneiss standard SY4 and bedrock samples from two mineral deposits by several commercially available methods has revealed that:

- Sodium peroxide sinter-ICPMS, LMB fusion-ICPMS, INAA and XRF are preferred methods for geochemical research because they produce the most accurate and precise data. Both 4 acid-ICPMS and AR-ICPMS analyses, while sufficiently precise for mineral exploration purposes, are inaccurate due to the inability of the acid to fully digest all rock-forming minerals and release all of the element in a sample.
- X-ray fluorescence is the most accurate technique for Zr, Hf, Y and Nb, but has a disadvantage of higher detection limits compared to sinter-ICPM and LMB fusion-ICPMS analysis. Accuracy and precision of lithium metaborate-tetraborate fusion-ICPMS approaches that of XRF and elements can be determined to lower detection limits. Mean values for Zr and Hf in the standard SY4 by 4

acid digest-ICPMS are much lower than the recommended value indicating that there is only a partial recovery of these elements from the standard.

- Instrumental neutron activation produces sufficiently accurate data for creating chondrite-normalized REE plots, but the high detection limits for some elements (Eu, Tb) are problematic for samples with low REE concentrations.
- Sodium peroxide sinter-ICPMS and LMB fusion-ICPMS analysis generate very similar chondrite-normalized REE profiles in contrasting rock types for all elements except for Ce.
- Analysis of other standard reference materials by the same methods would be a valuable complement to this study so that accuracy and precision of REE, RM and HFES elements can be determined over a wider concentration range.

ACKNOWLEDGMENTS

We very much appreciate the careful and constructive reviews of this paper by Graham Nixon, Senior Geologist, British Columbia Geological Survey and by Nick Massey, Emeritus Geoscientist, British Columbia Geological Survey.

REFERENCES

Bayon, G., Barrat, J.A. Etoublrau, J. Benoit, M., Bollinger, C and Revillon, S. (2009): Determination of rare earth elements, Sc, Y, Zr, Ba, Hf, and Th in geological samples by ICP-MS after Tm addition and alkaline fusion, *Geostandards and Geoanalysis Research, Volume 33*, pages 51-62.

Bowman, W.S. (1995): Canadian diorite gneiss SY-4: Preparation and certification by eighty-nine international laboratories; *Geostandards Newsletter*, volume 19, pages 101-124.

El-Teher, A. (2006): Rare earth elements in Egyptian granites by instrumental neutron activation analysis; in *Proceedings of the 2nd Environmental Physics conference, Alexandria*, pages 133-142.

Hall, G.E.M and Plant, J.A. (1992): Analytical errors in the determination of high field strength elements and their implications in tectonic interpretation studies; Chemical Geology, volume 95, pages 141-156.

Hall, E.M and Pelchat, J-C, (1990): Analysis of standard reference materials for Zr, Nb, Hf and Ta by ICP-MS after lithium metaborate fusion and cupferron separation; *Geostandards Newsletter*, volume 14, pages 197- 206.

Hoffman, E.L. (1992): Instrumental neutron activation in geoanalysis; *Journal of Geochemical Exploration*, volume 44, pages 297-320.

Logan, J.M, (2005): Alkaline magmatism and porphyry Cu-Au deposits at Glore Creek, Northwestern British Columbia, in Geological Fieldwork 2004, *BC Ministry of Energy, Mines and Petroleum Resources,* Paper 2005-1, pages 237-248.

Longerich, H.P., Jenner, G.A., Fryer, B.J. and Jackson, S.E. (1990): Inductively coupled plasma-mass spectrometric analysis of geological samples: A critical evaluation based on case studies; *Chemical Geology*, volume 83, pages 105-118.

Nakamura, N. (1974): Determination of REE, Ba, Fe, Mg, Na and K in carbonaceous and ordinary chondrites; *Geochimica et Cosmochimica Acta*, volume 38, pages 757-775.

Paterson, K. (2009): A lithogeochemical study of the Spanish Mountain Gold deposit, east central BC; Unpublished B.Sc. Thesis, *University of Victoria*, 46 pages.

Patterson, K. Lett, R.E and Telmer, K (2009): Lithogeochemistry of the Spanish Mountain Gold deposit, east central BC, (NTS 93A E11); in Geological Fieldwork 2008, *BC Ministry of Energy, Mines and Petroleum Resources,* Paper 2009-1, pages 163-168.

Potts, P.J. and Webb, P.C. (1992): X-ray Fluorescence spectrometry; *Journal of Geochemical Exploration*, volume 44, pages 250-296.

Carbonate-hosted, Nonsulphide Zn–Pb (supergene) Mineral Deposit Profile B09

by S. Paradis[1] and G.J. Simandl

IDENTIFICATION

SYNONYMS

Zinc-oxides, Calamines, Galman

COMMODITIES (*BYPRODUCTS*)

Zn, Pb *(Ag, Cu, barite, Cd)*

EXAMPLES

(British Columbia - *Canada*/*International*): Redbird (MINFILE 082FSW024), Lomond (MINFILE 082FSW018), Reeves MacDonald (MINFILE 082FSW026), Annex (MINFILE 082FSW219), Caviar (MINFILE 082FSW060), HB (MINFILE 082FSW004), Oxide (MINFILE 082FSW022), Cariboo Zinc (which comprises Canopener, DeBasher (MINFILE 093A 050), Flipper Creek, Dolomite Flats, Main (MINFILE 093A 065), Gunn, and Que (MINFILE 093A 062); *Leadville (Colorado, USA), Balmat (New York, USA), Sierra Mojada, Mapimi (Mexico), Accha, Mina Grande (Peru), Ariense (Brazil), Tynagh, Silvermines and Galmoy (Ireland), La Calamine (Belgium), Reocin (Spain), Silesia-Cracow district (Poland), San Giovanni (Italy), Lavrion (Greece), Touissit (Morocco), Um Gheig (Egypt), Zamanti district (Turkey), Jabali (Yemen), Angouran, Mehdiabad, Irankuh, Kuh-e-Surmeh (Iran), Shaimerden (Kazakhstan), Skorpion (Namibia), Padaeng (Thailand), Long Keng (Myanmar), Cho Dien (Vietnam), Jinding, Qiandong Shen Shen (China), Magellan (Australia).*

GEOLOGICAL CHARACTERISTICS

CAPSULE DESCRIPTION

Nonsulphide deposits are commonly hosted in carbonate rocks. The main minerals are hemimorphite, smithsonite, hydrozincite, cerussite, Fe-oxyhydroxides (including goethite), and hematite. The deposits are broadly divided into three subtypes: the more common – 1) direct replacement and 2) wallrock replacement; and the less common – 3) residual and karst-fill. Direct replacement deposits have similar shape as the sulphide protore from which they are derived and may contain vestiges of sulphide mineralization. Wallrock replacement deposits are located at various distances from the protore, have simpler mineralogy and higher Zn/Pb ratio than direct replacement deposits, and occur as irregular masses encrustations, tabular bodies, and open-space fillings. Residual and karst-fill deposits form generally small, high grade, irregular bodies of partly consolidated material that may have detrital component. Some nonsulphide deposits may share characteristics of more than one of these subtypes.

TECTONIC SETTING(S)

Supergene nonsulphide deposits derived from Mississippi Valley-type (MVT) and Irish-type deposits are located in carbonate platform settings, typically in relatively undeformed orogenic foreland rocks, commonly in foreland thrust belts inboard of clastic rock-dominated passive margin sequences, and in continental rift systems. Those derived from sedimentary exhalative (SEDEX) deposits are located in intracratonic or continental margin environments in fault-controlled basins and troughs. Volcanic-hosted massive sulphide (VHMS)-derived supergene nonsulphide deposits are emplaced under extensional crustal regime, such as oceanic or back-arc spreading ridges, continental rifts, back-arc basins, oceanic ridges close to continental margins, and rift environment within, or perhaps behind, an oceanic or continental margin arc.

DEPOSITIONAL ENVIRONMENT / GEOLOGICAL SETTING

Hostrocks of supergene nonsulphide Zn-Pb deposits are mostly deposited in platform successions within shallow and deep water environments. The nonsulphide deposits are found in both arid and tropical environments; however, many of the best supergene nonsulphide deposits recognized to date formed in semi-arid environments. Some are found in cold, wet climates at higher latitudes.

AGE OF MINERALIZATION

Ages of nonsulphide mineralization are commonly poorly constrained. Ore formation coincides with or postdates the exhumation of the hostrocks and generally postdates the main tectono-metamorphic event. Most of

[1] *Geological Survey of Canada, Sidney, BC*

This publication is also available, free of charge, as colour digital files in Adobe Acrobat® PDF format from the BC Ministry of Forests, Mines and Lands website at http://www.empr.gov.bc.ca/Mining/Geoscience/PublicationsCatalogue/Fieldwork.

the nonsulphide deposits formed during the late Cretaceous to late Tertiary *(i.e.,* Paleocene to Pliocene) and younger times.

HOST / ASSOCIATED ROCK TYPES

Dolostone, limestone, dolomitized limestone and argillaceous carbonate are the most common hostrocks. Siliciclastic rocks, such as calcsilicate rocks, carbonaceous black shale, siltstone, cherty argillite, quartz-rich conglomerate and arkosic meta-arenites, and volcaniclastic and metasedimentary rocks are also potential hosts.

DEPOSIT FORM

The direct replacement deposits (also referred to as "red ores") occur as a) irregular and poorly defined masses that replaced primary sulphides and carbonate hostrocks (Figure 1), whereby selective replacement within specific horizons may yield stratabound morphologies; and b) veins and open-space fillings within primary breccias of sulphide mineralization and carbonate hostrocks (Figure 2), where the morphologies of the

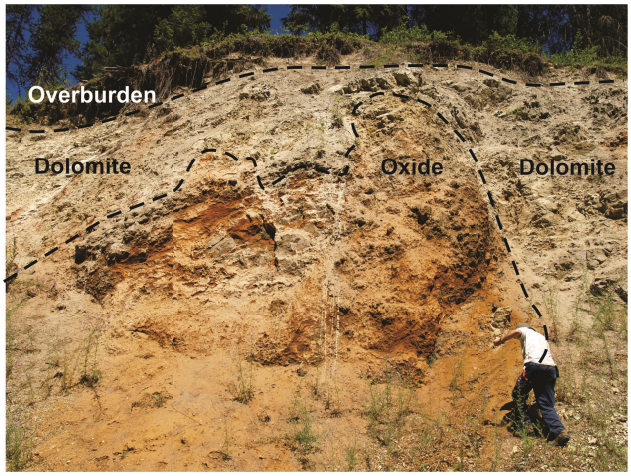

Figure 1. Lomond deposit; an example of a supergene direct replacement nonsulphide deposit, southeastern British Columbia.

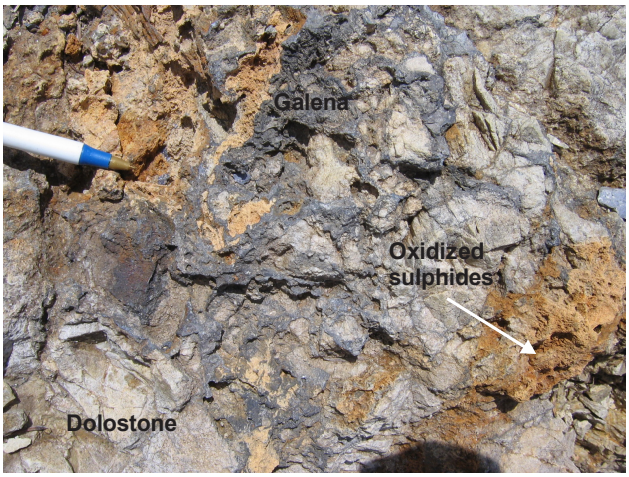

Figure 2. Galena and nonsulphides forming part of a vein-breccia system crosscutting the host dolostone, Cariboo Zinc property, east-central British Columbia.

nonsulphide zones are comparable to those of the related primary sulphides (*i.e.* stratabound zones and/or crosscutting pipes, fracture-fill zones, veins). The depth of oxidation can be variable from a few metres to several hundred metres. The wallrock replacement deposits are Zn-rich irregular and lens-shaped or tabular (subvertical to subhorizontal) bodies adjacent to or distal to direct replacement bodies. The residual and karst-fill deposits occur as accumulations of ferruginous, "earthy" and hemimorphite-clay mixtures, within karst cavities that cut through the replacement or open-space filling mineralization. These deposits have, irregular geometry, and can form high-grade nonsulphide bodies. Geometry is controlled by basement topography.

TEXTURE / STRUCTURE

Nonsulphides form irregular stratabound masses, pods or lenses; breccias of sedimentary and tectonic origin, disseminations, fracture fill, and veins are also very common. Due to intense oxidation, the primary textures of sulphides and hostrock are often obscured. Ore textures are varied and complex, ranging from massive to highly brecciated, from compact to powdery and from vuggy to dense. Nonsulphide minerals occur as earthy to crystalline aggregates replacing primary sulphides and/or carbonate hostrocks (Figures 3 and 4). They form crusts, concretions, and stalactites on outer surfaces, and botryoidal, colloform and crystalline aggregates of euhedral and subhedral crystals in intergranular voids, cavities, fractures, and breccias.

ORE MINERALOGY (Principal and *subordinate*)

Smithsonite, hemimorphite, hydrozincite, sauconite, cerussite, anglesite, litharge, pyromorphite, mimetite, and plumbojarosite, *minrecordite, zincian aragonite, willemite, goslarite, loseyite, descloizite, hetaerokite, hydrohetaerolite, chalcophanite, hopeite, aurichalcite, woodruffite, tarbuttite, scholzite.* Where the sulphide-bearing protolith was not entirely converted to nonsulphides, primary sulphides remain intermixed with

Figure 3. Hemimorphite-rich mineralization, Oxide deposit, southeastern British Columbia. The hemimorphite replaced the carbonate groundmass.

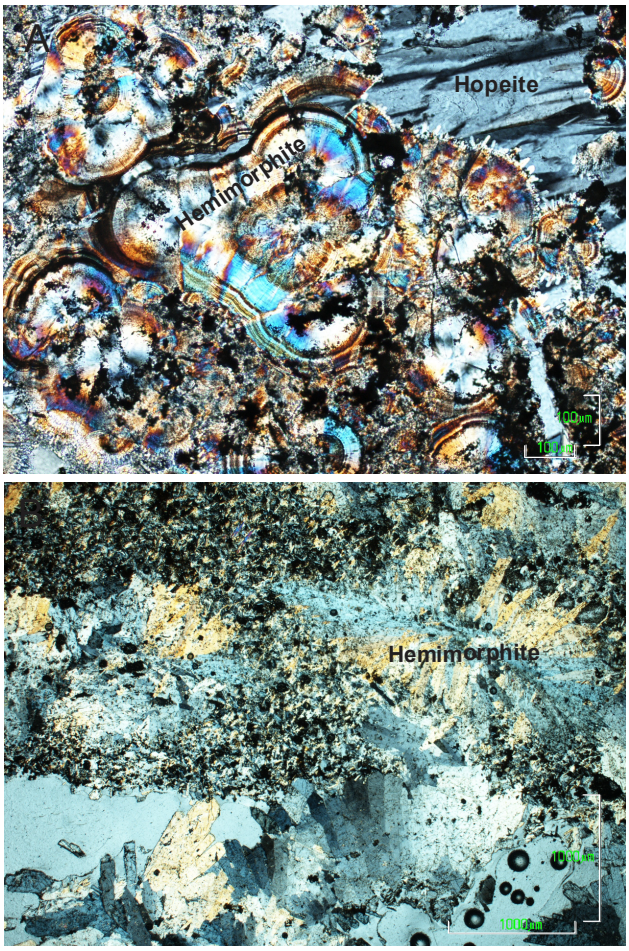

Figure 4. Microphotographs (polarised light) of A) concentric aggregates of radiating crystals of hemimorphite replacing the carbonate groundmass and tabular crystals of hopeite filling up crosscutting veinlets, and B) aggregates of tabular crystals of hemimorphite lining cavities.

the nonsulphide minerals to form "mixed ores". The primary sulphides may contain anglesite-coated nodules of galena and remnants of sphalerite. Chalcocite, malachite, and azurite are present in some deposits.

GANGUE MINERALOGY (Principal and *subordinate*)

Carbonates (dolomite, calcite, aragonite), hematite, goethite, other Fe-oxyhydroxides, *gypsum, minor quartz*.

ALTERATION MINERALOGY

Coarse crystalline dolomite spatially associated with MVT-type protore may survive in proximity to nonsulphide deposits and contrast with regional finely crystalline dolostone. Local alteration may also include silicification and rare secondary barite, both a result of the alteration and breakdown of feldspar (*e.g.,* Skorpion). The sulphide weathering and near surface alteration of protore corresponds to formation of supergene mineralization.

WEATHERING

The nonsulphide mineralization forms by weathering of sulphides. Multicyclic oxidation and leaching of nonsulphides is a part of the ore-forming process and may affect even previously formed wallrock replacement bodies (see genetic model). Such bodies may be gradually converted into porous brown to reddish smithsonite intergrown with hemimorphite. Further leaching may result in mixture of hemimorphite, sauconite, hematite- or goethite-dominated iron oxides, and hematitic chalcedonic silica, and ultimately transformed into a barren goethite-chalcedonic silica rock.

ORE CONTROLS

Most favourable conditions for oxidation are achieved in hot, arid or semiarid climates, which maximize the quantity of metals available for transport by supergene solutions. Sedimentary successions containing carbonate rocks are the most common regional hosts for nonsulphide lead and zinc deposits. In general, the oxidation of the protore takes place above water table. Karst, faulting, fracturing and to lesser extend porosity are important in enhancing the depth and intensity of the oxidation. Major faults represent channels for oxygenated solutions and permit oxidation to depths exceeding 500 m. Faults also increase the reactive surface of hostrocks (*i.e.* provoking changes in pH and Eh). Direct replacement deposits are confined to protore envelope. Wallrock replacement orebodies are commonly located near the level of the paleo and/or present water table.

GENETIC MODEL

Supergene nonsulphide Zn-Pb deposits form when base metal sulphide mineralization is subject to intense weathering and metals are liberated by the oxidation of sulphide minerals. The formation of nonsulphide minerals is influenced by the composition, size and morphology of the preexisting sulphide body. During the formation of a direct replacement deposit, primary ore (protore) is oxidized, and base metals pass into solution and are redistributed and trapped within space originally occupied by the protore. If the base metals liberated by the oxidation of sulphides are not trapped locally, they are transported by percolating waters down and/or away from the sulphide protore, and under favourable geological conditions may form wallrock replacement deposits. Wallrock replacement deposits can be located in proximity to protore or several hundreds of metres away. Lead is less mobile in the supergene environment than zinc, so in general, it is left behind as relict galena nodules and lead carbonate or lead sulphates. Wallrock replacement deposits tend to have higher Zn content and higher Zn/Pb ratios than direct replacement deposits. Residual and karst-fill deposits are formed as accumulations of mechanically and/or chemically transported zinc-rich material in karstic cavities or lows in basement topography. Some nonsulphide zinc deposits are assigned a hypogene origin. These deposits are

characterized by willemite or willemite-franklinite-zincite assemblages (Hitzman *et al.*, 2003) and formed at higher temperatures than the supergene deposits. Their temperature of formation is estimated from less than 100° to nearly 300°C.

ASSOCIATED DEPOSIT TYPES

Mississippi Valley-type Pb-Zn (E12), Irish-type carbonate-hosted Zn-Pb (E13), sedimentary exhalative Pb-Zn-Ag (E14), veins, and Pb-Zn skarns (K02); rarely volcanic-hosted massive sulphide (G04 to G06).

COMMENTS

British Columbia has prospective strata for supergene nonsulphide deposits in the miogeoclinal carbonate platform rocks of the Ancestral North America continental margin and in pericratonic rocks of the Kootenay terrane. The association of many known carbonate-hosted nonsulphide zones with directly underlying massive sulphide orebodies, in combination with nonsulphide mineralogical characteristics, suggests that a large proportion of known nonsulphide mineralized zones in southern and central British Columbia are of the direct replacement type.

EXPLORATION GUIDES

GEOCHEMICAL SIGNATURE

Colorimetric field test for secondary zinc minerals ("Zinc Zap") is very useful (Figure 5). Portable hand-held x-ray fluorescence spectrometry was successfully tested in British Columbia on supergene nonsulphide Pb-Zn deposits. Depletion in Zn, Pb, Cu, Fe, and Mn in and around former Zn-bearing sulphide gossans. Readily detectable positive anomalies of Zn and Pb in residual soils and stream sediments; elevated concentrations of Cu, Fe, Ag, Mn, As, and Cd can also be detected. Analysis of heavy mineral concentrates (identification of Zn-Pb nonsulphides) in stream and overburden may be effective

Figure 5. Typical bright red stain caused by reaction of "Zinc Zap" solution with zinc-rich mineralization, east-central British Columbia.

in areas lacking deep weathering. Where residual sulphide oxidation is taking place, soil gas geochemical techniques (SO2 surveys) may be an applicable exploration technique. Many supergene minerals, such as hydrozincite and smithsonite, give distinct spectral responses in the short-wave infrared portion of the spectrum. Hyperspectral imaging holds promise as a useful tool for accurate mapping of structures, lithologies, and alteration.

GEOPHYSICAL SIGNATURE

There is no simple approach to use geophysical methods in exploration for nonsulphide-bearing Pb-Zn deposits. The mineralogy, textures, homogeneity, friability, porosity, and degree of saturation by water vary widely. These properties affect the density, resistivity, magnetic susceptibility, and seismic properties of the rocks. Interpretation methodologies may be district specific. Where sulphide mineralization is present at depth, methodology used in exploration for MVT, VHMS, and SEDEX deposits applies.

OTHER EXPLORATION GUIDES

Most of the supergene nonsulphide base metal deposits are derived from the oxidation, or near-surface weathering, of primary carbonate-hosted sulphide deposits, such as Mississippi Valley-type, sedimentary exhalative, Irish-type or vein-type deposits and, to lesser extent, Pb-Zn skarns and rarely volcanic-hosted massive sulphide. Any carbonate-hosted, sulphide zinc district that has undergone geochemically mature weathering in semiarid to wet climatic (or paleoclimatic) conditions and concomitant tectonic uplift and/or water table depression is prospective for supergene nonsulphide deposits. Within these settings, exploration could be further focused on areas where favourable water table level, optimum oxido-reduction conditions, permissive hydrological characteristics (permeability and porosity of the hostrocks, karsts, and fracture and fault zones), rocks with ability to control the pH of the metal-bearing solutions, topography and slow(?) rate of uplift, coexisted. Discovery of outcropping supergene Zn-Pb nonsulphide deposits depends on recognition of common nonsulphide ore minerals. Areas not affected by glaciation have higher potential to contain preserved, soft, nonsulphide deposits than glaciated ones.

ECONOMIC FACTORS

TYPICAL GRADE AND TONNAGE

Tonnages for nonsulphide Zn-Pb deposits range from <1 Mt to 50 Mt with grades of 2% to more than 30% Zn. If mixed ores are considered, some deposits and districts have tonnages comparable to world-class sulphide deposits. Skorpion (Namibia) has 60 Mt of mixed resource grading 6–8% Zn and 1–2% Pb, and 24.6 Mt of oxide resource grading 10.6% Zn. Mehdiabad (Iran) has a mixed oxide-sulphide resource of 218 Mt grading 7.2% Zn, 2.3% Pb, and 51 g/t Ag. Direct replacement

nonsulphide Zn-Pb deposits could be also significant sources of Pb, as illustrated by the exploitation of the Magellan deposit, which has ore reserves of 8.5 Mt grading 7.12% Pb.

ECONOMIC LIMITATIONS

The economic value of nonsulphide ores is dependent on the physical setting of individual deposit, the specific characteristics of the mineralogical association and the nature of the gangue minerals. The large, near-surface deposits are amenable to high volume, open pit mining. Underground mining is less common. Depending on the type of ore and mineralogy, a dedicated processing plant may be required. However, there is also the possibility that limited quantities of zinc-rich carbonates or silicate-bearing material (with low levels of impurities) may be used by conventional smelters as a sweetener (instead of Ca carbonate that is commonly used to control the pH) or as source of silica; this should be investigated.

IMPORTANCE

Nonsulphide deposits were the main source of zinc prior to the 1930s. Following the development of differential flotation and breakthrough in smelting technology, the mining industry turned its attention almost entirely to sulphide ores. Today, most zinc is derived from sulphide ore. The nonsulphide deposits provided roughly 7% of the world's zinc production in 2009. The successful operation of a dedicated processing plant at the Skorpion mine to extract zinc, through direct acid leaching, solid-liquid separation, solvent extraction and electro winning from nonsulphide ore has attracted more attention to these types of deposits. These deposits are attractive targets because they are characteristically low in lead, sulphur and other deleterious elements, offer low-cost onsite production, and are environmentally friendly.

ACKNOWLEDGMENTS

This manuscript benefited from reviews by Donald Sangster (Geological Consultant, Ottawa) and David Lefebure (British Columbia Geological Survey Branch). The project started under the umbrella of the Cordilleran Targeted Geoscience Initiative-3 Program of the Geological Survey of Canada, and was done in collaboration with the British Columbia Geological Survey Branch. Geoscience BC is acknowledged and thanked for funding the laboratory component required to complete this project.

SELECTED BIBLIOGRAPHY

Gorzynski, G. (2001): REMAC zinc project, Reeves property and Redbird property – 2000 summary report, trenching and drilling program; *Redhawk Resources Inc*., 47 pages.

Heyl, A.V. and Bozion, C.N. (1962): Oxidized zinc deposits of the United States, Part 1, General geology; *United States Geological Survey*, Bulletin 1135-A, 52 pages.

Hitzman, M.W., Reynolds, N.A., Sangster, D.F., Cameron, R.A. and Carman, C.E. (2003): Classification, genesis, and exploration guides for nonsulphide zinc deposits; *Economic Geology*, Volume 98, Number 4, pages 685–714.

Paradis, S., Simandl, G.J., Bradford, J., Leslie, C., Brett, C., and Schiarizza, P. (2010): Carbonate-hosted sulphide and nonsulphide Pb-Zn Mineralization in the Barkerville area, British Columbia, Canada; *in* Geological Fieldwork 2009, *British Columbia Ministry of Energy, Mines and Petroleum Resources*, Paper 2010-1, pages 69-82.

Enkin, R, Paradis, S. and Simandl, G.J. (in press): Physical properties of carbonate-hosted nonsulphide Zn-Pb mineralization in southern (NTS 082F/03) and central British Columbia (NTS 093A/14E); in *Geoscience BC Summary of Activities*, Geoscience BC Report 2011-1.

Pirajno, F., Burlow, R. and Huston, D. (2010): The Magellan Pb deposit, Western Australia; a new category within the class of supergene non-sulphide mineral systems; *Ore Geology Reviews*, Volume 37, pages 101–113.

Reichert, J. (2009): A geochemical model of supergene carbonate-hosted nonsulphide zinc deposits; in Titley, S. R., ed., Supergene, Environments, Processes, and Products, Society of Economic Geologists, Special Publication number 14, pages 69-76.

Reichert, J. and Borg, G. (2008): Numerical simulation and geochemical model of supergene carbonate-hosted non-sulphide zinc deposits; *Ore Geology Reviews*, Volume 33, pages 134–151.

Sangster, D.F. (2003): A special issue devoted to nonsulphide zinc deposits: a new look; *Economic Geology*, Volume 98, Number 4, pages 683–684.

Simandl, G.J. and Paradis, S. (2009): Carbonate-hosted, nonsulphide, zinc-lead deposits in the Southern Kootenay Arc, British Columbia (NTS 082F/03); *in* Geological Fieldwork 2008, *British Columbia Ministry of Energy, Mines and Petroleum Resources*, Paper 2009-1, pages 205-218.